Investigating the role of phytohormones in Fusarium head blight and Fusarium root rot of *Brachypodium distachyon*

John Francis Haidoulis

A thesis submitted to the University of East Anglia

for the degree of Doctor of Philosophy (PhD)

Department of Crop Genetics

John Innes Centre

February 2021

Abstract

Fusarium graminearum causes Fusarium head blight (FHB) and Fusarium root rot (FRR) in small-grain cereals. Phytohormones are reported to affect host resistance to FHB. However the role of phytohormones on resistance to FRR is unknown. *Brachypodium distachyon* is an effective model for investigating both FHB and FRR. The role of phytohormones in the interaction between *B. distachyon* and *F. graminearum* was investigated.

Phytohormone treatment prior to *F. graminearum* infection assays were performed on *B. distachyon* floral and root seedling tissues. Jasmonic acid (JA), ethylene, auxin, cytokinin, and 3-aminobutanoic acid (BABA) induced the most significant effects on both FHB and FRR resistance. Tissue-specific effects of phytohormones were observed as JA and ethylene increased resistance to FRR but susceptibility to FHB. Salicylic acid (SA) only induced negative effects on FRR resistance. Tissue-independent effects were also observed. Auxin increased resistance whereas cytokinin and BABA increased susceptibility to both diseases.

An RNA-seq transcriptome analysis revealed that expression of genes associated with five phytohormones: JA, ethylene, auxin, cytokinin, and abscisic acid (ABA) were overrepresented in response to FHB and FRR. Generally, JA and ethylene associated genes showed similar expression patterns between tissues whereas auxin, cytokinin, and ABA associated genes showed dissimilar expression patterns between FHB and FRR. A transcriptome analysis of *F. graminearum* effectors with the same infected material revealed elevated expression of both core tissue-independent genes and several tissue-dependent genes during infection.

Ethylene signalling has been associated with *F. graminearum* susceptibility in wheat and *Arabidopsis thaliana*. The ability of *F. graminearum* to produce ethylene was demonstrated and the biosynthetic pathway used was identified. A candidate ethylene biosynthetic gene was identified through RNA-seq analysis and was deleted via a split-marker deletion method. No change in ethylene production, growth, or virulence was observed for the deletion strains.

Acknowledgments

Abbreviations

%	percentage
°C	degrees Celsius
µg	microgram(s)
µl	microlitre(s)
µM	micromolar
µm	micrometre(s)
ABA	abscisic acid
ACC	1-aminocyclopropane-1-carboxylic acid
AcDON	acetyldeoxynivalenol
ANOVA	analysis of variance
AOA	aminooxyacetic acid
Arg	arginine
At	*Arabidopsis thaliana*
AVG	2-aminoethoxyvinyl glycine
BABA	3-aminobutanoic acid
BAP	6-benzylaminopurine
BCA	bio-control agent
BCAT	branched chain amino acid transaminase
Bd3-1/Bd21	*Brachypodium distachyon* line 3-1 or line 21
bp	base pair
BR	brassinosteroid
Brz	brassinazole
CDL	czapek Dox Liquid
cDNA	complementary DNA
CKs	cytokinins
cm	centimetre(s)
Cq	quantitation cycle
CTAB	cetyltrimethylammonium bromide
cv.	cultivated variety
CWDE	cell wall degrading enzyme
DEGs	differentially expressed genes
diH$_2$O	deionized water
DMSO	dimethyl sulfoxide
dNTP	deoxynucleoside triphosphate
DON	deoxynivalenol
dpa	days post application
dpi	days post inoculation
ds	dilution series
DW	dry weight
eBL	epibrassinolide
ED	experimentally determined
EFE	ethylene-forming-enzyme
ER	endoplasmic reticulum
ET	ethylene
ETI	effector-triggered immunity
F	forward

Fc	*Fusarium culmorum*
FCR	Fusarium crown rot
Fg	*Fusarium graminearum*
FgPH1	*Fusarium graminearum isolate PH1*
FHB	Fusarium head blight
FID	flame Ionisation detector
FRR	Fusarium root rot
FW	fresh weight
g	gram(s)
GA	gibberellic acid
GABA	4-aminobutanoic acid
GC	gas chromatography
GC-MS	gas chromatography-mass spectrometry
gDNA	genomic DNA
GLM	generalised Linear Model
GOI	gene of interest
h	hour(s)
His	histidine
HK	housekeeping
hph	hygromycin-B-phosphotransferase
Hpi	hours post infection
HR	hypersensitive response
Hv	*Hordeum vulgare*
HYG	hygromycin selectable marker
IAA	indole-3-acetic acid
ID	identification
JA	jasmonic acid
JARIN-1	jasmonic acid inhibitor - 1
JIC	John Innes Centre
kbp	kilobase pair
KMBA	α-keto γ-methylthiobutyric acid
L	litre(s)
LB	Luria-Bertani media
Log	logarithm
LSD	least significant difference
M	molar
MB	mung Bean
Mbp	megabase pair
MeJA	methyl jasmonate/
Met	methionine
mg	milligram(s)
min	minute(s)
ml	millilitre(s)
mM	millimolar
mm	millimetre(s)
mV	millivolts
n	number of samples
NAA	1-naphthaleneacetic acid
NB-LRR	nucleotide-binding-leucine rich repeat

ng	nanogram(s)
NIV	nivalenol
nl	nanolitre
nmol	nanomole
Os	*Oryza sativa*
OXO	2-oxoglutarate
p-value	calculated probability
p-adj	adjusted p-value
PAMP	pathogen-associated molecular patterns
PCR	polymerase chain reaction
PDA	potato dextrose agar
Phx	prohexadione
PLP	pyridoxal 5 phosphate
pmol	picomole
ppb	parts per billion
ppm	parts per million
PRR	plant pattern recognition receptors
PTI	PAMP-triggered immunity
QTL	quantitative trait locus
R	reverse
RCBD	randomised complete block design
rcf	relative centrifugal force
RNA	ribonucleic acid
RNA-seq	RNA-sequencing.
RNL	root necrosis length
ROS	reactive oxygen species
rpm	revolutions per minute
RT-qPCR	reverse transcriptase-quantitative polymerase chain reaction
s	second(s)
SA	salicylic acid
SAR	systemic Acquired Resistance
SD	score-date
SE	standard error
SQRT	square root
Ta	*Triticum aestivum*
TMV	tobacco mosaic virus
tZ	*trans*-Zeatin
UTR	untranslated region
UVB	ultraviolet B
V	volts
WT	wild-type
Zm	*Zea mays*

Contents

Table of Figures

plants. (C) One pot of *F. graminearum*-infected Bd3-1 with individual spikes tagged for scoring growing in an 8 cm2 pot. Scale bar = 3 cm. (D-E) *F. graminearum*-infected Bd3-1 spikelets at 7 dpi with brown lesions on individual florets which were scored for all Bd trials (D) and heavily infected with aerial mycelia covering the entire spike (E). (C, D, and E) Taken from (Haidoulis & Nicholson, 2020).

distachyon tissues and were separately analysed through the RNA-seq pipeline with the respective inoculated sample tissues. The numbers besides the dendrogram represent cluster groups with similar expression patterns in response to FHB and FRR across samples. * Derived from (Jain et al., 2006a, Jain et al., 2006b). ** Derived from (Jain et al., 2005, Jain et al., 2006a) and was also responsive to auxin in (Kakei et al., 2015) with q < 0.05 and -2 ≤ Log2 ≥ 2. Some gene functions have a prefix (derived from *A. thaliana* (At) or *O. sativa* (Os)) and percentage homology (the percentage of *B. distachyon* sequence that matches the homologues sequence). Column abbreviations; HC (Head-FHB control), HF (Head-FHB fungus), RC (Root-FRR Control), RF (Root-FRR fungus).

light is important for the final conversion of KMBA to ethylene (Chagué et al., 2002, Zhu et al., 2012). Further information on the pathways can be found at MetaCyc.org (PWY-6853, ETHYL-PWY, PWY-6854) (Caspi et al., 2017). Abbreviations: ACC (1-aminocyclopropane-1-carboxylic acid), KMBA (α-keto γ-methylthiobutyric acid), EFE (ethylene-forming-enzyme). This figure is modified with permission from (Ansari et al., 2013).

(Arginine), Hist (Histidine), ACC (1-aminocyclopropane-1-carboxylic acid), and AOA (aminooxyacetic acid), KMBA (α-keto γ-methylthiobutyric acid), Met (Methionine).

replicates from one independent experiment. (C and D) Each bar is from one biological replicate (2 from bcat-J) from one independent experiment. Strains bcat-C, bcat-D, and bcat-L were not included in D due to software malfunction. Data for absence of methionine control treatments were not included as there was no ethylene detected. GLM-ANOVA significance level * $p < 0.05$.

Table of Tables

Table of Equations

Chapter 1 - General Introduction

1.1. Fusarium Diseases of Small Grain Cereals

Fusarium are fungi that cause disease of cereals in many areas of the world such as Europe, America, East Asia, and Australia (Parry et al., 1995, Xu & Nicholson, 2009). *Fusarium graminearum* is ranked as one of the most devastating fungal pathogens in the world (Dean et al., 2012). *F. graminearum* grows on both vegetative and reproductive organs of crops at any age, resulting in a range of diseases (Miedaner, 1997). Its main hosts are small grain cereals from the Poaceae family such as wheat (*Triticum aestivum*), barley (*Hordeum vulgare*), and rye (*Secale cereale*), on which they cause diseases such as Fusarium head blight (FHB, also known as ear blight/scab), Fusarium root rot (FRR), Fusarium crown rot (FCR), and seedling blight. There are many *Fusarium* species and several can cause FHB (Parry et al., 1995, Xu & Nicholson, 2009). However, the most economically important tend to be *Fusarium graminearum* (Teleomorph *Gibberella Zeae*) and *Fusarium culmorum* (Parry et al., 1995).

Wheat is one of the most important cereals in the world with 766 million tonnes produced on 216 million hectares worldwide in 2019 (FAO., 2020). By 2050, wheat production is required to increase between 25% and 70% in order to sustain the predicted human population size (Hunter et al., 2017). Reducing biotic-related reductions of wheat yield and grain quality is an important task to sustain a growing demand for wheat production. *Triticum* species appear to be the most susceptible to *F. graminearum* out of most cereal species (Langevin et al., 2004). Floral infection results in yield loss, quality loss (Parry et al., 1995, Osborne & Stein, 2007), and can also pose a threat to human and livestock health because of the accumulation of *Fusarium*-produced mycotoxins in grain (Antonissen et al., 2014, Salgado et al., 2014). The result of FHB epidemics costs billions of dollars in some parts of the world (McMullen et al., 2012). For example, the total cost of the disease on wheat and barley crops in the United States was estimated at $2.49 billion between 1998-2001 (Nganje et al., 2004). Furthermore, future climate and temperature changes may increase the risk of FHB epidemics (Sutton, 1982, Madgwick et al., 2011, Shah et al., 2014). Therefore employing strategies to control FHB is important for improving food security and health.

1.1.1. The Lifecycle of *Fusarium graminearum*

F. graminearum is a filamentous homothallic fungus in the Ascomycota division that can grow in soil or debris and lives either a non-host associated lifestyle or as a pathogen causing diseases on living hosts (Parry et al., 1995, Trail, 2009). *F. graminearum* remains haploid for most of its lifecycle (Trail, 2009). Depending on environmental conditions, asexual spores or sexual ascospores (Teleomorph *Gibberella zeae*) are produced (Goswami & Kistler, 2004, Kazan et al., 2012, Shah et al., 2018). *F. graminearum* is believed to reproduce sexually and asexually, whereas *F. culmorum* has only been observed to reproduce asexually (Doohan et al., 2003). There are three types of asexual spores but only two apply to *F. graminearum*. The first are macroconidia which are long and curved spores with hooked ends and several septa and are produced from a sporodochium. The second are round and thick cell walled chlamydospores that are produced from macroconidia or hyphae (Ma et al., 2013). Macroconidia or chlamydospores are transported through rain-splash or wind (Shah et al., 2018). *F. graminearum* macroconidia (Fig. 1.1) are optimally produced between 28°C - 32°C (Doohan et al., 2003). On the other hand, the sexual ascospores which are smaller and blunt-ended spores relative to macroconidia are optimally produced between 25°C - 28°C (Doohan et al., 2003). Black perithecia form on the debris surface (Fig. 1.2), and forcibly discharge ascospores onto cereal spikes in conducive environments such as under high humidity (Fig. 1.2; (Kazan et al., 2012, Keller et al., 2014). Chlamydospores and perithecia allow for *Fusarium* to overwinter and remain in the stubble of plant material from previous years (Shah et al., 2018) (Fig. 1.2) which is a major source of FHB inoculum (Bai & Shaner, 2004). Alternative sources of inoculum include grain infected with *Fusarium* or other *Fusarium* hosts (Parry et al., 1995). The most conducive environments for FHB are when the host flowers (anthesis) in moist environments (Bai & Shaner, 2004, Gautam & Dill-Macky, 2012, Kazan et al., 2012) and when temperatures are between 10°C - 30°C for ascospore release and 20°C - 30°C for macroconidia colonisation (Doohan et al., 2003). The environment has an important role in determining disease intensity and *Fusarium* biomass (Kriss et al., 2012).

Figure 1.1. *F. graminearum* PH1 macroconidia. Photo taken with iPhone 6 camera through the eyepiece of a light microscope. Scale bar = 50 µm.
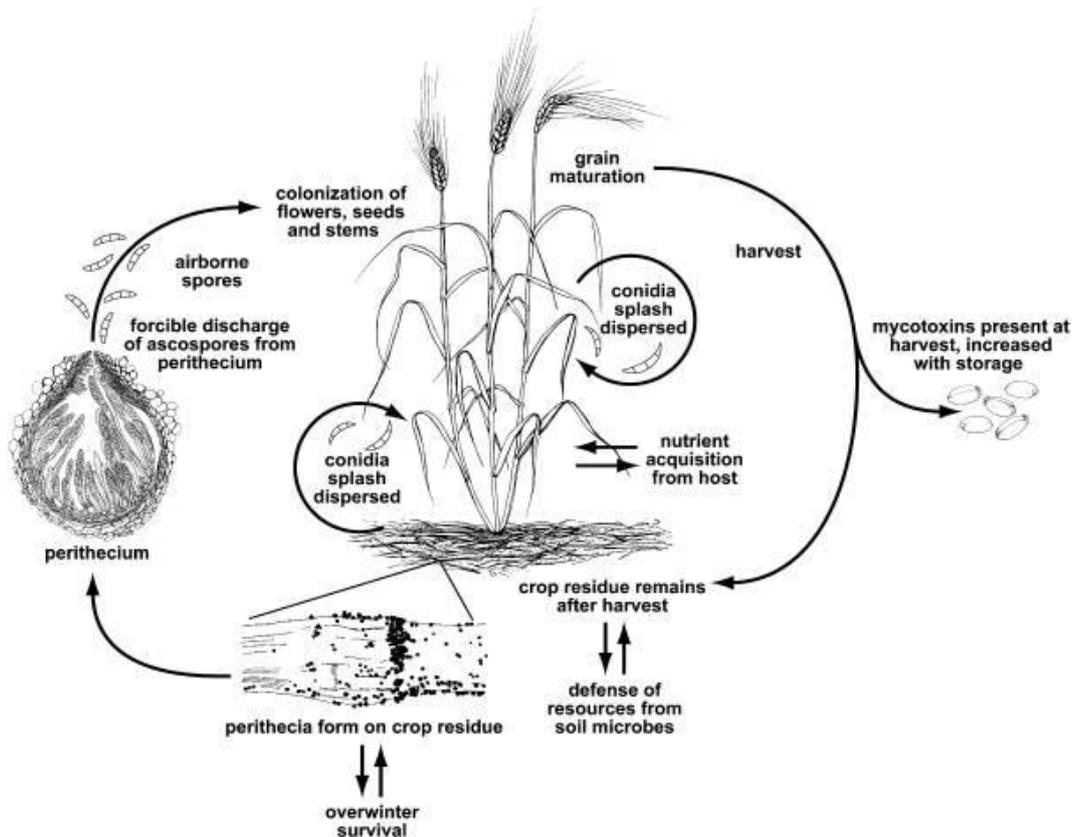
Figure 1.2. Overview of *F. graminearum* life cycle on a wheat plant. This figure has been taken with permission from one published by (Trail, 2009).

Fungi can exhibit different feeding lifestyles. Biotrophs often establish a constant feeding relationship with the host without killing host tissues, whereas necrotrophs directly kill host tissue for nutrient acquisition (Glazebrook, 2005). Hemi-biotrophs generally adopt an early biotrophic phase followed by a necrotrophic phase (Glazebrook, 2005). Aside from its predominantly saprotrophic life-style, *F. graminearum* is generally considered a facultative hemibiotroph exhibiting both biotrophy and necrotrophy (Parry et al., 1995, Jansen et al., 2005, Boddu et al., 2006, Brown et al., 2010, Kazan et al., 2012, Dweba et al., 2017). During initial infection of spike tissue at the advancing hyphal front, *F. graminearum* grows as a biotroph and feeds off apoplastic exudates whereas behind this, hyphae ramify through dead tissue (Brown et al., 2010, Dean et al., 2012). *F. graminearum* has the ability to infect nearly the entire plant (Miedaner, 1997), and as such there are slight differences in the infection process between different plant tissues. *Fusarium graminearum* is often associated with FHB, and as a result, other Fusarium diseases such as Fusarium root rot are not as well studied. The precise lifecycle of *F. graminearum* in different host tissues has not been investigated to the same extent.

1.1.2. Fusarium Head Blight

The most economically damaging Fusarium disease is FHB. As a result, much of the research has focussed exclusively on FHB. More than one species of *Fusarium* can co-infect a wheat spike (Xu & Nicholson, 2009) and the dominance of one species varies greatly at the field level (Xu et al., 2008b). *F. graminearum* is more competitive than the other *Fusarium* species (Xu et al., 2007). These species grow in various temperate environments, where *F. graminearum* is prevalent in humid and warm regions compared to infection by *Fusarium* species like *F. culmorum* that tend to occur in cooler and humid regions (Osborne & Stein, 2007, Xu et al., 2008a, Xu & Nicholson, 2009). However *F. graminearum* occurrence in cooler regions is becoming more prevalent (Xu & Nicholson, 2009).

Most wheat varieties consist of two-rowed spikelets on alternate sides of the rachis attached to rachis nodes. The floral bracts consist of a glume pair that encases at least four of the florets. Each floret has a palea and lemma that encases the grain. FHB is associated with floral tissue infection and results in considerable direct damage to the developing grain. On the abaxial surface of the glumes, macroconidia begin to germinate between 6 and 12 hours post infection (hpi) with thin hyphae that extend across the epidermis (Pritsch et al., 2000). Direct mechanical penetration of the floral bract is unlikely as there is a thick

external epidermis (Lewandowski et al., 2006), yet cell wall degrading enzymes secreted by the fungus can be used for penetration (Mary Wanjiru et al., 2002, Jansen et al., 2005, Kikot et al., 2009). Certain structures were identified at the end of peg-like structures on the glume's epidermis which might be involved in penetration and spread of the fungus (Pritsch et al., 2000, Goswami & Kistler, 2004, Boddu et al., 2006). Hyphae have been found to grow towards crevices between the lemma and palea to gain access to the organs inside the floret, since cell walls there are thinner and more susceptible to penetration (Pritsch et al., 2000, Mary Wanjiru et al., 2002, Lewandowski et al., 2006). Wheat anthers are an important target for *F. graminearum* (Parry et al., 1995). In addition, there is evidence that the fungal hyphae grow towards stomata between 12 hpi and 24 hpi (Pritsch et al., 2000).

F. graminearum can then grow intercellularly and intracellularly (Mary Wanjiru et al., 2002, Boddu et al., 2006). Dense hyphal mats resulting from intercellular growth usually occurs from 1 to 2 days post inoculation (dpi) in the subcuticular space under the epidermis. This is a prerequisite for parenchyma cell walls to be penetrated (Pritsch et al., 2000, Mary Wanjiru et al., 2002, Jansen et al., 2005). Subsequently, appressoria-like structures develop and intracellular growth in the cytosol of target cells occurs (Jansen et al., 2005). Once hyphae are in the cytosol and plasmolysis occurs, cell death quickly follows (Jansen et al., 2005, Brown et al., 2010). Extensive cell death manifests itself as lesions in the floral bract and then the caryopsis (Lewandowski et al., 2006). First visible symptoms are often brown discoloration of the lemma at 2 dpi up until 6 dpi (Boddu et al., 2006). Macroconidia developing from conidiophores became visible on the glumes (Pritsch et al., 2000) and caryopsis (Jansen et al., 2005) around 2 dpi to 4 dpi. The spread of hyphae between florets is thought to occur via the vascular tissues as hyphae were found in the rachis by 6 dpi (Jansen et al., 2005). Brown and colleagues (2010) describe systemic spread of *F. graminearum* in the rachis via intercellular and intracellular hyphal growth in the cortex and vascular bundle, respectively (Brown et al., 2010). Colonisation of the wheat peduncle and stem during late infection has also been reported (Guenther & Trail, 2005).

During later developmental stages, brown spots develop at the point of infection and spread throughout the rachis. The peduncle, which supports the inflorescence, becomes discoloured and over time the inflorescence bleaches (Fig. 1.3A), and the florets will then produce small and shrivelled kernels. This is due to the destruction of starch and protein (Sutton, 1982, Parry et al., 1995, Schmale III & Bergstrom, 2003, Goswami & Kistler, 2004,

Guenther & Trail, 2005). Extended periods of elevated temperatures and wetness can elevate FHB symptoms (Xu et al., 2007). During extensive humid periods, orange spore masses are visible on the floral bracts and caryopses (Goswami & Kistler, 2004) which consist of macroconidia (Shah et al., 2018).

Figure 1.3. FHB symptoms on wheat and barley ears. (**A**) Severe FHB symptoms on a wheat ear resulting in bleaching of almost the entire ear (**B**) FHB symptoms on a barley ear with one infected floret from each infection site. Scale bars: (**A**) 2 cm and (**B**) 1 cm. Photos kindly provided, with permission, from Dr Rachel Goddard.

Apart from affecting grain yield and quality of the cereal crop, a broad range of mycotoxins (sesquiterpenoid secondary metabolites) are produced by *Fusarium* species. There are numerous *Fusarium*-derived mycotoxins however prevalent *F. graminearum*-specific mycotoxins include trichothecenes and zearalenones (Ferrigo et al., 2016). There are broadly four groups of trichothecene mycotoxins but two mainly apply to *Fusarium* species (McCormick et al., 2011, Ferrigo et al., 2016). *Fusarium* species either produce Type A (e.g. T-2), and Type B (e.g. Deoxynivalenol (DON) and Nivalenol (NIV)), and the specific

toxin varies among *Fusarium* species and isolates (Ferrigo et al., 2016). Trichothecenes specific to *F. graminearum* are predominantly the type B trichothecenes; deoxynivalenol (DON), and nivalenol (NIV) (Ferrigo et al., 2016) that increase fungal virulence depending on the cereal species (Maier et al., 2006). DON may not be the most toxic trichothecene mycotoxin but is considered one of the most prevalent and economically damaging one (McCormick et al., 2011, McMullen et al., 2012) (Professor Paul Nicholson, personal communication). These toxins are thought to act as virulence factors for fungal infection (Bai et al., 2002). This is because *F. graminearum* strains that produce trichothecenes are generally more aggressive and result in more severe symptoms in wheat (Langevin et al., 2004). DON-producing species exacerbated the spread of infection throughout the wheat spike (Gosman et al., 2010). Furthermore, wheat grain colonisation by trichothecene-producing *F. graminearum* strains was found to be greater than non-producing *F. graminearum* strains (Nicholson et al., 1998). Likewise, an absence of DON production during infection resulted in reduced spread of infection in wheat (Bai et al., 2002), suggesting that DON promotes the spread of floral infection. There are also differences in pathogenesis depending on the trichothecene produced as DON producing *Fusarium* species were found to spread in the wheat heads faster and result in an increase in severity compared to NIV producing species (Gosman et al., 2010). The environment also has an important impact on the degree of type B mycotoxin contamination (Xu et al., 2007, Kriss et al., 2012).

The *Tri* gene cluster is involved in synthesis of trichothecene mycotoxins (Kimura et al., 2007). Trichothecene mycotoxins are amphipathic which can move passively through the membranes of cells (McCormick et al., 2011). It is thought that DON acts as a protein synthesis inhibitor by binding to ribosomes, affecting cell proliferation and apoptosis signalling through kinase activity modification, without triggering a defence response (Nishiuchi et al., 2006, Masuda et al., 2007, Blumke et al., 2015, Payros et al., 2016). Grains from *Fusarium*-infected plants can become contaminated with trichothecenes (Goswami & Kistler, 2004, Ferrigo et al., 2016). When contaminated grains are consumed by humans and livestock, symptoms of emesis ensue (DON is also known as vomitoxin), as well as several other problems such as immune response changes and anorexia (Antonissen et al., 2014, Payros et al., 2016). Furthermore DON contamination can result in potential rejection of the entire toxin-laden grain load since cereal grain DON limits have been imposed by many countries. For example, the European Commission (depending on the trichothecene,

species, and end-product), have set DON limits of 0.9 ppm - 12 ppm for livestock, and 750 ppb - 1,250 ppb for human consumption (Ferrigo et al., 2016).

1.1.3. Fusarium Crown Rot

Fusarium Crown Rot (FCR) is the infection of the crown and stem base of wheat (Fig. 1.4A) which can result in reduced grain yield and resulting economic loss (Liu & Ogbonnaya, 2015). FCR is predominantly caused by infection from *Fusarium pseudograminearum* but can also be caused by *F. graminearum* and *Fusarium culmorum* (Akinsanmi et al., 2006, Stephens et al., 2008, Beccari et al., 2011, Liu & Ogbonnaya, 2015). The inoculum source originates from previous years' contaminated plant material (Hogg et al., 2007). *F. graminearum* colonisation, biomass, and transcriptomic pathogen response during FCR were investigated in wheat (Stephens et al., 2008) and from *F. culmorum* (Beccari et al., 2011, Covarelli et al., 2012). Early *F. graminearum* expression patterns during FCR infection at the molecular level were relatively similar to that of early FHB infection (Stephens et al., 2008).

Figure 1.4. Fusarium crown rot (**A**) and Fusarium root rot (**B**) symptoms in wheat. (**A**) Four different wheat crowns infected with *Fusarium*. (**B**) The three images are infected primary roots at 1 dpi (a), 2 dpi (b), and 4 dpi (c), respectively. (**A**) Photos kindly provided, with permission, from Professor Paul Nicholson. (**B**) This figure has been taken with permission from one published by (Beccari et al., 2011).

F. graminearum-induced FCR in wheat progresses in three phases relatively slowly (Stephens et al., 2008): At 2 dpi, there is initial germination and hyphal growth at the infection point. Even after 14 dpi, no visible symptoms occur. Instead there is epidermal

penetration of the first leaf sheath following a fungal biomass drop as mycelia migrate down to the crown (below the soil). Lastly by 35 dpi, the crown vascular tissue and pith are colonised which is accompanied by a large increase in fungal biomass relative to the previous time point (Stephens et al., 2008). Visual FCR symptoms include necrosis of the crown (Stephens et al., 2008) and in severe cases, premature death of wheat heads. However the latter symptom is likely due to water stress or DON contamination rather than fungal contamination (Mudge et al., 2006, Hogg et al., 2007, Covarelli et al., 2012). *F. pseudograminearum*-induced FCR infection at the wheat stem base was found to progress as far as the floral tissues despite an absence of FHB symptoms (Mudge et al., 2006). *F. pseudograminearum* and *Fusarium culmorum*-induced FCR can lead to DON contamination of the crown, stem, and even the wheat rachis and grain (Mudge et al., 2006, Covarelli et al., 2012). *F. pseudograminearum, Fusarium culmorum*, and *F. graminearum* were shown to express DON biosynthesis genes during FCR (Mudge et al., 2006, Stephens et al., 2008, Beccari et al., 2011), indicating that DON probably has a role in stem colonisation (Mudge et al., 2006). All three species were recently shown to be similar in FCR pathogenesis, DON movement in the stem, and visual symptoms (Beccari et al., 2018).

1.1.4. Fusarium Root Rot

FRR is the necrosis of root tissue (Fig. 1.4B) in the soil leading to reduced root, shoot length, biomass, and yield loss (Mergoum et al., 1998, Beccari et al., 2011, Wang et al., 2015b). FRR in cereals can be caused *F. graminearum* and *F. culmorum* (Cook, 2001, Beccari et al., 2011, Wang et al., 2015b). The proliferation of FRR by *F. graminearum* and *F. culmorum* has been investigated previously (Beccari et al., 2011, Wang et al., 2015b). For *F. graminearum*, Wang and colleagues (2015b) analysed the pathogenesis of *F. graminearum* at the microscopic level in susceptible and resistant wheat varieties (Wang et al., 2015b). Infection was analysed between 0.5 dpi, 3 dpi, and 5 dpi encompassing three phases of infection: early infection, main infection, and sporulation. At 0.5 dpi, the macroconidia present on the surface of the root germinate, and by 1 dpi rapidly produced a dense network of hyphae that cover the entire longitudinal axis of the root. By 1 dpi, the first penetrations of the root epidermis also occur. The hyphae then grow from epidermal cells to cortical parenchyma cells while hyphopodia form (simple attachment and feeding structures). During the main infection stage (3 dpi), structures that are more complex appear and necrotized root cell symptoms are visible. Additionally, fungal biomass proliferation occurs together with appearance of other fungal structures like runner

hyphae. Hyphae did not invade the root hairs, endodermis, xylem, or phloem. The final stage of sporulation occurs around 5 dpi resulting in the appearance of sporodochia, macroconidia, and chlamydospores (Wang et al., 2015b). FHB and FCR can also manifest from FRR infection due to systemic migration via the vascular system (Beccari et al., 2011, Wang et al., 2015b). Like with FHB and FCR, there is evidence that *F. culmorum* can synthesise trichothecenes during FRR colonisation (Beccari et al., 2011), and DON was detected in wheat caused by *F. graminearum* at later stages of FRR infection (Wang et al., 2015b).

1.2. Control Strategies for Fusarium Diseases

1.2.1. Host Genetic Resistance

Genetic host resistance is an effective and durable control strategy. There are five types of resistance towards FHB, which are associated with the infection strategy of the fungus (Table 1). Type 1 and Type 2 resistance were identified first and show variation between wheat varieties (Schroeder & Christensen, 1963). Type 2 resistance is naturally found in a number of barley varieties (Langevin et al., 2004), which often results in only one bleached floret from the infection site (Fig. 1.3) due to limited internal hyphal spread (Jansen et al., 2005). The outcome of FHB in wheat is highly dependent on host background genetics (Buerstmayr et al., 2020). Identifying and breeding for resistance to FHB is complex due to resistance being quantitative (i.e. partial resistance attributed to many genes with small effects), as well as the pleiotropic effects of growth and development features (Buerstmayr et al., 2020). For example height-associated *Rht* genes play important roles in FHB resistance (Srinivasachary et al., 2008, Srinivasachary et al., 2009, Saville et al., 2012, He et al., 2016). Achieving complete resistance to FHB in wheat has not been successful, and breeding for resistance is slow.

Table 1.1. Types of host resistance to FHB.

Type	Form of Resistance
1	Initial fungal infection
2	Spread of infection throughout the head
3	Kernel Infection
4	Tolerance during infection
5	DON accumulation

Reference: (Boutigny et al., 2008).

Approximately 250 Quantitative Trait Loci (QTLs) associated with FHB resistance have been identified on all wheat chromosomes (Jia et al., 2018), however there are likely numerous false positives and only a few have been fine-mapped. The QTL research for FHB resistance has been nicely summarised in two literature reviews (Buerstmayr et al., 2009, Buerstmayr et al., 2020). Resistance or susceptibility is conferred to either FHB, or DON, or both. The predominant source of cultivars with naturally occurring FHB resistance originate

from East Asia, with the most prominent examples being cv. Sumai 3 and cv. Wangshuibai (Jia et al., 2018, Buerstmayr et al., 2020). An important wheat variety resistant to FHB spike infection, bleaching, and discoloration is the 'Sumai 3' Chinese wheat cultivar (Waldron et al., 1999, Anderson et al., 2001). Sumai 3 contains an important locus called *Fhb1* (synonym to *Qfhs.nau-3B*) located on chromosome 3BS which is an important source of breeding Type 2 resistance (Waldron et al., 1999, Cuthbert et al., 2006, Liu et al., 2006). *Fhb1* is also present in cv. Wangshuibai (Jia et al., 2018, Li et al., 2019) and this cultivar can provide both Type 1 and Type 2 resistance (Lin et al., 2004, Lin et al., 2006). There is still debate as to the exact nature of *Fhb1* resistance and the gene(s) responsible (Lagudah & Krattinger, 2019). Originally, the gene responsible within *Fhb1* was found to encode a chimeric lectin (Rawat et al., 2016). Later reports stated that the gene responsible is a histidine-rich calcium-binding-protein (Li et al., 2019, Su et al., 2019). Recently another candidate gene in the *Fhb1* QTL interval encoding a laccase was associated with increased FHB resistance (Soni et al., 2020).

Another gene *Fhb2* (synonym *Qfhs.nau-6B*) on chromosome 6BS likely functions in cell integrity and reinforcement while also providing type 2 resistance and possibly DON detoxification (Cuthbert et al., 2007, Dhokane et al., 2016). Subsequently the resistance QTLs *Fhb4* (synonym *Qfhi.nau-4B*) and *Fhb5* (synonym *Qfhi.nau-5A*), originally identified in cv. Wangshuibai and both providing Type 1 resistance (Lin et al., 2006), were also fine-mapped (Xue et al., 2010, Xue et al., 2011). Several candidate genes have been identified within this 5A QTL (Lucyshyn et al., 2007, Schweiger et al., 2013). Combining both *Fhb4* and *Fhb5* improved resistance to FHB compared to their effects alone (Jia et al., 2018). There is also evidence that combining Type 1 and Type 2 resistance produces additive effects on reducing FHB symptoms (Burt et al., 2015). Lastly multiple single nucleotide polymorphisms associated with lower FHB severity and DON accumulation were also found on seven wheat chromosomes (Arruda et al., 2016). Other sources of genetic resistance have been identified in wheat relatives and wild Poaceae species (Qi et al., 2008, Burt et al., 2015, Guo et al., 2015, Buerstmayr et al., 2020).

Type 5 mycotoxin resistance (Table 1) can be classified into either the chemical transformation by glucosylation, acetylation or de-epoxidation, or the mycotoxin accumulation reduction through inhibition (Boutigny et al., 2008). An increase in glucosylated DON (DON-3-*O*-glucoside) correlated with an increase in DON resistance

(Lemmens et al., 2005). Like with FHB, genomic regions or QTLs providing DON resistance have been identified (Lemmens et al., 2005, Hales et al., 2020). Lemmens and colleagues (2005), showed that the QTL for DON resistance was found to co-localise with type 2 resistance from *Fhb1* (Lemmens et al., 2005). Individual genes have also been identified to provide DON resistance in wheat and *Arabidopsis thaliana* (Poppenberger et al., 2003, Gunupuru et al., 2018, Mandalà et al., 2019).

Susceptibility-associated genes or chromosomal regions have also been discovered. Chromosome deletion experiments have identified ditelosomic deletion lines that positively or negatively affected FHB resistance and DON content in wheat (Ma et al., 2006). Chromosome regions containing predicted FHB susceptibility factors have also been identified in wheat (Garvin et al., 2015, Hales et al., 2020), and one was also associated with susceptibility to DON contamination (Garvin et al., 2015). Furthermore the *Fhb1*-associated gene *TaHRC* promoted FHB susceptibility and may be a susceptibility factor that has been disrupted in *Fhb1* resistant lines (Su et al., 2019). Generally host resistance can be quite effective at reducing FHB symptoms. However, producing highly resistant varieties that also produce high yield is rare (Professor Paul Nicholson, personal communication). Furthermore effectiveness of FHB resistance QTL's can be dependent on the host genotype (Salameh et al., 2011).

Genetic resistance to FRR and FCR are far less studied and implemented than that of FHB. There are partially FCR resistant wheat varieties (Desmond et al., 2005), and QTL resistance to *F. graminearum*-induced FCR has been identified (Ma et al., 2010) as well as to *F. culmorum*-induced FCR (Pariyar et al., 2020). Dissimilar to FHB resistances (Table 1), FRR resistance (reduced cell necrosis) is associated with increased time required by the pathogen to colonise the cortex (Wang et al., 2015b). Furthermore genetic resistance of certain varieties to FHB did not translate to effective FRR resistance (Wang et al., 2015b). Genetic resistance towards FRR has also been identified in wheat (Voss-Fels et al., 2018).

1.2.2. Fungicides

Most European wheat cultivars are susceptible to FHB (Parry et al., 1995, Simpson et al., 2001) (Professor Paul Nicholson, personal communication). Application of fungicides is one method for controlling FHB in the field. Different classes of fungicides are used to control FHB, each with different biochemical modes of action. Originally, fungicides acted

as multisite inhibitors however in the 1960s, newer fungicides operated at specific sites. The primary classes of fungicides used against FHB include demethylation inhibitors (DMIs), benzimidazoles, and Qo respiration inhibitors (QoIs)(Ma & Michailides, 2005). To date, no fungicide provides consistent complete resistance to *F. graminearum* (Dweba et al., 2017), and site-specific fungicides led to target fungi developing resistance at a higher rate, rendering entire classes of fungicides ineffective (Ma & Michailides, 2005).

Triazole and triazolinthione DMIs have been used since the 1980s (Becher et al., 2010). Commonly used DMIs for FHB control include metconazole, prothioconazole, propiconazole, tebuconazole, and prochloraz which have been shown to reduce FHB symptoms and trichothecene accumulation in the grain (Edwards et al., 2001, Maria Menniti et al., 2003, Mesterházy et al., 2003, Haidukowski et al., 2005, Blandino et al., 2006, Müllenborn et al., 2008, Paul et al., 2008, Yin et al., 2009, Paul et al., 2010). However, different triazoles/brands have different effects on the infection. Tebuconazole is one of the most effective and consistent at reducing FHB by up to 40% yet metconazole was most effective at reducing DON levels (Edwards et al., 2001, Paul et al., 2008). The target for these fungicides, cytochrome P450 sterol 14α-demethylase (*CYP51*), is involved in production of an important sterol (ergosterol) for cell membrane integrity (Becher et al., 2010). For example, mycelial growth is completely repressed within 5 days of applying tebuconazole (Yin et al., 2009). The triazolinthione prothioconazole is also effective at controlling FHB (Paul et al., 2008, Haidukowski et al., 2012). However prothioconazole differs to the triazoles as it binds as a competitive inhibitor and with less affinity to CYP51 (Parker et al., 2011). Instead its efficacy is attributed to the conversion and activity of the triazole prothioconazole-desthio (Parker et al., 2013). The efficacy of triazoles on FCR and FRR have not been investigated as thoroughly. However as an example, the compound combination, tebuconazole with β-cyclodextrin as preventative seed dressings, was shown to be effective against *F. culmorum* induced FCR and FRR (Balmas et al., 2006).

Benzimidazoles, like carbendazim, are one of the oldest used class of fungicide used to control FHB (Chen & Zhou, 2009, Tupe et al., 2014). Their mechanism of action is by interfering with microtubule function that inhibits cell division (Chen & Zhou, 2009). Resistance has been reported in many places with a history of heavy use of this type of fungicide (Chen & Zhou, 2009, Yin et al., 2009). Resistance to carbendazim is complex (Chen & Zhou, 2009, Yin et al., 2009), yet resistance to benzimidazoles is often the result of a point

mutation in the β-tubulin gene which modifies the amino acid sequence at the binding site for the benzimidazole (Ma & Michailides, 2005). Another class of fungicides effective against many plant pathogens include the strobulurins. These bind to cytochrome b at a specific site (Q_o), blocking electron transport and ATP production, halting mitochondrial respiration (Bartlett et al., 2002). Unfortunately the most commonly used ones, azoxystrobin and fluoxastrobin, were not as effective against *F. graminearum*, or DON levels (Edwards et al., 2001, Müllenborn et al., 2008). In some cases, application of azoxystrobin was found to increase wheat grain DON levels (Simpson et al., 2001).

Important factors that determine the effectiveness of the fungicide include cultivar resistance, climate, type of fungicide, fungicide dose, and agronomic management of field (Dweba et al., 2017). The best time to use these fungicides is at early to mid-anthesis, just as the anthers appear from the florets and the crop is most susceptible to FHB (Blandino et al., 2006, Yoshida et al., 2008, Yin et al., 2009, Becher et al., 2010, Dweba et al., 2017). FHB infection may respond differently based on timing of fungicide application. Applying fungicides too late (30 days after anthesis) might only reduce DON levels as opposed to FHB symptoms (Yoshida et al., 2008, Yoshida et al., 2012). However, fungicide application around the middle of anthesis (6 days) can sufficiently control both FHB and DON (D'Angelo et al., 2014). In addition, there are other variations to this based on the flowering type of the cereal variety used. Closed-flower (cleistogamous) cultivars were generally more resistant than open-flower (chasmogamous) cultivars (Yoshida et al., 2008). Wegulo and colleagues (2011) identified that applying fungicides during high severity years is economically profitable whereas applying during low severity years can result in a net loss (Wegulo et al., 2011). Dose is also important as sub-lethal levels of fungicides have been found to increase DON levels (Ramirez et al., 2004). In one case, prothioconazole stimulated fungal trichothecenes due to oxidative stress (Audenaert et al., 2010). Finally coupling fungicide application with the current climatic conditions, such as rainfall, is important because some of the major triazoles that are not completely rainfast (Andersen et al., 2014).

Unfortunately, resistance to triazoles can occur in *F. graminearum* (Becher et al., 2010), and resistance to tebuconazole has recently developed in certain *F. graminearum* populations (Spolti et al., 2013). Sources of resistance are because of either amino acid alterations or overexpression in the *CYP51* gene (Ma & Michailides, 2005). Furthermore, *F.*

graminearum is rapidly gaining resistance to newly discovered fungicides such as JS399-19 (Li et al., 2008, Chen & Zhou, 2009). Additionally, resistant isolates are equally as fit in non-fungicide environments (Chen et al., 2007, Chen & Zhou, 2009, Spolti et al., 2013), thus eliminating fungicide resistance from the population is even harder. Therefore, new fungicides with unique modes of action are required that are also non-toxic to humans and other non-target organisms. An antifungal target example is the conserved acetohydroxyacid synthase (*AHAS*) gene involved in synthesis of the branched-chained amino acid pathway conserved in fungi. Targeted deletion of two AHAS catalytic subunits (FgIlv2 and FgIlv6) in *F. graminearum* resulted in severely reduced virulence and DON production (Liu et al., 2015). Additionally, the novel amphiphilic aminoglycoside fungicide K20 was shown to reduce FHB in one field trial, as well as providing synergistic effects with the triazole, triazolinthione and strobilurin fungicides, and in one fungicide combination reduced DON content (Takemoto et al., 2018).

1.2.3. Other Control Strategies

Localising and identifying FHB symptoms in the field is a first step to disease control. Visual disease assessment is possible for FHB however this requires expertise and is time-consuming. Likewise it is also very challenging to assess FRR severity in wheat (Voss-Fels et al., 2018). *Fusarium* detection can be facilitated by modern tools such as spore sampling from the air and optical detection (West et al., 2017). There is also an investigation into the use of deep neural networks for automated FHB symptom detection (Jin et al., 2018). Identifying the causal *Fusarium* species is important and can be achieved with certain molecular tools (Nicholson et al., 1998, Nicholson et al., 2003).

Certain agronomic practises can help control FHB. In conducive conditions for FHB, crop rotation was shown to be effective at reducing *F. graminearum* FHB incidence and severity in wheat (Marburger et al., 2015). However only rotating crops that are hosts for *Fusarium*, like wheat and maize (*Zea mays*), can severely increase FHB incidence and severity (Dill-Macky & Jones, 2000). Crop rotation is also effective towards FCR (Desmond et al., 2005). Nitrogen fertilizer usage has been described as an important factor for FHB severity (Lemmens et al., 2004). Minimal/no-tillage practices should be avoided as they can result in a greater FHB incidence and severity due to a persistence of inoculum source from crop residues (Fig. 1.2) (Dill-Macky & Jones, 2000). Certain agronomic practices are also important for controlling mycotoxin contamination (Dill-Macky & Jones, 2000, Lemmens et

al., 2004, Ferrigo et al., 2016). However, local management of fields may be redundant in areas with substantial airborne inoculum (Schmale III & Bergstrom, 2003). Several cultural practices to treat root diseases have been described in (Cook, 2001).

Reducing DON contamination in wheat grains is also a highly important target for farmers due to strict regulations (Jansen et al., 2005, Yoshida et al., 2008). However there are relatively few compounds that exclusively reduce mycotoxin accumulation (Dr Egon Haden, personal communication). For example, zinc sulfate and zinc oxide nanoparticles were found to reduce the mycotoxin level in contaminated wheat grain and husks (Savi et al., 2015). Alternatively, chlorogenic acid and caffeic acid were also found to reduce trichothecene content but the effect depended on the *Fusarium* strain (Gauthier et al., 2016).

Bio-control agents (BCAs) are organisms that directly or indirectly reduces the presence of the target pest (Pal & McSpadden Gardener, 2006). There are numerous examples of BCAs that were successfully used to control FHB. Certain bacterial and fungal species were shown to be effective at reducing FHB symptoms in some wheat varieties (Schisler et al., 2002, Khan et al., 2004, Hu et al., 2014). Others have shown different BCA bacterial and fungal species were effective at reducing FHB disease symptoms and preventing/reducing DON accumulation in wheat (Palazzini et al., 2007, Zhao et al., 2014a, Palazzini et al., 2016). Lastly, several BCA strains were found to be effective at reducing symptoms of *F. graminearum*-induced FHB, FRR, and FCR in wheat (Wang et al., 2015a, Colombo et al., 2019). The efficacy of BCAs in controlling FHB was shown to be more effective when applied shortly before FHB infection (Khan & Doohan, 2009).

None of the control strategies mentioned provide complete durable resistance to FHB, therefore an integrative disease management approach coupling all control methods is required for long-term FHB control. For example, Salgado and colleagues (2014) found that combining moderate genetic resistance to *Fusarium* with appropriate fungicide treatments effectively reduced FHB symptoms and DON levels (Salgado et al., 2014).

As I have described, there is substantial evidence in the effectiveness of unconventional compounds in reducing FHB symptoms and DON contamination. Application of plant hormones (phytohormones) is another potential strategy to control *Fusarium* infection. The role of plant hormones in the host defence response to *Fusarium*, and the use of plant hormones as an effective control strategy by exogenous application are research areas that

are being investigated. This research is discussed in detail in the Introductions of Chapter 2, Chapter 3, and Chapter 4 with an emphasis on control of Fusarium diseases. The precise role of phytohormones in defence and especially *Fusarium* resistance is still unclear. In the following section (1.3.), I will discuss the background information on most plant hormones in their biosynthesis, signalling, and general role in plant resistance and defence response.

1.3. The Role of Phytohormones in Defence

Invading plant pathogens must overcome multiple layers of plant defences. The first barrier consists of constitutive/basal defences which can be physical or chemical pre-formed defences such as the epidermis, cuticle, and antimicrobial compounds (Agrios, 2005, van Loon et al., 2006b). Once surpassed, the pathogen often triggers induced defences by the plant. These defences encompass upregulation of defence-related genes, antimicrobial compounds, oxidative burst, and even programmed cell-death (Agrios, 2005, van Loon et al., 2006b, Bari & Jones, 2009). The success of countering infection relies upon effective detection of the invading pathogen and activation of the appropriate defence response (Jones & Dangl, 2006). Pathogens contain molecular signatures such as chitin in fungi which are described as pathogen-associated molecular patterns (PAMPs). Initially the invading pathogen's PAMPs are recognised by plant pattern recognition receptors (PRRs). The perception leads to PAMP-triggered immunity (PTI) which is effective at discontinuing pathogen colonisation through induced downstream resistance responses. However, successful pathogens can deploy effector molecules which can inhibit PTI or avoid PRR detection by binding to specific host proteins (De Jonge et al., 2010, Pieterse et al., 2012). As an additional defence layer, plants can respond to effectors by deploying R genes which encode molecules such as nucleotide-binding-leucine rich repeat (NB-LRRs) proteins that recognise effector molecules (DeYoung & Innes, 2006). This recognition of effectors causes effector-triggered immunity (ETI) which is faster and stronger than PTI and results in resistance through processes like the hypersensitive response (HR) (Jones & Dangl, 2006). It is thought that ETI is effective against biotroph and hemibiotroph pathogens and not towards necrotrophs since necrotrophs would benefit from programmed cell death induced by HR (Broekaert et al., 2006, Jones & Dangl, 2006).

Phytohormones are organic molecules that in small concentrations induce physiological processes in local or distal plant cells (Leyser, 1998, Davies, 2013). Almost all phytohormones play an important role in growth and development to varying degrees and differ in their presence and effectiveness throughout time and space. Downstream of pathogen recognition and early defence and signalling events, many phytohormones play important roles in initiating and regulating additional aspects of defence signalling (Pieterse

et al., 2012). There are numerous downstream targets of phytohormones that have important effects in resistance such as genes regulating antimicrobial compounds, induced-chemical defences, oxidative equilibrium, cell wall changes, and HR. These are described in the following sub-sections. Since changes in hormone equilibrium imposes a cost on growth and development (Walters & Heil, 2007, van Butselaar & Van den Ackerveken, 2020), plants are able to finely tune resistance via the synergistic and antagonistic nature of hormones (Pieterse et al., 2012). Therefore, the ultimate growth, development, and resistance are a manifestation of the timing and net effect of hormones in the host (Verhage et al., 2010, Davies, 2013).

In the following sub-sections, I shall briefly describe each major plant hormone, including their biosynthesis and their molecular signalling components, how they broadly affect plant defences, and how they interact with one another in defence. The strigolactone phytohormones that also function in defence (Marzec, 2016) are not described as they were not investigated in this thesis. Unless otherwise stated, most of the biosynthetic and signalling components correspond to *Arabidopsis thaliana* genes, except for gibberellic acid which was mostly described from rice (*Oryza sativa*) genes. The mechanisms and examples by which each hormone interacts with each other is discussed only after describing the molecular biosynthesis and signalling of both relevant phytohormones.

1.3.1. Salicylic Acid

The phenolic hormone salicylic acid (SA) (Fig. 1.5) is important for PTI and ETI response to pathogen infection and is crucial for resistance to pathogens that exhibit biotrophic or hemibiotrophic lifestyles (Fig. 1.6; (Glazebrook, 2005, Bari & Jones, 2009, Dempsey et al., 2011, Pieterse et al., 2012). SA can also regulate thermogenesis, plant growth, and several other developmental processes (Vlot et al., 2009, Dempsey et al., 2011, van Butselaar & Van den Ackerveken, 2020). The endogenous content of SA in untreated *A. thaliana* leaves is approximately between 70 ng/g to 4,000 ng/g of SA (Fresh weight (FW) and dry weight (DW)) (Klessig et al., 2016, Gupta et al., 2017). However in monocots like wheat, rice, and *Brachypodium distachyon*, the SA content (depending on the species and tissue) is approximately between 56 ng/g to 10,000 ng/g (FW and DW) (Chen et al., 1997, Buhrow et al., 2016, Klessig et al., 2016, Napoleão et al., 2017, Powell et al., 2017a, Brauer et al., 2019). Upstream of one SA biosynthesis gene *ISOCHORISMATE SYNTHASE 1* (*ICS1*), perception of PAMPs results in the activation of transcription factors calmodulin-binding

protein 60-like g (*CBP60g*) and *SAR-DEFICIENT 1* (*SARD1*). Activation of these genes depend on the activation of *SERINE/THREONINE PROTEIN KINASE 1/2* (*PCRK1/2*) and *TGACG SEQUENCE SPECIFIC BINDING PROTEIN 1/4* (*TGA1/4*), as well as *TRIHELIX TRANSCRIPTION FACTOR* (*GTL1*) for *CBP60g*. On the other hand, ETI response *TOLL-INTERLEUKIN-1* (*TIR*)-type R protein *NUCELOTIDE-BINDING LEUCINE-RICH REPEATS* (*NLR*s) target *ENHANCED DISEASE SUSCEPTIBILITY* (*EDS1*). *EDS1* together with *PHYTOALEXIN DEFICIENT 4* (*PAD4*) and helper *NLRs ACTIVATED DISEASE RESISTANCE 1* (*ADR1*), *ADR1-like1*, and *ADR1-Like2* activate *ICS1* and several additional sensor *NLRs*. Contrasting TIR-type R proteins, *COILED-COIL* (*CC*)-type R genes with *NON-RACE-SPECIFIC DISEASE RESISTANCE 1* (*NDR1*) and its interaction partner *RPM1-INTERACTING PROTEIN 4* (*RIN4*) have roles in both ETI and PTI (Vlot et al., 2009, Dempsey et al., 2011, Zhang & Li, 2019). Calcium signalling is also important for SA biosynthesis mediated by *CBP60g* (Pieterse et al., 2012, Zhang & Li, 2019).
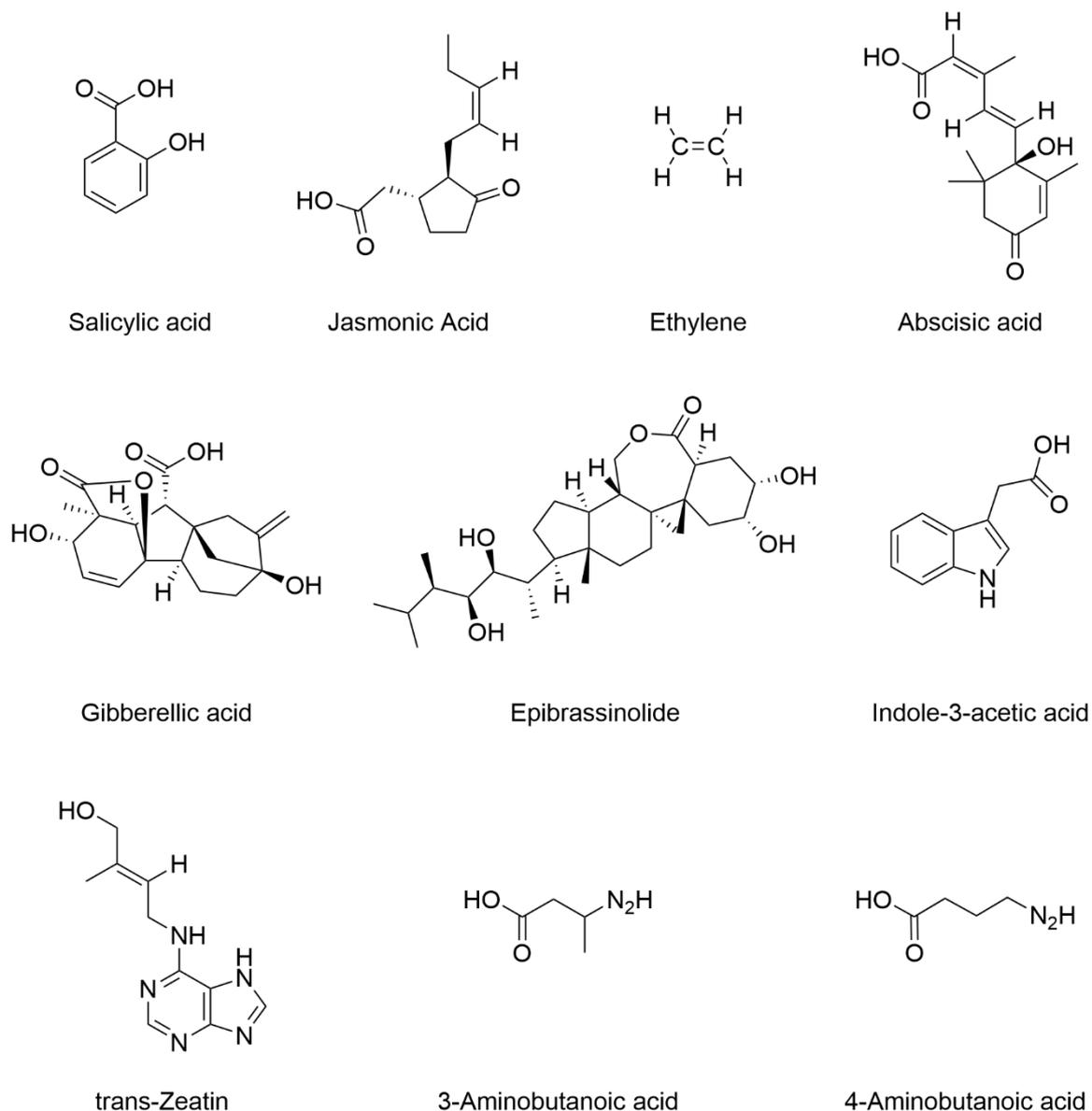
Figure 1.5. Chemical structures of main phytohormones investigated within this thesis. Structures were derived from PubChem (Kim et al., 2021) and drawn on ChemDraw Prime (V19.1.1.21).

Biosynthesis of SA is described in (Dempsey et al., 2011, Lefevere et al., 2020). Chorismate from the chloroplast (From the Shikimate pathway) is the starting compound for SA biosynthesis. Subsequently SA is synthesised from chorismite via two different pathways. The more established *PHENYLALANINE-AMMONIA LYASE* (*PAL*) pathway is preceded by chorismate conversion to phenylalanine by multiple *CHORISMATE MUTASE* (*CM*) genes. In the cytosol, phenylalanine is converted to trans-cinnamic acid (tCA) by non-oxidative deamination with the enzyme PAL. tCA is also a starting molecule for synthesis of important structural and defence compounds like lignin and flavonoids. Subsequently the

enzyme *ABNORMAL INFLORESNCE MERISTEM 1* (*AIM1*) converts tCA to benzoic acid. It is believed the final step for benzoic acid conversion to SA may be mediated by benzoic acid hydroxylase (Lefevere et al., 2020). The second pathway for SA biosynthesis, the *ICS* pathway, is primarily used in *Arabidopsis*. In the chloroplast, chorismate is converted to isochorismate via *ICS*. The product of *EDS5* transports isochorismate to the cytosol where it is converted to Isochrosimate-9-glutamate by the gene *avrPphB SUSCEPTIBLE 3* (*PBS3*). *PBS3* has to-date only been identified in *Arabidopsis*. Then either spontaneously or with *ENHANCED PSEUDOMONAS SUSCEPTIBLITY 1* (*EPS1*), SA is produced from Isochrosimate-9-glutamate (Dempsey et al., 2011, Lefevere et al., 2020). SA can also be modified by amino acid conjugation, glucosylation, sulphonation, hydroxylation, and methylation leading to inactivation or permitting transport (Vlot et al., 2009, Dempsey et al., 2011, Lefevere et al., 2020).

SA signalling is described in (Pieterse et al., 2012, Ding et al., 2018, Zhang & Li, 2019). SA is perceived by the ankyrin-repeat protein *NON-EXPRESSOR OF PATHOGENESIS-RELATED 1/3/4* (*NPR1/3/4*) that regulate SA biosynthesis (Ding et al., 2018, Zhang & Li, 2019). The NPR1 C-terminal interacts with SA and is involved in inducing transcription (Zhang & Li, 2019). NPR1 interacts with the basic leucine zipper (bZIP) transcription factor TGAs promoting SA transcription, whereas the co-repressors NPR3 and NPR4 interact with TGAs and repress SA transcription (Ding et al., 2018). In the absence of SA, NPR3 and NPR4 repress SA-related genes and NPR1 is sequestered and oligomerised in the cytosol or ubiquitinylated and degraded in the nucleus. In the presence of SA, NPR3 and NPR4 are released, the thioredoxins TRX-H3 and TRX-H5 change the redox state, monomerise NPR1 in the cytosol, and lead to an influx of NPR1 to the nucleus via nuclear pore *MODIFER OF snc1* (*MOS3/6/7*). In the nucleus, NPR1 interacts with either TGA2/5/6 via the ankyrin-repeat to bind to SA-responsive genes and NPR1 is ubiquitinylated and degraded (Pieterse et al., 2012, Zhang & Li, 2019). Other important transcription factors that promote SA-responsive genes include *RASS ASSOCIATED WITH DIABETES51D* (*RAD1D*), *SUPPRESSOR OF sni1 2* (*SSN2*), and *BREAST CANCER2A* (*BRCA2A*) which remove the negative regulator *SUPPRESSOR OF npr1 INDUCIBLE 1* (*SSN1*) from the target gene promoter. TGA on the other hand is inhibited by the negative regulator *NIM1 INTERACTING1* (*NIMIN1/2/3*) (Pieterse et al., 2012). Several other transcription factors that regulate *ICS1* are described in (Zhang & Li, 2019). *WRKY* transcription factors either function positively with SA (*WRKY18/53/54/70*) or negatively (*WKRY7/11/38/62*) (Vlot et al., 2009). The earliest genes expressed

downstream of SA, independent of perception, are *GLUTATHIONE S TRANSFERASE 6* (*GST6*) and *IMMEDIATE EARLY-INDUCED GLUCOSYLTRASNFERASE* (*IEGT*) (Vlot et al., 2009).

Important downstream SA gene targets include *PATHOGENESIS-RELATED* (*PR*) genes that encode numerous antimicrobial compounds and *WRKY* transcription factors (van Loon et al., 2006a, Makandar et al., 2011, Pieterse et al., 2012). Other potential SA downstream targets include callose deposition and lipid peroxidation (Sorahinobar et al., 2016). SA also has important roles in promoting oxidative burst (Vlot et al., 2009). Once a defence response is initiated, SA can be modified to methyl salicylate and back to SA at distal locations by *SAM-DEPENDENT CARBOXYL METHYLTRANSFERASE* (*BSMT1*) and *METHYLESTERASE* (*AtMES*), respectively, to induce resistance at undamaged distal parts of the plant. This mechanism is termed systemic acquired resistance (SAR), which is effective over a long time and in response to many other attacking pathogens (Park et al., 2007, Liu et al., 2011, Dempsey & Klessig, 2012). Another potential SAR mobile compound is N-hydroxyl pipecolic acid which is synthesised from pipecolic acid by the genes *L-LYSINE APLHA-AMINOTRASNFERASE* (*ALD1*), *SAR DEFICIENT 4* (*SARD4*), and *FLAVIN-DEPENDENT MONOOXYGENASE* (*FMO1*) (Dempsey & Klessig, 2012, Chen et al., 2018, Zhang & Li, 2019, Kachroo et al., 2020). The cuticle is believed to be important for SA storage and for SAR (Kachroo et al., 2020).

1.3.2. Jasmonic Acid

Jasmonates are a group of hormones involved in multiple growth and developmental processes as well as providing defences against tissue-damaging herbivores and necrotrophic pathogens (Fig. 1.6; (Lorenzo et al., 2003, Lorenzo & Solano, 2005, Bari & Jones, 2009, Pieterse et al., 2012, Wasternack & Hause, 2013). Elevated jasmonate levels can be induced by the mixing of components by wounding, breakdown products of plant and fungal cell walls, and the systemin peptide signal (Creelman & Mullet, 1997). The endogenous JA content is lower than that of SA. In untreated *A. thaliana* leaves, the concentration of JA varies between approximately 146 ng/g to 400 ng/g over time (DW) (Gupta et al., 2017), whereas concentration varies between approximately 10 ng/g to 77 ng/g (FW and DW) in wheat and *B. distachyon* tissues (Buhrow et al., 2016, Napoleão et al., 2017, Powell et al., 2017a, Brauer et al., 2019). Jasmonates are synthesised in photosynthetic tissue like leaves and also in non-photosynthetic tissues like roots (Acosta & Farmer, 2010). Oxylipin (oxygenated fatty acid) jasmonates in plants include

cyclopentenones like oxo-phytodienoic acid (OPDA) and dinor-OPDA and cyclopentanones like methyl jasmonate (MeJA), jasmonic acid (JA) (Fig. 1.5), jasmonyl-isoleucine (JA-Ile) (Acosta & Farmer, 2010). Jasmonate biosynthesis is described in detail in these reviews (Creelman & Mullet, 1997, Acosta & Farmer, 2010, Pieterse et al., 2012). Initially, α-linolenic acid is released from chloroplast cell membranes via phospholipase A1. In the cell plastid, α-linolenic acid is oxygenated at different positions by *LIPOXYGENASE* (*LOX*). These products are then converted to allene oxidase by *ALLENE OXIDASE SYNTHASE* (*AOS*) and are cyclized to by *ALLENE OXIDASE CYCLASE* (*AOC*). The resulting compounds, depending on where α-linolenic acid was oxygenated, OPDA and dn-OPDA are transported to the peroxisome and are reduced by *12-OXOPHYTODIENOATE-REDUCTASE 3* (*OPR3*) to OPC8 and OPC6, respectively. These are then oxidized to form JA. JA is then exported to the cytosol where it is modified to numerous different compounds including JA-Ile. (Seo et al., 2001, Schaller & Stintzi, 2009, Acosta & Farmer, 2010, Wasternack & Hause, 2013, Wasternack & Strnad, 2016, Yang et al., 2019). In fact JA-Ile, modified by the enzyme *JASMONOYL—L-AMINO ACID SYNTHETASE* (*JAR1*), is the active form of JA that induces JA-related transcription (Staswick & Tiryaki, 2004, Acosta & Farmer, 2010, Wasternack & Strnad, 2016).

JA signalling is described in detail by (Pieterse et al., 2012). In the absence of JA, *JASMONATE ZIM-DOMAIN* (*JAZ*) proteins function as JA-signalling repressors by binding to promoters of jasmonate-responsive genes. JAZ proteins are made up of a Jas motif and a ZIM domain. The JAZ ZIM domain interacts with the protein *NOVEL INTERACTOR OF JAZ* (*NINJA*) that associates with co-suppressors like *TOPLESS* (*TPL*). In the presence of Jasmonates, JA-Ile is recognised by the F-box protein *CORONATINE INSENSITIVE 1* (*COI1*) which together with RBX1 RING finger proteins, CULLIN1, ASK and SK2 adaptors forms an SCF ubiquitin E3 ligase. This complex then interacts with the Jas motif within the JAZ protein causing degradation by ubiquitination and activation of JA-suppressed genes. As a negative feedback loop, the repressor JAZ is activated in the presence of elevated jasmonic acid. JA presence also activates a positive feedback loop in that the biosynthetic genes *LOX*, *AOS*, *AOC*, and *OPR3* are upregulated.

JA-related downstream targets include antifungal proteins, ribosome inactivating proteins, phytoalexins, phenolics, and cell wall proteins (Creelman & Mullet, 1997). Importantly, there are two pathways of JA-related downstream defences that depend on

the type of attack. The first, mediated by *ETHYLENE RESPONSE FACTOR* (*ERF*) (ERF pathway), is the response to necrotrophic pathogens and involves *PLANT DEFENSIN 1* (*PDF1*) that has antimicrobial properties (Creelman & Mullet, 1997, Pieterse et al., 2012). The other is generally associated with resistance to insect herbivory, which is mediated by *MYC* transcription factors (MYC pathway) and affects downstream genes such as *VEGETATIVE STORAGE PROTEIN2* (*VSP2*) (Pieterse et al., 2012). JA also is critical for the activation of induced systemic resistance (ISR) in response to beneficial microorganisms (Wasternack & Hause, 2013, Pieterse et al., 2014).

JA and SA signalling pathways are mutually antagonistic (Fig. 1.6). This is thought to be important for fine-tuning resistance in a cost-effective way to multiple attacking pathogens with different lifestyles (Adie et al., 2007, Spoel & Dong, 2008, Acosta & Farmer, 2010, Leon-Reyes et al., 2010b, Pieterse et al., 2012). SA suppression of JA biosynthesis is predicted to occur at downstream regulatory genes. For example SA was shown to repress the downstream JA transcription of *PDF1.2* in wild-type and a JA biosynthesis mutant (Leon-Reyes et al., 2010b). Furthermore both MYC and ERF pathways are sensitive to SA suppression. The molecular components characterised as suppression co-factors that suppress JA signalling but promote SA signalling include *NPR1*, *WRKY* (e.g. *WRKY70*), *TGA* transcription factors. On the other hand, *JASMONATE INSENSITIVE 1* (*JIN1*)/*MYC2*, the *MITOGEN ACTIVATED PROTEIN KINASE 4* (*MPK4*), *SUPPRESSOR OF SA INSENSITIVITY* (*SSI2*), and *TGA* transcription factors (in the absence of SA), promoted JA signalling by suppressing SA signalling (Bari & Jones, 2009, Pieterse et al., 2012). *NPR1*, *EPS1*, and *WRKY70* and *WRKY53* are also involved in the SA-JA antagonism (Spoel et al., 2003, Bari & Jones, 2009, Dempsey et al., 2011). Certain *NAC* transcription factors can be activated by *MYC* resulting in suppression of SA biosynthesis (Yang et al., 2019).
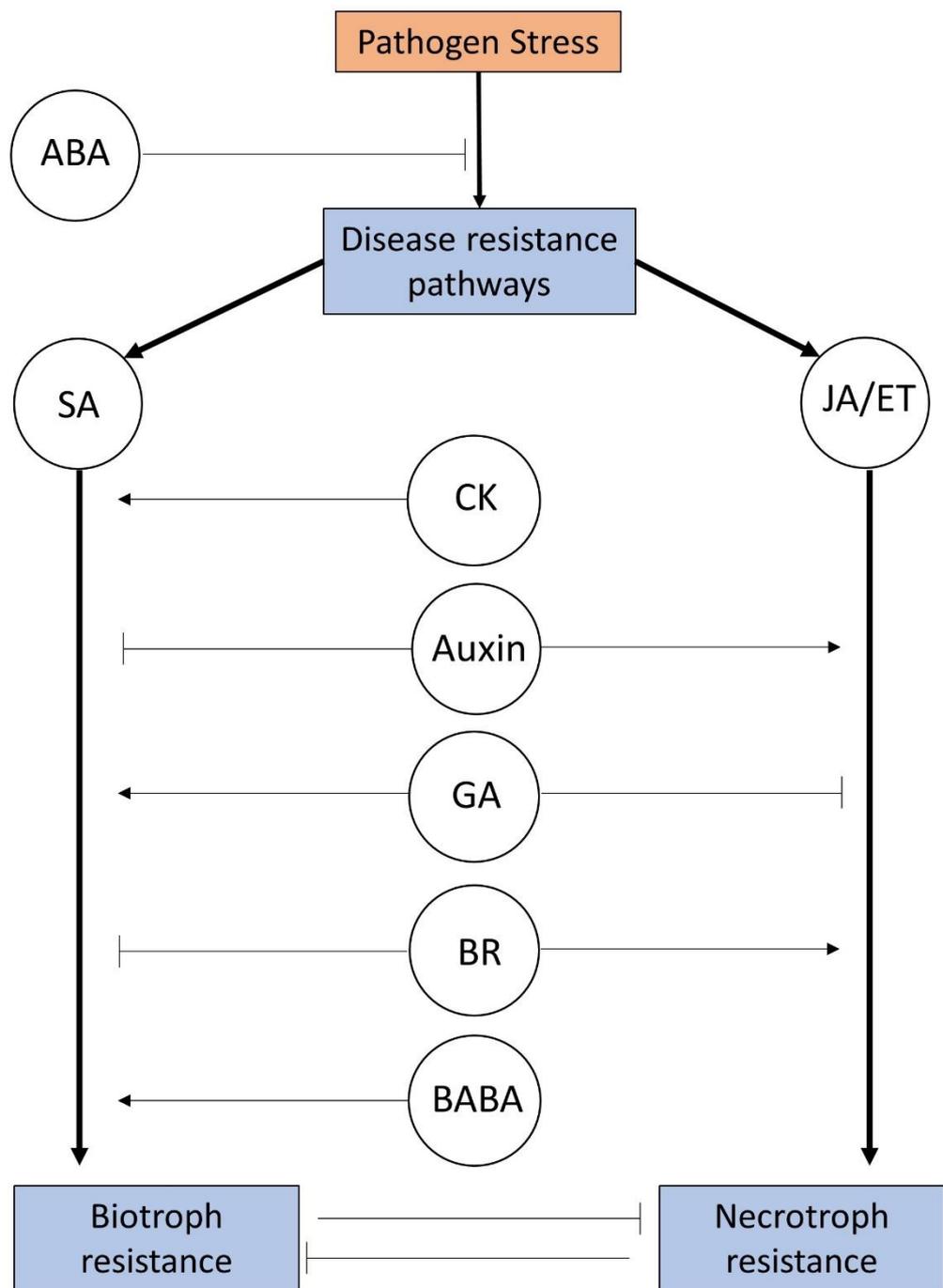
Figure 1.6. Simplified/generalisation overview of SA and JA/ethylene effects on pathogen resistance and the effect other phytohormones (and signalling molecule BABA) have on these pathways. More details are presented in the main text. The main pathway arrows for SA and JA/ethylene are in bold. Arrowed lines denote a positive/synergistic effect on resistance. Blunt-end arrow denote a negative effect/antagonistic effect on resistance. Phytohormones are circled. Abbreviations: ABA (abscisic acid), CK (Cytokinin), BABA (3-aminobutanoic acid), GABA (4-aminobutanoic acid), BR (Brassinosteroids), ET (Ethylene), GA (Gibberellic acid), JA (Jasmonic acid), SA (Salicylic acid). This figure has been adapted with permission from one published by (Robert-Seilaniantz et al., 2007).

1.3.3. Ethylene

Ethylene (Fig. 1.5) is a gaseous phytohormone which is known for its role in fruit ripening, leaf senescence, and abiotic stress responses, yet also has an important function in modulating biotic stress responses (van Loon et al., 2006a, Abeles et al., 2012, Davies, 2013). Ethylene content is approximately between 75 pmol/g/h to 175 pmol/g/h in *A. thaliana* tissues over time (Knoester et al., 1999), and between 0.1 nl/g/FW/h and 1.5 nl/g/FW/h in wheat spikes (Beltrano et al., 1994). Ethylene is synthesised in plants using a relatively simple pathway with only three enzymes. The amino acid methionine is converted to *S*-adenosylmethionine (SAM) catalysed by the enzyme SAM synthetase. The by-product is then salvaged to methionine via the Yang cycle. Subsequently the next rate-limiting step uses *ACC SYNTHASE* (*ACS*) (housing the important cofactor pyridoxal 5'-phosphate) to convert of S-AdoMet to 1-aminocyclopropane-1-carboxylic acid (ACC). ACC is then converted to ethylene by *ACC OXIDASE* (*ACO*) (Wang et al., 2002, Broekaert et al., 2006, van Loon et al., 2006a). ACC content is approximately between 10 ng/g to 147 ng/g (FW and DW) in wheat and *B. distachyon* leaves (Napoleão et al., 2017, Kretzler et al., 2020), and approximately 1 nmol/g to 26 nmol/g (FW) in *A. thaliana* tissues (Rodrigues-Pousada et al., 1993).

Much of the information of the molecular signalling cascade has been thoroughly investigated in *Arabidopsis* (Wang et al., 2002, Guo & Ecker, 2004, Broekaert et al., 2006, Ju & Chang, 2015). The ethylene receptors, *AtETR1*, *AtETR2*, *AtERS1*, *AtERS2*, and *AtEIN4* are functionally redundant and negatively regulate ethylene signalling in the presence of ethylene. The function of receptors requires copper which is supplied by the copper transporter *RAN1*. In the absence of ethylene, the C-terminus of ethylene receptors binds to the negative regulator Raf-like kinase *CONSTITUITIVE TRIPLE-RESPONSE1* (*CTR1*), suppressing the activity of the positive regulator *ETHYLENE INSENSITIVE2* (*EIN2*) by phosphorylation of its C-terminus and resulting in EIN2 degradation. As a result, F-box proteins EBF1/2 in the nucleus degrade the master ethylene signal regulator transcription factors *ETHYLENE INSENSITIVE 3* (*EIN3*) and *EIN3-LIKE 1* (*EIL*) required for downstream signalling. In the presence of ethylene, ethylene is perceived at the transmembrane receptor N-terminal which results in inactivation of the receptors, CTR1 inactivation, dephosphorylation of EIN2, and cleavage of the C-terminus of EIN2. Subsequently in the nucleus EBF1/2 repression of EIN3 is inhibited. Then the EIN2 C-terminus positively affects

the transcription family EIN3 which binds to the *ERF1* promoter for transcription of *ERF1* which is part of a large class of *APETELA2 AP2/ERF* transcription factors and a member of *ETHYLENE-RESPONSE-ELEMENT BINDING PROTEINS* (*EREBP*s). EREBPs can activate downstream ethylene-inducible genes containing a 5'-GCC-3' box promoter.

Ethylene is generated quickly, transiently, and faster than JA and SA resulting in an ethylene gradient throughout the plant (van Loon et al., 2006a). Similarly ACC can also function as a signalling molecule (Van de Poel & Van Der Straeten, 2014). There are many downstream targets involved in ethylene-dependent defence responses. Defence-related genes with ethylene responsive elements includes numerous PR proteins and phytoalexins as well as structural cell wall and xylem defences (Shinshi et al., 1995, Broekaert et al., 2006, Shinshi, 2008). Ethylene is reported to function synergistically with the plant hormone JA (Fig. 1.6 (Shinshi, 2008, Bari & Jones, 2009, Pieterse et al., 2012), and is particularly important for activating the specific branch of JA signalling involved with resistance to necrotrophic pathogens over herbivores (Lorenzo et al., 2003, Glazebrook, 2005, Pieterse et al., 2012). Downstream targets responsive to both JA and ethylene include chitinase and *PDF1.2* (Shinshi, 2008). It is believed the core network component responsible for interaction with JA and ethylene are *ERF*s (primarily *ERF1*) in which some are responsive to JA and ethylene and regulate numerous downstream ethylene and JA defence-related genes (Lorenzo et al., 2003, McGrath et al., 2005, Broekaert et al., 2006, Pieterse et al., 2012). As an example, the transcription factors *ERF1* and the *AP2/ERF ORA59* are activated by JA and ethylene and induce expression of downstream targets like *PDF1.2* (Pré et al., 2008, Pieterse et al., 2012). Defence to a necrotroph *Botrytis cinerea* is also improved when *ORA59* was overexpressed (Pré et al., 2008). *EIN3/EIL1* is also important for JA/ethylene synergism through its interaction with JAZ proteins (Zhu et al., 2011). Plants utilise ethylene signalling to further prioritise JA signalling over SA signalling, since early ethylene signalling can abolish subsequent SA suppression of JA signalling (Leon-Reyes et al., 2010a, Pieterse et al., 2012). The transcription factors *EIN3/EIL1* are also involved in repressing SA biosynthesis (Dempsey et al., 2011).

1.3.4. Abscisic Acid

Abscisic acid (ABA) (Fig. 1.5) is most known for its role in seed maturation germination, root architecture control, and abiotic stress responses (Dong et al., 2015). ABA concentrations in *A. thaliana* are approximately between 30 ng/g to 175 ng/g (FW and

DW) (Yu et al., 2012, Gupta et al., 2017). Similarly in tissues of monocots likes wheat and *B. distachyon*, the concentration of ABA ranges from approximately 4 ng/g to 330 ng/g (DW)(Buhrow et al., 2016, Napoleão et al., 2017, Brauer et al., 2019, Kretzler et al., 2020). The ABA biosynthetic, signalling, and regulation pathways are described by (Dong et al., 2015, Chen et al., 2020). Biosynthesis of ABA, like JA, begins in the plastid and primarily involves the carotenoid pathway. Initially, isopentenyl diphosphate (IPP) is synthesised from the methylerythritol pathway and leads to production of phytoene and lycopene. After lycopene cyclisation, the product β-carotene is hydroxylated to zeaxanthin. Then in a three or four-step process using *ZEAXANTHIN EPOXIDASE* (*ZEP*), *NEOXANTHIN SYNTHASE* (*NYP*), and isomerase, zeaxanthin is converted to 9'*cis*-violaxanthin or 9'*cis*-neoxanthin in the plastid. Then from either of these two compounds, in a rate-limiting step, xanthoxin is produced with the gene *9-cis-EPOXYCAROTENOID DIOXYGENASE* (*NCED*). Subsequently in the cytosol, xanthoxin is converted using an *ALCOHOL DEHYDROGENASE* (*ABA2*) to abscisic aldehyde and finally is oxidised to ABA by *ABSCISIC ACID OXIDASE* (*AAO3*). As a mechanism to effectively regulate ABA content, ABA can be degraded by four *CYTOCHROME P450 MONOOXYGENASE* 707A (*CYP707A*) enzymes by hydroxylation to phaseic acid and dihydrophaseic acid (DPA). Alternatively ABA can be glucosylated and stored to an inactive form ABA-glucosyl ester (ABA-GE) in the endoplasmic reticulum (ER) or vacuoles by uridine diphosphate glucosyltransferase (*UGT71C5*). ABA can then be made readily available again by hydrolysis using β-glucosidase (from *AtBG1* for the ER and *AtBG2* for the vacuole). ABA import and export is mediated by ABC transporters each with specific localisations and long-distance transport is believed to be accomplished via ABA-GE.

In the absence of ABA, the *PROTEIN PHOSPHATASE 2C* (*PP2C*) interacts with the *SNF1-RELATED PROTEIN KINASE* (*SnRK2*) which represses downstream ABA genes. In the presence of ABA, the intracellular soluble ABA receptor *PYRABACTIN-RESISTANCE/PYR-LIKE/REGULATORY COMPONENT OF ABA RECEPTOR* (*PYR/PYL/RCAR*) binds to ABA and forms a complex with PP2C which leads to the de-repression of *SnRK2*. Through either phosphorylation or autophosphorylation, downstream transcription factors and transporters are activated. Two other types of ABA receptors include the plasma membrane *G-PROTEIN COUPLED RECEPTOR* (*GPCR*) and the chloroplast localised Mg-chelatase H subunit (CHLH), both with roles in stomatal control and seed development (Dong et al., 2015). *PYR/PYL/RCARs*, *PP2C*, and *SnRK2* are also tightly regulated by phosphorylation or ubiquitination pathways (Chen et al., 2020).

ABA generally negatively affects resistance to plant pathogens (Fig. 1.6) but ABA can have positive or negative effects on defence depending on the phase of infection. Pre-penetration of pathogens, the closure of stomata has positive effects on resistance to those pathogens that penetrate via stomata (Ton et al., 2009, Chen et al., 2020). However post-penetration, ABA tends to have negative effects on resistance but the effect depends on the pathogen (Ton et al., 2009). ABA can have positive effects on resistance towards some necrotrophic fungi by inducing cell wall changes like callose deposition, but negative effects by reducing ROS levels (Ton et al., 2009). Reducing ABA biosynthesis and signalling can promote resistance, for example with the ABA signalling and biosynthesis antagonist *ARABIDOPSIS NAC DOMAIN CONTAINING PROTEIN* (*ATAF1*) that promotes pathogen penetration resistance (Jensen et al., 2008, Ton et al., 2009). During late infection, ABA is generally associated with susceptibly to pathogens by impacting the way ABA interacts with other hormones (Ton et al., 2009). ABA can suppress SA-related defences (Audenaert et al., 2002, Yasuda et al., 2008) and can divert resistance away from ethylene-JA resistance (Anderson et al., 2004, Lorenzo et al., 2004, Pieterse et al., 2012). Elevated ABA was shown to suppress JA/ethylene-related genes like *PDF1.2*, *PR4*, and a chitinase gene (*CHI*) (Anderson et al., 2004, Ton et al., 2009). On the other hand, ABA promotes resistance to insect herbivory and susceptibility to fungi through synergism with JA via the JA transcription factor *MYC2* (Pieterse et al., 2012).

1.3.5. Gibberellic Acid

The diterpene gibberellic acid (GA) (Fig. 1.5), most commonly produced by plants, is a growth hormone involved in processes like seed germination and stem growth (Davies, 2013). There are over 100 types of gibberellins in plants however only three, GA_1, GA_3, GA_4 are the most biologically active and are often synthesised at the target organ site (Yamaguchi, 2008, Hedden & Thomas, 2012). Different gibberellins in untreated *A. thaliana* tissues are approximately between 0.02 ng/g to 7 ng/g (FW and DW) (Gupta et al., 2017, Barro-Trastoy et al., 2020). This is a little higher in wheat, ranging from approximately 9 ng/g to 70 ng/g (DW) (Buhrow et al., 2016, Brauer et al., 2019). GA biosynthesis is described in detail by (Yamaguchi, 2008, Hedden & Thomas, 2012). All GAs are synthesised in the plastid from C20 geranylgeranyl diphosphate (GGDP) via the methylerythritol pathway. Initially, a two-step process using two terpene synthases *ent-COPALYL DIPHOSPHATE SYNTHASE* (*CPS*) and *ent-KAURENE SYNTHASE* (*KS*) convert GGDP to *ent*-Kaurene. Subsequently in a three-step reaction, *ent*-Kaurene is successively oxidised at C-19 to *ent*-

Kaurenoic acid by the cytochrome *CYP450 ent-KAURENE OXIDASE* (*KO*). In another three-step successive reaction in the ER, *ent*-Kaurenoic acid is successively oxidised at C-7 by another CYP450 enzyme *ent-KAURENOIC ACID OXIDASE* (*KAO*) to produce GA_{12}. Finally, different soluble *2-OXOGLUTARATE-DEPENDENT DIOXYGENASES* (*2OD*) (*GA20ox*, *GA13ox*, and *GA3ox*) are involved in oxidising different positions on GA_{12} in the cytosol resulting in the three main bioactive gibberellins GA_1, GA_3, and GA_4 (Yamaguchi, 2008). GAs can be modified to less bioactive forms by hydroxylation with GA2ox, epoxidation with *ELONGATED UPPERMOST INTERNODE* (*EUI*) and *CYP71D1*, conjugated with glucose, or methylated with *GAMT1/2* (Yamaguchi, 2008, Hedden & Thomas, 2012).

GA is perceived by soluble *GIBBERELLIN INSENSITIVE 1* (*GID1*) receptors, which when activated, bind to the DELLA domain of GA repressor DELLA proteins. An E3 ubiquitin ligase $SCF^{GID2/SLY1}$ (*AtSLY1* (*SLEEPY1*) is the F-box protein) ubiquitylates DELLA which is then degraded by the 26s proteasome. (Schwechheimer, 2008). Another negative regulator is *SPINDLY* (*SPY*) that may function together with DELLA. On the other hand, *REPRESSION OF ROOT GROWTH* (*RSG*) and *SCARECROW-LIKE3 3* (*SCL3*) function as GA positive regulators (Gomi & Matsuoka, 2003, Schwechheimer, 2008, Yamaguchi, 2008, Hedden & Thomas, 2012). GA feedback loops are likely regulated at GA 3-oxidase expression by *AT HOOK PROTEIN OF GA FEEDBACK REGULATION* (*AGF1*) and *YABBY1* (*OsYAB1*) (Yamaguchi, 2008, Hedden & Thomas, 2012). GA itself can also induce repression by upregulating or inducing *DELLA* expression and attenuating *GID1* and *SLY1* expression (Schwechheimer, 2008).

The consensus is that GAs affect defence response signalling indirectly by promoting necrotroph susceptibility and biotroph resistance (Fig. 1.6; (Navarro et al., 2008). This is most likely because of the way DELLA proteins interact with JA signalling repressors by binding to the JA transcriptional repressor *JAZ1*, which in turn allows activation of JA-related genes (Hou et al., 2010, Pieterse et al., 2012). Therefore, degradation of DELLA mediated by GA results in inhibition of JA gene signalling mediated by *JAZ* which indirectly upregulates SA signalling (Fig. 1.6; (Navarro et al., 2008, Pieterse et al., 2012). There is evidence suggesting that GA affects resistance independently of JA and SA signalling. For example DELLA proteins have been found to regulate ROS level through activation of detoxifying enzymes in response to *B. cinerea* (Achard et al., 2008). It is proposed that DELLA proteins play a key role in mediating different forms of defence (De Bruyne et al., 2014). Changes in GA content or perception through experimental mutation can affect

resistance as overexpression of *EUI* in rice, which normally deactivates GA, promoted resistance to the fungus *Magnaporthe oryzae* but susceptibility to the bacteria *Xanthomonas oryzae* (Yang et al., 2008). In another example, a *OsGID1* mutant was found to promote resistance to *Pyricularia grisea* in rice (Tanaka et al., 2006).

1.3.6. Brassinosteroid

The large family of Brassinosteroids (BRs) are structural analogues to animal steroids that have hormonal functions in plants on cell growth and development, gene expression control, abiotic, biotic, and photomorphogenic responses (Bajguz, 2007, Bari & Jones, 2009, Kim & Wang, 2010). There are 69 different BR compounds reported in plants to-date (Kim & Russinova, 2020). Depending on the type, brassinosteroids appear at very low concentrations in planta. For example in *A. thaliana*, the concentrations of several BRs range from approximately 0.025 ng/g to 2 ng/g (FW) (Bajguz & Tretyn, 2003, Yokota et al., 2017). Similarly in rice shoots, the concentrations of various BRs ranged from approximately 0.008 ng/g to 3 ng/g (FW) (Bajguz & Tretyn, 2003, Yokota et al., 2017). In most higher plants, BR biosynthesis (Described from (Bajguz et al., 2020)) starts from dimethylallyl pyrophosphate (DMAPP) and isopentenyl pyrophosphate (IPP) produced from the mevalonate (MVA) pathway. IPP and DMAPP are biochemically modified to farnesyl pyrophosphate. Squalene is then produced by the action of squalene synthase and is then oxidised and converted to the key compound cycloartenol in a two-step reaction. BRs are divided into groups based on carbon atoms as either C_{27}, C_{28}, C_{29}-type. These three types of BRs are derived from cycloartenol. For C_{27}, cycloartenol is converted to cycloartanol catalysed by *STEROL SIDE CHAIN REDUCTASE 2* (*SSR2*). In a nine-step reaction, cycloartanol is then converted to cholestanol by the enzymes C-4-sterol methyl oxidase 3, C-4 sterol methyl oxidase 4, sterol C-5(6) desaturase, 7-dehydrocholesterol reductase 2 and a 5a reductase (*DET2*), each at different steps. Subsequently the various C_{27} BRs are oxidised by *CYP90B1* and *CYP85A1/2*. For C_{28} type biosynthesis, a six-step reaction converts cycloartenol to 24-methylenelophenol with notable enzymes in this reaction including sterol *C-24 METHYLTRANSFERASE 1* (*SMT1*), *C-4 STEROL METHYL OXIDASE 1* (*SMO1*), cyclopropylsterol isomerase, *CYP51*, sterol C-14 reductase, and sterol 8,7 isomerase, sequentially. Then 24-methylenelophenol is converted to 24-methylenecholesterol in a three-step reaction with *SMO2, STEROL-5(6) DESATURASE 1* (*DWF7*), and *7-DEHYDROCHOLESTEROL REDUCTASE* (*DWF5*). From 24-methelenecholesterol, campesterol is synthesised via *SSR1*, sterol isomerase and *DET2* in a four step-reaction. Alternatively,

24-methelenecholerosterol is converted to 22S,24R-22-hydroxy-5a-ergostan-3-one with *CYP90A1* and *DET2* involved in the last two stages of the four-step reaction. From either of campestanol or 22S,24R-22-hydroxy-5a-ergostan-3-one (or a third derivative of 24-methelenecholerosterol, 22,23-dihydroxy-4-en-3-one), C_{28} BRs (e.g. castasterone and brassinolide) are synthesised by oxidation using various *CYP* enzymes; *CYP90A1/B1/C1/D1* and *CYP85A1/A2*. Lastly, C_{29} BRs are derived from an alternate pathway from 24-methyleneophenol in which beta-sitosterol is produced from a five-step reaction from *SMT2, SMO2, DWF7, DWF5*, and *SSR1*. The last step can also yield 22S-hydroxyisofucosterol which along with beta-sitosterol are required in synthesis of C_{29} which are oxidised by *CYP724B2, CYP90B3* and *CYP85A1/A2* along with other unknown enzymes. C_{27}, C_{28}, C_{29}-type BRs are can lead to synthesis of each other often from the end product BRs and in particular BR C_{28} castasterone acts as a funnel for biological activities (Bajguz et al., 2020). Campesterol (C_{28})-derived epibrassinolide (epiBL) (Fig. 1.5) is considered the most important BR (Nakashita et al., 2003). BRs can be conjugated with fatty acids or glucose (Bajguz et al., 2020).

BR signalling machinery is quite conserved between monocots and dicots (Kim & Russinova, 2020). BR signalling is summarised in (Zhu et al., 2013, Kim & Russinova, 2020). The BR receptor is the plasma-membrane localised *BRASSINOSTEROID INSENSITIVE 1* (*BRI1*) made up of an extracellular LRR domain, a transmembrane domain, and serine/threonine kinase in the cytosol. In the absence of BR, the BR receptors remain inactive through either auto-phosphorylation, kinase domain dephosphorylation from *PROTEIN PHOSPHATASE* (*PP2A*), or its interaction with *BRI1 KINASE INHIBITOR1* (*BKI1*). The transcription factors *BRASSINAZOLE RESISTANT 1* (*BZR1*)/*BRI1 EMS SUPPRESSOR* (*BES1*) are retained in the cytoplasm and impeded in DNA binding through phosphorylation by the negative regulator *BRASSINOSTEROID INSENSITIVE 2* (*BIN2*) and association with 14-3-3 proteins which results in BZR1/BES1 degradation with different E3 ligases. In the presence of BR, BR binds to BRI1 and forms a heterodimer complex with an LRR co-receptor kinase *BR1-ASSOCIATED KINASE* (*BAK1*) or the functionally redundant family proteins *SOMATIC EMBRYOGENESIS KINASE* (*SERK*) 1 and *SERK4* resulting in full activation from *trans*-phosphorylation of BKI1 from BRI1 resulting in their disassociation. Plasma membrane-bound *BR-SIGNALLING KINASE1* (*BSK1*) and *CONSTITUITIVE DIFFERENTIAL GROWTH1* (*CDG1*) are phosphorylated by the active BRI1. The BR positive signalling protein *BRI1 SUPPRESSOR/BSU-LIKEs* (*BSU1/BSLs*) is then activated by BSK1 scaffold association and CDG1 phosphorylation. The now activated

BSU1/BSL dephosphorylates BIN2 and homologues BIN2-LIKE1 and BIL2. BIN2 degradation is also mediated by *KINK SUPPRESSED IN BZR-1D* (*KIB1*). Repression of BIN2 permits BZR1/BES1 entry to the nucleus through activation by PP2 dephosphorylation. As a negative feedback loop, BZR1/BES1 binds to BR responsive elements (BRREs) as homodimers to repress expression of biosynthetic genes. Alternatively, BZR1/BES1 can bind to DNA E-box elements forming heterodimers with other transcription factors to activate BR biosynthetic genes (Zhu et al., 2013, Kim & Russinova, 2020).

BRs tend to have differing effects on resistance depending on the pathogen lifestyle, with generally positive effects on resistance to biotrophs and negative effects on resistance to necrotrophic and hemibiotrophic pathogens (Yu et al., 2018). The endogenous pool of BR may affect the balance between defence and or growth (Yu et al., 2018). The molecular pathway of BR in the defence pathway is described in (De Bruyne et al., 2014, Yu et al., 2018). There is some evidence for BR signalling components like *BAK1* having a role in plant defence and PAMP recognition (Bari & Jones, 2009) and *BAK1* is likely determining resistance or susceptibility depending of pathogen lifestyle (Yu et al., 2018). A mutation in *BRI1* was also shown to improve resistance to necrotrophic and hemibiotrophic pathogens (Ali et al., 2014, Goddard et al., 2014), in some cases linked to constitutive and induced defences like *PR1* and chitinases (Ali et al., 2014). Alternatively BR can regulate ROS levels or and secondary metabolites (De Bruyne et al., 2014). BRs can directly affect resistance, for example, pre-treatment with epiBL was found to increase resistance to a range of pathogens in tobacco (*Nicotiana tabacum*), without PR expression and independently of SA or SAR (Nakashita et al., 2003). However BR can also interact with other phytohormones. BR was shown to negatively affect SA defences (De Vleesschauwer et al., 2012) (Fig.1.4). Alternatively, BR was found to induce the expression of JA-related *OPR3* (Müssig et al., 2000) (Fig.1.4). Lastly there are molecular interactions with the growth hormone GA that can in turn affect resistance. For example, BR caused stabilisation of DELLA proteins which interfered with GA-related immune response (De Vleesschauwer et al., 2012).

1.3.7. Auxin

Auxins are important for many developmental processes such as shoot and root architecture, responses to light and gravity, and vascular development (Woodward & Bartel, 2005, Davies, 2013). Among four naturally occurring auxins, indole-3-acetic acid (IAA) is the main active auxin in plant tissues (Davies, 2013, Sauer et al., 2013). IAA levels

are substantially different between monocots and dicots. In untreated *A. thaliana* tissues (dicot), IAA levels range from approximately 10 ng/g to 50 ng/g (FW and DW) (Lewis et al., 2011, Gupta et al., 2017), whereas in dicots, IAA ranges from approximately 16 ng/g to 5160 ng/g (DW) in various tissues of wheat and *B. distachyon* (Buhrow et al., 2016, Napoleão et al., 2017). To-date IAA (Fig. 1.5) is believed to be synthesised in plants via four tryptophan (Trp)-dependent pathways or one Trp-independent pathway (Woodward & Bartel, 2005). These pathways are described in detail in (Woodward & Bartel, 2005, Zhao, 2014, Morffy & Strader, 2020). The most well-characterised and likely primary plant pathway is the relatively simple and highly conserved Trp-dependent Indole-3-pyruvate (IPA) pathway. The amino acid Trp is first deaminated by the aminotransferase family *TRYPTOPHAN AMINOTRANSFERASE OF ARABIDOPSIS* (*TAA*) to IPA. Subsequently in the rate-limiting step, IPA is turned into IAA with the enzyme *YUCCA* (*YUC*) flavin monooxygenases via oxidative decarboxylation (Mashiguchi et al., 2011, Zhao, 2012, Zhao, 2014). Other less characterised Trp-dependent pathways include the tryptamine (TAM) pathway in which Trp is converted to TAM via *TRYPTOPHAN DECARBOXYLASE* (*TDC*), then TAM to indole-3-acetaldehyde (IAAld), and IAAld to IAA with unknown enzymes for the last two steps. In the indoleacetamide (IAM) pathway, Trp is converted to IAM by an unknown mechanism and then to IAA via *AMIDASE 1* (*AMI1*). Lastly in the IAOx pathway, Trp is converted to IAOx via *CYP79B2/3*. IAOx is then converted via unknown mechanism to IAM or indole-3-acetonitrile (IAN) and then via the enzymes *AMI1* and *NITRILASE* (*NIT*), respectively, to IAA. The Trp-independent pathway is not well-characterised but is believed to utilise indole derived from the Trp precursor indole-3-glycerol phosphate which is then converted to IAA.

IAA levels are regulated at biosynthesis and post-translationally. In Arabidopsis, biosynthetic auxin genes are regulated by numerous transcription factors described in (Zhao, 2014). Furthermore IAA can be stored by being conjugated with glucose via IAA glucosyl-transferase or conjugated with different amino acids with *GRETCHEN HAGEN3* (*GH3*) and in turn released with amidohydrolase *IAA-LEUCINE RESISTANT 1* (*ILR1*)*-LIKE* family members (Staswick et al., 2005, Woodward & Bartel, 2005, Sauer et al., 2013). IAA can also be stored by conversion to indole-3-butryic acid (IBA) via IBA synthase and back to IAA via b-oxidation, or methylated with *IAA CARBOXYLMETHYLTRANSFERASE 1* (*IAMT1*) (Woodward & Bartel, 2005, Sauer et al., 2013). Auxin is transported between cells over long distances by polar transport which is mediated by the asymmetrical localisation of auxin influx (*AUX1*) and efflux *PIN-FORMED* (*PIN*) transmembrane proteins (Woodward & Bartel,

2005). Some PIN auxin carriers are localised in the ER and believed to function in auxin sequestration (Sauer et al., 2013).

In the absence of auxin, *AUXIN/INDOLE-3-ACETIC ACID* (*AUX/IAA*) proteins interact with the *AUXIN RESPONSE FACTOR* (*ARF*) transcription factors forming inhibitory heterodimers. In the presence of auxin, the F-box protein/receptor *TRANSPORT INHIBITOR RESISTANT1* (*TIR1*), which is part of an SKP-Cullin F-box (SCF) type ubiquitin E3 ligase, forms a complex with AUX/IAA and promotes its ubiquitination and targeted degradation by the 26s proteosome. This releases ARFs and allows for auxin-responsive gene expression (Woodward & Bartel, 2005, Sauer et al., 2013). Most ARFs do not interact with AUX/IAA and function as transcriptional repressors. Instead they compete with transcriptional activator ARFs to bind to auxin-responsive genes (Sauer et al., 2013). Other potential auxin receptors include *AUXIN-BINDING PROTEIN1* (*ABP1*) and *S-Phase kinase-associated 2A* (*SKP2A*) but are both less characterised than *TIR1* (Sauer et al., 2013). Downstream targets include the positive regulator *SMALLAUXIN-UPRNAs* (*SAURs*), *GH3*, and *AUXIN/INDOLE-3-ACETIC ACID* (*AUX/IAA*) for auxin response regulation (Woodward & Bartel, 2005).

Aside for their important role in growth and development, auxins are also involved in defence signalling. Direct application of auxins was found to increase disease symptoms likely through inhibiting defence responses, and resistance can occur when auxin signalling is repressed (Bari & Jones, 2009). *GH3.8* was shown to improve resistance to the rice pathogen *X. oryzae* independent of JA and SA signalling, likely through suppression of auxin-induced cell wall loosening (Ding et al., 2008, Bari & Jones, 2009). Alternatively, auxins can negatively affect SA-dependent defence responses, which may indirectly improve resistance to necrotrophs (Fig. 1.6; (Robert-Seilaniantz et al., 2007, Robert-Seilaniantz et al., 2011)). In turn, SA was also shown to regulate auxin by supressing expression of auxin transporters, receptors, and responsive genes (Wang et al., 2007). One common regulator between SA and auxin may be *GH3* since *GH3.5* regulates signalling of both auxin and SA (Zhang et al., 2007, Vlot et al., 2009, Chen et al., 2013b). Auxin is positively involved in the JA signalling pathway. The molecular JA components *JAZ*, *COI1*, *MYC2* function in the crosstalk between JA-auxin (Yang et al., 2019). For example, exogenous auxin and auxin signalling can induce JA-associated genes (Tiryaki & Staswick, 2002, Yang et al., 2019) like *JAZ/TIFY10A* (Grunewald et al., 2009). Lastly tryptophan conjugates of JA and IAA can inhibit function of auxin (Staswick, 2009). Alternatively, there

might be a negative cross-talk/fine-tuning as components of the E3-ubiquitin ligase complex are also used similarly with the auxin-related receptor *TIR1* which may result in a competition for component resources (Acosta & Farmer, 2010). Overall auxins likely have roles in defence towards necrotrophs due to their generally positive association with JA (Fig. 1.6). This is supported by evidence that necrotrophs were found to reduce auxin signalling (Llorente et al., 2008).

1.3.8. Cytokinin

Cytokinins are a group of hormones important for a range of developmental processes like floral development, cell division, specifying cell fate, and root development, (Davies, 2013, Wybouw & De Rybel, 2019). Natural cytokinins are purine base derivates and appear as either isoprenoid cytokinins (e.g. *N*-[2-isopentyl]adenine (iP), *trans*-Zeatin (tZ) (Fig. 1.5)) or aromatic cytokinins (e.g. Kinetin or *N*-benzyladenine (BA)) (Márquez-López et al., 2019). Cytokinin concentrations (specifically zeatin) are approximately between 1 ng/g and 7 ng/g (DW) in *Arabidopsis* leaves over time (Gupta et al., 2017), whereas in wheat and *B. distachyon* they were either not detected, or are between approximately 2 ng/g and 4 ng/g (DW) (Buhrow et al., 2016, Napoleão et al., 2017). Their biosynthesis, regulation, and transport is described in (Márquez-López et al., 2019). Isoprenoid cytokinin (iP, tZ, and dihydrozeatin (DZ)) synthesis starts from either the methylerythritol phosphate (MEP) pathway in the plastid that produces 4-hydroxy-3-methyl-2(E)-butenyl diphosphate (HMBDP) and subsequently dimethylallyl pyrophosphate (DMAPP) or through the MVA pathway in the cytosol that produces DMAPP directly. First ATP, ADP, or AMP are prenylated with the isoprenoid moiety from DMAPP using *ADENOSINE PHOSPHATE ISOPENTENYLTRANSFERASE* (*AP-IPT*), resulting in isopentenyl adenosine-5-triphosphate iPRTP, isopentenyladenosine-5-diphosphate iPRDP, or isopentenyladenosine-5-monophosphate iPRMP, respectively. Subsequently iPRTP, iPRDP, and iPRMP are hydroxylated to *trans*-Zeatin-riboside 5'-phosphates, tZRTP, tZRDP, or tZRMP, respectively, by *AtCYP735A1* and *AtCYP735A2*. The monophosphate ribonucleotides (i.e. iPRMP and tZRMP) are key precursors for the active cytokinins iP and tZ, respectively. The monophosphate ribonucleotide iPRMP can also be generated from dephosphorylation of IPRTP and iPRDP whereas the ribonucleotide tZRMP can also be produced from tZRPTP and tZRDP dephosphorylation. For the cytokinin DZ, the ribonucleotide DZRMP is produced from tZRMP. *cis*-Zeatin (cZ) is synthesised from tRNA in which the adenine at A37 is prenylated with tRNA-IPT, and after tRNA degradation, results in in the ribonucleotide

cZRMP. There are then two pathways that result in active cytokinins from the ribonucleotides described. The most known involves direct activation pathway that is catalysed by *LONELYGUY* (*LOG*) gene family converting the monophosphate ribonucleotides iPRMP, tZRMP, DZRMP, cZRMP to the active isoprenoid cytokinins iP, tZ, DZ, and cZ, respectively. Alternatively the monophosphate ribonucleotides can be converted to the active form via two-step pathway by converting the ribonucleotides iPRMP, tZRMP, DZRMP, cZRMP to ribonucleosides iPR, tZR, DZR, and cZR, respectively, before conversion to the active cytokinins. This alternate pathway is less characterised, and in *Arabidopsis* only one gene was characterised as *URIDINE RIBOHYDROLASE* (*URH1*) (a nucleoside N-ribohydrolase (NRH)) responsible for converting the ribonucleoside isopentenyladenine-riboside to iP. The biosynthesis of aromatic cytokinins is not well characterised.

Cytokinin levels can be regulated by conjugation or by oxidative breakdown. Cytokinins are conjugated at the O or N position with glucose catalysed by glucosyltransferases (*UGT*). N-conjugation is irreversible and is associated with cytokinin degradation whereas O-glucosylation is reversible with beta-glucosidase. Cytokinins can be degraded irreversibly through oxidative breakdown by cytokinin oxidase/dehydrogenase (*CKX*) (Albrecht & Argueso, 2017, Márquez-López et al., 2019). Cytokinins are transported long distance from root to shoot by ATP-binding cassette (ABC) transporters. The non-specific transporter *PUP* import apoplastic tZ and iP whereas *ENT* transporters import the respective apoplastic cytokinin ribonucleosides (Márquez-López et al., 2019).

Cytokinin signalling occurs through a two-component signalling pathway as described in (Nongpiur et al., 2012, Márquez-López et al., 2019). Cytokinins bind to CHASE domain of ER-localised *NON-ETHYLENE HISTIDINE KINASES* (*AHK*) receptors (*AtAHK2/3/4*) triggering histidine autophosphorylation. The phosphate group is then shuttled by the protein histidine phosphotransferase (HpT) from the cytoplasm to type B response regulators (RRs) in the nucleus. AHK4 also functions as a phosphatase and dephosphorylates HpT in the absence of cytokinin. Type-B RRs are made up of a receiver domain and a MYB-like DNA binding motif at the C-terminus which is important for activating downstream cytokinin-responsive genes such as the *type-A RRs*. Hpt positively interacts with other cytokinin-related transcription factors such as *CYTOKININ RESPONSE FACTORS* (*CRFs*) which share downstream targets with *type B RRs*. Cytokinin signalling is regulated at various steps in

this pathway. As a negative feedback loop, type A RRs that lack a DNA binding domain repress HpT and type B-RRs likely through competition for phosphate. Type B RRs are also regulated by *S-PHASE KINASE-ASSOCIATED PROTEIN1* (*SKP1*)/*CULLIN*/*F-BOX* (*SCF*) *E3*-ubiqutin with the F box *KISS ME DEADLY* (*KMD*) and 26S proteasome for degradation. Other transcription factors such as *SPY* and *GLABROUS1 ENHANCER-BINDING PROTEIN* (*GeBP/GPL*) can positively regulate cytokinin signalling.

There is relatively little known about the function cytokinins have in plant defences. Lower endogenous cytokinin levels were associated with susceptibility to the obligate biotroph *Plasmodiophora brassicae* in *A. thaliana* (Siemens et al., 2006), and cytokinin levels and signalling was found to increase in response to rice blast from *M. oryzae* (Jiang et al., 2013). Cytokinins are thought to promote susceptibility to obligate biotrophs in part through their association with 'green islands' in which a region of senescing tissue at infection sites remain photosynthetically active (Walters & McRoberts, 2006, Albrecht & Argueso, 2017). On the other hand, cytokinins were shown to promote resistance as cytokinins were found to elevate levels of phytoalexins (Großkinsky et al., 2011), and ROS scavenging compounds (Pogány et al., 2004), and induce callose deposition (Choi et al., 2010) in which pathogen resistance was inferred. However defence activation only occurred during co-application of cytokinins with elicitors/pathogen suggesting cytokinins act as priming agents (Albrecht & Argueso, 2017). Isoprenoid cytokinins were shown to affect tobacco resistance differently as tZ was more effective than cZ for reducing *Pseudomonas syringae* pv. *tabaci* symptoms (Großkinsky et al., 2013). Cytokinins may also have a more complex role in defence response signalling by functioning synergistically with other phytohormones. Cytokinins were shown to function synergistically with SA for defence (Fig. 1.6; (Robert-Seilaniantz et al., 2007, Choi et al., 2011, Naseem et al., 2012, Pieterse et al., 2012, Jiang et al., 2013, Albrecht & Argueso, 2017). For example, SA-related defence gene expression (i.e. Os*PR1b*) in rice was activated via the synergism from SA and cytokinin co-treatment (Jiang et al., 2013). Similarly the cytokinin negative regulator type-A RR was also found to suppress SA-related gene expression and downstream SA defences (Choi et al., 2010, Argueso et al., 2012). Cytokinin was found to have a priming effect on resistance before pathogen attack (Choi et al., 2010, Argueso et al., 2012). However, as a regulatory mechanism, SA was shown to negatively regulate cytokinin signalling (Argueso et al., 2012). Through modelling of *Arabidopsis* signalling networks, cytokinins were also

shown to function antagonistically to auxin in defence and the balance between these two hormones was shown to affect SA defences (Naseem et al., 2012).

1.3.9. Aminobutanoic Acids

Aminobutanoic acids (Synonym aminobutyric acids) are relatively newly recognised signalling molecules compared to the classic plant hormones. In terms of plant pathogen interactions the most important one is 3-aminobutanoic acid (BABA) (Fig. 1.5). BABA is a non-protein amino acid (Jakab et al., 2001, Cohen, 2002) which has been found naturally in plants at 6.4 ng/g (FW) in *A. thaliana*, and approximately 10 ng/g (FW) in wheat (Thevenet et al., 2017). To date only one BABA receptor has been identified as *IMPAIRED IN BABA-INDUCED IMMUNITY 1* (*AtIBI1*) encoding an aspartyl-tRNA synthetase. The R-enantiomer of BABA binds to aspartyl-tRNA synthetase binding domain, allowing for plant perception of BABA (Luna et al., 2014, Schwarzenbacher et al., 2014). Furthermore, *Atibi1* mutants displayed reduced BABA-induced resistance (Luna et al., 2014). It is suggested that *IBI1* (in the absence of BABA) contributes to resistance by sensing the dropping aspartic acid concentrations in the cytosol from invading biotrophic pathogens because of a reduction in its activity, resulting in elevated *IBI1* expression and basal defence. This scenario is mimicked by BABA binding to *IBI1* and priming basal resistance (Schwarzenbacher et al., 2014).

BABA is renowned for improving resistance in many plant species to a broad range of pathogens and insects without directly affecting the growth of the pathogen (Zimmerli et al., 2000, Jakab et al., 2001, Cohen, 2002, Cao et al., 2014). Remarkably BABA is known to increase resistance to both biotrophic and necrotrophic pathogens (Cohen, 2002, Ton & Mauch-Mani, 2004, Ton et al., 2005). BABA levels also increase in response to pathogen attack (Thevenet et al., 2017). BABA is reported to increase resistance via callose, ROS, lignin, phytoalexins, and phenols (Cohen, 2002, Olivieri et al., 2009). This resistance often leads to reduced host growth (Schwarzenbacher et al., 2014), iron deficiency (Koen et al., 2014) and even sterility (Cohen, 2002). BABA has the potential to be classed as a novel phytohormone (Baccelli & Mauch-Mani, 2017). Importantly the resistance and growth pathways induced by BABA are regulated by independent pathways (Luna et al., 2014). BABA-induced resistance pathways can also be pathogen-specific (Zimmerli et al., 2000, Cohen, 2002). There is a strong link between BABA and PAMP triggered immunity (PTI)

through SA signalling (Fig. 1.6) (Conrath et al., 2006). BABA has been shown to induce *PR1*, *PR2*, and *PR5* expression (Cohen, 2002, Flors et al., 2008). Additionally, BABA also increases resistance to necrotrophic pathogens by supporting ABA biosynthesis and signalling pathways which likely primes callose deposition (Ton & Mauch-Mani, 2004, Ton et al., 2005, Flors et al., 2008). Genes involved in this callose deposition include the ABA-associated *ZEP* and the activator protein 2 transcription factor *ABSCISIC ACID INSENSITIVE 4* (*ABI4*) (Ton & Mauch-Mani, 2004, Ton et al., 2009).

An important isomer of BABA is 4-aminobutanoic acid (GABA) (Fig. 1.5) which can also act as an extracellular signalling molecule in plants (Jakab et al., 2001, Shelp et al., 2006). GABA is found at a higher concentration than BABA at 7,790 ng/g (FW) in *A. thaliana* (Thevenet et al., 2017). Much less is known about the effect that GABA has on plant pathogen interactions compared to BABA (Kinnersley & Turano, 2000, Forlani et al., 2014, Shelp et al., 2017). GABA is important in the tricarboxylic acid pathway (TCA), specifically in the GABA shunt pathway which provides an alternative route to produce succinate from glutamate (Shelp et al., 2006, Bolton, 2009). The GABA shunt pathway was shown to be induced in *Lr34* resistant plants at 3 days post inoculation (dpi) (Bolton et al., 2008). Additionally, elevated GABA levels have been found in rice cultivars in response to rice blast *M. oryzae*, but while GABA levels continued to increase in resistant lines, GABA levels decreased in susceptible lines (Forlani et al., 2014). It is thought that GABA (through the GABA shunt pathway) provides resistance through maintaining NADH generation in the TCA cycle. This allows the host to circumvent enzymes that are sensitive to oxidative stress which often occurs during HR (Bolton, 2009). Additionally GABA might act as a stress response signal from decreasing pH levels in the cytosol and increased calcium signalling (Kinnersley & Turano, 2000). Expression of genes involved in primary amino acid metabolism, specifically the GABA biosynthetic genes were significantly increased in resistant mutants against necrotrophic pathogens (Seifi et al., 2013). Therefore the evidence suggests that GABA provides resistance to pathogens, specifically to necrotrophs, through primary metabolism and the reduction of disease symptoms. On the other hand, evidence shows that GABA might be used by pathogens as a nutrient source. GABA levels were found to increase in response to acidic pH from the compatible interaction with biotrophic fungi *C. fulvum* (Solomon & Oliver, 2002, Shelp et al., 2006). GABA level changes are also utilised by *F. graminearum* as self-defence mechanism against the toxicity of DON (Wang et al., 2018b).

1.4. The Biosynthesis of Phytohormones in Fungi

Almost all the phytohormones, either the same (Fig. 1.5) or novel compounds, are produced in fungi. Most phytohormone biosynthetic genes in fungi appear in clusters. The phytohormone GA was first identified in *Gibberella fujikuroi* (synonym *Fusarium monoliforme*) and the responsible biosynthetic pathway, controlled by a cluster of seven genes, is described in detail in (Tudzynski, 2005). The start of the fungal GA pathway is very similar to the pathway plants (Yamaguchi, 2008). In *G. fujikuroi*, *GGDP SYNTHASE-ENCODING GENE* (*GGS*), *CPS/KS*, *CYP450-4*, and *CYP450-1,* are key genes in the cluster involved at the start of GA biosynthesis from GGDP to GA_{12} aldehyde and GA_{14} aldehyde. The differences between *G. fujikuroi* and plants occurs after the GA_{12} aldehyde with the genes *CYP450-1*, *CYP450-2*, *CYP450-3*, and *GA4 1,2-DESATURASE* (*des*) and is generally to do with when the hydroxyl groups are added (Tudzynski, 2005). The gene *NADPH-CYTOCHROME P450 REDUCTASE* (*CPR*) is important for CYP450 enzyme function (Malonek et al., 2004). ABA is also produced in fungi like *B. cinerea*, *M. oryzae*, and *F. graminearum* (Siewers et al., 2006, Spence et al., 2015, Qi et al., 2016, Izquierdo-Bueno et al., 2018). In *B. cinerea*, the responsible genes include a four gene cluster (two *CYP450* genes (*aba1* and *aba2*), a gene of unknown function (*aba3*), and a *DEHYDROGENASE* (*aba4*)) as well as a fifth important gene (*SESQUITERPENE CYLASE* (*stc5/aba5*)) elsewhere in the genome (Siewers et al., 2006, Izquierdo-Bueno et al., 2018). Largely differing from the carotenoid pathway in plants (Chen et al., 2020), the direct ABA pathway in *B. cinerea* involves the conversion of farnesyl diphosphate, derived from IPP, to a-ionylideneethanol with *stc5/aba5*, which is then oxidised multiple times from the four gene cluster resulting in ABA (Inomata et al., 2004, Siewers et al., 2006, Izquierdo-Bueno et al., 2018).

Cytokinins are produced by two different pathways in fungi which match the different pathways for isoprenoid cytokinins in plants (Márquez-López et al., 2019). For the first pathway one of three forms of gene clusters are present in several fungal species like *F. pseudograminearum*, *Fusarium oxysporum*, and *Claviceps purpurea* (Sørensen et al., 2018)*.* Each cluster contains a different composition of genes but all contain the two key genes *IPT-LOG* fusion and a *CYP450*. Both genes are important for producing *trans*-zeatin, *cis*-zeatin, and three *Fusarium* specific cytokinins (e.g. Fusatinic acid) in *F.*

pseudograminearum (Sørensen et al., 2018) and *trans*-zeatin in *C. purpurea* (Hinsch et al., 2015). The second pathway involves a *tRNA-IPT* gene which is important for *cis*-Zeatin production is found in species like *M. oryzae*, *Colletotrichum graminicola* and *C. purpurea* (Chanclud et al., 2016, Hinsch et al., 2016, Eisermann et al., 2020). The *tRNA-IPT* protein is conserved in several Ascomycete fungi (Chanclud et al., 2016).

Fungi can also produce the auxin IAA generally using the one or more of the four tryptophan-dependent pathways, but often with genes resembling the ones found in bacteria, as described in (Morffy & Strader, 2020). A common pathway is the IAM pathway used by species like *Fusarium proliferatum* ET1 and *Colletotrichum gloeosporioides* f.sp *aeschynomene* (Robinson et al., 1998, Tsavkelova et al., 2012). In these species, the genes responsible are organised in a cluster containing a *TRYPTOPHAN MONOOXYGENASE* (*IaaM*) and an *IAM HYDROLASE* (*IaaH*) (Tsavkelova et al., 2012). Secondly, the IPA pathway is present in fungi like *Ustilago maydis*, *Neurospora crassa,* and likely also in *Leptosphaeria maculans* and *C. gloeosporioides* f.sp *aeschynomene* (Robinson et al., 1998, Reineke et al., 2008, Sardar & Kempken, 2018, Leontovyčová et al., 2020). In a manner connecting both the IPA and TAM pathway (Morffy & Strader, 2020), the most likely pathway is that tryptophan is converted to IPA with *TRYPTOPHAN AMINOTRANSFERASE* (*TAM*) genes (Reineke et al., 2008). Then IPA is likely converted to IAAld with *INDOLE-3-PYRUVATE DECARBOXYLASE* (*IPDC*) genes (Sardar & Kempken, 2018, Leontovyčová et al., 2020). *IPDC* orthologues are present in several ascomycete fungi (Leontovyčová et al., 2020). Lastly, IAAld is converted to IAA with *INDOLE-3-ACETYLALDEHYDE DEHYDROGENASE* (*IAD*) genes (Reineke et al., 2008). Interestingly *F. graminearum* is unique in that it likely uses the alternative IAN and TAM pathways for IAA biosynthesis (Luo et al., 2016).

The phytohormone ethylene is also produced by numerous fungi (Table 6.1) and the pathways responsible are described in detail in the introduction of chapter 6. Lastly, the phytohormones SA and JA can also be produced by fungi (Chanclud & Morel, 2016), including by *F. graminearum* (Ding et al., 2020). There are early descriptions of the JA pathway in fungi which is likely similar to the plant pathway (Eng et al., 2021), however the pathway for SA is still unidentified (Chanclud & Morel, 2016).

1.5. The Use of Phytohormones to Control Plant Diseases

Phytohormones can be exogenously applied to plants, generally before infection from microorganisms, to improve host resistance. The most well-studied phytohormone through exogenous application is SA. SA was shown to be effective in reducing disease from a wide range of bacterial, viral, and fungal pathogens in several species such as *Arabidopsis*, rice, and tomato (*Solanum lycopersicum*) (Mandal et al., 2009, Trusov et al., 2009, Koo et al., 2020). There are even commercial products, termed plant defence activators, that increase plant defence through SA-related plant defence pathways (Agrios, 2005, Bektas & Eulgem, 2015). For example the active component benzothiadiazole, in products like BION®, is a synthetic analogue of SA that primes plant defences through SAR and is used to reduce the severity of disease from several plant pathogens (Friedrich et al., 1996, Agrios, 2005, Sugano et al., 2013, Bektas & Eulgem, 2015). In a similar fashion, BABA could be considered a SAR-associated plant defence activator (Cohen, 2002, Agrios, 2005). Like SA, exogenous application of BRs can improve resistance to many plant and pathogen systems such as tobacco mosaic virus (TMV) in tobacco, *Magnaporthe grisea* and *X. oryzae* in rice, *phytophthora* in potato (*Solanum tuberosum*), and *P. syringae* and *Oidium* sp. in tobacco (Khripach et al., 2000, Nakashita et al., 2003, Yu et al., 2018). Importantly there is evidence of improved resistance to fungi from BR application in field trials of barley and cucumber (*Cucumis sativus L.*) (Khripach et al., 2000).

Despite the negative effects on resistance (Fig. 1.4), exogenous application of ABA can also improve resistance to species like *Plectosphaerella cucumerina* in *Arabidopsis*, *Cochliobolus miyabeanus* in rice, *Alternaria solani* in tomato, and can reduce TMV build-up in *Arabidopsis* (Ton & Mauch-Mani, 2004, De Vleesschauwer et al., 2010, Song et al., 2011, Chen et al., 2013a). For JA, exogenous application of the jasmonate MeJA has also been shown to increase resistance to several necrotrophic fungal pathogens, for example to *B. cinerea* and *P. cucumerina* in *Arabidopsis*, *Pythium arrhenomanes* in rice, and *Sclerotinia sclerotiorum* in dry bean (*Phaseolus vulgaris* L.) (Thomma et al., 2000, Oliveira et al., 2015, Verbeek et al., 2019). Exogenous application of ethylene or the precursor ACC have been shown to also improve resistance in soyabean (*Glycine max*) to *Phytophthora sojae* (Sugano et al., 2013), and tomato to *B. cinerea* (Díaz et al., 2002).

Exogenous application of cytokinins was also shown to improve resistance to bacteria, fungi, and an oomycete in species like *Arabidopsis*, rice, tobacco, and tomato (Naseem et al., 2012, Reusche et al., 2013, Albrecht & Argueso, 2017, Gupta et al., 2020). There is evidence that exogenous application of the auxin IAA increased resistance in cotton (*Gossypium hirsutum*) and tomato to certain *Fusarium* species (Sharaf & Farrag, 2004, Egamberdieva et al., 2015). Lastly exogenous application of GA has been shown to improve *phytoplasma* resistance in tomato (Ding et al., 2013). Exogenous application of phytohormones can also have negative effects on resistance and this depends on many factors such as the plant host and pathogen investigated (Díaz et al., 2002, Robert-Seilaniantz et al., 2007, Bari & Jones, 2009, De Vleesschauwer et al., 2010, Albrecht & Argueso, 2017, Yu et al., 2018, Koo et al., 2020). Thus the examining the effects of exogenous phytohormone application should be investigated in a case-by-case basis.

BCAs can be used as an alternative approach to improving host defences to pathogens through the modification of endogenous phytohormone content in host plants. The fungus *Trichoderma* is a good example of this. Root application of different *Trichoderma* species induced both JA and SA content in *Arabidopsis* and cucumber and reduced the symptoms of *B. cinerea* and *P. syringae*, respectively (Segarra et al., 2007, Contreras-Cornejo et al., 2011). Similarly, both JA and ethylene pathways were associated with the resistance-inducing properties of *Trichoderma asperellum* in cucumber to *P. syringae* (Shoresh et al., 2005). It is proposed that *Trichoderma* activates ISR against pathogens in distal tissues through the JA and ethylene pathway (Shoresh et al., 2005, Korolev et al., 2008, Pieterse et al., 2014). Similarly another BCA species, *Cryptococcus laurentii*, was shown to promote resistance to *B. cinerea* in cherry tomato through host-induced ethylene biosynthesis and signalling (Tang et al., 2019). Other phytohormones can also be affected by various BCA species. In melon (*Cucumis melo*), three other *Trichoderma* species were shown to reduce the disease symptoms from *F. oxysporum* which correlated with a reduction in hormone profiles like cytokinins (Martínez-Medina et al., 2014). In other BCAs like *Pseudomonas Fluorescence*, cytokinin signalling was shown to be important for effective biocontrol against *P. syringae* in *Arabidopsis* (Großkinsky et al., 2016). Lasty, the BCAs *Bacillus subtilis* and three *Trichoderma* species were shown to increase cucumber, melon, and tomato IAA content and provide resistance to different pathogens (Chen et al., 2010, Chowdappa et al., 2013, Martínez-Medina et al., 2014).

Overall, the manipulation of endogenous phytohormone content in several host species through exogenous application or BCAs are shown to be effective control strategies towards respective pathogens.

1.6. *Brachypodium distachyon* as a Model Organism for Studying Fusarium Diseases

Due to wheat having a large allohexaploid genome, long growth, and generation time, and relatively inefficient transformation resources (Brkljacic et al., 2011), wheat is not the best pathosystem for high throughput, small-scale experimental analysis of Fusarium diseases. Draper and colleagues (2001) described *Brachypodium distachyon* (purple false brome) as a useful model system for small-grained cereals (Draper et al., 2001). *B. distachyon* (2n_10) is a temperate monocotyledonous plant that belongs to the Pooideae sub-family. It is an inbreeding annual, with short generation times of less than four months, short height, and requires simple growth conditions (Fig. 1.7) (Draper et al., 2001, Brkljacic et al., 2011, Scholthof et al., 2018). In terms of resources, *B. distachyon* has a very simple genome of just 272 Mbp (high quality reads), high sequence collinearity and phylogenetic position with other important cereals, efficient transformation systems, and a wide array of other genetic resources (Vogel et al., 2006, Initiative, 2010, Brkljacic et al., 2011, Thole et al., 2012, Kellogg, 2015, Scholthof et al., 2018, Hus et al., 2020). Due to high similarity (anatomically and developmentally) to wheat, *B. distachyon* is a good model for studying shoot and root development (Watt et al., 2009), as well as similarities in grain development (Draper et al., 2001, Opanowicz et al., 2011) .

Figure 1.7. *B. distachyon* (Bd3-1) plants in pots growing in a controlled environment cabinet. Approximately 3-week old Bd3-1 in the front. Flowering Bd3-1 in the back (Approximately 6-week-old). Photos taken with an iPhone 6 camera.

In terms of *Fusarium* disease research, other hosts such as barley have inherent type 2 resistance (Fig. 1.3B, Table 1, (Langevin et al., 2004) which makes studying this type of resistance difficult. Although rice is a diploid with a small genome (Ensembl Genomes database (Howe et al., 2020)), it is not adapted to temperate climates, and is infected by alternative *Fusarium* species (Amatulli et al., 2010), which makes studying *F. graminearum* infection challenging. *A. thaliana* can be used (Urban et al., 2002) however it exhibits alternative FHB floral symptoms to those found in cereals and infection does not lead to accumulation of high DON concentrations in floral tissues (Professor Paul Nicholson, personal communication).

B. distachyon is also a good model for studying plant-pathogen interactions. Certain *B. distachyon* ecotypes display varying levels of susceptibility to a range of important cereal diseases (Draper et al., 2001, Routledge et al., 2004). Peraldi and colleagues (2011) and Pasquet and colleagues (2014) showed that *B. distachyon* is an important model for studying *F. graminearum* pathology on cereals (Peraldi et al., 2011, Pasquet et al., 2014). *F. graminearum* can infect all *B. distachyon* tissues with variation between *B. distachyon* ecotypes and germplasm (Peraldi et al., 2011, Su et al., 2018) (Fig. 2.2 and Fig. 3.2). The ecotype Bd3-1 was chosen for the present study due to it having slightly higher levels of susceptibility than Bd21 (Peraldi et al., 2011, Su et al., 2018). Furthermore *F. graminearum* was found to progress in a similar manner during *B. distachyon* FHB to that of wheat FHB, especially under elevated humidity (Su et al., 2018). Despite DON increasing susceptibility to *F. graminearum* in *B. distachyon* (Pasquet et al., 2014), pre-infection application of DON was shown to condition resistance to *F. graminearum* in *B. distachyon* (Blumke et al., 2015). Furthermore, a *B. distachyon* gene encoding a UDP-glucosyltransferase was shown to provide FHB and FRR resistance and DON resistance in *B. distachyon* and wheat (Pasquet et al., 2016, Gatti et al., 2019). Lastly, certain parts of the immune system are conserved between *B. distachyon* and other cereals such as with BR signalling (Goddard et al., 2014) or *PR* genes (Kouzai et al., 2016). Furthermore, many important phytohormone-associated *B. distachyon* genes have been investigated (Lyons et al., 2013, Kakei et al., 2015, Pearce et al., 2015, Yang et al., 2015, You et al., 2015, Chen et al., 2016, Gordon et al., 2016, Kouzai et al., 2016).

1.7. Project Aims

Most wheat varieties are susceptible to FHB and fungicides are not completely effective. Phytohormones are known to affect resistance to different plant pathogens. *Brachypodium distachyon* is an effective cereal model for investigating Fusarium diseases and phytohormone effects. The main aim of this project is to investigate the role of phytohormones in the interaction between *B. distachyon* and *F. graminearum*. Several sub-aims described below are important for addressing this aim. I want to compare the effects of each phytohormone on resistance to floral and root tissue diseases caused by *F. graminearum* (FHB and FRR, respectively). The effect of individual phytohormones on resistance will be investigated using exogenous hormone pre-application on FRR and FHB in Chapters 2 and 3, respectively. Phytohormones with the greatest effect on FRR and FHB disease resistance will be identified and discussed. I will then investigate the phytohormone-related transcriptomic response of *B. distachyon* during both FHB and FRR diseases in Chapter 4. Likewise, the expressed secretome and other important gene groups in *F. graminearum* during both FHB and FRR diseases will be investigated in Chapter 5. Lastly, it was reported that the host ethylene-signalling pathway is exploited by *F. graminearum*. Gas chromatography and transcriptomics will be used to investigate the biosynthesis of ethylene by *F. graminearum* in Chapter 6. Suitable predicted ethylene biosynthesis genes will then be deleted using a split-marker deletion method and ethylene production and virulence of deletion strains will be investigated.

Chapter Aims:

- Chapter 2: Determine which phytohormones are most effective at altering FRR resistance in *Brachypodium distachyon*.
- Chapter 3: Determine which phytohormones are most effective at improving FHB resistance in *Brachypodium distachyon* and wheat.
- Chapter 4: Investigate the phytohormone-associated transcriptome differences between FHB and FRR in *Brachypodium distachyon*.
- Chapter 5: Investigate the transcriptome differences of key *Fusarium graminearum* effectors and genes between FHB and FRR.
- Chapter 6: Determine whether *Fusarium graminearum* produces ethylene. Identify the responsible pathway. Determine whether *Fusarium graminearum*-derived ethylene has a role in virulence.

Chapter 2 - The Effect of Phytohormones on Fusarium Root Rot

Several figures and some of the writing in this chapter have been published previously in:

Haidoulis JF, Nicholson P, 2020. Different effects of phytohormones on Fusarium head blight and Fusarium root rot resistance in *Brachypodium distachyon*. *Journal of Plant Interactions* **15**, 335-44.

2.1 Introduction

Fungal root diseases in cereals caused by the fungi *Fusarium*, *Gaeumannomyces*, and *Rhizoctonia*, are widespread in wheat (*Triticum aestivum*) and barley (*Hordeum vulgare*) fields and are becoming more prevalent with the increased use of cereal crop rotation and no tillage practices (Cook, 2001). Fusarium root rot (FRR) in cereals can be caused by *Fusarium culmorum* and *Fusarium graminearum* (Cook, 2001, Beccari et al., 2011, Wang et al., 2015b). *F. graminearum* is often associated with the disease Fusarium head blight (FHB) as this is generally the first Fusarium symptom observed and is the most economically relevant (Parry et al., 1995). FRR on the other hand is not as well characterised as FHB due to the difficulty of studying root diseases (Voss-Fels et al., 2018). Fortunately wheat FRR caused by *F. graminearum* and *F. culmorum* has been the subject of some investigations (Wang et al., 2006, Beccari et al., 2011, Wang et al., 2015b, Wang et al., 2018c). Colonisation and sporulation can occur rapidly (Wang et al., 2015b) causing root browning and necrosis (Beccari et al., 2011, Peraldi et al., 2011). Control of FRR is also difficult due to limited effectiveness of fungicides, lack of genetic resistance, and persistence in the soil for many years facilitated by the predominantly saprotrophic lifestyle of *F. graminearum* (Parry et al., 1995, Cook, 2001).

Phytohormones induce different effects on Fusarium head blight (FHB) resistance in wheat and barley (Fig. 3.1). No research to my knowledge has investigated the effect of phytohormones in response to *F. graminearum* root disease in cereals. The effect of hormones on *F. oxysporum*-infection following root treatment has, however, been investigated previously (Sharaf & Farrag, 2004, Mandal et al., 2009, Trusov et al., 2009, Kidd et al., 2011). Unfortunately these experiments were performed on dicot hosts and only measured shoot disease symptoms. Therefore the effect of phytohormone on FRR

symptoms in cereals is relatively unknown. Certain *F. oxysporum formae specialis* are predominantly necrotrophic pathogens in many plant species that invade host roots and cause vascular wilt (Agrios, 2005). Generally salicylic acid (SA) root treatment improved *F. oxysporum* wilt resistance (Mandal et al., 2009, Trusov et al., 2009) and abscisic acid (ABA), 1-aminocyclopropane-1-carboxylic acid (ACC), and jasmonic acid (JA) root treatment increased *F. oxysporum* wilt susceptibility (Trusov et al., 2009).

Brachypodium distachyon is an effective cereal model for investigating cereal FRR due to the high anatomical similarity of roots to wheat (Watt et al., 2009, Chochois et al., 2012) and the fact that root tissues are highly susceptible to *F. graminearum* infection (Peraldi et al., 2011, Peraldi, 2012). *B. distachyon* was selected for FRR assays over wheat because of the fast and resource-saving method. There is also a reduction in random experimental variation because of the larger density of *B. distachyon* plants that are grouped together for a single treatment. Furthermore the *B. distachyon* FRR data can be more accurately compared to FHB assays using *B. distachyon* (Chapter3), and the small *B. distachyon* genome (Initiative, 2010) is useful to ease the subsequent investigation of transcriptomics in FRR (Chapter 4). Therefore *B. distachyon* was used to efficiently test the effect of phytohormones on FRR resistance on many roots simultaneously in a short timeframe. This has been investigated once before. Exogenous ACC application on *B. distachyon* roots was shown to increase *F. culmorum*-induced FRR symptoms (Cass et al., 2015).

The objective of this chapter is to determine which phytohormones have the most significant effect on *F. graminearum*-induced FRR resistance when applied exogenously. *B. distachyon* root tissues from seedlings were treated with a range of phytohormones before inoculation with *F. graminearum*. All phytohormones, excluding strigolactones but including aminobutanoic acids, were investigated. Since phytohormones interact with other hormones at the molecular level, two compounds with substantial effects on FRR resistance were then assessed for their effects on endogenous phytohormone and defence changes during late FRR infection with the use of hormone responsive markers.

Aim: Identify the phytohormones that are most effective at altering FRR resistance in *Brachypodium distachyon*.

2.2 Materials and Methods

2.2.1. Plant Material and Growth Conditions

The *Brachypodium distachyon* line Bd3-1 was obtained from the John Innes Centre, Norwich, UK. To soften the floret, seeds were soaked in water (sterile diH_2O) for 10 to 30 min. Subsequently, the lemma and palea were peeled off the individual seeds. Peeled seeds were placed between two layers of dampened filter paper (9 cm, Sartorius Grade 292) with 5 ml water (sterile diH_2O) in a Petri-dish. Seeds were then stratified at 5°C for five days in the dark. Then the top filter paper layer covering the seeds was removed and the seeds were incubated for one day at 22°C (16 h/8 h light/dark photoperiod, variable humidity) in controlled environment cabinets (Snijders Labs MicroClima-series, Economic LUX chambers) (Peraldi et al., 2011).

2.2.2. Maintenance of *F. graminearum*

Fusarium graminearum PH1 (obtained from John Innes Centre, UK) was maintained on 20 ml solidified potato dextrose agar (PDA) (41 g/L) (The PDA solution was prepared by the JIC media kitchen) in circular 9 cm diameter plastic Petri-dishes in controlled environment cabinets (Snijders Labs MicroClima-series, Economic LUX chambers or in a walk-in controlled environment growth room) at 22°C under 16 h/8 h light/dark photoperiod (Fig. 2.1).
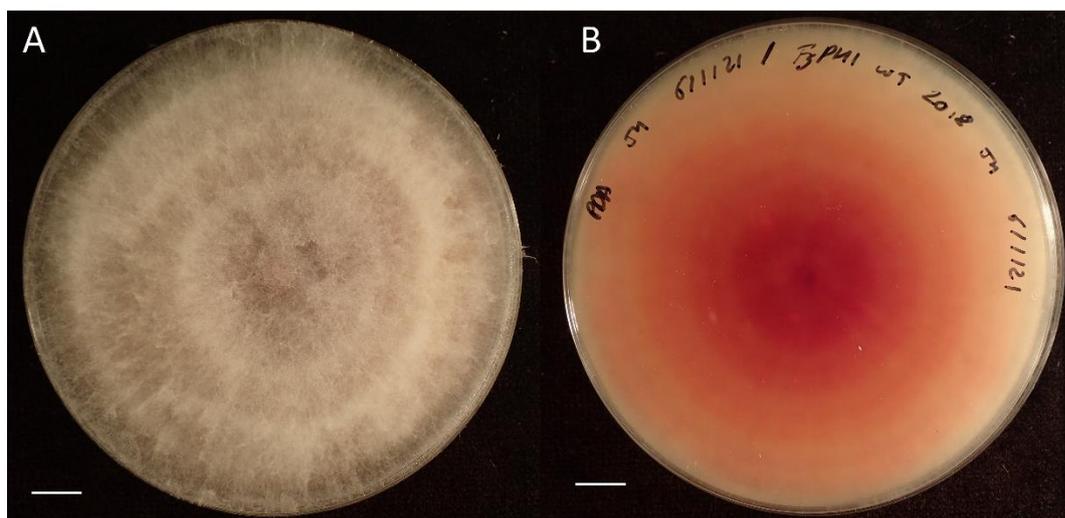
Figure 2.1. *F. graminearum* PH1 mycelial growth on PDA (6 dpa) from an agar plug. Both images (**A** and **B**) are the same Petri-dish viewed from the top (lid) (**A**) and the bottom (PDA base) (**B**). Scale bars = 1 cm.

2.2.3. Root Rot Assay

Aspects of the FRR assay were derived from (Peraldi et al., 2011, Goddard et al., 2014) and were modified for chemical amendment experiments. A sterile 9 cm^2 filter paper square (cut from Chromatography Paper 46 cm x 57 cm from Slaughter Ltd R & L) was placed on square plastic square Petri-dishes (10 x 10 cm) containing 50 ml autoclaved 0.8% agar (Fischer Science). Under sterile conditions, ten cold-stratified and germinated Bd3-1 seeds were placed on the filter paper. A minimum of 30 seedlings were used for each treatment. All plates were placed, angled at 70° from the horizontal to ensure uniform downward root growth, in covered plant propagators containing wetted paper towel to maintain high humidity (Supp. Fig. S1). Plant propagators with square Petri-dishes were incubated at 22°C (16h/8h light/dark photoperiod, variable humidity) in controlled environment cabinets (Snijders Labs MicroClima-series, Economic LUX chambers). After three days, the filter paper with seedlings attached was carefully transferred to different square Petri-dishes containing 0.8% agar amended with phytohormone or control solvent alone and returned to controlled environment growth cabinets. All compounds were ordered from Merck/Sigma-Aldrich UK unless otherwise stated. All non-water solvent concentrations in final treatment were at or below 0.1%. The same concentration of solvent was applied to respective control treatment 0.8% agar plates. Additionally the

compounds were applied to Bd3-1 roots in the absence of disease (Supp. Fig. S2) to make sure no visual browning occurred over time that might interfere with FRR measurements.

Table 2.1. Summary of each phytohormone exogenously applied for *B. distachyon* FRR assays.

Plant Hormone*	Working Concentration (µM)	Solvent**	References***
Salicylic acid	100	Ethanol (0.1%)	DS + (Kakei et al., 2015)
Jasmonic acid	1	Ethanol (0.1%)	DS + Dr Antoine Peraldi, unpublished
1-aminocyclopropane-1-carboxylic acid (ACC)	100	Water	DS + (Peraldi, 2012, Van de Poel & Van Der Straeten, 2014)
Auxin (Indole-3-acetic acid) sodium salt	10	Water	(Kakei et al., 2015)
Auxin (1-Naphthaleneacetic acid)	5	Ethanol (0.1%)	****
Cytokinins (*trans*-Zeatin)	10	DMSO (0.1%)	(Großkinsky et al., 2013, Kakei et al., 2015)
Cytokinin (Kinetin)	10	Water	****
Gibberellic acid (GA)	10	Water	DS + (Tanaka et al., 2006)
epiBrassinolide	0.1	Ethanol	DS + (Peraldi, 2012)
Prohexadione-calcium	100	Water	(Kakei et al., 2015)
Brassinazole	10	DMSO (0.02%)	(Nahar et al., 2012)
3-aminobutanoic acid (BABA)	9000	Water	DS + (Cohen, 2002, De Vleesschauwer et al., 2010)
4-aminobutanoic acid (GABA)	9000	Water	****

* All compounds were ordered from Sigma-Aldrich/Merck ** Final solvent concentration applied to 0.8% autoclaved agar in control plates (ELGA water). ***The source for the respective working concentrations were derived either from a publication, previous lab member notes, or a dilution series (DS) (Data not shown). **** The concentration for NAA, Kinetin and GABA was based on the concentrations used with IAA, *trans*-zeatin, and BABA respectively. A slightly lower concentration of NAA was chosen because of evidence that NAA is more stable than IAA and primarily passively diffuses into plant cells (Dunlap et al., 1986, Hošek et al., 2012).

Roots were inoculated six hours after transfer to hormone-amended medium (Fig. 2.2). Inoculum was prepared by blending mycelium and PDA from one-week old cultures (adding 1 ml water (sterile diH$_2$0) per PDA plate). Subsequently, approximately 0.1 ml to 0.2 ml of homogenized slurry was transferred with a 10 ml syringe (Terumo syringe without needle) onto the root tip. Inoculated plants were then incubated at 22°C (16h/8h light/dark photoperiod, variable humidity) in controlled growth cabinets (Snijders Labs MicroClima-series, Economic LUX chamber or a Snijders Scientific cabinet). The slurry was removed when necrosis was visible at the root tip, generally at 1-day post inoculation (dpi) (Fig. 2.2). Roots were photographed at intervals to monitor disease development. For repeated independent experiments with different measurement dates, the days were combined and denoted as 'Score Date' 1 to 3 with each measurement at 3-day intervals (Fig. 2.5B, Fig. 2.5C). Unless otherwise stated, all photographs were taken with either an Olympus C-750 Ultra Zoom Digital compact camera or an Olympus Stylus TG-4 camera.
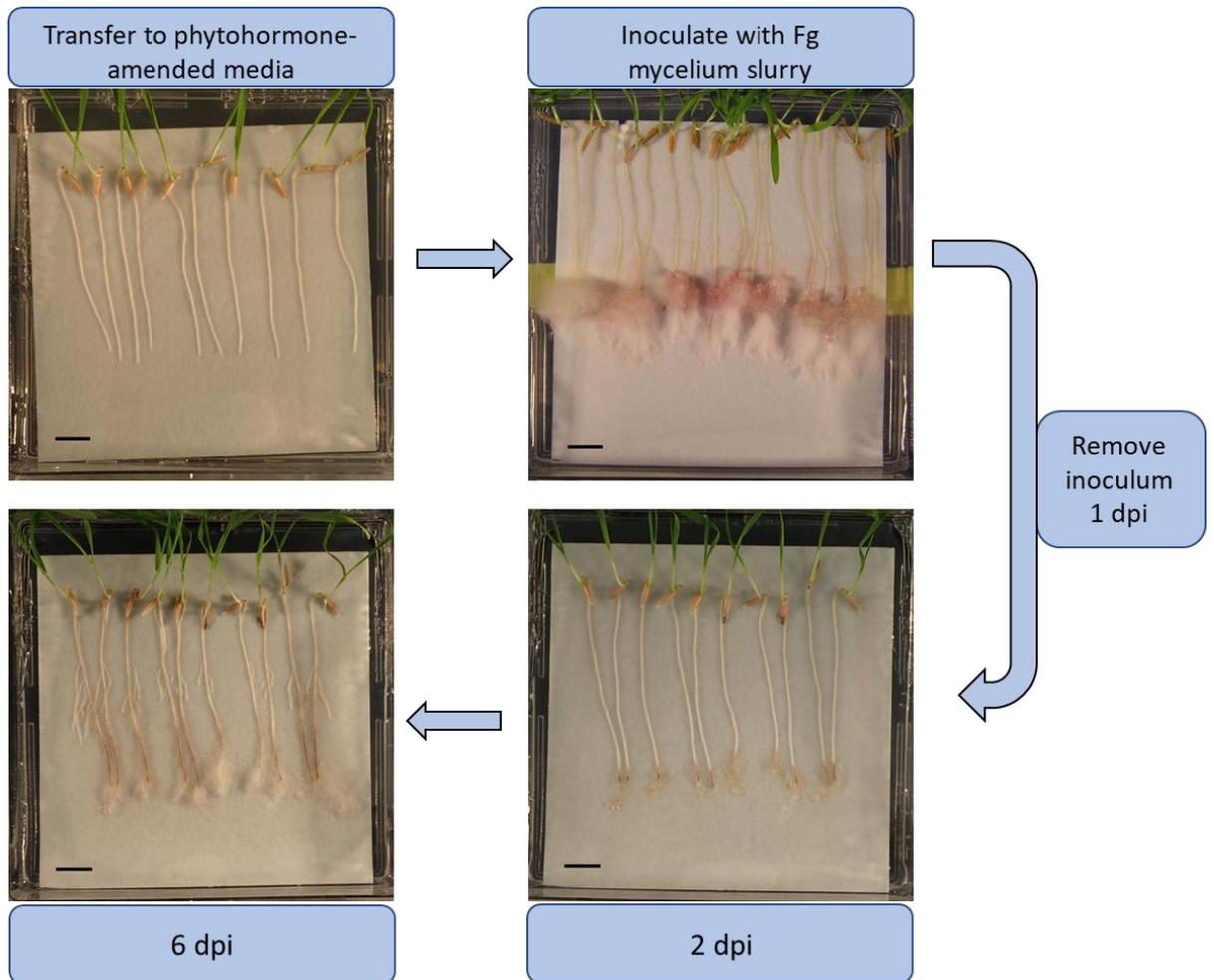
Figure 2.2. Fusarium root rot assay protocol summary. Pictures were taken from different experiments except for 2 dpi and 6 dpi pictures. The second step/mycelial slurry inoculum picture was taken at 3 dpi (three days after inoculation) and does not normally show aerial mycelia during application. Scale Bars = 1 cm.

2.2.4. Antimicrobial Activity against *F. graminearum*

Potential effects of phytohormones on fungal growth were assessed. PDA mycelial plugs (5 mm) of five- or seven-day old *F. graminearum* PH1 were transferred to 9 cm diameter Petri-dishes with 20 ml chemically amended PDA agar or to a control treatment with equal concentration of respective solvent (Table 2.2). Plates were stored at 22°C/22°C, 16 h/8 h (light/dark) (in controlled environment cabinets Snijders Labs MicroClima-series, Economic LUX chambers) and measured across two perpendicular diameters every day for three days.

Table 2.2. Summary of each phytohormone in amended PDA for *F. graminearum* antimicrobial test.

Plant Hormone	Working Concentration (μM)	Solvent
Indole-3-acetic acid	10	Water
3-aminobutanoic acid	10000	Water
trans-Zeatin	10	DMSO (0.1%)
Salicylic acid	100	Ethanol (0.1%)
Jasmonic acid	1	Ethanol (0.001%)
ACC	100	Water
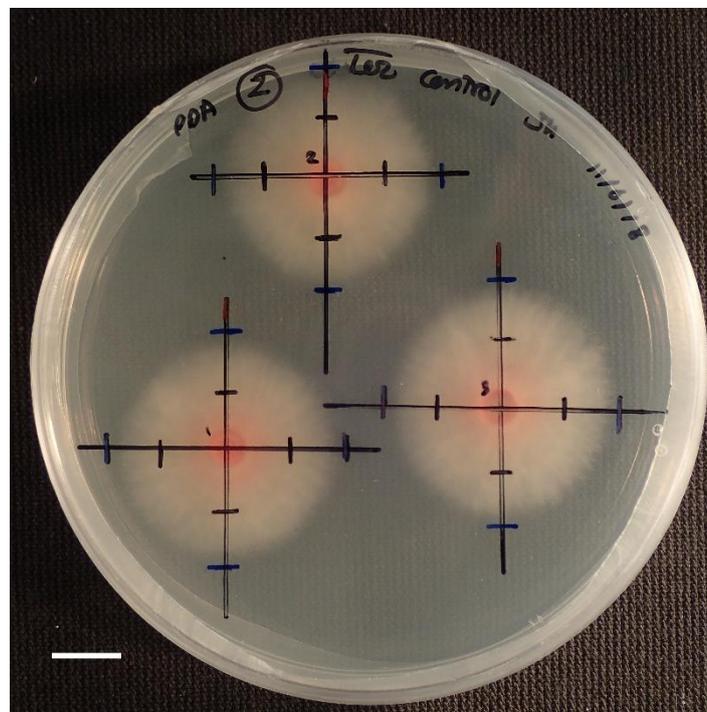
Figure 2.3. Two-day old *F. graminearum* PH1 mycelial plugs growing radially along the marked grid. Black marks on the grid represent 1 dpa, blue 2 dpa, and red is for orientation purposes. Scale bar = 1 cm.

2.2.5. Differential Gene Expression of Marker Genes

Bd3-1 leaves and floret tissue were harvested, flash frozen in liquid nitrogen, and DNA was extracted using a Qiagen DNeasy Plant Mini Kit. Once material was ground to a powder with a mortar and pestle with a small amount of acid-washed sand, 400 µl of Buffer AP1 and 4 µl RNaseA were pipetted into the material. The mixture was vortexed and incubated at 65°C for 10 min. Then 130 µl of P3 buffer was mixed the mixture was incubated for 5 min on ice and was subsequently centrifuged at 18,200 rcf. The lysate was centrifuged in a QIAshredder spin column for 2 min at 18,200 rcf. Then 400 µl of AW1 buffer was added to the supernatant (Approximately 200 µl) and mixed. The mixture was added to a DNeasy Mini spin column and was centrifuged at 5,900 rcf for 1 min twice while discarding the supernatant. In a new collection tube, 500 µl of AW2 buffer was then added and the mixture was centrifuged at 5,900 rcf for 1 min, subsequently discarding the flow-through. This step was repeated but at 18,200 rcf for 2 min. The Qiagen spin column was then placed in a 1.5 ml Eppendorf tube and the DNA was eluted with 50 µl or 100 µl buffer AE, incubated at room temperature for 5 min, and centrifuged at 5,900 rcf for 1 min. This step was repeated using the eluate from the previous step.

Primers (Supp. Table S11) were ordered from Merck/Sigma Aldrich UK. In order to test primer efficacy and annealing temperature, PCR was then carried out on a Gstorm PCR machine (Table 2.3 and Table 2.4). Quality of PCR amplicons was determined using gel electrophoresis with 1% agarose (Melford) in 1 x TAE buffer and 6 µl of ethidium bromide. Then 10 µl of PCR product was pipetted to each well with 100 bp DNA ladder in one lane. The electrophoresis power supply was set at 80 V to 100 V. The gel was visualised in a Bio-Rad Gel Imaging System.

Table 2.3. PCR reagents for primer quality assays.

Reagent	Concentration (µm)	Volume per well (µl)
Buffer 5x		3
MgCl$_2$	25	0.9
dNTPs	10000	0.3
TaqPol*		0.05
Primer F	10	1
Primer R	10	1
DNA template		3
dH$_2$O		5.75
Total		15

* TaqPol (Gotaq G2 Flexi DNA polymerase from Promega). Abbreviations: F (Forward), R (Reverse).

Table 2.4. The PCR thermo-cycling parameters for Bd3-1 DNA amplification.

Step	Temperature (°C)	Number of Cycles	Time (s)	Activity
1	94	1	300	Denaturation
2	94	35	35	Denaturation
3	58	35	35	Annealing
4	72	35	50	Extension
5	72	1	600	Extension
6	10	1	Indefinitely	Storage

Reference: Dr. Marianna Pasquariello, personal communication.

For RT-qPCR of FRR root tissues (Control and hormone treated roots with root rot), FRR roots of BABA or IAA at 6 dpi were cut at the top of the roots near the seed (Fig. 2.4), collected, and stored in 2 ml Eppendorfs in liquid nitrogen. Approximately 10 roots (all the roots in a square box (Fig. 2.2) were pooled into one biological sample (replicate). RNA samples were prepared using Qiagen RNeasy Mini Kit. Biological material was ground with liquid nitrogen with a small amount of acid-washed sand for approximately 1 ml of fungal material powder or approximately 200 µl plant material powder. Then 450 µl of Buffer RLT (for all plant material) or Buffer RLC (for all fungal material) was added to the frozen

samples and the tubes were vortexed. The lysate was then transferred to the QIAshredder spin column and was centrifuged for 2 min at 18,200 rcf. Approximately 400 µl of supernatant was transferred to new Eppendorf tubes. Afterwards, 200 µl of absolute ethanol was added to the lysate, mixed by pipetting, and the mixture was immediately transferring to an RNeasy mini spin column. The column was centrifuged for 15 seconds at 9,300 rcf and the flow-through was discarded. Then 700 µl of buffer RW1 was added to the spin column and centrifuged for 15 seconds at 9,300 rcf. The flow-through was discarded. Then 500 µl of buffer RPE was added to the spin column and centrifuged for 15 seconds at 9,300 rcf. The flow-through was discarded. Then 500 µl of buffer RPE was added to the spin column again and centrifuged for 2 min at 9,300 rcf. The RNeasy spin column was placed in a new collection tube and centrifuged at 18,200 rcf for 1 min to dry the column membrane. Finally, the RNeasy spin column was placed in a new Eppendorf tube, and 30 µl of RNase-free water was added directly to the spin column membrane. The samples were incubated for 1 to 4 min at room temperature and then centrifuged for 1 min at 9,300 rcf to elute the RNA. This last step was repeated using the eluate obtained from the first elution and RNA was quantified using a NanoDrop 2000 Spectrophotometer (Thermo Scientific).
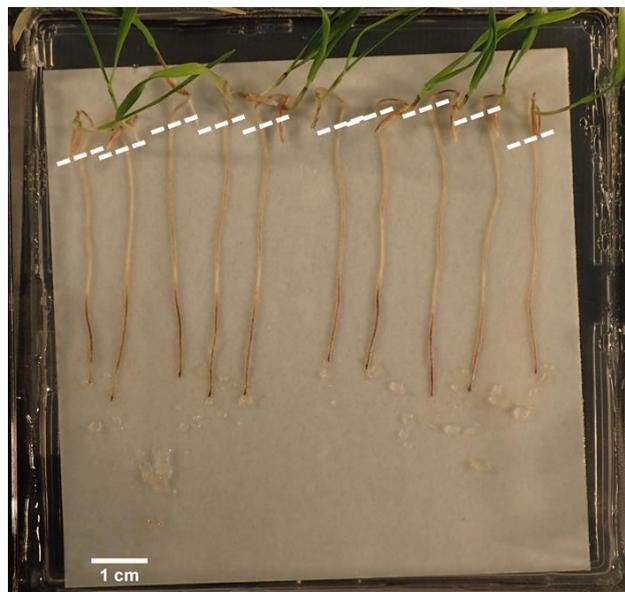
Figure 2.4. Root harvesting method for RT-qPCR. White dashed lines denote location where roots were cut. Plate is from BABA treated Bd3-1 FRR assay at 6 dpi.

DNA was eliminated using Turbo DNA-free kits (Invitrogen). Then 2 µl of Turbo DNAse buffer and 1.5 µl of Turbo DNAse was added to 20 µl RNA and mixed gently. The mixture was incubated at 37°C for 30 min (Thermo Scientific Heratherm incubator). Then another 1.5 µl of DNAse was added and the mixtures were incubated for another 30 min at 37°C.

Subsequently, 5 µl of DNAse inactivation buffer was added to the samples and samples were mixed well. The samples were then incubated at room temperature for 5 min while mixing a few times. Samples were then centrifuged at 10,000 g for 1.5 min and the RNA (Approximately 22 µl) was transferred to fresh Eppendorfs. RNA was quantified again using a NanoDrop 2000 Spectrophotometer (Thermo Scientific) and samples were stored at -70°C.

Once RNA was cleaned of DNA and re-quantified using a NanoDrop 2000 Spectrophotometer (Thermo Scientific), cDNA was prepared by first strand synthesis using Superscript 3 reverse transcriptase (Invitrogen). A mixture was prepared containing 3 µl of sample RNA, 1 µl of 50 µM oligoDt, 1 µl of 50 ng/µl random hexamers, 1 µl of 10 mM dNTPs and then DECP-treated water to a total of 10 µl. This mixture was incubated for 5 min at 65°C and kept on ice for at least 1 min. The cDNA synthesis mix was prepared in a different Eppendorf; In the indicated order, 2 µl of 10x buffer, 4 µl of 25 mM $MgCl_2$, 2 µl of 0.1 M DTT, 2 µl of 400U/µl RNase OUT, and 200U/µl of Superscript 3 was added. A total of 10 µl of cDNA synthesis mix was pipetted to each RNA/primer mixture and then the combination was incubated at room temperature for 10 min, followed by 50°C for 50 min. The reaction was terminated at 85°C for 5 min, and the mixture was then chilled on ice. Lastly, the mixture was centrifuged briefly and 1 µl of RNase H was added followed by a 20 min incubation at 37°C.

cDNA from each treatment was used for RT-qPCR reactions (Table 2.5 and Table 2.6). Samples were pipetted into a 96-well plate with a BioRAD microseal B adhesive sealer and centrifuged briefly. Standard curves were made for *B. distachyon* Actin housekeeping gene (Supp. Table S11) using a cDNA dilution series of 1/5, 1/10, 1/20, 1/50, 1/100. *Actin7* was primarily used over *GAPDH* (Supp. Table S11) because of smaller Cq (Quantitation cycle) standard deviation between the treatments.

Table 2.5. Reagent list for RT-qPCR.

Reagent	Concentration (µm)	µl/well
SYBR green*	2x	5
Primer F	10	0.6
Primer R	10	0.6
cDNA	**	2
H_2O		1.8
Total		10

*SYBR Green JumpStart Taq ReadyMix from Sigma-Aldrich. ** A 1/50 cDNA dilution from stock was experimentally determined. Abbreviations: F (Forward), R (Reverse).

Table 2.6. The PCR thermo-cycling parameters for Bd3-1 RT-qPCR gene expression analysis.

Step	Temperature (°C)	Number of cycles	Time (s)	Activity
1	95	1	240	Denaturation
2	94	39	10	Denaturation
3	60	39	10	Annealing
4	72	39	30	Extension/Picture
5	72	1	600	Extension
6	65-95		5	Meltcurve capture

Carried out on a CFX96 TouchTM Real-Time PCR detection system (BioRad) using the Scan mode SYBR/FAM only.

Once Cq values were obtained for target genes and the housekeeping gene *Actin7* from BioRad CFX Manager Software V3.1, the log-fold change in expression was then calculated (Equation 2.1). The primer efficiency (Equation 2.1) for each primer pair, unless otherwise stated, was experimentally determined in a dilution series experiment using the same PCR protocol (Table 2.5 and Table 2.6). The standard curve for the housekeeping genes was automatically calculated from this by the BioRad CFX Manager Software V3.1 with the

output results. A minimum primer efficiency of 1.8 was used however in one case the efficiency was slightly under 1.8.

Equation 2.1. Calculation for log-fold change in expression for target gene from Cq values between two treatments using a housekeeping gene as a reference. Cq (Quantitation cycle), GOI (Gene of Interest), HK (Housekeeping gene). Primer efficiency calculated from standard curve with primers. Equation from (Dr Marianna Pasquariello, personal communication).

$$\Delta\,\text{Cq} = (\text{GOI Cq} \; - \; \text{HK gene Cq})$$
$$\Delta\Delta\,\text{Cq} = (\text{Hormone Treatment}\,\Delta\,\text{Cq} - \text{Control Treatment}\,\Delta\,\text{Cq})$$
$$\text{Log2fold change} = \; \text{Log2}(\text{Primer Efficiency}^{\wedge}\Delta\Delta\,\text{Cq})$$

2.2.6. Software, Data Processing, and Statistics

Microsoft office (Excel, Word, and Powerpoint) 2016 was used for writing, data collection, images, and analysis. EndNote X8/X9 was used throughout the thesis as the reference manager. All graphs were prepared using Graphpad Prism (V5.04). ImageJ was used for measuring root necrosis length and preparing scale bars for photographs (1 pixel/aspect ratio) (Abràmoff et al., 2004). All FRR data statistics were performed on GENSTAT v.19.1.0.21390 (VSN international Ltd). A generalised linear model (GLM) with normal distribution and identity link function parameters was used to analyse each FRR experiment (Supp. Table S2). Time points were analysed separately. The model 'Experiment + Treatment / Replicate' against the response variate data was used for all assays ("Replicate" denotes each square Petri-dish per treatment (Fig. 2.2)). After model checking for normal distribution and equal variance, data was either kept normal or transformed before recording ANOVA results (Supp. Table S2). A few ANOVA's for combined independent experiments showed a significant interaction between the independent experiment and the hormone treatment ($p < 0.05$) at specific time points (Supp. Table S2). However for all the remaining time points, no such interaction was observed ($p > 0.05$) and as such the interaction factors (aside from "Treatment / Replicate") were excluded from the GLM ANOVA test. The qRT-PCR gene expression data (Fig. 2.16) was analysed on Microsoft Excel using a standard student t.test.

2.3. Results

2.3.1. The Effect of Phytohormones on Fusarium Root Rot

Salicylic acid (SA) increased root necrosis length (RNL) symptoms at all time points (Fig. 2.5A, $p < 0.01$). In contrast, JA application resulted in a significant decrease in RNL at every time point (Fig. 2.5B, $p < 0.01$). Like JA, the plant precursor to ethylene (ACC) also decreased RNL at all time points (Fig. 2.5C, $p < 0.01$) however the effect was less pronounced at second score date. Interestingly, the difference in RNL for all three compounds at each time point remained similar with the regression lines remaining parallel rather than diverging over time. The classic defence hormones had significant effects on FRR resistance however the direction of effect depended on the particular phytohormone.
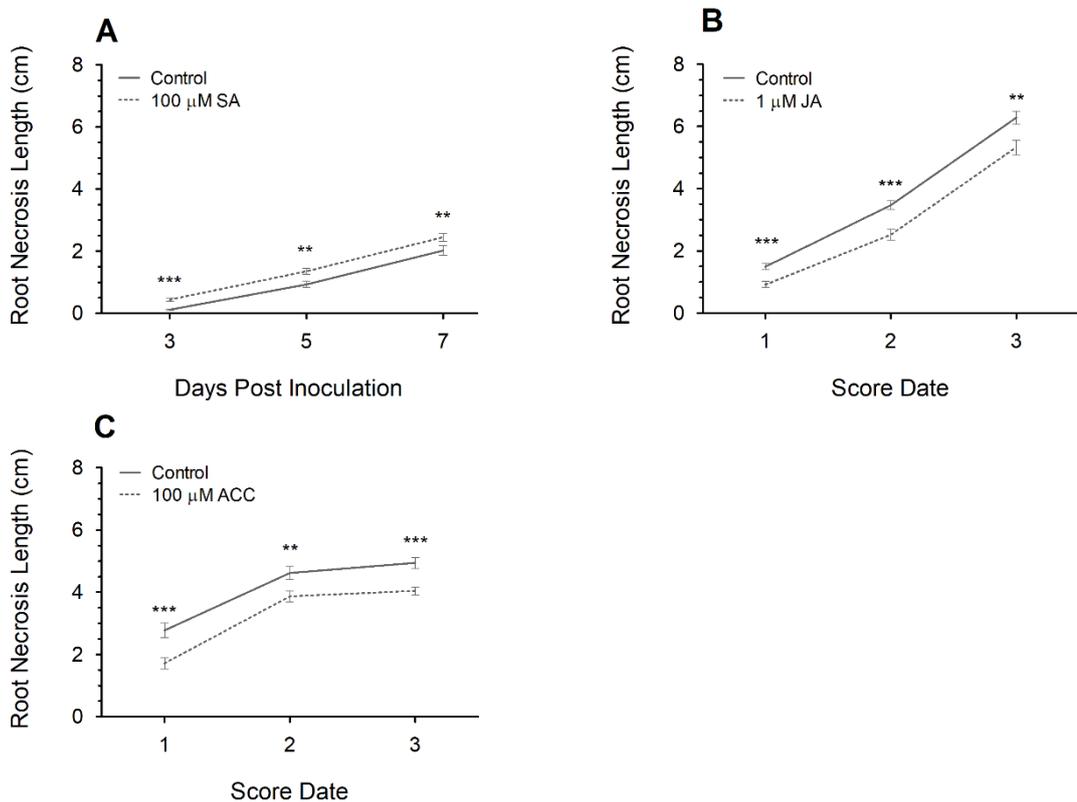
Figure 2.5. The change in *F. graminearum*-induced FRR necrosis after application of 100 μM SA (**A**), 1 μM JA (**B**), 100 μM ACC (**C**) on Bd3-1 seedling roots. Each data point is the mean RNL ± SE from two independent experiments, except score date 3 from **C** which was from one independent experiment. Score Date numbers (3-day intervals between each number) for **B** and **C** are the combined dpi from different experiments. Significance levels: ** $p < 0.01$, *** $p < 0.001$ compared to control. Taken and modified from (Haidoulis & Nicholson, 2020).

There was no significant effect of gibberellic acid (GA) on RNL at any time point (Fig. 2.6A, $p < 0.05$). According to (Kakei et al., 2015), endogenous GA levels are likely to be saturated in *B. distachyon* and thus might not respond to exogenous hormone application. Therefore, GA-deficient conditions were generated by application of the GA biosynthesis inhibitor prohexadione (Phx) (Nahar et al., 2012, Kakei et al., 2015). Exogenous application of Phx had no significant effect at 2 dpi ($p = 0.294$). However RNL symptoms increased at 4 dpi (Fig. 2.6B; $p < 0.01$) and continued to do so with the greatest effect on RNL observed at 6 dpi ($p < 0.001$). This suggests that inhibition of GA biosynthesis increased FRR susceptibility with the effect becoming more pronounced at later time points.
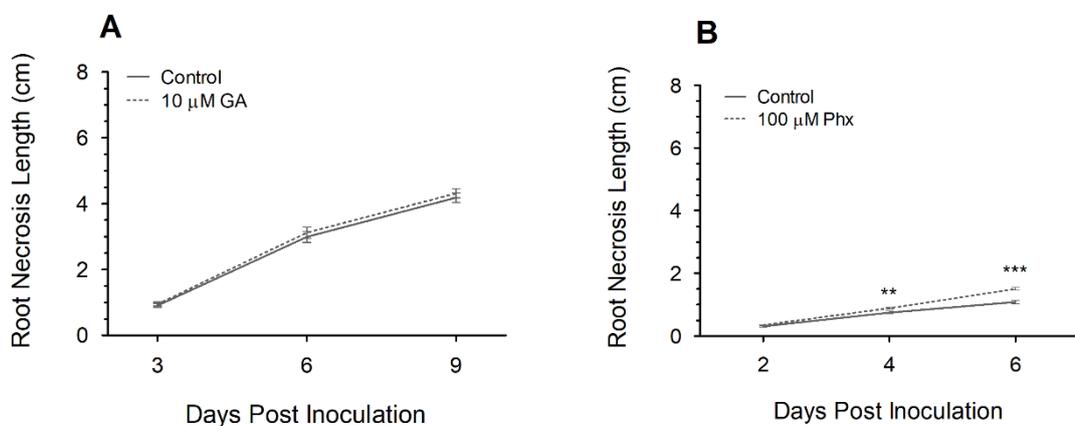
Figure 2.6. The change in *F. graminearum*-induced FRR necrosis after application of GA (**A**) and Phx (**B**) on Bd3-1 seedling roots. Each data point is the mean RNL ± SE from one (**A**) or two (**B**) independent experiments. Significance levels: ** $p < 0.01$, *** $p < 0.001$ compared to control. (**A**) Taken and modified from (Haidoulis & Nicholson, 2020).

There was no significant effect of epibrassinolide (eBL) on RNL at any time point (Fig. 2.7A, $p < 0.05$). Similar to GA, eBL levels are also likely saturated in *B. distachyon* (Kakei et al., 2015), therefore BR-deficient conditions were generated by exogenous treatment with the biosynthesis inhibitor Brassinazole (Brz) (Asami et al., 2000). Like Phx, there was no significant effect on RNL at 2 dpi ($p < 0.05$) (Fig. 2.7B). However RNL was reduced by Brz application relative to the control at 4 dpi ($p < 0.01$) and the effect continued to intensify with the most pronounced effect observed at 6 dpi ($p < 0.001$). This suggests that inhibition of BR biosynthesis improved resistance to FRR at later time-points.
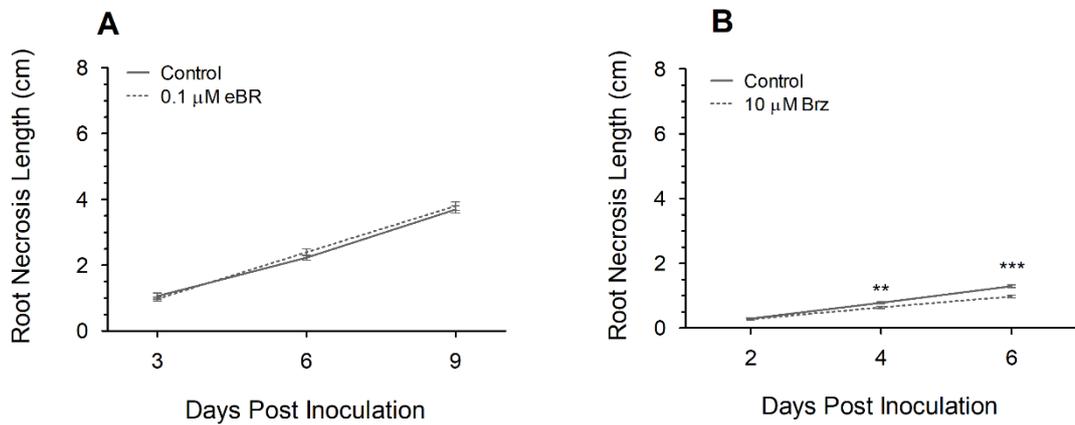
Figure 2.7. The change in *F. graminearum*-induced FRR necrosis after application of eBR (**A**) and Brz (**B**) on Bd3-1 FRR progression. Each data point is the mean RNL ± SE from one (**A**) or two (**B**) independent experiments. Significance levels: ** $p < 0.01$, *** $p < 0.001$ compared to control. **A** Taken and modified from (Haidoulis & Nicholson, 2020).

IAA-amended media had the most pronounced effect on RNL compared to all other phytohormones at all time points since RNL symptoms were reduced by half compared to the control treatment at all time points (Fig. 2.8A p<0.001 and Fig. 2.9). Like IAA, the synthetic auxin NAA also significantly reduced RNL at all time points (Fig. 2.8B; p<0.001) but auxin-induced FRR resistance was most pronounced with IAA. With both auxins, the increased resistance was observed as early as 2 dpi yet the regression lines diverged over time with a greater reduction in RNL at later time points (Fig. 2.8 and Fig. 2.9). Auxins produced a very positive effect on FRR resistance.
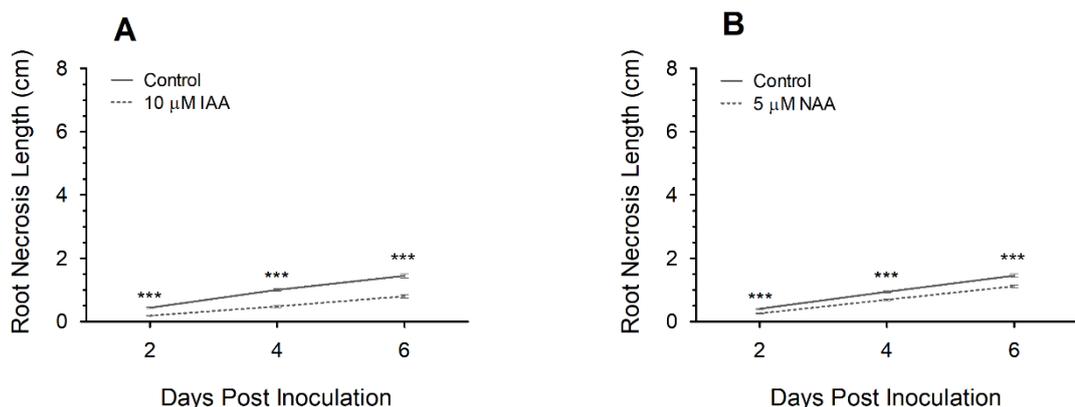
Figure 2.8. The change in *F. graminearum*-induced FRR necrosis after application of 10 µM IAA (**A**) 5 µM NAA (**B**) on Bd3-1 roots. Each data point is the mean RNL ± SE from two independent experiments. Significance level ** $p < 0.01$, *** $p < 0.001$ compared to control. Taken and modified from (Haidoulis & Nicholson, 2020).
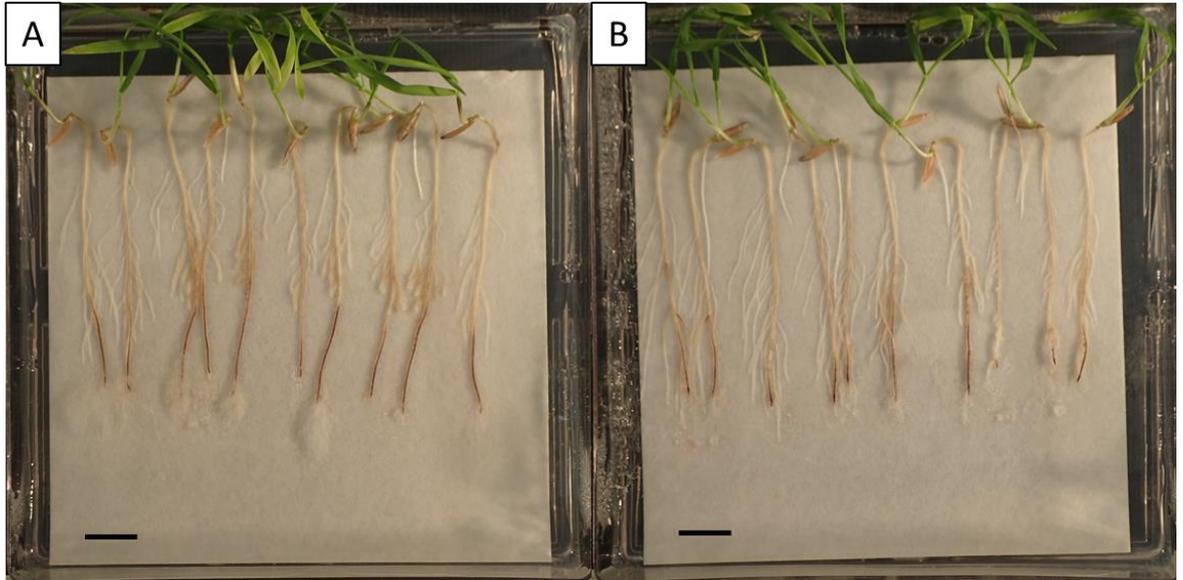
Figure 2.9. The decrease in RNL after IAA (Indole-3-acetic acid) application (**B**) compared to the control (**A**) at 6 dpi. Scale bars = 1 cm. Taken from (Haidoulis & Nicholson, 2020).

The cytokinin *trans*-Zeatin (tZ) induced the most severe FRR symptoms compared almost all other phytohormones (Fig. 2.10A). The difference in RNL between the control and treated roots increased from a relatively small but significant difference at 2 dpi (p < 0.001) followed by a dramatic increase in RNL by 4 dpi (p < 0.001). The extent of necrosis was twice that in the control by 6 dpi (Fig. 2.10A p<0.001; Fig. 2.11). Like *trans*-Zeatin, the cytokinin kinetin also showed a pronounced increase in RNL like tZ (Fig. 2.10B). Kinetin exhibited no significant effect on symptoms at 2 dpi (p = 0.785) but increased the rate of RNL so that the differential increased over time (Fig. 12B, 4 dpi and 6 dpi p < 0.01, p < 0.001 respectively). Like auxins, the cytokinin-induced RNL difference increased over time from 2 dpi to the largest effect at 6 dpi. Overall cytokinin amendment appeared to have a very negative effect on FRR resistance which became more pronounced as the disease progressed
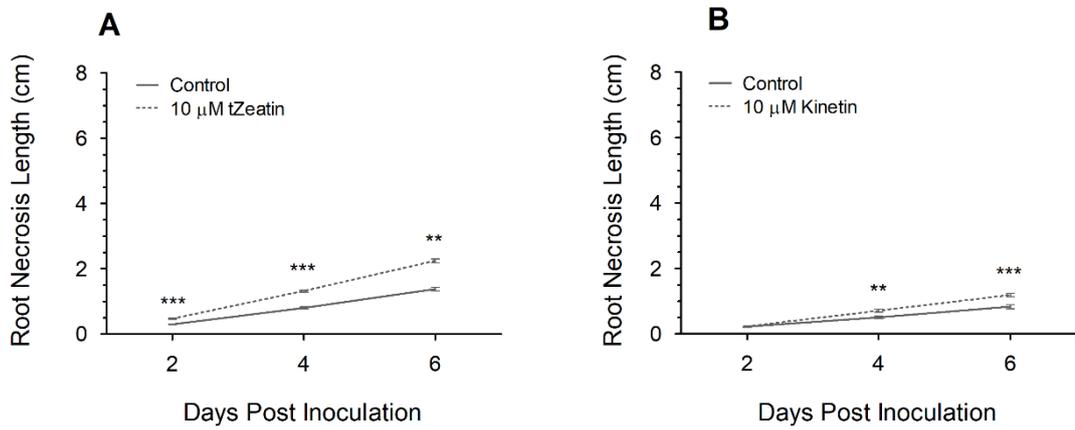
Figure 2.10. The change in *F. graminearum*-induced FRR necrosis after application of 10 µM *trans*-Zeatin (**A**) and 10 µM Kinetin (**B**) on Bd3-1 seedling roots. Each data point is the average RNL ± SE from three (**A**) or one (**B**) independent experiments. Significance levels: ** $p < 0.01$, *** $p < 0.001$ compared to control. Taken and modified from (Haidoulis & Nicholson, 2020).
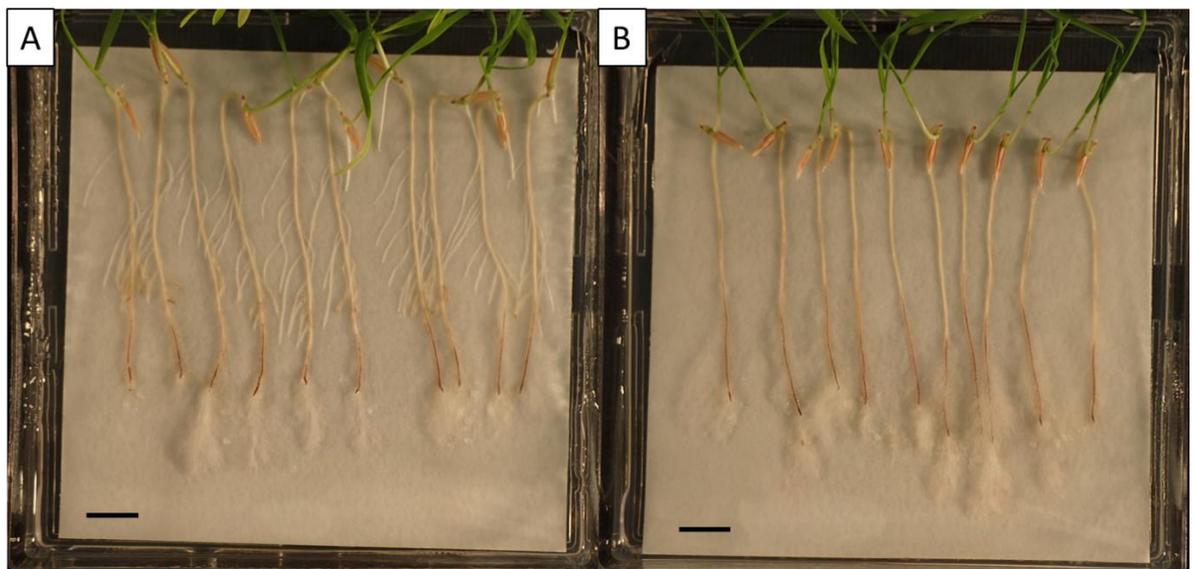
Figure 2.11. The increase in RNL after *trans*-Zeatin application (**B**) compared to the DMSO control (**A**) at 6 dpi. Scale bars = 1 cm. Taken from (Haidoulis & Nicholson, 2020).

The compound BABA had one of the greatest effects in increasing RNL compared to other defence-related hormones (Fig. 2.12A, Fig. 2.13). The differential RNL symptoms resulting from pre-application of BABA increased over time with the least significant effect on RNL at 2 dpi ($p < 0.05$) but similar to cytokinins there was near doubling of necrosis at 4 dpi and 6 dpi ($p < 0.001$) relative to the control. On the other hand, GABA had no significant effect on RNL at any time point (Fig. 2.12B, $p > 0.05$).
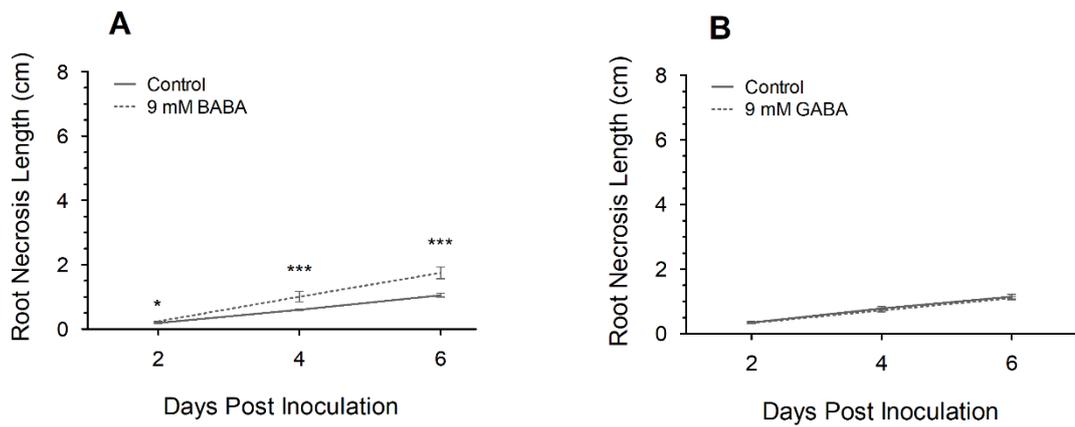
Figure 2.12. The change in *F. graminearum*-induced FRR necrosis after application 9 mM BABA (**A**) and 9 mM GABA (**B**) on Bd3-1 seedling roots. Each data point is the average RNL ± SE from three (**A**) or two (**B**) independent experiments. Significance levels: * $p < 0.05$, ** $p < 0.01$, *** $p < 0.001$ compared to control. (**A**) Taken and modified from (Haidoulis & Nicholson, 2020).
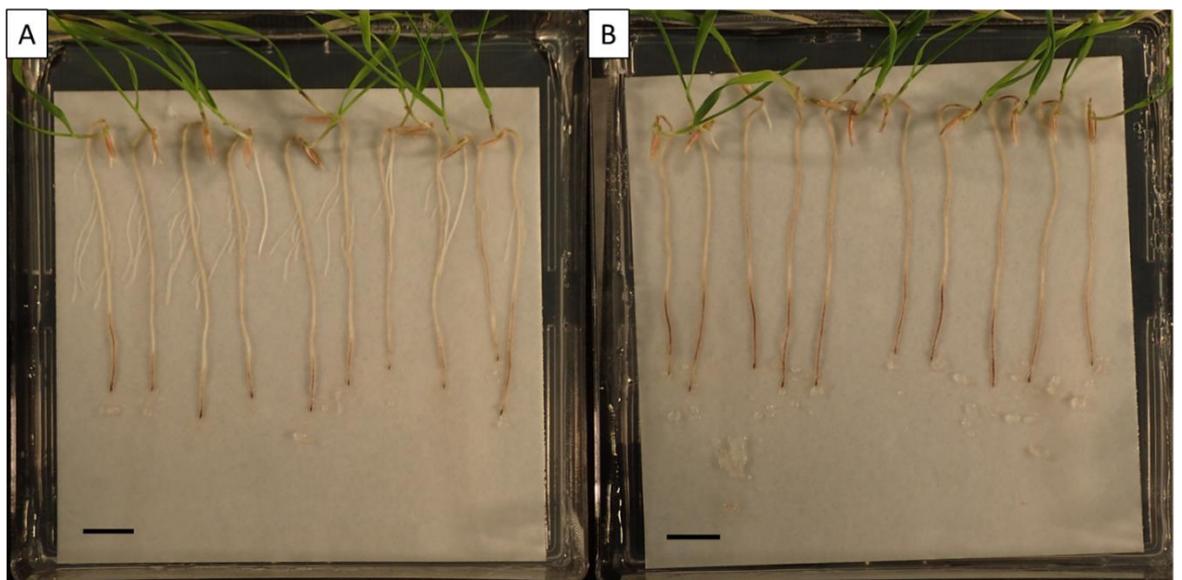
Figure 2.13. The increase in RNL after BABA treatment (**B**) compared to the water control (**A**) at 6 dpi. Scale Bars = 1 cm.

The phytohormone ABA was also tested on FRR response however it induced extensive root discoloration which was indistinguishable from FRR symptoms and so prevented assessment (Fig. 2.14).

Figure 2.14. The effect of 10 µM abscisic acid on 7-day old Bd3-1 roots (after stratification) in the absence of *F. graminearum* treatment. Scale Bar = 1 cm. Taken from (Haidoulis & Nicholson, 2020).

A summary of the effects that each phytohormone has on FRR resistance is summarised in Table 2.7.

Table 2.7. Summary of all FRR assay results.

Phytohormone	Compound	Overall Effect on FRR Resistance*	Effect on FRR Progression**
SA	SA	—	Parallel
JA	JA	+	Parallel
Ethylene	ACC	+	Parallel
Auxin	IAA	+	Divergent
Auxin	NAA	+	Divergent
Cytokinin	*trans*-Zeatin	—	Divergent
Cytokinin	Kinetin	—	Divergent
GA	GA	N	
GA inhibitor	Prohexadione	—	Divergent
BR	Epibrassinolide	N	
BR inhibitor	Brassinazole	+	Divergent
Aminobutanoic acid	BABA	—	Divergent
Aminobutanoic acid	GABA	N	

* Symbols for generalised effects: '—' denotes a negative effect, '+' denotes a positive effect, and 'N' denotes no effect on resistance. ** See section 2.4.4. for explanation on the two different groups. Abbreviations: ACC (1-aminocyclopropane-1-carboxylic acid), BABA (3-aminobutanoic acid), BR (Brassinosteroid), GA (Gibberellic acid), GABA (4-aminobutanoic acid), IAA (Indole-3-aceticacid), JA (Jasmonic acid), NAA (1-Naphthaleneacetic acid), SA (Salicylic acid).

2.3.2. The Effect of Phytohormones on *F. graminearum* Growth

To ascertain whether the effects of phytohormones on FRR reflected an altered plant response or an effect on the fungus itself, hormones at the same concentrations as used in the experiments (Section 2.3.1) were applied to *F. graminearum* growth medium to detect any changes in growth over time. Compared to the respective control treatments there was no significant effect on *F. graminearum* growth by any of the tested phytohormones (Fig. 2.15).
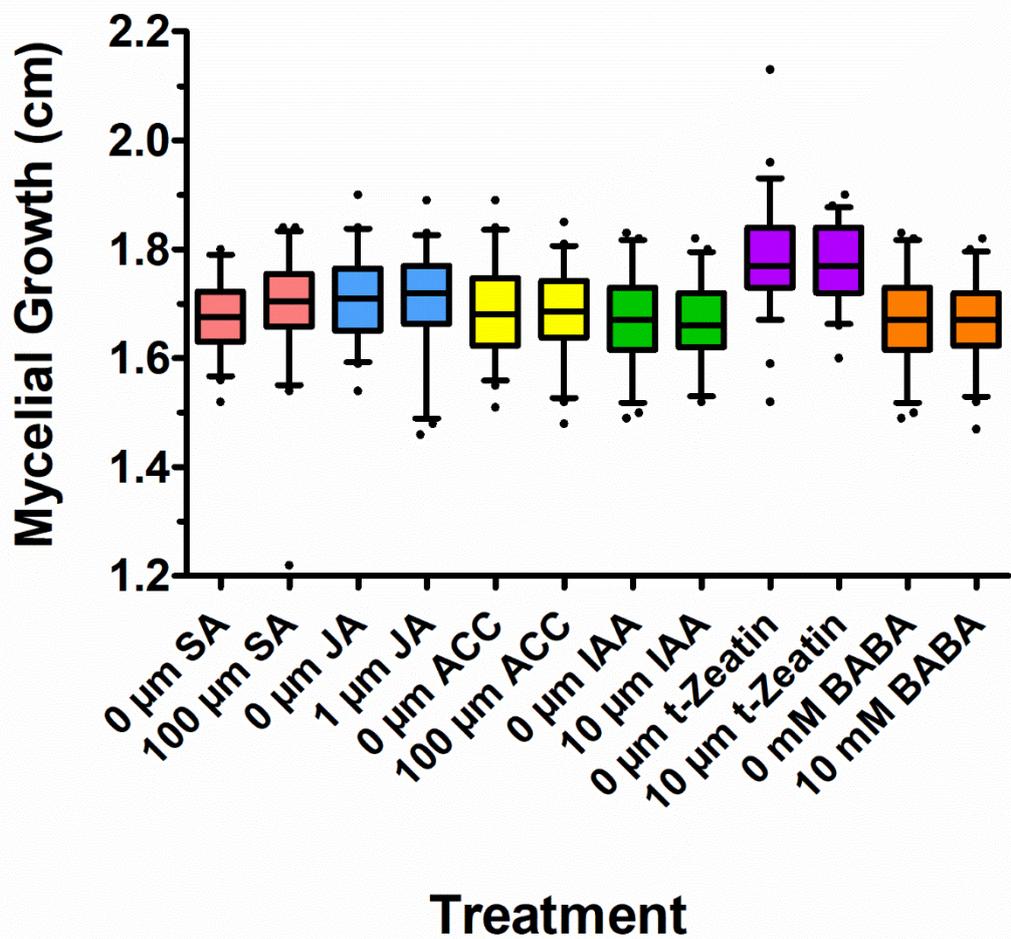
Figure 2.15. The growth (measured as radius from mycelial epicentre) of *F. graminearum* on hormone-amended PDA at 2 dpa. Each data point is the average of approximately 46 measurements from 12 biological replicates (4 measurements per biological replicate) ± SE. A 95th percentile whisker end cap was used for all treatments. GLM-ANOVA comparing compound to respective control; $p = 0.247$ (SA), $p = 0.364$ (JA), $p = 0.918$ (ACC), $p = 0.568$ (IAA), $p = 0.729$ (BABA), $p = 0.475$ (tZ). Abbreviations; SA (Salicylic acid), JA (Jasmonic acid), ACC (1-aminocyclopropane-1-carboxylic acid), and BABA (β-aminobutyric acid), t-Zeatin (*trans*-zeatin). Taken from (Haidoulis & Nicholson, 2020).

2.3.4. The Induction of Hormone and Defence Related Genes in Response to Exogenous Hormone Treatment during FRR

In order to determine the potential mechanism involved in the large effects of IAA and BABA on FRR, the expression of a panel of hormone and defence – related genes were analysed in response to treatments with IAA and BABA. Using two SA and JA related biosynthesis and signalling marker genes, I could also identify whether the effect on FRR was due to an indirect activation of JA or SA pathways. No marker gene was significantly expressed or repressed in response to IAA at 6 dpi (Fig. 2.16A $p < 0.05$). However according to Fig. 2.16B, BABA caused a significant 4-fold downregulation of the SA-related *MES1* (*Methyl Salicylate Esterase 1*) gene at 6 dpi ($p = 0.005$). On the other hand, expression of the JA-related biosynthetic gene *12-oxophytodienoate reductase 3* (*OPR3*) was significantly upregulated at 6 dpi by approximately 0.8-fold change ($p < 0.05$). However when the housekeeping gene *GAPDH* was used for comparison, there was no significant difference for *OPR3* ($p = 0.199$, data not shown). No other gene tested was significantly expressed or repressed in response to BABA ($p < 0.05$).
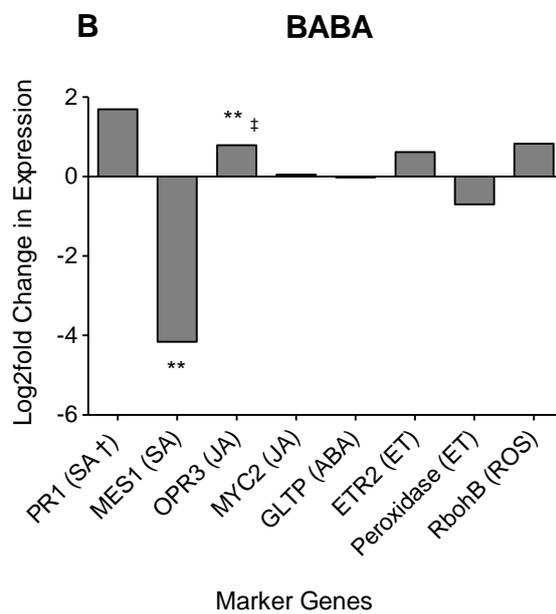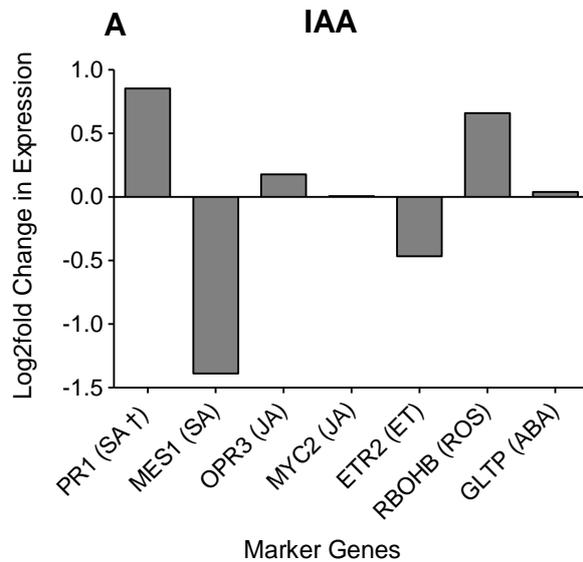
Figure 2.16. Change in expression of hormone-related or general defence-related marker genes in response to IAA (**A**) or BABA (**B**) 6 days after inoculation with *F. graminearum*. In all instances, expression shown is relative to that in control treated roots (0-Log fold change). Gene expression was normalised with *Actin7*. Each bar is the average of two biological replicates (with three technical replicates for each), and each are from independent experiments. (**B**) Markers *MES1*, *MYC2*, peroxidase, and *RBOHB* are from a different PCR experiment than the other markers and were compared to a different *Actin7* housekeeping reading. Student t-test significance level for Cq values: ** $p < 0.01$. Compared to respective solvent control: (**A**) p = 0.307 (*PR1*), p = 0.166 (*MES1*), p = 0.521 (*OPR3*), p = 0.993 (*MYC2*), p = 0.409 (*ETR2*), p = 0.443 (*RBOHB*), p = 0.699 (*GLTP*). (**B**) p = 0.209 (*PR1*), p = 0.005 (*MES1*), p = 0.009 (*OPR3*), p = 0.988 (*MYC2*), p = 0.956 (*GLTP*), p = 0.181 (*ETR2*), p = 0.661 (Peroxidase), p = 0.236 (*RBOHB*). Primers used are described in (Supp. Table S11). All genes (Except *RbohB*) were responsive to respective phytohormones (Kakei et al., 2015). Abbreviations in (Supp. Table S11). † Originally believed to be SA responsive but is JA responsive in *B. distachyon* (Kouzai et al., 2016). ‡ No significance (p > 0.05) compared to *GAPDH*. Gene expression for *PR1*, *OPR3*, *GLTP*, *ETR2* in BABA treatment (**B**) was also normalised with *GAPDH* (data not shown).

2.4. Discussion

2.4.1. The Classic Defence Hormones Suggest a Necrotrophic-Focussed Lifestyle of *F. graminearum* in Bd3-1 Roots.

The data shows that almost all phytohormones have significant effects on FRR resistance at concentrations used herein. There have been no reports on exogenous phytohormone-induced changes to *F. graminearum* FRR resistance published previously. SA was found to promote susceptibility to FRR (Fig. 2.5A). This contrasts with evidence from (Makandar et al., 2011, Qi et al., 2012, Sorahinobar et al., 2016) where SA promoted resistance to *F. graminearum* in *A. thaliana* and wheat. Additionally this contrasts with evidence suggesting a role of SA in resistance to *F. oxysporum* in *Arabidopsis thaliana* and *Solanum lycopersicum* (Mandal et al., 2009, Trusov et al., 2009). These apparent contradictions may be due to differences in application time, the tissue and disease assessed, or the organism used (Mandal et al., 2009, Trusov et al., 2009, Makandar et al., 2011, Sorahinobar et al., 2016). For example, in the studies of Makandar and colleagues (2011) and Sorahinobar and colleagues (2016), root tissue was treated with SA prior to infection but symptoms were assessed on shoot tissue rather than root tissue (Makandar et al., 2011, Sorahinobar et al., 2016). The effectiveness on resistance caused by phytohormones may differ between tissues. Furthermore, making inferences based upon shoot symptoms following root treatments may be confounding due to the effects of systemic acquired resistance (SAR) and induced systemic resistance (ISR) (Park et al., 2007, Liu et al., 2011, Dempsey & Klessig, 2012, Pieterse et al., 2014). Contrary to SA, the positive effect of JA on FRR resistance (Fig. 2.5B) supports other studies that investigated the effect of JA on FHB (Li & Yen, 2008, Qi et al., 2016, Sun et al., 2016). Makandar and colleagues (2010) have found that JA can promote susceptibility to *F. graminearum* in A*. thaliana* leaves if applied during or shortly after inoculation but promotes resistance if applied at least a day after inoculation (Makandar et al., 2010). Exogenous application of Methyl jasmonate (MeJA) to *A. thaliana* seedling roots also elevated Fusarium wilt susceptibility to *F. oxysporum* (Trusov et al., 2009). Together this suggests that the effects on JA are dependent on one or more factors like timing of application or the fungal pathogen used.

Like JA, ACC also increased resistance to FRR (Fig. 2.5C). ACC is a precursor to ethylene and the data (Fig. 2.5B and Fig. 2.5C) supports the reported synergism of ethylene with JA in *Arabidopsis* (Bari & Jones, 2009, Pieterse et al., 2012). Furthermore the results are consistent with the evidence that JA and ET signalling is antagonistic to SA signalling (Spoel & Dong, 2008, Pieterse et al., 2012). The results of ACC on FRR support numerous studies that also investigated the effect of ethylene on FHB (Li & Yen, 2008, Sun et al., 2016, Foroud et al., 2018). However contrary to the results here, exogenously applied ACC has been shown to increase *F. culmorum*-induced FRR symptoms in *B. distachyon* (Cass et al., 2015). Though a different *B. distachyon* line was used, and the concentration of ACC was at least 5-fold higher which may suggest there is a concentration-dependent effect of ACC on FRR resistance. Furthermore the data in the present study also contradicts (Chen et al., 2009) who found that ethylene promoted susceptibility to FHB and leaf colonisation in wheat and *A. thaliana*, and Trusov and colleagues (2009) who found that exogenous application of ACC on *A. thaliana* seedling roots increased Fusarium wilt symptoms caused by *F. oxysporum* (Trusov et al., 2009). van Loon and colleagues (2006) described how the effect of ethylene on plant resistance to pathogens is sensitive to numerous factors including type of pathogen, timing of application and importantly the tissue type (van Loon et al., 2006a). Additionally, many of these previous studies utilised ethephon to exogenously apply ethylene as opposed to exogenous application of ACC which was performed here. However evidence shows that ACC and ethephon induced similar effects on FHB in most wheat varieties (Foroud et al., 2018). The effects of these three defence phytohormones on FRR resistance are unlikely to be due to antimicrobial effects on *F. graminearum* mycelial growth (Fig. 2.15) but rather likely due to the influence of hormones on host root hormone signalling and defence responses.

The differences observed between the FRR studies undertaken by me and those of studies on FHB and leaf infection may be because of a unique FRR response. *F. graminearum*-induced FRR is not very well characterised but evidence suggests that *F. graminearum* progresses in a unique manner in root tissues (Wang et al., 2015b). The SA pathway is generally considered to promote resistance to biotrophic pathogens and susceptibility to necrotrophic pathogens whereas JA and ethylene pathways generally promote resistance to necrotrophic pathogens and susceptibility to biotrophic pathogens (Glazebrook, 2005, Bari & Jones, 2009, Pieterse et al., 2012). Phytohormones were applied shortly before inoculation thus their effect on resistance should have begun and continued

(from continuous phytohormone exposure) during the early stages of infection where the reported biotrophic stage would be expected to occur. The increase in resistance due to JA and ACC application (Fig. 2.5B and Fig. 2.5C) suggests that *F. graminearum* is acting primarily as a necrotroph or has a much shorter biotrophic phase in Bd3-1 roots compared to its reported hemibiotrophic life-style in floral tissues (Brown et al., 2010). This view is compatible with the negative effect of SA application on resistance of root tissues (Fig. 2.5A). Differences in trophic state on host tissues been observed for other plant pathogens. Marcel and colleagues (2010) found that *M. oryzae* behaves as a biotroph during rice (*Oryza sativa*) root infection despite adopting a hemibiotrophic lifestyle on leaves (Marcel et al., 2010). Wang and colleagues (2015) found that wheat Sumai3 roots were susceptible to FRR despite this variety being known for its potent FHB resistance (Wang et al., 2015b). Furthermore, Lyons and colleagues (2015) identified differing gene expression patterns between root and leaf infection following *Fusarium oxysporum* (Lyons et al., 2015). These examples suggest a unique tissue-specific defence mechanism might be occurring in roots, in turn, which promotes a different trophic lifestyle in *Fusarium* when infecting these tissues. Hypothetical reasons for switching to necrotrophy may be due to a demand for a change in the resource acquisition method, the time required to overcome defences, or a change in plant defence response (Kabbage et al., 2015, Zeilinger et al., 2016). One or more of these factors may be causing this difference in fungal lifestyle between roots and shoots in the *B. distachyon - F. graminearum* pathosystem. For example the speed at which FRR progress may be the cause as FRR resistance was characterised by time required to penetrate the root cortex (Wang et al., 2015b) rather than the numerous types of resistances present in FHB (Table 1.1). The observation of rapid progression of *F. graminearum* in wheat roots (Wang et al., 2015b) was also observed with *B. distachyon* as half the root was necrotic by 6 dpi. To understand this difference in resistance between tissues, a combination of host and pathogen -omic responses to early infection root infection are necessary.

2.4.2. Auxins and Cytokinins Induced the Most Substantial Effect on FRR Resistance.

The development-associated hormones induced the most significant effect on FRR resistance compared to the classic defence hormones. Both IAA and NAA increased resistance to FRR. The greater effectiveness of IAA over NAA is probably because twice the

concentration of IAA was used (Fig. 2.8A and Fig. 2.8B). The positive effects of auxins has also been reported for *F. culmorum*-induced FHB in barley (Petti et al., 2012) and to *F. oxysporum*- induced FRR in tomato roots after application of a soil drench (Sharaf & Farrag, 2004). A low concentration of IAA of 0.01 µM was also found to reduce FRR symptoms caused by *Fusarium solani* in cotton (*Gossypium hirsutum*) (Egamberdieva et al., 2015). It is possible that IAA is having a detrimental effect on *F. graminearum* growth as was shown by (Luo et al., 2016). However, I did not observe an antimicrobial effect of auxin on *F. graminearum* mycelial growth (Fig. 2.15) suggesting that the positive effect of auxins on FRR found in my studies are probably due to an effect on the plant. Llorente and colleagues describe how necrotrophs reduced auxin signalling (Llorente et al., 2008). Given that auxins promoted resistance to FRR as early as 2 dpi, the data provides additional evidence towards *F. graminearum* behaving as a necrotroph in FRR. In contrast to auxin, both cytokinins *trans*-Zeatin and kinetin substantially increased FRR susceptibility. The greater effect of *trans*-Zeatin may be due to the higher activity of *trans*-Zeatin because of its highly reactive allylic hydroxy group (Chauhan, 2008). There is no evidence to date of cytokinins affecting *F. graminearum* FRR symptoms. Contrary to other studies, exogenous application of certain cytokinins was found to promote resistance to *Verticillium longisporum, Pseudomonas syringae*, and *Hyaloperonospora arabidopsis* (Choi et al., 2010, Argueso et al., 2012, Naseem et al., 2012, Reusche et al., 2013)*.* However, like other studies with SA, above-ground symptoms where measured rather than root symptoms because the diseases were different. This further suggests a different form of host-pathogen interaction occurring in roots. The effect of cytokinins on resistance was also reported to be concentration-dependent (Argueso et al., 2012). The mechanism for the effects of auxin and cytokinin on FRR resistance in *B. distachyon* is unknown and will need further investigation.

Surprisingly both auxins and cytokinins exhibited greater effects on resistance compared to the classic defence hormones. It is therefore plausible that they are both affecting FRR resistance in an SA/JA independent manner. IAA had no significant effect on SA or JA marker genes (Fig. 2.16B) suggesting the effect of auxins was SA/JA independent. To further support these results, the expression of additional hormone marker genes for SA signalling would need to be examined as well as assessing expression shortly after IAA and *F. graminearum* co-application. Despite the numerous links of auxins and cytokinins to synergism or repression with JA and SA (Wang et al., 2007, Choi et al., 2010, Naseem et al., 2012) this independent effect has also been observed in previous research. For example

(Qi et al., 2016) found that exogenous application of IAA did not lead to an increase in endogenous levels of SA or JA. Furthermore auxin signalling independent of JA and SA was found to be important for *A. thaliana* resistance to two other necrotrophic pathogens (Llorente et al., 2008). Additionally, the effect of auxin signalling mutant *A. thaliana* plants was found to be independent of SA-related *PR1* expression (Kidd et al., 2011). In another example, elevated expression of a the IAA-amido synthetase gene *GH3-8* that regulates IAA levels promoted resistance to *X. oryzae* in rice independently of SA and JA (Ding et al., 2008). Auxin had no significant effect on the ABA-responsive gene *GLTP*, ethylene receptor *ETR2* expression, and ROS signalling-related *RbohB* (Fig. 2.16B). Cytokinins were also found to improve *Nicotiana tabacum* resistance to *Pseudomonas syringae* in an SA and JA independent manner (Großkinsky et al., 2011). Overall given their large effect, auxins and cytokinins are likely very important for the interaction between *F. graminearum* and are likely not having a direct effect on defence hormone signalling. The role of auxin in its role in resistance is further complicated given that *F. graminearum* has been reported to possess the capacity to produce IAA (Luo et al., 2016) whereas this is likely not the case for cytokinins (Sørensen et al., 2018).

The different effect of development-associated hormones may be related to either phytohormone homeostasis, antimicrobial production linked to metabolic pathways of development hormones, or trade-offs with growth (Kazan & Manners, 2009, Naseem et al., 2012, Huot et al., 2014, Albrecht & Argueso, 2017, Powell et al., 2017b). Additionally, the opposite response observed between cytokinins and auxins may be due to an antagonism between the two response networks (Naseem & Dandekar, 2012, Naseem et al., 2012). Overall, the effect of development-associated hormones on FHB and FRR may depend on their influence on basal resistance or specific growth/defence trade-offs independent of the trophic lifestyle of the pathogen. In contrast, the role of the classic defence hormones may be dependent on the trophic lifestyle of the pathogen. For example exogenous application of auxins and cytokinins induced substantial changes to root development. In the absence of infection, both IAA and NAA inhibited primary root elongation and caused increased lateral root branching compared to the control (Supp. Fig. S2A, S2E, and S2F). This supports previous evidence for this effect of auxins on lateral root development in *Arabidopsis* (Casimiro et al., 2003, Laplaze et al., 2007). The root tip is responsible for regulating auxin homeostasis by generating auxin (Müller et al., 1998) and acting as an auxin sink (Overvoorde et al., 2010). The root tip was the point of inoculation for all FRR

assays (Fig. 2.2). If we assume infection and necrosis of the root tip is the equivalent of removing the root tip, a disruption of auxin homeostasis may be one of many potential reasons for its effect on FRR resistance (Kerk et al., 2000). Due to these observations, it would be useful to compare the effect of auxins on FRR with inoculation away from the root tip. Contrary to auxin and regardless of infection, application of the cytokinins Zeatin or kinetin caused an inhibition of branching (Fig. 2.11, Supp. Fig. S2A, Fig. S2G, Fig. S2H). Cytokinin is known to inhibit lateral root growth (Laplaze et al., 2007) which was observed in response to FRR (Fig. 2.11B) and under disease-free conditions (Supp. Fig. S2A, Fig. S2G, Fig. S2H). Further investigation is required to understand the interactions between root development, infection, and auxins and cytokinins.

2.4.3. The Aminobutanoic Acid BABA Severely Increased FRR Susceptibility

The aminobutanoic acid BABA has not been previously tested on *F. graminearum*-induced FRR to my knowledge. The highly negative effect of BABA on FRR resistance (Fig. 2.12A and Fig. 2.13) contrasts with evidence showing that BABA increases resistance to both necrotrophs and biotrophs (Cohen, 2002, Singh et al., 2012) and especially root pathogens (Cohen, 2002, Olivieri et al., 2009). The contrasting effect may be dependent on the type of pathogen as was hypothesised by (Cohen, 2002). The substantial effect of BABA on FRR susceptibility could be due to synergism of SA and ABA signalling (Conrath et al., 2006). BABA was reported to function synergistically with SA, as evidenced by upregulation of *PR1* genes, or impairing immunity in lines with SA deficient mutations (Siegrist et al., 2000, Cohen, 2002, Conrath et al., 2006). Supporting this synergism, SA also increases FRR susceptibility (Fig. 8A). Furthermore BABA was shown to negatively affect *MES1* (*MethylEsterase 1*) expression at 6 dpi (Fig. 2.16A). *MES1* is important for SAR response and is known to be repressed at the site of infection. This allows for a further increase the levels of MeSA for transport to distal plant cells for preparation of SA-related defences (Park et al., 2007, Liu et al., 2011, Dempsey & Klessig, 2012). Therefore I hypothesise that BABA induced a SAR response in *F. graminearum*-infected roots. Indeed BABA is known to function as a priming agent (Conrath et al., 2006, Singh et al., 2012). Ament and colleagues (2010) identified that silencing of *MesA* promotes resistance to *F. oxysporum* in tomato (*Solanum lycopersicum*) (Ament et al., 2010). Therefore, the activity of *MES1* may promote susceptibility to *F. graminearum*. In order to investigate this hypothesis, the expression of

MES1 in distal tissues, like shoot tissue, during the FRR assays treated with BABA and *F. graminearum* would need to be analysed. Unlike the effect on *MES1*, the predicted downstream SA-responsive gene *PR1* (Bradi1g57590) was not significantly upregulated (Fig. 2.16A). However *PR1-5* (Bradi1g57590) was identified as more responsive to JA than SA (Kouzai et al., 2016). Therefore, a different downstream signalling SA marker gene would have been more appropriate. Nonetheless the JA biosynthetic gene *OPR3* was slightly but significantly upregulated (Fig. 2.16A). This would suggest that BABA slightly induced JA biosynthesis. The influence of BABA on JA-related genes has been reported (Hamiduzzaman et al., 2005). Due to destructive nature of measuring marker gene expression, expression was only recorded at 6 dpi in which half the root was necrotised and FRR symptoms were very severe. The expression of SA and JA related genes might be different at earlier time points, thus it would be important to test expression of hormone-related genes in response to co-inoculation of hormone and *F. graminearum* at an earlier FRR time point.

Given the larger effect of BABA on FRR susceptibility compared to SA it is possible that BABA is also affecting FRR resistance in an SA-independent manner. Aside from roles in plant defence, BABA can also affect plant development through reduction of growth and endogenous iron content (Wu et al., 2010, Koen et al., 2014). Therefore, BABA may be functioning similarly to the classic development-associated hormones auxin and cytokinin. BABA induced negative effects on lateral root branching (Fig. 2.13B) as well as the inhibition of root tip elongation in the absence of the pathogen (Supp. Fig. S2A and Fig. S2K). BABA can be phytotoxic at high concentrations however it is reported that roots are more tolerant than shoots (Jakab et al., 2001). Up to 100-fold lower concentrations of BABA were found to also increase susceptibility to FRR with minimal effects on development (Data not shown). BABA functions synergistically with the ABA defence pathway (Ton & Mauch-Mani, 2004) and there is evidence suggesting that ABA promotes FHB susceptibility (Buhrow et al., 2016, Qi et al., 2016). Alternatively BABA also activates the ABA signalling pathway (Ton & Mauch-Mani, 2004) and there is evidence that ABA increases susceptibility to FHB (Buhrow et al., 2016, Qi et al., 2016). Unfortunately, there was no significant effect of BABA on the expression of ABA responsive-*GLTP* (Fig. 2.16). Therefore this suggests that BABA-induced ABA signalling (Ton & Mauch-Mani, 2004) was not involved in FRR resistance or that *GLTP* was not the appropriate marker. Alternatively BABA can induce iron deficiency state in *A. thaliana* (Koen et al., 2014) and changes to iron content can promote susceptibly

to necrotrophs (Laluk & Mengiste, 2010). If *F. graminearum* is behaving as a necrotroph during FRR, then it is possible that a reduced iron content caused by BABA promoted FRR hyper-susceptibility.

Unlike BABA, the same concentration of its isomer GABA did not affect FRR resistance (Fig. 2.12B). This contrasts with evidence where GABA has been shown to be involved in plant resistance (Solomon & Oliver, 2002, Bolton et al., 2008). Given the high concentration of GABA applied, it is unlikely that other concentrations will affect resistance. Furthermore no difference was observed in root growth in the absence of disease (Supp. Fig. S2A and Fig. S2L). Overall, these results show that BABA and GABA have contrasting effects on resistance of *B. distachyon* to FRR, and it provides evidence that a lesser-known plant signalling molecule (BABA) can have substantial effects on *Fusarium* resistance.

2.4.4. The Different Phytohormone-Dependent Root Infection Trends

Multiple time points were recorded and as such there were differences in slope regression in response to phytohormones. All phytohormones with significant effects on FRR resistance were separated into two broad groups (Table 2.7). The first 'parallel' group are those compounds that induced a significant difference in resistance at the first time point, and that differential remained similar at later time points. For examples all defence-associated phytohormones appeared to have this effect (SA, JA, ACC) (Fig. 2.5). This trend implies that these compounds have an effect on initial *F. graminearum* infection, after which the absence of deviation relative to the first time point suggests that the effect on FRR colonisation was much reduced or absent. On the other hand, the second 'divergent' group are those that have relatively minor effects at the first time point, but where the differential in resistance increased at later time points. The growth and development-associated phytohormones auxins, cytokinins, and BABA exhibited this (Fig. 2.8A-B, Fig. 2.10A-B, Fig. 2.12A). This trend implies that these compounds have a minimal effect on initial infection but affect the ability of the host to restrict *F. graminearum* colonisation. Together the evidence supports the idea of fundamental differences in the functioning of growth/development associated phytohormones compared to the classic defence phytohormones in resistance to FRR. It further supports the hypothesis that the development hormones auxin and cytokinin, including BABA, are functioning largely in an SA/JA independent manner. Importantly, speculation about the two distinct 'slope

differential' groups is under the assumption that the ultimate effect on FRR resistance is independent of the dose applied.

2.4.5. Endogenous GA and BR Levels Affect Resistance to FRR

Exogenous application of either GA or eBR had no significant effect on FRR resistance (Fig. 2.6A and Fig. 2.7A). However, their inhibitors (Phx and Brz respectively) induced effects on resistance at later time points (Fig. 2.6B and Fig. 2.7B). Phx functions as a growth retardant by inhibiting late stage biosynthesis of GA (Brown et al., 1997). Similarly Brz also behaves as an inhibitor of BR biosynthesis (Asami et al., 2000) and Brz at 10 μM was found to be effective at reducing Brz content in barley leaves and roots (Bajguz et al., 2019). Bd3-1 roots were continuously exposed to these inhibitors throughout the duration of the FRR experiment. I hypothesise that GA and BR deficient conditions would manifest during late-infection due to the naturally high availability of GA and BR in *B. distachyon* (Kakei et al., 2015). Therefore, non-depleted endogenous levels of respective hormones did not affect resistance at 2 dpi until differences in resistance became visible by 4 dpi and 6 dpi when endogenous GA and BR were likely near-depleted. If a low GA content after Phx treatment caused increased FRR susceptibility (Fig. 2.6B), it suggests that GA promotes resistance to *F. graminearum* in *B. distachyon* roots. Positive effects of GA on FHB have been previously reported (Buhrow et al., 2016). The decrease in FRR symptoms after BR biosynthesis inhibition from BRZ (Fig. 2.7B) suggests that BR promotes susceptibility to *F. graminearum* in *B. distachyon* roots. This result contrasts with the evidence that exogenous BR increased FHB resistance to *F. culmorum* in barley (Ali et al., 2013). Furthermore, disruption of BR perception in barley promoted resistance to *F. culmorum*, perhaps as a result of increased levels of BR in the signalling mutant (Ali et al., 2014, Goddard et al., 2014). The effect of Brz was not investigated on *F. graminearum* growth but increased resistance from antimicrobial effects of Brz on *F. graminearum* is unlikely given that there was no significant effect on resistance at 2 dpi (Fig. 2.7B).

2.4.6. Root Rot Assay Limitations

The FRR assay results are likely dependent on numerous factors. I have only investigated the effect of a single concentration of phytohormone on FRR, but it should be borne in mind that there may be concentration-dependent effects. This should be key for investigating specific phytohormones such as auxins or cytokinins. Furthermore it would be beneficial to investigate the FRR response to phytohormones after inoculation as this was shown to be important for final disease resistance outcome (Makandar et al., 2010). The age of seedlings is also relevant given how resistance can change between adult and seedling plants. In several studies investigating root disease caused by *F. oxysporum*, phytohormones and inoculation were applied by soil drench, physical removal of roots from soil or use of hydroponics to enable investigation of adult plants (Mandal et al., 2009, Trusov et al., 2009, Kidd et al., 2011). This may be an option for investigating hormone effect on adult root systems. Lastly it would be interesting to investigate the effect of interesting phytohormones like auxin, cytokinin, and BABA on wheat seedling roots using a variation of the FRR assay method to compare the effects between the two species.

2.4.7. Conclusion

The FRR experimental results addressed the initial objective of the chapter. I showed that the phytohormones auxins, cytokinins, and BABA induced the most significant effects on FRR. In fact almost all phytohormones tested affected FRR resistance in one way or another. The phytohormones JA, ethylene, auxin, and GA were associated with FRR resistance whereas SA, cytokinins, BR, and BABA were associated with FRR susceptibility. Secondly the data provides supporting evidence for an antagonistic effect between the classic defence hormone SA and JA/ethylene and hints at a unique infection strategy of *F. graminearum* in *B. distachyon* roots in that it adopts a more necrotrophic-focused lifestyle than that reported for infection of floral tissues. Furthermore, the data shows an important role of development-associated hormones auxin and cytokinins on FRR resistance and hints at their potential SA/JA-independent effects. The data revealed two resistance groups focussed on initial infection or colonisation and that these broad groups were dependent on the 'class' of phytohormone applied. Defence-associated phytohormones appeared to play a more significant role in initial infection whereas growth-associated phytohormones

played a greater role in colonisation. Together the data suggests that phytohormones can affect FRR resistance and suggests an important role phytohormones during *F. graminearum* infection of roots. The effects of phytohormones on FRR resistance can then be compared to their effects on *B. distachyon* FHB resistance which is investigated in chapter 3. Future experiments are required to examine the host and pathogen transcriptome response during FRR (Investigated in chapters 4 and 5) to provide additional evidence on the mode of trophism within infected tissues and *B. distachyon* hormone-related gene expression changes.

Chapter 3 - The Effects of Phytohormones on Fusarium Head Blight

Several figures and some of the writing in this chapter have been published previously in:

3.1. Introduction

Fusarium graminearum is a facultative hemibiotroph that causes numerous diseases on small grain cereals (Jansen et al., 2005, Boddu et al., 2006, Brown et al., 2011). The most important *F. graminearum* disease is Fusarium head blight (FHB) caused by the infection of the cereal spike (Parry et al., 1995, Jansen et al., 2005, Boddu et al., 2006, Brown et al., 2010). Wheat (*Triticum aestivum*) and *Brachypodium distachyon* plants are most susceptible to FHB during mid-anthesis (Fig. 3.1). Therefore, this is a critical time for controlling FHB. A potential target for tackling FHB is to find compounds that can reduce susceptibility to FHB at this critical developmental stage and reduce the total content of the associated *Fusarium* mycotoxin deoxynivalenol (DON) that accumulates in the grain. Current control methods rely on genetic host resistance and fungicides (Dweba et al., 2017). Phytohormones are important components of plant defence signalling and their impact on resistance to *F. graminearum* has been investigated in numerous studies on *A. thaliana*, wheat, and barley (*Hordeum vulgare*) (Table 3.1). Furthermore phytohormones have also been shown to affect mycotoxin content in infected grains (Makandar et al., 2011, Buhrow et al., 2016) and to directly affect *F. graminearum* (Qi et al., 2012). It is conceivable that a useful measure of disease control can be achieved by application of selected phytohormones(s) to reduce or eliminate the peak of susceptibility at mid-anthesis. In this chapter, I will investigate the use of phytohormones as FHB controlling agents in susceptible *B. distachyon* lines as well as the effects of some phytohormones on control of FHB in wheat.
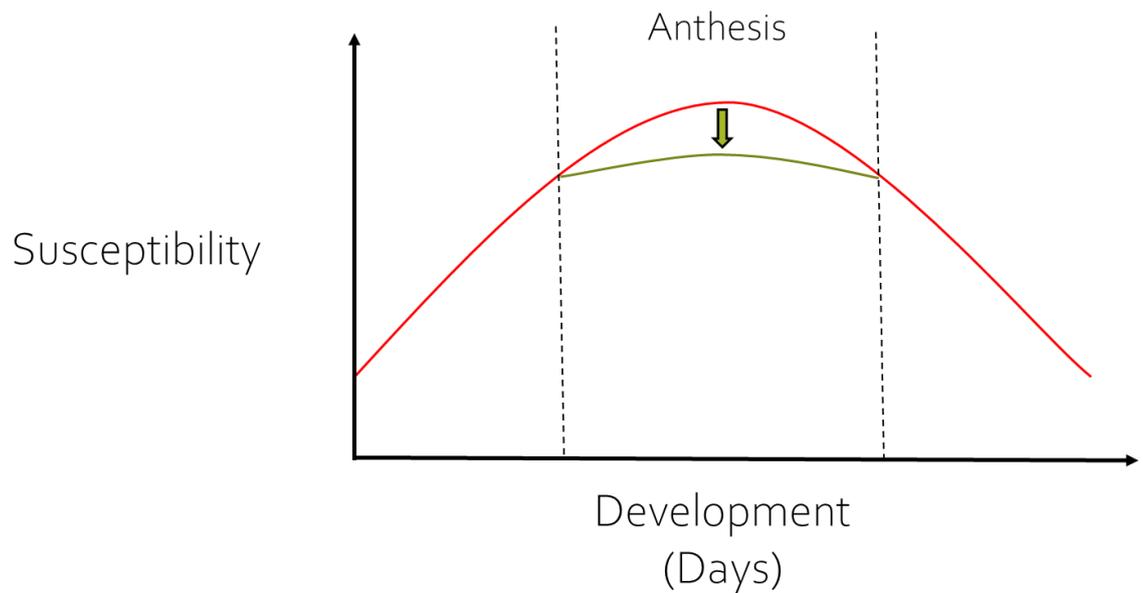
Figure 3.1. The aim to transiently increase resistance towards FHB during mid-anthesis of cereals. Describes the change in susceptibility (red line) during the lifespan of cereals. Window of heightened susceptibility is denoted between the two dotted lines. Green arrow and line are the potential transient reduction in susceptibility during heightened level of susceptibility. Heightened mid-anthesis susceptibility concept influenced from (Parry et al., 1995, Bai & Shaner, 2004, Xu et al., 2008b, Peraldi et al., 2011).

Exogenous application of salicylic acid (SA) or methyl salicylate has been shown to have positive effects on FHB resistance in wheat (Makandar et al., 2011, Qi et al., 2012, Sorahinobar et al., 2016) and on DON reduction (Makandar et al., 2011). Application of methyl salicylate also showed positive effects on wheat leaf resistance to *F. graminearum* (Ameye et al., 2015). There is extensive evidence in the literature of the effectiveness of SA against a range of pathogenic species. Initially, Makandar and colleagues (2010) showed that endogenous SA and SAR were important for resistance to *F. graminearum* in *Arabidopsis thaliana* (Makandar et al., 2010). SA biosynthesis mutants such as s*id2* exhibited higher *F. graminearum*-induced disease severity in *A. thaliana* (Makandar et al., 2010). However, SA was also shown to have no effect on FHB resistance (Li & Yen, 2008), and SAR is likely not involved in FHB resistance in wheat (Li & Yen, 2008) or barley (Hao et al., 2018). The increased resistance to *F. graminearum* may also be due to a direct damage to fungal cells by SA as (Qi et al., 2012) found that growth, germination, and DON production were significantly reduced with increased exogenous SA levels *in vitro*.

Reports on the effect of Jasmonic acid (JA) and methyl jasmonate (MeJA) on FHB are inconclusive. JA and MeJA application was reported to have a positive effect on FHB

resistance in wheat (Li & Yen, 2008, Qi et al., 2016, Sun et al., 2016). In contrast, exogenous MeJA (metabolised from JA) vapours were found to increase susceptibility to *F. graminearum* by attenuating SA signalling in *A. thaliana* and wheat during early infection (Makandar et al., 2010, Makandar et al., 2011), however positive effects were observed during late infection in *A. thaliana* (Makandar et al., 2010). Similar results were reported in wheat where pre-infection application of methyl-jasmonic acid promoted susceptibility, whereas post-infection application promoted resistance of wheat leaves to *F. graminearum* (Ameye et al., 2015). Exogenous application of MeJA also provided a reduction in disease severity (Li & Yen, 2008, Sun et al., 2016). Similar to SA, exogenous JA likely also directly reduces *F. graminearum* growth *in vitro*, which was associated with reduced wheat FHB symptoms (Qi et al., 2016). Inherent antagonism between SA and JA hormone pathways (Fig. 1.6) suggests a contradiction in the response of wheat to *F. graminearum* (Table 3.1). This may, however, be explained by the plant responding to the different trophic lifestyles of *F. graminearum* at different stages of infection (Bari & Jones, 2009, Brown et al., 2010).

The precise role of ethylene on resistance to *Fusarium* also remains unclear. Chen and colleagues (2009) identified that overexpression and reduction of ethylene signalling resulted in increased susceptibility or resistance, respectively, in *A. thaliana* to *F. graminearum*. Furthermore, silencing of a core ethylene signalling gene (*EIN2*) reduced disease symptoms and mycotoxin content in wheat grains. It was also suggested that the virulence factor DON utilises ethylene signalling for modulating cell death response (Chen et al., 2009). However, (Li & Yen, 2008) reported that externally applied ethylene treatment provided resistance equivalent to the resistant control Sumai3. Similarly Foroud and colleagues (2018) found that ethylene-promoting compounds improved resistance and the opposite was true for ethylene-inhibiting compounds (Foroud et al., 2018). This effect of ethylene is further complicated given that Sun and colleagues (2016) found no significant change in FHB susceptibility in response to exogenous ethylene on wheat spikes (Sun et al., 2016).

More recently other important hormones were shown to have roles in defence and contribute significantly to the infection response. Exogenous application of gibberellic acid reduced FHB spread in wheat heads (Buhrow et al., 2016). Dwarf wheat varieties (mutant *Rht* genes) which produce constitutively active DELLA proteins and whose sensitivity to GA is decreased have been associated with necrotrophic FHB resistance (Saville et al., 2012,

He et al., 2016). However there is evidence that effects on *Fusarium* resistance may not link directly to GA and DELLA proteins but are rather associated with plant height (Chen et al., 2014a). Exogenous application of the phytohormone abscisic acid negatively affected resistance to FHB (Buhrow et al., 2016, Qi et al., 2016). A study by Ali and colleagues (2013) found that exogenously applied epiBL reduced *Fusarium culmorum* disease severity and grain-associated weight loss in barley (*H. vulgare*) (Ali et al., 2013). Goddard and colleagues (2014) found that disrupting the main BR receptor (*BRI1*) in barley resulted in increased resistance in most tissues to a range of non-biotrophic pathogenic fungi, including *F. culmorum* (Goddard et al., 2014). The same *BRI1* mutant barley cultivars also showed increased resistance to FHB (Ali et al., 2014). The auxins indole-3-acetic acid (IAA) had positive effects on FHB spikelet infection and yield loss in barley (Petti et al., 2012), negative effects on FHB in wheat (Su et al., 2020), and was even found to reduce *Fusarium* growth *in vitro* (Luo et al., 2016).

There are hormones that have not been investigated regarding exogenous application and response to *F. graminearum* infection. These include cytokinins which have been implicated in plant defence (Choi et al., 2010, Choi et al., 2011, Albrecht & Argueso, 2017) and the recently classed non-protein amino acid and signalling molecule 3-aminobutryric acid (BABA) (Cohen, 2002, Thevenet et al., 2017). A summary of exogenous phytohormone's effects on *Fusarium*-induced FHB and DON is described in Table 3.1.

Table 3.1. Summary of the effects each phytohormone (investigated in this thesis) has on *F. graminearum* and *F. culmorum* infection response from exogenous application in different hosts.

Plant Hormone	Effect on *Fusarium* infection	References
Salicylic acid (SA)	Reduced FHB and leaf infection symptoms, and mycotoxin levels (*Ta* and *At*). No effect on FHB resistance (*Ta*).	(Li & Yen, 2008, Makandar et al., 2010, Makandar et al., 2011, Qi et al., 2012, Ameye et al., 2015, Sorahinobar et al., 2016)
Jasmonic acid (JA)	Increased symptoms at early leaf infection (*Ta* and *At*). Increased resistance at early and late infection (*Ta* and *At*).	(Li & Yen, 2008, Makandar et al., 2010, Ameye et al., 2015, Qi et al., 2016, Sun et al., 2016)
Ethylene (ET)	Susceptibility (*Ta* and *At*). Resistance or no effect (*Ta*).	(Li & Yen, 2008, Chen et al., 2009, Sun et al., 2016, Foroud et al., 2018)
Brassinosteroid (BR)	Reduced FHB (*F. culmorum*) and seed weight loss (Hv).	(Ali et al., 2013)
Gibberellic acid (GA)	FHB resistance and reduced mycotoxin (*Ta*).	(Buhrow et al., 2016)
Abscisic acid (ABA)	Increased FHB symptoms (*Ta*).	(Buhrow et al., 2016, Qi et al., 2016)
Auxin	Reduced FHB (*F. culmorum*) severity and yield loss (*Hv*). Increased FHB and leaf (*F. graminearum*) severity (*Ta*).	(Petti et al., 2012, Su et al., 2020)
Cytokinin (CK)	N/A	N/A
3-aminobutrytic acid (BABA)	N/A	N/A
4-aminobutrytic acid (GABA)	N/A	N/A

Abbreviations; *Ta* (*Triticum aestivum*), *At* (*Arabidopsis thaliana*), *Hv* (*Hordeum vulgare*). "N/A" means that there is no study to my knowledge that has investigated the exogenous effect of the respective phytohormone or compound.

There is evidence for *Fusarium* inducing FHB in *B. distachyon* with the accessions tested shown to be susceptible at mid-anthesis and pathogenesis of floral tissues progressed similarly to wheat FHB (Peraldi et al., 2011). Research in the effects of phytohormones on FHB is rising (Table 3.1) however none have investigated the effects in *B. distachyon* FHB. The aim of this chapter is to identify hormones that can transiently improve cereal resistance to FHB in *B. distachyon*. Phytohormones were exogenously applied during mid-anthesis (Fig. 3.1) in FHB susceptible *B. distachyon* lines Bd3-1 and Bd21, and Perigee wheat floral tissues. Many of the compounds chosen were shown previously to have positive effects on FRR (Chapter 2). From the information of individual phytohormones, hormone antagonists were then tested on *B. distachyon* Bd21 and wheat FHB. Aside from reducing visual FHB symptoms I also investigated the effect of phytohormones on wheat grain DON content to identify any DON reducing phytohormone-associated compounds.

Aims:

1. Identify which phytohormones or phytohormone antagonists can transiently increase FHB resistance in *B. distachyon* and wheat.
2. Identify which phytohormones or phytohormone antagonists can reduce DON content in wheat grains.

3.2. Materials and Methods

3.2.1. Plant Material and Growth Conditions

The *Brachypodium distachyon* accession Bd3-1 was obtained from the John Innes Centre (JIC), Norwich, UK. The Bd3-1 seed peeling preparation and stratification method was followed as described in Section 2.2.1. Bd3-1 seeds were sown in 50% Peat/Sand and 50% John Innes mix 2 (two seeds per 8 cm^2 pot). Plants were kept for the remainder of the experiment at 22°C (20 h/4 h light/dark photoperiod, 70% humidity) in controlled environment cabinets (Snijders Scientific Jumo Imago F3000 chambers, or walk-in controlled environment rooms (Gallenkamp)) (Peraldi et al., 2011). For the FHB assay with Bd21 (from BASF Agricultural Centre, Limburgerhof, Germany), approximately five unpeeled seeds per one litre pot were grown for six weeks at 20 h/4 h 22°C day/night in soil under Autumn glasshouse conditions. The FHB susceptible line wheat (*T. aestivum*) Perigee variety (from BASF Agricultural Centre, Limburgerhof, Germany) was grown for 52 days at 16 h/8 h day/night length at 22°C in Autumn glasshouse conditions. Approximately 10 wheat seeds were sown per one litre pot in soil.

3.2.2. Maintenance and Preparation of *F. graminearum* Inoculum

The *Fusarium graminearum* isolate PH1 was used for all Bd3-1 FHB assays. To produce mycelial inoculum for FRR assays, *F. graminearum* was maintained on approximately 20 ml potato dextrose agar (PDA) (The PDA solution was prepared by the JIC media kitchen) in 9 cm diameter plastic Petri-dishes in controlled environment cabinets (Snijders Labs MicroClima-series, Economic LUX chambers or in a walk-in controlled environment growth room) at 22°C under 16 h/8 h light/dark photoperiod. Conidial *F. graminearum* inoculum (Fig. 1.1) was cultured in Mung Bean (MB) broth (Makandar et al., 2006) from a 1 cm^2 mycelial plug. MB broth was prepared by seeping 1 L of hot water (ELGA) with 40 g of mung beans for 10 min. The extract was filtered through multiple layers of sterile cheesecloth, decanted into 100 ml conical flasks, and then autoclaved. A mycelial plug was placed in each flask and the cultures were incubated in a shaker (New Brunswick Scientific Series 25 or Model G25) at 200 rpm and 23°C - 25°C in the dark or with minimal natural light. After seven to eight days, the conidia were filtered through cheesecloth,

centrifuged at 1,800 rcf for 5 min (removing most supernatant), and the concentration of the pellet was adjusted to 1 x 10^6 conidia/ml using a Thoma haemocytometer (Hawksley England) (Equation 3.1). Inoculum was stored at 5°C for up to 2 weeks before inoculation.

Equation 3.1. Method used to count *F. graminearum* conidia in a haemocytometer. This calculation depends on the haemocytometer grid and square size used. Counting method derived from (Caprette, 2006).

$$0.004 \: mm^3 = 0.04 \: mm^2 (square \: area) \times 0.1 \: mm \: (depth)$$
$$0.064 \: mm^3 \: (total \: volume) = 16 \: (number \: of \: squares) \times \: 0.004 \: mm^3$$
$$\frac{Conidia}{mm^3} = \frac{x \: (Number \: of \: conidia \: counted)}{0.064 \: mm^3}$$
$$\frac{Conidia}{ml} = \frac{Conidia}{mm^3} \times 1000$$

For Bd21 and Perigee wheat FHB assays, *F. graminearum* isolate Li600 was grown for two weeks at alternating every two weeks on Malt agar and Oatmeal agar in a 9 cm diameter plastic Petri-dish. Conidia were harvested in 10 ml of water amended with approximately 0.05% Tween 20 (10 drops to 1 L diH$_2$0) and then filtered through cheesecloth. Conidia were counted using a disposable Neubauer Improved DHC-N01 C-chip (NanoEntek) haemocytometer. A 100-fold stock conidia suspension was prepared. A different calculation was used for the conidial concentration where the concentration was calculated from the average conidial count per haemocytometer grid (Only two values if relatively similar counts) which was then multiplied by 100 x 10^4 for a conidia/ml concentration. The inoculum was immediately used.

3.2.3. FHB assay with Chemical Pre-Treatment

Numerous features of the FHB assay were derived from (Peraldi et al., 2011). For Bd3-1 FHB assays (JIC) once extruding anthers were visible around mid-anthesis (at least four weeks after sowing), the entire Bd3-1 plant (Fig. 3.2C) was sprayed using a Juvale fine mist atomiser spray bottles with 50 ml of phytohormone or solvent control (Table 3.2), amended with 0.05% Tween 20 surfactant onto a tray of 10 to 11 pots (Table 3.2). The phytohormones ABA and BR were not tested due to their non-significant effect or absence of results in the investigation into Fusarium root rot (Chapter 2). All compounds were ordered from Merck/Sigma-Aldrich UK unless otherwise stated. The same concentration of

solvent was applied to respective control treatment groups (Table 3.2). All compounds were applied with minimal adjuvants to identify the effect of the respective target compound alone. Unless otherwise stated, the effects described were from a single dose of phytohormone pre-treatment as opposed to continual exposure as during the FRR assays (Chapter 2). As a result, a higher concentration of phytohormone was applied to maximise the dose of phytohormone received by the plant. Twenty-four hours later the soil and base matting was watered heavily, and Bd3-1 spikes were sprayed to run-off using one Juvale fine mist atomiser spray bottles (6-12 sprays, two plants at a time) with a total of 30 ml *F. graminearum* PH1 (0.25 - 1 x 10^6 conidia/ml) amended with 0.05% Tween 20. A control pot without inoculum was included for each treatment. Approximately 30 ml of inoculum was sprayed onto a total of 20 plants' spikelets per treatment. Inoculum spraying was performed immediately before the dark period. In order to maximise humidity, plants were collectively held in a large plastic bag (Fig. 3.2A) or a humidity chamber (Fig. 3.2B) for three days. Symptoms were scored every three or four days by counting the number of infected florets per spike (Fig. 3.2D, Fig. 3.2E). Bd3-1 plants were tagged before any compound application to monitor and score the same spike over time (Fig. 3.2C). For repeated independent experiments with different measurement dates, the days were combined to 'Score Date' 1-3 with each measurement at 4-day intervals (Fig. 3.5A, Fig. 3.6A).

Table 3.2. Summary of the phytohormones exogenously sprayed onto *B. distachyon* Bd3-1.

Plant Hormone	Concentration (mM)	Solvent*	Reference**
Salicylic acid	0.2	Ethanol (0.2%)	***
Jasmonic acid	0.05	Ethanol (0.053%)	ED
ACC****	1	Water	ED
trans-Zeatin	0.01	DMSO (0.1%)	FRR
BABA	10	Water	FRR
GABA	10	Water	FRR
Auxin (IAA) sodium salt	0.05	Water	ED
Auxin (NAA)	0.005	Ethanol (0.1%)	FRR

*Includes final solvent concentration applied to water-based (diH$_2$0) spray. ** ED denotes the concentration was experimentally determined. FRR denotes the concentration was derived from FRR assays (Table 2.1). *** Concentration derived from (Mandal et al., 2009, Makandar et al., 2010, Makandar et al., 2011, Sorahinobar et al., 2016). ****ACC is the precursor of ethylene (Van de Poel & Van Der Straeten, 2014). Abbreviations in Table 2.1.
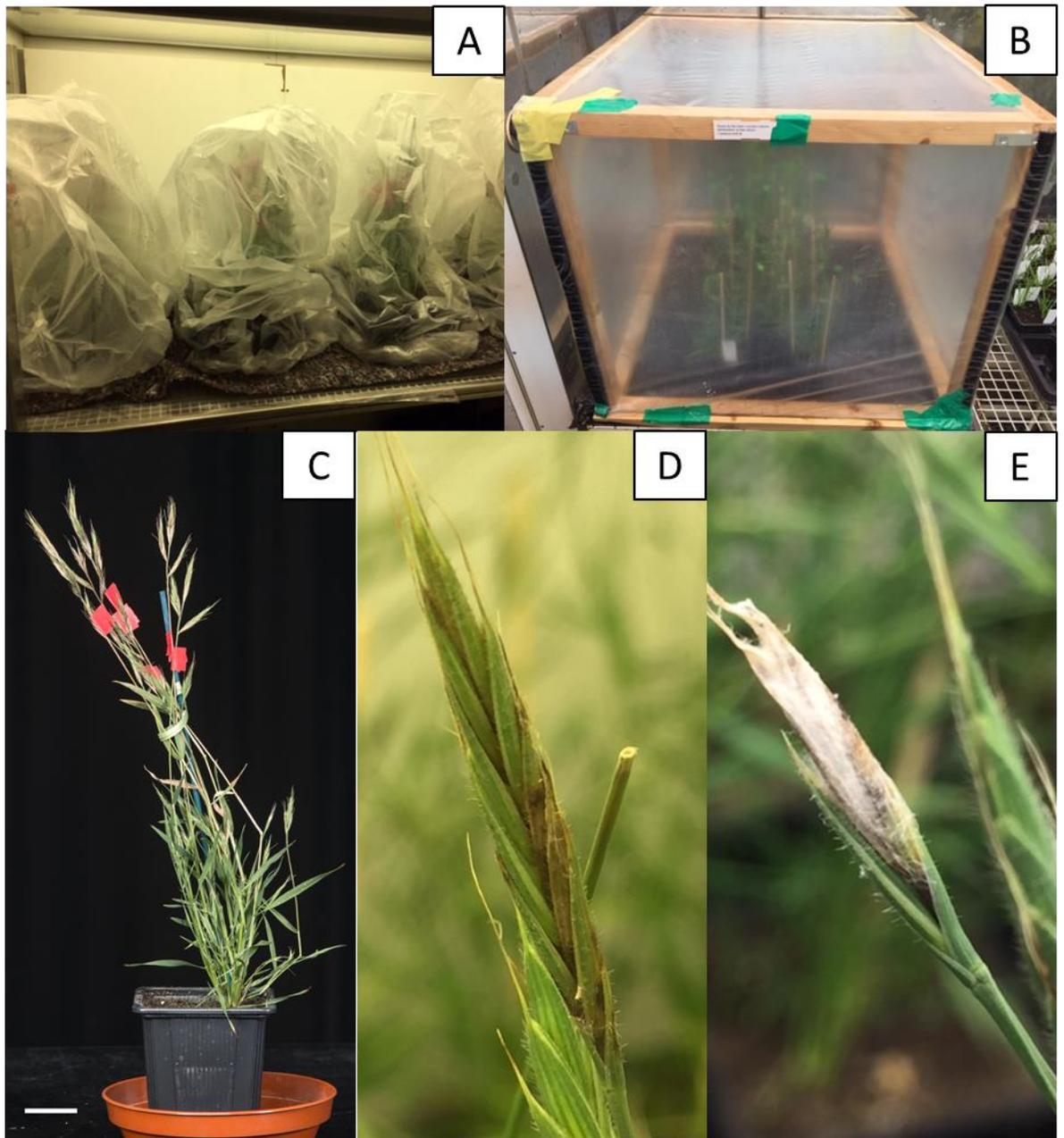
Figure 3.2. Pictures of various Bd3-1 FHB trials at the John Innes Centre, Norwich UK. (**A**) The heavy-duty plastic bags covering individually treated trays of Bd3-1 plants after inoculation in climate-controlled growth cabinet. (**B**) Humidity chamber (inside a climatically controlled chamber) holding an individually treated tray of Bd3-1 plants. (**C**) One pot of *F. graminearum*-infected Bd3-1 with individual spikes tagged for scoring growing in an 8 cm^2 pot. Scale bar = 3 cm. (**D**-**E**) *F. graminearum*-infected Bd3-1 spikelets at 7 dpi with brown lesions on individual florets which were scored for all Bd trials (**D**) and heavily infected with aerial mycelia covering the entire spike (**E**). (**C**, **D**, and **E**) Taken from (Haidoulis & Nicholson, 2020).

All Bd21 and wheat trials were performed in collaboration with BASF Agricultural Centre, Limburgerhof, Germany. Bd21 and Bd3-1 are both highly susceptible to FHB and exhibit a similar DON response as wheat (Peraldi et al., 2011). For wheat (Fig. 3.3A) and Bd21 (Fig. 3.3C), 50 and 80 pots were used for each trial, respectively. Once at mid-anthesis, 50 ml of test compound or solvent control (Table 3.3) amended with 0.05% of the surfactant Wettol was applied to the entire plant shoot until run-off. Selected compounds (up to four per trial) were applied sequentially in an automatic chemical spray chamber (BASF). Aside from the standard water and solvent controls (Table 3.3), all trials included the positive triazole control prothioconazole (at 0.175 mM (25 ppm) or 0.365 mM (125 ppm)) and the concentration of acetone solvent) (obtained from BASF Agricultural Centre, Limburgerhof) which displayed reduced FHB symptoms, as well as a negative control that was not sprayed with any compound or solvent (Data not shown). Prothioconazole concentrations were derived from ppm concentrations. After 24 h, a working concentration of $5x10^5$ conidia/ml for *B. distachyon* or $1x10^4$ conidia/ml for wheat of *F. graminearum* LI600 was prepared in 0.05% Tween 20 water solution, and 175 ml of inoculum was evenly sprayed above the entire plant in an automatic inoculation tunnel (BASF). The base matting was watered until run-off and plants were enclosed (Fig. 3.3C) for three (wheat) or six (Bd21) days in an elevated humidity glasshouse room until the first score date. Trolleys with pots were moved back to a conventional glasshouse after first score date and were not watered again until harvesting.

Table 3.3. Summary of each phytohormone exogenously sprayed onto *B. distachyon* Bd21 and/or wheat.

Compound	Conc. (mM)	Solvent*	Reference**
Salicylic Acid (SA)	0.5	Acetone	Table 3.2 + ED + (Qi et al., 2012)
Indole-acetic acid (IAA)	0.05, 0.5, 4, 8	Acetone	Table 3.2 + ED
Naphthaleneacetic acid (NAA)	0.5, 2, 4, 8	Acetone	*** + ED
Gibberellic acid (GA)	1	Acetone	(Buhrow et al., 2016)
Aminoethoxyvinylglycine hydrochloride (AVG)	0.035, 0.35, 0.8	Water	(Cohen et al., 1986, Ma et al., 1998, Bregoli et al., 2002, Saltveit, 2005)
Jasmonic acid inhibitor (JARIN-1)	0.3	Acetone	(Meesters et al., 2014)
Brassinazole (BRZ)	0.02, 0.2	Acetone	FRR + (Asami et al., 2000)

*Solvent applied to water-based spray. Acetone concentration less than 5% in final solution. ** ED: Concentrations were experimentally determined. *** Concentration initially derived from the IAA concentration. All compounds were ordered from Sigma-Aldrich/Merck except for JARIN-1 which was ordered from AOBIUS (AOB6436).

The tallest heads for each pot were scored for both wheat and Bd21 plants (Fig. 3.3B and Fig. 3.3D) since it was certain they were exposed to inoculum. The percentage of infection was scored for each wheat spike (Fig. 3.3B) whereas the number of infected florets per spike was scored for Bd21 and Bd3-1 (Fig. 3.2D, Fig. 3.3E, Fig. 3.3D). Several compounds were tested per experiment (Supp. Table S4, Supp. Table S5, Supp. Table S6), thus several control treatments are the same data between graphs (Fig 3.9A, 3.9G, 3.10A), (Fig. 3.9E, Fig. 3.10B), (Fig. 3.11A, 3.11G, 3.12A), and (Fig. 3.11E, 3.12B). Unless otherwise stated, all FHB experiments were repeated at least once.
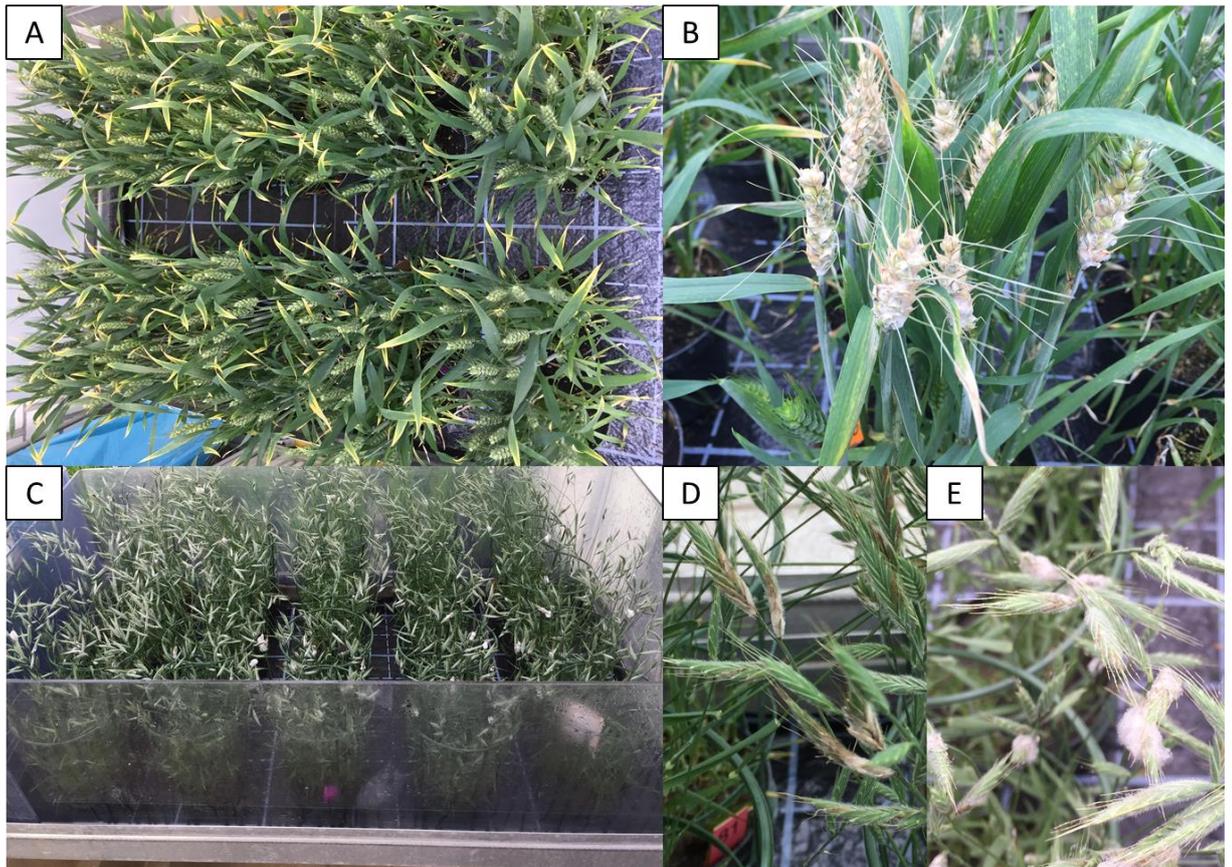
Figure 3.3. Pictures of various Perigee wheat and Bd21 FHB trials at BASF Agricultural Centre, Limburgerhof, Germany. (**A**) Randomised complete block design (RCBD) design for wheat plants before inoculation. There are two blocks in each trolley with 10 pots per block (two blocks shown). Regions without plants have low inoculum coverage. (**B**) Ten heavily infected Perigee wheat plants in one pot completely covered in aerial mycelia. (**C**) Similar RCBD design as wheat for Bd21 including plastic walls on trolleys (Excluding lid) to elevate humidity shortly after inoculation. (**D** and **E**) *F. graminearum*-infected Bd21 spikelets with brown lesions (**D**) and/or aerial mycelia (**E**) on florets.

3.2.4. DON Quantification Test

After the second scoring date and when sufficiently dry, wheat spikes from each pot were harvested by cutting below the spike of the tallest tillers. Approximately ten wheat spikes of the same pot were harvested per biological replicate. Cut spikes were placed in a paper drying bag and stored in a drying cabinet at 42°C for a minimum of 4 days. Some trials were stored at -20°C immediately after drying and then dried again for over an hour before use. Wheat samples were threshed in a machine using a rotor and air displacement (BASF Agricultural Centre, Limburgerhof). The pool of grains from ten spikes from one pot were then then milled in a Retsch MM 400. Grains were placed in a metal holder with a large ball bearing and pulverised for 1 min at the maximum speed (30) until a fine flour was obtained. The DON content reading per treatment was from four independent pools (biological replicates) of grains, each from approximately 10 spikes grown together in one pot. A mixture of 1 g of flour and 50 ml of diH_2O was mixed using a magnetic stirrer for 2 min at 400 rpm. Subsequently 1 ml of each sample was centrifuged for 1 min and 50 µl of supernatant was added to 1 ml of DONQ2 buffer (ROSA DONQ2 Quantitative Test - CharmScience kit). Samples with predicted high DON content were first diluted 10-fold in water before adding to DONQ2 buffer. Then 300 µl of this mixture was added to a ROSA DONQ2 test trip (CharmScience inc) and was incubated on a ROSA Incubator for 2 min at 46°C. The DON content for each sample was measured on a calibrated CharmEZ M reader. All readings from the reader were multiplied by 10 and then again by 10 for diluted samples.

3.2.5. Experiment Design, Statistics, and Graphs

A randomised complete block design (RCBD) was generated from the R-studio (V1.2.1335) package 'agricolae' for Bd21 (8 blocks) and wheat (5 blocks). Before chemical application, wheat and *B. distachyon* pots were numerically labelled and grouped per treatment according to RCBD design. Immediately after chemical application, wheat and Bd21 pots were randomised on trolleys. Each blocks (two per trolley) was defined by the inoculation tunnel spray pattern (Fig. 3.3A). Bd3-1 pot were separated by treatment before

chemical and inoculum application and kept in the same tray throughout the duration of the experiment (Fig. 3.2A and Fig. 3.2B).

All statistical tests were performed using the software package GENSTAT v.19.1.0.21390 (VSN international Ltd). A Generalised liner model (GLM) was used for all FHB assays. Either a normal distribution with an identity-link function was used for wheat and DON data, or a Poisson distribution with a log-link function was used for all Bd data (Supp. Table S3-S6). A few ANOVA's for combined independent experiments showed a significant interaction between the independent experiment and the hormone treatment at specific time points ($p < 0.05$), however for all the remaining time points, no such interaction was observed ($p > 0.05$) (Supp. Table S3, Supp. Table S4, Supp. Table S6). As such the interaction factors with "Experiment" for these remaining ANOVA tests were excluded from the GLM ANOVA test. For all data, the values were either collectively untransformed or transformed before GLM analysis according to the best fit model with the best normal distribution and equal variance. For wheat FHB assays, unless otherwise stated (Supp. Table S4), the data was logit transformed using the function 'log(Percentage_infection+0.25)/(100-Percentage_Infection+0.25) (McGrann et al., 2014) to account for large amounts of 0's and 100's scored. For all data analysed, individual time points were analysed separately.

Microsoft office (Excel, Word, and Powerpoint) was used for writing, data collection, images, and analysis. All graphs were prepared using Graphpad Prism (V5.04). All photos were taken using and iPhone 6 except Fig. 3.2C which was taken by the photography team at the JIC.

3.3 Results

3.3.1. The Effect of Phytohormones on FHB Disease Progression in *B. distachyon*

Although pre-inoculation treatment with SA marginally increased FHB symptoms (Fig. 3A), the increase was not statistically significant at any time point ($p > 0.05$, Fig. 3.4A). In additional experiments, SA was applied repeatedly (four applications) before, during, and after inoculation on Bd3-1 but again, no significant effect on resistance was observed ($p > 0.05$, Fig. 3.4B).
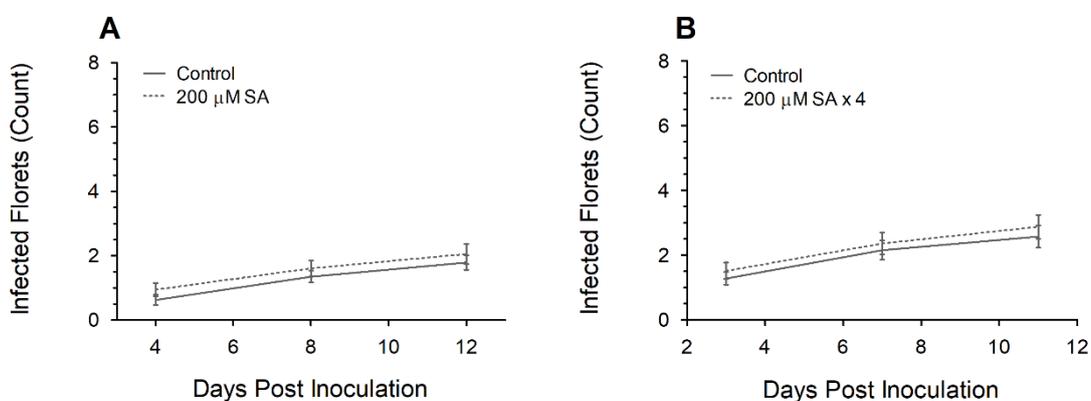
Figure 3.4. The change in number of *F. graminearum*-infected florets after pre-application of salicylic acid (SA) on Bd3-1 over time. (**A**) One SA application 24 h before inoculation. (**B**) Four applications of SA before (- 1 dpi), during (0 dpi), and after inoculation (3 dpi and 7 dpi). Each data point is the mean number of florets infected ± SE from one independent experiment each. Abbreviations: SA (Salicylic acid). Taken and modified from (Haidoulis & Nicholson, 2020).

Pre-inoculation treatment with JA resulted in an increase in the number of infected florets at all time points (p < 0.05, Fig. 3.5A). There was a significant increase in infected florets at the first score date (p = 0.009) and third score date (p = 0.011), however the effect was most prominent at the ScoreDate 2 (p < 0.001). Similarly, pre-treatment with ACC (Fig. 3.5B) also significantly increased the number of infected florets at all time points (p < 0.05), but the effect on symptoms diminished over time, and by 11 dpi the effect was not significant (p = 0.102). The compound 2-aminoethoxyvinyl glycine (AVG) acts as an inhibitor of ACC synthase which reduces ethylene biosynthesis (Schaller & Binder, 2017) and was found most effective at lowering ethylene before inoculation (Robison et al., 2001). I exogenously applied three concentrations of AVG on Bd21 florets before inoculating with *F. graminearum* (Fig. 3.5C and Fig. 3.5D). Given that ACC increased the number of florets infected, it was anticipated that application of AVG would reduce susceptibility. However all concentrations of AVG (35 µm, 350 µm, and 800 µm) significantly increased the number of infected florets at the first score date (p < 0.001 Fig. 3.5C, p < 0.05 Fig. 3.5D).
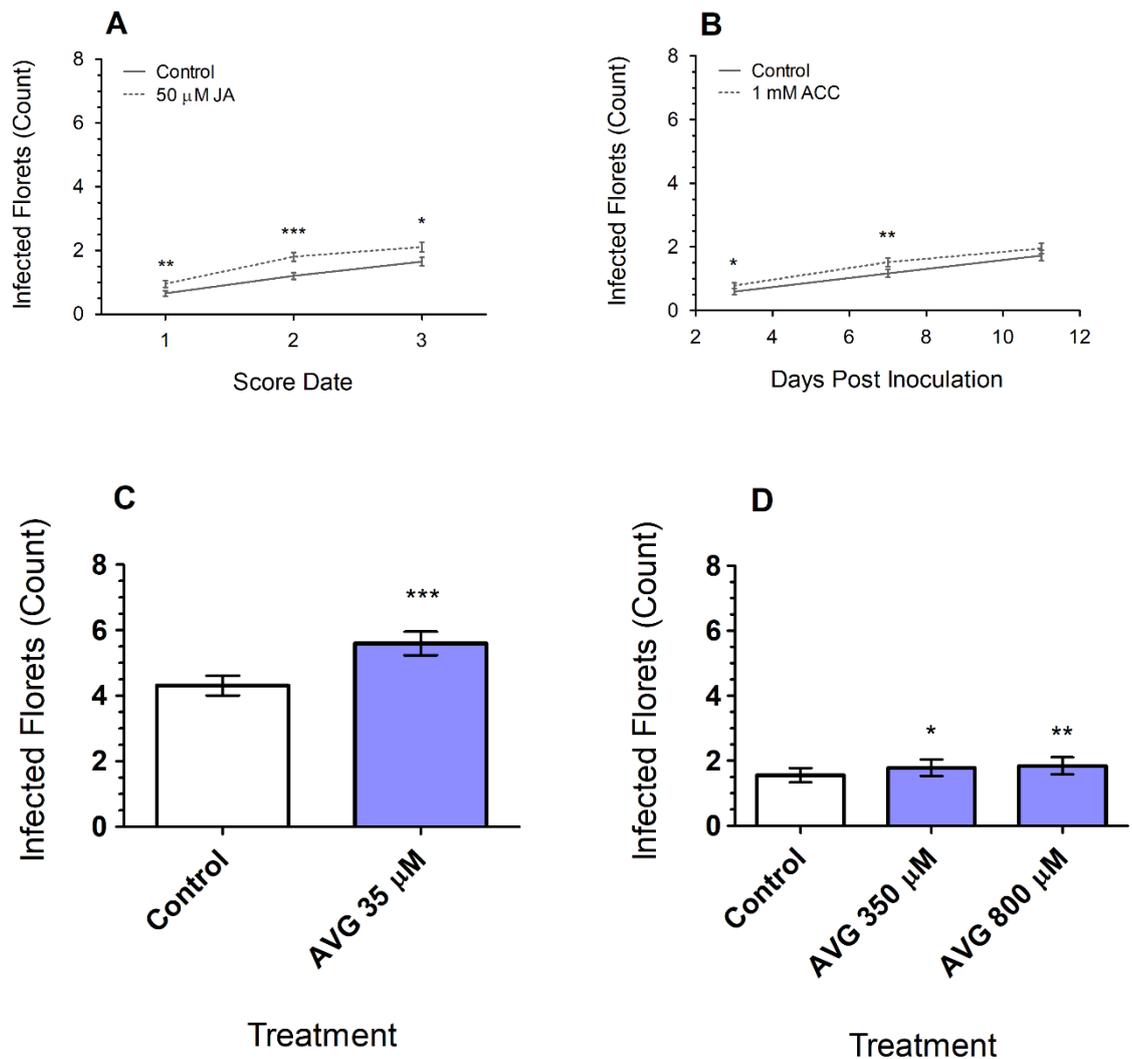
Figure 3.5. The change in number of *F. graminearum*-infected florets after pre-application of JA (**A**)*,* the ethylene precursor ACC (**B**) over time on Bd3-1, and the ethylene inhibitor AVG at 7 dpi (**C**) and 8 dpi (**D**) on Bd21. (**A** and **B**) Each data point is the mean number of florets infected ± SE from two independent experiments. (**C** and **D**) White bars denote controls whereas blue bars denote a test compound. Each bar is the mean number of florets infected ± SE from one independent experiment. This data was generated at BASF. (**All**) Significance levels * $p < 0.05$, ** $p < 0.01$, *** $p < 0.001$ compared to control. Abbreviations: JA (jasmonic acid), ACC (1-aminocyclopropane-1-carboxylic acid) AVG (2-aminoethoxyvinyl glycine). **A** and **B** Taken and modified from (Haidoulis & Nicholson, 2020).

Pre-inoculation with the compound BABA at 10 mM (Fig. 3.6A) significantly increased the number of infected florets at all time points (p< 0.001). The largest difference compared to the control was observed at the third score date (Fig. 3.6A). Applying the isomer of BABA, GABA (Cohen, 2002), at the same concentration (Fig. 3.6B) significantly increased the number of infected florets at 4 dpi only (p = 0.036) however this increase was relatively small compared to the control. After 4 dpi, there was no significant change in number of infected florets at any other time point (p > 0.05).
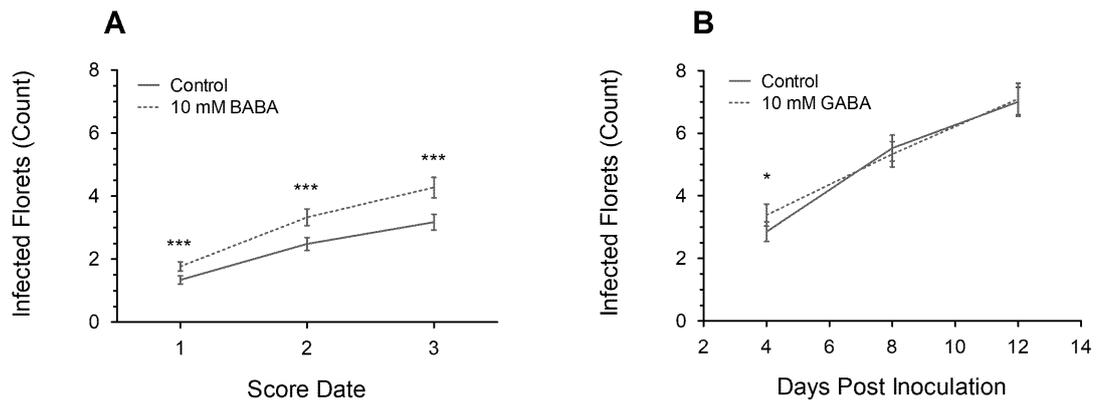
Figure 3.6. The change in number of *F. graminearum*-infected florets after pre-application of BABA (**A**) and GABA (**B**) on Bd3-1 over time. Each data point is the mean number of florets infected ± SE from three (**A**) or one (**B**) independent experiments. Significance levels: * p < 0.05, *** p < 0.001 compared to control. Abbreviations: BABA (3-aminobutanoic acid), GABA (4-aminobutanoic acid). (**A**) Taken and modified from (Haidoulis & Nicholson, 2020).

trans-Zeatin (10 μm) (Fig. 3.7) caused the largest increase in infected florets relative to the control treatment (p < 0.001) and showed one of the largest increases in FHB symptoms compared to all other hormone treatments. *trans*-Zeatin induced susceptibly early on at 3 dpi and the difference to the control increased slightly over time relative to that at the first time point.
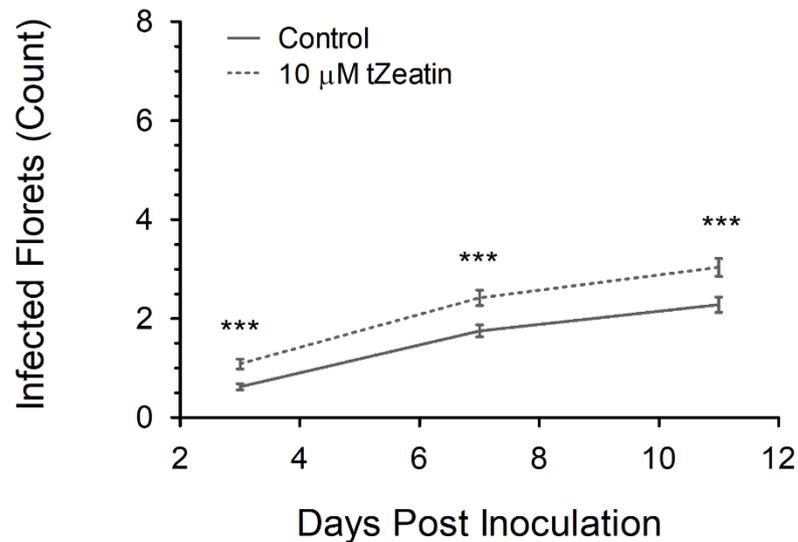
Figure 3.7. The change in number of *F. graminearum*-infected florets after pre-application of *trans*-Zeatin on Bd3-1 over time. Each data point is the mean number of florets infected ± SE from two independent experiments. Significance level *** p < 0.001 compared to control. Taken and modified from (Haidoulis & Nicholson, 2020).

The two auxins IAA at 50 µm and NAA at 5 µm (NAA was applied repeatedly with four applications before, during, and after inoculation) showed no significant effect on the number of infected florets at any time point (p > 0.05 Fig. 3.8A and Fig. 3.8B). To test whether these concentrations were too low, a much higher concentration of IAA and NAA was exogenously applied to Bd21 plants before inoculation with *F. graminearum* (Fig. 3.8C). Pre-application of synthetic auxin NAA at 8 mM resulted in the most significant decrease in the number of infected florets (p < 0.001) compared to IAA. Even 4 mM NAA significantly decreased the number of infected florets (p < 0.01) but to a lesser extent. The auxin IAA appeared to be less effective than NAA since 8 mM IAA showed a similar reduction in infected florets as 4 mM NAA (p < 0.01), and at 4 mM IAA the reduction in the number of infected florets was not significant (p = 0.33). Overall, these data indicate that auxins have a positive effect on FHB resistance when applied at relatively high concentrations prior to inoculation.
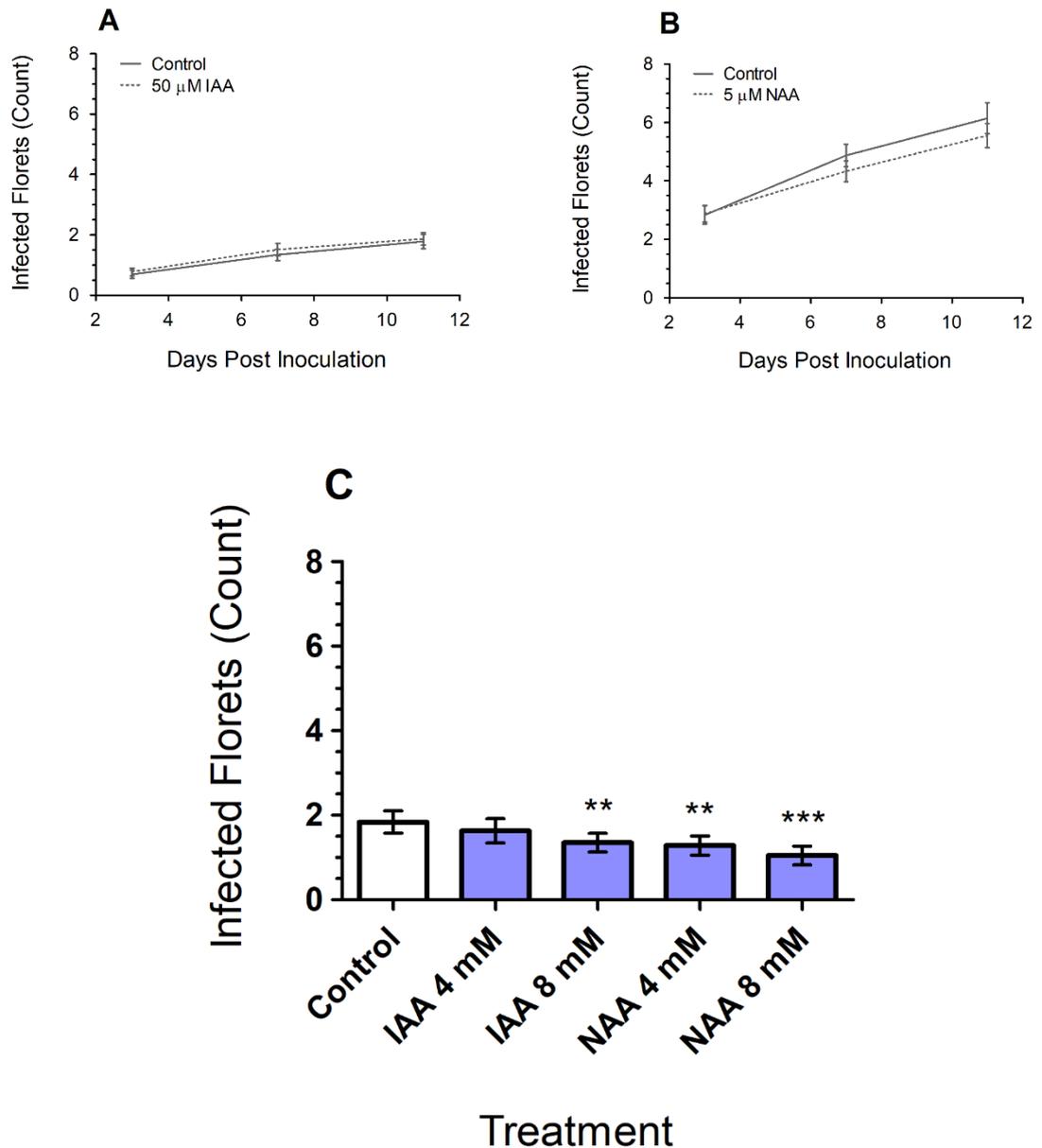
Figure 3.8. The change in number of *F. graminearum*-infected florets after application of IAA and NAA at different concentrations on Bd3-1 over time (**A**-**B**) and Bd21 (**C**) at 8 dpi. Each data point (**A**-**B**) and bar (**C**) is the mean number of florets infected ± SE from one experimental replicate. (**A** and **C**) One IAA application 24 h before inoculation. (**B**) Four applications of NAA before (- 1 dpi), during (0 dpi), and after inoculation (3 dpi and 7 dpi). White bars denote controls whereas blue bars denote a compound. LSD test significance levels ** $p < 0.01$, *** $p < 0.001$ compared to control. Data from **C** was generated at BASF. Abbreviations: IAA (Indole-3-acetic acid), NAA (1-Naphthaleneacetic acid). (**C**) Taken and modified from (Haidoulis & Nicholson, 2020).

To ascertain whether the reduction in FHB reflected an altered plant response or an effect on the fungus itself, an antimicrobial assay was performed by applying auxins or solvent controls to filter disks at four equidistant points from a mycelial plug of *F. graminearum* PH1 (Supp. Fig. S3). There was no difference in mycelial growth near any of the auxin-treated filter disks. Overall following the application of phytohormones on Bd3-1, most promoted FHB susceptibility whereas at a high concentration, the auxins IAA and NAA improved FHB resistance.

3.3.2. The Effect of Phytohormones and Phytohormone-Related Compounds on FHB in Wheat

A number of phytohormones that were tested with *B. distachyon* were re-tested on wheat spikes in addition to some additional phytohormone-associated compounds. Given that some compounds increased the number of infected florets in Bd3-1, respective hormone antagonists were also exogenously applied on wheat spikes before inoculation. The main aim was to verify the effect of phytohormones on FHB in a second temperate grass, and to identify additional compounds that can transiently increase resistance to FHB.

As for the *B. distachyon* SA trials (Fig. 3.4), pre-application of 500 µM SA showed no significant effect on percentage spike infection at either 7 dpi or 15 dpi ($p > 0.05$, Fig. 3.9A). Given that JA increased the number of infected florets in *B. distachyon* (Fig. 3.5A), a novel inhibitor of JA called JARIN-1 (Meesters et al., 2014) was exogenously applied to wheat plants before inoculation. Application of 300 µM JARIN-1 did not significantly change the percentage spike infection at 7 dpi ($p = 0.773$, Fig. 3.9B). The ethylene inhibitor ethylene AVG was also exogenously applied to wheat spikes before inoculation (Fig. 3.9C) at a similar concentration to that used in the *B. distachyon* trial (Fig. 3.5D). There was no significant change in percentage infection after pre-treating shoots with 35 µM AVG ($p = 0.668$) however there was a significant increase in symptoms when the concentration was increased to 175 µM ($p < 0.001$, Fig. 3.10D) and 350 µM at 15 dpi ($p < 0.01$, Fig. 3.9D).

Two auxins were also exogenously applied to wheat spikes before inoculation. There was no significant change in percentage spike infection after pre-application of 50 µM IAA at either time point ($p > 0.05$, Fig. 3.9E). Similarly there was no significant change in FHB symptoms after 500 µm IAA at any time point ($p > 0.05$, Fig. 3.10A). This was also observed

with 500 µM NAA on wheat FHB at all time points ($p > 0.05$, Fig. 3.10B). However, 2 mM NAA significantly reduced the percentage spike infection ($p = 0.006$, Fig. 3.9F). The effect of 2 mM NAA was independently and repeatedly assessed on FHB severity in wheat (Fig. 3.10C). There was a slight reduction in spike infection comparable to Fig. 3.9F, however this difference was not statistically significant ($p > 0.05$, Fig. 3.10C). I previously described how GA had no significant effect on FRR resistance (Chapter 2). Similarly, 1 mM GA had no significant effect on percentage spike infection at 7 dpi and 15 dpi ($p > 0.05$, Fig. 3.9G). Given how the brassinosteroid inhibitor brassinazole (Brz) (Asami et al., 2000) promoted resistance in FRR (Chapter 2) I predicted that Brz might also improve FHB resistance. According to Fig. 3.9H, Brz at 20 µM significantly increased percentage spike infection at 8 dpi ($p < 0.01$) and 15 dpi ($p < 0.05$). However, there was no significant change in infection of 200 µM Brz at 7 dpi and 15 dpi ($p > 0.05$). Finally, there was no obvious difference in symptom differential over time between the control and test compounds (Fig. 3.9A, Fig. 3.9D, Fig. 3.9E, Fig. 3.9G, Fig. 3.9H).
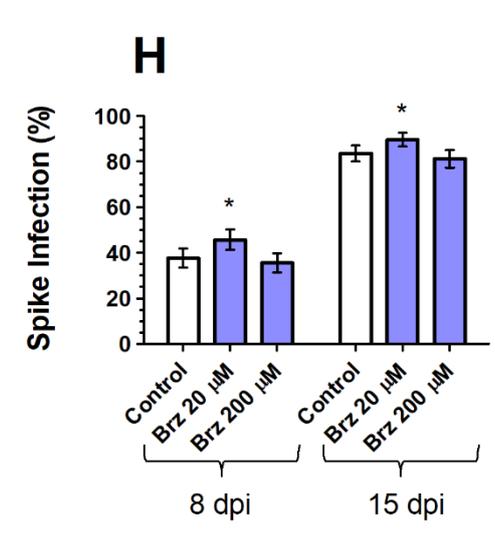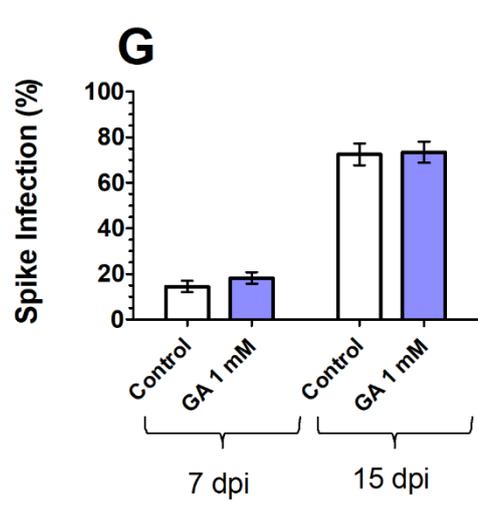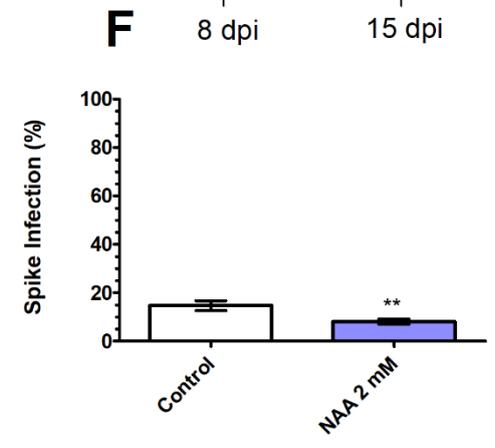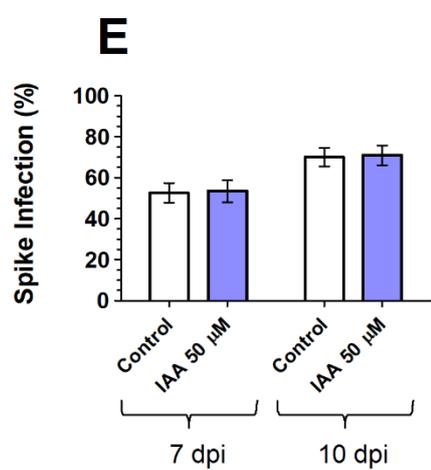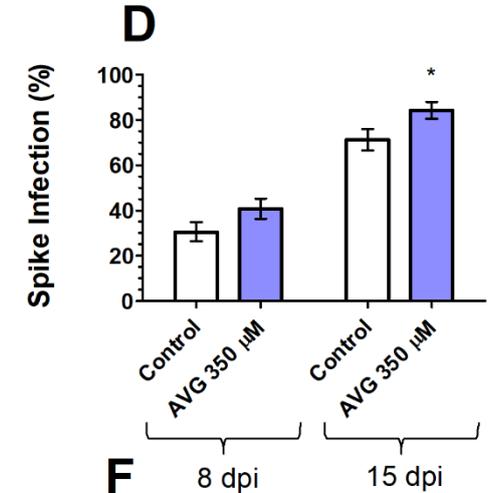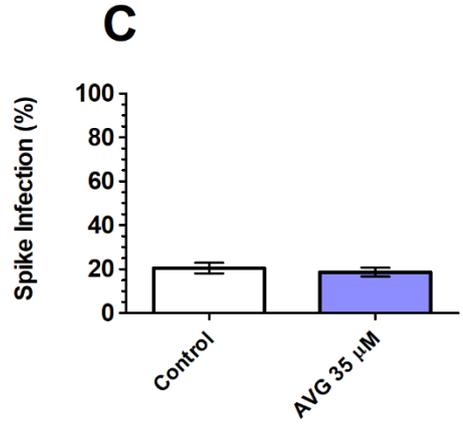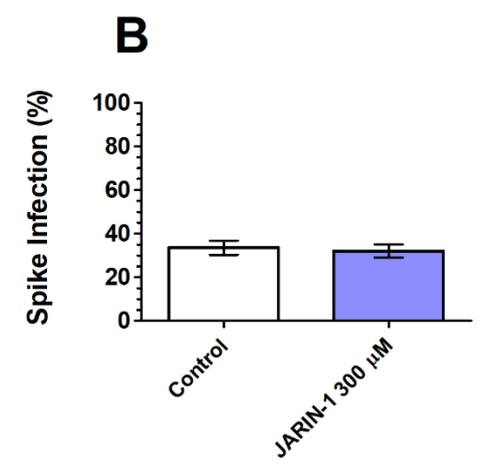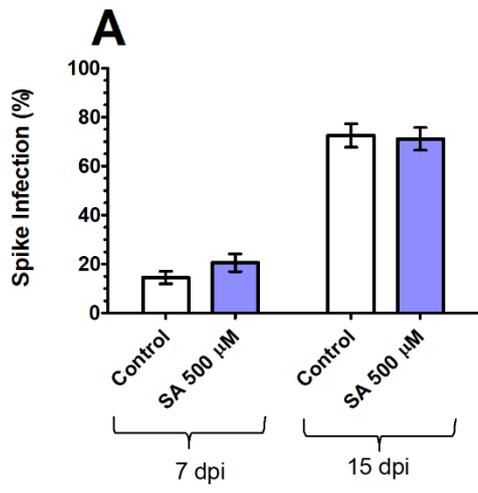
Figure 3.9. The effect of exogenous pre-application of phytohormone or phytohormone antagonists on visual FHB symptoms in wheat spikes at one or two time points. (**B**) is at 7 dpi, (**C**) are combined time point 7 and 8 dpi, (**F**) is at 7 dpi. The horizontal axis is treatments (compounds or solvents) exogenously applied (at different days in some cases). White bars denote controls whereas blue bars denote a compound. Each bar is the average spike infection percentage ± SE from one (**A**, **D**, **E**, **F**, **G**, **H**) or two (**B** and **C**) independent experiments. Data from **D** is part of the same experiment as C. Significance levels (LSD test for multiple treatments) * $p < 0.05$ ** $p < 0.01$ compared to controls. This data was generated at BASF Agricultural Centre, Limburgerhof, Germany. Abbreviations: AVG (2-aminoethoxyvinyl glycine), Brz (Brassinazole), GA (Gibberellic acid), IAA (Indole-3-acetic acid), JARIN-1 (JA inhibitor), NAA (1-Naphthaleneacetic acid), SA (Salicylic acid).
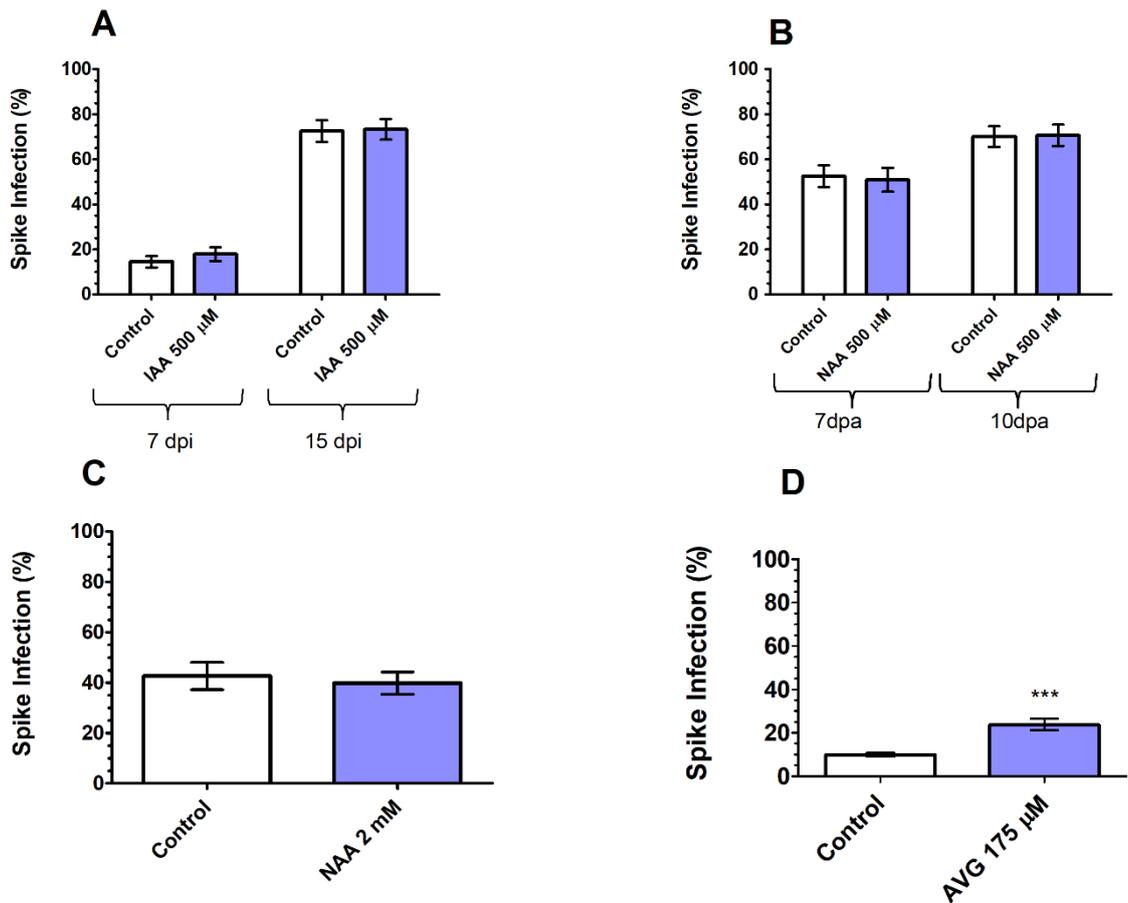
Figure 3.10. Additional FHB experiments with IAA, NAA, and AVG at different concentrations in wheat. (**A**) The change in FHB symptoms after IAA pre-treatment at 7 and 15 dpi. (**B** and **C**) Different concentrations of NAA used for wheat FHB assays. (**B**) The change in FHB symptoms after NAA (First concentration used) pre-treatment at 7 and 10 dpi. (**C**) A repeat experiment with NAA at 8 dpi (Fig. 3.9F). (**D**) Another concentration of AVG pre-treatment before FHB symptoms measurements at 7 dpi. The horizontal axis is treatments (compounds or solvents) exogenously applied (at different days in some cases). White bars denote controls whereas blue bars denote a compound. Each bar is the mean number of florets infected ± SE from one independent experiment. Significance levels: *** $p < 0.001$ compared to control. This data was generated at BASF Agricultural Centre, Limburgerhof, Germany. See Fig. 3.9 for compound abbreviations.

The grain DON content (Fig. 3.11) was measured for each phytohormone treatment (Fig. 3.9). The high concentration for Brz was chosen for analysis (Fig. 3.11H) since it caused the greatest reduction in FHB symptoms out of the two concentrations tested (Fig. 3.9H). In the majority of instances, DON levels were extremely high in both the control and treated samples. There was no significant change in wheat grain DON content for any compound tested ($p > 0.05$, Fig. 3.11, Fig. 3.12). Nonetheless, 2 mM NAA caused a slight reduction in grain DON content (Fig. 3.11F) that mirrored the reduced visual symptoms in the spike (Fig. 3.9F). There was also no reduction in grain DON content when NAA was applied at a lower concentration of 500 µM ($p > 0.05$, Fig. 3.12B). Similarly 500 µM IAA did not cause any change in grain DON content either ($p > 0.05$, Fig. 3.12A).
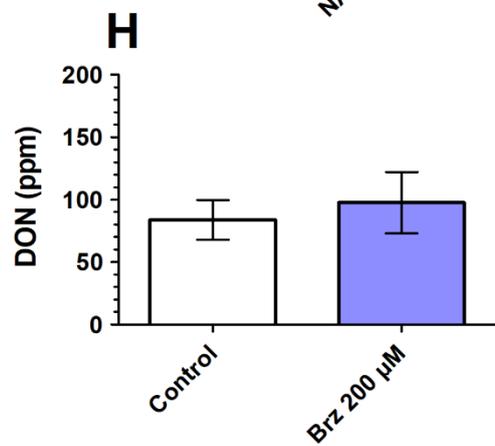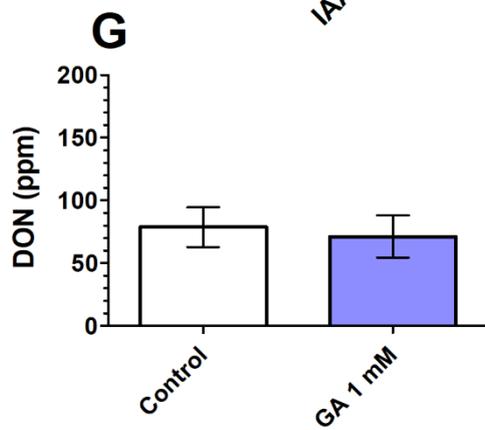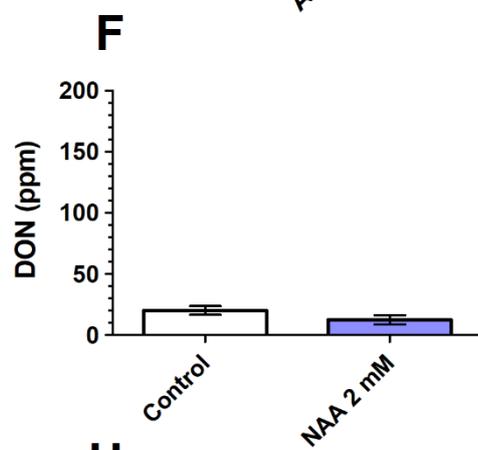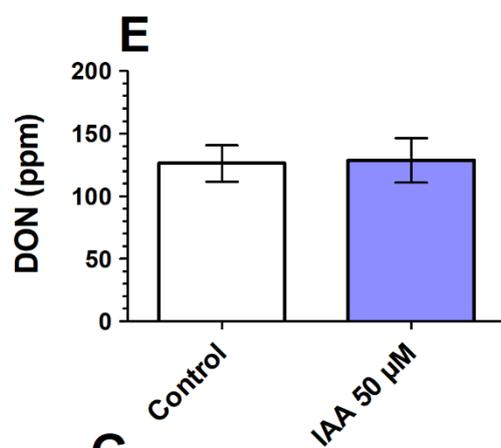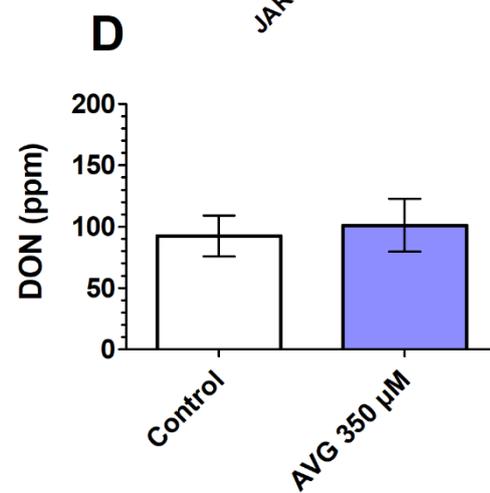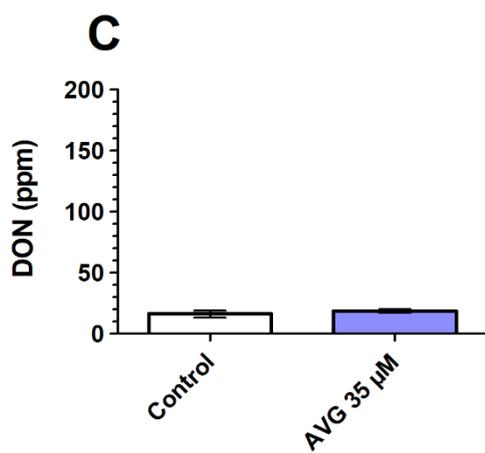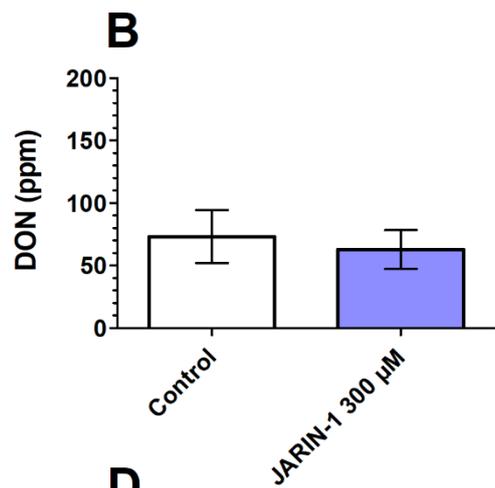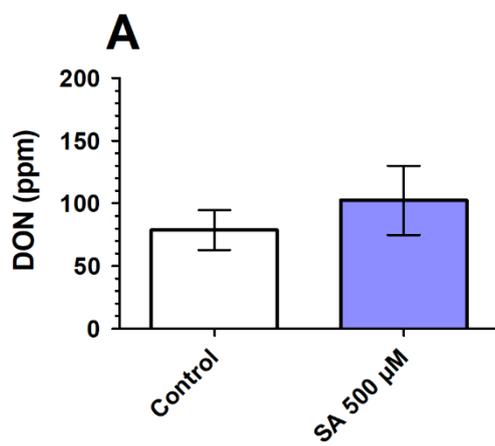
Figure 3.11. The effect of exogenous pre-application of phytohormone or phytohormone antagonists on the wheat grain DON content of infected grains. The horizontal axis is treatments (compounds or solvents) exogenously applied. White bars denote controls whereas blue bars denote a compound. Each graph is from the same trial material as FHB test (Fig. 3.9). All graphs are from one experimental replicate except for **B** which is from two. See Fig. 3.9 for compound abbreviations.
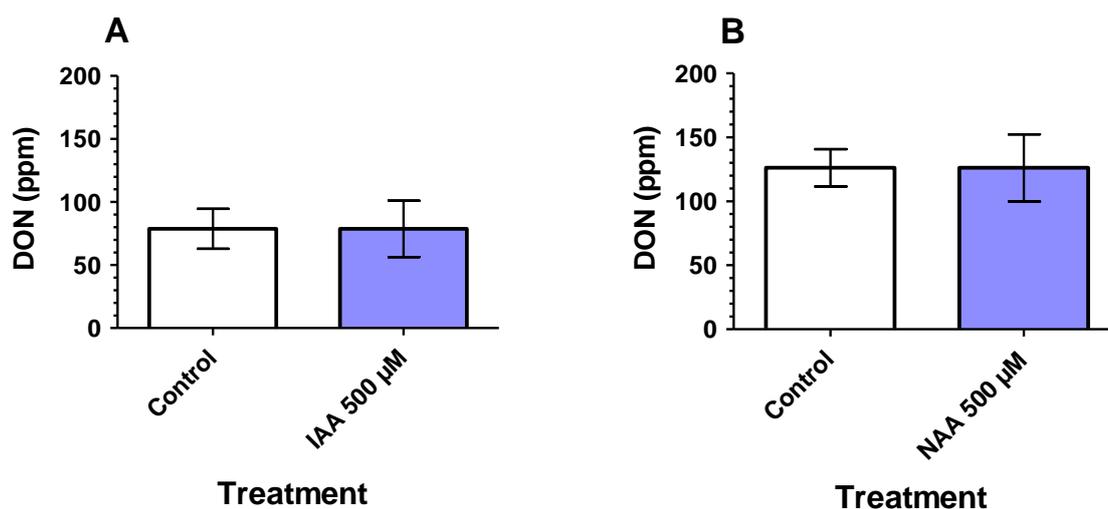
Figure 3.12. The effect of exogenous pre-application of auxins (repeated) on the wheat grain DON content of infected grains. (**A**) Grain DON content after application of IAA. (**B**) Grain DON content after application of NAA. (**A** and **B**) Each DON content graph is from one experimental replicate and is from the same trial material as the FHB test; Fig. 3.12A for Fig. 3.10A, and Fig. 3.12B for Fig. 3.10B. See Fig. 3.9 for compound abbreviations.

A summary of the effects that each phytohormone or phytohormone antagonist has on FHB resistance in both wheat and *B. distachyon* and DON content in wheat is summarised in Table 3.4.

Table 3.4. Summary of all FHB assay results.

Phytohormone	Compound	Species*	Overall Effect on FHB Resistance**	Effect on DON Content
SA	SA	Bd/Ta	N	N
JA	JA	Bd	—	
JA inhibitor	JARIN-1	Ta	N	N
Ethylene	ACC	Bd	—	
Ethylene inhibitor	AVG	Bd/Ta	—	N
Auxin	IAA	Bd/Ta†	+	N
Auxin	NAA	Bd/Ta	+	N
Cytokinin	*trans*-Zeatin	Bd	—	
GA	GA	Ta	N	N
BR inhibitor	Brassinazole	Ta	—	N
Aminobutanoic acid	BABA	Bd	—	
Aminobutanoic acid	GABA	Bd	N	

* Tested either in *B. distachyon* (Bd) and/or in *T. aestivum* (Ta). ** Symbols for generalised effects: '—' denotes a negative effect, '+' denotes a positive effect, 'N' denotes no effect, and a blank space denotes that the DON content was not tested. † No significant effect on FHB in Ta at the concentrations tested. Abbreviations: ACC (1-aminocyclopropane-1-carboxylic acid), AVG (Aminoethoxyvinylglycine hydrochloride), BABA (3-aminobutanoic acid), BR (Brassinosteroid), DON (Deoxynivalenol), GA (Gibberellic acid), GABA (4-aminobutanoic acid), IAA (Indole-3-aceticacid), JA (Jasmonic acid), JARIN-1 (Jasmonic acid inhibitor), NAA (1-Naphthaleneacetic acid), SA (Salicylic acid).

3.4 Discussion

3.4.1. Auxins Generally Improved Resistance to FHB in Wheat and *B. distachyon*

The data suggests that auxins improved resistance in wheat and *B. distachyon* but only at relatively high concentrations (Fig. 3.8C). Both IAA and NAA were most effective at 8 mM in improving FHB resistance in *B. distachyon* whereas a lower concentration of 2 mM NAA was shown to increase resistance in wheat but only in one experimental replicate (Fig. 3.9F, Fig. 3.10C). It should be pointed out that the FHB disease levels in wheat were very high (Fig. 3.10C), and this high disease pressure may have prevented the detection of any effect of treatment. For example NAA (2 mM) was most effective when symptoms were lower (15% spike infection in control, Fig. 3.9F) rather than higher symptoms (40% in control, Fig. 3.10C) at around the same time point. Nonetheless the results with *B. distachyon* and wheat supports the initial objectives in finding a compound that improves FHB resistance and provides evidence that auxins can promote resistance in cereals to *F. graminearum*. These findings support evidence by Petti and colleagues (2012) who found that exogenous IAA application reduced yield loss and general symptoms of *F. culmorum*-induced FHB in barley (Petti et al., 2012). On the contrary, there is evidence that exogenous IAA application increased *F. graminearum*-induced FHB and leaf susceptibility in wheat (Su et al., 2020). However, in this study, a lower concentration (100 µM) was used with a different method whereby severed spikes and leaves were in contact with auxin for a longer duration with no apparent time gap between auxin and *Fusarium* application. These factors may have affected the final disease outcome. The mechanism for the effects of auxin in FHB response are not clear given that *F. graminearum* can also produce IAA (Luo et al., 2016). However, my data suggest that the effects of both auxins were due to an effect on the plant response as opposed to an effect on the fungus itself (Supp. Fig. S3). Both the type of auxin and the concentration of auxin were important for the ultimate FHB resistance outcome in both host species. Phytohormones are generally physiologically effective at low concentrations (Davies, 2013). In the present study, however, low concentrations of NAA and IAA between 5 µM and 50 µM in *B. distachyon* (Fig. 3.8A and Fig. 3.8B), and 500 µM for IAA and NAA in wheat (Fig. 3.10A and Fig. 3.10B) did not induce a significant effect on FHB resistance. The high concentrations of auxin may be required

and tolerated by wheat and *B. distachyon* because of their reported low effectiveness on monocot species like wheat and *B. distachyon* (McSteen, 2010, Sauer et al., 2013). Alternatively, high concentrations may be required in order to observe an effect due to restricted uptake of the compound by the plant.

NAA was more effective than IAA in *B. distachyon* in controlling FHB as a two-fold higher concentration of IAA (8 mM) was required to have similar resistance effects as 4 mM NAA (Fig. 3.8C). IAA is the most abundant natural auxin present in plants whereas NAA is a synthetic auxin that is more stable and primarily passively diffuses into plant cells (Dunlap et al., 1986, Hošek et al., 2012, Sauer et al., 2013). Therefore, the difference in effectiveness observed is likely due to more efficient uptake of NAA through passive transport and its longer persistence. Endogenous auxin content after exogenous application of different micro- and milli- molar concentrations of auxins would need to be investigated to test this hypothesis. Despite evidence from Luo and colleagues (2016) that IAA can reduce DON accumulation *in vitro* (Luo et al., 2016), there was no significant effect of auxins on DON content of wheat grain in the current study (Fig. 3.11F).

3.4.2. The Canonical Defence Hormones SA, JA, and Ethylene Did Not Promote FHB Resistance in Wheat and *B. distachyon*

Evidence from other research groups have identified that SA increases resistance to FHB in wheat and *A. thaliana* (Makandar et al., 2010, Makandar et al., 2011, Qi et al., 2012, Sorahinobar et al., 2016). I was not able to replicate the positive FHB effect of SA at 200 µM with either a single application (Fig. 3.4A) or four applications (Fig. 3.4B) on Bd3-1 despite using the same concentration as some of these studies. It is possible that the concentration of SA was too low. Qi and colleagues (2012) found that a 2-fold higher concentration of 400 µM was effective at reducing disease susceptibility in wheat (Qi et al., 2012). To confirm this, I pre-treated wheat cv. Perigee with a higher concentration of 500 µM SA (Fig. 3.9A) but this also failed to have any significant effect on FHB symptoms. Consistent with the findings in the present study, previous research by Li and Yen (2008) showed an absence of effect on FHB resistance after a high concentration of 3 mM SA was exogenously applied to wheat spikes (Li & Yen, 2008). Therefore, the concentration of SA is likely not reason for these differences in effects. In earlier studies, SA (200 µM) was applied as a soil drench (Makandar et al., 2011, Sorahinobar et al., 2016). This application method could have more pronounced effects on resistance due to initial uptake in roots as

opposed to florets and because the phytohormone remained in contact with the roots throughout the experiment. Furthermore prolonged exposure to SA may influence the JA/ethylene dependent induced systemic resistance (ISR) pathway (Pieterse et al., 2014) which might impact the observed resistance response to FHB. Alternatively, it was reported that monocot rice (*Oryza sativa*) shoots had a higher level of endogenous SA (Chen et al., 1997). Thus, exogenous SA application could have minimal impact on the endogenous SA levels. In addition, there was no significant change in wheat grain DON content following SA application to wheat spikes prior to inoculation. This contrasts previous reports where the same concentration of SA resulted in reduced DON content (Makandar et al., 2011). The reason for this is unclear given that both lines being compared are considered susceptible (Bobwhite and Perigee), but may be again due to the difference in application of the phytohormone (Makandar et al., 2011).

Contrary to the effects of SA, 50 µm JA was found to increase susceptibility to FHB (Fig. 3.5A). This finding is similar to a study by Makandar and colleagues (2010) who identified that JA promoted leaf susceptibility to early *F. graminearum* infection in *A. thaliana* after application of 200 µM MethylJasmonate (MeJA) (Makandar et al., 2010). In contrast however, other studies found that exogenously applied JA or MeJA induced positive effects on wheat FHB resistance (Li & Yen, 2008, Qi et al., 2016, Sun et al., 2016). The reasons for these differences are unclear. Sun and colleagues (2016) pretreated wheat with a 200 µM MeJA continuously for multiple days before inoculating susceptible cv. Alondra wheat spikes (Sun et al., 2016). Qi and colleagues (2016) showed that concentrations of JA greater than 3.5 mM led to increased resistance in cv. Roblin wheat (Qi et al., 2016). These results may reflect the use of a higher concentration of JA in these studies and perhaps higher JA concentrations promote resistance while lower concentrations increase susceptibility. The difference may also be due to the application method. Qi and colleagues (2016) point-inoculated individual florets with *F. graminearum* rather than spraying the spike (Qi et al., 2016). Injecting high levels of inoculum into florets may have resulted in a by-passing or severe shortening of the biotrophic phase of infection/colonisation (Jansen et al., 2005, Brown et al., 2010). Lastly, the timing of JA application could also be important for final disease severity outcome as *A. thaliana* treated with 200 µM MeJA after inoculation was more resistant to *F. graminearum* leaf infection (Makandar et al., 2010). Together the evidence suggests that the ultimate effect of JA on FHB resistance is sensitive to many factors.

Given the negative effect of JA on FHB susceptibility in *B. distachyon*, I tested a novel inhibitor of JA biosynthesis inhibitor, JARIN-1 in wheat FHB. Meesters and colleagues (2014) describe how 10 µM to 30 µM JARIN-1 was effective at reducing JA-Ile production in *A. thaliana* (Meesters et al., 2014). Unfortunately, 300 µM JARIN-1 had no significant effect on wheat FHB resistance (Fig. 3.9B). It is possible that a reduction in wheat JA-Ile biosynthesis and signaling had no effect on wheat FHB resistance, or that the precursor JA rather than JA-Ile (Acosta & Farmer, 2010) affects the FHB resistance response. However, I cannot confidently comment on the properties of JA inhibition given that I can't be sure that JARIN-1 efficiently entered the plant and was biologically active following exogenous spraying. In order to validate any impact JARIN-1 had, endogenous JA content would need to be measured post-JARIN-1 application.

Like JA, I found that application of the plant precursor to ethylene, ACC, promoted FHB susceptibility (Fig. 3.5B). Supporting my FHB results, (Chen et al., 2009) found that ethylene (from 50 mM ethephon chemical feeding - ethylene releasing compound) promoted susceptibility to colonisation in wheat, barley, and *A. thaliana* leaf infection. However contrary to the present FHB results, evidence from (Sun et al., 2016) found that 1 mM ethephon had no effect on any wheat line tested. Contrary to both studies, (Li & Yen, 2008) found that 1 mM ethephon promoted FHB resistance in a susceptible wheat line compared to the Sumai-3 resistant control. More recently (Foroud et al., 2018) showed that ACC and ethephon application also led to increased resistance in dip-inoculated detached wheat heads. Differences in the experimental procedures may also affect important factors for ethylene response. In some reports detached head assays were performed (Chen et al., 2009, Foroud et al., 2018) which might influence senescence processes as well as defence responses. Ethephon was used instead of ACC as the ethylene treatment in some studies (Li & Yen, 2008, Chen et al., 2009, Sun et al., 2016). Foroud and colleagues (2018), however, found that ethephon and ACC had similar effects on FHB in most wheat varieties tested (Foroud et al., 2018). The gaseous hormone ethylene is known to function synergistically with JA in terms of resistance (Bari & Jones, 2009, Pieterse et al., 2012). The similar effect of these compounds on response to *F. graminearum* infection may reflect this relationship (Fig. 3.5A and Fig. 3.5B). Both JA and ACC are that are associated with resistance to necrotrophs but negatively affect resistance to biotrophs (Bari & Jones, 2009, Pieterse et al., 2012). JA and ACC were applied before inoculation, and thus would be most active during the early stages of infection. Given that *F. graminearum* is a hemibiotroph and

primarily biotrophic during initial infection (Jansen et al., 2005, Boddu et al., 2006), JA and ethylene could promote susceptibility during the biotophic phase of *F. graminearum* possibly via its antagonistic relationship with SA signalling (Robert-Seilaniantz et al., 2007).

Understanding the role of ethylene is further complicated given that I also showed that application of the ethylene inhibitor AVG (Schaller & Binder, 2017) in *B. distachyon* and wheat also promoted susceptibility. In *B. distachyon*, 35 µM AVG induced the most significant increases in susceptibility (Fig. 3.5C). In wheat the concentration most effective on *B. distachyon* FHB (35 µM) had no significant effect (Fig. 3.9C), however at higher concentrations of 175 µM in wheat and 350 µM in wheat and *B. distachyon*, there was an increased susceptibility (Fig. 3.5D, Fig. 3.9D, Fig. 3.10D). Consistent with my results, Robison and colleagues (2000) described how both 100 µM AVG and 100 µM ACC promoted *Verticillium* resistance in tomato despite these compounds having opposite effects on ethylene accumulation (Robison et al., 2001). Likewise, 2 µM AVG was shown to promote FRR resistance in *B. distachyon* roots infected with *F. culmorum* (Cass et al., 2015). Similar to my findings, Foroud and colleagues (2018) also identified that ethylene antagonists promoted susceptibility in wheat (Foroud et al., 2018). However, Foroud and colleagues (2018) did not use AVG, but rather two antagonists that affect the ethylene biosynthesis and perception. Only the receptor inhibitor (1-Methylcyclopropene, MCP) significantly increased FHB symptoms in both resistant and susceptible wheat lines whereas the biosynthesis inhibitor (Cyclopropane-1,1-dicarboxylic acid, CDA) was only effective at increasing susceptibility in the resistant wheat line (Foroud et al., 2018). Given that Bd3-1 is susceptible to FHB, there may be a different effect on resistance if an ethylene receptor inhibitor was used. Ethylene-induced susceptibility (Fig. 3.5B) may be due to the role of ethylene in accelerated senescence (van Loon et al., 2006a, Abeles et al., 2012), or in cell death with mycotoxins (Moore et al., 1999, Chen et al., 2009) which can make hosts more susceptible to pathogens feeding necrotrophically (Häffner et al., 2015). However, as a potential alternate function, inhibition of ethylene from AVG might also induce susceptibility due to some positive links ethylene has to the defense response (Robison et al., 2001, van Loon et al., 2006a). Chen and colleagues (2009) found that inhibition of ethylene signaling reduced DON accumulation in wheat (Chen et al., 2009), but in the current study, inhibition of ethylene production with AVG had no significant effect on DON production (Fig. 3.11D).

The effects of ethylene on *F. graminearum* infection has proven complex with seemingly contradictory effects between different studies and within this study. van Loon and colleagues (2006) describes how the role of ethylene is dependent on many factors such as pathogen type, timing, tissue (van Loon et al., 2006a). These reported studies into the role of ethylene in *Fusarium* infection used varying experimental procedures which likely affected the outcome on resistance since the effect of ethylene is sensitive to many factors. In conclusion, it is too early to define precisely the role of ethylene on FHB resistance. Further trials are required to test many of these seemingly important factors for the role of ethylene on *F. graminearum* resistance.

3.4.3. *trans*-Zeatin, BABA, GABA, and Brassinazole Promoted FHB Susceptibility in Wheat and *B. distachyon*

The cytokinin *trans*-zeatin had the greatest effect on *B. distachyon* FHB susceptibility compared to most other hormones (Fig. 3.7). Few studies have investigated the role of cytokinins in defense and even fewer have investigated the exogenous application of cytokinins on disease resistance. Unlike our results, other studies found that exogenous application of cytokinins zeatin, kinetin, and 6-benzylaminopurine (BAP) at similar concentrations promoted resistance in response to *Pseudomonas syringae* and *Hyaloperonospora arabidopsis* on *A. thaliana* (Choi et al., 2010, Argueso et al., 2012, Naseem et al., 2012). Similarly (Reusche et al., 2013) found that 50 µM BAP was effective at reducing *Verticillium longisporum* disease symptoms in *A. thaliana*. This apparently contradictory evidence may be due to differences in the plant and pathogen pathosystem being investigated. For example, a study by Jiang and colleagues (2013) found that exogenous application of cytokinins kinetin and iP had no significant effect on rice seedling resistance to the hemibiotrophic *M. oryzae* (Jiang et al., 2013). There could also be a concentration-dependent effect as Argueso and colleagues (2012) describes how lower concentrations of applied cytokinins were found to promote susceptibility (Argueso et al., 2012).

High concentrations of 10 mM BABA substantially increased FHB susceptibility (Fig. 3.6A). This is surprising given that BABA has been shown to increase resistance to both biotroph and necrotroph pathogens (Cohen, 2002, Ton & Mauch-Mani, 2004, Ton et al., 2005). No study to date has investigated the effect of BABA on *F. graminearum* in cereal species

however there is evidence that it can have positive effects on resistance to other *Fusarium* species (Cohen, 2002, Olivieri et al., 2009). Furthermore, the molecular mechanisms by which BABA affects resistance are still being investigated. In addition to activating the SA pathway (Conrath et al., 2006), BABA can also activate the abscisic (ABA) pathway (Ton & Mauch-Mani, 2004, Jakab et al., 2005), and there is evidence suggesting that ABA promotes FHB susceptibility (Buhrow et al., 2016, Qi et al., 2016). This is a potential reason why BABA had a negative effect on FHB resistance. BABA and cytokinins are thought to function synergistically with SA (Conrath et al., 2006, Choi et al., 2010, Argueso et al., 2012, Naseem et al., 2012, Jiang et al., 2013). The relatively large effect of BABA and *trans*-zeatin compared to the non-significant SA susceptibility (Fig. 3.6A) implies that in the *Fusarium-B. distachyon* interaction, both BABA and zeatin (Fig. 3.7) are functioning in an SA-independent manner. BABA displayed maximum susceptibility at later time points in infection (Fig. 3.6A). This suggests the effect of BABA persisted in *B. distachyon* days after application and affected *F. graminearum* colonisation rather than the initial infection.

GABA, an isomer of BABA, increased susceptibility to early infection (Fig. 3.6B). There are only a few cases where GABA has been shown to be involved in plant resistance (Solomon & Oliver, 2002, Bolton et al., 2008, Forlani et al., 2014, Yu et al., 2014). In contrast to my results, GABA was found to have no effect on resistance to the same pathogen as BABA (Cohen, 2002) or had positive effects on resistance (Yu et al., 2014). The reasons for the relatively small increase in susceptibility (Fig. 3.6B) are not clear.

Brassinazole (Brz) application is effective at reducing BR content *in planta* (Asami et al., 2000). Surprisingly, Brz application increased FHB symptoms in wheat at the lower (20 µM) concentration but had no significant effect when applied at 200 µM (Fig. 3.8H). The reasons for the greater effectiveness of the lower Brz dose are unknown and the experiment would need repeating again. Ali and colleagues found the BR epibrassinolide reduced FHB disease symptoms in barley (Ali et al., 2013). Therefore, an FHB trial with a BR instead of Brz might also promote FHB resistance. Altogether the evidence for *F. graminearum* supports the hypothesis in line with other reports that brassinosteroids are positively involved in plant defence (Nakashita et al., 2003).

Gibberellic acid was predicted to increase resistance to wheat FHB given evidence from Buhrow and colleagues (2016) that showed a decrease in spread of FHB and DON content (Buhrow et al., 2016). Unfortunately, at the same concentration, 1 mM GA had no effect

on FHB symptoms or DON content on wheat (Fig. 3.9G). Like previous research investigating SA and JA, a different application method was used. Buhrow and colleagues (2016) applied GA and *F. graminearum* per spikelet via point-inoculation (Buhrow et al., 2016). Not only would this affect the type of FHB resistance (Table 1.1), but also make cellular uptake of GA much more efficient than exogenous application of GA on the floral cuticle. To confirm this, endogenous GA content would need to be compared between point and spray application methods. I previously found that the GA biosynthesis inhibitor Prohexadione-calcium (Phx) modified FRR resistance while GA had no effect (Fig. 2.6). An FHB experiment with Phx may reveal a change in FHB symptoms that would have been masked to GA treatment if wheat shares an elevated GA content as *B. distachyon* (Kakei et al., 2015).

3.4.4. *B. distachyon* is an Effective Model for Chemically-Screening Compounds for FHB Resistance in Cereals

Overall, the results presented here on the severity of FHB in *B. distachyon* in response to phytohormones were broadly in line with those from studies on the response to auxins, JA, and ethylene in barley and *Arabidopsis* (Chen et al., 2009, Makandar et al., 2010, Petti et al., 2012, Ali et al., 2013). Compounds that were tested on wheat and *B. distachyon* generally showed a similar effect on FHB response: SA (Fig. 3.4 and Fig. 3.9A), AVG (Fig. 3.4D and Fig. 3.9D), IAA (Fig. 3.8A and Fig. 3.9E) and NAA (Fig. 3.8C to Fig. 3.9F). Any small differences in response such with AVG at 35 µM (Fig. 3.4C and Fig. 3.9C) was likely due to differences in experimental design: JIC trials with Bd3-1 were performed in climatically controlled cabinets whereas at BASF Agricultural Centre Bd21 and wheat trials were performed under Autumn glasshouse conditions. Additionally, there was instances where a higher concentration was required to induce an effect in *B. distachyon* compared to wheat (NAA - Fig. 3.8C and Fig. 3.9H). This difference may be attributed to the highly cleistogamous floral morphology of *B. distachyon* compared to cv. Perigee wheat which may make uptake of compounds more difficult (Fig. 3.2D and Fig. 3.3B). Overall, my data provides evidence that *B. distachyon* is an effective model for screening the effect of exogenous application of phytohormones on FHB resistance.

3.4.5. Conclusion

To address my initial aims, many of the compounds tested at their respective concentrations did not transiently improve FHB resistance in *B. distachyon* or wheat, and none had any significant DON reducing effects. In most cases, exogenous application phytohormones caused negative effect on FHB resistance. Most hormones, especially *trans*-zeatin and BABA, promoted susceptibility to FHB in *B. distachyon*. Brz, JA and ethylene (promoting or inhibiting compounds) also promoted susceptibility to FHB. The only phytohormone with positive effects on FHB resistance were the auxins IAA and NAA. Auxins generally improved resistance to FHB in wheat and *B. distachyon*. Lastly, SA and GA showed no significant effect on FHB in wheat or *B. distachyon*. To understand the differences in effects of each hormone on FHB in *B. distachyon*, the transcriptomic changes of phytohormone regulated genes during infection will need to be investigated (Investigated in Chapter 4).

Chapter 4 - Investigation of the Phytohormone-Associated Transcriptome Responses Between Fusarium Head Blight and Fusarium Root Rot

4.1. Introduction

Plant defence responses to pathogens are multi-layered and range from physical to molecular defences (Agrios, 2005, van Loon et al., 2006b, Bari & Jones, 2009). Effective defence depends on an appropriate and coordinated resistance response (Glazebrook, 2005, Jones & Dangl, 2006, Verhage et al., 2010). In response to infection, plants elevate defences to perceive the pathogen and counter pathogenesis. Cereals hosts have been shown to respond to infection by *Fusarium* species through the deployment of defences like deoxynivalenol (DON) detoxication, phytohormone signalling, host metabolism changes, cell wall development changes, and antimicrobial compounds such as phenylpropanoid and *PATHOGENESIS-RELATED* (*PR*) proteins (Boddu et al., 2006, Jia et al., 2009, Pasquet et al., 2014, Ameye et al., 2015, Powell et al., 2017a, Powell et al., 2017b). Successful plant defences rely upon signalling to activate appropriate downstream defence responses. In plants, these signals are often transduced using phytohormones, which are important mobile molecules that activate numerous other antimicrobial compounds, structural changes, or even programmed cell death depending on the pathogen (Glazebrook, 2005, Pieterse et al., 2012, Davies, 2013).

In Chapters 2 and 3, I determined which phytohormones induced the most significant effect on *Fusarium graminearum*-induced FHB and FRR in *B. distachyon*, respectively. I provide evidence that most phytohormones induced significant effects on resistance after exogenous application. However I showed that the phytohormones SA, JA, ethylene, cytokinin, auxin, BABA either induced similar or different effects on FHB and FRR resistance. This poses the important question as to whether these significant yet different effects between diseases is reflected in the expression of genes associated with the biosynthesis of these phytohormones and/or any phytohormones-associated genes.

This question has been touched on in previous transcriptomic studies of *Fusarium* infection. Of the canonical defence phytohormones, the consensus is that salicylic acid (SA) -regulated responses are often associated with resistance to biotrophic pathogens whereas

jasmonic acid (JA) and ethylene associated responses are linked to resistance to necrotrophic pathogens (Glazebrook, 2005, Pieterse et al., 2012). Likely owing to the hemibiotrophic lifestyle of *F. graminearum*, SA and JA/ethylene have been shown to be important for defence towards *F. graminearum* through exogenous application studies (Table 3.1) and through transcriptomic investigation (Li & Yen, 2008, Jia et al., 2009, Makandar et al., 2010, Ding et al., 2011, Makandar et al., 2011, Gottwald et al., 2012, Pasquet et al., 2014, Ameye et al., 2015, Sun et al., 2016, Hao et al., 2018, Pan et al., 2018, Wang et al., 2018a, Wang et al., 2018c, Su et al., 2020). Most other phytohormones including abscisic acid (ABA), gibberellic acid (GA), auxin, and cytokinin have been implicated in response to *F. graminearum* infection through the investigation of transcriptome change of phytohormones during *Fusarium* infection (Pasquet et al., 2014, Powell et al., 2017a, Powell et al., 2017b, Pan et al., 2018, Wang et al., 2018a, Buhrow et al., 2020, Su et al., 2020). Most studies investigating the role of phytohormones in resistance to *Fusarium* species were focussed on the disease Fusarium head blight (FHB). However Fusarium root rot (FRR) is one of multiple diseases caused by the same *Fusarium* species responsible for FHB, with evidence of unique infection pathogenesis and host resistances (Wang et al., 2015b). The transcriptome response of phytohormones to FRR infection has been investigated in response to wheat (*Triticum aestivum*) FRR (Wang et al., 2018c) but none to our knowledge have investigated *B. distachyon* transcriptome response to FRR.

One method for investigating phytohormone responses during pathogenesis is the use of transcriptomics. There have been studies that investigated *F. graminearum*-induced changes in gene transcription during infection of cereals using methods such as microarray analysis and RT-qPCR (Boddu et al., 2006, Li & Yen, 2008, Jia et al., 2009, Pasquet et al., 2014, Ameye et al., 2015, Sorahinobar et al., 2016, Sun et al., 2016). Investigating the molecular responses to disease under different biotic stresses is more accessible using ever-improving transcriptomic technologies. RNA-seq is a revolutionary transcriptome analysis technology that permits the high-throughput sequencing of the complete set of RNA transcripts in a given cell or tissue by aligning the complete transcript population to a reference genome (Wang et al., 2009). With respect to the many years of FHB research, RNA-seq has recently been deployed for wheat and barley (*Hordeum vulgare*) responses to FHB (Hofstad et al., 2016, Huang et al., 2016, Powell et al., 2017a, Pan et al., 2018, Wang et al., 2018a, Buhrow et al., 2020). Applying RNA-seq technology would be useful in

comparing the expression of defence-related or phytohormone-related genes in FHB and FRR and to identify commonalities and specificities in response to infection of the two tissues.

The genetic resources required for RNA-seq have become increasingly abundant. The genome of *B. distachyon* is very accessible as it is just 272 Mbp in size with high sequence collinearity and phylogenetic position with other cereal species, and importantly has an ever-growing array of genetic resources available (Initiative, 2010, Brkljacic et al., 2011, Kellogg, 2015, Scholthof et al., 2018, Hus et al., 2020). Importantly, *B. distachyon* is an excellent model for investigating FHB and FRR as both roots and florets are susceptible to *F. graminearum* infection (Peraldi et al., 2011, Pasquet et al., 2014). RNA-seq is also being used for Fusarium diseases in *B. distachyon*. For example, Powell and colleagues (2017b) describes how Fusarium crown rot (FCR) caused by *F. pseudograminearum* in *B. distachyon* shares common transcriptional responses to wheat such as tryptophan and phenylalanine biosynthesis (Powell et al., 2017b). Ding and colleagues also identified *F. graminearum* genes expressed during FRR infection in of *B. distachyon* (Ding et al., 2020).

I previously showed that FHB and FRR disease severity in *B. distachyon* did not always respond in a similar manner to application of a range of phytohormones, and it is unclear as to the mechanisms involved in the disease severity outcome (Chapter 2 and Chapter 3). The aim of this chapter was to uncover and compare the phytohormone-related gene transcriptome response of *B. distachyon* to FHB and FRR. This provides the first example of obtaining and comparing RNA-seq data of both FHB and FRR in *B. distachyon*. The first objective was to perform an RNA-seq analysis on *B. distachyon* FHB at mid-anthesis and seedling FRR at early time-points in infection to identify the transcription patterns and differences in response between the two diseases. For both diseases, the time of the first observation of disease symptoms was selected for sampling. For FHB, this occurred three days after inoculation while for FRR this was one day after inoculation. The second objective was to identify whether observed differences in phytohormone-related gene expression are consistent between diseased tissues over time. Selected phytohormone-related genes displaying differential expression in the RNA-seq experiment were analysed over time between FHB and FRR using a RT-qPCR time-course analysis in a separate experiment. The global difference in transcriptomes between FHB and FRR is also briefly described.

Aim: Investigate the transcriptome of *Brachypodium distachyon* in response to FHB and FRR focussing on similarities and differences in expression of phytohormone-related genes.

4.2. Materials and Methods

4.2.1. Plant Material and Growth Conditions

The *Brachypodium distachyon* accession Bd3-1 was obtained from the John Innes Centre (JIC), Norwich, UK. The Bd3-1 seed peeling preparation and stratification method was followed as described in Section 2.2.1. For FHB assays, stratified seeds were sown in 50% peat/sand and 50% John Innes mix 2, with two seeds per 8 cm^2 pot. Plants were kept for the remainder of the experiment at 22°C (20 h/4 h light/dark photoperiod, 70% humidity) in controlled environment cabinets (Snijders Scientific Jumo Imago F3000 chambers) (Peraldi et al., 2011).

4.2.2. Maintenance of Fungus and Preparation of Inoculum

For mycelium inoculum, *F. graminearum* PH1 (John Innes Centre, Norwich, UK) was maintained on 20 ml potato dextrose agar (PDA) (The PDA solution was prepared by the JIC media kitchen) in a petri-dish in a 22°C (16 h/8 h - light/dark photoperiod) in controlled environment cabinets (Snijders Labs MicroClima-series, Economic LUX chambers or in a walk-in controlled environment growth room). Seven-day old plates were then blended with 5% water (sterile diH$_2$0) for a mycelium slurry for the FRR assay. For the FHB assay, preparation of the *F. graminearum* conidial suspension from Mung Bean (MB) broth was as described in Section 3.2.2. Fresh inoculum was prepared at 1 x 10^6 conidial suspension (using a Thoma haemocytometer (Hawksley England) (Equation 3.1)) in water (sterile diH$_2$0) with 0.05 % Tween 20.

4.2.3. RNA-seq Sample Inoculation and Preparation

For FRR assays, ten stratified seeds were placed on 9 cm^2 filter paper square on a 50 ml 0.8% water (ELGA) agar inside square Petri dishes (Fig. 4.1). All plates were angled at 70° from the horizontal in covered plant propagators with wetted paper towel to maintain high humidity, and incubated for 3 days in controlled environment cabinets (Snijders Labs MicroClima-series, Economic LUX chamber or a Snijders Scientific cabinet) at 22°C (16h/8h - light/dark photoperiod) before inoculation. Roots were inoculated at three positions with

mycelial PDA slurry, or mock PDA slurry using a 10 ml syringe (Terumo syringe without needle) (Fig. 4.1). After one day, the inoculum slurry was removed once infection was visible and roots were rinsed with water. For each biological replicate, ten roots were cut (Like in Fig. 2.4) and immediately frozen in liquid nitrogen (Fig. 4.1). For FHB assays, six-week-old Bd3-1 spikes at mid-anthesis were evenly sprayed with conidial suspension using a hand-held spray bottle (Juvale fine mist atomiser spray bottles) before returning to the controlled environment cabinet dark photoperiod. Pots and matting were watered prior to inoculation. Both inoculum suspension and mock water control contained 0.05% Tween 20. Plants were all immediately covered with a large heavy-duty plastic transparent bag for 3 days to increase humidity. After three days, for each biological replicate, three infected spikelets (Fig. 3.2C-E) from randomly selected plants and pots were cut and immediately frozen in liquid nitrogen.

RNA was extracted using QIAGEN RNeasy kit as per standard protocol (Described in section 2.2.5). RNA was then immediately cleaned using Turbo DNA-free kits as per standard protocol with two rounds of Turbo DNAse (Invitrogen) treatment (Described in section 2.2.5). RNA samples were quantified and quality checked at the JIC and at Genewiz before RNA-seq using a NanoDrop 2000 Spectrophotometer (Thermo Scientific) (Internal and Genewiz), Qubit (Genewiz), and Tapestation (Genewiz).
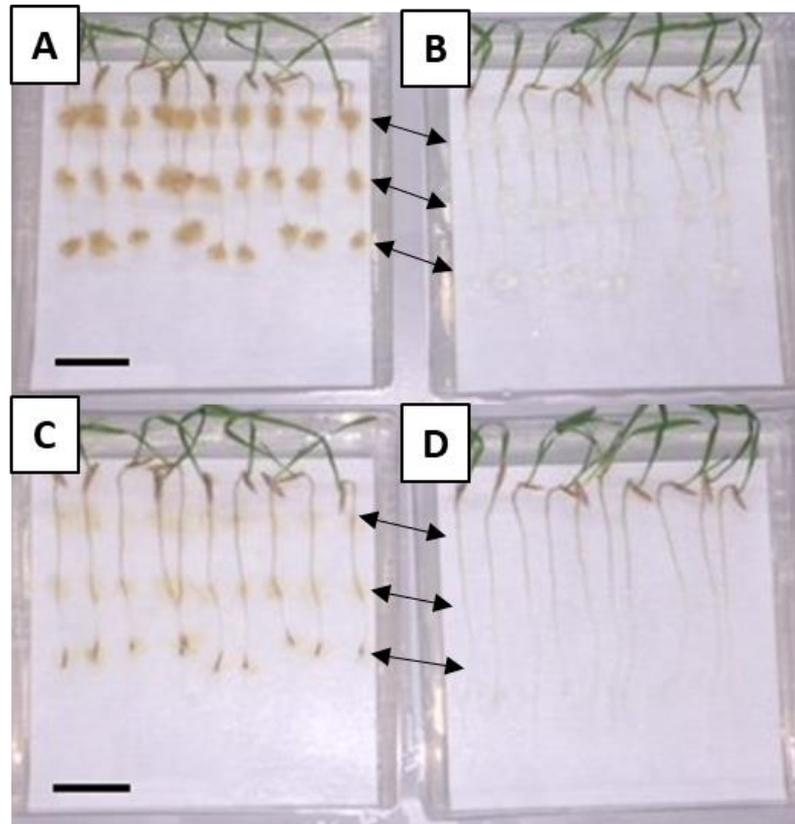
Figure 4.1. FRR assay root samples at 1 dpi for RNA-seq. Location of PDA slurry with 7-day-old *F. graminearum* mycelia (at the time of infection) (**A** and **C**) or PDA slurry mock control (**B** and **D**) on Bd3-1 roots. Removal of *F. graminearum* slurry (**C**) and control slurry (**D**) at 1 dpi. Arrows indicate the three locations where the slurry was applied on the root between treatment and control plates. Roots were cut just below the seed for each plant like in (Fig. 2.4). Scale Bars = 2 cm. Photo taken with iPhone 6 camera.

4.2.4. Library Preparation RNA-seq Bioinformatics Analysis

Library preparation was performed at Genewiz and libraries were sequenced using an Illumina HiSeq, 2x150 bp sequencing configuration with a single index per lane. RNA-seq Illumina reads FASTA data, obtained from Genewiz, was uploaded and analysed to the Galaxy web browser on the Galaxy platform (Afgan et al., 2016). The RNA-seq pipeline used is described in Figure 4.2. FastQC (G.V.0.72) was employed on sample FASTA reads as a quality check. Using Trimmomatic (G.V.0.36.5), paired-end FASTA reads trimmed with default 'Sliding window' (4 bases), 'leading' and 'trailing' ends (3 bases), and TrueSeq3 Illumina clip was used to remove Illumina adaptor sequences. Trimmed FASTA reads were quality checked again with FASTQC (G.V.0.72). Trimmed FASTA reads were aligned to the Bd21 JGI v3.0 assembly (Phytozome JGI V12.1.5 (Initiative, 2010, Goodstein et al., 2012)) using HISAT2 (G.V.2.10). Gene annotations were assigned using Stringtie v3.1 (G.V.1.3.4) with annotations (Phytozome JGI, *B. distachyon* v3.1 (Initiative, 2010, Goodstein et al.,

2012)). Stringtie gene counts for FHB and FRR were differentially compared to respective controls samples with DEseq2 (G.V.2.11.40.2). The tool Venny V2.1 was used for Venn diagrams and sorting treatment groups (Oliveros, 2018).
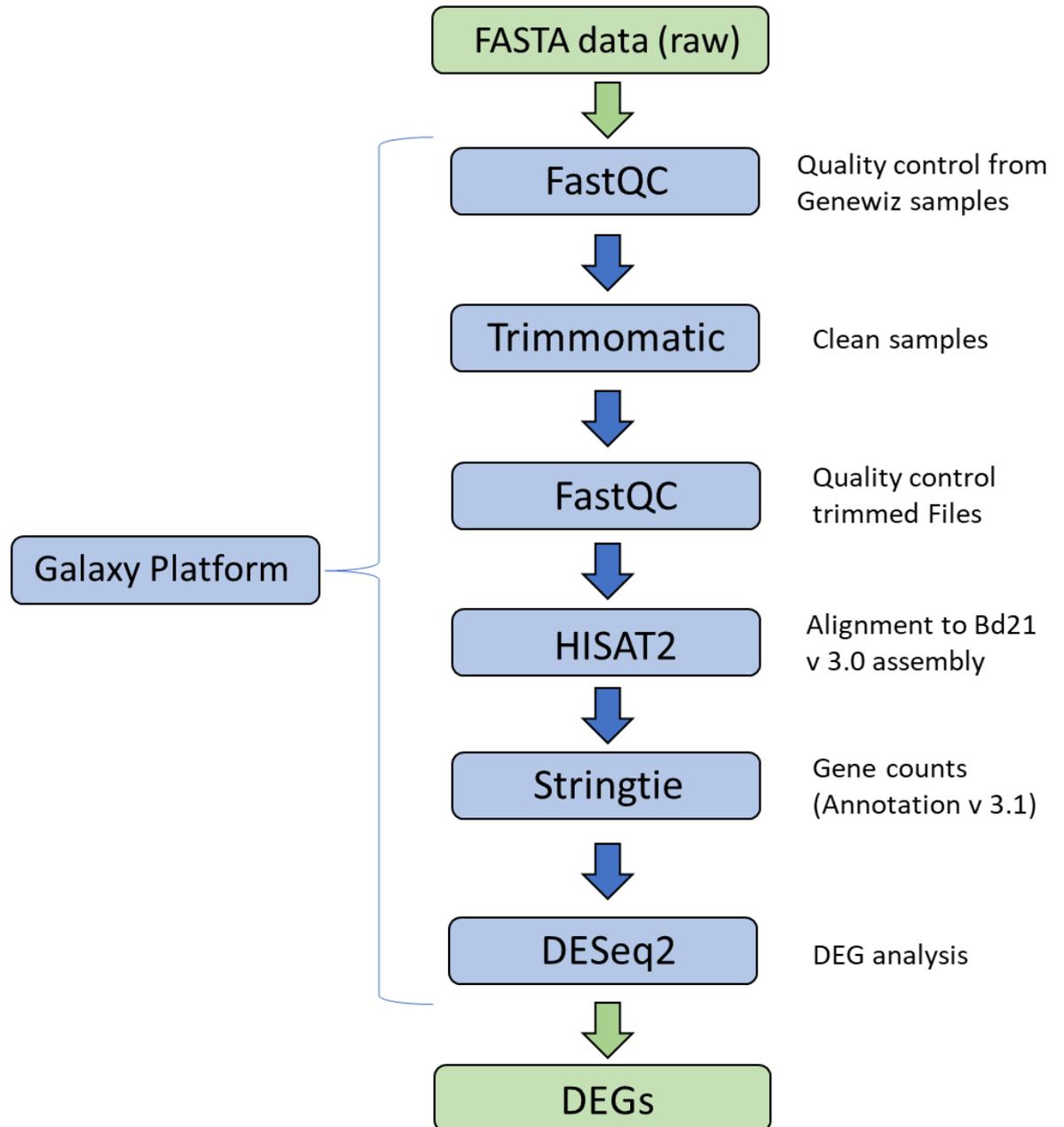
Figure 4.2. Pipeline used for RNA-seq bioinformatic analysis on Galaxy platform. Abbreviation: DEG (Differentially expressed gene). Derived from Galaxy platform guide (Afgan et al., 2016).

4.2.5. Time-Course RT-qPCR

FHB and FRR RNA samples were prepared as per previous protocols. Biological samples from different plants were harvested at 3 dpi, 5 dpi, and 7 dpi for FHB and 1 dpi, 3 dpi, 5 dpi for FRR, with at least three biological replicates per treatment and time-point. After extraction and DNase treatment, first strand synthesis of RNA was performed with Invitrogen SuperScript III Reverse Transcriptase (Invitrogen) as per standard protocol (Described in section 2.2.5). For the time-course experiment, reverse transcriptase qPCR was performed with 2 µl cDNA, 5 µl of 2x SYBR Green JumpStart Taq ReadyMix (Sigma-Aldrich), 0.6 µl of 10 µM for each primer, and water (sterile diH$_2$0) to 10 µl final volume. PCR reactions were prepared in a Framestar-480/384 well plate with BioRAD microseal B adheasive film. Thermocycling was carried out on a Roche LightCycler LC480 on SYBR green 1 scan mode with the following parameters; 300 s 95°C, 45x(94°C 10 s, 58°C (or 60°C for Bradi1g57590) 10 s, 72°C 10 s, 75C 2 s (single acquisition)), 95°C 5s, 60°C 60 s, 97°C, 40°C for 30 s. LC480 raw data was converted to Excel format with LC480 conversion software and analysed for primer efficiency and Cq values on LinRegPCR tool (Ruijter et al., 2009). Log fold changes were calculated from Cq values (Equation 2.1).

All PCR primers were ordered from Sigma Aldrich UK. Primers (Supp. Table S12) for gene targets, unless otherwise stated, were prepared using Primer 3 (Koressaar & Remm, 2007, Untergasser et al., 2012, Kõressaar et al., 2018) on a single coding sequence exonic region and avoiding untranslated regions (UTRs). Oligocalc (Kibbe, 2007) was used to verify properties and quality. Primer quality was checked following methods described in (Chapter 2.2.5, Table 2.3 and Table 2.4). Primers were tested with Bd3-1 gDNA including gel electrophoresis quality tests using methods from Section 2.2.5 (Table 2.3 and Table 2.4). The best housekeeping gene *GAPDH* (Supp. Table S12) for these samples was experimentally determined and analysed on NormFinder in GenEx V6 using cDNA obtained from both control and infected root and floret material (Both the same and different biological replicates of RNA as those sent for RNA-seq). Bd3-1 gDNA was obtained from four-week-old Bd3-1 leaf material obtained using a DNeasy Plant Mini Kit (Section 2.2.5), as well as from Bd3-1 gDNA extracted by Ms Elizabeth Bankes-Jones, and through Cetyltrimethylammonium bromide (CTAB) extraction. CTAB was prepared using 2% cetyl

trimethylammonium bromide, 1% polyvinyl pyrrolidone, 100 mM Tris-HCl, 1.4 M NaCl, 20 mM EDTA. Frozen leaf material was mixed with 1 ml of warm CTAB solution (Prepared by Ms Martha Clarke). Samples were mixed and incubated at 65°C for 90 min with frequent shaking and inverting. After incubation, 340 µl of 5 M KAC and 350 µl chloroform/IAA mix (24:1) were added to samples, mixed thoroughly, and placed in at -20°C for 15 min. Samples were then centrifuged at 13,400 rcf for 15 min and 900 µl of supernatant was added to equal volumes of pre-chilled isopropanol and shaken gently. The mixture was incubated overnight at 4°C and then centrifuged at 13,400 rcf for 10 min. Isopropanol was then discarded and the DNA pellet was washed with 1 ml of cold 70% ethanol. Samples were shaken and centrifuged at 13,400 rcf for 5 min and the ethanol was discarded. The ethanol wash was repeated again. gDNA was left to dry at room temperature and the DNA was resuspended in 30-50 µl sterile water water (sterile diH$_2$0). DNA quantity and quality were verified on a NanoDrop 2000 Spectrophotometer (Thermo Scientific).

4.2.6. Statistics, Software, and Graphs

All RNA-seq data was analysed using Microsoft Excel. All heatmaps were prepared in Rstudio (Version 1.2.1335) using 'pheatmap' and 'rcolorbrewer' packages. To make the heatmaps, the normalised transcript counts (reads) were transformed (Log2 (x + 1)) and then scaled per gene (row). The data was scaled by the standard error from the total mean denoted as a Z-score (legend). Hierarchical clustering of genes (rows) used Euclidean distance metric with complete-linkage clustering. Genes within the heatmaps with a prefix and percentage homology (Percentage of *B. distachyon* sequence that matches the orthologous sequence, Ensembl Genomes (Howe et al., 2020)) were derived from Chapter 1 (Section 1.3), the Arabidopsis Information Resource (TAIR10) database (Berardini et al., 2015), and (Yazaki et al., 2004, Jain et al., 2006a, Jain et al., 2006b, Yamaguchi, 2008, Vlot et al., 2009, Dempsey et al., 2011, Tsai et al., 2012, Lyons et al., 2013, Pearce et al., 2015, Bajguz et al., 2019). Then, if necessary, the *B. distachyon* homologue/s were identified within the Ensembl Genomes database (Howe et al., 2020) (At: *A. thaliana* TAIR10, Os: *O. sativa* RGSP-1.0, Hv: *H. vulgare* IBSC_v2Zm, or *Z. mays* B73_RefGen_v4)) and were then searched for within the RNA-seq dataset. Unless otherwise stated, the predicted functions for the remaining *B. distachyon* genes were obtained from Ensembl Genomes (Howe et al.,

2020), UniProt (Consortium, 2018), BrachyPan (Goodstein et al., 2012, Gordon et al., 2017) and *B. distachyon* v3.1 from Phytozome JGI (V12.1.5) (Initiative, 2010, Goodstein et al., 2012). Microsoft Word and PowerPoint were used for writing and diagram preparation (Fig. 4.1, Fig. 4.2). Graphs for time-course experiment (Fig. 4.11) were prepared on GraphPad Prism (V5.04). The Venn diagram (Fig. 4.4) was obtained using the Venny V2.1 tool (Oliveros, 2018). Figure 4.3 is an output from Galaxy platform DEseq2 (Afgan et al., 2016). RNA-seq statistics were outputs from Galaxy DEseq2. A standard students t-test was used for time-course RT-qPCR Cq data using Microsoft Excel.

4.3. Results

4.3.1. Fusarium Head Blight and Fusarium Root Rot Display Distinct Global Transcriptome Responses to Infection

Differential gene expression was performed on total gene counts of diseased *B. distachyon* floral and root tissues, FHB and FRR respectively, in comparison to respective mock-inoculated treatments. The time points 3 dpi and 1 dpi for FHB and FRR, respectively, represent the earliest stage at which symptoms were visible. Coverage of the Bd21 assembly was between 80-95%. With no log-fold change threshold, there were 6,158 genes significantly differentially expressed in response to FHB (p-adj < 0.05), whereas 8,568 genes were significantly differentially expressed in response to FRR (p-adj < 0.05).

The global transcriptome change patterns were substantially different between infected tissues (Fig. 4.3). The number of genes upregulated and downregulated in response to FRR were proportionally similar (Fig. 4.3B) whereas the proportion of upregulated genes for FHB infection was much greater than downregulated genes (Fig. 4.3A). However approximately 17% of the significantly differentially expressed genes in response to FRR were within the Log-fold change threshold (Fig. 4.4). On the other hand, 29% of the significantly differentially expressed genes were within the Log-fold change threshold in response to FHB (Fig. 4.4).
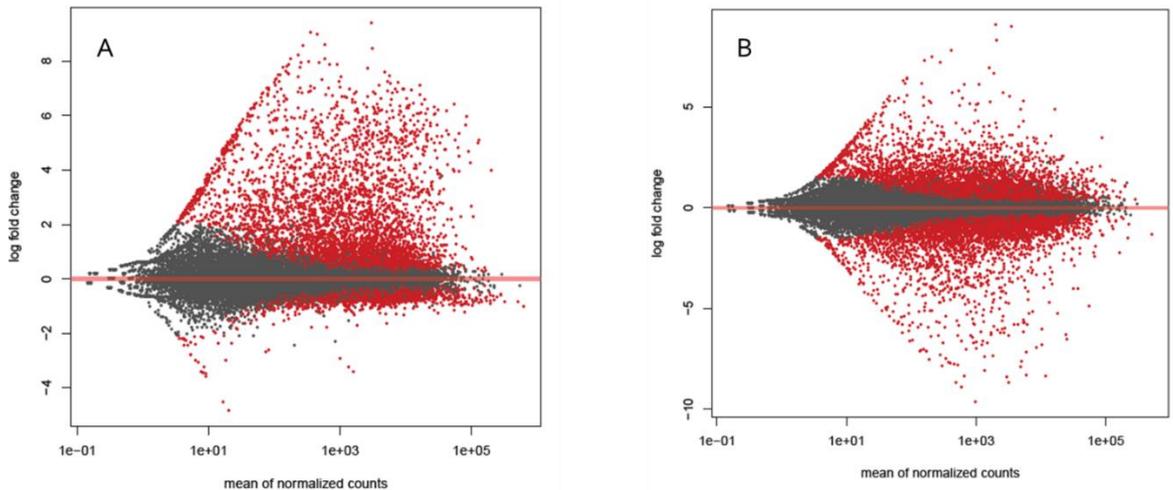
Figure 4.3. The global transcriptome changes of FHB (**A**) and FRR (**B**) compared to respective controls. Each red dot represents a single gene. Red dots denote genes significantly expressed whereas grey dots are genes below the significance threshold. Low expressor genes that might have big log fold changes are accounted for by shrinking the log fold change. The significance threshold is therefore denoted by genes with an appropriate log fold change for its respective gene count. (**A** and **B**) Output graphs from Galaxy platform DEseq2 (Afgan et al., 2016).

The transcriptome response between FHB and FRR was then compared (Fig. 4.4). There were relatively few genes that were upregulated or downregulated in response to both FHB and FRR with only 266 genes upregulated and only one gene downregulated. On the other hand, there were more genes exclusively upregulated (466 genes) and downregulated (707 genes) in response to FRR. Furthermore, half the total observable gene counts (50%) were exclusively expressed in response to FHB. A small group of 24 genes were upregulated in response to FHB and downregulated in response to FRR (Fig. 4.4). Of these 24, notable genes include a xyloglucan endotransglucosylase (Bradi3g31767), a pathogenesis-related protein 1 (Bradi3g53681), a disease resistance protein RPP13-related (Bradi1g29381), a peroxidase (Bradi5g27150), an endoglucanase (Bradi3g36210), a RING-type E3 ubiquitin transferase (Bradi3g52120), and an expansin (Bradi3g09960).
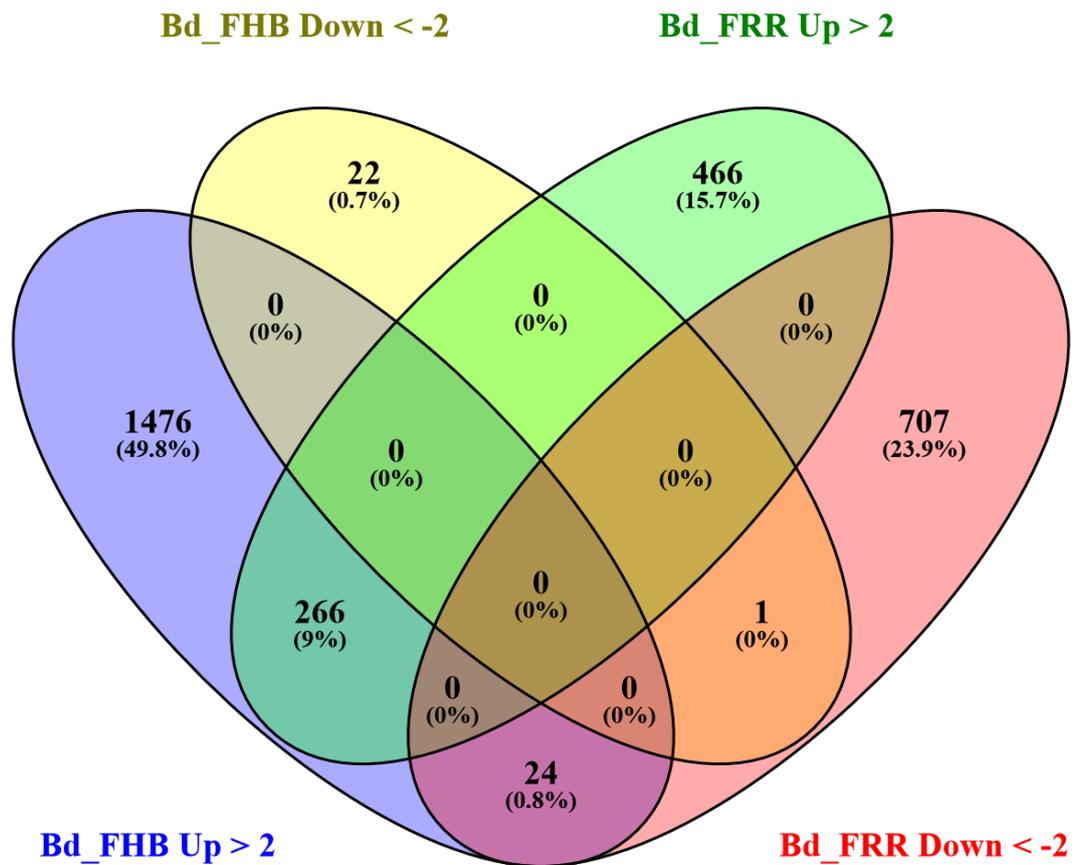
Figure 4.4. Summary of all significantly upregulated or downregulated *B. distachyon* genes in response to FHB and FRR. The threshold of -2 ≤ x ≥ 2 Log-fold change and p-adj < 0.05 was applied to all genes. Abbreviations: Bd (*B. distachyon*), Up (Upregulated), Down (Downregulated), FRR (Fusarium Root Rot), FHB (Fusarium Head Blight).

4.3.2. Phytohormone-Related Genes are Important in Response to FHB and FRR

Significantly upregulated or downregulated hormone-related *B. distachyon* genes (p-adj < 0.05) were grouped based on predicted function and compared between FHB and FRR. The predicted *B. distachyon* phytohormone genes with roles in either biosynthesis, signalling, or homeostasis found in the RNA-seq data has been presented as heatmaps (Fig. 4.5-4.10). The data signifies that the genes are likely associated with the respective phytohormone. The functional description of many of the genes identified in the heatmaps is presented in Chapter 1 under the respective phytohormone (Section 1.3.).

Unless otherwise stated, the threshold for a gene to be considered significantly responsive is having a Log2-fold expression change of greater than 2 or less than -2 and a p-adj < 0.05. In some cases, gene expression pattern exceptions were noted if they had a Log2-fold change of greater than 1 but less than 2 and were still statistically significant. Transcriptionally similar clusters of genes were identified as either exclusively responsive to FHB, exclusively responsive to FRR, or responsive to both FHB and FRR. No phytohormone-related gene in the following heatmaps was significantly downregulated in response to FHB whereas there was approximately an equal distribution of upregulated and downregulated phytohormone-related genes in response to FRR. In some cases a gene is mentioned twice in two different heatmaps as it was predicted to be responsive to both phytohormones. Many *B. distachyon* genes whose predicted function is in pathogen sensing and are believed to precede phytohormone signalling (DeYoung & Innes, 2006, Jones & Dangl, 2006, Pieterse et al., 2012) were also differentially expressed in response to FHB and FRR (Supp. Fig. S4). The phytohormones SA, JA, ethylene, auxin, cytokinins, and ABA were the main phytohormones significantly responsive to FHB and FRR in the RNA-seq data.

There were 18 predicted SA-related genes with two expression-pattern clusters (Fig. 4.5). Over half the SA-related genes (13 genes) were upregulated in response to FHB and were found in both clusters (1 and 2) that are predicted to encode *PR1-4/5* genes, chorismate synthase, *AGD2-LIKE DEFENCE RESPONSE PROTEIN* (*ALD1*), *SAR-DEFICIENT 1* (*AtSARD1*)*, NON-EXPRESSOR OF PATHOGENESIS-RELATED 4 (OsNPR4), 4-Coumarate:CoA ligase* (*4CL*), two *AtGRX480*, and *METHYLESTERASE 1* (*MES1*). However in cluster 1, Bradi3g47110 and Bradi3g47120 (phenylalanine-ammonia lyase, *AtPAL1/2/3/4*) were significantly upregulated in response to both FHB and FRR (Log2-fold change greater than 2). Furthermore Bradi4g05360 (calmodulin-binding protein 60-like g, *AtCBP60g*), Bradi2g54340 (*OsNPR4)* in cluster 2, and all of cluster 1 were significantly upregulated in response to FRR with a Log-fold change of greater than 1 but less than 2 (p-adj < 0.05). Only Bradi3g43920 (*SUPPRESSOR OF SA INSENSITIVITY* (*AtSSI2*)) and Bradi2g52110 (*MES1* predicted) and Bradi2g52000 (*GRETCHEN HAGEN 3* (*AtGH3.5*)) were exclusively upregulated in response to FRR. Lastly Bradi3g53681 encoding *PR1* was the only gene significantly upregulated in response to FHB but downregulated in response to FRR. Although Bradi1g71530 encoding *ALD1* was significantly upregulated in response to FHB it was not significantly downregulated in response to FRR (p-adj > 0.05). Overall most SA-

related genes were differentially expressed between FHB and FRR as the majority were exclusively responsive to FHB. There were also substantial differences between floral and root tissues in untreated conditions. The genes Bradi2g41070, Bradi2g08400, Bradi2g52110, Bradi3g53681, Bradi1g71530, had lower basal expression in non-inoculated spikes compared to non-inoculated roots, whereas Bradi3g43920 had a very low number of transcript counts in non-inoculated roots but not in non-inoculated spikes.
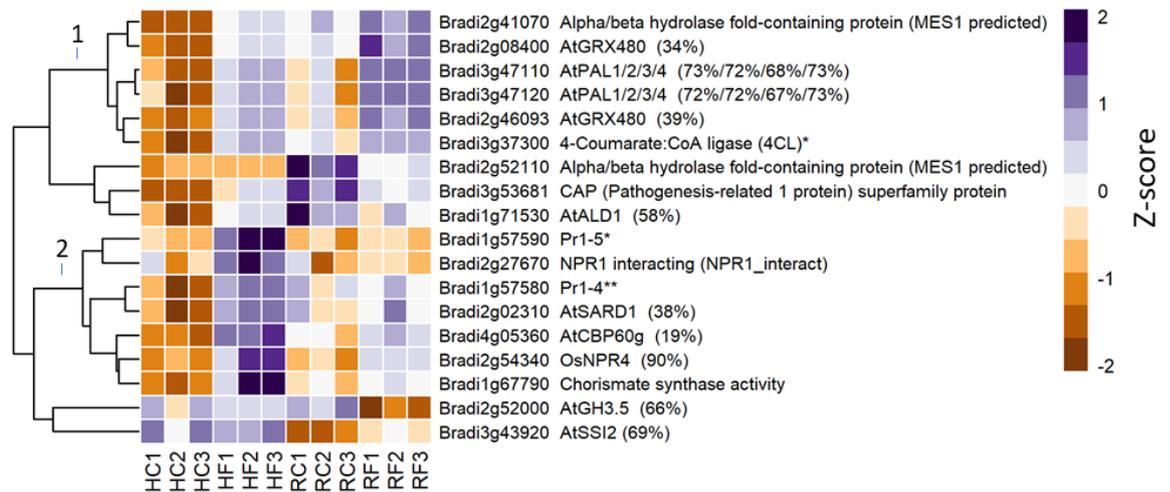
Figure 4.5. The upregulated or downregulated SA-related *B. distachyon* genes in response to FHB and FRR. These genes showed a log-fold change of -2 ≤ Log2 ≥ 2 with a p-adj < 0.05 in response to either FHB, FRR, or both. Three biological replicates for each of the four treatments are displayed as columns. The control samples (HC1-HC3, RC1-RC3) are normalised transcript counts from mock inoculated head (Water with Tween 20) and root (PDA slurry) *B. distachyon* tissues and were separately analysed through the RNA-seq pipeline with the respective inoculated sample tissues. The numbers besides the dendrogram represent cluster groups with similar expression patterns in response to FHB and FRR across samples. * Derived from (Kouzai et al., 2016). ** Derived from (Kakei et al., 2015, Kouzai et al., 2016). Some gene functions have a prefix (derived from *A. thaliana* (At) or *O. sativa* (Os)) and percentage homology (the percentage of *B. distachyon* sequence that matches the homologues sequence). Column abbreviations; HC (Head-FHB control), HF (Head-FHB fungus), RC (Root-FRR Control), RF (Root-FRR fungus).

A total 35 JA-related genes were identified with seven gene expression clusters (Fig. 4.6) which was the second largest number of phytohormone-related genes in the entire RNA-seq dataset. Most of cluster 3 (13 genes) which was the largest cluster and contained all five *12-OXOPHYTODIENOATE-REDUCTASE* (*OPR*) genes, were upregulated in response to FHB. Genes in cluster 7 (three genes) were also upregulated in response to FHB. Cluster 1

(Bradi1g12360 and Bradi1g42760) was also exclusively upregulated in response to FHB but to a lesser extent. Four genes from cluster 4 Bradi1g57590 (*PR1-5*), Bradi3g12566 and Bradi3g15084 (*ETHYLENE RESPONSE FACTOR 1/ORA59* (*AtERF1b/ORA59*)), Bradi4g20220 (*Arabidopsis thaliana* Phospholipase A1-Ialpha2) were also exclusively upregulated in response to FHB. However in cluster 3, Bradi3g37300 (*4CL*), Bradi2g08400/Bradi2g46093 (*GRX480*), Bradi3g48840 (*PAL*), Bradi1g05880 (*OPR*) and cluster 7 gene Bradi1g72610 (*JASMONATE-ZIM DOMAIN* (*JAZ*)) were slightly upregulated in response to FRR with a Log-fold change greater than 1 but less than 2 (P-adj < 0.05). Only the two genes in cluster 6 (Bradi2g14240 (*Pr1-6*) and Bradi3g43920 (*SSI2*)) were exclusively upregulated in response to FRR. Clusters 2 and 5 (four genes) were exclusively downregulated in response to FRR including two predicted *LIPOXYGENASE* (*LOX*) genes (Bradi1g09260 and Bradi1g11680), *PR1-8* (Bradi3g53637), and *JASMONATE O-METHYLTRANSFERASE* (*JMT*) (Bradi1g43080). Lastly, seven genes from cluster 4, which was the second largest cluster, contained most of the JAZ and *AtERF/ORA59* genes and were significantly upregulated in response to both FHB and FRR. Three of these genes were significantly upregulated in response to FRR with a log-fold change of greater than 1 but less than 2 (p-adj < 0.05) (Bradi3g23180 (*JAZ*), Bradi1g72590 (*JAZ*), Bradi1g00666 (*ERF1*). Generally JA-related gene expression appears important in response to both FHB and FRR. Lastly, genes in clusters 1, 2, and 3 were more highly expressed in non-inoculated roots than in non-inoculated spike tissue while genes in clusters 6 and 7 were more highly expressed in non-inoculated spike tissues than in roots.

Certain genes are associated with both JA and SA (Pieterse et al., 2012). For example Bradi2g08400 and Bradi2g46093 are homologous to *AtGRX480* which were both expressed in response to FHB and FRR but to a lesser extent in response to FRR (Log-fold change of greater than 1 but less than 2). On the other hand, the *AtSSI2* homologue Bradi3g43920 was exclusively upregulated in response to FRR (Fig. 4.5 and Fig. 4.6). Due to several significantly expressed *WRKY* genes, a separate heatmap was created encompassing all predicted *WRKY* transcription factors (Supp. Fig. S5). These included important phytohormone related *WRKY* genes such as *WRKY70*, *WRKY50*, and *WRKY45-2* (Vlot et al., 2009, Pieterse et al., 2012). For example, Bradi2g44270 encoding *WRKY45-2*, responsive to SA, JA, and ethylene (Kakei et al., 2015, Kouzai et al., 2016), was upregulated in response to FHB and to a lesser extent in FRR (Supp. Fig. S5). In most cases, *WRKY* genes were upregulated in response to both FHB and FRR (Supp. Fig. S5).
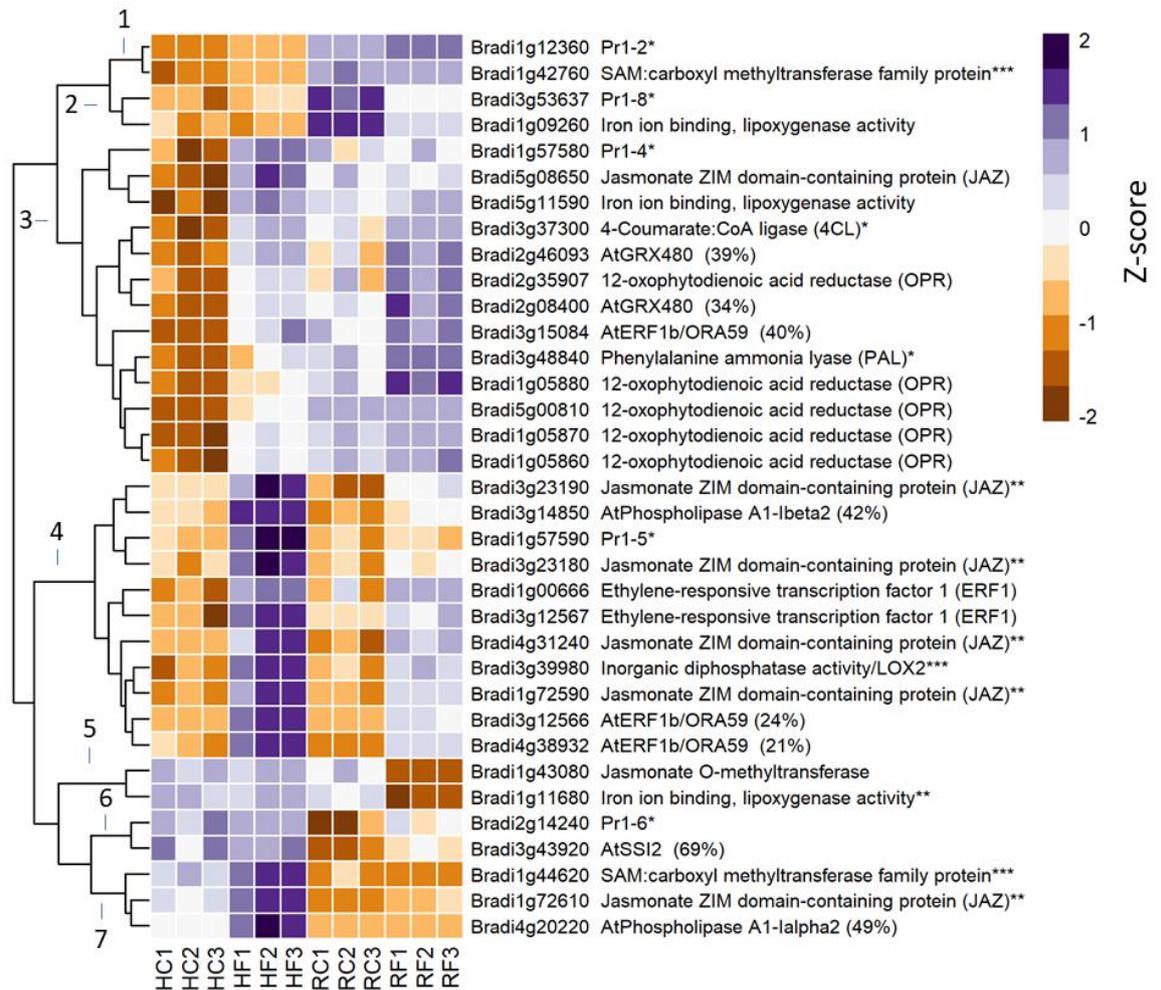
Figure 4.6. The upregulated or downregulated JA-related *B. distachyon* genes in response to FHB and FRR. These genes showed a log-fold change of -2 ≤ Log2 ≥ 2 with a p-adj < 0.05 in response to either FHB, FRR, or both. Three biological replicates for each of the four treatments are displayed as columns. The control samples (HC1-HC3, RC1-RC3) are normalised transcript counts from mock inoculated head (Water with Tween 20) and root (PDA slurry) *B. distachyon* tissues and were separately analysed through the RNA-seq pipeline with the respective inoculated sample tissues. The numbers besides the dendrogram represent cluster groups with similar expression patterns in response to FHB and FRR across samples. * Derived from (Kouzai et al., 2016). ** Also responsive to JA in (Kakei et al., 2015) with q < 0.05 and -2 ≤ Log2 ≥ 2. *** Derived from but was not significantly expressed in (Kakei et al., 2015). Some gene functions have a prefix (derived from *A. thaliana* (At)) and percentage homology (the percentage of *B. distachyon* sequence that matches the homologues sequence). Column abbreviations; HC (Head-FHB control), HF (Head-FHB fungus), RC (Root-FRR Control), RF (Root-FRR fungus).

A total of 21 ethylene-related genes with four gene clusters were identified in the RNA-seq data (Fig. 4.7). Many of the genes did not fall into clear gene expression-pattern clusters. Many of the genes in cluster 4 were exclusively upregulated in response to FHB (Fig. 4.7). In addition the gene Bradi3g12566 (*AtERF1b/ORA59*), in cluster 2 and those not found in clusters (Bradi1g57580 *PR1-4*, Bradi5g19100 *ACC SYNTHASE* (*ACS*)) were also exclusively upregulated in response to FHB. Furthermore several genes were significantly upregulated in response to FRR but had a log-fold change of less than 2: Bradi1g00666 (*ERF1*), Bradi4g41616 (*ERF15-related*), Bradi3g37300 (*4CL*), and Bradi1g10030 (*ACS11-related*) (P-adj < 0.05). Cluster 3 showed two genes primarily upregulated in response to FRR, however Bradi2g35860 (*ACC OXIDASE* (*ACO5*)) was also significantly upregulated in response to FHB (Less than log-fold 2, p-adj < 0.05). Genes in cluster 1 including Bradi3g53637 (*Pr1-8*) were exclusively downregulated in response to FRR. These three genes including Bradi2g05790 (*AtACS7*) had very high basal expression in non-inoculated root tissues compared to non-inoculated spike tissues. Lastly, cluster 2 contained four genes upregulated in response to both FHB and FRR except for Bradi3g12566 (*AtERF1b/ORA59*) which was not significantly expressed in response to FRR. Despite these identified genes, many other ethylene-related *B. distachyon* genes (Yang et al., 2015) were not significantly expressed in response to either FHB or FRR. There were 25 differentially expressed genes that encoded *APETELA2* (*AP2*) domain genes and three *ETHYLENE-RESPONSE-ELEMENT BINDING PROTEIN* (*EREBP*) genes which are also predicted to be ethylene responsive (Table 4.1) (Broekaert et al., 2006). Taken together, ethylene-related genes are the largest group of phytohormone-related genes in the RNA-seq data set. Many of the *EREBP/AP2* domain genes (nine) were significantly upregulated in response to FHB and FRR. Another five *EREBP/AP2* domain genes were similarly significantly expressed but with less than 2-fold-change in response to either FHB or FRR (p-adj < 0.05). Nine *EREBP/AP2* domain genes were exclusively upregulated in response to FHB. Lastly six *EREBP/AP2* domain genes were upregulated and two were downregulated in response to FRR. Generally ethylene-related genes were mostly responsive to FHB however many genes appeared either responsive to both FHB and FRR or were slightly upregulated in response to FRR.

146
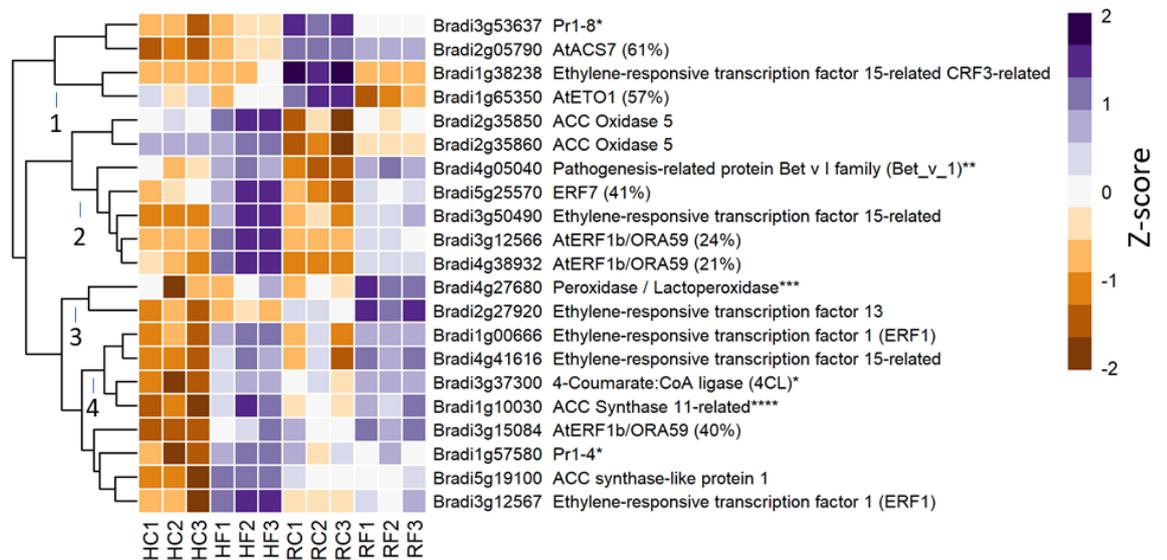
Figure 4.7. The upregulated or downregulated ethylene-related *B. distachyon* genes in response to FHB and FRR These genes showed a log-fold change of -2 ≤ Log2 ≥ 2 with a p-adj < 0.05 in response to either FHB, FRR, or both. Three biological replicates for each of the four treatments are displayed as columns. The control samples (HC1-HC3, RC1-RC3) are normalised transcript counts from mock inoculated head (Water with Tween 20) and root (PDA slurry) *B. distachyon* tissues and were separately analysed through the RNA-seq pipeline with the respective inoculated sample tissues. The numbers besides the dendrogram represent cluster groups with similar expression patterns in response to FHB and FRR across samples. * Derived from (Kouzai et al., 2016). ** Derived from (Kouzai et al., 2016) but was not significant. *** Derived from (Kakei et al., 2015). *** Derived from (Kakei et al., 2015). **** Also significantly expressed in response to ACC (Kakei et al., 2015) with q < 0.05 and -2 ≤ Log2 ≥ 2. Some gene functions have a prefix (derived from *A. thaliana* (At)) and percentage homology (the percentage of *B. distachyon* sequence that matches the homologues sequence). Column abbreviations; HC (Head-FHB control), HF (Head-FHB fungus), RC (Root-FRR Control), RF (Root-FRR fungus).

Table 4.1. Ethylene-associated AP2 domain and EREBP-like transcription factor genes that were upregulated or downregulated in response to FHB or FRR.

Gene ID	Predicted function*	FHB Log fold change**	FHB p-adj	FRR Log fold change**	FRR p-adj
Bradi2g11890	AP2 domain	3.14	<.001	3.31	<.001
Bradi4g38932	AP2 domain	5.22	<.001	3.43	<.001
Bradi1g49560	AP2 domain	2.51	0.005	2.34	0.003
Bradi2g02710	AP2 domain containing protein RAP2.8 (DREB)	2.73	0.019	2.13	<.001
Bradi3g18070	AP2 domain	5.69	<.001	3.69	<.001
Bradi2g25050	AP2 domain	8.63	<.001	3.67	<.001
Bradi2g56145	AP2 domain	2.38	<.001	3.27	<.001
Bradi5g17490	EREBP-like factor	6.23	<.001	3.11	<.001
Bradi3g12566	AP2 domain	5.33	<.001	1.15	0.195
Bradi3g15084	AP2 domain	4.05	<.001	1.13	0.103
Bradi2g57201	AP2 domain	5.57	<.001	1.55	0.017
Bradi4g38941	AP2 domain	6.62	<.001	1.40	0.09
Bradi2g24175	AP2 domain	3.06	<.001	1.15	0.005
Bradi5g21250	AP2 domain	2.09	<.001	1.20	<.001
Bradi5g25570	EREBP-like factor	2.12	<.001	1.53	<.001
Bradi3g56801	AP2 domain	2.47	<.001	-0.10	0.93
Bradi3g58015	AP2 domain	4.22	<.001	0.36	0.745
Bradi3g12565	AP2 domain	4.13	<.001	0.04	0.974
Bradi2g60340	AP2 domain	2.05	0.011	0.13	0.84
Bradi4g35650	AP2 domain	4.90	<.001	0.85	0.106
Bradi3g38140	AP2 domain	7.90	<.001	-0.28	0.758
Bradi2g17610	AP2/ERF and B3 domain-containing transcription repressor RAV2-related	1.55	<.001	2.21	<.001
Bradi3g18073	AP2 domain	1.90	0.135	3.55	<.001
Bradi2g21067	AP2 domain	0.11	0.867	2.53	<.001
Bradi3g41543	AP2 domain	0.02	0.959	2.13	<.001
Bradi1g17961	EREBP-like factor (EREBP)	-0.26	0.736	6.94	<.001
Bradi1g67350	AP2 domain	0.19	0.879	-2.55	<.001
Bradi5g17620	AP2 domain	1.17	0.438	-3.09	<.001

* All predicted functions obtained from Phytozome (V12.1.5) (Goodstein et al., 2012). **Log fold changes sorted based on expression between FHB and FRR. Abbreviations: *AP2* (*APETELA2*), EREBP (*ETHYLENE-RESPONSE-ELEMENT BINDING PROTEIN*), *ERF* (*ETHYLENE RESPONSE FACTOR 1*).

A total of 26 auxin-related genes with four main expression cluster groups were identified in the RNA-seq data (Fig. 4.8). This was the third largest hormone-related group of genes identified in the RNA-seq data set. Five genes: Bradi5g15810 (*SMALLAUXIN-UPRNAs* (*OsSAUR18*)) and Bradi4g11580 (*SUPEROOT1* (*AtSUR1*)), Bradi3g49020 (*AUXIN RESPONSE FACTOR* (*ARF*)), and Bradi1g73230 (*ARF*) were exclusively upregulated in response to FHB. Only Bradi1g13115 (*SAUR15/17*) and Bradi1g00587 (*YUCCA3/7* (*AtYUC3/7*)) from cluster 3 were exclusively upregulated in response to FRR. All genes from cluster 1, cluster 2 (together 10 genes) were exclusively downregulated in response to FRR: Three *SAUR* genes, one *GH3* gene, two *TRYPTOPHAN DECARBOXYLASE* (*OsTDC*) genes, an *AUXIN/INDOLE-3-ACETIC ACID* (*AUX/IAA*), two *ARF*, and a pin-formed transporter. Genes from cluster 3 were exclusively upregulated in response to FRR. Three genes from cluster 4 were significantly upregulated in response to FHB and FRR. Several genes (including two from cluster 4) were significantly upregulated in response to FHB and slightly in response to FRR (FRR: Log fold change of less than 2, p-adj < 0.05): Bradi2g50840 (*OsGH3-2*), Bradi1g34250 (*SAUR*), Bradi1g32400 (*SAUR*), Bradi3g14490 (*TRYPTOPHAN SYNTHASE BETA 1/2* (*AtTSB1/2*)), and Bradi3g49010 (*ARF*). Lastly, the genes in cluster 2 showed high basal expression in non-inoculated roots compared to non-inoculated spikes.
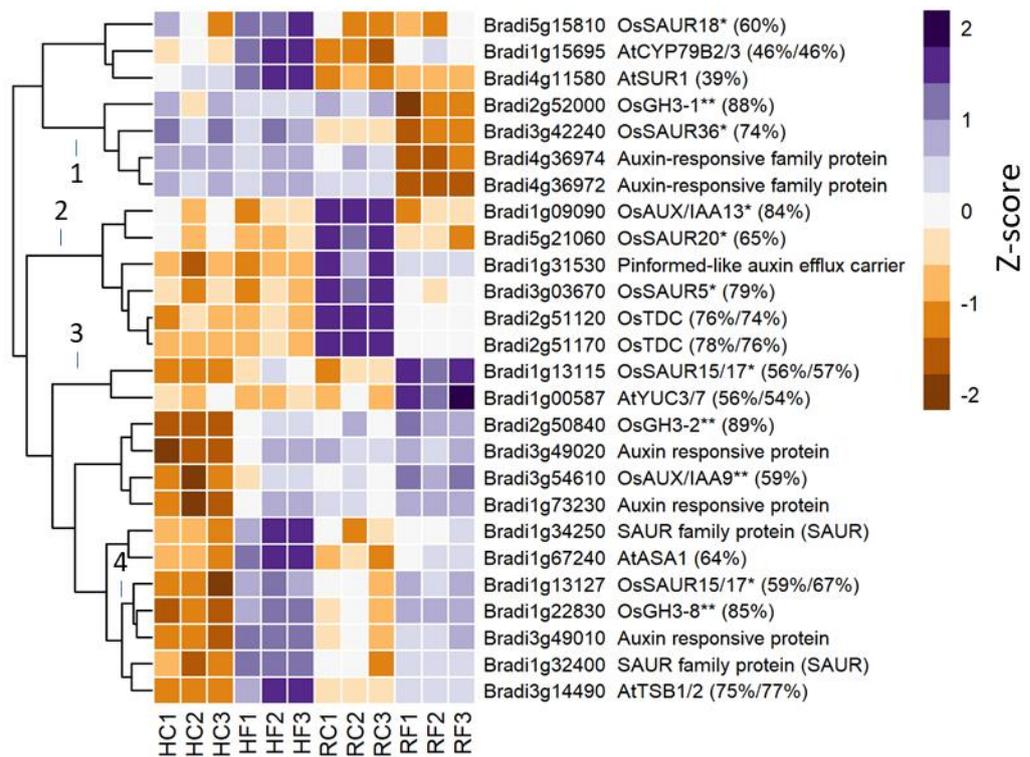
Figure 4.8. The upregulated or downregulated auxin-related *B. distachyon* genes in response to FHB and FRR. These genes showed a log-fold change of -2 ≤ Log2 ≥ 2 with a p-adj < 0.05 in response to either FHB, FRR, or both. Three biological replicates for each of the four treatments are displayed as columns. The control samples (HC1-HC3, RC1-RC3) are normalised transcript counts from mock inoculated head (Water with Tween 20) and root (PDA slurry) *B. distachyon* tissues and were separately analysed through the RNA-seq pipeline with the respective inoculated sample tissues. The numbers besides the dendrogram represent cluster groups with similar expression patterns in response to FHB and FRR across samples. * Derived from (Jain et al., 2006a, Jain et al., 2006b). ** Derived from (Jain et al., 2005, Jain et al., 2006a) and was also responsive to auxin in (Kakei et al., 2015) with q < 0.05 and -2 ≤ Log2 ≥ 2. Some gene functions have a prefix (derived from *A. thaliana* (At) or *O. sativa* (Os)) and percentage homology (the percentage of *B. distachyon* sequence that matches the homologues sequence). Column abbreviations; HC (Head-FHB control), HF (Head-FHB fungus), RC (Root-FRR Control), RF (Root-FRR fungus).

A total of 16 cytokinin-related genes with four predicted expression clusters were identified in the RNA-data (Fig. 4.9). All genes from clusters 1 and 2 (seven genes), including Bradi2g42190 (*LONELYGUY 1* (*OsLOG1*)) from cluster 3, were highly upregulated in response to FHB. In addition, the genes Bradi1g53527 (OsCytokinin-N-glucosyltransferase1), Bradi3g58670 (glucosyltransferase 85A1 (*AtUGT85A1*)), and Bradi2g60456 (cytokinin oxidase/dehydrogenase (*OsCKX4*)) were partially and significantly upregulated in response to FRR (Log2 fold change less than 2, p-adj < 0.05). The transporter Bradi5g19720 (*AtPUP11*) was exclusively upregulated in response to FRR. All genes from cluster 3 and 4 (seven genes) except for Bradi2g42190 were exclusively downregulated in response to FRR. Cluster 4 which included four rice (*Oryza sativa*) *Type A RESPONSE REGULATORS* (*OsType A-RRs*) showed the most substantial downregulation of genes out of any cytokinin-related gene in response to FRR. Lastly, the genes in cluster 3 and Bradi4g43090 and Bradi1g28726 from cluster 4 were much more highly expressed in the non-inoculated root tissues than in non-inoculated spike tissues.
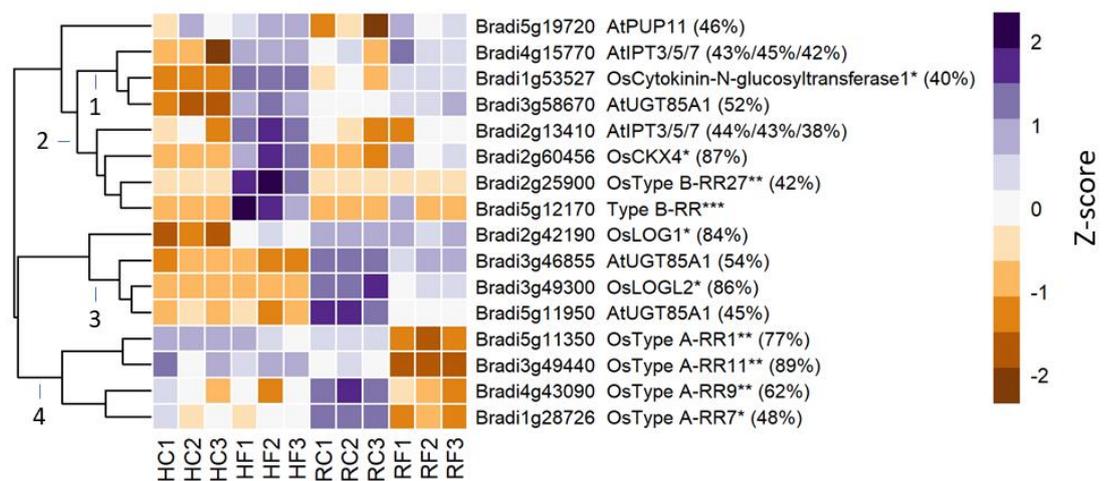
Figure 4.9. The upregulated or downregulated cytokinin-related *B. distachyon* genes in response to FHB and FRR. These genes showed a log-fold change of -2 ≤ Log2 ≥ 2 with a p-adj < 0.05 in response to either FHB, FRR, or both. Three biological replicates for each of the four treatments are displayed as columns. The control samples (HC1-HC3, RC1-RC3) are normalised transcript counts from mock inoculated head (Water with Tween 20) and root (PDA slurry) *B. distachyon* tissues and were separately analysed through the RNA-seq pipeline with the respective inoculated sample tissues. The numbers besides the dendrogram represent cluster groups with similar expression patterns in response to FHB and FRR across samples. * Derived from (Tsai et al., 2012). ** Derived from (Tsai et al., 2012) but also responsive to cytokinin in (Kakei et al., 2015). *** Derived from (Kakei et al., 2015) but was not significantly expressed. Some gene functions have a prefix (derived from *A. thaliana* (At) or *O. sativa* (Os)) and percentage homology (the percentage of *B. distachyon* sequence that matches the homologues sequence). Column abbreviations; HC (Head-FHB control), HF (Head-FHB fungus), RC (Root-FRR Control), RF (Root-FRR fungus).

A total of 18 ABA-related genes with two distinct expression clusters were identified withing the RNA-seq-data (Fig. 4.10). Genes from cluster 2 (seven genes) except for Bradi1g64987 (Xanthoxin dehydrogenase) but including Bradi5g25570 (*AtERF7*) were significantly upregulated in response to FHB. Two of the three 9-*cis*-epoxycarotenoid dioxygenase *AtNCED2/3/5/9* genes (Bradi1g13760 and Bradi1g58580) were moderately upregulated in response to FRR (Log2 fold less than 2, p -adj < 0.05). On the other hand only Bradi2g36687 (*H. vulgare* Glucose and ribitol dehydrogenase homolog 1-related) and Bradi1g17870 (Peroxidase (*OsPOX8.1*)) were exclusively upregulated in response to FRR. Three genes from cluster 1 encoding abscisic acid oxidase (*AtAAO1/2/3/4*) and two *ROOT CAP PROTEINS* (*RCP2*) genes were exclusively downregulated in response to FRR. Three genes (Bradi2g43056, Bradi2g60490, and Bradi2g60441) predicted to encode beta-glucosidase 1 (*AtBG1*), a chitinase (Bradi2g45610, *ZmPrm3*), and xanthoxin dehydrogenase (Bradi1g64987) were upregulated in response to both FHB and FRR. Generally ABA-related genes were not similarly expressed in response to FHB and FRR and most were significantly upregulated in response to FHB only. Lastly, the genes in cluster 1, including Bradi1g51850 and Bradi4g23640, were highly upregulated in non-inoculated root tissues compared to non-inoculated spike tissues.
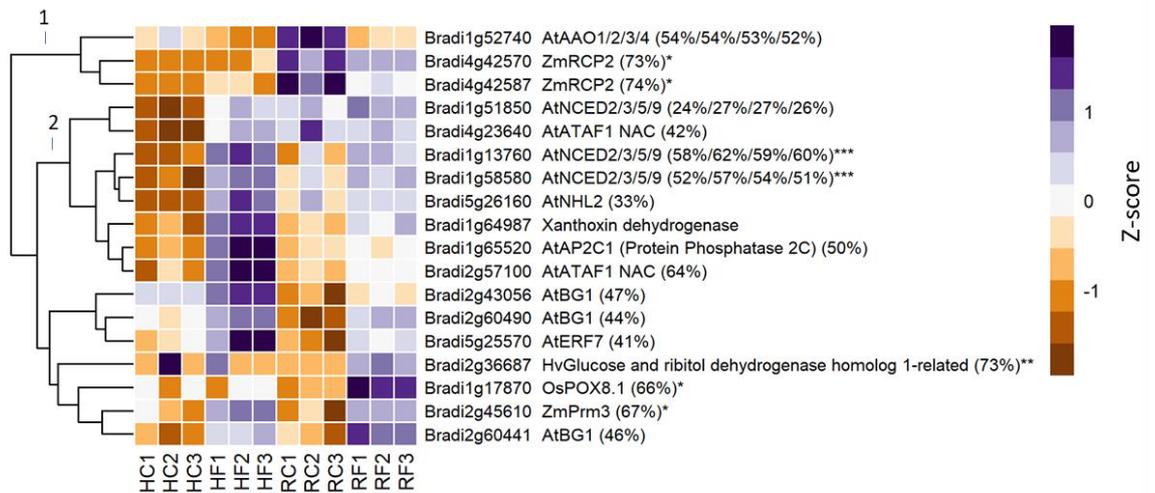
Figure 4.10. The upregulated or downregulated ABA-related *B. distachyon* genes in response to FHB and FRR. These genes showed a log-fold change of -2 ≤ Log2 ≥ 2 with a p-adj < 0.05 in response to either FHB, FRR, or both. Three biological replicates for each of the four treatments are displayed as columns. The control samples (HC1-HC3, RC1-RC3) are normalised transcript counts from mock inoculated head (Water with Tween 20) and root (PDA slurry) *B. distachyon* tissues and were separately analysed through the RNA-seq pipeline with the respective inoculated sample tissues. The numbers besides the dendrogram represent cluster groups with similar expression patterns in response to FHB and FRR across samples. * Derived from (Yazaki et al., 2004). ** Derived from (Yazaki et al., 2004) but also significantly responsive to ABA in (Kakei et al., 2015) with q < 0.05 and -2 ≤ Log2 ≥ 2. *** Also significantly expressed in response to ABA (Kakei et al., 2015). Some gene functions have a prefix (derived from *A. thaliana* (At), *O. sativa* (Os), *H. vulgare* (Hv), *Z. mays* (Zm)) and percentage homology (the percentage of *B. distachyon* sequence that matches the homologues sequence). Column abbreviations; HC (Head-FHB control), HF (Head-FHB fungus), RC (Root-FRR Control), RF (Root-FRR fungus).

There were only a few genes responsive to GA in the RNA-seq data (Table 4.2). The GA biosynthetic genes Bradi2g50280, Bradi1g59570 which encode 2-oxoglutarate-dependent dioxygenases (2OD) were upregulated and downregulated in response to FRR, respectively, but were not responsive to FHB. Bradi3g49390 which encodes the predicted homologue *OsGA2ox9* (58%) was significantly and exclusively upregulated in response to FRR. Furthermore, Bradi2g22050 which encodes the predicted epoxidation homeostasis homologue *ELONGATED UPPERMOST INTERNODE* (*OsEUI* (75%)) was only significantly upregulated in response to FHB and slightly downregulated in response to FRR (Log fold change -1.5). Despite the low number of GA-related genes responding to these treatments, the data suggests that GA biosynthesis increased in response to FRR while GA was being inactivated in response to FHB. Only one brassinosteroid (BR) gene was identified as responding to either FHB or FRR. Bradi2g22967 that encodes the predicted homologue *AtCDG1* (30%) was significantly downregulated in response to FRR. This suggests that BR was not particularly responsive to FHB and FRR in *B. distachyon*. No genes associated with 3-aminobutanoic acid (BABA) (Section 1.3.9) were identified within the RNA-seq data.

Table 4.2. Gibberellic acid and brassinosteroid-associated phytohormone genes that were upregulated or downregulated in response to FHB or FRR.

Phytohormone	Gene ID	Predicted function	FHB Log fold change	FHB p-adj	FRR Log fold change	FRR p-adj
GA	Bradi2g50280	Gibberelin 2-beta-dioxygenase 2-related*	-0.29	0.770	3.60	<0.001
GA	Bradi1g59570	Gibberelin 2-beta-dioxygenase 2-related*	0.01	0.996	-3.96	<0.001
GA	Bradi2g22050	*OsEUI* (75%)**	2.20	<0.001	-1.52	0.002
GA	Bradi3g49390	*OsGA2ox9* (58%)**	0.09	0.953	3.29	<0.001
BR	Bradi2g22967	*AtCDG1* (30%)**	-0.07	0.945	-2.28	<0.001

*Predicted gene function derived from Phytozome (V12.1.5) (Goodstein et al., 2012). ** Derived from Ensembl Genomes orthologue comparison (Howe et al., 2020). Abbreviations: At (*Arabidopsis thaliana*), BR (Brassinosteroid), CDG1 (*CONSTITUITIVE DIFFERENTIAL GROWTH1*), EUI (*ELONGATED UPPERMOST INTERNODE*), GA (Gibberellic acid), GA2ox9 (*2-OXOGLUTARATE-DEPENDENT DIOXYGENASES*), Os (*Oryza sativa*),.

For all phytohormones investigated, no respective phytohormone receptor (Section 1.3.) was identified within the RNA-seq data.

4.3.3. Time-Course Expression Analysis of Phytohormone-Related Genes

Many genes described from each heatmap generated from the RNA-seq data were differentially expressed between FHB and FRR, and others were moderately but significantly upregulated in response to FRR (Log-fold change of greater than 1 but less than 2). It remains important to confirm these findings in separate experiments and to identify whether the differential expression between FHB and FRR extended beyond the early time points obtained for the RNA-seq experiment (Section 4.2.3). FHB and FRR assays were repeated with the addition of two more later time-points for validation using RT-qPCR. Most of the phytohormone-related genes selected either had important roles with phytohormones and/or were differentially expressed between FHB and FRR in the RNA-seq experiment. Genes involved in the biosynthesis or signalling of JA, SA, auxin, and cytokinin were investigated as these represented the phytohormones showing most evidence for differential regulation in response to FHB and FRR.

In every instance (with exception of Bradi4g31240 in FRR), the expression differential at the first time point (Fig. 4.11) was like that observed in the RNA-seq experiment (Section 4.3.2.). The SA responsive Bradi2g30695 (*BdWRKY45*) (Kouzai et al., 2016) showed no change in expression in response to FHB and FRR (Fig. 4.11A). The expression at the first time point for *BdWRKY45* was like the RNA-seq results in both FHB and FRR. In response to FRR, *WRKY* was not differentially expressed at 1 dpi (p = 0.473), however it was downregulated to -2.6-fold change at 3 dpi (p = 0.012), and then to -3.9-fold change at 5 dpi (p = 0.017). *BdWRKY45* was not differentially expressed (p = 0.085) in response to FHB at 3 dpi but declined significantly (p < 0.05) by 5 dpi before returning to a similar starting expression change at 7 dpi (p = 0.244). *MES1* is important for Systemic Acquired Resistance (SAR). Like the RNA-seq data, Bradi2g52110 (*MES1*) was significantly downregulated in FRR by -1.9-fold at 1 dpi (p = 0.012). *MES1* continued to be downregulated to -4.1 fold change at 3 dpi (p < 0.001) and -3.9-fold change at 5 dpi (p < .001)(Fig. 4.11B). On the other hand,

MES1 showed no marked change in expression at any time point in FHB (p = 0.629 at 3 dpi, p = 0.551 at 5 dpi, p = at 0.375 7 dpi). *NPR4* is a repressor of SA-associated defence gene expression (Ding et al., 2018). Bradi2g54340 (*NPR4*) was more highly expressed at 1 dpi to 1.2-fold change (p = 0.026) in response to FRR (Fig. 4.11C). Expression increased by 3 dpi to 2.7-fold change (p = 0.001) before declining by 5 dpi to 1.2-fold change which was not significant (p = 0.112). In a similar trajectory, *NPR4* was significantly expressed at 3 dpi in response to FHB to over 1.3-fold change (p = 0.003), but then declined to near background levels at 5 and 7 dpi (Fig. 4.11C).

The expression of the SA and JA responsive Bradi1g57590 (*BdPR1-5*) (Kakei et al., 2015, Kouzai et al., 2016) was significantly enhanced in response to FHB and FRR (Fig. 4.11D). *PR1* expression was not significantly altered to FRR at 1 dpi (p = 0.546) but increased markedly and peaked at 3 dpi at around 5.4-fold expression (p = 0.003). By 5 dpi expression dropped to 2.5-fold change FRR (p = 0.004). In a similar trajectory as FRR, *PR1-5* in response to FHB was highly expressed at 3 dpi at 5.2-fold change (p < 0.001) and declined to non-significant levels at approximately 1.8-fold change (p = 0.180). However at 7 dpi expression of FHB increased again to over 4.5-fold upregulation (p = 0.002).

Both JA responsive genes (*LOX2 and JAZ*) showed similar expression patterns (Fig. 4.11F and Fig. 4.11E). Expression of the JA biosynthetic gene Bradi3g39980 (*LOX2*) was significantly increased at all time points in response to FRR with 2.6-fold increase at 1 dpi (p = 0.010) that increased to the peak expression at 3 dpi at approximately 7.2-fold change for FRR (p = 0.005). Subsequently expression declined to 4.6-fold change by 5 dpi (p = 0.002). On the other hand *LOX2* was only significantly responsive to FHB at 3dpi at 5.2-fold change (p < .001), after which expression rapidly declined to non-significant levels at later time points (p = 0.158 5 dpi, and 0.343 7 dpi). The JA transcription repressor Bradi4g31240 (*JAZ*) (Fig. 4.11F) was significantly downregulated at 1 dpi to -1.3-fold change in response to FRR (p = 0.013) although expression had been increased at the same time point in the RNA-seq experiment. Expression rose to approximately 2.8-fold expression at 3 dpi (p < 0.001) and the level of expression was maintained at 5 dpi (p = 0.008). In response to FHB, *JAZ* expression was elevated at 3 dpi at 2.4-fold change (p = 0.002) however by 5 dpi and 7 dpi, expression declined to non-significant levels at near 0-fold change (p = 0.927 5 dpi and p = 0.321 7 dpi).

Bradi1g09090 (*BdAUX/IAA*) is a homologue of the auxin repressor gene *OsAUX/IAA13* (Jain et al., 2006a). In response to FRR, *AUX/IAA* expression (Fig. 4.11G) was downregulated by 2.1-fold at 1 dpi (p = 0.018) and continued to decrease over time to -2.8-fold at 3 dpi (p = 0.024) and -4.1 fold at 5 dpi (p = 0.028). In contrast, although *AUX/IAA* was significantly downregulated at 3 dpi by -1.2-fold change (p = 0.050) in response to FHB, expression returned to background levels by 5 dpi and 7 dpi where expression was close to 0-fold change (p = 0.144 5 dpi, p = 0.530 7 dpi). Like the RNA-seq, *AUX/IAA* was downregulated at 3 dpi in FHB only (Fig. 4.11). The *GH3* gene is responsible for auxin homeostasis (Jain et al., 2005). In response to FRR, Bradi2g50840 (*BdGH3*) (Fig. 4.11H) was slightly upregulated to 0.9-fold expression at 1 dpi (p = 0.048). Peak expression occurred at 3 dpi with a 2.2-fold change (p = 0.010) but then declined slightly to 1.7-fold change (p = 0.020). In response to FHB, *GH3* peak expression also occurred at 3 dpi with a 2.9-fold change (p = 0.005) however expression remained high thereafter at 2.6-fold change at 5 dpi (p = 0.005) and then to 1.8-fold change at 7 dpi (p = 0.006).

The cytokinin biosynthesis gene Bradi2g42190 (*LOG1*) (orthologous to Os01g0588900 - (Tsai et al., 2012)) (Fig. 4.11I) was not differentially expressed at 1 dpi in response to FRR (p = 0.474) but increased after this time to be significant at or at 5 dpi at 1.7-fold increase (p = 0.003). In contrast, *BdLOG1* peak expression at 3 dpi in response to FHB was at 1.9-fold change (p = 0.003). Subsequently expression declined to near 0-fold change at 5 dpi (p = 0.752) and then slightly increased to 0.9-fold change at 7 dpi (p = 0.273). Like the RNA-seq analysis at the first documented time-point (Fig. 4.9), *LOG1* was exclusively expressed in FHB. The orthologue of type *OsA-RR* (Tsai et al., 2012) Bradi4g43090 (Fig. 4.11J) was significantly downregulated at all time points in response to FRR (Fig. 4.11). At 1 dpi in response to FRR, *RR9* was downregulated by -1.2-fold change (p = 0.008). Subsequently *RR9* was further downregulated at 3 dpi to -1.8-fold change (p = 0.042), and then again to -2.1-fold change at 5 dpi (p = 0.003). On the other hand, there was no significant change in expression of *RR9* in FHB at any time point (p = 0.108 3 dpi, p = 0.128 5 dpi, p = 0.912 7 dpi).

Overall the qRT-PCR fold change of differentially expressed genes was generally in accord with the RNA-seq observations at 1 dpi and 3 dpi for FRR and FHB, respectively (Fig. 4.5, Fig. 4.6, Fig. 4.8, Fig. 4.9). FRR expression at 3 dpi for Bradi1g57590, Bradi2g54340, Bradi2g50840, Bradi4g31240, Bradi3g39980 (Fig. 4.11) resembled expression levels of FHB at 3 dpi. The increased expression of genes in response to FHB tended to decline after the

first timepoint suggesting that the increase was transient. In contrast, expression of many of those genes differentially expressed in response to FRR continued to diverge from the controls overtime (Fig. 4.11).
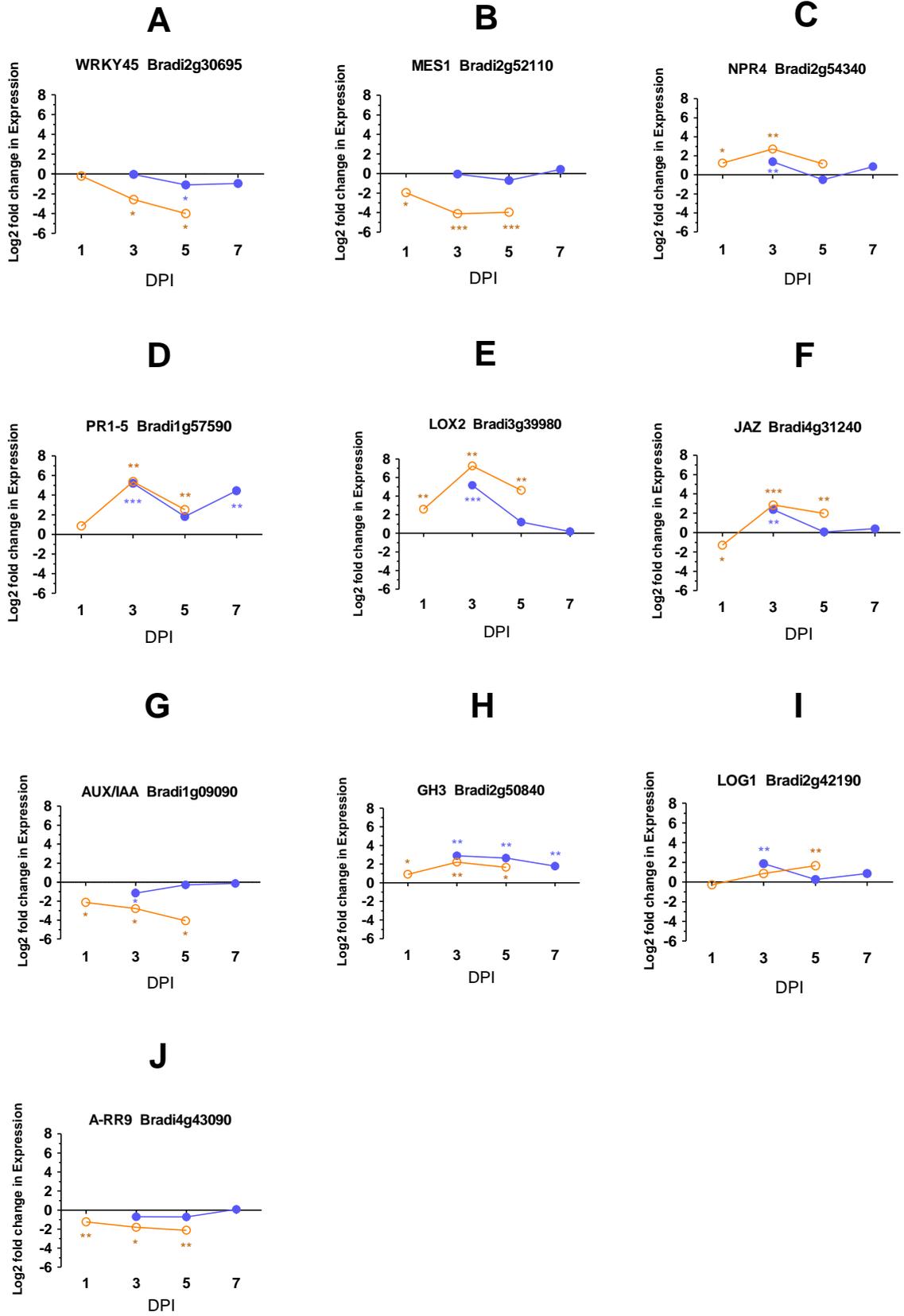
Figure 4.11. Time-course RT-qPCR on differentially expressed hormone-related genes. Gene function and ID are given for each tissue disease. Blue lines with solid circles denote FHB and orange lines with open circles denote FRR. Log values presented are calculated by comparing infected tissue against mock-inoculated treatments. Furthermore, all treatments are calculated with the reference housekeeping gene *GAPDH*. Each point is the average of three biological replicates and 2-3 technical replicates. Level of significance relative to the mock-control, Cq t-test *p<0.05, **p<0.01, *** p < 0.001.

4.4. Discussion

FHB and FRR displayed dissimilar global transcriptome changes during early infection. FRR exhibited an equal number of upregulated and downregulated genes whereas most of the genes in FHB were upregulated (Fig. 1). Likewise, FCR also displayed more upregulated genes than downregulated (Powell et al., 2017a, Powell et al., 2017b). This suggests that the transcriptional response to FHB is more like FCR than FRR. Similar to the FRR results, Chen and colleagues (2014b) identified many more repressed genes in *A. thaliana* root response to *Fusarium oxysporum* infection (Chen et al., 2014b). Most significant genes were exclusively expressed or repressed in response to FHB or FRR (Fig. 4.4). Similarly, *F. oxysporum* infection caused around half of genes to display root or leaf-specific expression in *A. thaliana* (Lyons et al., 2015). This suggests that there are substantial differences in host expression between *Fusarium*-infected tissues. Like with *A. thaliana*, *B. distachyon* roots and shoots display transcriptionally unique responses to *Fusarium* infection (Fig. 4.3-4.10). The differences between FHB and FRR were observed consistently over time for several genes (Fig. 4.11A, Fig. 4.11B, Fig. 4.11G, Fig. 4.11I, and Fig. 4.11J). Furthermore, it was observed that expression of many phytohormone-associated genes showed drastically different transcript count levels in non-inoculated *B. distachyon* spikes and roots (Fig. 4.5-4.10). Most of these genes showed a much higher level of transcript counts in non-inoculated root tissues. This reflected the tissue-specific differences in expression in response to infection for some of the genes. The similarities and differences between phytohormone-associated genes are discussed.

4.4.1. SA is Likely Not Responsive to FHB and FRR in *B. distachyon*

SA is synthesised from either the isochorismate (ICS) pathway or the PAL pathway (Lefevere et al., 2020). In the current study, SA biosynthesis regulators homologs, *AtCBP60g* and *AtSARD1*, which are key for ICS-related transcription (Zhang & Li, 2019) were both highly expressed in response to FHB but showed very limited change in FRR (Fig. 4.5). It has been reported that the ICS pathway for SA production in barley was important for leaf and floral resistance to *F. graminearum* (Hao et al., 2018). There was no ICS pathway-related

gene altered in expression in response to either FHB or FRR (Fig. 4.5) Chorismate synthase (involved in the biosynthesis of chorismate, a phenylalanine precursor) and three *PAL* genes were upregulated in response to FHB (Fig. 4.5). Similarly, the *PAL* gene Bradi3g7110 was similarly upregulated in response to *F. graminearum*-induced FHB in *B. distachyon* (Pasquet et al., 2014). However only two *PAL* genes were significantly upregulated in response to FRR (Fig. 4.5). These genes can also affect resistance as a *PAL* gene was shown to positively affect resistance to *Fusarium culmorum* in *B. distachyon* leaves and roots (Cass et al., 2015). Given the absence of ICS and the expression of PAL genes, it suggests that SA is being produced in response FHB and FRR through the PAL pathway (Lefevere et al., 2020). SA content increased in response to *F. pseudograminearum*-induced FCR in wheat at 1 dpi (Powell et al., 2017a), although PAL and chorismate synthase were not substantially expressed in response to *F. pseudograminearum*-induced FCR in *B. distachyon* (Powell et al., 2017b). The two *B. distachyon AtPAL*-like genes (Bradi3g7110 and Bradi3g7120) that were responsive to both FHB and FRR (Fig. 4.5) may also function independently of the SA pathway in *B. distachyon*. For example, a third *PAL* gene (Bradi3g48840) which was exclusively expressed in response to FHB (Fig. 4.6), was responsive to JA but not SA (Kouzai et al., 2016). The antimicrobial-related phenylpropanoid pathway, that requires *PAL* and several other genes, was induced in response to FHB and FCR in *B. distachyon* (Pasquet et al., 2014, Powell et al., 2017b), and in response to FHB in barley (Boddu et al., 2006). Numerous antimicrobial compound-related genes were identified within the RNA-seq data (Supp. Fig. S6). Therefore, the *PAL* genes (Fig. 4.5 and Fig. 4.6) may be linked to JA signalling and predominantly activated for antimicrobial defences. The same may be true for the chorismate synthase gene however this gene was not investigated for phytohormone responsiveness in (Kouzai et al., 2016).

There was evidence for FHB-responsive SA-associated signalling. The genes *PR1-4*, *Pr1-5*, Bradi3g53681 (a *PR1*), Bradi2g54340 (*NPR4*) and Bradi2g27670 (*NPR1-interacting protein*) were responsive to FHB (Fig. 4.5). In agreement with these findings, there is evidence for elevated SA-related gene expression in response to FHB (Makandar et al., 2010, Ding et al., 2011, Makandar et al., 2011, Ameye et al., 2015). However as for the *PAL* genes, *Pr1-4*, *Pr1-5*, and *4CL* (Fig. 4.5) have also been shown to be responsive to JA (Kouzai et al., 2016). There was no strong indication of SA biosynthetic or downstream signalling genes in response to either FHB or FRR at 3 dpi and 1 dpi respectively. The key SA signalling regulator *NPR1* (the homologue Bradi2g05870) which was shown to be important for FHB

resistance in wheat (Makandar et al., 2011) was not found to differentially expressed within the RNA-seq experiment (FHB: -0.4-foldchange p-adj > 0.05. FRR: 0.8-fold change, p-adj = 0.01). In fact there appeared to be a downregulation of SA-related defences in response to FRR. The gene *AtGH3.5* which acts as positive regulator for SA (Vlot et al., 2009) was exclusively downregulated in response to FRR (Fig 4.5), and *BdWRKY45* which is classed as an effective SA-responsive gene in *B. distachyon* (Kakei et al., 2015, Kouzai et al., 2016), was progressively more downregulated over time in response to FRR and slightly at 5 dpi with FHB (Fig. 4.11A). Consistent with these observations, *NPR4* was expressed in response to both FHB and FRR at 3 dpi but at a greater level in response to FRR (Fig. 4.11C). *NRP4* along with *NPR3* function as co-repressors for SA-related gene transcription (Ding et al., 2018). Together, the time course experiments suggest that SA-related transcription was suppressed in response to FHB and even more so in response to FRR. Similarly, Kidd and colleagues (2011) also identified suppression of SA-responsive *AtPR1* in roots at the latest time point following infection (Kidd et al., 2011). An absence or a very low amount of SA-related gene transcription was also identified in wheat, *B. distachyon,* and *Arabidopsis* in response to *Fusarium* infection (Kidd et al., 2011, Lyons et al., 2015, Sun et al., 2016, Powell et al., 2017b) as well as no significant increase in SA content at 3 dpi in *B. distachyon* (Powell et al., 2017b).

Despite the suggested absence of SA biosynthesis and signalling components in response to FHB and FRR, there is evidence for SA-related systemic acquired resistance (SAR) in response to FHB. SAR is an important component of SA-induced resistance (Park et al., 2007, Liu et al., 2011, Dempsey & Klessig, 2012). Several SA-responsive *BdMES1* genes, associated with SAR (Park et al., 2007, Dempsey et al., 2011) were primarily expressed in response to FHB (Fig. 4.5, Fig. 4.11B). The *MES1* enzyme methyl salicylate (MeSA) esterase converts MeSA to SA (Dempsey & Klessig, 2012). At the site of infection, a repression of *MES1* suggests higher MeSA levels and SA levels since SA can repress *MES1* leading to MeSA accumulation whereas at distal sites, an upregulation of *MES1* suggests an increase in SA content required for SAR (Liu et al., 2011, Dempsey & Klessig, 2012). This either suggests that a SAR response is occurring in distal undamaged florets, as these were also harvested among the pool of floral RNA, or that SAR initiation is being repressed in infected floral tissue. On the contrary, the recently described SAR mobile signal pipecolic acid may also be active in response to FHB as the related gene homologue *AtALD1* (Chen et al., 2018, Zhang & Li, 2019, Kachroo et al., 2020), was also expressed in *B. distachyon*

FHB (Fig. 4.5). Similarly *TaALD1* was also upregulated in response to FHB at 3 dpi (Wang et al., 2018a). Other research concluded that SAR contributed little to FHB resistance in wheat (Li & Yen, 2008) and barley (Hao et al., 2018). In contrast to the situation in FHB, the three *MES1* genes were either not substantially expressed or downregulated in response to FRR (Fig. 4.5; Fig. 4.11B). These differences in FRR compared to FHB are partly because of the much higher transcript count level of *MES1* (Bradi2g41070, Bradi2g52110) and *ALD1* (Bradi1g71530) in non-inoculated root tissues (Fig. 4.5). Therefore despite displaying higher or equal transcript counts in FRR compared to FHB, there would not be a substantial fold-change increase for FRR. The presence of SAR is unclear given the underrepresentation of SA-associated gene expression in FHB and FRR. However there is evidence that MeSA and SAR are positively regulated by JA (Truman et al., 2007, Dempsey & Klessig, 2012). Given the overrepresentation of JA-related genes as opposed to SA signalling (Fig. 4.6), JA may be involved in propagating the potential SAR signals observed. Overall, the evidence suggests that SA signalling is not initiated extensively in defence response to FHB or FRR in the susceptible accession Bd3-1. On the contrary, there is evidence that SAR-associated signalling is likely occurring in both FHB and FRR, however the mechanisms and role of SAR here are unclear.

4.4.2. JA Transcriptional Responses Are Similar between FHB and FRR

JA-related genes were one of the most overrepresented groups of phytohormone genes in the RNA-seq experiment. Numerous JA biosynthetic genes were identified (Fig. 4.6). Two phospholipase homologs (Bradi4g20220, Bradi3g14850) were upregulated in response to FHB and FRR or FHB alone, respectively. This suggests α-linolenic acid was released as a wounding response and for JA signalling (Creelman & Mullet, 1997, Pieterse et al., 2012) in response to both FHB and FRR. Numerous JA biosynthetic *LOX* (Bradi5g11590, Bradi3g39980, Bradi1g11680), and *OPR* (Bradi1g05880, Bradi5g00810, Bradi1g05870, Bradi1g05860, Bradi2g35907) genes were primarily upregulated in response to FHB (Fig. 4.6). *LOX* genes are important for JA biosynthesis (Acosta & Farmer, 2010), and the *BdLOX* gene Bradi5g11590 was found to be responsive to JA (Kakei et al., 2015). This implies that JA is being synthesised in response to FHB. *BdLOX2* (Bradi3g39980) was the only *LOX* gene significantly upregulated in response to both FHB and FRR (Fig. 4.6) and at 3 dpi for both FHB and FRR (Fig. 4.11E). Supporting the findings, the *LOX* genes Bradi3g39980

and Bradi5g11590, were also upregulated in response to FgPH1 in *B. distachyon* in response to FHB (Pasquet et al., 2014). Similarly, *TaLOX* genes were also expressed in the wheat response to *Fusarium* infection (FHB and FRR) (Li & Yen, 2008, Sun et al., 2016, Pan et al., 2018, Wang et al., 2018a, Wang et al., 2018c). The *LOX* gene Bradi1g11680 which is also responsive to JA in *B. distachyon* (Kakei et al., 2015) was downregulated in response to FRR (Fig. 4.6). This is contrary to findings that another *LOX* gene, *TaLOX2*, was highly expressed in response to FHB and FRR in the FRR-resistant and FHB-susceptible Florence-Aurore genotype (Wang et al., 2018c).

The FHB-responsive and JA biosynthetic *BdOPR* genes Bradi2g35907, Bradi1g05870, Bradi1g05880 (Fig. 4.6), were also upregulated in response to *B. distachyon* FCR (Powell et al., 2017b). In other studies the biosynthetic genes *TaOPR* genes were also expressed in the wheat response to *Fusarium* infection (FHB and FCR) (Jia et al., 2009, Sun et al., 2016, Powell et al., 2017a, Pan et al., 2018, Wang et al., 2018a, Buhrow et al., 2020). Several studies have also noted an increase JA accumulation in response to FHB (Buhrow et al., 2016, Qi et al., 2016, Powell et al., 2017b, Wang et al., 2018a) but not in response to wheat FCR (Powell et al., 2017a). However many of the *OPR* genes were not expressed in response to FRR (Fig. 4.6). The reason may be due to the earlier timing of FRR samples due to the low expression change at 1 dpi for JA-related genes *JAZ* (Bradi3g23190) and *LOX2* (Bradi3g39980) (Fig. 4.11E-F). By 3 dpi, both genes were similarly expressed between FHB and FRR at 3 dpi (Fig. 4.11E-F). The expression the majority of transcripts in barley (*H. vulgare*) peaked at 3 dpi in response to FHB (Boddu et al., 2006). Furthermore the expression of *TaLOX2* and *TaJAZ9* genes were found to peak between 2 dpi and 3 dpi in response to FRR in the FRR resistant wheat line (Wang et al., 2018c). Therefore it is likely that at later time points for FRR, many more JA-related genes will be upregulated as for FHB. Lastly, the *JMT* homologous genes involved in methyl jasmonate biosynthesis (Seo et al., 2001), Bradi1g42760 and Bradi1g44620, were exclusively upregulated in response to FHB whereas Bradi1g43080 was exclusively downregulated in response to FRR (Fig. 4.6). Despite this differential expression, these genes were not found previously to be significantly responsive to JA treatment (Kakei et al., 2015). The more pronounced log-fold change of *OPR* genes in FHB is because of the much lower transcript counts of all the *OPR* genes in non-inoculated spike tissues (Fig. 4.6). The same was also true for two *LOX* genes (Bradi5g11590 Bradi1g09260) and *JMT* homologues (Bradi1g42760) (Fig. 4.6). These JA biosynthesis genes showed higher transcript count levels in non-inoculated roots and FRR

samples (Fig. 4.6), therefore JA levels may already be elevated in both non-inoculated roots and infected roots. Overall JA-related biosynthetic genes identified were primarily expressed in response to FHB but there was evidence for JA biosynthesis at later time points in response to FRR.

Most downstream signalling JA-related genes were upregulated in response to both FHB and FRR. Six *JAZ* genes were highly upregulated in response to FHB and five of these (except for Bradi5g08650) were moderately upregulated in response to FRR (despite a few with a slightly lower fold change in response to FRR) (Fig. 4.6). *BdJAZ* (Bradi4g31240) was also similarly expressed between FHB and FRR at 3 dpi (Fig. 4.11F). *BdJAZ* (Bradi4g31240) expression was downregulated at 1 dpi in response to FRR in the time course experiment while expression had been moderately increased in the RNA-seq experiment but was similar to *LOX2* at 3 dpi (Fig. 4.11E). This may be due a lag response in the time course experiment as *JAZ* expression may have increased to regulate JA production that increased rapidly after 1 dpi from the biosynthetic *LOX2*. The *JAZ* genes Bradi3g23180, Bradi3g23190, Bradi1g72590, and Bradi4g31240 have been shown to be responsive to exogenous JA treatment in *B. distachyon* (Kakei et al., 2015). Supporting the present findings, *BdJAZ* genes Bradi3g23180, Bradi1g72610, Bradi3g23190, Bradi1g72590 were also upregulated in response to *F. graminearum* PH1 compared to the control on *B. distachyon* FHB (Pasquet et al., 2014). *TaJAZ* genes were also upregulated in response to wheat FHB (Sun et al., 2016, Pan et al., 2018, Wang et al., 2018a, Wang et al., 2018c), and *TaJAZ9* was shown to be highly expressed at 1 dpi in response to wheat FRR (Wang et al., 2018c). Together the information suggests that JA biosynthesis and signalling is similarly occurring between wheat and *B. distachyon* FHB. JA signalling is also similarly occurring between FHB and FRR in *B. distachyon* but to a greater extent in the former interaction. All the JA- related genes (*PR1-5*, *JAZ*, and *LOX2*) showed similar trends over time between FHB and FRR with peak expression for JA-related genes likely at 3 dpi (Fig. 4.11D-F).

Dissimilar responses between FHB and FRR were observed with the *PR* genes. *Pr1-2* (Bradi1g12360), *Pr1-4* (Bradi1g57580), *Pr1-5* (Bradi1g57590), and *Pr1-8* (Bradi3g53637) are reported to be JA-responsive in *B. distachyon* (Kouzai et al., 2016). While *Pr1-4* and *Pr1-5* were highly upregulated in response to FHB but showed no altered expression to FRR, expression of *Pr1-2* was moderately increased in both FHB and FRR (Fig.4.6). On the other hand *Pr1-8* expression was markedly reduced in response to FRR (Fig. 4.6). Like *OPR* genes,

the lower expression of *PR* genes (Bradi1g12360, Bradi1g57580, Bradi3g53637, and the FHB and FRR differentially expressed Bradi3g53681) in FRR is also due to the higher transcript counts in non-inoculated root tissues (Fig. 4.5 and Fig. 4.6). Given the responsiveness of most of these *PR1* genes to JA (Kouzai et al., 2016), their heightened expression may be associated with the heightened expression of *OPR* genes in non-inoculated roots (Fig. 4.6). Powell and colleagues (2017b) found *Pr1-2*, *Pr1-4*, and *Pr1-5* genes differentially expressed in *B. distachyon* in response to FHB (Powell et al., 2017b). The observed difference between FHB and FRR may also be due to a delay in observed response due to the earlier time point for FRR. For example, the gene *BdPR1-5* (Bradi1g57590) (Fig. 4.5, Fig. 4.6), was upregulated in response to both FHB and FRR by 3 dpi (Fig. 4.11D). Given Bradi1g57590 is more responsive to JA than SA (Kouzai et al., 2016), and the activation of JA-responsive genes appears to be more extensive than for SA-responsive genes (Fig. 4.5), it may be that the upregulation of *PR1-5* (Fig. 4.6) is linked to JA signalling rather than SA signalling. *TaPR1* genes were also upregulated in response to wheat FHB (Makandar et al., 2011, Wang et al., 2018a, Buhrow et al., 2020) and to *F. pseudograminerum* FCR in wheat (Powell et al., 2017a). The gene *TaPR1-4* was observed to be upregulated in response to wheat FHB in FHB resistant and susceptible lines but only in the FRR-resistant wheat line response to FRR (Wang et al., 2018c).

Lastly other genes like Bradi3g48840 (*PAL*) and Bradi3g37300 (*4CL*) which are responsive to JA (Kouzai et al., 2016) were markedly differentially expressed in response to FHB but to a lesser extent in response to FRR (Fig. 4.6). The lower increase in expression of Bradi3g48840 in FRR compared to FHB is also because of the heightened transcript levels in non-inoculated roots (Fig. 4.6) like the *PR* genes described above. *TaPAL* genes were also expressed in response to wheat FHB (Li & Yen, 2008, Buhrow et al., 2020) as well as several in response to wheat *F. pseudograminearum* FCR (Powell et al., 2017a). Furthermore the homologue encoding *AtSSI2* (Bradi3g43920) which functions as a co-factor in promoting JA signalling over SA signalling (Pieterse et al., 2012) was exclusively upregulated in response to FRR (Fig. 4.5 and Fig. 4.6). This may be because of the lower transcript counts in non-inoculated root tissues (Fig. 4.5 and Fig. 4.6). Generally the data for FHB and FRR (Fig. 4.6) supports the role of JA-related transcription in response to Fusarium diseases of cereals (Li & Yen, 2008, Makandar et al., 2010, Ding et al., 2011, Makandar et al., 2011, Gottwald et al., 2012, Pasquet et al., 2014, Ameye et al., 2015, Sun et al., 2016, Wang et al., 2018a, Wang et al., 2018c, Su et al., 2020) and *Arabidopsis* (Lyons et al., 2015). Overall, the data

from the present study suggests that JA-related transcription is increased in response to FHB and perhaps also to FRR if analysed at a later infection time point. Given the defence-response transcriptome evidence in FHB and FRR (Fig. 4.5, Fig. 4.6, and Fig. 4.11) and the evidence from other research groups, JA, rather than SA, is the predominant hormone involved in the response towards FHB and FRR in this susceptible accession of *B. distachyon*.

4.4.3. Ethylene is Likely Functioning Synergistically with JA Signalling in Both FHB and FRR

Like JA, ethylene-related genes were overrepresented for both FHB and FRR in the RNA-seq data (Fig. 4.7). The three biosynthetic *ACS* genes (Bradi5g19100, Bradi1g10030, and Bradi2g05790) were upregulated in response to FHB whereas two ACC oxidase (*ACO5*) genes Bradi2g35850 and Bradi2g35860 were upregulated in response to FHB and FRR, respectively (Fig. 4.7). The greater expression of the *ACS* gene Bradi2g05790 in FHB is because from the lower level of transcript counts in non-inoculated spike tissues as opposed to non-inoculated root tissue (Fig. 4.7). Hence the log-fold increase in response to FRR is not as large as in FHB (Fig. 4.7). Together, the evidence suggests that ethylene biosynthesis is occurring in both FHB and FRR. *TaACS* genes were expressed in wheat in response to FHB (Sun et al., 2016, Pan et al., 2018, Wang et al., 2018a, Buhrow et al., 2020) and likewise with *TaACO* (Sun et al., 2016, Buhrow et al., 2020). Furthermore ACC levels in all wheat varieties increased in response to FHB (Wang et al., 2018a). In a similar trend to JA, downstream ethylene signalling components primarily *ERF* and *AP2/EREBP* domain genes (Broekaert et al., 2006) were mostly upregulated in response to both FHB and FRR, except for Bradi1g38238 (ethylene-responsive *ERF15*-related (AP2/ERF) transcription factor) that was highly downregulated in response to FRR (Fig. 4.7). There was a significant upregulation of *AtERF1/ORA59* homologs Bradi3g12567 and Bradi4g38932 in response to both FHB and FRR (Fig. 4.7). An ERF gene Bradi3g50490 was also found to be upregulated in response to *B. distachyon* in response to FCR (Powell et al., 2017b). Similarly an ethylene responsive transcription factor was also upregulated in numerous wheat genotypes in response to FHB (Pan et al., 2018). Furthermore eight *AP2/EREBP* domain genes were upregulated in response to both FHB and FRR (Table 4.1). Likewise three *AP2* containing protein genes (Bradi2g25050, Bradi3g18070, and Bradi5g17490) which were upregulated in response to both FHB and FRR, and Bradi3g38140 responsive to FHB exclusively (Table

4.1) have previously been show to increase in expression in response to FgPH1 FHB in *B. distachyon* (Pasquet et al., 2014).

Ethylene functions synergistically with JA signalling in plants by prioritizing JA signalling and fine-tuning resistance to necrotrophic pathogens (Bari & Jones, 2009, Pieterse et al., 2012). *ERF* transcription factors are also involved in the necrotrophic pathogen specialisation from JA signalling and *ERF1/ORA59* functions in JA/ethylene synergism (Lorenzo et al., 2003, McGrath et al., 2005, Pieterse et al., 2012). Given the abundance of ethylene-related transcription factors (Fig. 4.7 and Table 4.1) the data suggests that the ethylene branch of JA signalling is activated in response to both FHB and FRR and that the JA/ethylene synergism is important in FHB and FRR response. Many core ethylene signalling genes in *B. distachyon*, like the ethylene receptors, were identified from *Arabidopsis* homologues (Yang et al., 2015). However all the *B. distachyon* genes described by Yang and colleagues (2015) were not expressed in response to FHB and FRR (Data not shown, Log-fold change $-2 > x \leq 2$ and in most cases p-adj > 0.05). Lyons and colleagues (2015) also described limited expression of ethylene in response to *F. oxysporum* infection of *A. thaliana* (Lyons et al., 2015). Furthermore, the two *B. distachyon* ethylene-responsive exclusive genes identified by (Kouzai et al., 2016) were not expressed in response to FHB or FRR. Overall, the data suggests that the role of ethylene in response to FHB and FRR is predominantly for JA synergism and prioritisation. JA and ethylene expression were found to be co-occurring in *B. distachyon* in response to FHB (Pasquet et al., 2014), and wheat FHB (Li & Yen, 2008, Jia et al., 2009, Gottwald et al., 2012). In summary, the data suggests that ethylene signalling is activated in response to FHB and FRR, but it is likely having a more supportive role with JA signalling towards the FHB and FRR defence response.

4.4.4. Auxin Transcription is Important for Response to FHB and FRR

Numerous auxin-related genes were differentially expressed between FHB and FRR. The genes Bradi1g67240 (*ANTHRANILATE SYNTHASE ALPHA SUNUNIT 1* (*AtASA1*)), Bradi3g14490 (*AtTSB1/2*), Bradi1g15695 (*CYTOCHROME P450 B2/3* (*CYP79B2/3*)) were upregulated in response to both FHB and FRR (Fig. 4.8). There are four IAA biosynthetic pathways in Arabidopsis, and *CYP79B2*/3 is associated with the indole-3-acetonitrile (IAN) pathway for auxin biosynthesis (Zhao, 2014, Morffy & Strader, 2020). This suggests that the auxin precursor tryptophan and the final downstream product IAA are being synthesised in response to both FHB and FRR through the IAN pathway (Morffy & Strader, 2020).

However, the YUC pathway may also be functional in response to FRR given the exclusive upregulation of Bradi1g00587 (*AtYUC3/7*) in response to FRR (Fig. 4.8). The tryptamine (TAM) pathway appeared repressed in response to FRR given the strong downregulation of Bradi2g51120 and Bradi2g51170 (*OsTDC*) in response to FRR (Fig. 4.8) (Morffy & Strader, 2020). This downregulation is more pronounced due to the very high transcript counts in in non-inoculated root tissues compared to spike tissues (Fig. 4.8) which indicates a heightened expression in non-inoculated root tissue. The RNA-seq data indicates that auxin biosynthesis generally increases in response to FHB and FRR and it would be expected that this would result in a higher content of auxin in *B. distachyon* tissues infected with FHB and FRR. This outcome is supported by the observation of IAA and conjugated IAA in response to FHB infection in a susceptible wheat line (Qi et al., 2016), and in Sumai3 in response to *F. graminearum* FHB at 4 dpi which was accompanied by an upregulation of auxin biosynthesis genes (Wang et al., 2018a). However, an increase in auxin content has not been reported in all studies. No significant change of auxin content was observed in resistant or susceptible wheat lines in response to FHB in the study of Buhrow and colleagues (Buhrow et al., 2016).

The main differentially expressed auxin-related signalling and homeostasis genes included *AUX/IAA*, *GH3*, *ARF*, and *SAUR* genes. *AUX/IAAs* (*OsIAA*) are one of two co-receptors that repress *AUXIN RESPONSE FACTORS* (ARFs) that control transcription of auxin-regulated genes in a concentration dependent manner (Hagen & Guilfoyle, 2002, Sauer et al., 2013, Nemhauser, 2018). Bradi3g54610 (*OsIAA9* orthologue) was upregulated in response to both FHB and FRR (Fig. 4.8). The upregulation of the ARF repressor *AUX/IAA* may be a negative feedback mechanism to dampen the heightened levels of auxin. This is because Bradi3g54610 was highly responsive to auxin treatment in *B. distachyon* (Kakei et al., 2015). Similarly, Jain and colleagues (2006a) showed that *OsIAA9* was the most upregulated to exogenous synthetic auxin and displayed relatively similar mRNA contents in different tissues (Jain et al., 2006a). The *OsIAA13* (*AUX/IAA13*) homologue Bradi1g09090 was significantly repressed in response to FRR (Fig. 4.8) and only slightly repressed at one time point in FHB (Fig. 4.11G). However *OsIAA13* in rice was not substantially responsive to synthetic auxin (Jain et al., 2006a) nor in *B. distachyon* (Kakei et al., 2015). Its function was localised to root tissue and has likely functions in root growth and development (Liscum & Reed, 2002). Root growth was affected after FRR infection (Fig. 4.1) so exclusive downregulation in roots may be linked to this (Fig. 4.11G). The AUX/IAA proteins form

structures with ARF transcription factors leading to inhibition of auxin-related transcription (Sauer et al., 2013). In the RNA-seq experiment carried out here, there was an absence of altered expression of *OsARF* homologues or the *BdARF* genes described in (Zhou et al., 2018) in response to either FHB or FRR. There were however three different *ARFs*: Bradi3g49010, Bradi3g49020, and Bradi1g73230, which were exclusively upregulated in response to FHB (Fig. 4.8). Two of these, Bradi3g49010 and Bradi3g49020, were also expressed in *B. distachyon* in response to *F. graminearum* isolate PH1 FHB (Pasquet et al., 2014).

GH3 genes, encoding IAA-amido synthetases, conjugate IAA with amino acids which maintains auxin homeostasis (Staswick et al., 2005). Both Bradi1g22830 (*OsGH3-8*) and Bradi2g50840 (*OsGH3-2*) (Jain et al., 2005) were expressed in response to both FHB and FRR (Fig. 4.8 and Fig. 4.11H). Both the rice homologs of these *B. distachyon* genes were responsive to the synthetic auxin 2,4-D (Jain et al., 2005) and the *B. distachyon* genes were significantly responsive to IAA in *B. distachyon* (Kakei et al., 2015). The expression of these *GH3* genes may be linked to the Bd3-1 defence response to *F. graminearum*. For example, the rice homologue of Bradi2g50840, *OsGH3-2*, was responsive to IAA and positively affected basal resistance to the fungus *Magnaporthe grisea* in rice (Fu et al., 2011). Overexpression of *GH3-8* was also linked to increased resistance to *X. oryzae* and it was suggested that this was partly due to expansin repression (Ding et al., 2008). Contrary to the other two *GH3* genes, Bradi2g52000 (*OsGH3-1*) was exclusively downregulated in response to FRR (Fig. 4.8) yet this gene was also auxin responsive in rice and *B. distachyon* (Jain et al., 2005, Kakei et al., 2015) and associated with resistance to *M. grisea* in rice (Domingo et al., 2009). It is unclear why there is differential expression of the three *GH3* auxin-related genes. Generally, given the upregulation of auxin biosynthesis genes, auxin responsive genes (*ARF*s), auxin repressors (*AUX/IAA*), and *GH3* genes, the data suggests that FHB and FRR affected processes that interfere with auxin homeostasis within the two tissues.

The two genes Bradi4g36974 and Bradi4g36972 which were exclusively and highly downregulated in response to FRR (Fig. 4.8) are predicted homologs of *AtSAUR62/63/64*. In fact many of the differentially expressed auxin-related genes were identified as *SAUR* genes (Fig. 3). Many of the *SAUR* genes were downregulated in response to FRR except for Bradi1g13115 and Bradi1g13127 (homologs of *OsSAUR15/17*) (Fig. 4.8). One *SAUR* genes,

Bradi1g32400 (*SAUR26*) (Fig. 4.8), was also found to be upregulated in *B. distachyon* in response to *F. graminearum* PH1 FHB (Pasquet et al., 2014). Of all the *SAUR* genes described (Fig. 4.8), only Bradi3g03670 (*OsSAUR5*) was responsive to synthetic auxin in rice and possessed an auxin responsive element (Jain et al., 2006b). *OsSAUR5* was shown to be root tissue localised in rice (Jain et al., 2006b). Bradi3g03670 was downregulated exclusively in response to FRR (Fig. 4.8). If Bradi3g03670 (homologue *OsSAUR5*) is also root localised in *B. distachyon*, then is may explain the exclusive downregulation of Bradi3g03670 (homologue *OsSAUR5*) in *B. distachyon* FRR (Fig. 4.8). The other *SAUR* genes may possess other functions (Ren & Gray, 2015). For example, 9 out of the 17 *SAUR* genes identified in wheat spikes infected with *F. graminearum* were associated with susceptibility in wheat (Pan et al., 2018). Similar to *OsSAUR*5, root localised *AtPIN3* (*pinformed inflorescence*) homologue Bradi1g31530 which regulates auxin transport and development (Bandyopadhyay et al., 2007) was downregulated in response to FRR (Fig 4.7). In support of this finding, influx and efflux auxin genes were also shown to be downregulated in all wheat genotypes tested in response to FHB (Pan et al., 2018). Similar to the FRR results but contrasting to those for FHB (Fig. 4.8), there was downregulation of auxin signalling genes in response to wheat FHB, which was associated with susceptibility (Wang et al., 2018a). It is important to note that the *SAUR* genes (Bradi3g03670 (*SAUR5*), Bradi5g21060 (*SAUR20*)) and *PIN3* (Bradi1g31530), had very high transcript count levels in non-inoculated roots compared to non-inoculated spikes (Fig. 4.8) which partly explains their more apparent downregulated in roots. Together the data suggests there was differential expression between FHB and FRR for auxin-related gene signalling which is partly explained by different levels of expression between non-inoculated tissues.

Biosynthesis and signalling of auxins can affect resistance to plant pathogens (Bari & Jones, 2009, Kazan & Manners, 2009). Auxin-related genes were substantially affected in response to both FHB and FRR (Fig. 4.8 and Fig 4.11H-I). In support of my findings, Lyons and colleagues (2015) identified using RNA-seq analysis that auxins were important components of defence responses to *F. oxysporum* in both shoot and root tissues (Lyons et al., 2015). In summary, based on the expression patterns of genes (Fig. 4.8) and associated function and sensitivity to auxins (Jain et al., 2005, Jain et al., 2006a, Jain et al., 2006b), auxin levels are predicted to be elevated in response to both FHB and FRR. There are also similarities between FHB and FRR in interference with auxin homeostasis-associated genes

but also differences in auxin signalling with an upregulation in response to FHB but a suppression in response to FRR.

4.4.5. Cytokinin-Related Gene Transcription is Different between FHB and FRR

Expression of *B. distachyon* cytokinin-related genes generally increased in response to FHB but decreased in response to FRR (Fig. 4.9). Two cytokinin biosynthesis *ISOPENTENYLTRANSFERASE* (*IPT*) homologs Bradi2g13410 and Bradi4g15770 were exclusively upregulated in response to FHB (Fig. 4.9). Likewise, Bradi2g13410 was also found to be upregulated in *B. distachyon* in response to *F. graminearum* PH1 FHB (Pasquet et al., 2014). The cytokinin biosynthetic *LOG* genes showed differential expression with Bradi2g42190 (*OsLOG1*) exclusively upregulated in response to FHB, whereas Bradi3g49300 (*OsLOGL2*) was exclusively downregulated in response to FRR (Fig. 4.9). Together this would suggest that cytokinin content increases in FHB more than in FRR. However, Bradi2g42190 (*OsLOG1*) eventually displayed high levels of expression in response to FRR comparable to FHB at 5 dpi (Fig. 4.11I). This suggests cytokinin biosynthesis is very delayed in response to FRR compared to FHB and that the response at later time points is relatively similar. Bradi3g49300 (*OsLOGL2*) might show a similar expression pattern and become upregulated at later time points in response to FRR. Furthermore, Bradi3g49300 showed higher levels of transcript counts in non-inoculated roots leading to significant downregulation in FRR (Fig. 4.9). This partly explains the differential expression of *LOG* genes at the early time points. Other important genes include Bradi2g60456 which is the *B. distachyon* homologue of a cytokinin homeostasis regulator *OsCKX4* (Albrecht & Argueso, 2017, Márquez-López et al., 2019) which was also exclusively expressed in response to FHB (Fig. 4.9). Unlike *LOG1* and *LOGL2*, *CKX4* was transcriptionally responsive to cytokinin treatment in rice roots and shoots (Tsai et al., 2012). Additionally a cytokinin 7-beta-glucosyltransferase (Bradi1g53527), was exclusively upregulated in response to FHB (Fig. 4.9) and this gene was similarly upregulated in response to FCR in *B. distachyon* (Powell et al., 2017b).

There was an absence of altered expression of *B. distachyon* cytokinin receptors orthologous to *Arabidopsis* or rice genes (Nongpiur et al., 2012, Tsai et al., 2012) identified in the RNA-seq dataset. However type A and B *RRs* were the most responsive cytokinin-related genes. Only two *type B RR*s, Bradi2g25900 (*OsRR27*) and Bradi5g12170 were exclusively upregulated in response to FHB (Fig. 4.9). *Type B RRs* activate target genes in

the presence of cytokinin (Nongpiur et al., 2012). However both the *type B RRs* identified were not reported to be responsive to cytokinin in *B. distachyon* (Kakei et al., 2015). Downstream of *type B RR*, *type A RRs* function as negative regulators of cytokinin response (To et al., 2007, Kieber & Schaller, 2018). Surprisingly *type A RR*s were highly and exclusively downregulated in response to FRR (Fig. 4.9). Bradi4g43090 homologue of Os*RR9/10* was significantly downregulated in response to FRR at all time points but not to FHB (Fig. 4.11J). Of the *type A RR* genes identified (Fig. 4.9), the homologues of Bradi5g11350 and Bradi4g43090, *OsRR1* and *OsRR9/10*, respectively, have been shown to be transcriptionally responsive to exogenous cytokinin in both rice root and shoot tissues, while *OsRR11* (Bradi3g49440) was exclusively responsive to cytokinin in rice shoot tissue and *OsRR7* (Bradi1g28726) was exclusively responsive in rice root tissue (Tsai et al., 2012). In *B. distachyon*, only Bradi5g11350 and Bradi4g43090 (*OsRR1* and *OsRR9/10*) were found to be transcriptionally responsive to cytokinin treatment (Kakei et al., 2015). Importantly two of the *type A RRs* (Bradi4g43090, Bradi1g28726) had a higher level of transcript counts in roots (Fig. 4.9) which partly explains their substantial downregulation in FRR. Given the function of *type A RRs*, it suggests there was some repression of cytokinin-related genes in non-inoculated root tissue. Together this suggests that there was a repression of cytokinin signalling repression in response to FRR.

Interestingly, the rice homologue of Bradi1g28726 (Os*RR7*) was also been shown to responsive to auxin (Tsai et al., 2012). Furthermore Bradi2g60456 (*CKX4*) was responsive to auxin treatment rather than cytokinin treatment in *B. distachyon* (Kakei et al., 2015). These could be examples of the direct interactions between auxin and cytokinin signalling and reflect the effects of auxin rather than cytokinin signalling (Naseem et al., 2012). Despite evidence for a positive synergism of cytokinins with SA (Choi et al., 2010, Argueso et al., 2012, Naseem et al., 2012) and given the lack of SA-responsive genes in the RNA-seq datasets, there did not appear to be co-expression of SA genes and cytokinin genes in either tissue, suggesting that cytokinin-related gene expression is occurring independently to SA. In summary, the data provides evidence in that cytokinin-related genes are responsive to both FHB and FRR. Different sets of genes, however, were involved in response to the two diseases. Several genes were highly upregulated to FHB while a second set were significantly downregulated in response to FRR (Fig. 4.9).

4.4.6. ABA Biosynthesis is Responsive to FHB and FRR

Several ABA-related genes were differentially expressed in response to FHB and FRR (Fig. 4.10). ABA synthesis genes identified include *NCEDs*, xanthoxin dehydrogenase, and *ABSCISIC ACID OXIDASE* (*AAO3*) (Chen et al., 2020). Three ABA biosynthetic *AtNCED* homologs (Bradi1g13760, Bradi1g58580, and Bradi1g51850) were highly upregulated in response to FHB while Bradi1g58580 and Bradi1g13760 showed a moderate increase in response to FRR (Fig. 4.10). The increase in expression for Bradi1g51850 was not as apparent in FRR because of the higher transcript counts in non-inoculated root tissues (Fig. 4.10). As observed for JA (Fig. 4.11E-F) and cytokinin biosynthesis genes (Fig. 4.11I), the apparent delay in expression of ABA biosynthesis genes may reflect differences due to the single time point analysed. However a time-course analysis of ABA-related genes was not performed. The *AtNCED* homologs Bradi1g51850 and Bradi1g13760 were also upregulated in *B. distachyon* in response to *F. graminearum* PH1 FHB (Pasquet et al., 2014). For other biosynthetic genes, xanthoxin dehydrogenase was upregulated in response to both FHB and FRR whereas *AtAAO1/2/3/4* (homologue Bradi1g52740) was exclusively downregulated in response to FRR, partly because of a high endogenous transcript count level in non-inoculated roots (Fig. 4.10). Despite the repression of Bradi1g52740 in response to FRR, there is evidence for ABA biosynthesis in response to both FHB and FRR, but to a greater extent in FHB. This supports evidence from Powell and colleagues (2017b) who found that there was a significant increase in ABA content in *B. distachyon* FCR following inoculation with *F. pseudograminearum* (Powell et al., 2017b). Likewise, an increase in ABA metabolites occurred to the susceptible response to *F. graminearum* FHB (Qi et al., 2016) and an increase in ABA content was also found in response to FHB in certain wheat lines (Buhrow et al., 2016, Wang et al., 2018a). ABA can also be derived from ABA conjugates from the endoplasmic reticulum (ER) or vacuole with AtBG1 and AtBG2, respectively (Chen et al., 2020). *AtBG1* homologs Bradi2g43056, Bradi2g60441, and Bradi2g60490 were highly upregulated in response to both FHB and FRR (Fig. 4.10). This may suggest that ABA is predominantly being derived from ABA conjugates in the ER rather than de-novo synthesis as a response to infection. Interpretation of the change in levels of ABA is complicated given evidence that *F. graminearum* can synthesise ABA (Qi et al., 2016).

Despite evidence for an increase in ABA content, there was no evidence for upregulated ABA signalling components (Dong et al., 2015), or the *PYRABACTIN-RESISTANCE/PYR-LIKE/REGULATORY COMPONENT OF ABA RECEPTOR* (*PYR/PYL/RCAR*) ABA receptors (Gordon et al., 2016). There was however the upregulation of one ABA negative regulator homologue *PROTEIN PHOSPHATASE 2C* (*AtAP2C1*) (Bradi1g65520), predicted to encode a PP2C-type phosphatase (Ensembl Genomes (Howe et al., 2020)), which was exclusively upregulated in response to FHB. Secondly, the gene Bradi5g25570 (*AtERF7* orthologue) was also significantly upregulated in response to FHB, and slightly in response to FRR (Fig. 4.7). The transcription factor *AtERF7* is a negative regulator of ethylene signalling (Song et al., 2005). Given the inhibitory role of *AtERF7* and *PP2C* in ABA signalling (Song et al., 2005, Chen et al., 2020), the data suggest an absence or repression of ABA signalling in response to FHB and FRR. This is supported by a lack in expression change for ABA-associated signalling genes in response to *F. graminearum*-induced FHB in wheat (Buhrow et al., 2020). In summary, there is evidence for ABA biosynthesis and endogenous content increase but no strong evidence for an increase in ABA perception or signalling in both FHB and FRR.

4.4.7. Transcription of GA - and BR - Associated Genes are Not Altered in Response to FHB and FRR

Both GA and BR-related genes were the least responsive to FHB and FRR compared to all the other phytohormones. For GA, there was evidence for a change in expression of three biosynthetic *2-OXOGLUTARATE-DEPENDENT DIOXYGENASES* (*2OD*) genes in response to FRR only (Bradi2g50280, Bradi1g59570, Bradi3g49390) whereas there was evidence for epoxidation in response to FHB from upregulation of Bradi2g22050 *ELONGATED UPPERMOST INTERNODE* (*OsEUI*) (Yamaguchi, 2008, Hedden & Thomas, 2012) (Table 4.2). Another group of *2OD* genes, *GA20ox*, were expressed in response to wheat FCR (Powell et al., 2017a), and gibberellin oxidases were also upregulated in response to *F. graminearum* treatment in wheat (Pan et al., 2018). However no significant change in GA content was observed in resistant or susceptible wheat lines in response to FHB (Buhrow et al., 2016). Only one BR gene was expressed, Bradi2g22967, the *B. distachyon* homologue of *CONSTITUITIVE DIFFERENTIAL GROWTH1* (*AtCDG1*) (Table 4.2). The receptor-like kinase *AtCDG1* functions as a positive BR regulator functioning together with the BR receptor *BRASSINOSTEROID INSENSITIVE 1* (*BRI1*) (Kim & Russinova, 2020). It is worth noting that *AtCDG1* had a low percentage sequence similarity to the *B. distachyon* gene Bradi2g22967

(Table 4.2). Despite the link of *AtCDG1* to BR signalling, the respective receptor, *BRI1*, was not identified. There is evidence of a role of BR signalling in *Fusarium* resistance since the *Bdbri1* receptor mutants in *B. distachyon* and barely were shown to increase resistance to FHB and FRR in *B. distachyon* (Goddard et al., 2014). Unlike the results observed here, recent data suggests that *F. graminearum* induced both an upregulation and downregulation of several GA and BR biosynthetic genes (Buhrow et al., 2020). It is unclear why GA- and BR-associated genes were more responsive in wheat than in *B. distachyon* from this study. It is possible that constitutively elevated GA and BR content in *B. distachyon* may be the reason for a low expression change in response to infection (Kakei et al., 2015).

4.4.8. Limitations and Future Studies

FHB and FRR are diseases in which symptoms progress at different rates (Wang et al., 2015b). Based on the observation of first visual symptoms (Chapter 1 and Chapter 2) rather than transcriptomic activity, the time-point of 1 dpi for FRR and 3 dpi for FHB were selected to represent the equivalent points in the interaction. I show through time course analysis that most phytohormone-related genes peaked in expression at 3 dpi (Fig. 4.11). Likewise the majority of transcripts were expressed at 3 dpi of FHB in barley (Boddu et al., 2006). However, it is unclear whether 1 dpi was appropriate for FRR sample analysis and comparison with the 3 dpi for FHB. The evidence suggests that 3 dpi may also be relevant for peak expression for FRR since genes (Bradi2g54350, Bradi1g57590, Bradi4g31240, Bradi3g39980, Bradi1g09090, and Bradi2g50840) which displayed similar gene expression levels between FHB and FRR at 3 dpi (Fig. 4.11C, Fig. 4.11D, Fig. 4.11F, Fig. 4.11E, Fig. 4.11G, Fig. 4.11H). However, there is evidence that supports the time-point decision in this study for FRR and FHB time-points. For example, JA-related genes *TaLOX2* and *TaJAZ9* were all highly expressed at 1 dpi in wheat seedling rot and moreover the expression of *TaPR1-4*, and *TaJAZ9* was highest past 3 dpi in FHB (Wang et al., 2018c). This suggests 1 dpi for FRR, which was done in this RNA-seq was also a relevant time-point to assess for phytohormone-related genes. For future studies, it would be interesting to analyse FRR samples collected at 3 dpi. Alternatively, 1 dpi FHB samples could be analysed to compare to 1 dpi for FRR.

There is evidence that certain genes described in the heatmaps (Section 4.3.2) are responsive to the respective hormone in *B. distachyon* and rice (Jain et al., 2005, Jain et al., 2006a, Jain et al., 2006b, Tsai et al., 2012, Kakei et al., 2015, Kouzai et al., 2016). However it cannot be confidently assumed that all of the genes described are truly responsive to the respective phytohormone, as several respond to more than one phytohormone, as was shown previously (Kouzai et al., 2016). Further analysis of important FHB and FRR-responsive genes identified within the RNA-seq data would need to be functionally characterised for phytohormone responsiveness. Furthermore, there are numerous studies that have investigated the change in phytohormone content following *Fusarium* infection (Buhrow et al., 2016, Powell et al., 2017a, Powell et al., 2017b, Wang et al., 2018a). It would also be of interest to carry out similar metabolite analyses for *B. distachyon* FHB and FRR to compare to the RNA-seq data.

These experiments were only performed on one susceptible accession of *B. distachyon* (Peraldi et al., 2011) so it cannot be determined whether the transcriptome response are resistance or susceptibility-associated responses. Numerous other studies looked at expression of phytohormone-associated genes in FHB susceptible and resistant wheat lines (Li & Yen, 2008, Jia et al., 2009, Gottwald et al., 2012, Sun et al., 2016, Pan et al., 2018, Wang et al., 2018a, Wang et al., 2018c). The difference between resistant and susceptible outcomes may relate more to the timing of phytohormone responses rather than global differences in phytohormone profiles. For example, several phytohormone-related pathways from transcriptomic data were upregulated at 2 dpi in moderately susceptible wheat spikelets in response to FHB, whereas in resistant wheat lines, they started earlier at 1 dpi (Wang et al., 2018a). Similarly, JA-associated genes were expressed earlier in the resistant wheat line Sumai 3 to FHB (Wang et al., 2018c). It would be interesting to compare different resistant and susceptible *B. distachyon* accessions for resistant-specific phytohormone gene expression.

4.4.9. Conclusion

The biosynthesis, signalling, and homeostasis gene expression response of five phytohormones were substantially affected in response to FHB and FRR in *B. distachyon*. The phytohormones JA and ethylene-associated genes had the most significant expression change in response to FHB and FRR suggesting an important role in response to both

diseases. On the other hand, expression of the defence-related hormone SA genes did not appear significantly transcriptionally affected in response to either FHB or FRR despite some evidence for changes in SAR signalling in response to FHB and FRR. Both ABA and auxin-related biosynthesis genes were expressed in response to both FHB and FRR however ABA and auxin signalling was differentially expressed between FHB and FRR. Auxin was also one of the most overrepresented phytohormone-related gene groups. Lastly, and relatively little documented, cytokinin biosynthesis and signalling was also differentially expressed in response to FHB and FRR. These results suggest an important role of the development associated phytohormones (ABA, auxin, cytokinin) in the defence response to two Fusarium diseases in *B. distachyon*. The expression of several genes was greatly influenced by levels of transcript counts in non-inoculated tissues, which were generally much higher in non-inoculated roots compared to spikes. There was no evidence that phytohormones GA, BR, and BABA were significantly differentially expressed in response to FHB or FRR. These results provide novel important information for the phytohormone transcriptome responses to FHB and the lesser known FRR disease in the model grass species *B. distachyon*. Future work into comparing resistant and susceptible *B. distachyon* lines at different time-points would be important to further investigate phytohormone gene expression and roles in resistance.

Chapter 5 - Comparing the *Fusarium graminearum* Transcriptome between Fusarium Head Blight and Fusarium Root Rot

5.1. Introduction

During plant disease, certain fungal pathogens deploy virulence factors and effectors for establishment and colonisation. *Fusarium graminearum* is known to utilise a combination of cell wall-degrading enzymes and the toxin deoxynivalenol (DON) to overcome host defences in small-grain cereals. Infection is also accompanied by an increase in secreted effectors, changes to pathogen molecular transport and signalling, and changes to secondary metabolite and nutrient metabolism (Kikot et al., 2009, Brown et al., 2011, Lysøe et al., 2011, Harris et al., 2016, Ding et al., 2020). Many plant pathogens can also interfere with resistance through manipulation of plant phytohormone biosynthesis and signalling (Kazan & Lyons, 2014). This can be achieved either through effector-induced activation or inhibition of phytohormone biosynthesis and signalling (Kazan & Lyons, 2014), or by altering the balance of phytohormones through fungal-derived phytohormone biosynthesis (Summarised in Chapter 6 section 6.1).

In chapters 2 and 3 I show that different exogenously applied phytohormones differently affect *F. graminearum* infection of *B. distachyon* depending on the tissues. Furthermore in chapter 4, I provide evidence that there are differences in *B. distachyon* tissue responses, in terms of phytohormone-associated genes, to *F. graminearum* infection. An important question arising from these results is whether these tissue-specific differences reflect differences in the transcriptome of *F. graminearum* between tissues during infection.

Several studies have investigated the transcriptome of *F. graminearum* during Fusarium head blight (FHB) disease of small grain cereals, in most cases through microarray analysis (Lysøe et al., 2011, Harris et al., 2016, Brown et al., 2017). The transcriptome of *F. graminearum* between FHB and Fusarium crown rot (FCR) has been compared (Stephens et al., 2008). However the *F. graminearum* secretome during Fusarium root rot (FRR) is relatively unknown and has only recently been investigated in *Brachypodium distachyon* (Ding et al., 2020). The complete *F. graminearum* genome (Cuomo et al., 2007, King et al., 2015) has been sequenced revealing a small (36.1 Mbp) genome with only four

chromosomal regions (Cuomo et al., 2007). The predicted *F. graminearum* secretome was also generated and investigated (Brown et al., 2012). Together these resources allow for whole-genome transcriptomics and the identification of key pathogenicity-related genes during pathogenesis. RNA-seq technology (Wang et al., 2009) has been used to-date, in terms of *F. graminearum* disease transcriptomics, for FRR (Ding et al., 2020) and FHB (Pan et al., 2018, Buhrow et al., 2020).

F. graminearum-specific reads were obtained from the same RNA-seq library as in Chapter 4. Thus the time points are identical to those in FHB and FRR as reported in Chapter 4. This permits a direct comparison of *F. graminearum* genes and induced *B. distachyon* responses between FHB and FRR. Effector-specific genes can be filtered from the results which were then utilised to identify any tissue-specific activity. Additionally, *F. graminearum* phytohormone-related genes and DON-related genes were identified within the RNA-seq data and were collated. The similarities and differences of these genes and effectors between FHB and FRR were investigated and discussed. This is the first study to my knowledge that compares key *F. graminearum* effectors and genes during diseases of different tissues in the same host.

<u>Aim</u>: Investigate *Fusarium graminearum* transcriptome similarities and differences during infection of spike (Fusarium head blight) and root (Fusarium root rot) tissues.

5.2. Materials and Methods

5.2.1. Maintenance of *F. graminearum*, Preparation of Inoculum, and Inoculation

The material described in this chapter is from the same RNA-seq experiment in Chapter 4. *F. graminearum* PH1 maintenance and inoculum preparation was as described in section 4.2.2. The *B. distachyon* Bd3-1 root and head inoculation protocol was the same as described in section 4.2.3. The *F. graminearum in vitro* control samples were the same as from section (6.2.3).

5.2.2. Library Preparation RNA-seq Bioinformatics Analysis

Both infected samples and *in vitro* control samples were sent to Genewiz for library preparation as part of independent experiments, as described in sections (4.2.4 and 6.2.3). The same pipeline (Fig. 4.2) was used with the same data. Library reads were aligned to the *F. graminearum* PH1 genome assembly and gene annotation (European Nucleotide Archive; GCA_900044135.1, study PRJEB5475 (King et al., 2015). FHB and FRR sample gene counts were separately compared against the same *F. graminearum in vitro* control samples (The treatment without methionine (termed C samples) from the RNA-seq experiment in Chapter 6 described in Section 6.2.3) using DEseq2 tool on the Galaxy Platform (Fig. 4.2). The average transcript counts from the *in vitro* control samples was slightly higher from the FRR DEseq2 analysis but the difference to the FHB DEseq2 transcript counts was still proportional, thus the average of each biological replicate control treatment was taken for the heatmap value (Fig. 5.2). Differentially expressed *Fusarium* genes in FHB and FRR were filtered for potential effectors using PH1 v5.0 secretome prediction script (Brown et al., 2012). To compare gene expression results with other research datasets, *F. graminearum* str. PH1 gene IDs (FGRAMPH1_01G) were converted to (FG_05) *F. graminearum* str. CS3005 (GCA_000599455) (EMBL) and (FGSG_) *F. graminearum* PH1 (GCA_000240135) Ensembl Genome IDs (Howe et al., 2020) using UniProt data (Consortium, 2018). For absent gene conversion IDs, the gene IDs in *F. graminearum* str. CS3005 (GCA_000599455) and (FGSG_) *F. graminearum* PH1 (GCA_000240135) were identified by protein sequence Basic Local Alignment Search Tool (BLAST) (Sayers et al., 2020).

5.2.3. Time-Course RT-qPCR

The same materials and methods for RT-qPCR was used from Section 4.2.5 and Section 6.2.3, but with a different set of primers (Supp. Table S13). Only one time point was used for the *in vitro* control which was subsequently compared to all three infected FHB and FRR time-point samples (Fig. 5.3) using Equation 2.1.

5.2.4. Statistics, Software, and Graphs

The same method was used as 4.2.6 for respective data. However the online databases Ensembl Genomes (Howe et al., 2020), UniProt (Consortium, 2018), and protein sequence BLAST (Sayers et al., 2020) were only used for *F. graminearum* gene function identification.

5.3. Results

Between 8% to 15% of the FHB and FRR transcript reads mapped to the *F. graminearum* PH1 assembly. A total of 4,567 *F. graminearum* genes were significantly responsive in FHB or FRR, or in both (Fig. 5.1). However only 6% of these were functionally characterised on UniProt (Consortium, 2018). A total of 3,499 genes were differentially expressed in spike infection (FHB), of which 55% were upregulated (Fig. 5.1). On the other hand 3,214 genes were differentially expressed during root infection (FRR), of which 56% were upregulated (Fig. 5.1). A total of 26% of the genes were upregulated and 21% were downregulated in both root and spike tissues, respectively, relative to axenic culture medium (Fig. 5.1). Only 1% of genes were upregulated in one tissue but downregulated in the other (Fig. 5.1).

Figure 5.1. Summary of all significantly upregulated or downregulated *F. graminearum* genes in FHB and FRR. The number and percentage of *F. graminearum* genes are displayed. The threshold of -2 ≤ x ≥ 2 Log-fold change and p-adj < 0.05 was applied to all genes. Abbreviations: Fg (*F. graminearum*), Up (Upregulated), Down (Downregulated), FRR (Fusarium Root Rot), FHB (Fusarium Head Blight).

All the significantly differentially expressed genes were then filtered by association with the *F. graminearum* secretome database (Brown et al., 2012). Only 3% of FHB-responsive genes (Fig. 5.1) were classed as effectors and 40% of these were exclusively expressed or repressed in FHB. On the other hand, 2% of FRR-responsive genes (Fig. 5.1) were classed as effectors and 21% of these were exclusively expressed or repressed in root tissues (FRR) (RNA-seq dataset not shown). Approximately 54% of all these effector-associated genes had a predicted function (From *F. graminearum* (UniProt (Consortium, 2018) or through protein homology in different fungal species (BLAST (Sayers et al., 2020)), RNA-seq dataset not shown). For both FHB and FRR, 79% of these effector-associated genes were upregulated. Only upregulated genes were then filtered since they were predicted to be the effectors playing important roles in FHB and FRR virulence. A total of 80 *F. graminearum* genes were highly upregulated (Log-fold ≥ 3) in FHB and/or FRR with four main expression

clusters (Fig. 5.2). A total of 21 genes in cluster 3 were upregulated in FHB. Likewise, 20 genes in cluster 4 were also upregulated in FHB however these were slightly more upregulated in FRR. Most of the genes in cluster 2 (30 genes) were similarly upregulated in FHB and FRR. Lastly 9 genes in cluster 1 were upregulated in FRR. There was a tendency for genes that were similarly expressed between FHB and FRR (Clusters 2 and 4) to have a much lower baseline expression in control treatments than differentially expressed effectors (Cluster 1 and 3).

Here I shall describe notable effectors that were upregulated (Fig. 5.2). Many of the effectors were upregulated in both FHB and FRR. Genes encoded cell wall degrading enzymes (CWDEs) were generally upregulated in both FHB and FRR (Fig. 5.2). Examples include endo-1,4-beta-xylanase (FGRAMPH1_01G20977 and FGRAMPH1_01G13319), acetylxylan esterase (FGRAMPH1_01G08665), cutinase (FGRAMPH1_01G12927, FGRAMPH1_01G08583, FGRAMPH1_01G12551), a pectate lyase (FGRAMPH1_01G11755 and FGRAMPH1_01G16515), and a hydrolytic enzyme (FGRAMPH1_01G12629). Other notable effectors upregulated in FHB and FRR (Fig. 5.1) include a rhamnogalacturonan acetylesterase precursor (FGRAMPH1_01G16469), two effectors encoding gegh16 proteins (FGRAMPH1_01G08931, FGRAMPH1_01G27287), a chorismate mutase 2 gene (FGRAMPH1_01G22073), a hypersensitive response (HR)-inducing gene (FGRAMPH1_01G16209), two CFEM domain containing genes (FGRAMPH1_01G05255 FGRAMPH1_01G13253) (Log2 fold > 2), and a hydrophobin gene (FGRAMPH1_01G28003).

In contrast there were several genes showing differential expression between tissues. Four genes encoding *TOX* effectors were differentially expressed (Fig 5.2). *TOX1* (FGRAMPH1_01G00197), *TOX2* (FGRAMPH1_01G00199) were upregulated only in FHB (Log-fold > 3). *TOX3* (FGRAMPH1_01G00201) was upregulated in both FHB and FRR but to a lesser extent in FRR. In contrast, *TOX4* (FGRAMPH1_01G08389) was upregulated in FRR. The two cutinase (FGRAMPH1_01G12927, FGRAMPH1_01G08583) and one pectate lyase (FGRAMPH1_01G16515) were only upregulated in FHB. Lasty, FGRAMPH1_01G08399 has a low identity similarity to a metalloprotease, and FGRAMPH1_01G09079 is predicted to encode a myroilysin precursor which has metalloprotease attributes (Xu et al., 2017). Both metalloprotease-like effectors were exclusively upregulated in FRR. In fact, FGRAMPH1_01G08399 was highly upregulated in FRR but highly downregulated in FHB.
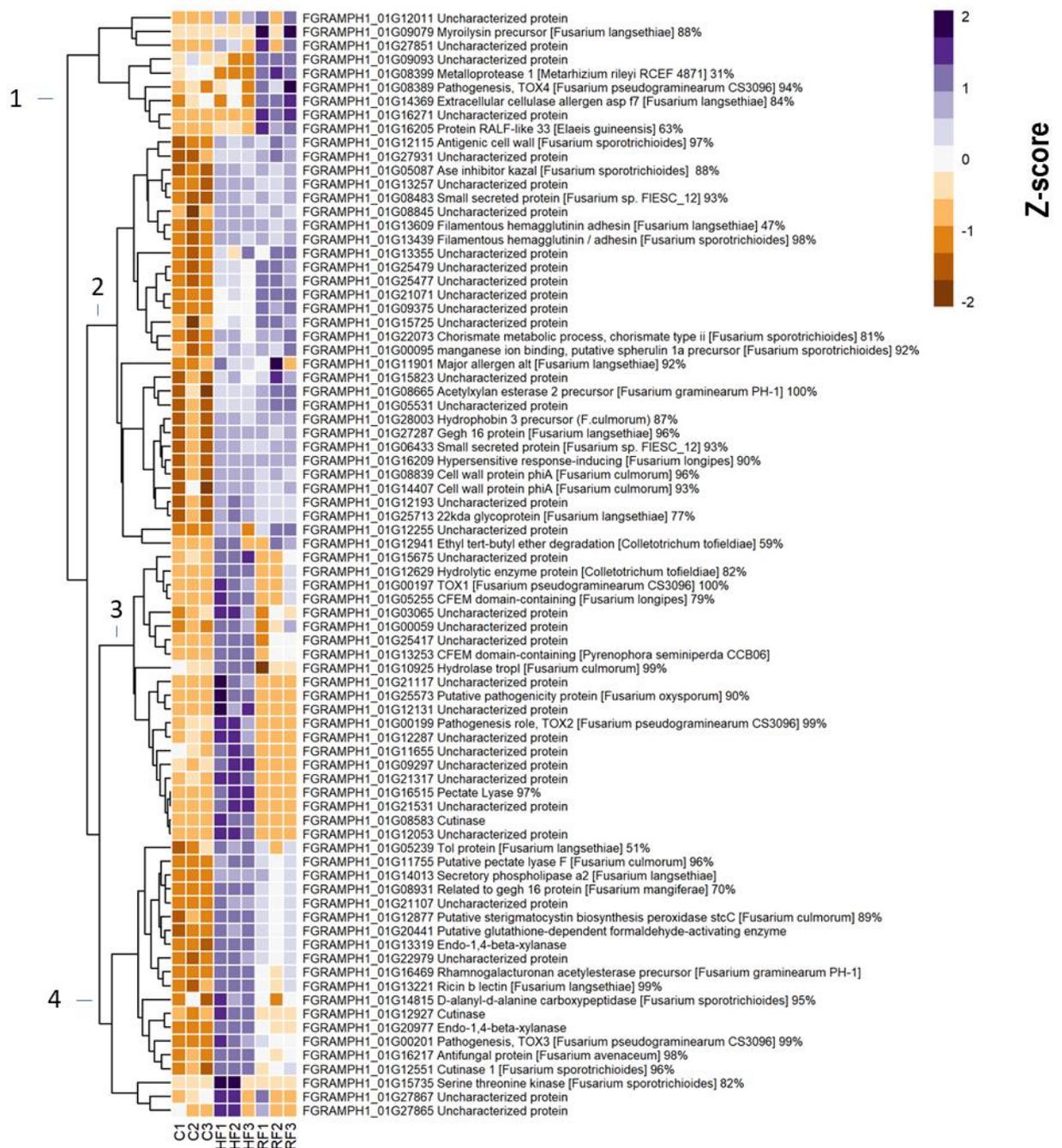
Figure 5.2. The most upregulated *F. graminearum* predicted-effector genes in FHB and FRR. These genes have an expression of Log-fold increase ≥ 3 in FHB and/or FRR. Three biological replicates for each of the three treatments are displayed as columns. Control Treatment (C1-3) is the average normalised gene counts (two values per column/biological replicate) of *in vitro* treatments (four-day-old samples grown in Czapeks Dox Liquid media). The same *in vitro* sample was analysed separately (DESeq) with the FHB and FRR samples. Some gene function includes the most homologous protein sequence BLAST query hit (Sayers et al., 2020) with respective genus and species and percentage homology. If no percentage sign is visible, then the gene was identified from UniProt (Consortium, 2018). Abbreviations: C (*In vitro* control respective to FHB and FRR), HF (Head-FHB fungus), RF (Root-FRR fungus).

189

The expression of two effector genes that showed differential expression between FHB and FRR in the RNA-seq data set (Fig. 5.2), were examined using RT-qPCR (Fig 5.3A). During FRR, FGRAMPH1_01G00199 (*TOX2*) was downregulated at all time points by -5.3-fold change at 1 dpi (p = 0.004), -6.7-fold change at 3 dpi (p = 0.004), and -4.1-fold change at 5 dpi which was not statistically significant (p = 0.130). On the other hand, *TOX2* was not significantly expressed at 3 dpi in FHB (p = 0.388). However, *TOX2* was upregulated to 3.3-fold change at 5 dpi (p = 0.024), and then to 4.1-fold change by 7 dpi (p = 0.027) in FHB. Differential expression between FHB and FRR was maintained at all time points (Fig. 5.3A) which is in accordance with the differential expression in the RNA-seq data of FHB and FRR (Fig. 5.2). Although the absolute expression values differed between experiments for the same gene at 1 dpi for FRR and 3 dpi for FHB (Fig. 5.2 and 5.3A), the differential expression between tissues was maintained over time (Fig. 5.3A).

The effector FGRAMPH1_01G16515, predicted to encode a pectate lyase, also showed differential expression between FHB and FRR (Fig. 5.3B). In FRR, pectate lyase was downregulated to -3.1-fold change (p = ND) and then to non-significant baseline levels at 3 dpi (p = 0.674) and 5 dpi (p = 0.715). In contrast, pectate lyase was significantly upregulated by 2.9-fold change at 3 dpi in FHB (p = 0.031). Despite a slight increase in expression at 5 dpi at 3.1-fold change, it was not significantly expressed (p = 0.060). By 7 dpi, expression decreased to baseline levels (p = 0.078). Similarly pectate lyase also displayed FHB-specific upregulation in the RNA-experiment at 3 dpi (Fig. 5.2), but to much a reduced level. Despite a lower log-fold proportion at the first time point for FHB (Fig. 5.3B) relative to the RNA-seq data (Fig. 5.2), the differential in expression for FHB at 3 dpi and FRR at 1 dpi supports the RNA-seq results for both FHB and FRR.
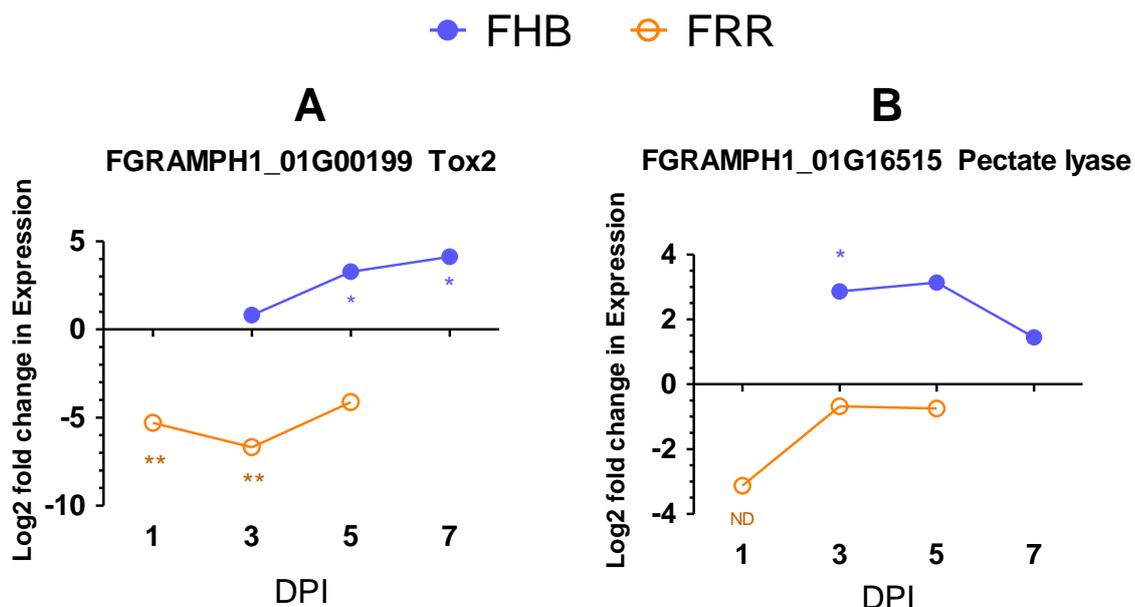
Figure 5.3. Time-course validation RT-qPCR on two differentially expressed *F. graminearum* genes identified in RNA-seq. Gene function and gene ID are given for each tissue disease. Blue lines with solid circles denote FHB and orange lines with open circles denote FRR. Log values presented are calculated by comparing infected tissue against mock-inoculated treatments. Furthermore, all treatments are calculated with the reference Housekeeping gene *GzUBH*. Each point is the average of three biological replicates (except for the *in vitro* control where two biological replicates were used) and two to three technical replicates (except for one biological replicate from FRR 3 dpa *TOX2* with only one). Level of significance relative to the mock-control: Cq t-test *p < 0.05, **p < 0.01. "ND" denotes no statistical comparison due to the absence of expression in control.

Trichothecene production is regulated by a cluster of *Tri* genes (Kimura et al., 2003, Kimura et al., 2007). *F. graminearum* PH1 is a 15-acetylDON (ADON) producer (Kimura et al., 2007) (Professor Paul Nicholson, personal communication). The expression of the *Tri5*-gene cluster was investigated to identify any difference in transcription of DON associated genes between FHB and FRR. The essential DON biosynthetic triplet of genes (*Tri4*, *Tri5*, *Tri11*) were the most upregulated genes in both FHB and FRR (Table. 5.1). The transcriptional regulators (*Tri6*, *Tri10*), and *Tri12* transporter were also upregulated in both FHB and FRR (Table 5.1). There were also high levels of expression of non-essential *Tri9* and *Tri14* in both FHB and FRR (Table 5.1). *Tri14* may have a role in DON synthesis and virulence (Dyer et al., 2005). Furthermore there was high expression of *Tri3* (Alexander et al., 2011) in both FHB and FRR (Table. 5.1). Despite the low but significant expression in FHB, *Tri8* was the only gene exclusively expressed in FHB (Table. 5.1). *Tri8* encodes a C-3 deacetylase that

is involved in 15-ADON production (Alexander et al., 2011). The expression of *Tri7* and *Tri13*, involved in the biosynthesis of nivalenol trichothecenes (Lee et al., 2002, Kimura et al., 2003), were below the significant log-fold threshold in both FHB and FRR as expected as *F. graminearum* PH1 is a DON producing strain (Table. 5.1).

Table 5.1. Expression change of *F. graminearum Tri* gene cluster in *B. distachyon* FHB and FRR relative to *in vitro* control.

Tri gene	Gene ID	Gene function	FHB Log-fold change	p-adj	FRR Log-fold change	p-adj
FgTri8	FGRAMPH1_01G13101	C-3 deacetylase	2.7	< 0.001	0.01	0.990
FgTri7	FGRAMPH1_01G13103	4-O- Acetyltransferase	1.8	0.433	0.02	0.994
FgTri3	FGRAMPH1_01G13105	15-O- Acetyltransferase	11.1	< 0.001	9.1	< 0.001
FgTri4	FGRAMPH1_01G13107	Multifunctional Oxygenase	7.9	< 0.001	6.9	N/A
FgTri6	FGRAMPH1_01G13109	Transcription regulator	3.0	N/A	3.1	0.023
FgTri5	FGRAMPH1_01G13111	Trichodiene synthase	8.8	< 0.001	7.0	< 0.001
FgTri10	FGRAMPH1_01G13113	Transcription regulator	3.7	0.008	2.8	0.522
FgTri9	FGRAMPH1_01G13115	Unknown polypeptide	6.2	< 0.001	6.6	< 0.001
FgTri11	FGRAMPH1_01G13117	3-ADON biosynthesis	8.3	< 0.001	7.0	< 0.001
FgTri12	FGRAMPH1_01G13119	Transporter	5.4	N/A	4.3	< 0.001
FgTri13	FGRAMPH1_01G13121	C-4 hydroxylase	1.5	0.530	1.5	N/A
FgTri14	FGRAMPH1_01G13123	Uncharacterised	6.3	< 0.001	5.0	N/A

Light red highlighted cell denote p-adj > 0.05. N/A denotes that p-value and p-adj were unavailable. Gene Id and function were obtained from; (Kimura et al., 2003, Kimura et al., 2007) and Ensembl Genomes (Howe et al., 2020)).

Several *F. graminearum* genes identified by Ding and colleagues (2020) were postulated to be phytohormone-related mostly through homology (Ding et al., 2020). These were compared to the *F. graminearum* RNA-seq data (Data no shown) in FHB and FRR in the present study. A total of 14 salicylic acid (SA) hydroxylases were significantly expressed in FHB and/or FRR. FGRAMPH1_01G13395, FGRAMPH1_01G16999, and FGRAMPH1_01G07837 were upregulated in both FHB and FRR. Seven other salicylate hydroxylases were expressed in FRR whereas four others were upregulated in FHB. Lastly an SA-related *ENHANCED PSEUDOMONAS SUSCEPTIBLITY 1* (*EPS1*) homologue FGRAMPH1_01G00633 was significantly upregulated in FRR (Table 5.2). There were no JA-related *Fusarium* genes significantly upregulated in FHB, however an *Arabidopsis thaliana* 2OG oxygenase homologue (FGRAMPH1_01G05547), involved in JA hydroxylation (Ding et al., 2020), was significantly upregulated in FRR (Table 5.2). The ethylene biosynthetic gene homologue *ACC SYNTHASE 1* (*ACS1*) (FGRAMPH1_01G17303) was significantly upregulated in FHB whereas the homologue *ACS2* (FGRAMPH1_01G25199) was significantly upregulated in FRR, both with relatively low expression (Table 5.2). Lastly, a cytokinin biosynthetic gene homologue tRNA-IPT transferase (FGRAMPH1_01G28119) was significantly upregulated in FHB although displaying a relatively low log-fold change level (Table 5.2).

Table 5.2. Significantly upregulated phytohormone-related *F. graminearum* genes in FHB and FRR relative to *in vitro* control.

Hormone	Gene ID	Gene Function homologs	FHB Log-fold change	p-adj	FRR Log-fold change	p-adj
SA	FGRAMPH1_01G22073 (FGSG_11442)	Chorismate mutase	3.09	< 0.001	3.42	< 0.001
SA	FGRAMPH1_01G00633 (FGSG_00237)	*EPS1*	4.21	N/A	2.90	0.022
SA	FGRAMPH1_01G09151 (FGSG_08116)	Salicylate hydroxylase	1.96	NA	8.39	< 0.001
SA	FGRAMPH1_01G13395 (FGSG_03657)	Salicylate hydroxylase	5.00	< 0.001	3.98	< 0.001
SA	FGRAMPH1_01G08529 FGSG_10612)	Salicylate hydroxylase	0.88	0.436	5.00	< 0.001
SA	FGRAMPH1_01G13567 (FGSG_03729)	Salicylate hydroxylase	9.84	< 0.001	0.72	NA
SA	FGRAMPH1_01G16769 (FGSG_04969)	Salicylate hydroxylase	3.59	< 0.001	-1.03	0.488
SA	FGRAMPH1_01G13679 (FGSG_03775)	Salicylate hydroxylase	-0.60	0.702	1.97	< 0.001
SA	FGRAMPH1_01G25101 (FGSG_07562)	Salicylate hydroxylase	2.11	< 0.001	0.83	0.233
SA	FGRAMPH1_01G16999 (FGSG_05063)	Salicylate hydroxylase	3.37	< 0.001	2.97	< 0.001
SA	FGRAMPH1_01G25249 (FGSG_07628)	Salicylate hydroxylase	1.67	0.098	2.04	0.040
SA	FGRAMPH1_01G16165 (FGSG_04722)	Salicylate hydroxylase	1.23	NA	4.62	< 0.001
SA	FGRAMPH1_01G28011 (FGSG_09063)	Salicylate hydroxylase	8.52	< 0.001	3.18	0.055
SA	FGRAMPH1_01G07837 (FGSG_10330)	Salicylate hydroxylase	6.59	< 0.001	7.05	< 0.001
SA	FGRAMPH1_01G09151 (FGSG_08116)	Salicylate hydroxylase	1.96	N/A	8.39	< 0.001
SA	FGRAMPH1_01G15123 (FGSG_04368)	Salicylate hydroxylase	-1.33	0.287	1.91	< 0.001
JA	FGRAMPH1_01G05547 (FGSG_02301)	Arabidopsis 2OG oxygenases	N/A	N/A	5.59	0.009
Ethylene	FGRAMPH1_01G17303 (FGSG_05184)	*ACS1*	2.47	< 0.001	0.86	0.142
Ethylene	FGRAMPH1_01G25199 (FGSG_07606)	*ACS2*	0.65	0.403	1.39	0.031
Cytokinin	FGRAMPH1_01G28119 (FGSG_09015)	tRNA-IPT transferase	1.56	< 0.001	0.67	0.163

All genes and predicted function were derived from (Ding et al., 2020). Genes presented are those that were significantly expressed (p-adj < 0.05) in either FHB or FRR, or both. Green highlight signifies significant difference in expression p-adj < 0.05. N/A signifies that there was no log-foldchange or p-adj value output (DEseq2). Abbreviations: *EPS1* (*ENHANCED PSEUDOMONAS SUSCEPTIBLITY 1*), *ACS* (*ACC SYNTHASE*), *IPT* (*ISOPENTENYLTRANSFERASE*).

Lastly, a group of eight non-effector genes were found to be differentially expressed between FHB and FRR (Table 5.3). These genes comprise a cluster of genes predicted to be involved in the synthesis of the red pigment aurofusarin (Table 5.3). For most of these genes, they were significantly downregulated in response to FHB but upregulated in FRR (Table 5.3). Both FGRAMPH1_01G05593 (*PKS12*) and FGRAMPH1_01G05587 (*aurO*) (Table 5.3) were among these 30 genes that were highly upregulated in FRR and downregulated in FHB (Fig. 5.1). FGRAMPH1_01G05599 (*aurF*) and FGRAMPH1_01G05601 (*GIP1*) also display this differential in expression but the effect was not statistically significant for FHB (Table 5.3). The exceptions to this differential trend were FGRAMPH1_01G05605 (*aurL2*) which was significantly upregulated in both FHB and FRR, and both FGRAMPH1_01G05589 (*aurT*) and FGRAMPH1_01G05591 (*aurR2*) which were downregulated in response to FHB but were not significantly upregulated in response to FRR (Table 5.3). Likewise, FGRAMPH1_01G05585 (*aurR1*) was significantly downregulated in both FHB and FRR, but to a lesser degree in FRR (Table 5.3)

Table 5.3. The change in expression of *F. graminearum* aurofusarin genes in FHB and FRR.

Gene ID	Predicted Function	FHB Log-fold change	p-adj	FRR Log-fold change	p-adj
FGRAMPH1_01G05585	Aurofusarin biosynthesis regulatory protein aurR1 (Aurofusarin biosynthesis cluster protein R1) (Gibberella pigment protein 2)	-8.2	< 0.001	-1	0.002
FGRAMPH1_01G05587	FAD-linked oxidoreductase aurO (Aurofusarin biosynthesis cluster protein O) (Gibberella pigment protein 3)	-5.1	< 0.001	2.5	< 0.001
FGRAMPH1_01G05589	Rubrofusarin-specific efflux pump aurT (Aurofusarin biosynthesis cluster protein T) (Gibberella pigment protein 4)	-6.5	< 0.001	0.5	0.646
FGRAMPH1_01G05591	Aurofusarin cluster transcription factor aurR2 (Aurofusarin biosynthesis cluster protein R2) (Gibberella pigment protein 5)	-5.9	< 0.001	0.7	0.247
FGRAMPH1_01G05593	Non-reducing polyketide synthase PKS12 (Aurofusarin biosynthesis cluster protein PKS12)	-5.2	< 0.001	4.37	< 0.001
FGRAMPH1_01G05599	Monooxygenase aurF (Aurofusarin biosynthesis cluster protein F) (Gibberella pigment protein 8)	-5.4	NA	4.7	< 0.001
FGRAMPH1_01G05601	Multicopper oxidase GIP1 (Aurofusarin biosynthesis cluster protein GIP1) (Gibberella pigment protein 1) (Laccase-1)	-5.0	NA	4.6	< 0.001
FGRAMPH1_01G05605	Multicopper oxidase aurL2 (Aurofusarin biosynthesis cluster protein L2) (Gibberella pigment protein 10) (Laccase-2)	5.3	< 0.001	4.9	< 0.001

Gene function was derived from Ensembl Genomes (Howe et al., 2020)). Green highlight signifies significant difference in expression p-adj < 0.05. N/A signifies that the p-adj value was unavailable.

5.4. Discussion

The secretome of *F. graminearum* is important during pathogenesis (Brown et al., 2012) however whether *F. graminearum* deploys tissue-specific effectors within the same host is unclear. Effectors were originally believed to be biotroph-specific however evidence is accumulating suggesting to their importance for hemibiotrophic and necrotrophic pathogens (Amselem et al., 2011, Guyon et al., 2014, Kabbage et al., 2015). Many effector-like genes were upregulated in *F. graminearum* during growth in spike and root tissues (FHB and FRR, respectively) (Fig. 5.2). Nearly half of the *F. graminearum* predicted effector genes were exclusively expressed or repressed in FHB. This suggests that expression of a large proportion of the *F. graminearum* secretome is controlled in a tissue-specific manner following infection of *B. distachyon* tissues. A similar proportion of non-effector genes were also differentially expressed between tissues (Fig. 5.1). Many of the genes identified were uncharacterised (Fig. 5.1, Fig. 5.2). This was also observed by (Lysøe et al., 2011, Harris et al., 2016). Here I shall compare both the notable upregulated effectors (Fig. 5.2) as well as DON (Table 5.2) and phytohormone-related (Table 5.2) genes which show similarities or differences between FHB and FRR.

5.4.1. Tissue-Independent *F. graminearum* Effectors and Genes

Genes that encode CWDEs are highly associated with necrotrophic and hemibiotrophic attack (Laluk & Mengiste, 2010, Zhao et al., 2014b, Kabbage et al., 2015, Zeilinger et al., 2016). *F. graminearum* is known to express an abundance of CWDE genes (Cuomo et al., 2007, Kikot et al., 2009) in symptomatic tissue (Brown et al., 2017). The role of CWDEs is likely as a means for nutrient acquisition and/or as effectors (Walton, 1994, Cuomo et al., 2007). Indeed many CWDE genes were predicted as effectors (Fig. 5.2). Two endo-1,4-beta-xylanase genes (FGRAMPH1_01G20977 (FGSG_10999), FGRAMPH1_01G13319 (FG05_03624)) were upregulated in both spike (FHB) and root (FRR) tissues (Fig. 5.2). Xylanases degrade xylan which is abundant in hemicellulose that is a major component of the monocot cell wall (Kikot et al., 2009). The gene FGRAMPH1_01G20977 was previously found to be upregulated in *F. graminearum*-induced FHB in wheat (*Triticum aestivum*), barley (*Hordeum vulgare*), and maize (*Zea mays*) (Lysøe et al., 2011, Harris et

al., 2016, Pan et al., 2018). Likewise FGRAMPH1_01G13319 was also upregulated during FHB in these same three host species (Harris et al., 2016), in wheat FHB (Brown et al., 2017, Pan et al., 2018, Buhrow et al., 2020), and in *F. graminearum*-induced FRR *B. distachyon* (Ding et al., 2020). The acetylxylan esterase 2 precursor (FGRAMPH1_01G08665, FGSG_10670) was also upregulated in spike and root tissues (Fig. 5.2). Similarly, this gene was upregulated in *F. graminearum* causing FHB in wheat, barley, and maize (Harris et al., 2016, Brown et al., 2017, Pan et al., 2018, Buhrow et al., 2020). A hydrolytic enzyme FGRAMPH1_01G12629 that may have a role in cell wall depolymerisation was upregulated in spike tissues (FHB) and to a lesser extent in in root tissues (FRR) (Fig 5.2). This gene was also observed to be upregulated in *F. graminearum* causing FHB in wheat and barley (Harris et al., 2016, Brown et al., 2017, Pan et al., 2018). Many other CWDE genes were also upregulated during infection of spikes of wheat and barley (Lysøe et al., 2011) and during infection of roots of *B. distachyon* (Ding et al., 2020).

Another gene family involved in cell-wall depolymerisation and induced in *F. graminearum* in both spikes and root tissues were pectin degradation enzymes (Fig. 5.2). Pectate lyase enzymes degrade pectin, which is present in the middle lamellae and the cell wall, resulting in tissue maceration (Walton, 1994, Agrios, 2005). A pectate lyase gene FGRAMPH1_01G11755 (FGSG_02977), upregulated in response to both FHB and FRR (Fig. 5.2), has previously been reported to be significantly upregulated in *F. graminearum* infecting roots of *B. distachyon* (Ding et al., 2020). However a different pectate lyase gene (FGRAMPH1_01G16515, FGSG_04864) was found to be exclusively upregulated in spikes in the present study (Fig. 5.2). FGRAMPH1_01G16515 was only significantly expressed in FHB at 3 dpi (Fig. 5.3B) which implies that its expression was short-lived during spike infection. Similarly this gene was also found to be upregulated in *F. graminearum* PH1 causing wheat and barley FHB (Lysøe et al., 2011). Both pectate lyase genes, FGRAMPH1_01G16515 and FGRAMPH1_01G11755, were also observed to be upregulated in *F. graminearum* causing FHB in wheat and barley but not in ears of maize (Harris et al., 2016, Brown et al., 2017, Pan et al., 2018). FGRAMPH1_01G11755 was also found to be upregulated in *F. graminearum* in a separate study of FHB in wheat (Lysøe et al., 2011). Pectate lyase has been associated with virulence in several plant pathogens, but to a lesser extent in fungi like *Fusarium* (Walton, 1994). Whether the pectate lyase genes presented here are involved in virulence is unknown. One *F. graminearum* effector-like gene that was highly upregulated in FHB tissue, (FGRAMPH1_01G16469, FGSG_04848) (Fig. 5.2), is predicted to

encode a rhamnogalacturonan acetylesterase precursor, that likely has a role in degrading rhamnogalacturonan components of pectin (Kauppinen et al., 1995). FGRAMPH1_01G16469 was also upregulated in FHB and FRR (Fig. 5.2). These findings are supported by other studies. This gene was also significantly upregulated in *F. graminearum* infecting roots of *B. distachyon* (Ding et al., 2020), and spikes of wheat and barley (Lysøe et al., 2011, Brown et al., 2017, Pan et al., 2018, Buhrow et al., 2020). Pectin degradation-related genes were also found to be upregulated in an FHB and crown rot microarray study of wheat (Stephens et al., 2008). Overall, the results show that most CWDEs were expressed in a tissue-independent manner for *F. graminearum*.

The type B trichothecene DON is believed to act as a virulence factor for *F. graminearum* during colonisation of spikes in wheat (Bai et al., 2002, Maier et al., 2006) and *B. distachyon* (Peraldi et al., 2011). Almost all the important DON biosynthesis and transport genes from the *Tri5* cluster (Kimura et al., 2003) were upregulated in both FHB and FRR (Table 5.1). In terms of FHB, *Tri3* (FGRAMPH1_01G13105, FGSG_03534), *Tri5* (FGRAMPH1_01G13111, FGSG_03537), *Tri10* (FGRAMPH1_01G13113, FGSG_03538), *Tri11* (FGRAMPH1_01G13117, FGSG_03540), and *Tri14* (FGRAMPH1_01G13123, FGSG_03543) have previously been found to be upregulated in wheat, barley, and maize FHB (Lysøe et al., 2011, Harris et al., 2016, Brown et al., 2017, Pan et al., 2018, Buhrow et al., 2020). These were some of the most highly expressed *Tri* genes identified in the present study (Table 5.1). *Tri6* (FGRAMPH1_01G13109, FGSG_03536) and *Tri12* (FGRAMPH1_01G13119, FGSG_03533) were upregulated in FHB of wheat (Lysøe et al., 2011, Brown et al., 2017, Pan et al., 2018, Buhrow et al., 2020). Lastly the genes *Tri8* (FGRAMPH1_01G13101, FGSG_03532), *Tri4* (FGRAMPH1_01G13107, FGSG_03535), *Tri9* (FGRAMPH1_01G13115, FGSG_03539), were also upregulated in wheat, barley, and maize FHB (Harris et al., 2016, Brown et al., 2017, Pan et al., 2018, Buhrow et al., 2020). Only *Tri5* and *Tri14* were upregulated in both FHB and FCR in wheat (Stephens et al., 2008). In FRR, Ding and colleagues (2020) also identified that *Tri4*, *Tri5*, *Tri6*, *Tri8*, *Tri10*, and *Tri11* were upregulated by *F. graminearum* in *B. distachyon* roots (Ding et al., 2020). Supporting these findings, Wang and colleagues (2015b) reported DON presence in root tissues (Wang et al., 2015b). Overall, there is strong evidence that *F. graminearum* PH1 produced DON in both *B. distachyon* floral and root tissue during infection. However there is evidence that despite DON being produced by *F. graminearum* in *B. distachyon* roots, it does not act as a virulence factor like its role in spike tissues (Ding et al., 2020). Furthermore DON does not act as a virulence factor in barley and

maize (Maier et al., 2006). Together these findings suggest that the virulence of DON is species- and tissue-specific despite its species- and tissue-independent production.

Several *F. graminearum* phytohormone-related genes, associated with SA, JA, ethylene, and cytokinin, were found to be significantly upregulated in the present study (Table 5.2). SA-related genes were the most overrepresented phytohormone-related group identified (Table 5.2). Many salicylate hydroxylase genes, involved in SA degradation (Qi et al., 2019), were upregulated in FHB and/or FRR (Table 5.2). The SA hydroxylase genes FGRAMPH1_01G08529, FGRAMPH1_01G13567, FGRAMPH1_01G16769, FGRAMPH1_01G13679, FGRAMPH1_01G25101 were also reported to be upregulated during infection of *B. distachyon* roots (Ding et al., 2020). Similarly, FGRAMPH1_01G25101 was upregulated in FHB of wheat and barley (Lysøe et al., 2011). Similar to the results in Figure 5.2, many of the SA hydroxylases were upregulated in *F. graminearum*-induced FHB in floral tissues of wheat, barley, and maize (Harris et al., 2016, Brown et al., 2017, Pan et al., 2018). FGRAMPH1_01G13395 (FGSG_03657) has been shown to be responsive to SA treatment and to degrade SA but did not play a role in FHB virulence (Hao et al., 2019). In contrast, FGRAMPH1_01G09151 (FGSG_08116) was shown to affect SA degradation and to affect FHB resistance (Qi et al., 2019). Overall, despite tissue-specific expression of some salicylate hydroxylases (Fig. 5.2), SA hydroxylases appear to play an important function during pathogenesis in FHB and FRR. A chorismate mutase FGRAMPH1_01G22073 (FGSG_11442) was upregulated in both FHB and FRR (Fig. 5.2, Table 5.2). This gene was also previously shown to be upregulated in *F. graminearum* causing FHB of wheat, barley, and maize (Harris et al., 2016, Brown et al., 2017, Pan et al., 2018) and FRR of *B. distachyon* (Ding et al., 2020). This enzyme is a known effector enzyme involved in metabolite redirection which can affect SA biosynthesis (Djamei et al., 2011). Together with information on SA hydroxylases, the data suggests that *F. graminearum* may be affecting host SA production in both FHB and FRR. Further complicating the story, *F. graminearum* has been shown to produce SA *in vitro* and in *B. distachyon* FRR (Ding et al., 2020). The *AtEPS1* homologue (FGRAMPH1_01G00633, FGSG_00237) (Table 5.2), which in plants is involved in plant SA biosynthesis (Lefevere et al., 2020), was significantly upregulated in FRR in the present study (Table 5.2). This gene was also upregulated in response to *B. distachyon* FRR (Ding et al., 2020) and also in response to FHB in wheat (Harris et al., 2016). Unfortunately it is not possible to compare the expression of *F. graminearum* homologues of *AtEPS1* in FHB given the absent p-adj value in this study (Table 5.2). The role of SA-

manipulation and production by *F. graminearum* is unclear and requires further investigation.

In terms of ethylene-related genes, *F. graminearum*-associated ethylene biosynthesis *ACS* genes (FGRAMPH1_01G17303 (FGSG_05184) and FGRAMPH1_01G25199 (FGSG_07606)) were upregulated in FHB and FRR, but with a different *ACS* gene upregulated in spike and root tissues (Table 5.2). These two *ACS* genes have also been reported to be upregulated by *F. graminearum* infecting spikes of wheat and barley, and also in maize for FGRAMPH1_01G17303 (Harris et al., 2016). Only FGRAMPH1_01G17303 was upregulated studies of FHB in wheat (Pan et al., 2018, Buhrow et al., 2020). However these genes are unlikely to play a role in ethylene manipulation since they lacked activity on ethylene precursor substrates (Svoboda et al., 2019). In contrast, the two ethylene-associated *ACS* genes (Table 5.2) were not differentially expressed in *F. graminearum* causing FRR (Ding et al., 2020).

Several other effector genes may play important roles as pathogenicity factors for *F. graminearum*. The two genes FGRAMPH1_01G08931 (FGSG_08021) and FGRAMPH1_01G27287 (FGSG_09353) which encode gegh16 proteins were one of the most highly upregulated effectors in both FHB and FRR of *B. distachyon* (Fig. 5.2). *Gegh* genes are thought to have a role in penetration and pathogenicity (Xue et al., 2002, Brown et al., 2012). Both FGRAMPH1_01G08931 and FGRAMPH1_01G27287 genes were upregulated in *F. graminearum*-inducing FHB in wheat, barley, and maize (Harris et al., 2016, Pan et al., 2018), and to FHB and FCR in wheat (Stephens et al., 2008). Only FGRAMPH1_01G08931 was upregulated in *F. graminearum*-inducing FHB in wheat (Brown et al., 2017). In a separate study, only FGRAMPH1_01G27287 was also upregulated in *F. graminearum* causing wheat and barley FHB (Lysøe et al., 2011). Both genes were also upregulated in response to wild-type *F. graminearum* induced FRR in *B. distachyon* (Ding et al., 2020). Together these findings suggest that these effectors serve an important function during *F. graminearum* pathogenesis. Expression of another effector, the HR gene FGRAMPH1_01G16209 (FGSG_04741), was increased in FHB and FRR of *B. distachyon* (Fig. 5.2). FGRAMPH1_01G16209 was also reported to be significantly upregulated in *F. graminearum* causing wheat, barley, and maize FHB (Harris et al., 2016, Brown et al., 2017, Pan et al., 2018, Buhrow et al., 2020) and in roots of *B. distachyon* (Ding et al., 2020). Two genes that encode CFEM domain-containing protein genes, (FGRAMPH1_01G05255

(FGSG_02181) and FGRAMPH1_01G13253 (FGSG_03599)), were highly upregulated in both FHB and FRR, but to a lesser extent in FRR (Log-fold change = 2.97, Fig. 5.2). CFEM domains are fungus-specific domains that likely have roles in infection (Kulkarni et al., 2003). FGRAMPH1_01G05255 was also upregulated in *F. graminearum* infected roots of *B. distachyon* (Ding et al., 2020), and crowns and spikes of wheat (Stephens et al., 2008, Brown et al., 2017) whereas FGRAMPH1_01G13253 was upregulated in other studies of FHB in wheat and barley (Harris et al., 2016, Brown et al., 2017, Pan et al., 2018, Buhrow et al., 2020).

Lastly, there were several other genes that were upregulated in both FHB and FRR (Fig. 5.2) and have also been reported to be significantly upregulated in at least four other *F. graminearum* infection transcriptome studies (Lysøe et al., 2011, Harris et al., 2016, Brown et al., 2017, Pan et al., 2018, Buhrow et al., 2020, Ding et al., 2020). These include two cell wall protein phiA (FGRAMPH1_01G14407 (FGSG_04074) and FGRAMPH1_01G08839 (FGSG_07988)), an antifungal protein (FGRAMPH1_01G16217 (FGSG_04745)), a putative sterigmatocystin biosynthesis peroxidase stcC (FGRAMPH1_01G12877 (FGSG_03436)), a ricin b lectin (FGRAMPH1_01G13221 (FGSG_03584)), a secretory phospholipase a2 (FGRAMPH1_01G14013 (FGSG_03911)), a tol protein (FGRAMPH1_01G05239 (FGSG_12081)), and a 22 kda glycoprotein (FGRAMPH1_01G25713 (FGSG_07807)). These eight genes merit further investigation. Many other uncharacterised genes were also similarly expressed between (Fig 5.2) and (Lysøe et al., 2011, Harris et al., 2016, Brown et al., 2017, Pan et al., 2018, Buhrow et al., 2020, Ding et al., 2020).

Many effectors, DON-related genes, and phytohormone-related genes that were upregulated in *F. graminearum*-induced FHB in *B. distachyon* (Fig. 5.2, Table 5.1, Table 5.2) were similarly expressed during *F. graminearum*-induced wheat and barley FHB (Lysøe et al., 2011, Harris et al., 2016, Brown et al., 2017, Pan et al., 2018). This suggests there are similarities and consistencies in the spectrum of effectors secreted by *F. graminearum* during infection of floral tissues of *B. distachyon*, wheat, and barley.

5.4.2. Tissue-Dependent *F. graminearum* Effectors and Genes

In addition to the large number of effectors expressed by *F. graminearum* during infection of both spike and root tissues of *B. distachyon*, there were also some notable differences (Fig. 5.2). Four *TOX* genes were upregulated by *F. graminearum* during *B.*

distachyon infection (Fig. 5.2), however the combination of them was tissue specific. *TOX1* (FGRAMPH1_01G00197, FGSG_00060)*, TOX2* (FGRAMPH1_01G00199, FGSG_00061), and *TOX3* (FGRAMPH1_01G00201, FGSG_00062) comprise a cluster of genes. This three-gene cluster was expressed in FHB (Fig. 5.2). Supporting these findings for FHB, this *TOX* cluster was reported to be upregulated in FHB of wheat and barley (Lysøe et al., 2011, Harris et al., 2016, Pan et al., 2018). *TOX3* was the only *TOX* gene upregulated in both FCR and FHB of wheat (Stephens et al., 2008). In contrast, expression of *TOX1*, *TOX3*, and *TOX4* (FGRAMPH1_01G08389, FGSG_10551) was enhanced in FRR, but to a lesser extent than in FHB (Fig. 5.2). *TOX2* and *TOX4* displayed tissue-specific expression (Fig. 5.2) and differential expression of *TOX2* was maintained over time (Fig. 5.3A)). Expression of *TOX4* was not found to be significantly enhanced in *F. graminearum* causing FHB in wheat, barley, or maize in one study (Harris et al., 2016), while it was found to be exclusively expressed in wheat in a second report (Lysøe et al., 2011), including a third study on wheat FHB, but only at 4 dpi instead of 2 dpi (Pan et al., 2018). In contrast to the present results (Fig. 5.2), Ding and colleagues (2020) did not identify expression of any of the four *TOX* genes in FRR of *B. distachyon* (Ding et al., 2020). These differences may be due to a different *Fusarium* isolate that was used in previous studies which may show differences in effector expression. The present study is the only one to use a common host accession and pathogen isolate. Alternatively, this difference may be due to a slightly altered method whereby roots were in contact with *F. graminearum* for a much longer period of five days (Ding et al., 2020) as opposed to one day in the present study (Section 4.2.3). However, taken together, the data suggests that there was selective expression of *TOX* genes in different *B. distachyon* tissues (Fig. 5.2) and between different species (Lysøe et al., 2011, Harris et al., 2016). It is unclear why *F. graminearum* would express different *TOX* gene combination depending on the host tissue. All four *TOX* genes are predicted to share a common "Killer Toxin KP4/SMK" domain (IPR011329 (Consortium, 2018)). Killer Toxin KP4/SMK proteins have antifungal properties and are involved in killing other fungal species (UniProt (Consortium, 2018)). Thus I can speculate that *TOX* genes may be responding directly to the different rhizosphere and phyllosphere microflora instead of the *B. distachyon* host tissues. However, Lu and Faris (2019) have shown that *F. graminearum* KP4 proteins may promote virulence towards seedling rot (Lu & Faris, 2019). This suggests that *TOX* genes may be important for *F. graminearum* virulence in FHB and FRR.

Cutins are polymers found on the external surfaces on plants (Agrios, 2005). Cutinases, that degrade cutin to monomers, are present in relatively large numbers in hemibiotrophic and necrotrophic pathogens such as *Gaeumannomyces graminis* and *Magnaporthe* oryzae (Zhao et al., 2014b). FGRAMPH1_01G12927 (FGSG_03457), FGRAMPH1_01G08583 (FGSG_10634) and FGRAMPH1_01G12551 (FGSG_03304), encoding cutinase, were upregulated in FHB, but only FGRAMPH1_01G12551 was upregulated in both FHB and FRR (Fig. 5.2). The two former genes encoding cutinases were reported to be upregulated in wheat and barley FHB (Lysøe et al., 2011), while in separate studies, and all three cutinases were found to be upregulated in FHB of wheat and barley (Harris et al., 2016, Pan et al., 2018). FGRAMPH1_01G12551 was the only cutinase upregulated in another study of FHB of wheat (Brown et al., 2017). FGRAMPH1_01G12927 was also reported to be upregulated in FCR and FHB of wheat (Stephens et al., 2008). None of these cutinase genes were upregulated in response to *F. graminearum* induced FRR in *B. distachyon* (Ding et al., 2020). Together this provides evidence for tissue-specific cutinase expression whereby most are exclusively upregulated during infection of floral tissues. This difference between tissues is likely due to the cutin layer being present only on the epidermis of shoot tissues (Walton, 1994). The expression of cutinase in roots (FGRAMPH1_01G12551) may also be associated with a different pathogenicity-associated role (Walton, 1994).

Two phytohormone-related genes also showed tissue-dependent expression. JA-hydroxylation-related (FGRAMPH1_01G05547, FGSG_02301) (Ding et al., 2020) was highly upregulated in FRR but not in FHB (Table 5.2). This gene was also reported to be significantly upregulated in *B. distachyon* FRR (Ding et al., 2020) but it was also upregulated in FHB of wheat (Harris et al., 2016, Brown et al., 2017). In contrast, the cytokinin-related tRNA-IPT, involved in cytokinin biosynthesis (Márquez-López et al., 2019) (FGRAMPH1_01G28119, FGSG_09015), was significantly upregulated only in FHB (Table 5.2). Supporting this, FGRAMPH1_01G28119 was not reported to be upregulated in FRR of *B. distachyon* (Ding et al., 2020), but was upregulated in wheat FHB (Pan et al., 2018). Whether these genes play a significant role in influencing *B. distachyon* hormone profiles is uncertain. Ding and colleagues (2020) show that despite *F. graminearum* possessing the ability to synthesise JA, there was no significant change in JA content in infected *B. distachyon* roots (Ding et al., 2020) suggesting an absence of JA manipulation during FRR. Given the amount of uncharacterised genes (Fig. 5.1, complete dataset not shown), and the abundance of pathogen strategies to manipulate phytohormones *in planta* (Kazan &

Lyons, 2014), there are potentially many more *F. graminearum* phytohormone-related genes in this dataset that are uncharacterised and would be interesting to investigate.

F. graminearum can produce the naphthoquinone aurofusarin, which is a red pigment (Fig. 2.1B), and is synthesised by the aurofusarin gene cluster (Malz et al., 2005, Frandsen et al., 2006). There were tissue-specific differences in expression of this gene cluster in *F. graminearum* during infection of *B. distachyon* (Table 5.3). All the genes were highly downregulated in FHB, except for FGRAMPH1_01G05605 (FGSG_02330) which was upregulated (Table 5.3). FGRAMPH1_01G05605, however, is not necessary for aurofusarin biosynthesis (Frandsen et al., 2006) which explains this gene being differentially expressed compared to the other seven preceding genes in FHB (Table 5.3). Similarly, all the genes (except FGRAMPH1_01G05593 (FGSG_12040) and FGRAMPH1_01G05605 (FGSG_02330)) appeared downregulated in *F. graminearum* inducing symptomatic wheat FHB (Brown et al., 2017). In another study, however, the entire gene cluster (Table 5.3) was upregulated in *F. graminearum* inducing FHB in wheat, barley, and/or maize (Harris et al., 2016). In contrast to the FHB results, several of the genes in the cluster were significantly upregulated in FRR (Table 5.3). The key genes required for aurofusarin biosynthesis (Kim et al., 2005, Frandsen et al., 2006), FGRAMPH1_01G05587 *aurO* (FGSG_02321), FGRAMPH1_01G05593 *PKS12*, FGRAMPH1_01G05599 *aurF* (FGSG_02327), and FGRAMPH1_01G05601 *GIP1* (FGSG_02328)) were highly upregulated in FRR (Table 5.3). This suggests aurofusarin is being produced by *F. graminearum* during FRR pathogenesis of *B. distachyon*. However the positive regulator FGRAMPH1_01G005585 encoding *aurR1*/*GIP2* (FGSG_02320) and the regulator with an undetermined function FGRAMPH1_01G05591 *aurR2* (FG05_02323) (Frandsen et al., 2006, Kim et al., 2006, Westphal et al., 2018) were downregulated or unchanged, respectively, in FRR (Table 5.3). The reason for the difference in expression between the two transcription factors and the biosynthetic genes is unclear. In contrast to the results in my study, none of the eight genes (Table 5.3) were significantly upregulated in *F. graminearum* inducing FRR in *B. distachyon* (Ding et al., 2020). The differences and similarities to other studies may be due to the *F. graminearum* isolate used. The isolates used to investigate *F. graminearum* FRR (Ding et al., 2020) and FHB (Harris et al., 2016) were CS3005 and DAOM180378, respectively. This is different to the *F. graminearum* isolate PH1 used in this study and by Brown and colleagues (2017) who generally showed similar transcription results for FHB (Brown et al., 2017) (Table 5.3). The comparison between different studies suggests that aurofusarin

regulation is *Fusarium*-isolate specific. The role of aurofusarin in FRR is unclear as it was shown to not affect FHB virulence in wheat and barley (Kim et al., 2005, Malz et al., 2005). However like with the *TOX* gene cluster, the primary function of aurofusarin may be as an antimicrobial compound (Westphal et al., 2018). Therefore I speculate that aurofusarin produced by *F. graminearum* isolate PH1 is important for competing with the microbiota on the *B. distachyon* rhizosphere but not those present on the *B. distachyon* phyllosphere.

Another effector class displaying tissue-specific expression were those predicted to encode metalloproteases. The two predicted metalloprotease effectors, FGRAMPH1_01G08399 (FGSG_10554) and FGRAMPH1_01G09079 (FGSG_08085), were exclusively upregulated in FRR (Fig. 5.2). Metalloproteases are enzymatic effectors that have chitinase inhibitory properties (Naumann et al., 2011, Jashni et al., 2015, Franceschetti et al., 2017). Supporting the findings in this study, none of the metalloprotease predicted effector genes (Fig. 5.2) were upregulated in a study with wheat FHB (Pan et al., 2018). However in other studies, both were upregulated in *F. graminearum* infecting wheat but not in barley or maize (Harris et al., 2016) or instead only FGRAMPH1_01G08399 or FGRAMPH1_01G09079 were upregulated in *F. graminearum* infecting wheat FHB (Buhrow et al., 2020) or (Brown et al., 2017), respectively. Instead of these two metalloproteases (Fig. 5.2), a different metalloprotease gene (FGRAMPH1_01G00105 (FGSG_00028)), was upregulated in *F. graminearum* isolate CS3005 during infection of roots of *B. distachyon* (Ding et al., 2020). FGRAMPH1_01G00105 was also upregulated in wheat, barley, and maize FHB (Lysøe et al., 2011, Harris et al., 2016, Brown et al., 2017, Pan et al., 2018, Buhrow et al., 2020). Likewise another predicted metalloprotease (FGRAMPH1_01G12949 (FGSG_03467) was also upregulated in wheat, barley, and maize FHB (Lysøe et al., 2011, Harris et al., 2016, Brown et al., 2017, Pan et al., 2018) and in *B. distachyon* FRR (Ding et al., 2020). FGRAMPH1_01G00105 and FGRAMPH1_01G12949 are classed as a non-effector metalloprotease (Brown et al., 2012) and are thus absent from Figure 5.2, however both also showed high expression in both FHB and FRR in the present study (Log fold change > 8, RNA-seq dataset not shown). Overall, the results from the current and previous studies indicate that there may be tissue-specific expression of metalloproteases however the evidence is not sufficient to draw conclusions. The reasons for the differences between studies are unclear and further investigation is required using a single *F. graminearum* isolate to infect different host

tissues and different hosts. Nonetheless, metalloproteases appear important for *F. graminearum* infection.

There were several other uncharacterised genes that showed significant large differential expression between tissues (Fig. 5.2) and these merit further investigation once characterised.

5.4.3. Conclusion

Most characterised or predicted genes and effectors were similarly upregulated in *F. graminearum* causing FHB and FRR. These core processes appear to be associated with CWDEs, DON production, SA-modification genes, as well as several other predicted pathogenicity factors. However, there were subtle differences for specific effectors and non-effector genes that were differentially expressed in FHB and FRR. These include *TOX* genes, cutinase, the aurofusarin gene cluster, and possibly JA and cytokinin-related genes. The examples above and the expression of many tissue-specific genes (Fig. 5.1 and Fig. 5.2) provide some evidence that *F. graminearum* is deploying a specialised secretome consisting of a different array of effectors when infecting different tissues. This would suggest that *F. graminearum* has the capacity to recognise the type of host tissue and adjust its' secretome accordingly as an infection strategy.

Chapter 6 - Ethylene production by *Fusarium graminearum*

6.1. Introduction

It is well documented that many microbial symbionts from the soil produce phytohormones to aid their colonisation and in turn support plant defence and nutrition (Jameson, 2000, Zamioudis & Pieterse, 2011, Fusconi, 2014). For example, up to 80% rhizosphere microbes can synthesise the auxin indole-3-acetic acid (IAA) (Jameson, 2000). On the opposite end of the symbiotic-parasitic spectrum (Zeilinger et al., 2016), certain plant pathogens have been shown to exploit phytohormone pathways (Dörffling et al., 1984, Murphy et al., 1997, Maor et al., 2004). One of the best-known cases of this is related to the bacterium *Rhizobium radiobacter* (formerly known as *Agrobacterium tumefaciens*) that causes crown-gall disease. On infected plant cells, auxin and cytokinin biosynthetic genes integrate into the host genome and induce excessive plant cell proliferation (Jameson, 2000). This is considered to contribute to the virulence strategy in order to redirect the plants' metabolites (Jameson, 2000), a form of manipulation and suppression of the plants defence response (Hedden et al., 2001, Robert-Seilaniantz et al., 2007).

Several *Fusarium* species can synthesise phytohormones. *Gibberella fujikuroi* (synonym *Fusarium monoliforme*) is known to induce 'bakanae' disease in rice (*Oryza sativa*) (Amatulli et al., 2010). It can produce a gibberellic acid (GA) isoform similar to the plant GA, and with similar effects on plant physiology (Malonek et al., 2004). With the example of GA biosynthesis, pathogen hormonal biosynthetic pathways are thought to have evolved independently in higher plants and fungi, with slightly different biosynthetic pathways (Hedden et al., 2001).

Some isolates of *Gibberella fujikuroi* have been shown to synthesise cytokinins (Van Staden & Nicholson, 1989). Similarly, *Fusarium pseudograminearum* can synthesise *Fusarium*-specific cytokinins (Sørensen et al., 2018). The responsible cluster was expressed during *B. distachyon* infection and one of these cytokinins promoted cytokinin-associated signalling in *B. distachyon* (Sørensen et al., 2018). Furthermore another *Fusarium*-specific cytokinin was induced at hyphae that were in close proximity to wheat tissue (Blum et al., 2019). Cytokinins produced by biotrophs and hemibiotrophs very likely contribute to green-

island formation where the fungus promotes delayed senescence in tissues surrounding the fungus, and forms a nutrient sink at infection sites (Murphy et al., 1997, Walters & McRoberts, 2006, Albrecht & Argueso, 2017). Indeed a *Fusarium*-derived cytokinin was shown to slightly delay senescence in *B. distachyon* leaves (Sørensen et al., 2018). ABA can also be produced by some *forma speciales* of *Fusarium oxysporum* (Dörffling et al., 1984). More recently, *Fusarium graminearum* was discovered to possess the biosynthetic machinery to synthesise and metabolise IAA (Luo et al., 2016, Qi et al., 2016) as well being able to produce ABA, SA, and JA *in vitro* (Qi et al., 2016, Ding et al., 2020).

Ethylene has been reported to be produced by numerous fungi (Table 6.1). At the start of the project in this Chapter, there was no evidence that *F. graminearum* and *Fusarium culmorum* could synthesise ethylene. However at study by Svoboda and colleagues (2019) observed ethylene production by *F. graminearum in vitro* but the authors did not identify the pathway responsible (Svoboda et al., 2019). Ethylene biosynthesis can be achieved through one or a combination of three pathway (Fig. 6.1). Two of the three pathways have been reported in a few *Fusarium* species (Table 6.1): the α-keto γ-methylthiobutyric acid (KMBA) pathway or the ethylene-forming-enzyme (EFE) pathway (Fig. 6.1). Most pathogenic fungi predominantly use the KMBA pathway for ethylene biosynthesis (Fig. 6.1). The KMBA pathway requires only methionine as a precursor (Fig. 6.1) and is mainly found in bacteria but is also present in fungi such as *Botryotinia fuckeliana* (synonym *Botrytis cinerea*) and *F. oxysporum* (Billington et al., 1979, Tzeng & DeVay, 1984, Chagué et al., 2002, Cristescu et al., 2002, Qadir et al., 2011). *Penicillium digitatum* is the only organism recorded in which both the EFE and KMBA pathways are present (Table 6.1). The ACC pathway also utilises methionine as a precursor in plants (Fig. 6.1) however in many cases this pathway was proven to not be utilised for ethylene biosynthesis in fungi (Wilkes et al., 1989, Chagué et al., 2002, Cristescu et al., 2002, Daundasekera et al., 2003, Qadir et al., 2011, Zhu et al., 2017).
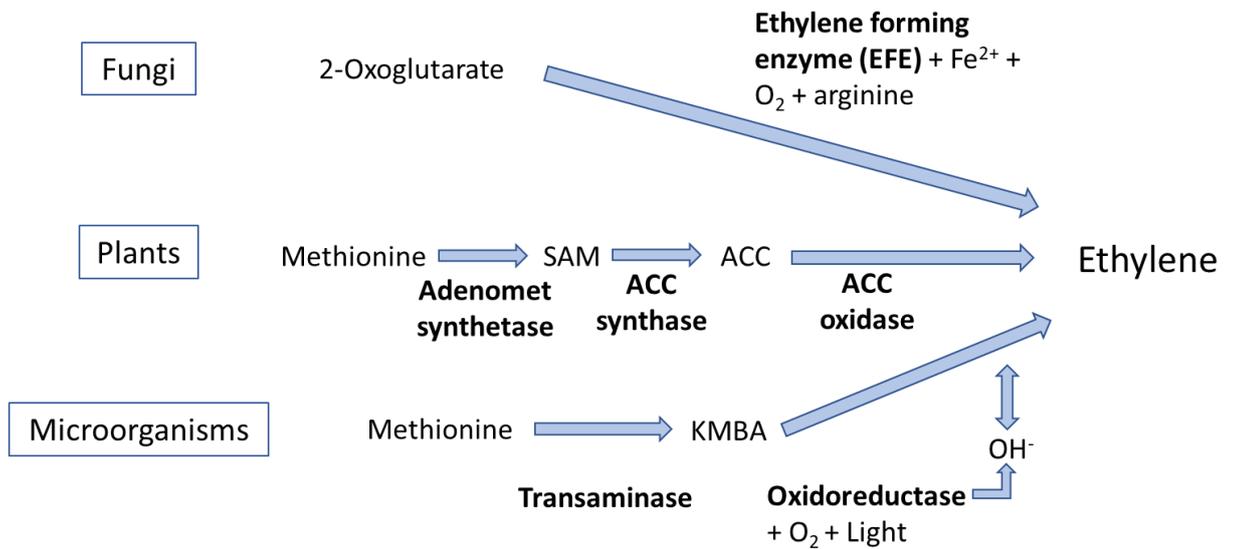
Figure 6.1. The three ethylene biosynthetic pathways. Enzymes are in bold. Hereafter the fungal pathway will be referred to as the EFE pathway, the plant pathway as the ACC pathway, and the microorganism one as the KMBA pathway. Note that the second step of the KMBA pathway is believed to be non-enzymatic (Fukuda et al., 1989) and light is important for the final conversion of KMBA to ethylene (Chagué et al., 2002, Zhu et al., 2012). Further information on the pathways can be found at MetaCyc.org (PWY-6853, ETHYL-PWY, PWY-6854) (Caspi et al., 2017). Abbreviations: ACC (1-aminocyclopropane-1-carboxylic acid), KMBA (α-keto γ-methylthiobutyric acid), EFE (ethylene-forming-enzyme). This figure is modified with permission from (Ansari et al., 2013).

Signalling processes in response to ethylene production have been linked to susceptibility in *Arabidopsis thaliana* to *Fusarium graminearum* (Chen et al., 2009). Therefore, it is plausible that *Fusarium* might be able to harness the ability to produce its own ethylene to increase susceptibility of the host. There are links between ethylene signalling and cell death in plant defence responses (Moore et al., 1999). Additionally, the virulence factor deoxynivalenol (DON) is thought to modulate cell death via ethylene signalling (Chen et al., 2009), and increased ethylene production by *B. cinerea* correlated with increased disease symptoms (Zhu et al., 2012). Ethylene also accelerates senescence (Abeles et al., 2012, Davies, 2013). These physiological effects from the phytohormone could indirectly predispose the plant to infection and colonisation by a necrotrophic pathogen that benefits from dead tissue for nutrients (Glazebrook, 2005, Cristescu et al., 2007, Pieterse et al., 2012). Furthermore, an EFE supplementary amino acid arginine has been associated with trichothecene biosynthesis (Gardiner et al., 2009, Gardiner et al., 2010). Ethylene production by the fungus could act as a virulence factor used to stimulate

and redirect the host's metabolism in a manner that aids host colonisation through suppression of defence, resulting in increased susceptibility to *Fusarium*.

Table 6.1. The fungal pathogens (to my knowledge) which have been found produce ethylene and their predicted pathway used.

Fungal Pathogen	Pathway	References
Botrytis cinerea	KMBA	(Qadir et al., 1997, Chagué et al., 2002, Cristescu et al., 2002, Qadir et al., 2011, Zhu et al., 2012)
Fusarium oxysporum f. sp. vasinfectum	KMBA*	(Tzeng & DeVay, 1984)
Alternia alternata	KMBA	(Zhu et al., 2017)
Verticillium dahliae	KMBA	(Tzeng & DeVay, 1984)
Colletotrichum musae	KMBA	(Daundasekera et al., 2003)
Colletotrichum dematium var truncatum	KMBA*	(Tzeng & DeVay, 1984)
Sclerotinia sclerotiorum	KMBA*	(Al-Masri et al., 2006)
Endothia gyrosa	KMBA	(Wilkes et al., 1989)
Cytospora eucalipticola	KMBA	(Wilkes et al., 1989)
Penicillium cyclopium	EFE	(Pažout & Pažoutová, 1989)
Fusarium oxysporum f. sp. tulipae	EFE	(Hottiger & Boller, 1991)
Fusarium mangiferae	**	(Ansari et al., 2013)
Penicillium digitatum	KMBA + EFE	(Chalutz et al., 1977, Billington et al., 1979, Fukuda et al., 1986)

The pathways are described in Fig. 6.1. *Methionine-dependent but not fully determined to be the KMBA pathway. **The authors did not identify which pathway was being utilised, only that ethylene was present. Abbreviations: EFE (Ethylene forming enzyme), KMBA (α-keto γ-methylthiobutyric acid).

It was reported that the ethylene-signalling pathway is exploited by *F. graminearum* (Chen et al., 2009). I hypothesise that this exploitation by *F. graminearum* may be the result of *F. graminearum*-derived ethylene as opposed to ethylene originating exclusively from the host plant. Gas chromatography and transcriptomics will be used to investigate the potential biosynthesis of ethylene by *F. graminearum* and identify the pathway and genes responsible. Any suitable candidate biosynthesis gene will then be deleted using a split-marker deletion method and ethylene production and virulence of deletion strains will be investigated. Like other *Fusarium* species (Table 6.1) if ethylene is produced by *F. graminearum*, it is probable that this is achieved through either the EFE or KMBA biosynthetic pathway.

1. Determine whether *F. graminearum* produces ethylene.

2. Identify which ethylene biosynthetic pathway is being used.

3. Identify potential ethylene biosynthesis genes and validate their function.

4. Determine whether ethylene production acts as a virulence factor.

6.2. Materials and Methods

6.2.1. Preparation and Maintenance of *F. graminearum*

All *Fusarium graminearum* isolates (Table 6.3) were obtained from stocks at the John Innes Centre, Norwich, UK. *F. graminearum* PH1 was maintained on 20 ml potato dextrose agar (PDA), unless otherwise stated, in 9 cm plastic Petri-dishes in controlled environment cabinets (Snijders Labs MicroClima-series, Economic LUX chambers or in a walk-in controlled environment growth room) at 22°C, 16 h/8 h light/dark photoperiod. For the different experiment with different *Fusarium* species and isolates (Fig. 6.9), the isolates were grown on ½ V8 agar for 1 week at the same growth conditions. ½ V8 agar was made by separately preparing 3% Bactoagar (9 g in 300 ml) and then 50 ml V8 Vegetable Juice with 150 ml diH$_2$0 (ELGA). The two mixtures were combined after autoclaving. For gene deletion experiments, *F. graminearum* PH1, obtained from Rothamsted Research, was maintained on PDA under a mixture of white light and UVA light at room temperature. Subsequently cultures were also grown on PDA in controlled growth cabinet at 22°C, 16 h/8 h light/dark photoperiod for experiments with transformants.

6.2.2. Gas Chromatography for *F. graminearum* Ethylene Production

Low nitrogen Czapek Dox Liquid (CDL) medium modified (Oxoid) was prepared (33.4 g/L ELGA water) and autoclaved. Once cooled, the necessary filter sterilised co-factor chemicals were added to respective treatments (Table 6.2). The media was then divided into aliquots for each replicate into 50 ml (Fig. 6.2A) or 10 ml (Fig. 6.2B). Then 0.1% volume of a 200 µM streptomycin and penicillin mixture (Solution prepared by Dr Laetitia Chartrain) was added to each flask individually to prevent any potential bacterial growth. Subsequently, *F. graminearum* PH1 conidial stock was pipetted into each flask to a working concentration of 1 x 10^4 conidia/ml (Fig. 6.2A). Alternatively, one mycelial plug (size) from a 7-day-old *F. graminearum* plate was placed in each flask (Fig. 6.2B). For the experiment with many transformants (Fig. 6.14C and 6.14D), a sterile toothpick was used to gather a large clump of mycelia from a plate. The toothpick and mycelia were then placed in the appropriate CDL medium container. Aerated flasks were then placed in a shaker (New

Brunswick Scientific Series 25 or Model G25 or Innova 44 model) at 200 rpm, 25°C (In one experiment up to 30°C for a short period due to machine malfunction) in either natural or artificial light (Tzeng & DeVay, 1984). In one experiment, the settings were set to 220 rpm at 28°C for the first incubation day before returning to standard conditions for the last incubation day (Fig. 6.8B, Fig. 6.8C, Fig. 6.8H, and Fig. 6.8I). After one day of shaking, flasks were sealed with three layers of duct tape (Fig. 6.2A) or Suba Seal rubber septa (Fig. 6.2B) (Sigma-Aldrich). Ethephon (Sigma-Aldrich/Merck) was used as a positive control for gas chromatography (GC) experiments since under a basic pH, it breaks down to ethylene. Ethephon was dissolved in water (sterile diH$_2$0) to a 50 mM stock (Chen et al., 2009). Using a pH meter, the pH of the solution was adjusted to approximately pH 11 with the slow addition of a few drops of 1 M NaOH. Then 4 ml of this was aliquoted into individual Vacutainers.

Table 6.2. The supplements required and used for each ethylene pathway to function under aerobic conditions assuming the organism has the biosynthetic capacity to synthesise ethylene (Fig. 6.1).

Supplements*	Conc. (mM)	EFE pathway	KMBA pathway**	ACC Pathway**
2-Oxoglutarate	0.25	+	-	-
L-Arginine	0.2	+	-	-
L-Histidine	10	+	-	-
L-Methionine	10	-	+	+
KMBA	1	-	+	-
ACC	10	-	-	+

The three pathways are described in Fig. 6.1. *Working concentration included for each supplement. ** Only one of the two supplements are required for ethylene production. The most effective concentration of each supplement was derived from (Nagahama et al., 1991, Chagué et al., 2002)). A plus symbol denotes the compound is necessary for the pathway above whereas a minus symbol denotes that it is not. A lower concentration of KMBA was used because of a low starting stock. The transaminase inhibitor AOA (Aminooxyacetic acid) was also utilised in Fig. 6.8 at 10 mM (Qadir et al., 2011). The concentration of ACC and AOA were chosen to match the concentration of methionine. Abbreviation: ACC (1-aminocyclopropane-1-carboxylic acid), KMBA (α-keto γ-methylthiobutyric acid). All compounds were ordered from Sigma-Aldrich/Merck.

After another day of shaking and once the GC (Perkin Elmer Clarus 480 gas chromatograph) was set up, 1 ml of headspace gas from the flasks was extracted using a 1 ml syringe (Terumo) attached to a fine long injection needle (Agani needle 25G Terumo,

0.5 x 25 mm). The gas was injected relatively fast into the rubber seal of one of the GC channels before running the GC and was repeated for each individual sample. Each sample was individually recorded, and the output was subsequently analysed. To set up the GC for detection (as per the user guide written by members of Professor Phil Poole's group at the JIC), the nitrogen carrier gas was turned on and the GC was turned on before waiting for each component (Oven, Injector, and Detector) to reach the appropriate temperature. Then both the hydrogen and oxygen, used as the FID fuel, were also turned on. The carrier gas was set at a flow rate of approximately 25 ml/min (or approximately 8 ml/min was used for Fig 6.8H, Fig. 6.8I and Fig. 6.14 because the machine settings were updated). Then the Flame Ionisation Detector (FID) was ignited and set at approximately 0.08 mV after turning off and on the hydrogen and oxygen gas. The GC column used was a HayeSep N 80-100 mesh. The software (TotalChrom Workstation) was set up as per the user guide and the detection sensitivity was set to the highest detection sensitivity (FID range 1, INT attenuation -6). All ethylene volumes were calculated from ethylene peak data on GC software using the percentage volume from 1 ml total volume input.
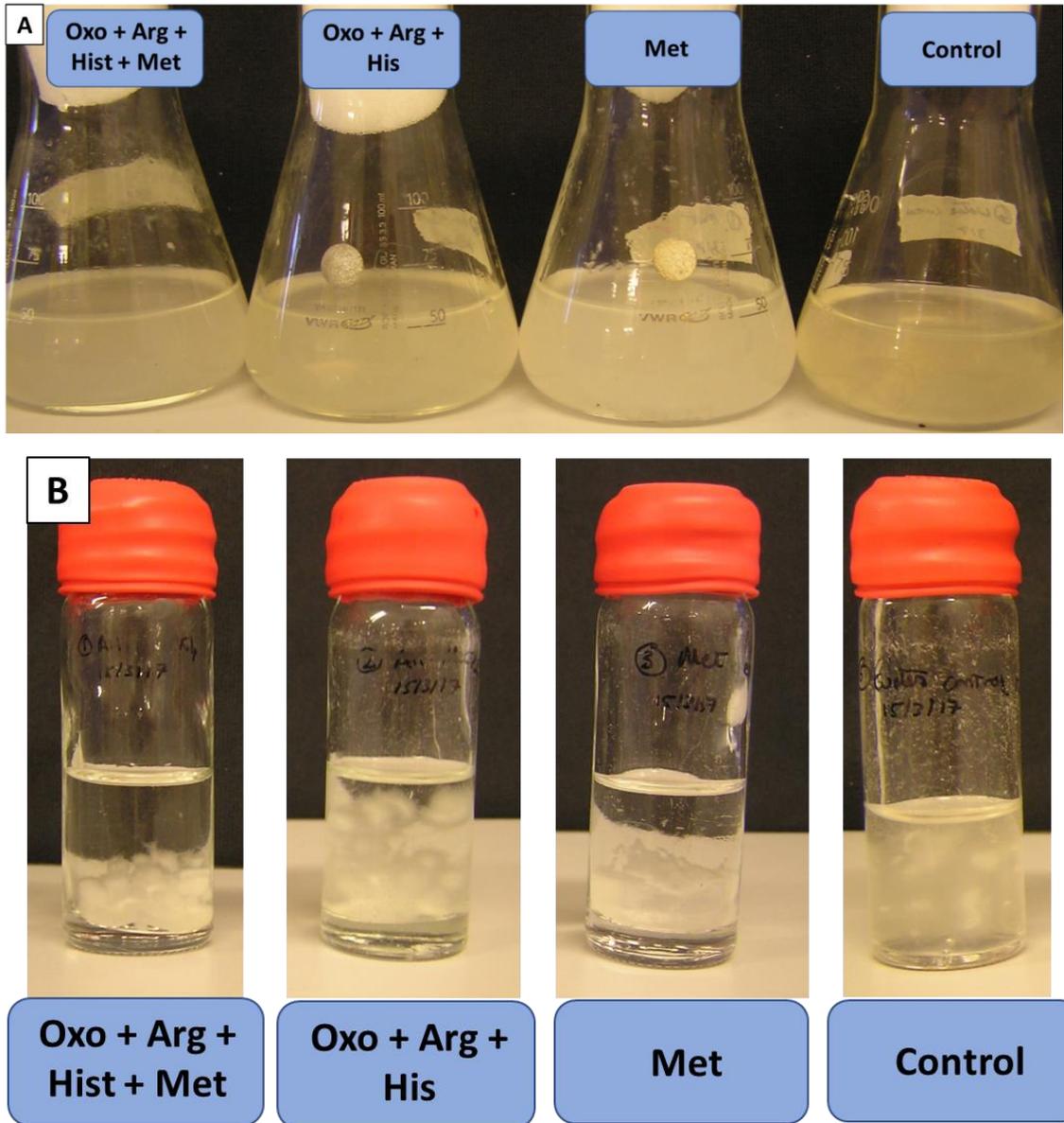
Figure 6.2. The two effective methods for ethylene GC with *F. graminearum* using 100 ml conical flasks (**A**) or Universal flasks (**B**). Ultimately most experiments were carried out using method **B**. Pictures were taken immediately after measuring ethylene content at 2 dpa. Abbreviations: OXO (2-oxoglutarate), Arg (Arginine), His (Histidine), Met (Methionine).

The same method for ethylene detection was used for all other *Fusarium* species and isolates (Table 6.3).

Table 6.3. The list of *F. graminearum* and *F. culmorum* isolates with respective chemotypes used for testing ethylene emission in ethylene-producing defined media.

Species	Isolate ID	Chemotype*
F. graminearum	PH1	15Ac DON
F. graminearum	K1/4	15Ac DON
F. graminearum	CC120	15Ac DON
F. graminearum	F86	NIV
F. graminearum	F500	NIV
F. culmorum	2076	3Ac DON
F. culmorum	2037	3Ac DON
F. culmorum	CC52	3Ac DON
F. culmorum	F77	3Ac DON
F. culmorum	F710	NIV
F. culmorum	F712	NIV
F. culmorum	F713	NIV

Abbreviations: Ac DON (Acetyldeoxynivalenol), NIV (Nivalenol). *Derived from Professor Paul Nicholson, personal communication.

6.2.3. RNA-seq Preparation and Analysis and qRT-PCR Validation

Samples were grown in minimal media with methionine (termed M samples) or without methionine (termed C samples) with 200 μM of streptomycin and penicillin mixture for four days in a shaker at 200 rpm (New Brunswick Scientific Series 25 or Model G25 or Innova 44 model). Immediately after verifying ethylene presence (Data not shown), mycelia were frozen and DNA-free RNA was prepared excluding the cDNA first strand synthesis protocol (RT-qPCR section). Sample libraries were prepared and sequenced by Ms Grittney Tam at Genewiz. Initially mRNA was enriched and fragmented then underwent random priming. Then first and second strand cDNA synthesis of the mRNA was performed. Subsequently strand ends were repaired, the 5' ends were phosphorylated and the 3' ends were adenylated. Finally, the adaptor sequences were ligated to the 3' ends (sequencing via polyA selection), enriched with PCR and then sequenced using Illumina HiSeq, PE 2x150bp. RNA-seq Bioinformatics analysis was performed by Mr Brian Sereni at Genewiz: Initially sequence quality was evaluated by checking the number of reads and yield giving a mean quality score for each sample. Subsequently the per base sequence quality and per

sequence GC content was measured. Using Trimmomatic v.0.36, Sequence reads were trimmed to remove adapter sequences and nucleotides with poor quality. Using STAR aligner v.2.5.2b (splice aligner that detects splice junctions and incorporates them to align the entire read sequence), the sequence reads were mapped to the reference genome of *Fusarium graminearum* str. PH-1 which was available on Ensembl Genomes (Howe et al., 2020). From this, BAM files were generated. Unique reads found within exon regions were counted using Subread package v.1.5.2 featureCounts giving unique gene hit counts. Differential gene expression was analysed using the gene hit counts table. A comparison of gene expression between groups of C and M samples was analysed using DESeq2. Using the Wald test, p-values and log2fold change were calculated. In order to accurately determine differential gene expression, values were normalised and then dispersion of variance values were shrunk to a common mean by leveraging dispersion information across all genes.

For qRT-PCR validation of RNA-seq data (Fig. 6.10), RNA samples that were not sent for RNA-seq from the method described above (Samples were from the same experiment) were used to test FGRAMPH1_01G00157 fold change in the presence of methionine as per the protocol in (Chapter 2 method section 2.2.5). The primers for FGRAMPH1_01G00157, forward 5'-ACATCCGCCCATTTGCATTT-3' and reverse 5'-CTCCACTTGATAACAGGCGC-3' (Tm 59.1°C and 58.99°C, 211 bp amplicon size) and the housekeeping gene *gzUBH* (Supp. Table S13) were tested using the same protocol as in Chapter 2 (Method Section 2.2.5, Table 2.5, Table 2.6) on cDNA. The appropriate concentration of cDNA and the primer efficiency for FGRAMPH1_01G00157 and *gzUBH* were experimentally determined through a dilution series qRT-PCR experiment (Described Section 2.2.5 but using a 5-fold dilution series). The Log fold change was calculated using Equation 2.1. The primers for *gzUBH* were quality tested using the same protocol as in Chapter 2 (Method Section 2.2.5, Table 2.3, Table 2.4) using *F. graminearum* PH1 DNA from 7 day old plates, frozen in liquid nitrogen, and extracted using the CTAB protocol (Method Section 4.2.5).

6.2.4. *F. graminearum* Gene Deletion: Split-Marker Deletion

Several protocols, resources, and assistance for this following section were provided by Dr Martin Urban at Rothamsted Research as part of a collaboration.

6.2.4.1 Cloning

Fourteen primers were prepared (Supp. Table S14) for either the 3' or 5' of the flanking region or the hph (Hygromycin-B-phosphotransferase) selectable marker using the Gibson assembly (Gibson et al., 2009). The hph gene also contains the respective upstream promoter. The NEBuilder Assembly Tool V1 (https://nebuilderv1.neb.com/) was used to design primers (Supp. Table S14) with overlapping regions of the vector and the respective adjacent primers (Fig. 6.3).
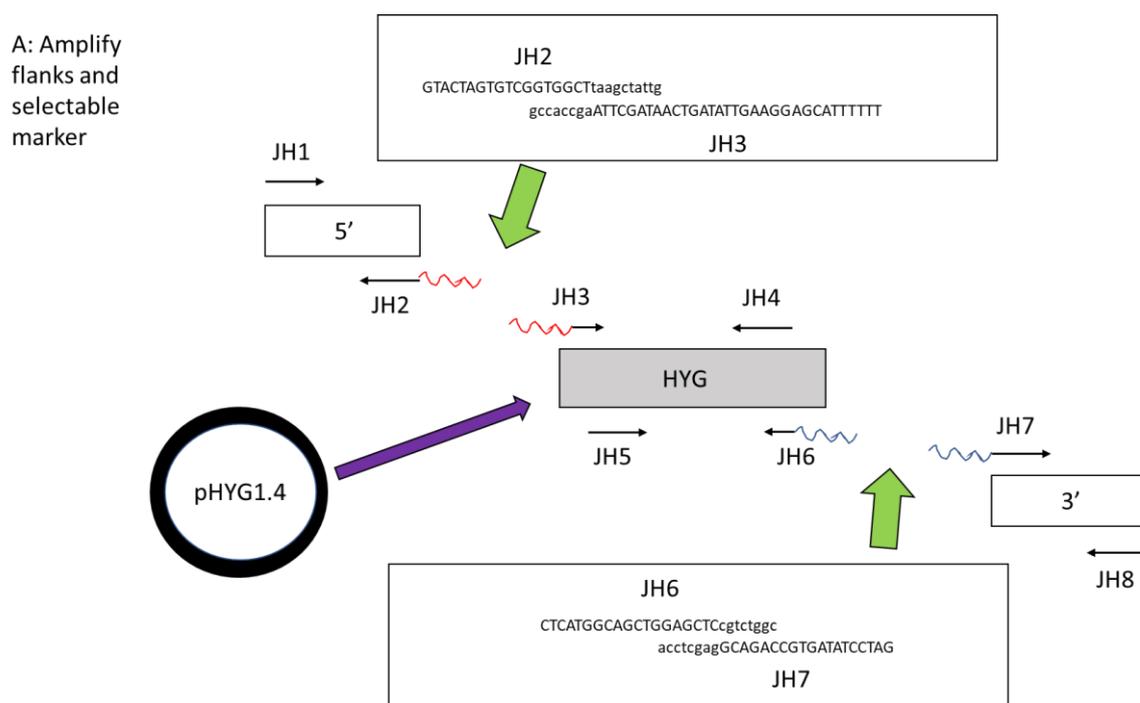
Figure 6.3. *F. graminearum* gene deletion step A: First PCR to amplify gene target flanks and selectable marker from plasmid pHYG1.4. Primer Sequences at Supp. Table S14. This figure is taken and modified with permission from (Catlett et al., 2003).

A standard PCR was first used to amplify the target gene and the selectable marker resistance gene (Table 6.4 and Table 6.5).

Table 6.4. *F. graminearum* gene deletion step A: Fragment amplification.

Reagent	Concentration	μl/well
Phusion Master Mix	2x	12.5
Primer F	10 μm	0.5
Primer R	10 μm	0.5
DMSO	100%	0.75
cDNA	50 ng/μl	0.5
dH$_2$O		10.25
Total		25

Phusion Master Mix (New England BioLabs) was prepared using 2 X HF buffer, 3 mM MgCl2, 400 μm dNTPs, and 0.04 units/μl Phusion Polymerase. Associated with Fig. 6.3. Primer pairs JH1 + JH2, JH3 + JH4, JH5 + JH6, JH7 + JH8 (Supp. Table S14).

Table 6.5. Gradient PCR for *F. graminearum* gene deletion step A.

Step	Temperature (°C)	Number of Cycles	Time (s)	Activity
1	98	1	30	Denaturation
2	98	40	10	Denaturation
3	55-68	40	30	Annealing
4	72	40	45	Extension
5	72	1	600	Extension
6	10	1	Indefinitely	Storage

Four combinations of primers used at different annealing temperatures: JH1 +JH2 (62.8°C), JHF3 + JH4 (67.8°C), JH5 + JH6 (60.4°C), JH7 + JH8 (55.8°C) (Supp. Table S14). Associated with Fig. 6.3 and Table 6.4.

After amplification, PCR products (9 μl) were visualised in a Bio-Rad Gel Imaging System. on a 1% gel with 6 μl Ethidium Bromide (Merck/Sigma Aldrich) at 80 V to 100 V and using 6 X loading buffer (New England Bioscience). Amplified fragments of the correct size were then excised from the gel using a transilluminator and were purified using a gel extraction kit (QIAGEN). In Eppendorf, 350 μl of Buffer QG was added to fragment and then kept at 50°C for 10 min and vortexed every 3 min. Then 350 μl of isopropanol was added to the samples and mixed. The DNA was then bound to the column by having the samples centrifuged for 1 min in a QIAquick column at 15,700 rcf and the flow-through was discarded. Subsequently, 0.5 ml Buffer QG was added to the same column and centrifuged again for 1 min at 15,700 rcf and the flow-through was discarded. Then 0.75 ml Buffer PE was added to the sample column and incubated at room temperature for 5 min,

centrifuged for 1 min, and the flow through was discarded. The column was centrifuged at 15,700 rcf for 1 min and placed in a microcentrifuge tube. Finally, 12 µl of water (sterile diH$_2$0) was added to the Qiaquick membrane, incubated at room temperature for 4 min and centrifuged for 1 min at 15,700 rcf. This step was repeated with remaining eluate. Another PCR with 40 µl total (Table 6.4 and Table 6.5) for samples with low yield (5' flank) were pooled and the concentration was increased using a Savant Speed Vac SPD121p with a Universal Vacuum System Plus UV5400A.

Step B consisted of fusing the 5' Flank with HY fragment, and the 3' Flank with the YG fragment. The EcoRV linearized vector PGEMt-easy system 1 (Promega) was used for the fragment fusions. The reaction (Table 6.6) was incubated in a water bath for 60 min at 50°C.
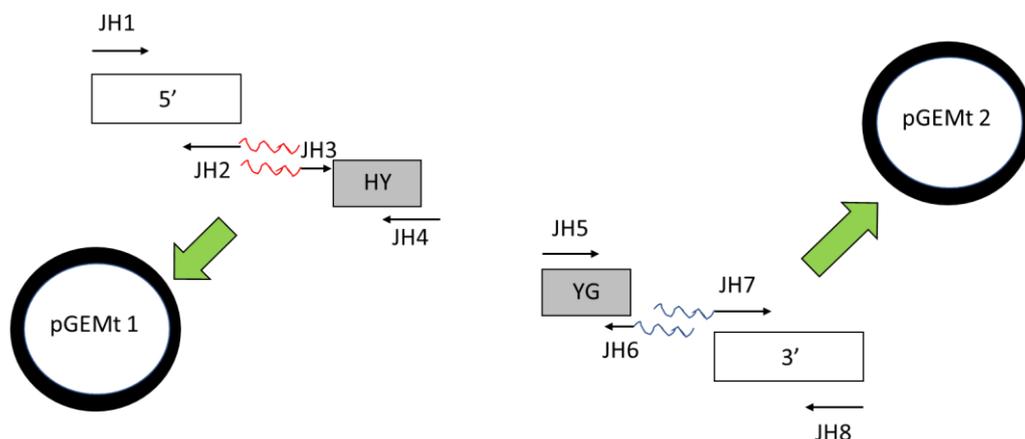
Figure 6.4. *F. graminearum* gene deletion step B illustration of fusing target gene flanks with selectable marker fragments. Primer Sequences at Supp. Table S14. This figure is taken and modified with permission from (Catlett et al., 2003).

Table 6.6. *F. graminearum* gene deletion step B: 5'+HY and 3'+YG fragment fusion.

Reagent	Concentration	Volume per well (µl)
Gibson master Mix	2x	5
HY/YG fragment	35/50 ng/µl	2
5'/3' fragment	11/25 ng/µl	2
pGEMt easy vector	50 ng/µl	1
dH$_2$O		10.25
Total		25

Associated with Fig. 6.4.

After PCR amplification, the vectors were cloned in *E. coli* competent cells (Subcloning EFF DH5-alpha competent cells 2 ml (Life Technologies Ltd (Invitrogen Division)). Beforehand, 1.5 ml Eppendorfs were chilled on ice, and then 5 μl of respective Gibson reaction (5'+HY and 3'+YG, Table 6.6) was added to each tube. The competent cells were thawed on ice and 35 μl was transferred to the chilled culture tube. The mixture was then kept on ice for 25 min. The cells were carefully transferred to a water bath at exactly 42°C and heat-shocked for 50 sec. The tubes were then immediately placed on ice for 2 min. Then 250 μl of cold SOC medium (20 g tryptone (peptone from casein), 5 g yeast extract, 0.58 g NaCl, 0.186 g KCL, 2.03 g MgCl$_2$ 6H$_2$O, 2.46 g MgSO$_4$ 7H$_2$O, and 3.6 g glucose to 1 L water) (Prepared by the JIC media kitchen) was added to each reaction. The mixture was then incubated at 37°C for 60 min (Thermo Scientific Heratherm incubator). Then 100 μl and 200 μl of *E. coli* clones were spread onto LB plates (Fast-media Amp, XGAL with Amplicillin, Invitrogen), dried for 5 min, sealed with parafilm and incubated overnight at 37°C (Thermo Scientific Heratherm incubator). The next morning, any white colonies were first streaked onto a gridded plate of the same LB media using a clean pipette tip, and then the tip was placed in PCR wells with PCR reaction (Table 6.7).

Table 6.7. Colony PCR for cloned *Escherichia coli* colonies.

Reagent	Concentration (μm)	Volume per well (μl)
Buffer 5x		3
MgCl$_2$	25	0.9
dNTPs	10000	0.3
TaqPol*		0.05
M13 Primer F	10	1
M13 Primer R	10	1
E. coli colony**		
dH$_2$O		8.75
Total		15

Negative control also included with 1 μl plasmid template (replaces 1 μl of water (diH$_2$0)). *TaqPol (Gotaq G2 Flexi DNA polymerase from Promega). ** DH5-alpha competent cells.

Cloned colonies with inserts were visualised on a gel (as described above) using all the PCR product from the colony PCR, and inserts with the correct size were excised from the agarose gel with a transilluminator. The gel extraction protocol, as described above, was repeated with these excised PCR inserts. For each insert, two tubes of 5 μl of purified DNA, 2 μl of forward or reverse M13 primers, and 8 μl water (sterile diH$_2$0) were sent for

sequencing (Eurofins). This is important to check that the *HYG* sequences were correct. The chromatogram quality was assessed first and then ClustalW was used to compare to detect any nucleotide changes compared to the reference sequences using BioEdit (Hall, 1999). Uniprot UGENE v1.31 (Okonechnikov et al., 2012) was used to check for any amino acid sequence changes at all potential frames.

Once the sequences of the inserts were validated, positive transformed colonies from colony PCR plate were transferred to new LB plates (LB agar Miller, prepared by the JIC media kitchen) containing 100 µg/ml carbenicillin. A sterile toothpick was used to transfer the colony and this was then placed in a 20 ml sterile universal flask containing 10 ml liquid LB broth (25g LB Broth Miller) with 100 µg/ml carbenicillin. The flask was left overnight at 37°C in a shaker at 220 rpm (New Brunswick Scientific Innova 44 model).

A Miniprep protocol was used on colonies that grew. A 2 ml aliquot of the overnight culture was centrifuged at 5,900 rcf for 3 min at room temperature. The pellet was then resuspended in 250 µl Buffer P1 and transferred to a microcentrifuge tube. Then 250 µl of Buffer P2 was mixed in and the tube was incubated at room temperature and inverted occasionally for a maximum of 5 min until the solution cleared. Then 350 µl of Buffer N3 was mixed in thoroughly by inversion. The mixture was centrifuged at 15,700 rcf for 10 min. The 800 µl of supernatant was then placed in a QIA2.0 spin column and centrifuged for 60 seconds and 15,700 rcf. The remnants were then washed with buffer PB and centrifuged for 60 s at 15,700 rcf. A further wash was performed by adding 0.75 ml Buffer PE to the spin column and this was then centrifuged for 60 s at 15,700 rcf and then again for 1 min to remove residual wash buffer. The column was then placed in an Eppendorf tube where 50 µl of water (sterile diH$_2$0) was added followed by incubation at room temperature for 1 min and was subsequently centrifuged for 1 min. The sample quantity and quality were then measured on a NanoDrop 2000 Spectrophotometer (Thermo Scientific).

Before transformation, the insert fusions were amplified using a Bulk PCR protocol. A minimum of six reactions per insert was amplified (Table 6.8). A new reverse primer (A2) for 5' and HY fusion was used as a replacement for primer JH4 due to amplification issues.

Table 6.8. Bulk PCR mix for *F. graminearum* transformation preparation.

Reagent	Concentration (µm)	Volume per well (µl)
HotStarTaq		25
Primer F	10	1
Primer R	10	1
Plasmid DNA	50 ng/µl	0.5
dH$_2$O		22.5
Total		50

Primers used were JH1 and A2 for 5' and HY fusion, and JH5 and JH8 for YG and 3' fusion (Supp. Table S14).

The optimum PCR annealing temperature (Table 6.9) for each fusion was identified using a gradient PCR. It is worth noting a new primer (A2) was used to increase yield of PCR product. The samples were run on a 1% agarose gel (Melford) with 2 µl of 6X loading buffer to 10 µl PCR product at 80 V to 100 V for 40 min. Once the PCR product size was validated, all six reactions were pooled into a 2 ml Eppendorf (approximately 300 µl total volume). Then 200 µl of dH$_2$O was added to the tube. An equal volume (500 µl) of phenol/chloroform/isoamyalcohol (25:24:1) was pipetted in and mixed. The mixture was centrifuged at 15,900 rcf for 5 min and kept on ice. The upper phase of DNA was pipetted into a clean 2 ml Eppendorf and water (sterile diH$_2$0) was added up to 500 µl if necessary. Then 500 µl of chloroform was added, mixed thoroughly and centrifuged for 5 min at 15,900 rcf. Again, the upper DNA phase was placed into another new 2 ml Eppendorf. Then 2 volumes (1 ml) of cold Ethanol was added and mixed by inverting four to eight times. The mixtures were kept on ice for 15 min and then centrifuged at 16,400 rcf for 15 min. The ethanol was removed by pipetting and then the tube was washed by with 300 µl 70% ethanol. Ethanol traces were removed by incubating tubes for a minimum of 5 min at room temperature. The pellet was resuspended in 30 µl of water (sterile diH$_2$0), vortexed, and measured on a NanoDrop 2000 Spectrophotometer (Thermo Scientific). Each sample had at least 1 µg/µl of DNA. As a final validation step, individual samples aliquots were sent for sequencing (Eurofins) with respective primers combinations (Supp. Table S14, JH 1 and JH 12, JH 14 and JH 8, JH 1 and JH 4, JH 5 and JH 8). Furthermore, a dilution of 200 ng/µl was run on a 1% agarose gel (Melford) for 30 min – 50 min at 80 V to 100 V. (Sample components: 5.5 µl DNA, 2 µl 6X Loading dye (New England BioLabs), 3.5 µl water (sterile diH$_2$0)).

Table 6.9. Bulk PCR mix program for *F. graminearum* transformation preparation.

Step	Temperature (°C)	Number of Cycles	Time (s)	Activity
1	95	1	900	Denaturation
2	94	34	60	Denaturation
3	52	34	30	Annealing
4	72	35	150	Extension
5	72	1	600	Extension

6.2.4.2 Transformation

The Fg PH1 conidia were prepared for transformation by pipetting $2x10^5$/ml conidia onto four to five PDA plates and were incubated for two days at room temperature under a mixture of UVA and white light. The growth on plates was gently scraped with 10 ml dH_2O using a glass stirrer and collected in a 50 ml falcon tube. The spore suspension was filtered through two layers of miracloth into a sterile bottle. Spores were counted with a haemocytometer to $1x10^6$. The mixture was transferred into 300 ml TB3 (0.3% Yeast extract, 0.3% Bacto Peptone, 20% Sucrose) flasks and the spore concentration was counted again. The mixture was gently stirred overnight at 16°C in the dark. The following day, using a haemocytometer, the germ tubes of the cultured conidia were assessed so that approximately 80% of conidia had hyphae that were eight times longer than the original conidium in length. Depending on yield and germ tube length, the mixture was stirred at room temperature for 40 min to 3 h.

To prepare protoplasts, an enzyme mix was prepared (200 mg Sigma Lysing Enzyme and 500 mg Driselase in 20 ml 1.2 M KCL). Once reagents were mixed, they were centrifuged at 4,600 rcf for 5 min to separate the enzyme from the carrier. The supernatant was then placed in a separate 50 ml tube. The centrifugation was repeated, and the supernatant was placed into new tube up to approximately 30 ml. The TB3 mix of germlings was harvested using two small sheets of miracloth through a pump. The harvest was then washed with 100 ml water (sterile diH_20) and 20 ml of 1.2 M KCL. The miracloth plus fungus was weighed to obtain 0.7 g - 1.2 g dry weight of mycelium. This was then placed into the prepared enzyme mix and the combination was mixed gently to separate the miracloth from the mycelial clump. Once the miracloth was removed, the conidia were mixed thoroughly to resuspend. The mixture was placed in a shaker at 80 rpm, 30°C for a minimum of 1-2 h depending on weight. Protoplasts were verified with a haemocytometer. To dilute, STC-sucrose (20% sucrose; 50 mM Tris/HCl, pH 8.0; 50 mM $CaCl_2$) was added up to 50 ml. The

tube was mixed gently and centrifuged at 2,100 rcf for 10 min to harvest protoplasts. The supernatant was discarded without disturbing the pellet.

The protoplasts (Fig. 6.5) were resuspended in 25 ml STC-sucrose, were mixed gently with a cut pipette tip manually, and centrifuged again at 2,100 rcf for 10 min. The supernatant was discarded without disturbing pellet. The pellet was resuspended again in 1 ml STC-sucrose. Using a cut pipette tip, the protoplasts were transferred to a 2 ml Eppendorf tube and centrifuged for 5 min at 2,300 rcf and the supernatant was carefully removed. The protoplast pellet was resuspended in 1 volume STC sucrose, mixed manually with the pipette tip and then stored at room temperature or at 5°C. To check the quality, a small volume of protoplasts in a new Eppendorf was diluted 1:100 in STC-sucrose with 0.5 µl Evans Blue (1% weight/volume in normal saline). A concentration of 1×10^8 protoplasts/ml was achieved with a maximum of 5% ghosts (Fig. 6.5).
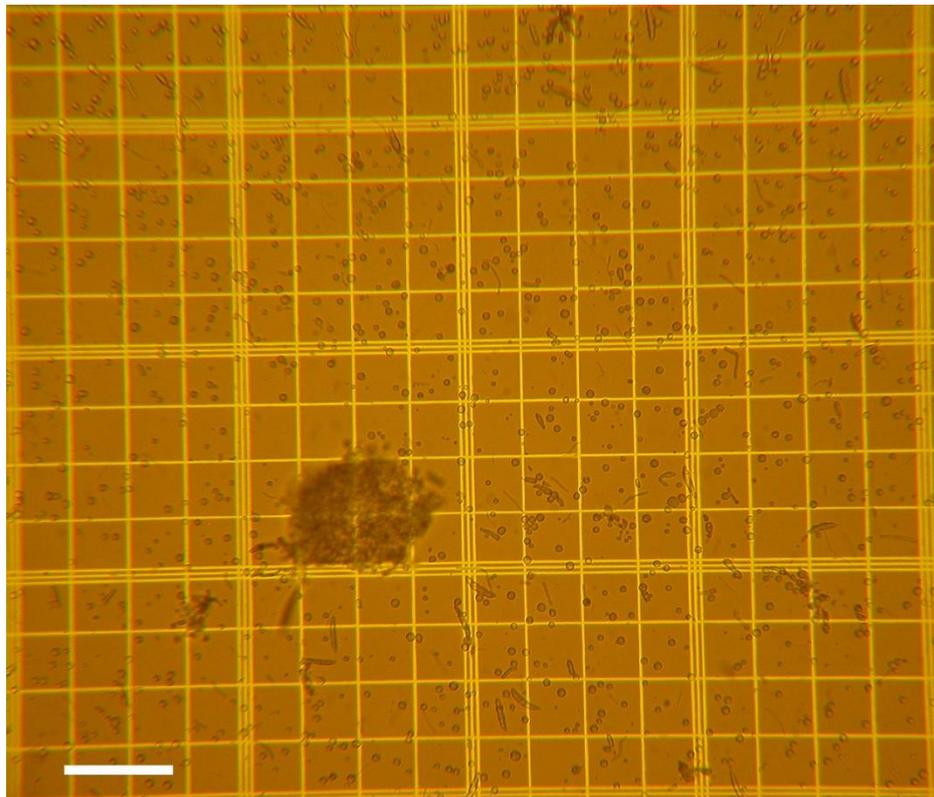
Figure 6.5. *F. graminearum* PH1 protoplasts (small circles) immediately after enzymatically removing their cell walls. 'Ghosts' are the conidia that still look intact (Fig. 1.1) but are in fact empty. Photo taken with mounted microscope camera on a light microscope. Scale bar = 100 µm.

For the transformation (Fig. 6.6), Both 5' and 3' DNA fragments were pooled into a new Eppendorf. One positive control tube with pHYG1.4 and a negative control (only STC) were

also prepared. In a 15 ml falcon tube, a mixture of 90 µl of STC-sucrose and 10 µl of DNA was added. Then with cut end pipette tip, 100 µl of protoplast suspension was mixed in gently and the mixture was incubated at room temperature for 20 min. Then 1 ml of 40% PEG in STC-sucrose (40 g PEG8000 + 100 ml STC sucrose) was carefully pipetted into the 15 ml falcon tube and mixed manually. The mixture was incubated for 20 min at room temperature. Then 5 ml of TB3 was pipetted into the mixture and then the tube was placed on a turntable overnight. Once the mixture appeared cloudy the following day, the regeneration agar (0.7g of low melting temperature agarose dissolved in 100 ml of media (50 ml of 2x REG (0.4% Yeast Extract, 0.4% Casein-Hydrolysate (N-Z-Amine A)) + 50 ml of 1.6 M sucrose) (100 ml for each treatment) was prepared and kept in a pre-heated water bath set to 45°C. When the 2x REG media was at 40°C, hygromycin was added to a final concentration of 75 µg/ml while stirring. For each treatment, four 25 ml Petri-dishes were prepared. The protoplast solution was divided into two separate 50 ml falcon tubes and then regeneration agar was added to a final volume of 45 ml. The solution was mixed by inversion and poured into respective plates. After resting for 2 h to solidify, the plates were stored at 28°C in the dark face up.
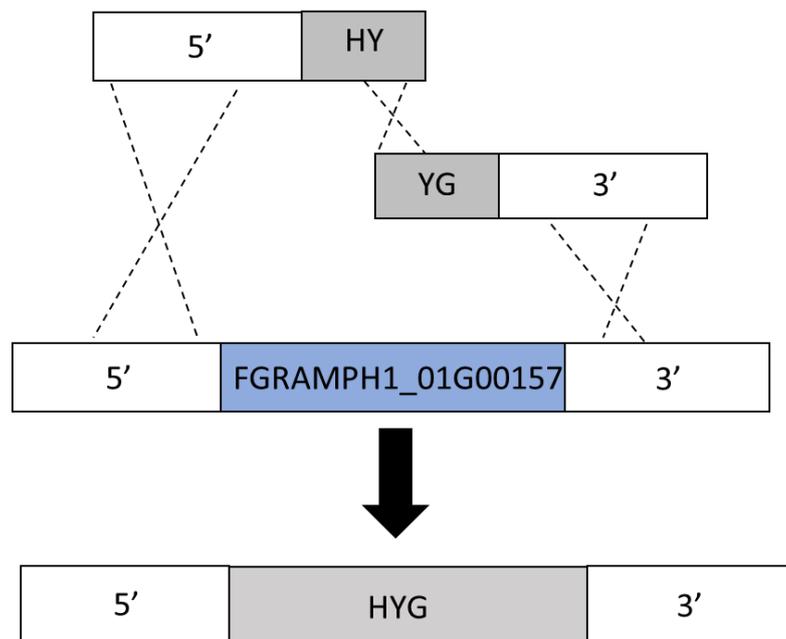
Figure 6.6. Transformation by homologous recombination. Modified from (Catlett et al., 2003).

6.2.4.3 Validation

Dead colonies were visible at 1 to 2 days and transformants were visible after 6 days. With a sterile toothpick, colonies were transferred to six-well square plates containing SNA media (synthetic nutrient poor agar: 0.1% KH_2PO_4, 0.1% KNO_3, 0.1% $MgSO_4$ x 7 H_2O, 0.05% KCl, 0.02% Glucose, 0.02% Saccharose, 2% Bacto Agar (Difco)) + 20 µg/ml hygromycin. After sufficient growth, colonies were transferred again to new SNA agar plates + 20 µg/ml hygromycin. Then after sufficient growth, transformants were stable and were transferred to PDA plates for 6 d at 22°C.
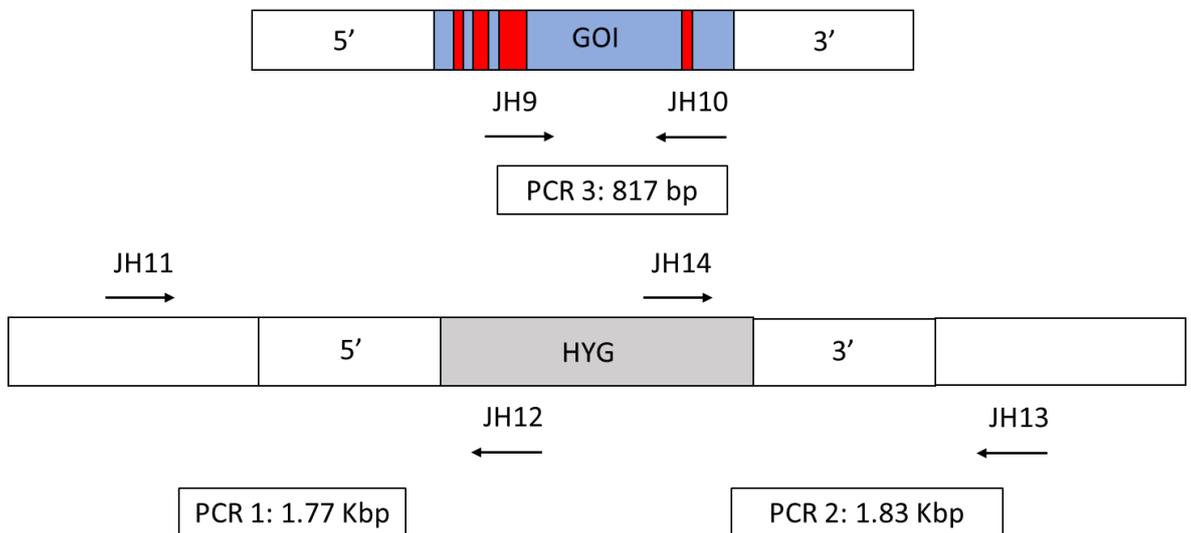
Figure 6.7. Deletion validation including respective primer combinations for the three different PCRs. GOI (Gene of Interest). *HYG* (Hygromycin resistance gene). Red bars denote the approximate location of all introns in the GOI sequence. Primer sequences at Supp. Table S14.

Using Qiagen DNeasy plant mini kit, a whole fungal plate (6 dpa or 8 dpa) of mycelia was extracted from each strain (1-12 transformants) and DNA was harvested. After PCR (Table 6.9 and Table 6.10) of each sample with either of three combination of primers (Fig. 6.7), each PCR product was visualised on a 1% agarose gel (Melford) at 80 V to 100 V for 40 min to 1 h with 2 µl loading buffer 6X, 10 µl of PCR product. Plugs from each strain were stored

at -70 in 20% glycerol. 1 Kb ladder and 1 kb ladder Plus (Fig. 6.11-6.13) are from New England Biolabs (NEB).

Table 6.10. PCR protocol to validate *F. graminearum* gene deletion.

Reagent	Concentration (µm)	Volume per well (µl)
HotStarTaq		5
Primer F	10	0.2
Primer R	10	0.2
DNA	10 ng/ul	0.5
dH$_2$O		4.1
Total		10

Primers used were JH1 and A2 for 5' and HY fusion, and JH5 and JH8 for YG and 3' fusion (Supp. Table S14).

6.2.5. *B. distachyon* FRR assay

The same root rot assay was performed as described in section 2.2.3 without moving seeds to new chemical amended boxes. Instead of three boxes per treatment, four boxes of 10 Bd3-1 roots were prepared for each *F. graminearum* genotype. A total of six genotypes were tested. After three days on the filter paper, a slurry prepared from 7-day *F. graminearum* (WT and *bcat* knockouts) in PDA circular plastic Petri-dishes was applied as per standard protocol (Section 2.2.3). Due to number of plastic Petri-dish boxes, the experiment was divided into two separate propagator trays (Two plates of each genotype per tray). Each genotype was equally represented within these propagator trays. Unless otherwise stated, all photographs were taken with an Olympus Stylus TG-4 camera.

6.2.6. Growth of Transformants *in Vitro*

This assay was derived from that used in the antimicrobial test as described in Chapter 2 (section 2.2.4) but with no chemical amendment. Each Petri-dish contained three mycelial plugs from only one genotype and each genotype-specific plate was repeated a total of four times (A total of twelve plugs for each genotype).

6.2.7. Software, Data Processing, and Statistics

Microsoft office (Excel, Word, and Powerpoint) 2016 was used for writing, data collection, images, and analysis. All graphs were prepared using Graphpad Prism (V5.04) unless otherwise stated. Scale bars were created using ImageJ (Abràmoff et al., 2004). The TcNAV software was used for GC graph generation, respective peak data, and for quantifying ethylene volume.

Primers used for split-marker deletion of target ethylene gene were developed with the help of Dr Martin Urban at Rothamsted Research using the NEBuilder Assembly tool v1.12.17 (New England BioLabs). Primer preference parameters were set as following: product (E2611 Gibson Assembly Master Mix), number of fragments (2-3 fragments including vector), total construct length (less than 10 kb), minimum overlap (15 nucleotides), allow linear assembly (no), PCR product group (Phusion), PCR product (Phusion High fidelity PCR kit (GC buffer), PCR primer concentration (400), minimum primer length (18 nucleotides). The gene sequences used were generated from Ensembl Genomes (Howe et al., 2020) whereas the selectable *HYG* marker was obtained from Dr Martin Urban (Rothamsted Research). Primers JH9 to JH14, and A2, and those used for qRT-PCR were generated using Primer 3 (Koressaar & Remm, 2007, Untergasser et al., 2012, Kõressaar et al., 2018) on a single CDS exonic region and avoiding untranslated regions (UTRs) and checked for quality and dimerization using Oligocalc (Kibbe, 2007). M13 primers were obtained from Dr Marianna Pasquariello (JIC). Ensembl Genomes (Howe et al., 2020)), BLAST (Sayers et al., 2020), and MetaCyc (Caspi et al., 2017) were used for individual *F. graminearum* genes and the RNA-seq dataset identification and analysis.

Statistics was performed using GENSTAT v.19.1.0.21390 (VSN international Ltd) for all experiments. Unless otherwise stated (Supp. Table S7-S10), the normal distribution was used for all data. Logit transformation was accomplished using the calculation 'Log(('response variate')/(100 - 'response variate'))' based on (McGrann et al., 2014). A standard students t-test was used for time-course RT-qPCR Cq data using Microsoft Excel (Fig. 6.10) but with only two biological replicates for the mock control since in the one, no transcripts were detected (no Cq value).

6.3. Results

6.3.1. *F. graminearum* Produces Ethylene *in Vitro*

Liquid media with supplements required for ethylene biosynthesis were used to determine whether *F. graminearum* produces ethylene *in vitro*. Ethylene production was measured in headspace using gas chromatography (Fig. 6.8). In a basic pH ethephon releases ethylene. Therefore, the positive control ethephon denotes that ethylene has a retention time of approximately 0.41 min (Fig. 6.8A). However due to the high FID sensitivity (Section 5.2.2), the voltage for ethylene emitted from ethephon was much higher (Fig. 6.8A). No ethylene peak was detected in non-amended CDL media (Fig. 6.8B). In the presence of the ethylene precursor ACC only, no ethylene peak was observed (Fig. 6.8C). This suggests ACC does not induce ethylene production. When all supplements necessary for either the EFE- or KMBA-related ethylene pathways were present in the CDL media, a ~35 mV ethylene peak was observed with a retention time of 0.40 min (Fig. 6.8D) Peak area = 41.8%, n = 4. This suggests that one or a combination of the supplements are used by *F. graminearum* to produce ethylene and that either the EFE or KMBA pathways was being used to produce ethylene. When one of the supplements (methionine) necessary for the KMBA pathway was omitted, the ethylene peak was not present (Fig. 6.8E), suggesting that the EFE pathway is not being used by *F. graminearum* to produce ethylene. Furthermore, when methionine was the only supplement added to the CDL media, a relatively strong ~250 mV ethylene peak was identified at 0.40 min (Fig. 6.8F). In the presence of methionine, *F. graminearum* PH1 produced 4.02 ± 0.086 μl of ethylene (n = 24 biological replicates, eight independent experiments, peak area = 92.2%, n = 4). Ethylene was produced from mycelia or conidia starter solution (Fig. 6.8, Fig. 6.2 methods). This suggests the main requirement for *F. graminearum* to produce ethylene was methionine and that the KMBA pathway was being used to produce ethylene. To verify this, KMBA the product produced from methionine precursor by the action of a transaminase (Fig. 6.1) was added to the CDL media and a smaller ~40 mV ethylene peak appeared at 0.41 min, Peak area = 85.5% n = 4) (Fig. 6.8G). This provides evidence that the KMBA and not the EFE biosynthetic pathway is being used by *F. graminearum* to produce ethylene. To further

verify this result, the transaminase inhibitor aminooxyacetic acid (AOA) (Qadir et al., 2011) at 10 mM was added to CDL media and no ethylene peak was observed with or without methionine added (Fig. 6.8H and Fig. 6.8I). The results also a show a peak at ~0.2 mV of an unknown gas that tended to be negatively associated with the ethylene peak (Fig. 6D-G). Overall, the results showed that *F. graminearum* PH1 has the biosynthetic capacity to produce ethylene in small amounts from both primary and intermediate ethylene precursors using the KMBA pathway (Fig. 6.1).
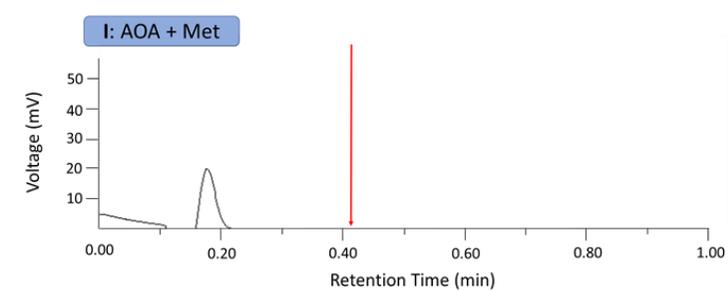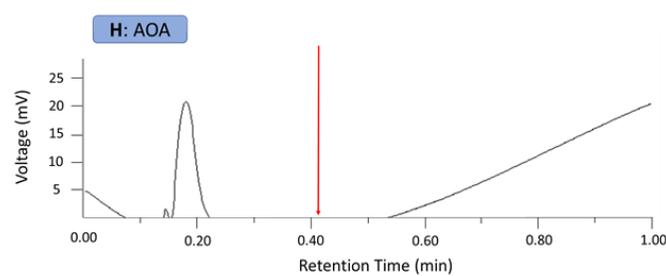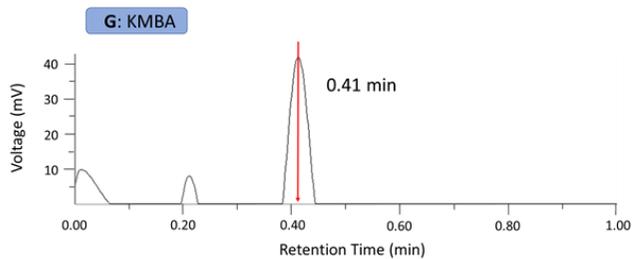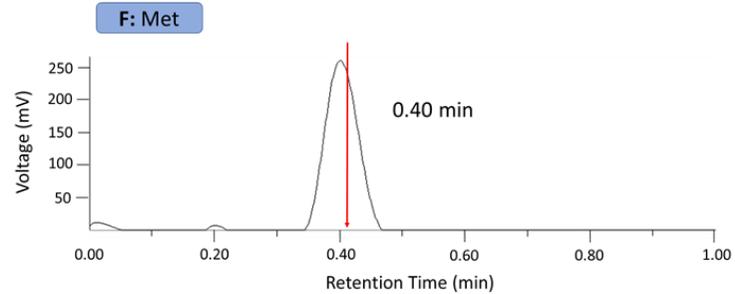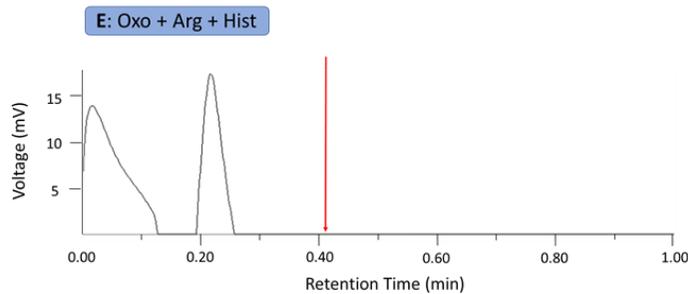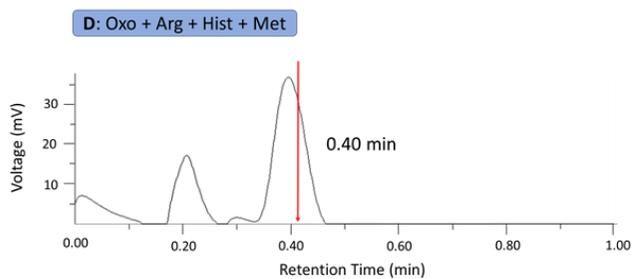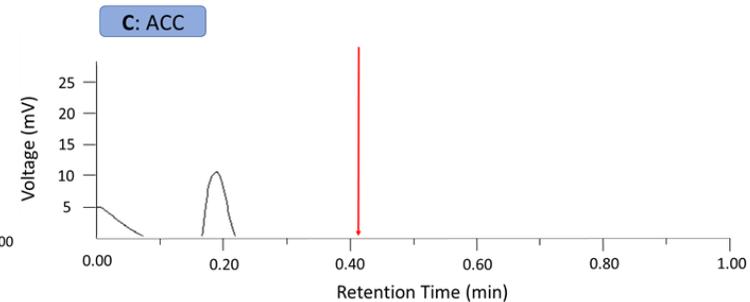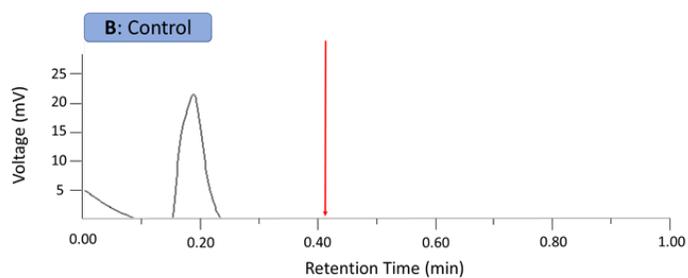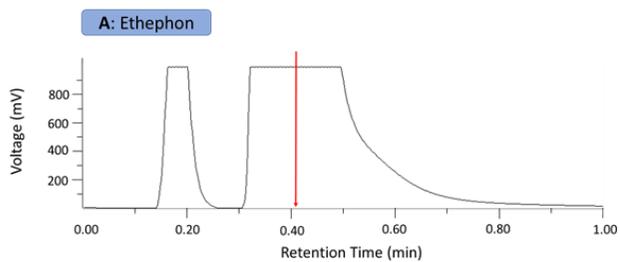
Figure 6.8. Gas chromatograms of sealed Czapek Dox Liquid (CDL) samples containing 2-day-old 1 x 10^5 *F. graminearum* PH1 conidia or 6 dpa mycelial plugs. Relative retention time of ethylene derived from ethephon control is denoted with a red arrow. Each graph (Except **A**) is the output of a gas sample from different CDL media compositions (Table 6.2). The result from each treatment (**B-I**) was found in all 4 biological replicates (three times for B, **C**, **H**, **I**) and the experiment was repeated three times (once for **B**, **C**, **H**, **I**). **B**, **C**, **H**, and **I** (Conidia) were obtained from a different experiment than **A**, **D**, **E**, and **G** (Plug). (**B**, **C**, **H**, and **I**) Performed with an updated GC protocol, low natural light treatment, and Clarus 480 system update. (**B**) is FgPH1 in CDL media with water (added before autoclaving) as the supplement. In a few biological replicates between experiments, a very small peak around 0.4 min was present in the negative control (**B**) (< 5 mV, Data not shown) but was often attached to an equally small peak at a higher or lower retention time. AOA (**H** and **I**) slightly inhibited growth in CDL media. Abbreviations: OXO (2-oxoglutarate), Arg (Arginine), Hist (Histidine), ACC (1-aminocyclopropane-1-carboxylic acid), and AOA (aminooxyacetic acid), KMBA (α-keto γ-methylthiobutyric acid), Met (Methionine).

6.3.2. Ethylene Production was Species, Isolate, and Chemotype Independent

It is unclear whether other *Fusarium* species and isolates also produce ethylene. Like *F. graminearum*, *F. culmorum* is also major cause of FHB in cereals (Parry et al., 1995). Therefore ethylene production in these two species needed to be confirmed. Furthermore isolates of both *F. graminearum* and *F. culmorum* differ in the trichothecenes they produce (Ferrigo et al., 2016). Isolates that produce type B trichothecenes 3-AcDON, 15-AcDON, and NIV (Ferrigo et al., 2016) were selected (Table 6.3). The aim was to determine whether different species and trichothecene chemotypes were able to produce ethylene to identify any association between trichothecene chemotype and the level of DON production.

Several *F. graminearum* isolates and *F. culmorum* isolates that produce different trichothecene mycotoxins were cultured with or without methionine and analysed using the same GC protocol and with the ethephon positive control (Fig. 6.9). All isolates tested showed an ethylene peak at approximately 0.45 min retention time (which is approximately where ethylene peaked for the ethephon control, data not shown) only in the presence of methionine. For GC chromatograms, peak area is a proportion of each compound from the sample added to the GC. Ethylene was the most abundant compound in the flask headspace for each isolate since over 80% of the compounds detected in headspace were ethylene (except for Fc 713 due to malfunction with chromatography software) (Fig. 6.9A). There was no significant difference between the peak area for any of the isolates (p = 0.324). The approximate ethylene volume was derived from the peak area using the GC software and was between 5 µl to 15 µl ethylene gas (Fig. 6.9B). Like the peak

area, there was no significant difference in ethylene volume emitted (p = 0.301). Therefore, the data showed that both *F. graminearum* and *F. culmorum* isolates produced ethylene in the presence of methionine. Furthermore, there was no significant difference in ethylene production between chemotypes (NIV or either 3 or 15 acetyl-DON) suggesting that the chemotype did not affect the presence or amount of ethylene produced (Fig. 6.9).
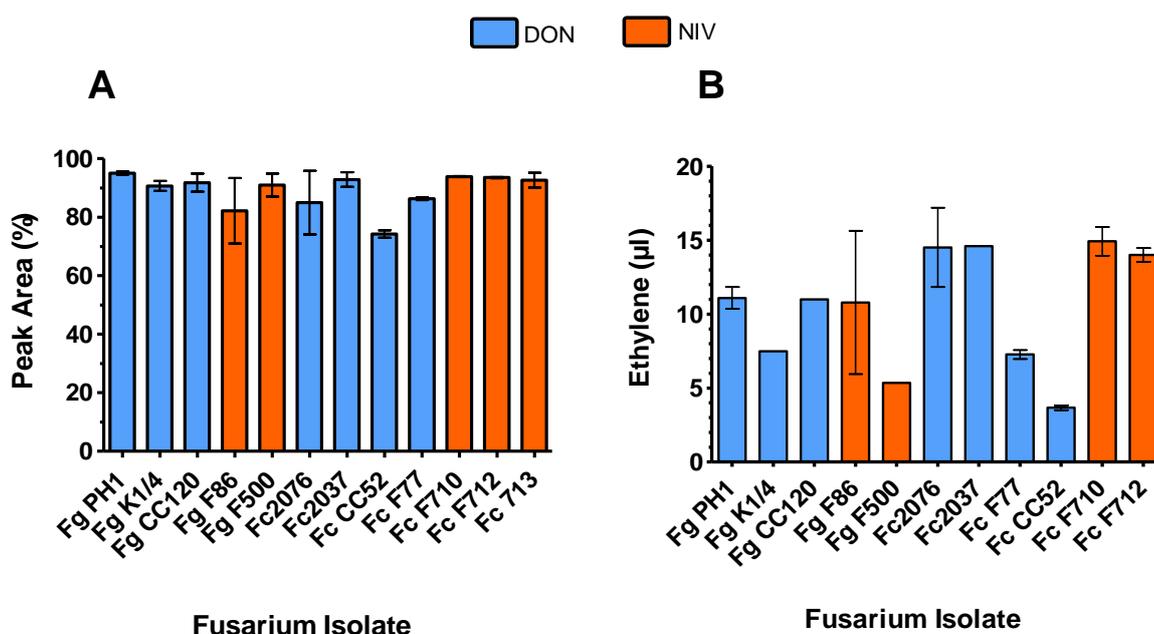
Figure 6.9. The ethylene GC peak area (**A**) and predicted ethylene volume (**B**) is similar between five *F. graminearum* (Fg) and seven *F. culmorum* (Fc) isolates in the presence of 10 mM methionine. Trichothecene chemotype distinguished by bar colour. Note that Fc 713 is absent from **B** since no prediction was made by the GC software. Each bar is the average ± SE of between two and five biological replicates (**A**) and 1 (denoted by absence of error bar) to three biological replicates (**B**). Each bar is the summary from one intendent experiment, however FgPH1, K1/4, and CC120 are from a different intendent experiment (**A** and **B**). Data for absence of methionine control treatments were not included as there was no ethylene detected.

6.3.3. Identifying Genes Involved in Ethylene Production in *F. graminearum*

RNA-seq offers a potential means of identifying genes involved the production of ethylene. Numerous candidate genes were identified by investigating the change in gene expression in samples grown in defined media (Table 6.2) with or without the essential precursor methionine for ethylene production. A total of 845 genes were significantly and differentially expressed between methionine and control treatments (RNA-seq dataset not

shown). The genes upregulated in the presence of methionine were used to identify genes involved in ethylene production. Given the distinct switch to ethylene production in the presence of methionine, one would expect that the target gene would change from negligible or very low read counts to very high read counts in the presence of methionine.

Despite many studies describing the KMBA pathway (Fig. 6.1), the exact genes involved are still unclear in many instances. With reference to the potential KMBA biosynthetic pathway, all candidate transaminase or oxidoreductase genes were collated (Table 6.11). The objective was to narrow down the gene list to a select few candidate genes responsible for ethylene production. Transaminases and oxidoreductases are important components of the KMBA pathway (Fig. 6.1). Seven oxidoreductase genes were highly upregulated in response to methionine as well as showing a relatively low number of reads in the control treatment (Table 6.11). Several other oxidoreductases were also identified but were below the threshold assigned (RNA-seq dataset not shown). However, KMBA is converted to ethylene via a non-enzymatic reaction facilitated by oxidoreductases rather than requiring their function (Fig. 6.1). As a result, the transaminase genes are the only remaining candidate enzymes. Only four genes annotated as transaminases were highly expressed in response to methionine (Table 6.11). Of these four genes, FGRAMPH1_01G13965 and FGRAMPH1_01G18173 were excluded since they are predicted to be ornithine transaminases class 3, with no known function described in the literature for methionine transamination. Instead two branched chain amino acid transaminases (*BCAT*) FGRAMPH1_01G00157 and FGRAMPH1_01G15607 were more promising as they were predicted to encode class 4 BCAT genes. Class 4 BCAT enzymes have been reported to catalyse the transamination of methionine (Engels et al., 2000, Yvon et al., 2000, Bondar et al., 2005, Schuster et al., 2006). No other *BCAT* gene was identified among all the 844 significantly expressed genes responding to methionine treatment. Out of the two remaining *BCAT* genes, FGRAMPH1_01G00157 was the most highly upregulated (p < 0.001) and had the lowest number of transcript reads in the control treatment (19 reads) (Table 6.11). Therefore FGRAMPH1_01G00157 was chosen over FGRAMPH1_01G15607 as the primary gene responsible for ethylene production. This gene was also selected for the RNA-seq validation test using RT-qPCR (Fig. 6.10). FGRAMPH1_01G00157 displayed a very similar log-fold change in expression under methionine conditions when assessed by RT-qPCR as compared to the RNA-seq data (Fig. 6.10, Table 6.11).

Table 6.11. Summary of all potential genes with the highest fold-expression and lowest control read count that could be important in the KMBA pathway for ethylene biosynthesis.

Gene ID	Predicted gene function	Closest Homologue	Mean Control counts	Mean Methionine counts	Log-fold change	p-adj	Log-fold change FHB	Log-fold change FRR
FGRAMPH1_01G00157	*BCAT* Transaminase class 4 (aminotransferase apf4)	*F. culmorum* 88%	19	12002	9.32	> 0.001	-4.5	5.74**
FGRAMPH1_01G15607	*BCAT* Transaminase class 4		342	1026	1.6	0.011	2.5	3.08
FGRAMPH1_01G13965	Transaminase class 3/Ornithine aminotransferase	*F. culmorum* (99%)/ F. fujikuroi 84%	153	111159	9.5	> 0.001	-2.4	-6.38
FGRAMPH1_01G18173	Transaminase class 3/Ornithine aminotransferase		1489	9465	2.7	0.031	1.1*	-0.8*
FGRAMPH1_01G00155	Oxidoreductase (2OG+AC0-FE II OXYGENASE FAMILY PROTEIN+ACI)		12	6457	9.1	> 0.001	-4.4	6.7**
FGRAMPH1_01G00129	Oxidoreductase		62	2447	5.3	> 0.001	-6.5	3.8**
FGRAMPH1_01G14253	Oxidoreductase//FMN binding/catalytic activity		69	3346	5.6	> 0.001	2.6	4.1
FGRAMPH1_01G12523	FAD-dependent Oxidoreductase	*Alistipes* sp. marseille 42%	211	1595	2.9	> 0.001	-7.6	-0.6**
FGRAMPH1_01G00145	Oxidoreductase		248	7162	4.9	> 0.001	-7.4	3.1**
FGRAMPH1_01G11491	Oxidoreductase		420	11193	4.7	0.001	-0.9*	1.5
FGRAMPH1_01G09063	NADH: Flavin oxidoreductase		616	20379	5.1	> 0.001	2.2	4.7

Data is from the RNA-seq analysis comparing *F. graminearum* grown in the presence or absence of methionine. Includes the expression of each gene in response to *B. distachyon* FHB and FRR (Chapter 4 RNA-seq experiment). Candidate genes were filtered to 154 genes cut-off based on p-adj significance, genes with a minimum of 1000 transcript count difference between the control and methionine treatment, and with a relatively low control read count (RNA-seq dataset not shown). The exception was FGRAMPH1_01G15607 which was identified by function Predicted gene function derived from either Ensembl Genomes (Howe et al., 2020) description and/or protein Basic Local Alignment Search Tool (BLAST) (with most homologous species if used to identify function) (Sayers et al., 2020). The log-fold change response to FHB and FRR (p-adj < 0.05) was derived by cross-referencing gene ID with *F. graminearum* expressed genes in response to FHB and FRR (Chapter 5 (Section 5.2) RNA-seq method and data). * Genes have a p-adj > 0.05. **Significance level = NA.

The most promising candidate *BCAT* gene FGRAMPH1_01G00157 (FGSG_00049) was differentially expressed in response to Fusarium head blight (FHB) and Fusarium root rot (FRR) in *B. distachyon* (Table 6.11), and the same gene was also expressed in response to FHB in wheat (*Triticum aestivum*) and maize (*Zea mays*) (Boedi et al., 2016, Harris et al., 2016, Brown et al., 2017, Buhrow et al., 2020). This provides additional support to FGRAMPH1_01G00157 being the most important ethylene producing gene. It is worth noting that the candidate gene was chosen before performing the FHB and FRR RNA-seq experiments (Chapter 4 and Chapter 5). Two other transaminases were also significantly expressed during *B. distachyon* pathogenesis. The second class three ornithine aminotransferase FGRAMPH1_01G13965 was significantly downregulated in both FHB and FRR infections. The class 4 *BCAT* gene, FGRAMPH1_01G15607, was the only transaminase significantly upregulated in response to FHB and FRR at relatively low level of 2-fold and 3-fold change respectively. Overall the data suggests that these transaminases may serve an important function during pathogenesis in both Fusarium diseases.
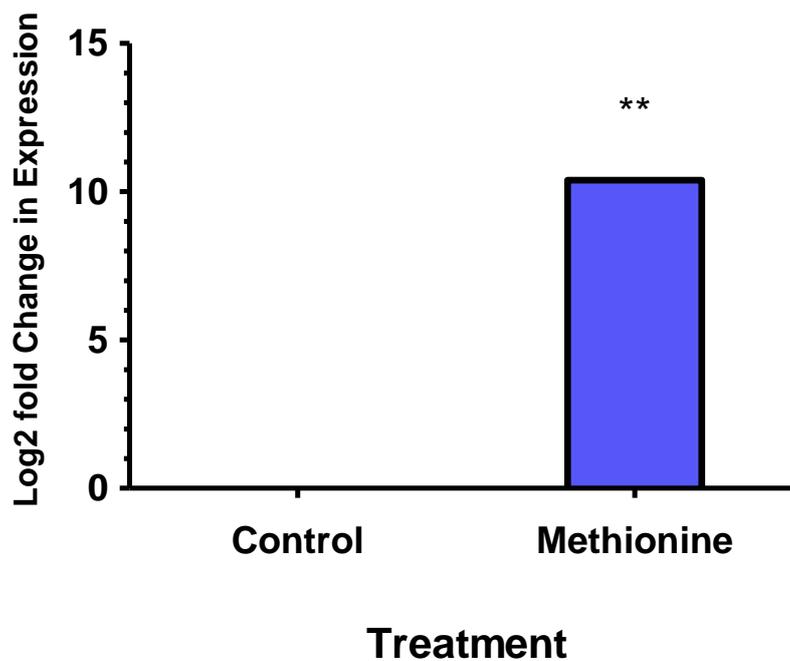
Figure 6.10. The change in expression of FGRAMPH1_01G00157 in response to 10 mM methionine using RT-qPCR. *gzUBH* was used as the reference housekeeping gene. Each bar is the average of three biological (Methionine) and two (Control) replicates and 2-3 (Methionine) and one (Control) technical replicates. Level of significance relative to the control, Cq t-test **p<0.01.

6.3.4. Deletion of Candidate Transaminase Gene

To investigate whether ethylene production is important for virulence, a knockout strain, unable to produce ethylene, would first need to be generated. This would be followed by virulence assays with the ethylene knockout strain. The *BCAT* class 4 gene FGRAMPH1_01G00157 was chosen as the primary candidate ethylene producing gene (Table 6.11). *F. graminearum* deletion strains were produced with the help of Dr Martin Urban from Rothamsted Research as part of a collaboration. Twelve transformants were successfully produced following use of the split-marker deletion protocol. Hereafter, the twelve deletion strains shall be called *bcat-A* to *bcat-L*. The split-marker deletion validation experiments (Fig. 6.11, 6.12, and 6.13) showed that from the twelve FgPH1 transformant strains tested for the deletion, four strains (*bcat-E*, *bcat-G*, *bcat-I*, *bcat-L*) presented the deletion at the FGRAMPH1_01G00157 *BCAT* gene (PCR 3, Fig. 6.11, Fig. 6.13). Here, there was no amplification of the *BCAT* gene PCR product (PCR 3) in strains *bcat-E*, *bcat-G*, *bcat-I*, *bcat-L* (Fig. 6.11, Fig. 6.13). The PCR product for the *HYG* selectable marker (PCR 1 and PCR 2), predicted to be approximately 1.8 kbp for both flanks (Fig. 6.7), was only amplified

in strains *bcat-E*, *bcat-G*, *bcat-I*, *bcat-L* (Fig. 6.11, Fig. 6.13). Therefore the *BCAT* FGRAMPH1_01G00157 gene was replaced with the *HYG* selectable marker in the transformant strains *bcat-E*, *bcat-G*, *bcat-I*, *bcat-L* (PCR 1 and PCR 2, Fig. 6.11). The wild-type strain FgPH1 was used as a negative control (Fig. 6.11, 6.12, and 6.13). The *BCAT* gene PCR product (PCR 3) which was predicted to be 817 bp (Fig. 6.7) was still present for all the remaining strains like the wild-type Fg PH1 (Fig. 6.11, 6.12, and 6.13). Unusually, there was poor amplification for the *BCAT* gene PCR product (PCR 3) in the strain *bcat-J* (Fig. 6.12 and Fig. 6.13). The *HYG* selectable marker PCR products (PCR 1 and PCR 2) were absent for all the remaining strains like the wild-type Fg PH1 (Fig. 6.11, 6.12, and 6.13) suggesting no selectable marker was inserted at FGRAMPH1_01G00157. Therefore, the strains *bcat-A*, *bcat-B*, *bcat-C*, *bcat-D*, *bcat-F*, *bcat-H*, and *bcat-J*, and *bcat-K* had the same genotype as the wild-type FgPH1.
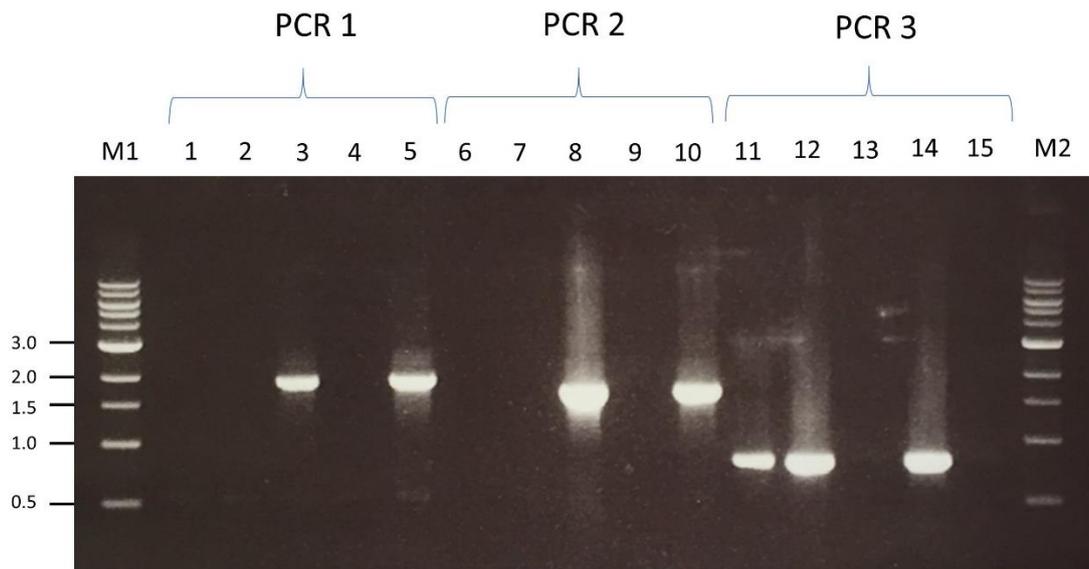
Figure 6.11. Gene deletion validation of four *BCAT* transformant strains. Agarose gel post-electrophoresis showing the presence or absence of products from three PCR validation experiments. PCR 1 (1.77 kbp) and PCR 2 (1.83 kbp): *HYG* amplification, PCR 3 (817 bp): *BCAT* amplification (Fig. 6.7). Lanes 1, 6, and 11 are wild-type FgPH1. Lanes 2, 7, and 12 are *bcat-C*. Lanes 3, 8, and 13 are from *bcat-E*. Lanes 4, 9, and 14 are from *bcat-H*. Lanes 5, 10, and 15 are from *bcat-L*. Lanes M1 and M2 are the 1 kb DNA ladder (Values are in kilobases).
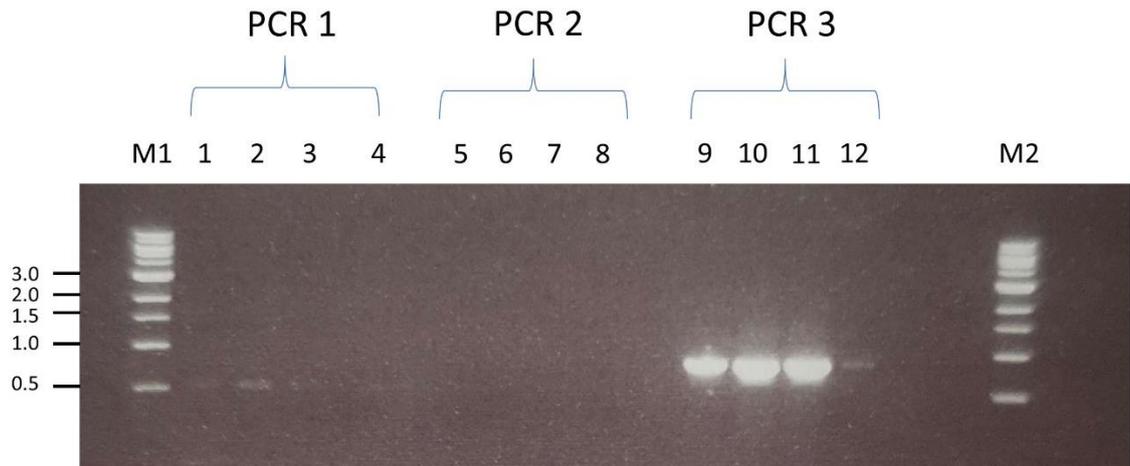
Figure 6.12. Gene deletion validation of three *BCAT* transformant strains. Agarose gel post-electrophoresis showing the presence or absence of products from three PCR validation experiments. PCR 1 (1.77 kbp) and PCR 2 (1.83 kbp): *HYG* amplification, PCR 3 (817 bp): *BCAT* amplification (Fig. 6.7). Lanes 1, 5, and 9 are wild-type FgPH1. Lanes 2, 6, and 10 are *bcat-B*. Lanes 3, 7, and 11 are from *bcat-D*. Lanes 4, 8, and 12 are from *bcat-J*. Lanes M1 and M2 are the 1 kb DNA ladder (Values are in kilobases).
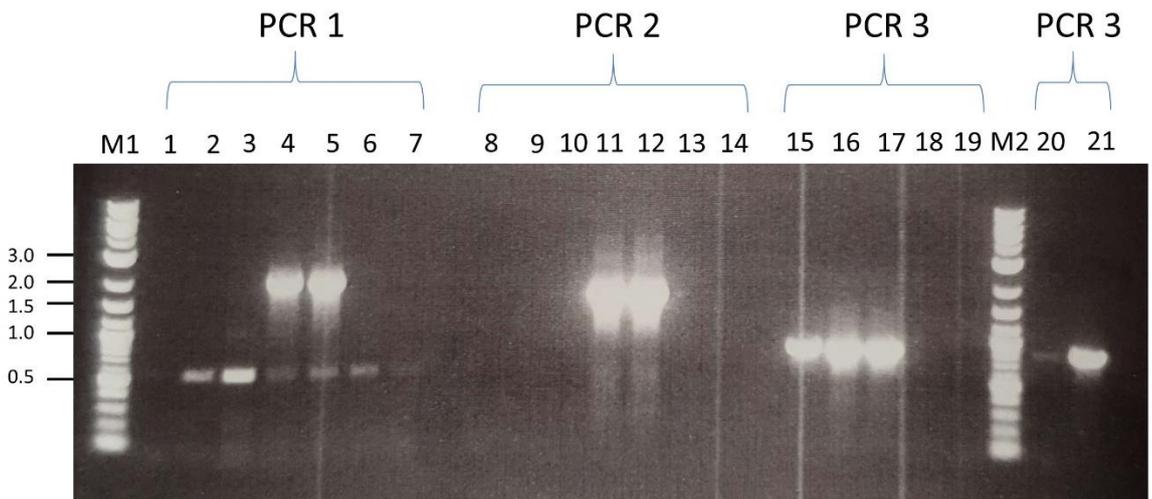
Figure 6.13. Gene deletion validation of six *BCAT* transformant strains. Agarose gel post-electrophoresis showing the presence or absence of products from three PCR validation experiments. PCR 1 (1.77 kbp) and PCR 2 (1.83 kbp): *HYG* amplification, PCR 3 (817 bp): *BCAT* amplification (Fig. 6.7). Lanes 1, 8, and 15 are wild-type FgPH1. Lanes 2, 9, and 16 are *bcat-A*. Lanes 3, 10, and 17 are *bcat-F*. Lanes 4, 11, and 18 are from *bcat-G.* Lanes 5, 12, and 19 are from *bcat-I*. Lanes 6, 13, and 20 *bcat-J*. Lanes 7, 14, and 21 bcat-K. Lanes M1 and M2 are the 1 kb Plus DNA ladder (Values are in kilobases).

Gas chromatography was then undertaken on the *bcat-E* deletion strain (Fig. 6.14A and Fig. 6.14B). The strain *bcat-H* was used as a negative control since *bcat-H* and *bcat-E* were transformants from the same selection plate. The *BCAT* wild-type strain Fg PH1 (JIC stock) was also included as a second negative control. Both *bcat-E* and *bcat-H* had a similar ethylene peak which accounted for approximately 60% of total compounds in the vial headspace (Fig. 6.14A). This demonstrated that ethylene production was unaffected by deletion of FGRAMPH1_01G00157. The ethylene peak in PH1 was significantly smaller than that in *bcat-E* ($p < 0.05$) (Fig. 6.14A) but there was no difference in peak area between PH1 and *bcat-H* ($p > 0.05$). No significant difference in ethylene volume in vial headspace was observed for any of the strains compared to each other ($p > 0.05$, Fig. 6.14B). The experiment was repeated with all remaining strains (Fig. 6.12 and Fig. 6.13), including a retest for *bcat-E*, *bcat-H* and PH1 (Fig. 6.14C and Fig. 6.14D). Like the first experiment, there was no significant difference in the proportion of ethylene ($p > 0.05$, Fig. 6.14C) and the volume of the ethylene in the gas sample for *bcat-E* and any of the other *bcat* strains ($p > 0.05$, Fig. 6.14D). The ethylene volume for strain *bcat-L* was not shown (Fig. 6.14D) due to a technical malfunction with the gas chromatography software. Overall the data implies that deletion of the *BCAT* gene (FGRAMPH1_01G00157) had no significant effect on the ethylene biosynthesis in *F. graminearum* PH1 under methionine rich conditions.
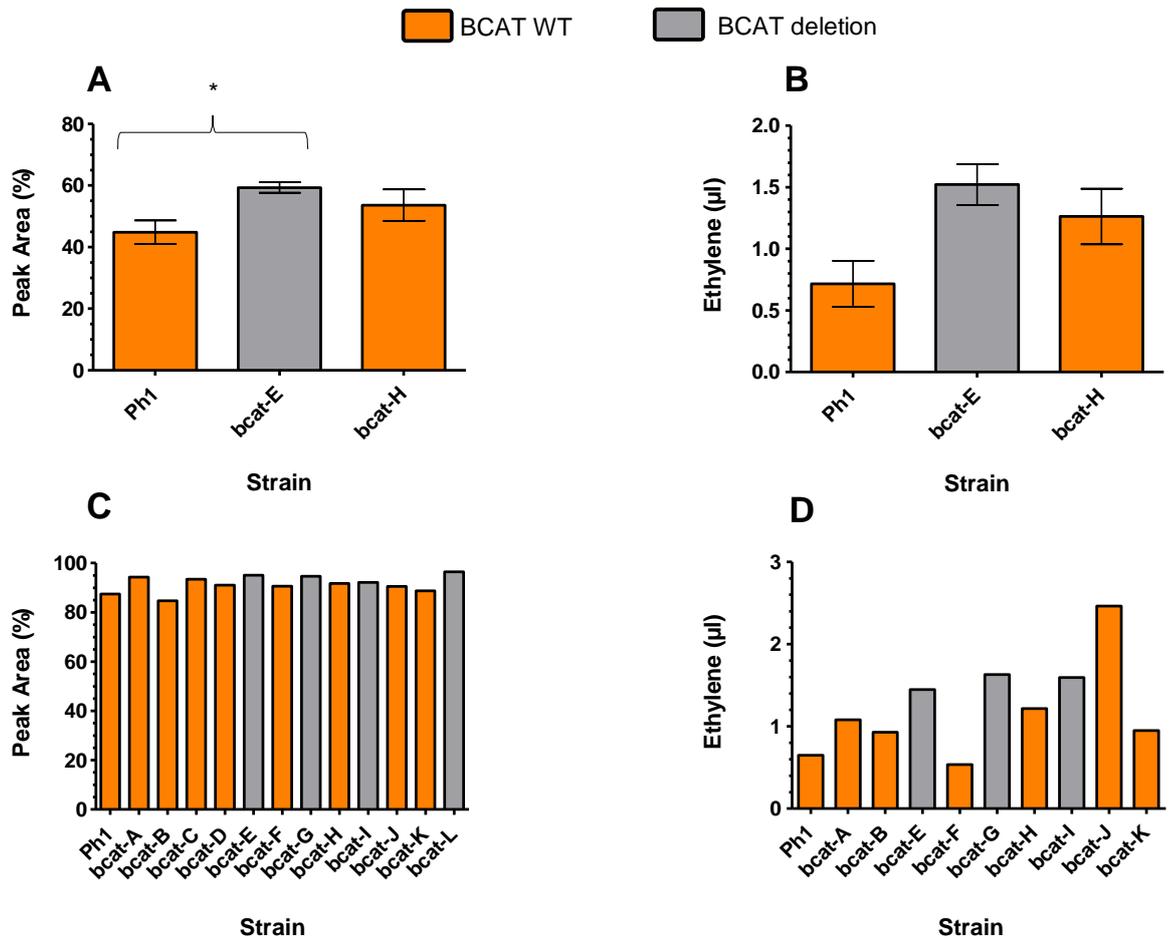
Figure 6.14. All strains including the validated deletion strains have similar peak areas (**A** and **C**) and ethylene volume (**B** and **D**) in the presence of 10 mM methionine. The bar colour type was derived from Fig. 6.11, 6.12, and 6.13. (**A** and **B**) Each bar is the mean ± SE of 4 to 5 biological replicates from one independent experiment. (**C** and **D**) Each bar is from one biological replicate (2 from *bcat-J*) from one independent experiment. Strains *bcat-C*, *bcat-D*, and *bcat-L* were not included in **D** due to software malfunction. Data for absence of methionine control treatments were not included as there was no ethylene detected. GLM-ANOVA significance level * $p < 0.05$.

Four strains that were validated for the presence or absence of the *BCAT* gene were also examined for any changes to mycelial growth (Fig. 6.15). All *bcat* strains grew less than the PH1 strain at all time points ($p < 0.001$). There were also significant differences between individual strains at different time points. The strain *bcat-E* showed the most notable reduction in mycelial growth at 2 dpa compared to *bcat-C* and *bcat-H* as well as to *bcat*-L at 3 dpa (Fig. 6.15). The strain *bcat-L* with a similar *bcat* genotype to *bcat-E* showed no significant difference to the other strains at 2 dpa and 3 dpa. *bcat-L* was only significantly different to *bcat-H* at 1 dpa. Overall the data suggests that there was no substantial effect of FGRAMPH1_01G00157 deletion on mycelial growth and that the variation observed is likely due to factors unrelated to *bcat*.
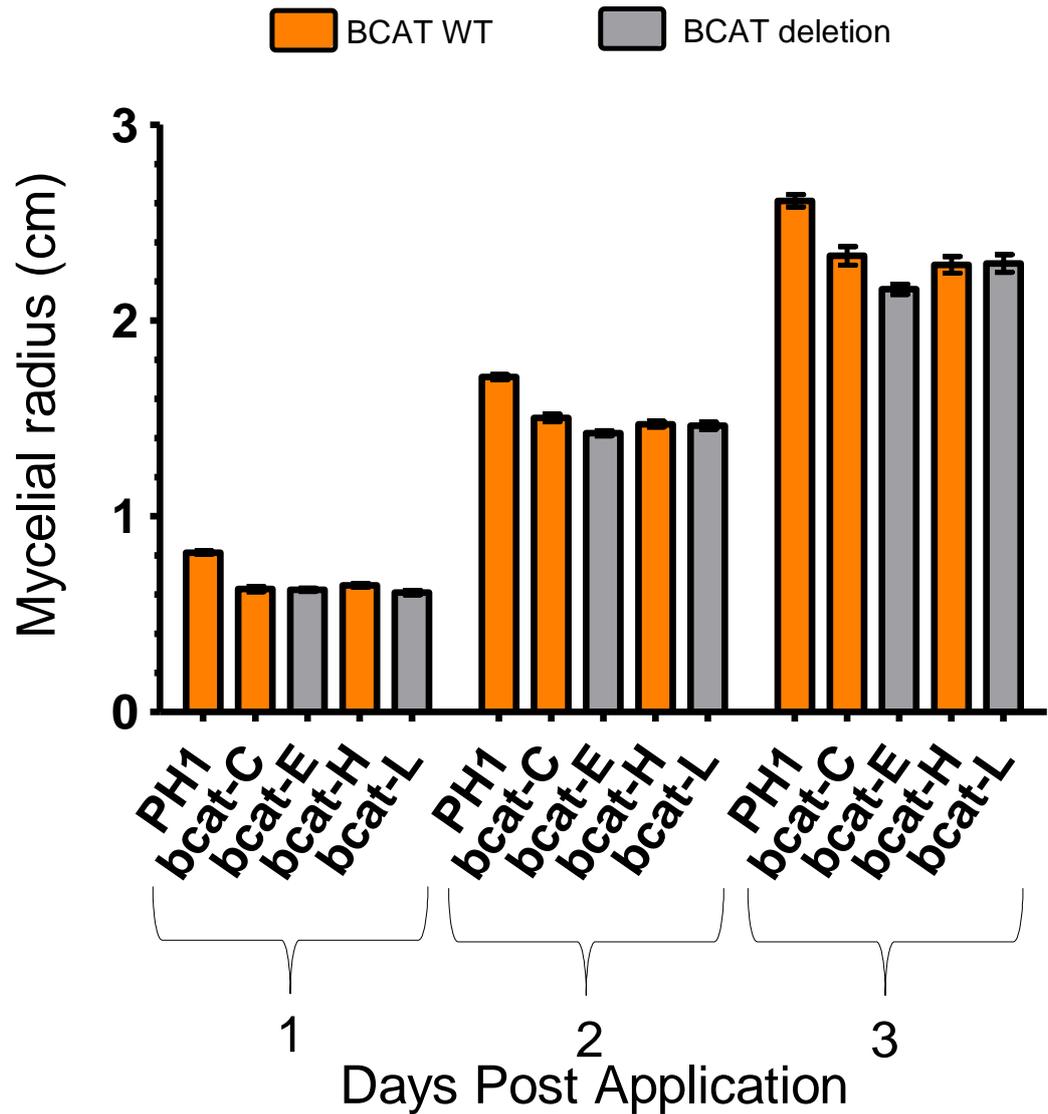
Figure 6.15. Total growth of all *F. graminearum* PH1 transformants at three time points. *bcat-C* and *bcat-H* transformants don't have the deletion whereas *bcat-E* and *bcat-L* do contain the *bcat* gene deletion. Each data point is the average of approximately 12 biological replicates with four different measurement per biological rep ± SE. The bar colour type was derived from Fig. 6.11, 6.12, and 6.13. GLM ANOVA LSD test results: All *bcat* strains – PH1 at all time points ($p < 0.001$), bcat-H – bcat-L at 1 dpa ($p < 0.05$), bcat-E - bcat-C at 2 dpa ($p < 0.001$), bcat-E – bcat-H at 2 dpa ($p < 0.01$), bcat-E – bcat-L at 3 dpa ($p < 0.05$), bcat-E – bcat-C at 3 dpa ($p < 0.01$).

The virulence of four strains, three with the deletion of FGRAMPH1_01G00157 and three without, was also examined on Bd3-1 FRR resistance (Fig. 6.16). The *F. graminearum* deletion strain *bcat-E* showed a decrease in root necrosis length (RNL) compared to *bcat-H* ($p < 0.05$) and *bcat-L* ($p < 0.01$) at 2 dpi (Fig. 6.16). However by 4 dpi and 6 dpi, there was no significant difference in RNL for any of the *bcat* strains ($p > 0.05$) (Fig. 6.16). Given that was no significant difference in RNL for the majority of transformants at all time points, the data suggests that deletion of FGRAMPH1_01G00157 did not affect virulence on Bd3-1 roots.
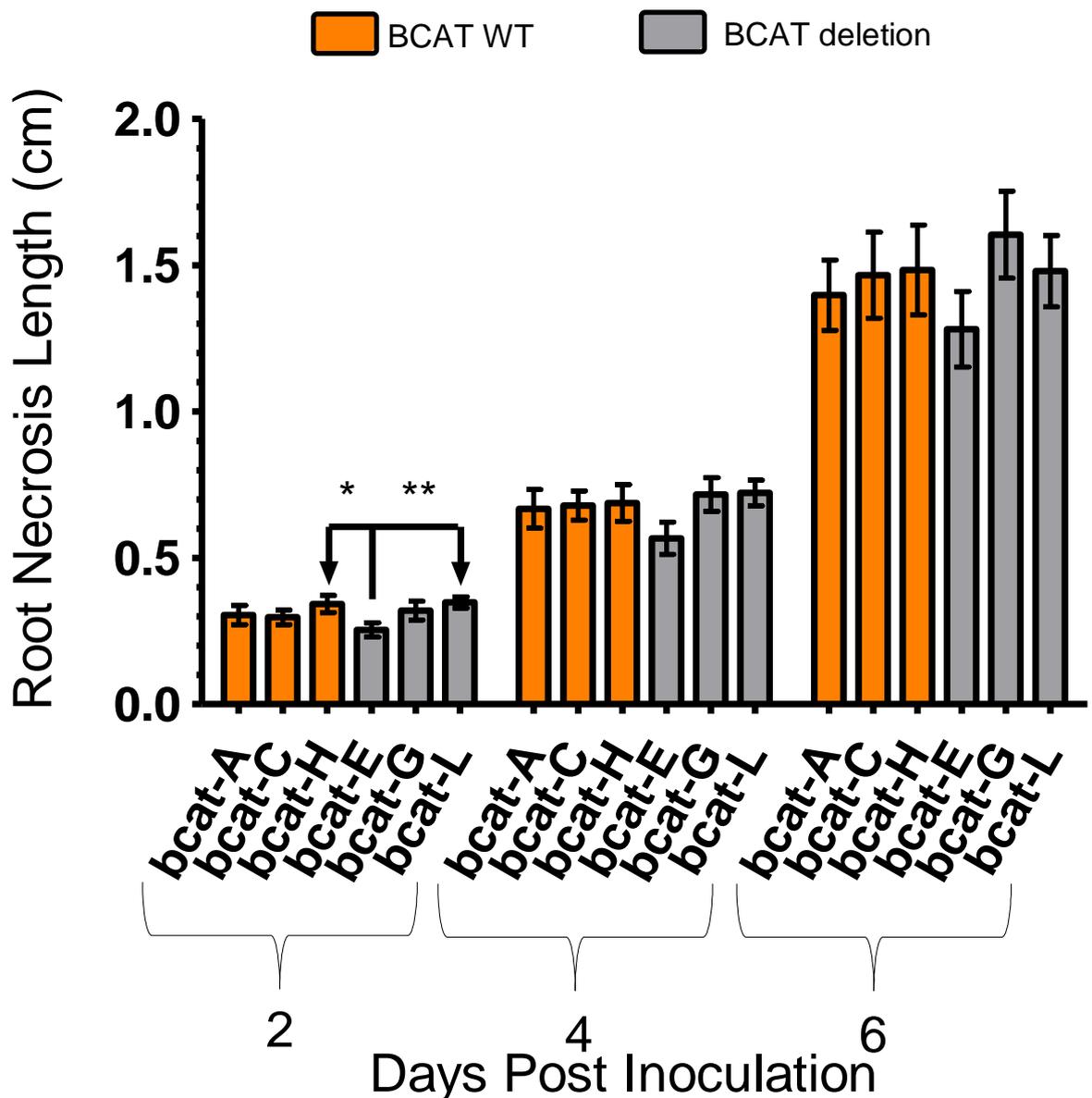
Figure 6.16. Effect of bcat deletion on Bd3-1 root virulence at three time points. Each data point is the average of approximately 40 biological replicates ± SE from one independent experiment (Except n = 39 for *bcat-L* at 2 dpi). The bar colour type was derived from Fig. 6.11, 6.12, and 6.13. GLM-ANOVA LSD test significance level * $p < 0.05$, ** $p < 0.01$.

6.4. Discussion

Through a process of elimination of important prerequisite compounds from the three ethylene producing pathways (Fig. 6.1 and Fig. 6.8), it was determined that *F. graminearum* and *F. culmorum* isolates can produce ethylene *in vitro* exclusively in the presence of 10 mM methionine. Recently Svoboda and colleagues (2019) also noted that *F. graminearum* can produce ethylene in the presence of 20 mM methionine but did not identify the pathway or genes responsible (Svoboda et al., 2019). We also show that *F. graminearum* produces ethylene using the KMBA pathway (Fig. 6.1) with either of the compounds methionine or KMBA (Fig. 6.8). This is similar to the situation observed in *B. cinerea* (Qadir et al., 1997, Cristescu et al., 2002, Qadir et al., 2011). Unlike *F. oxysporum* and other fungi which produce ethylene using the EFE pathway (Fig. 6.1 and Table 6.1), the results verify that *F. graminearum* does not produce ethylene using the EFE biosynthetic pathway (Fig. 6.1 and Fig. 6.8). In support of this finding, Svoboda and colleagues (2019) were not able to identify any good EFE candidate gene in *F. graminearum* (Svoboda et al., 2019). Methionine is also the prerequisite for ethylene biosynthesis in plants (Fig. 6.1). However, the evidence suggests that the plant ACC pathway (Fig. 6.1) was not responsible for ethylene production in *F. graminearum* (Fig. 6.8). Svoboda and colleagues identified two *F. graminearum* PH1 ACC synthase genes (FGRAMPH1_01G17303 and FGRAMPH1_01G25199) as well as two ACC deaminase genes involved in the degradation of ACC (FGRAMPH1_01G06417 and FGRAMPH1_01G16927) (Svoboda et al., 2019). However none of these genes were significantly expressed in response to methionine treatment (Supp. Table S1). Taken together, the data show that neither EFE or ACC pathways are responsible for ethylene production and that KMBA is the sole pathway responsible for ethylene production in *F. graminearum*. Overall the first and second objective were addressed in that I identified that *F. graminearum* produces ethylene in axenic conditions and have identified the pathway responsible.

Due to the non-enzymatic nature of oxidoreductases (Fig. 6.1) and the numerous oxidoreductase genes expressed in response to methionine (Table. 5.11), the focus shifted towards the transamination step of the KMBA pathway (Fig. 6.1). The most expressed transaminase genes identified in the RNA-seq dataset that went from few transcript-reads in the control to over 1000 in methionine conditions were exclusively *BCAT* genes (Table

6.11). As a result, I predicted that *BCAT* genes were responsible for the first step of converting methionine to KMBA (Fig. 6.1). *BCAT* genes are reported to be associated with methionine catabolism in bacteria (Engels et al., 2000, Yvon et al., 2000, Bondar et al., 2005) and also found in KMBA production in *Arabidopsis* (Schuster et al., 2006). However, none have been characterised in fungi despite the numerous reports of KMBA-related ethylene biosynthesis in fungi (Table 6.1). A *BCAT* gene (YALI0_D01265g) in *Y. lipolytica* was found to convert methionine to KMBA (Bondar et al., 2005). Based on homology, the respective enzyme from YALI0_D01265g appears to have the same molecular function, similar catalytic sites, and protein size as FGRAMPH1_01G00157 (Ensembl Genomes (Howe et al., 2020)). BCAT enzymes function on both the branched chain amino acids leucine, isoleucine and valine as well as methionine which is not a branched chain amino acid. Despite this, BCAT class 4 enzymes (Table 6.11) can catalyse the transamination of methionine (Yvon et al., 2000, Schuster et al., 2006). *BCAT4* involved in ethylene production (MetaCyc PWY-6854) (Caspi et al., 2017) was involved in methionine transamination (Schuster et al., 2006). Indeed FGRAMPH1_01G00157 is predicted to encode a class 4 BCAT (Table 6.11) and along with three out of the five oxidoreductases, were all highly expressed in a small region on chromosome 1 (Table 6.11 and Ensembl Genomes (Howe et al., 2020)). Furthermore, the activity of FGRAMPH1_01G00157 is predicted to be pyridoxal 5 phosphate (PLP) dependent (Ensembl Genomes (Howe et al., 2020)). Yvon and colleagues (2000) mention that BCAT class 4 aminotransferases are also PLP dependent (Yvon et al., 2000). When the PLP cofactor activity was inhibited by AOA, ethylene production was almost eliminated (Qadir et al., 2011). Similarly I showed that ethylene production is also inhibited by AOA even in methionine rich conditions (Fig. 6.8). This confirms that the target candidate enzyme involved in ethylene production is PLP-dependent, like FGRAMPH1_01G00157. Two *BCAT* class 4 genes were identified but FGRAMPH1_01G00157 was by far the most highly expressed of the two in response to addition of methionine (Table 6.11). Overall, the information supports the view that the *BCAT* gene FGRAMPH1_01G00157 is the gene responsible in the transamination of methionine to KMBA.

Despite all the evidence suggesting FGRAMPH1_01G00157 was the gene responsible for ethylene production, I showed that in the absence of FGRAMPH1_01G00157 (Fig. 6.11), ethylene production was not different to non-deletion transformant strains (Fig. 6.14). Therefore, the *BCAT* gene FGRAMPH1_01G00157 is not responsible for ethylene production at least on its own. Yvon and colleagues identified that mutation of the target

BCAT gene involved in transamination of methionine only reduced aminotransferase activity by 40% (Yvon et al., 2000). Bondar and colleagues (2005) also mention that most fungal species have two *BCAT* genes with different localisations (Bondar et al., 2005), which suggests that there may also be genetic redundancy for *BCAT* genes in *F. graminearum*. Indeed, there was one other class 4 *BCAT* gene (FGRAMPH1_01G15607) that was significantly upregulated in expression in the presence of methionine but to a relatively small extent (1.6 log-fold change) in comparison to that of FGRAMPH1_01G00157 (9.3 log-fold change, 632-fold transcript read increase) (Table 6.11). On the contrary, two other *BCAT* class 3 genes were upregulated (Table 6.11) and one of the two (FGRAMPH1_01G13965) had the highest expression levels (9.5 log-fold change, 727-fold transcript read increase) and transcript read counts (over 100,000) compared to all the other *BCAT* genes in the presence of methionine (Table 6.11). There is, however, no evidence in the literature to-date that *BCAT* class 3 genes have any affinity to methionine or catalyse the conversion of methionine to KMBA. In fact the main function attributed to FGRAMPH1_01G13965 is predicted to encode an ornithine aminotransferase. Ornithine aminotransferases are involved in arginine metabolism (Dzikowska et al., 2015). Despite this, it is possible that *BCAT* class 3 genes (particularly FGRAMPH1_01G13965) are also involved in ethylene biosynthesis because of the evidence of a very high fold change in expression (Table 6.11), and the presence of a PLP binding domain in the BCAT protein (Ensembl Genomes (Howe et al., 2020)). Therefore there is a possibility that all four *BCAT* genes (Table 6.11) function redundantly in the transamination of methionine to KMBA. To test this, future experiments would need to examine the expression change of FGRAMPH1_01G15607, FGRAMPH1_01G13965, and FGRAMPH1_01G18173 with *bcat* strains under ethylene production conditions to identify any increase in expression in the absence of FGRAMPH1_01G00157. Secondly, if all *BCAT* genes show equal affinity towards methionine, then it will be difficult to generate a quadruple mutant inhibited in ethylene production. The substantial difference in transcript counts and fold change in expression in the presence of methionine between *BCAT* genes (Table 6.11) may, however, be an indication of different affinities of the four gene products. Due to the high expression and the low transcript read count in the control treatment (Table 6.11), FGRAMPH1_01G13965 is the most promising second *BCAT* candidate gene involved in ethylene biosynthesis. Overall I have addressed the third objective in identifying potential gene candidates involved in ethylene biosynthesis but I was unsuccessful in validating their function. As a

result it was not possible to directly address the fourth objective through the gene disruption approach.

Ethylene has been documented as a virulence factor (Cristescu et al., 2007, Chen et al., 2009, Zhu et al., 2012). The candidate *BCAT* gene FGRAMPH1_01G00157 (i.e. FGSG_00049) was also found to be upregulated during early infection in cereals (Harris et al., 2016), and was also expressed in *F. graminearum* during wheat infection (Boedi et al., 2016). Furthermore the other two *BCAT* genes FGRAMPH1_01G15607 and FGRAMPH1_01G18173 were also expressed during wheat infection (Boedi et al., 2016). I predicted that FGRAMPH1_01G00157 may be a virulence factor because of its role in ethylene production. Supporting this I showed an upregulation of FGRAMPH1_01G00157 *in planta* following infection of roots (FRR) (Table 6.11) which implies a possible role in virulence. However there was no significant change in FRR virulence from the deletion of FGRAMPH1_01G00157. Given that we were unable to inhibit ethylene production by gene deletion (Fig. 6.14) the potential role of ethylene produced by *F. graminearum* acts as a virulence factor *in planta* is still unknown.

Chen and colleagues identified that an absence of ethylene signalling from silencing of the relevant genes in the plant host resulted in reduced DON content in wheat (Chen et al., 2009). Ethylene production might promote DON production as a virulence strategy. The entire *FgTri* cluster involved in DON production was not induced in response to methionine treatment (Supp. Table S1) and no significant change in DON content was observed in media when methionine was added as a substrate (Supp. Fig. S7). Together this would suggest that *Fusarium*-derived ethylene does not affect DON content *in vitro*. Furthermore I showed that the chemotype of the *Fusarium* isolate did not affect ethylene production (Fig. 6.9). Whether ethylene production affects DON content *in planta* would require further gene expression and DON content tests *in planta*.

In conclusion, I demonstrated that *F. graminearum* and *F. culmorum* isolates produce ethylene via the KMBA biosynthetic pathway. Utilising information from an RNA-seq dataset, gene function databases, and results from other studies, a very likely candidate transaminase involved in ethylene production was chosen for split-marker deletion. However in the absence of this candidate gene, ethylene production was unaffected and an increase in FRR virulence was not observed. It is believed that this may be due to genetic

redundancy. The role of ethylene production is still unknown and future work is necessary to ascertain the role of *Fusarium*-derived ethylene during plant pathogenesis.

Chapter 7 - General Discussion

One figure and some of the writing in this chapter have been published previously in:

Haidoulis JF, Nicholson P, 2020. Different effects of phytohormones on Fusarium head blight and Fusarium root rot resistance in *Brachypodium distachyon*. *Journal of Plant Interactions* **15**, 335-44.

In the absence of robust genetic resistance, strategies for controlling Fusarium head blight (FHB) rely predominantly on chemical control methods to reduce FHB symptoms and mycotoxin accumulation in grain. Wheat is most susceptible to FHB at mid-anthesis (Parry et al., 1995, Bai & Shaner, 2004, Xu et al., 2008b, Peraldi et al., 2011). Phytohormones are important for plant defence responses (Bari & Jones, 2009, Pieterse et al., 2012). Numerous studies have identified the impact of phytohormones on endogenous defences to *Fusarium* at the molecular level (Chapter 4.1. Introduction), and their effects on *Fusarium* resistance following exogenous application (Table 3.1). Given this information, phytohormones have to potential to be used as a control strategy to transiently reduce susceptibility to FHB at mid-anthesis when the wheat host is most vulnerable.

Brachypodium distachyon is an effective model cereal for *Fusarium* research (Peraldi et al., 2011, Peraldi, 2012) with evidence for phytohormones affecting this *Fusarium* resistance (Peraldi, 2012, Goddard et al., 2014, Pasquet et al., 2014, Powell et al., 2017b). The central aim and theme of this thesis was to investigate the role of phytohormones in the *B. distachyon-Fusarium graminearum* pathosystem and their potential for use as disease control chemicals. The phytohormones investigated throughout the thesis include salicylic acid (SA), jasmonic acid (JA), ethylene, auxin, cytokinin, abscisic acid (ABA), gibberellic acid (GA), brassinosteroid (BR), and the defence signalling molecule 3-aminobutanoic acid (BABA). The role of phytohormones in response to FHB and FRR in *B. distachyon* was investigated by exogenous application experiments in Chapters 2 and 3, and transcriptomic investigation experiments in Chapter 4 and Chapter 5. The likelihood of ethylene being a virulence factor for *F. graminearum* was then investigated in Chapter 6.

Aside from the economically important FHB disease of cereals, *F. graminearum* can infect any tissue of the host. There is, however, an under-representation of research on resistance to other Fusarium diseases. Fusarium root rot (FRR) is an important disease caused by different *Fusarium* species, including *F. graminearum*. Relative to FHB, few studies have investigated control strategies for FRR. Furthermore, the role of

phytohormones in *F. graminearum*-induced FRR has not been previously investigated. This topic was investigated in Chapter 2. FRR has been studied in wheat (Beccari et al., 2011, Wang et al., 2015b, Wang et al., 2018c) however there are time and space constraints associated with studying wheat root tissues. *B. distachyon* seedlings offered an efficient time and space saving method for investigating FRR resistance. An optimised protocol was adapted from (Peraldi et al., 2011, Goddard et al., 2014) that allowed for consistent and time-course cataloguing experiments for the effect of phytohormones on FRR symptoms. The majority of phytohormones affected the severity of FRR symptoms (Chapter 2). The defence-associated hormone SA increased susceptibility to FRR whereas JA and ethylene increased resistance (Fig. 2.5). Given the positive resistance role of SA with biotrophs and JA/ethylene with necrotrophs (Glazebrook, 2005, Bari & Jones, 2009, Pieterse et al., 2012), I hypothesised that *F. graminearum* may be adopting a more necrotrophic lifestyle in roots due to the positive role of JA and ethylene on FRR resistance. Strikingly, the growth and development associated phytohormones induced the most significant changes to FRR resistance with auxins strongly increasing FRR resistance, whereas cytokinins and BABA severely increased FRR symptoms. None of the latter three phytohormones have been previously studied for their role in *F. graminearum*-induced FHB or FRR. Together the results from Chapter 2 suggest that many phytohormones are important for FRR resistance. The reasons for the significant effects of each hormone on FRR, especially with auxins, cytokinins, and BABA, are unclear and merit further investigation. These results on FRR response to phytohormones provide important information that can be used to study the similarities in wheat FRR response to phytohormones. Their use as potential FRR chemical control compounds also merits further investigation.

Changes to FHB resistance in response to phytohormones has been previously investigated in wheat and barley (*Hordeum vulgare*) (Li & Yen, 2008, Chen et al., 2009, Petti et al., 2012, Qi et al., 2012, Ali et al., 2013, Buhrow et al., 2016, Qi et al., 2016, Sorahinobar et al., 2016, Sun et al., 2016, Foroud et al., 2018). However there is a lack of information on the effect of exogenous phytohormones on *B. distachyon* FHB resistance. Therefore the main aim of Chapter 3 was to identify which phytohormones had the greatest effect on FHB in the model cereal *B. distachyon*. Surprisingly the majority of phytohormones tested (JA, ethylene, *trans*-Zeatin, BABA) increased FHB symptoms (Chapter 3.3. Results). It is unclear why this occurred. The phytohormones SA, GA, and auxins, as well as the phytohormone inhibitors for JA, ethylene, and BR were also tested on wheat response to

FHB for comparison. Most showed no significant effect on wheat FHB and none significantly altered grain deoxynivalenol (DON) content. Only auxins at relatively high concentrations reduced FHB symptoms in wheat and *B. distachyon*. Together with the positive effect of auxin on FRR, I show that auxin has a promising potential to be used to transiently control FHB and FRR symptoms. An important observation mentioned in the discussion of Chapter 3 is the contrasting effects observed in the current work with those reported in previous studies. The reasons for these contradictions are still unclear. Phytohormone outcomes on defence are complicated due to their interconnectedness (Bari & Jones, 2009, Verhage et al., 2010, Pieterse et al., 2012). Altering the endogenous balance of one hormone through exogenous application may negatively affect another phytohormone that positively affects FHB resistance (Fig. 1.6, Table 3.1) (Verhage et al., 2010, Pieterse et al., 2012). For example, JA and SA which are known to act antagonistically (Spoel & Dong, 2008, Leon-Reyes et al., 2010b, Pieterse et al., 2012) share a large number of co-responsive genes in rice (*Oryza sativa*) (Tamaoki et al., 2013), and this may also be true for *B. distachyon* (Kouzai et al., 2016). This is complicated further by the hemibiotrophic lifestyle of *F. graminearum* in floral tissues (Brown et al., 2010) which may activate both SA and JA defences (Glazebrook, 2005, Pieterse et al., 2012). Many more of these exogenous phytohormone FHB studies that incorporate different experimental designs and environmental conditions are necessary to fully explain the role of phytohormones in resistance to FHB and FRR. Lastly, despite the contradictory effects (Discussed in Chapter 3) on FHB resistance of the ethylene inhibitor aminoethoxyvinylglycine (AVG) and the BR inhibitor Brassinazole (BRZ) on resistance (Fig. 3.5C-D, 3.9D, 3.9H), there is a plethora of different phytohormone inhibitors that may induce antagonistic effects on FHB in addition to the phytohormones tested in this study. These could be trialled on *B. distachyon* to transiently promote FHB resistance. It is still too early to state whether phytohormones can be effectively used to control FHB.

One important observation made in Chapters 2 and 3, was the tissue-dependent and tissue-independent effect of particular phytohormones on *Fusarium* resistance. Similarly, defence and resistance to different *Fusarium* tissue-diseases has been shown to be tissue-specific (Lyons et al., 2015, Wang et al., 2015b). The tissue-specific effects of phytohormones on resistance has not been investigated within this *B. distachyon - F. graminearum* pathosystem before. The effect of exogenous application of six phytohormones on *B. distachyon* FRR and FHB symptoms was compared (Fig. 7.1). The data showed that the canonical defence-associated phytohormones SA, JA, and ethylene

induced tissue-specific changes to resistance (Fig. 7.1). It is unclear why these tissue-specific effects occurred. SA application had no effect on FHB symptoms but increased FRR disease symptoms (Fig. 7.1). Tissue-specific resistance may be the result of differences in the endogenous phytohormone concentrations between tissues. For example, endogenous free SA levels were higher in rice (*Oryza sativa*) floral tissues than in root tissues (Chen et al., 1997). In contrast to SA, JA, and ethylene increased FHB susceptibility but decreased FRR susceptibility (Fig. 7.1). This again supports my hypothesis that *F. graminearum* adopts a more necrotrophic lifestyle in root tissues than in floral tissues. The increase in FHB susceptibility may have been observed because JA and ethylene were applied shortly before the short early biotrophic phase of the predominantly hemibiotrophic lifestyle of *F. graminearum* when infecting and colonising floral tissues in FHB (Brown et al., 2010).
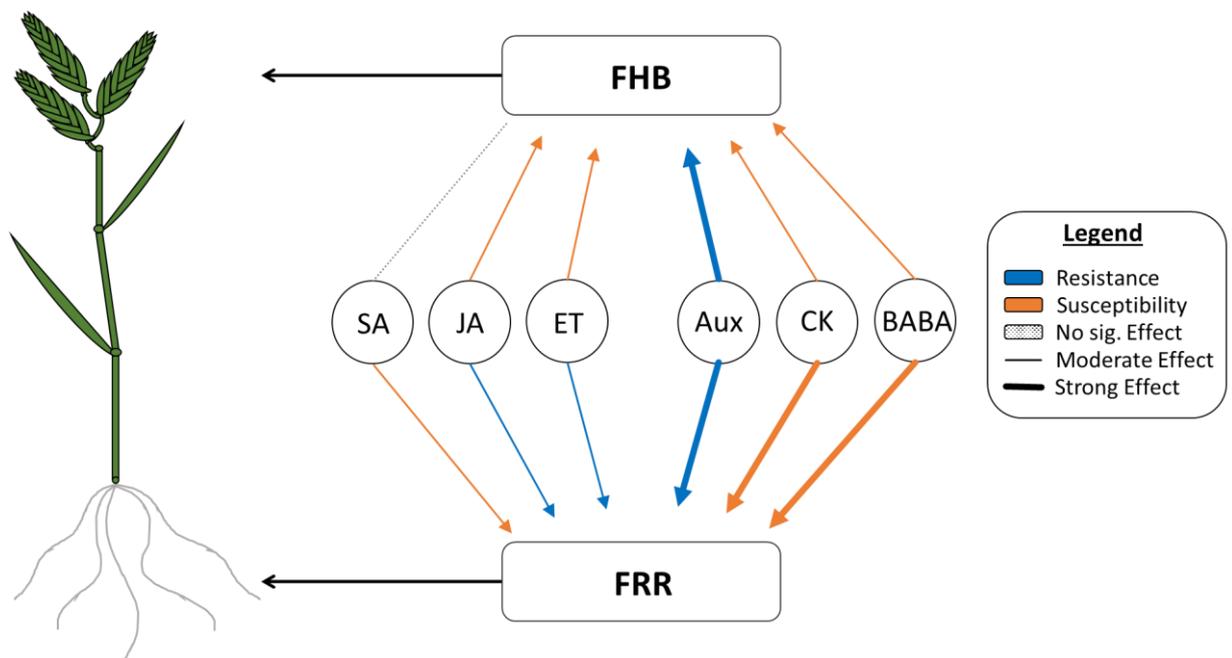
Figure 7.1. The tissue-dependent or tissue-independent effects on six phytohormones on FHB and FRR symptoms in *B. distachyon*. This summary is a generalisation of the trend over time of data from Chapter 2 (FRR) and Chapter 3 (FHB). Different arrow thicknesses are shown based on the potency of response caused by each phytohormone. The cartoon on the left is a representation of an adult *B. distachyon* plant but the roots denote seedling roots. Novel abbreviations: ET (ethylene), Aux (auxins), CK (cytokinins). Taken and modified from (Haidoulis & Nicholson, 2020).

Novel advances in transcriptomics has permitted increased understanding of the numerous defence pathways important for disease resistance. The transcriptome response of *B. distachyon* has been investigated in response to FHB and FCR infection by different *Fusarium* species (Pasquet et al., 2014, Powell et al., 2017b), but the *B. distachyon* response to *F. graminearum*-induced FRR has not. The reasons for the tissue-specific effects of

canonical defence phytohormones (Fig. 7.1) was unclear. I wanted to investigate this further by comparing phytohormone-related gene expression responses between FHB and FRR in *B. distachyon*. The results from Chapter 4 show the phytohormone-specific similarities and differences between FHB and FRR. There was a distinct change in the expression of JA and ethylene-associated genes but not to the same extent for SA-associated genes. Contrary to evidence of an important role of SA in FHB resistance (Makandar et al., 2010, Ding et al., 2011, Makandar et al., 2011, Ameye et al., 2015, Sorahinobar et al., 2016, Wang et al., 2018a), the transcriptomic data revealed few SA-related genes expressed in response to both FHB and FRR. This is supported by data from Chapter 3 on the absence of effect of exogenous SA on FHB resistance (Fig. 7.1), and is also supported by several other studies on resistance to Fusarium diseases (Kidd et al., 2011, Qi et al., 2012, Lyons et al., 2015, Sun et al., 2016, Powell et al., 2017b, Hao et al., 2018, Pan et al., 2018). Taken together I conclude that SA-controlled gene expression is unlikely to play a major role in FHB and FRR resistance in *B. distachyon*. It has been shown that in response to FHB from *Fusarium* infection, SA-associated pathways were expressed earlier in the resistant wheat line Sumai3 than susceptible lines (Wang et al., 2018a) and Sumai3 showed greater endogenous SA levels (Sorahinobar et al., 2016, Wang et al., 2018a). The *B. distachyon* line Bd3-1 chosen in this study is susceptible to *Fusarium* (Peraldi et al., 2011, Su et al., 2018). An early SA-response may be more pronounced in a resistant *B. distachyon* line. This would merit further investigation.

JA and ethylene-associated genes were generally similarly expressed between FHB and FRR (Fig. 4.6 and Fig. 4.7). Exogenous application of JA and ethylene had similar effects on resistance in both tissues (Fig. 7.1). This supports the consensus that JA and ethylene function synergistically in defence against fungal pathogens (Fig. 1.6) (Pieterse et al., 2012) and that they both play important roles in resistance to FHB and FRR in *B. distachyon*. This is supported by several other studies (Li & Yen, 2008, Makandar et al., 2010, Ding et al., 2011, Makandar et al., 2011, Gottwald et al., 2012, Pasquet et al., 2014, Ameye et al., 2015, Sun et al., 2016, Wang et al., 2018c). However there appears to be a contradiction with their tissue-specific effects on resistance from exogenous application of JA and ethylene (Fig. 7.1) but similar endogenous JA- and ethylene-associated expression between tissues (Fig. 4.6 and Fig. 4.7). There were considerable differences in levels of basal expression (Control samples) of several phytohormone-related genes between spikes and roots (Fig.

4.5 - 4.10). These differences in the absence of any pathogen attack may help explain these contradictory results described above.

To further investigate the tissue-specific differences, the transcriptome of *F. graminearum* in FHB and FRR was investigated in Chapter 5. This has not been performed previously with different tissues in the same host. Other fungal pathogens like *Magnaporthe oryzae* (Dean et al., 2012) show tissue-specific pathogenesis and different host resistance outcomes (Jansen et al., 2006, Marcel et al., 2010). I previously proposed a hypothesis that *F. graminearum* is behaving predominantly as a necrotroph in root tissues of *B. distachyon*. Among several interesting effectors and non-effectors potentially involved in pathogenicity (Fig. 5.2), I show that the key genes highly expressed in both tissues encoded cell-wall degrading enzymes (CWDEs) and the mycotoxin DON (Fig. 5.2 and Table 5.1). CWDEs and toxins are key signatures for necrotrophy by pathogenic fungi (Laluk & Mengiste, 2010, Zhao et al., 2014b, Kabbage et al., 2015, Zeilinger et al., 2016). This paired with the activation of necrotrophy-associated JA and ethylene biosynthesis and signalling to both FHB and FRR by *B. distachyon* (Fig. 4.6 and Fig. 4.7) suggests that *F. graminearum* is behaving as a necrotroph in both tissues at the time points sampled. However it is unclear if there is an absence of biotrophy-related activities by *F. graminearum* in root tissues. This requires further investigation using transcriptomics and microscopy at even earlier time-points. The comparison of host-pathogen interactions in different tissues is relatively unstudied and the information gathered in this study may be useful for additional research into other types of tissue-specific diseases in other small-grain cereal crops.

Chapter 5 revealed both similarities and differences in *F. graminearum* gene expression during spike and root infection (Fig. 5.1, Fig. 5.2, Fig. 5.3, Table 5.3). Given that *B. distachyon* is susceptible to *Fusarium* (Peraldi et al., 2011) and is similarly deploying JA and ethylene defences to FHB and FRR (Fig 4.6 and Fig 4.7), and that *F. graminearum* is deploying several tissue-specific effector and non-effector genes (Fig. 5.1 and Fig. 5.2), I hypothesise that *F. graminearum* may be better at detecting the environment it's in and reacting accordingly than the *B. distachyon* host is at mounting an appropriate defence response in each tissue. The *Fusarium* transcriptome during infection may also help in understanding the tissue-specific differences of the effects of phytohormones SA, JA, and ethylene (Fig. 7.1). Within the set of genes upregulated by *F. graminearum*, several

phytohormone-related genes were differentially upregulated in FHB and FRR (Table 5.2). One of these was a JA-related homologue of an *Arabidopsis thaliana* 2OG oxygenase (Table 5.2) involved in JA-hydroxylation (Ding et al., 2020). This gene was highly upregulated in FRR but not in FHB (Table 5.2). Given the positive effects JA has on FRR resistance (Fig 7.1) and the upregulation of JA biosynthetic genes in FRR (Fig. 4.6), I hypothesise that *F. graminearum* is attempting to decrease the JA content to create a more suitable environment for colonisation in root tissues. Given the large number of uncharacterised *F. graminearum* genes (Chapter 5 Results section), there may be more uncharacterised phytohormone manipulation genes that are upregulated in FHB and FRR. An SA biosynthetic homologue *EPS1* was also upregulated in response to FRR only (Table 5.2) and there is evidence that *F. graminearum* can synthesise SA (Ding et al., 2020). Given the negative effect of SA on FRR resistance (Fig. 7.1) I speculate that *F. graminearum* may be attempting to synthesise SA during its necrotrophic infection of root tissue given the negative role SA has on necrotrophic resistance (Fig. 1.6). Several SA degradation-related genes were also upregulated in response to both FHB and FRR (Table 5.2). It is unclear why both SA biosynthetic and degradation genes were upregulated given I show minimal SA-related biosynthetic gene expression in FHB and FRR (Fig. 4.5). Together this information highlights the complexity of interactions between *F. graminearum* and *B. distachyon* and that phytohormones play an important role in this interaction.

Phytohormone manipulation by plant pathogens is an effective virulence strategy. Exogenous application of ethylene had contrasting effects on FHB and FRR (Fig. 7.1). However it was unclear whether *F. graminearum* was able to produce ethylene and use it as a virulence factor. I show in Chapter 6 conclusive evidence that *F. graminearum* can produce ethylene with the appropriate substrates, and that *F. graminearum* synthesises ethylene via the α-keto γ-methylthiobutyric acid (KMBA) pathway. The important question remains as to whether *F. graminearum*-derived ethylene functions as virulence factor. Unfortunately there was no effect on ethylene production, growth, or FRR virulence of *F. graminearum* when the predicted target gene (FGRAMPH1_01G00157) was deleted (Fig. 6.13, Fig. 6.14, Fig. 6.15). Future work is required to identify the gene/s responsible for ethylene production and their role, if any, in virulence. There may be genetic redundancy for ethylene production. Other candidates like FGRAMPH1_01G13965 may also be involved in ethylene biosynthesis and is a prime candidate for producing a double knockout given its very high expression under ethylene-producing conditions (Table 5.11). Ethylene is

clearly an important phytohormone for both FHB and FRR, and further research is necessary to determine its role in the *F. graminearum* and *B. distachyon* interaction.

One of the most important findings from this thesis was the importance of non-defence phytohormones in *F. graminearum* resistance. The development-associated phytohormones auxin and cytokinin induced the most significant but tissue-independent effects (Fig. 7.1). Furthermore data from Chapter 4 show that auxin and cytokinin-associated genes were also important in response to FHB and FRR (Fig. 4.8, Fig. 4.9, and Fig. 4.11G-J). This suggests that these two phytohormones are functioning independently of the *F. graminearum* trophic state proposed previously. In chapter 4, some auxin-related biosynthetic and homeostasis genes were relatively similarly expressed between tissues however the downstream signalling genes were not. Given that application of auxin increased resistance to both FHB and FRR (Fig. 7.1), and the elevated expression of auxin biosynthetic genes in response to infection (Chapter 4), I hypothesise that the endogenous auxin content affects FHB and FRR resistance. Similarly other studies have shown that auxin content were elevated in susceptible wheat lines as a result of FHB (Qi et al., 2016, Wang et al., 2018a). The data in Chapter 2, 3, and 4 highlight the potential importance of auxin in *B. distachyon* FHB and FRR. Exogenous application of auxin increased resistance to FHB and FRR (Fig. 7.1), expression of auxin-related signalling genes differs in *B. distachyon* in response to FHB and FRR (Chapter 4 - Discussion auxin 4.4.4.). Auxin is generally associated with FHB susceptibility (Qi et al., 2016, Pan et al., 2018, Wang et al., 2018a), and *F. graminearum* has the capacity to synthesise IAA (Luo et al., 2016). The definitive role of auxin in FHB and FRR is still unclear and requires further research. In contrast to auxin, cytokinins severely increased susceptibility to both FHB and FRR (Fig. 7.1). There are no previous reports in the literature for the effect of exogenous application of cytokinins on *F. graminearum*-induced FHB and FRR. There is, however, emerging evidence from transcriptomic studies for a role of cytokinins in *Fusarium* resistance (Powell et al., 2017a). However the role of cytokinin-related gene transcription was unclear with a delayed expression of two cytokinin-related genes (*LONELYGUY* (*LOG1*) and *Type-A Response Regulator* (*RR*)) in response to FRR (Fig. 4.11I and Fig. 4.11J). Both auxin and cytokinin are of particular interest given their significant effects on resistance. An important question arises from these results (Fig. 7.1). Why do auxin and cytokinin have contrasting effects on resistance in a tissue-independent manner? The antagonism of auxin and cytokinin in resistance has been reported previously (Naseem & Dandekar, 2012, Naseem et al., 2012)

but it is unclear if the results presented here are due to a direct antagonism. Additional study of role of auxin and cytokinin in *Fusarium* resistance is required.

Like the use of exogenous phytohormones on FHB and FRR resistance, it is conceivable that the use of BCAs with phytohormone profile-modifying properties can be used affect FHB and FRR resistance. BCAs are known to change the content of JA, ethylene, IAA, and cytokinin and improve pathogen resistance in several host species (Segarra et al., 2007, Chen et al., 2010, Contreras-Cornejo et al., 2011, Chowdappa et al., 2013, Martínez-Medina et al., 2014, Tang et al., 2019). Given the positive and negative effects of auxin and cytokinin, respectively, on FHB and FRR (Fig. 7.1), the BCA species which were shown to increase auxin or reduce cytokinin levels in hosts (Chen et al., 2010, Chowdappa et al., 2013, Martínez-Medina et al., 2014) may improve FHB and FRR resistance. On the contrary, given that some BCA species were shown to increase JA content (Segarra et al., 2007, Contreras-Cornejo et al., 2011) or ethylene content (Tang et al., 2019), this may have positive effects on FRR resistance but negative effects on FHB resistance (Fig. 7.1). This is all assuming the BCA species investigated can modify the phytohormone content similarly in *B. distachyon*. Furthermore, due to the direct growth antagonism of BCAs like *Trichoderma* on *Fusarium* species (Martínez-Medina et al., 2014, Tian et al., 2018), typical application of *Trichoderma* on roots (Segarra et al., 2007, Korolev et al., 2008, Contreras-Cornejo et al., 2011) may provide an additional resistance mechanism towards FRR. The use of BCAs that influence phytohormones in wheat and *B. distachyon* would be valuable to investigate as an alternative means for FHB and FRR control.

Several other phytohormones and a signalling compound were investigated for their role in *Fusarium* resistance throughout the thesis. The role of the signalling molecule BABA on *F. graminearum* resistance has not been investigated before. There is strong evidence in other host-pathogen interactions that BABA promotes disease resistance (Jakab et al., 2001, Cohen, 2002, Ton & Mauch-Mani, 2004, Ton et al., 2005, Olivieri et al., 2009). However evidence from Chapters 2 and 3 revealed a significant susceptibility promoting effect from exogenous application, particularly on FRR (Fig. 2.12A). Relatively little is known about the BABA signalling pathway (Luna et al., 2014), and no BABA-related genes were identified within Chapter 4. This supports the hypothesis made in chapter 3 that BABA is indirectly affecting resistance either though synergism with other phytohormones, or through effects from growth and development changes. This was supported in Chapter 2

as BABA was shown to significantly upregulate the expression with the SAR-associated gene *BdMES1* (Fig.2.15B). Given the substantially large yet unclear effects of BABA on both FHB and FRR (Fig. 7.1), this compound merits further investigation. GA did not alter resistance when exogenously applied on FRR in *B. distachyon* (Chapter 2), or on FHB in wheat (Chapter 3). Furthermore, differential expression of GA-responsive genes were relatively underrepresented in response to the same diseases (Chapter 4). This is contrasts with evidence of GA being associated with FHB resistance (Buhrow et al., 2016). Similarly BR application did not affect FRR resistance (Chapter 2) and genes associated with this pathway were not represented within the RNA-seq data for FHB or FRR (Chapter 4). This contrasts to reports indicating that BR is important for *Fusarium* resistance in wheat and barley (Ali et al., 2013, Ali et al., 2014, Goddard et al., 2014). However a BR inhibitor did significantly affect resistance to FRR in *B. distachyon* and FHB in wheat (Fig. 2.7B and Fig 3.9H). Overall the data suggests that some aspect of GA and BR signalling is important for Fusarium disease response and it may be via their association with other phytohormones (Sections 1.3.5 and 1.3.6) that induced more significant effects on resistance (Fig. 7.1). Lastly, there was evidence of altered expression of genes associated with ABA biosynthesis in line with reports that application of ABA negatively influences FHB resistance (Buhrow et al., 2016, Pan et al., 2018, Wang et al., 2018a). It is unfortunate that despite the transcriptome findings, no equivalent exogenous ABA assays could be successfully performed on FHB and FRR for comparison. Further research is required to study the role of all non-defence phytohormones in Fusarium diseases and their potential use as chemical control agents for *F. graminearum* resistance.

To summarise, I show that phytohormones play an important role in *Fusarium* resistance in both roots and spikes of *B. distachyon*. The phytohormones JA, ethylene, auxin, and cytokinin played the most prominent roles in *B. distachyon* resistance. This information will be important for future work to investigate novel chemical control strategies for both FHB and FRR. A key point of future research will be to determine the function of each phytohormone in resistance to FHB and FRR and the extent of phytohormone interactions. These aims become more complex given the discovery from this study and other reports of *Fusarium* having the capacity to synthesise several plant phytohormones. Determining how much of a role these *Fusarium*-derived phytohormones play in virulence will also need to be investigated. The information within this thesis confirms the complexity of the *F. graminearum – B. distachyon* pathosystem and highlights the need for additional research

into other tissue-specific diseases as well as the key challenges that they pose for disease control.

Bibliography

Abeles FB, Morgan PW, Saltveit Jr ME, 2012. *Ethylene in plant biology.* San Diego, CA: Academic press. 176-187.

Abràmoff MD, Magalhães PJ, Ram SJ, 2004. Image processing with ImageJ. *Biophotonics international* **11**, 36-42.

Achard P, Renou J-P, Berthomé R, Harberd NP, Genschik P, 2008. Plant DELLAs restrain growth and promote survival of adversity by reducing the levels of reactive oxygen species. *Current Biology* **18**, 656-60.

Acosta IF, Farmer EE, 2010. Jasmonates. *The arabidopsis book* **8**, e0129-e.

Adie BaT, Pérez-Pérez J, Pérez-Pérez MM*, et al.*, 2007. ABA Is an Essential Signal for Plant Resistance to Pathogens Affecting JA Biosynthesis and the Activation of Defenses in Arabidopsis. *The Plant Cell* **19**, 1665-81.

Afgan E, Baker D, Van Den Beek M*, et al.*, 2016. The Galaxy platform for accessible, reproducible and collaborative biomedical analyses: 2016 update. *Nucleic acids research* **44**, W3-W10.

Agrios G, 2005. Plant pathology 5th Edition: Elsevier Academic Press. *Burlington, Ma. USA*, 144-63, 210-32, 315-6.

Akinsanmi O, Backhouse D, Simpfendorfer S, Chakraborty S, 2006. Genetic diversity of Australian Fusarium graminearum and F. pseudograminearum. *Plant Pathology* **55**, 494-504.

Al-Masri M, Elad Y, Sharon A, Barakat R, 2006. Ethylene production by Sclerotinia sclerotiorum and influence of exogenously applied hormone and its inhibitor aminoethoxyvinylglycine on white mold. *Crop Protection* **25**, 356-61.

Albrecht T, Argueso CT, 2017. Should I fight or should I grow now? The role of cytokinins in plant growth and immunity and in the growth–defence trade-off. *Annals of Botany* **119**, 725-35.

Alexander NJ, Mccormick SP, Waalwijk C, Van Der Lee T, Proctor RH, 2011. The genetic basis for 3-ADON and 15-ADON trichothecene chemotypes in Fusarium. *Fungal Genetics and Biology* **48**, 485-95.

Ali SS, Gunupuru LR, Kumar GS*, et al.*, 2014. Plant disease resistance is augmented in uzu barley lines modified in the brassinosteroid receptor BRI1. *Bmc Plant Biology* **14**, 1-15.

Ali SS, Kumar GBS, Khan M, Doohan FM, 2013. Brassinosteroid Enhances Resistance to Fusarium Diseases of Barley. *Phytopathology* **103**, 1260-7.

Amatulli MT, Spadaro D, Gullino ML, Garibaldi A, 2010. Molecular identification of Fusarium spp. associated with bakanae disease of rice in Italy and assessment of their pathogenicity. *Plant Pathology* **59**, 839-44.

Ament K, Krasikov V, Allmann S, Rep M, Takken FLW, Schuurink RC, 2010. Methyl salicylate production in tomato affects biotic interactions. *The Plant Journal* **62**, 124-34.

Ameye M, Audenaert K, De Zutter N*, et al.*, 2015. Priming of Wheat with the Green Leaf Volatile *Z*-3-Hexenyl Acetate Enhances Defense against *Fusarium graminearum* But Boosts Deoxynivalenol Production. *Plant Physiology* **167**, 1671-84.

Amselem J, Cuomo CA, Van Kan JA*, et al.*, 2011. Genomic analysis of the necrotrophic fungal pathogens Sclerotinia sclerotiorum and Botrytis cinerea. *PLoS genetics* **7**, e1002230.

Andersen KF, Morris L, Derksen RC, Madden LV, Paul PA, 2014. Rainfastness of Prothioconazole + Tebuconazole for Fusarium Head Blight and Deoxynivalenol Management in Soft Red Winter Wheat. *Plant Disease* **98**, 1398-406.

Anderson JA, Stack R, Liu S*, et al.*, 2001. DNA markers for Fusarium head blight resistance QTLs in two wheat populations. *Theoretical and Applied Genetics* **102**, 1164-8.

Anderson JP, Badruzsaufari E, Schenk PM*, et al.*, 2004. Antagonistic Interaction between Abscisic Acid and Jasmonate-Ethylene Signaling Pathways Modulates Defense Gene Expression and Disease Resistance in Arabidopsis. *The Plant Cell* **16**, 3460-79.

Ansari MW, Shukla A, Pant RC, Tuteja N, 2013. First evidence of ethylene production by Fusarium mangiferae associated with mango malformation. *Plant Signaling & Behavior* **8**, e22673.

Antonissen G, Martel A, Pasmans F*, et al.*, 2014. The Impact of Fusarium Mycotoxins on Human and Animal Host Susceptibility to Infectious Diseases. *Toxins* **6**, 430-52.

Argueso CT, Ferreira FJ, Epple P*, et al.*, 2012. Two-component elements mediate interactions between cytokinin and salicylic acid in plant immunity. *PLoS genetics* **8(1)**, e1002448-e.

Arruda MP, Brown P, Brown-Guedira G*, et al.*, 2016. Genome-Wide Association Mapping of Fusarium Head Blight Resistance in Wheat using Genotyping-by-Sequencing. *The Plant Genome* **9**, plantgenome2015.04.0028.

Asami T, Min YK, Nagata N*, et al.*, 2000. Characterization of Brassinazole, a Triazole-Type Brassinosteroid Biosynthesis Inhibitor. *Plant Physiology* **123**, 93-100.

Audenaert K, Callewaert E, Höfte M, De Saeger S, Haesaert G, 2010. Hydrogen peroxide induced by the fungicide prothioconazole triggers deoxynivalenol (DON) production by Fusarium graminearum. *BMC Microbiology* **10**, 1-14.

Audenaert K, De Meyer GB, Höfte MM, 2002. Abscisic Acid Determines Basal Susceptibility of Tomato toBotrytis cinerea and Suppresses Salicylic Acid-Dependent Signaling Mechanisms. *Plant Physiology* **128**, 491-501.

Baccelli I, Mauch-Mani B, 2017. When the story proceeds backward: The discovery of endogenous β-aminobutyric acid as the missing link for a potential new plant hormone. *Communicative & Integrative Biology* **10**, 552-9.

Bai G-H, Desjardins A, Plattner R, 2002. Deoxynivalenol-nonproducing Fusarium graminearum causes initial infection, but does not cause DiseaseSpread in wheat spikes. *Mycopathologia* **153**, 91-8.

Bai G, Shaner G, 2004. Management and resistance in wheat and barley to Fusarium head blight. *Annu. Rev. Phytopathol.* **42**, 135-61.

Bajguz A, 2007. Metabolism of brassinosteroids in plants. *Plant Physiology and Biochemistry* **45**, 95-107.

Bajguz A, Chmur M, Gruszka D, 2020. Comprehensive Overview of the Brassinosteroid Biosynthesis Pathways: Substrates, Products, Inhibitors, and Connections. *Frontiers in Plant Science* **11**, 1034.

Bajguz A, Orczyk W, Gołębiewska A, Chmur M, Piotrowska-Niczyporuk A, 2019. Occurrence of brassinosteroids and influence of 24-epibrassinolide with brassinazole on their content in the leaves and roots of Hordeum vulgare L. cv. Golden Promise. *Planta* **249**, 123-37.

Bajguz A, Tretyn A, 2003. The chemical characteristic and distribution of brassinosteroids in plants. *Phytochemistry* **62**, 1027-46.

Balmas V, Delogu G, Sposito S, Rau D, Migheli Q, 2006. Use of a complexation of tebuconazole with β-cyclodextrin for controlling foot and crown rot of durum wheat incited by Fusarium culmorum. *Journal of Agricultural and Food Chemistry* **54**, 480-4.

Bandyopadhyay A, Blakeslee J, Lee OR, *et al.*, 2007. Interactions of PIN and PGP auxin transport mechanisms. In.: Portland Press Ltd.

Bari R, Jones JDG, 2009. Role of plant hormones in plant defence responses. *Plant Molecular Biology* **69**, 473-88.

Barro-Trastoy D, Carrera E, Baños J, *et al.*, 2020. Regulation of ovule initiation by gibberellins and brassinosteroids in tomato and Arabidopsis: two plant species, two molecular mechanisms. *The Plant Journal* **102**, 1026-41.

Bartlett DW, Clough JM, Godwin JR, Hall AA, Hamer M, Parr-Dobrzanski B, 2002. The strobilurin fungicides. *Pest Management Science* **58**, 649-62.

Beccari G, Covarelli L, Nicholson P, 2011. Infection processes and soft wheat response to root rot and crown rot caused by Fusarium culmorum. *Plant Pathology* **60**, 671-84.

Beccari G, Prodi A, Pisi A*, et al.*, 2018. Development of three fusarium crown rot causal agents and systemic translocation of deoxynivalenol following stem base infection of soft wheat. *Plant Pathology* **67**, 1055-65.

Becher R, Hettwer U, Karlovsky P, Deising HB, Wirsel SGR, 2010. Adaptation of Fusarium graminearum to Tebuconazole Yielded Descendants Diverging for Levels of Fitness, Fungicide Resistance, Virulence, and Mycotoxin Production. *Phytopathology* **100**, 444-53.

Bektas Y, Eulgem T, 2015. Synthetic plant defense elicitors. *Frontiers in Plant Science* **5**, 804-.

Beltrano J, Carbone A, Montaldi ER, Guiamet JJ, 1994. Ethylene as promoter of wheat grain maturation and ear senescence. *Plant Growth Regulation* **15**, 107-12.

Berardini TZ, Reiser L, Li D*, et al.*, 2015. The Arabidopsis information resource: making and mining the "gold standard" annotated reference plant genome. *genesis* **53**, 474-85.

Billington DC, Golding BT, Primrose SB, 1979. Biosynthesis of ethylene from methionine. Isolation of the putative intermediate 4-methylthio-2-oxobutanoate from culture fluids of bacteria and fungi. *Biochemical Journal* **182**, 827-36.

Blandino M, Minelli L, Reyneri A, 2006. Strategies for the chemical control of Fusarium head blight: Effect on yield, alveographic parameters and deoxynivalenol contamination in winter wheat grain. *European Journal of Agronomy* **25**, 193-201.

Blum A, Benfield AH, Sørensen JL*, et al.*, 2019. Regulation of a novel Fusarium cytokinin in Fusarium pseudograminearum. *Fungal Biology* **123**, 255-66.

Blumke A, Sode B, Ellinger D, Voigt CA, 2015. Reduced susceptibility to Fusarium head blight in Brachypodium distachyon through priming with the Fusarium mycotoxin deoxynivalenol. *Molecular Plant Pathology* **16**, 472-83.

Boddu J, Cho S, Kruger WM, Muehlbauer GJ, 2006. Transcriptome Analysis of the Barley-Fusarium graminearum Interaction. *Molecular Plant-Microbe Interactions* **19**, 407-17.

Boedi S, Berger H, Sieber C*, et al.*, 2016. Comparison of Fusarium graminearum transcriptomes on living or dead wheat differentiates substrate-responsive and defense-responsive genes. *Frontiers in microbiology* **7**, 1113.

Bolton MD, 2009. Primary Metabolism and Plant Defense—Fuel for the Fire. *Molecular Plant-Microbe Interactions* **22**, 487-97.

Bolton MD, Kolmer JA, Xu WW, Garvin DF, 2008. Lr34-Mediated Leaf Rust Resistance in Wheat: Transcript Profiling Reveals a High Energetic Demand Supported by Transient Recruitment of Multiple Metabolic Pathways. *Molecular Plant-Microbe Interactions* **21**, 1515-27.

Bondar DC, Beckerich J-M, Bonnarme P, 2005. Involvement of a branched-chain aminotransferase in production of volatile sulfur compounds in Yarrowia lipolytica. *Applied and Environmental Microbiology* **71**, 4585-91.

Boutigny A-L, Richard-Forget F, Barreau C, 2008. Natural mechanisms for cereal resistance to the accumulation of Fusarium trichothecenes. *European Journal of Plant Pathology* **121**, 411-23.

Brauer EK, Rocheleau H, Balcerzak M*, et al.*, 2019. Transcriptional and hormonal profiling of Fusarium graminearum-infected wheat reveals an association between auxin and susceptibility. *Physiological and Molecular Plant Pathology*.

Bregoli AM, Scaramagli S, Costa G*, et al.*, 2002. Peach (Prunus persica) fruit ripening: aminoethoxyvinylglycine (AVG) and exogenous polyamines affect ethylene emission and flesh firmness. *Physiologia Plantarum* **114**, 472-81.

Brkljacic J, Grotewold E, Scholl R*, et al.*, 2011. Brachypodium as a Model for the Grasses: Today and the Future. *Plant Physiology* **157**, 3-13.

Broekaert WF, Delauré SL, De Bolle MF, Cammue BP, 2006. The role of ethylene in host-pathogen interactions. *Annu. Rev. Phytopathol.* **44**, 393-416.

Brown NA, Antoniw J, Hammond-Kosack KE, 2012. The predicted secretome of the plant pathogenic fungus Fusarium graminearum: a refined comparative analysis. *Plos One* **7**, e33731.

Brown NA, Bass C, Baldwin TK*, et al.*, 2011. Characterisation of the Fusarium graminearum-wheat floral interaction. *Journal of pathogens*, 9 pages.

Brown NA, Evans J, Mead A, Hammond-Kosack KE, 2017. A spatial temporal analysis of the Fusarium graminearum transcriptome during symptomless and symptomatic wheat infection. *Molecular Plant Pathology*.

Brown NA, Urban M, Van De Meene AML, Hammond-Kosack KE, 2010. The infection biology of Fusarium graminearum: Defining the pathways of spikelet to spikelet colonisation in wheat ears. *Fungal Biology* **114**, 555-71.

Brown RG, Kawaide H, Yang YY, Rademacher W, Kamiya Y, 1997. Daminozide and prohexadione have similar modes of action as inhibitors of the late stages of gibberellin metabolism. *Physiologia Plantarum* **101**, 309-13.

Buerstmayr H, Ban T, Anderson JA, 2009. QTL mapping and marker-assisted selection for Fusarium head blight resistance in wheat: a review. *Plant Breeding* **128**, 1-26.

Buerstmayr M, Steiner B, Buerstmayr H, 2020. Breeding for Fusarium head blight resistance in wheat—Progress and challenges. *Plant Breeding* **139**, 429-54.

Buhrow LM, Cram D, Tulpan D, Foroud NA, Loewen MC, 2016. Exogenous Abscisic Acid and Gibberellic Acid Elicit Opposing Effects on Fusarium graminearum Infection in Wheat. *Phytopathology* **106**, 986-96.

Buhrow LM, Liu Z, Cram D*, et al.*, 2020. Wheat transcriptome profiling reveals abscisic and gibberellic acid treatments regulate early-stage phytohormone defense signaling, cell wall fortification, and metabolic switches following Fusarium graminearum-challenge. *bioRxiv*.

Burt C, Steed A, Gosman N*, et al.*, 2015. Mapping a Type 1 FHB resistance on chromosome 4AS of Triticum macha and deployment in combination with two Type 2 resistances. *Theoretical and Applied Genetics* **128**, 1725-38.

Cao HH, Zhang M, Zhao H*, et al.*, 2014. Deciphering the Mechanism of beta-Aminobutyric Acid-Induced Resistance in Wheat to the Grain Aphid, Sitobion avenae. *Plos One* **9**, e91768.

Caprette DR, 2006. Using a Counting Chamber. In. Experimental Biosciences, Rice University. ([Updated: 2012][Accessed: 2017].)

Casimiro I, Beeckman T, Graham N*, et al.*, 2003. Dissecting Arabidopsis lateral root development. *Trends in Plant Science* **8**, 165-71.

Caspi R, Billington R, Fulcher CA*, et al.*, 2017. The MetaCyc database of metabolic pathways and enzymes. *Nucleic acids research* **46**, D633-D9.

Cass CL, Peraldi A, Dowd PF*, et al.*, 2015. Effects of PHENYLALANINE AMMONIA LYASE (PAL) knockdown on cell wall composition, biomass digestibility, and biotic and abiotic stress responses in Brachypodium. *Journal of Experimental Botany* **66**, 4317-35.

Catlett NL, Lee B-N, Yoder O, Turgeon BG, 2003. Split-marker recombination for efficient targeted deletion of fungal genes. *Fungal Genetics Reports* **50**, 9-11.

Chagué V, Elad Y, Barakat R, Tudzynski P, Sharon A, 2002. Ethylene biosynthesis in Botrytis cinerea. *FEMS microbiology ecology* **40**, 143-9.

Chalutz E, Lieberman M, Sisler HD, 1977. Methionine-induced ethylene production by Penicillium digitatum. *Plant Physiology* **60**, 402-6.

Chanclud E, Kisiala A, Emery NRJ*, et al.*, 2016. Cytokinin production by the rice blast fungus is a pivotal requirement for full virulence. *PLoS pathogens* **12**, e1005457.

Chanclud E, Morel JB, 2016. Plant hormones: a fungal point of view. *Molecular Plant Pathology* **17**, 1289-97.

Chauhan B, 2008. *Principles of biochemistry and biophysics*. New Delhi, India: University Science Press, 369.

Chen C, Wang J, Luo Q, Yuan S, Zhou M, 2007. Characterization and fitness of carbendazim-resistant strains of Fusarium graminearum (wheat scab). *Pest Management Science* **63**, 1201-7.

Chen F, Wang M, Zheng Y, Luo J, Yang X, Wang X, 2010. Quantitative changes of plant defense enzymes and phytohormone in biocontrol of cucumber Fusarium wilt by Bacillus subtilis B579. *World Journal of Microbiology and Biotechnology* **26**, 675-84.

Chen G, Yan W, Liu Y*, et al.*, 2014a. The non-gibberellic acid-responsive semi-dwarfing gene uzu affects Fusarium crown rot resistance in barley. *Bmc Plant Biology* **14**, 1-8.

Chen K, Li GJ, Bressan RA, Song CP, Zhu JK, Zhao Y, 2020. Abscisic acid dynamics, signaling, and functions in plants. *Journal of Integrative Plant Biology* **62**, 25-54.

Chen L, Han J, Deng X*, et al.*, 2016. Expansion and stress responses of AP2/EREBP superfamily in Brachypodium Distachyon. *Scientific Reports* **6**, 21623.

Chen L, Zhang L, Li D, Wang F, Yu D, 2013a. WRKY8 transcription factor functions in the TMV-cg defense response by mediating both abscisic acid and ethylene signaling in Arabidopsis. *Proceedings of the National Academy of Sciences* **110**, E1963-E71.

Chen X, Steed A, Travella S, Keller B, Nicholson P, 2009. Fusarium graminearum exploits ethylene signalling to colonize dicotyledonous and monocotyledonous plants. *New Phytol* **182**, 975-83.

Chen Y-C, Holmes EC, Rajniak J*, et al.*, 2018. N-hydroxy-pipecolic acid is a mobile metabolite that induces systemic disease resistance in Arabidopsis. *Proceedings of the National Academy of Sciences* **115**, E4920-E9.

Chen Y, Shen H, Wang M, Li Q, He Z, 2013b. Salicyloyl-aspartate synthesized by the acetyl-amido synthetase GH3.5 is a potential activator of plant immunity in Arabidopsis. *Acta Biochimica et Biophysica Sinica* **45**, 827-36.

Chen Y, Zhou M-G, 2009. Characterization of Fusarium graminearum Isolates Resistant to Both Carbendazim and a New Fungicide JS399-19. *Phytopathology* **99**, 441-6.

Chen YC, Wong CL, Muzzi F, Vlaardingerbroek I, Kidd BN, Schenk PM, 2014b. Root defense analysis against Fusarium oxysporum reveals new regulators to confer resistance. *Scientific Reports* **4**, 5584.

Chen Z, Iyer S, Caplan A, Klessig DF, Fan B, 1997. Differential Accumulation of Salicylic Acid and Salicylic Acid-Sensitive Catalase in Different Rice Tissues. *Plant Physiology* **114**, 193-201.

Chochois V, Vogel JP, Watt M, 2012. Application of Brachypodium to the genetic improvement of wheat roots. *Journal of Experimental Botany* **63**, 3467-74.

Choi J, Choi D, Lee S, Ryu C-M, Hwang I, 2011. Cytokinins and plant immunity: old foes or new friends? *Trends in Plant Science* **16**, 388-94.

Choi J, Huh SU, Kojima M, Sakakibara H, Paek K-H, Hwang I, 2010. The Cytokinin-Activated Transcription Factor ARR2 Promotes Plant Immunity via TGA3/NPR1-Dependent Salicylic Acid Signaling in Arabidopsis. *Developmental Cell* **19**, 284-95.

Chowdappa P, Kumar SM, Lakshmi MJ, Upreti K, 2013. Growth stimulation and induction of systemic resistance in tomato against early and late blight by Bacillus subtilis OTPB1 or Trichoderma harzianum OTPB3. *Biological Control* **65**, 109-17.

Cohen R, Riov J, Lisker N, Katan J, 1986. Involvement of ethylene in herbicide-induced resistance to Fusarium oxysporum f. sp. melonis. *Phytopathology* **76**, 1281-5.

Cohen YR, 2002. β-Aminobutyric Acid-Induced Resistance Against Plant Pathogens. *Plant Disease* **86**, 448-57.

Colombo EM, Kunova A, Pizzatti C, Saracchi M, Cortesi P, Pasquali M, 2019. Selection of an endophytic Streptomyces sp. strain DEF09 from wheat roots as a biocontrol agent against Fusarium graminearum. *Frontiers in microbiology* **10**, 2356.

Conrath U, Beckers GJM, Flors V*, et al.*, 2006. Priming: Getting Ready for Battle. *Molecular Plant-Microbe Interactions* **19**, 1062-71.

Consortium TU, 2018. UniProt: a worldwide hub of protein knowledge. *Nucleic acids research* **47**, D506-D15.

Contreras-Cornejo HA, Macías-Rodríguez L, Beltrán-Peña E, Herrera-Estrella A, López-Bucio J, 2011. Trichoderma-induced plant immunity likely involves both hormonal-and camalexin-dependent mechanisms in Arabidopsis thaliana and confers resistance against necrotrophic fungi Botrytis cinerea. *Plant Signaling & Behavior* **6**, 1554-63.

Cook RJ, 2001. Management of wheat and barley root diseases in modern farming systems. *Australasian Plant Pathology* **30**, 119-26.

Covarelli L, Beccari G, Steed A, Nicholson P, 2012. Colonization of soft wheat following infection of the stem base by Fusarium culmorum and translocation of deoxynivalenol to the head. *Plant Pathology* **61**, 1121-9.

Creelman RA, Mullet JE, 1997. Biosynthesis and action of jasmonates in plants. *Annual Review of Plant Biology* **48**, 355-81.

Cristescu SM, De Martinis D, Te Lintel Hekkert S, Parker DH, Harren FJM, 2002. Ethylene Production by Botrytis cinerea In Vitro and in Tomatoes. *Applied and Environmental Microbiology* **68**, 5342-50.

Cristescu SM, Woltering EJ, Harren FJ, 2007. Real time monitoring of ethylene during fungal-plant interaction by laser-based photoacoustic spectroscopy. *MYCOLOGY SERIES* **25**, 27-43.

Cuomo CA, Güldener U, Xu J-R*, et al.*, 2007. The Fusarium graminearum Genome Reveals a Link Between Localized Polymorphism and Pathogen Specialization. *Science* **317**, 1400-2.

Cuthbert PA, Somers DJ, Brulé-Babel A, 2007. Mapping of Fhb2 on chromosome 6BS: a gene controlling Fusarium head blight field resistance in bread wheat (Triticum aestivum L.). *Theoretical and Applied Genetics* **114**, 429-37.

Cuthbert PA, Somers DJ, Thomas J, Cloutier S, Brulé-Babel A, 2006. Fine mapping Fhb1, a major gene controlling fusarium head blight resistance in bread wheat (Triticum aestivum L.). *Theoretical and Applied Genetics* **112**, 1465-72.

D'angelo DL, Bradley CA, Ames KA, Willyerd KT, Madden LV, Paul PA, 2014. Efficacy of Fungicide Applications During and After Anthesis Against Fusarium Head Blight and Deoxynivalenol in Soft Red Winter Wheat. *Plant Disease* **98**, 1387-97.

Daundasekera M, Joyce D, Aked J, Adikaram N, 2003. Ethylene production by Colletotrichum musae in vitro. *Physiological and Molecular Plant Pathology* **62**, 21-8.

Davies P, 2013. *Plant hormones: physiology, biochemistry and molecular biology.* Berlin/Heidelberg, Germany: Springer Science & Business Media. 1-12.

De Bruyne L, Höfte M, De Vleesschauwer D, 2014. Connecting growth and defense: the emerging roles of brassinosteroids and gibberellins in plant innate immunity. *Molecular Plant* **7**, 943-59.

De Jonge R, Van Esse HP, Kombrink A*, et al.*, 2010. Conserved fungal LysM effector Ecp6 prevents chitin-triggered immunity in plants. *Science* **329**, 953-5.

De Vleesschauwer D, Van Buyten E, Satoh K, *et al.*, 2012. Brassinosteroids antagonize gibberellin-and salicylate-mediated root immunity in rice. *Plant Physiology* **158**, 1833-46.

De Vleesschauwer D, Yang Y, Cruz CV, Höfte M, 2010. Abscisic acid-induced resistance against the brown spot pathogen Cochliobolus miyabeanus in rice involves MAP kinase-mediated repression of ethylene signaling. *Plant Physiology* **152**, 2036-52.

Dean R, Van Kan JaL, Pretorius ZA, *et al.*, 2012. The Top 10 fungal pathogens in molecular plant pathology. *Molecular Plant Pathology* **13**, 414-30.

Dempsey DMA, Klessig DF, 2012. SOS–too many signals for systemic acquired resistance? *Trends in Plant Science* **17**, 538-45.

Dempsey DMA, Vlot AC, Wildermuth MC, Klessig DF, 2011. Salicylic Acid biosynthesis and metabolism. *The arabidopsis book* **9**, e0156-e.

Desmond OJ, Edgar CI, Manners JM, Maclean DJ, Schenk PM, Kazan K, 2005. Methyl jasmonate induced gene expression in wheat delays symptom development by the crown rot pathogen Fusarium pseudograminearum. *Physiological and Molecular Plant Pathology* **67**, 171-9.

Deyoung BJ, Innes RW, 2006. Plant NBS-LRR proteins in pathogen sensing and host defense. *Nature immunology* **7**, 1243-9.

Dhokane D, Karre S, Kushalappa AC, Mccartney C, 2016. Integrated Metabolo-Transcriptomics Reveals Fusarium Head Blight Candidate Resistance Genes in Wheat QTL-Fhb2. *Plos One* **11**, e0155851.

DíAz J, Ten Have A, Van Kan JA, 2002. The role of ethylene and wound signaling in resistance of tomato to Botrytis cinerea. *Plant Physiology* **129**, 1341-51.

Dill-Macky R, Jones R, 2000. The effect of previous crop residues and tillage on Fusarium head blight of wheat. *Plant Disease* **84**, 71-6.

Ding L, Xu H, Yi H, *et al.*, 2011. Resistance to hemi-biotrophic F. graminearum infection is associated with coordinated and ordered expression of diverse defense signaling pathways. *Plos One* **6**, e19008-e.

Ding X, Cao Y, Huang L, *et al.*, 2008. Activation of the Indole-3-Acetic Acid–Amido Synthetase GH3-8 Suppresses Expansin Expression and Promotes Salicylate- and Jasmonate-Independent Basal Immunity in Rice. *The Plant Cell* **20**, 228-40.

Ding Y, Gardiner DM, Kazan K, 2020. Transcriptome analysis reveals infection strategies employed by Fusarium graminearum as a root pathogen. *bioRxiv*.

Ding Y, Sun T, Ao K*, et al.*, 2018. Opposite Roles of Salicylic Acid Receptors NPR1 and NPR3/NPR4 in Transcriptional Regulation of Plant Immunity. *Cell* **173**, 1454-67.e15.

Ding Y, Wei W, Wu W*, et al.*, 2013. Role of gibberellic acid in tomato defence against potato purple top phytoplasma infection. *Annals of applied biology* **162**, 191-9.

Djamei A, Schipper K, Rabe F*, et al.*, 2011. Metabolic priming by a secreted fungal effector. *Nature* **478**, 395-8.

Dmochowska-Boguta M, Nadolska-Orczyk A, Orczyk W, 2013. Roles of peroxidases and NADPH oxidases in the oxidative response of wheat (T riticum aestivum) to brown rust (P uccinia triticina) infection. *Plant Pathology* **62**, 993-1002.

Domingo C, Andrés F, Tharreau D, Iglesias DJ, Talón M, 2009. Constitutive expression of OsGH3. 1 reduces auxin content and enhances defense response and resistance to a fungal pathogen in rice. *Molecular Plant-Microbe Interactions* **22**, 201-10.

Dong T, Park Y, Hwang I, 2015. Abscisic acid: biosynthesis, inactivation, homoeostasis and signalling. *Essays in biochemistry* **58**, 29-48.

Doohan F, Brennan J, Cooke B, 2003. Influence of climatic factors on Fusarium species pathogenic to cereals. In. *Epidemiology of mycotoxin producing fungi.* Springer, 755-68.

Dörffling K, Petersen W, Sprecher E, Urbasch I, Hanssen H-P, 1984. Abscisic acid in phytopathogenic fungi of the genera Botrytis, Ceratocystis, Fusarium, and Rhizoctonia. *Zeitschrift für Naturforschung C* **39**, 683-4.

Draper J, Mur LaJ, Jenkins G*, et al.*, 2001. Brachypodium distachyon. A New Model System for Functional Genomics in Grasses. *Plant Physiology* **127**, 1539-55.

Dunlap JR, Kresovich S, Mcgee RE, 1986. The effect of salt concentration on auxin stability in culture media. *Plant Physiology* **81**, 934-6.

Dweba CC, Figlan S, Shimelis HA*, et al.*, 2017. Fusarium head blight of wheat: Pathogenesis and control strategies. *Crop Protection* **91**, 114-22.

Dyer RB, Plattner RD, Kendra DF, Brown DW, 2005. Fusarium graminearum TRI14 Is Required for High Virulence and DON Production on Wheat but Not for DON Synthesis in Vitro. *Journal of Agricultural and Food Chemistry* **53**, 9281-7.

Dzikowska A, Grzelak A, Gawlik J*, et al.*, 2015. KAEA (SUDPRO), a member of the ubiquitous KEOPS/EKC protein complex, regulates the arginine catabolic pathway and the expression of several other genes in Aspergillus nidulans. *Gene* **573**, 310-20.

Edwards SG, Pirgozliev SR, Hare MC, Jenkinson P, 2001. Quantification of trichothecene-producing Fusarium species in harvested grain by competitive PCR to determine efficacies

of fungicides against Fusarium head blight of winter wheat. *Appl Environ Microbiol* **67**, 1575-80.

Egamberdieva D, Jabborova D, Hashem A, 2015. Pseudomonas induces salinity tolerance in cotton (Gossypium hirsutum) and resistance to Fusarium root rot through the modulation of indole-3-acetic acid. *Saudi journal of biological sciences* **22**, 773-9.

Eisermann I, Motyka V, Kümmel S*, et al.*, 2020. CgIPT1 is required for synthesis of cis-zeatin cytokinins and contributes to stress tolerance and virulence in Colletotrichum graminicola. *Fungal Genetics and Biology* **143**, 103436.

Eng F, Marin JE, Zienkiewicz K, Gutiérrez-Rojas M, Favela-Torres E, Feussner I, 2021. Jasmonic acid biosynthesis by fungi: derivatives, first evidence on biochemical pathways and culture conditions for production. *PeerJ* **9**, e10873.

Engels WJ, Alting AC, Arntz MM*, et al.*, 2000. Partial purification and characterization of two aminotransferases from Lactococcus lactis subsp. cremoris B78 involved in the catabolism of methionine and branched-chain amino acids. *International dairy journal* **10**, 443-52.

Fao., 2020. FAO.FAOSTAT.Production.Crops. [Latest update: 22/10/2020][Accessed: 13/02/2021] In. [http://www.fao.org/faostat/en/#data/QC].

Ferrigo D, Raiola A, Causin R, 2016. Fusarium toxins in cereals: Occurrence, legislation, factors promoting the appearance and their management. *Molecules* **21**, 627.

Flors V, Ton J, Van Doorn R, Jakab G, García-Agustín P, Mauch-Mani B, 2008. Interplay between JA, SA and ABA signalling during basal and induced resistance against Pseudomonas syringae and Alternaria brassicicola. *The Plant Journal* **54**, 81-92.

Forlani G, Bertazzini M, Giberti S, 2014. Differential accumulation of gamma-aminobutyric acid in elicited cells of two rice cultivars showing contrasting sensitivity to the blast pathogen. *Plant Biology* **16**, 1127-32.

Foroud NA, Pordel R, Goyal RK*, et al.*, 2018. Chemical activation of the ethylene signalling pathway promotes Fusarium graminearum resistance in detached wheat heads. *Phytopathology*, 109: 796-803.

Franceschetti M, Maqbool A, Jiménez-Dalmaroni MJ, Pennington HG, Kamoun S, Banfield MJ, 2017. Effectors of filamentous plant pathogens: commonalities amid diversity. *Microbiol. Mol. Biol. Rev.* **81**, e00066-16.

Frandsen RJ, Nielsen NJ, Maolanon N*, et al.*, 2006. The biosynthetic pathway for aurofusarin in Fusarium graminearum reveals a close link between the naphthoquinones and naphthopyrones. *Molecular microbiology* **61**, 1069-80.

Friedrich L, Lawton K, Ruess W*, et al.*, 1996. A benzothiadiazole derivative induces systemic acquired resistance in tobacco. *The Plant Journal* **10**, 61-70.

Fu J, Liu H, Li Y*, et al.*, 2011. Manipulating broad-spectrum disease resistance by suppressing pathogen-induced auxin accumulation in rice. *Plant Physiology* **155**, 589-602.

Fukuda H, Fujii T, Ogawa T, 1986. Preparation of a Cell-free Ethylene-forming System from Penicillium digitatum. *Agricultural and Biological Chemistry* **50**, 977-81.

Fukuda H, Takahashi M, Fujii T, Tazaki M, Ogawa T, 1989. An NADH: Fe(III) EDTA oxidoreductase from Cryptococcus albidus: an enzyme involved in ethylene production in vivo? *FEMS Microbiology Letters* **60**, 107-11.

Fusconi A, 2014. Regulation of root morphogenesis in arbuscular mycorrhizae: what role do fungal exudates, phosphate, sugars and hormones play in lateral root formation? *Annals of Botany* **113**, 19-33.

Gardiner DM, Kazan K, Manners JM, 2009. Nutrient profiling reveals potent inducers of trichothecene biosynthesis in Fusarium graminearum. *Fungal Genetics and Biology* **46**, 604-13.

Gardiner DM, Kazan K, Praud S, Torney FJ, Rusu A, Manners JM, 2010. Early activation of wheat polyamine biosynthesis during Fusarium head blight implicates putrescine as an inducer of trichothecene mycotoxin production. *Bmc Plant Biology* **10**, 1-13.

Garvin DF, Porter H, Blankenheim ZJ, Chao S, Dill-Macky R, 2015. A spontaneous segmental deletion from chromosome arm 3DL enhances Fusarium head blight resistance in wheat. *Genome* **58**, 479-88.

Gatti M, Cambon F, Tassy C*, et al.*, 2019. The Brachypodium distachyon UGT Bradi5gUGT03300 confers type II fusarium head blight resistance in wheat. *Plant Pathology* **68**, 334-43.

Gautam P, Dill-Macky R, 2012. Impact of moisture, host genetics and Fusarium graminearum isolates on Fusarium head blight development and trichothecene accumulation in spring wheat. *Mycotoxin Res* **28**, 45-58.

Gauthier L, Bonnin-Verdal M-N, Marchegay G*, et al.*, 2016. Fungal biotransformation of chlorogenic and caffeic acids by Fusarium graminearum: new insights in the contribution of phenolic acids to resistance to deoxynivalenol accumulation in cereals. *International Journal of Food Microbiology* **221**, 61-8.

Gibson DG, Young L, Chuang R-Y, Venter JC, Hutchison Iii CA, Smith HO, 2009. Enzymatic assembly of DNA molecules up to several hundred kilobases. *Nature Methods* **6**, 343-5.

Glazebrook J, 2005. Contrasting mechanisms of defense against biotrophic and necrotrophic pathogens. *Annu. Rev. Phytopathol.* **43**, 205-27.

Goddard R, Peraldi A, Ridout C, Nicholson P, 2014. Enhanced Disease Resistance Caused by BRI1 Mutation Is Conserved Between Brachypodium distachyon and Barley (Hordeum vulgare). *Molecular Plant-Microbe Interactions* **27**, 1095-106.

Gomi K, Matsuoka M, 2003. Gibberellin signalling pathway. *Current Opinion in Plant Biology* **6**, 489-93.

Goodstein DM, Shu S, Howson R*, et al.*, 2012. Phytozome: a comparative platform for green plant genomics. *Nucleic acids research* **40**, D1178-D86.

Gordon CS, Rajagopalan N, Risseeuw EP*, et al.*, 2016. Characterization of Triticum aestivum Abscisic Acid Receptors and a Possible Role for These in Mediating Fusairum Head Blight Susceptibility in Wheat. *Plos One* **11**, e0164996.

Gordon SP, Contreras-Moreira B, Woods DP*, et al.*, 2017. Extensive gene content variation in the Brachypodium distachyon pan-genome correlates with population structure. *Nature Communications* **8**, 1-13.

Gosman N, Srinivasachary, Steed A, Chandler E, Thomsett M, Nicholson P, 2010. Evaluation of type I fusarium head blight resistance of wheat using non-deoxynivalenol-producing fungi. *Plant Pathology* **59**, 147-57.

Goswami RS, Kistler HC, 2004. Heading for disaster: Fusarium graminearum on cereal crops. *Molecular Plant Pathology* **5**, 515-25.

Gottwald S, Samans B, Luck S, Friedt W, 2012. Jasmonate and ethylene dependent defence gene expression and suppression of fungal virulence factors: two essential mechanisms of Fusarium head blight resistance in wheat? *Bmc Genomics* **13**, 1-22.

Großkinsky D, Edelsbrunner K, Pfeifhofer H, Van Der Graaff E, Roitsch T, 2013. Cis- and trans-zeatin differentially modulate plant immunity. *Plant Signaling & Behavior* **8**, e24798.

Großkinsky DK, Naseem M, Abdelmohsen UR*, et al.*, 2011. Cytokinins mediate resistance against Pseudomonas syringae in tobacco through increased antimicrobial phytoalexin synthesis independent of salicylic acid signaling. *Plant Physiology* **157**, 815-30.

Großkinsky DK, Tafner R, Moreno MV*, et al.*, 2016. Cytokinin production by Pseudomonas fluorescens G20-18 determines biocontrol activity against Pseudomonas syringae in Arabidopsis. *Scientific Reports* **6**, 1-11.

Grunewald W, Vanholme B, Pauwels L*, et al.*, 2009. Expression of the Arabidopsis jasmonate signalling repressor JAZ1/TIFY10A is stimulated by auxin. *EMBO reports* **10**, 923-8.

Guenther JC, Trail F, 2005. The development and differentiation of Gibberella zeae (anamorph: Fusarium graminearum) during colonization of wheat. *Mycologia* **97**, 229-37.

Gunupuru LR, Arunachalam C, Malla KB, *et al.*, 2018. A wheat cytochrome P450 enhances both resistance to deoxynivalenol and grain yield. *Plos One* **13**, e0204992.

Guo H, Ecker JR, 2004. The ethylene signaling pathway: new insights. *Current Opinion in Plant Biology* **7**, 40-9.

Guo J, Zhang X, Hou Y, *et al.*, 2015. High-density mapping of the major FHB resistance gene Fhb7 derived from Thinopyrum ponticum and its pyramiding with Fhb1 by marker-assisted selection. *Theoretical and Applied Genetics* **128**, 2301-16.

Gupta A, Hisano H, Hojo Y, *et al.*, 2017. Global profiling of phytohormone dynamics during combined drought and pathogen stress in Arabidopsis thaliana reveals ABA and JA as major regulators. *Scientific Reports* **7**, 1-13.

Gupta R, Pizarro L, Leibman-Markus M, Marash I, Bar M, 2020. Cytokinin response induces immunity and fungal pathogen resistance, and modulates trafficking of the PRR LeEIX2 in tomato. *Molecular Plant Pathology* **21**, 1287-306.

Guyon K, Balagué C, Roby D, Raffaele S, 2014. Secretome analysis reveals effector candidates associated with broad host range necrotrophy in the fungal plant pathogen Sclerotinia sclerotiorum. *Bmc Genomics* **15**, 1-18.

Häffner E, Konietzki S, Diederichsen E, 2015. Keeping control: The role of senescence and development in plant pathogenesis and defense. *Plants* **4**, 449-88.

Hagen G, Guilfoyle T, 2002. Auxin-responsive gene expression: genes, promoters and regulatory factors. *Plant Molecular Biology* **49**, 373-85.

Haidoulis JF, Nicholson P, 2020. Different effects of phytohormones on Fusarium head blight and Fusarium root rot resistance in Brachypodium distachyon. *Journal of Plant Interactions* **15**, 335-44.

Haidukowski M, Pascale M, Perrone G, Pancaldi D, Campagna C, Visconti A, 2005. Effect of fungicides on the development of Fusarium head blight, yield and deoxynivalenol accumulation in wheat inoculated under field conditions with Fusarium graminearum and Fusarium culmorum. *Journal of the Science of Food and Agriculture* **85**, 191-8.

Haidukowski M, Visconti A, Perrone G, *et al.*, 2012. Effect of prothioconazole-based fungicides on Fusarium head blight, grain yield and deoxynivalenol accumulation in wheat under field conditions. *Phytopathologia Mediterranea*, 236-46.

Hales B, Steed A, Giovannelli V, *et al.*, 2020. Type II Fusarium head blight susceptibility conferred by a region on wheat chromosome 4D. *Journal of Experimental Botany* **71**, 4703-14.

Hall TA. BioEdit: a user-friendly biological sequence alignment editor and analysis program for Windows 95/98/NT. *Proceedings of the Nucleic acids symposium series*, *1999*: [London]: Information Retrieval Ltd., c1979-c2000., 95-8.

Hamiduzzaman MM, Jakab G, Barnavon L, Neuhaus J-M, Mauch-Mani B, 2005. β-Aminobutyric acid-induced resistance against downy mildew in grapevine acts through the potentiation of callose formation and jasmonic acid signaling. *Molecular Plant-Microbe Interactions* **18**, 819-29.

Hao G, Naumann TA, Vaughan MM*, et al.*, 2019. Characterization of a Fusarium graminearum salicylate hydroxylase. *Frontiers in microbiology* **9**, 3219.

Hao QQ, Wang WQ, Han XL*, et al.*, 2018. Isochorismate-based salicylic acid biosynthesis confers basal resistance to Fusarium graminearum in barley. *Molecular Plant Pathology* **19**, 1995-2010.

Harris LJ, Balcerzak M, Johnston A, Schneiderman D, Ouellet T, 2016. Host-preferential Fusarium graminearum gene expression during infection of wheat, barley, and maize. *Fungal Biology* **120**, 111-23.

He XY, Singh PK, Dreisigacker S, Singh S, Lillemo M, Duveiller E, 2016. Dwarfing Genes Rht-B1b and Rht-D1b Are Associated with Both Type I FHB Susceptibility and Low Anther Extrusion in Two Bread Wheat Populations. *Plos One* **11**, e0162499.

Hedden P, Phillips AL, Rojas MC, Carrera E, Tudzynski B, 2001. Gibberellin Biosynthesis in Plants and Fungi: A Case of Convergent Evolution? *Journal of Plant Growth Regulation* **20**, 319-31.

Hedden P, Thomas SG, 2012. Gibberellin biosynthesis and its regulation. *Biochemical Journal* **444**, 11-25.

Hinsch J, Galuszka P, Tudzynski P, 2016. Functional characterization of the first filamentous fungal tRNA-isopentenyltransferase and its role in the virulence of Claviceps purpurea. *New Phytologist* **211**, 980-92.

Hinsch J, Vrabka J, Oeser B, Novák O, Galuszka P, Tudzynski P, 2015. De novo biosynthesis of cytokinins in the biotrophic fungus C laviceps purpurea. *Environmental Microbiology* **17**, 2935-51.

Hofstad AN, Nussbaumer T, Akhunov E*, et al.*, 2016. Examining the Transcriptional Response in Wheat Fhb1 Near-Isogenic Lines to Fusarium graminearum Infection and Deoxynivalenol Treatment. *Plant Genome* **9**, plantgenome2015.05.0032.

Hogg A, Johnston R, Dyer A, 2007. Applying real-time quantitative PCR to Fusarium crown rot of wheat. *Plant Disease* **91**, 1021-8.

Hong S-Y, Seo PJ, Yang M-S, Xiang F, Park C-M, 2008. Exploring valid reference genes for gene expression studies in Brachypodium distachyonby real-time PCR. *Bmc Plant Biology* **8**.

Hošek P, Kubeš M, Laňková M*, et al.*, 2012. Auxin transport at cellular level: new insights supported by mathematical modelling. *Journal of Experimental Botany* **63**, 3815-27.

Hottiger T, Boller T, 1991. Ethylene biosynthesis in Fusarium oxysporum f. sp. tulipae proceeds from glutamate/2-oxoglutarate and requires oxygen and ferrous ions in vivo. *Archives of Microbiology* **157**, 18-22.

Hou X, Lee LYC, Xia K, Yan Y, Yu H, 2010. DELLAs Modulate Jasmonate Signaling via Competitive Binding to JAZs. *Developmental Cell* **19**, 884-94.

Howe KL, Contreras-Moreira B, De Silva N*, et al.*, 2020. Ensembl Genomes 2020—enabling non-vertebrate genomic research. *Nucleic acids research* **48**, D689-D95.

Hu W, Gao Q, Hamada MS*, et al.*, 2014. Potential of Pseudomonas chlororaphis subsp. aurantiaca strain Pcho10 as a biocontrol agent against Fusarium graminearum. *Phytopathology* **104**, 1289-97.

Huang YD, Li L, Smith KP, Muehlbauer GJ, 2016. Differential transcriptomic responses to Fusarium graminearum infection in two barley quantitative trait loci associated with Fusarium head blight resistance. *Bmc Genomics* **17**, 1-16.

Hunter MC, Smith RG, Schipanski ME, Atwood LW, Mortensen DA, 2017. Agriculture in 2050: recalibrating targets for sustainable intensification. *Bioscience* **67**, 386-91.

Huot B, Yao J, Montgomery BL, He SY, 2014. Growth–defense tradeoffs in plants: a balancing act to optimize fitness. *Molecular Plant* **7**, 1267-87.

Hus K, Betekhtin A, Pinski A*, et al.*, 2020. A CRISPR/Cas9-based mutagenesis protocol for Brachypodium distachyon and its allopolyploid relative, Brachypodium hybridum. *Frontiers in Plant Science* **11**, 614.

Initiative IB, 2010. Genome sequencing and analysis of the model grass Brachypodium distachyon. *Nature* **463**, 763-8.

Inomata M, Hirai N, Yoshida R, Ohigashi H, 2004. The biosynthetic pathway to abscisic acid via ionylideneethane in the fungus Botrytis cinerea. *Phytochemistry* **65**, 2667-78.

Izquierdo-Bueno I, González-Rodríguez VE, Simon A*, et al.*, 2018. Biosynthesis of abscisic acid in fungi: identification of a sesquiterpene cyclase as the key enzyme in Botrytis cinerea. *Environmental Microbiology* **20**, 2469-82.

Jain M, Kaur N, Garg R, Thakur JK, Tyagi AK, Khurana JP, 2006a. Structure and expression analysis of early auxin-responsive Aux/IAA gene family in rice (Oryza sativa). *Functional & Integrative Genomics* **6**, 47-59.

Jain M, Kaur N, Tyagi AK, Khurana JP, 2005. The auxin-responsive GH3 gene family in rice (Oryza sativa). *Functional & Integrative Genomics* **6**, 36.

Jain M, Tyagi AK, Khurana JP, 2006b. Genome-wide analysis, evolutionary expansion, and expression of early auxin-responsive SAUR gene family in rice (Oryza sativa). *Genomics* **88**, 360-71.

Jakab G, Cottier V, Toquin V*, et al.*, 2001. β-Aminobutyric Acid-induced Resistance in Plants. *European Journal of Plant Pathology* **107**, 29-37.

Jakab G, Ton J, Flors V, Zimmerli L, Métraux J-P, Mauch-Mani B, 2005. Enhancing Arabidopsis salt and drought stress tolerance by chemical priming for its abscisic acid responses. *Plant Physiology* **139**, 267-74.

Jameson PE, 2000. Cytokinins and auxins in plant-pathogen interactions – An overview. *Plant Growth Regulation* **32**, 369-80.

Jansen C, Von Wettstein D, Schäfer W, Kogel K-H, Felk A, Maier FJ, 2005. Infection patterns in barley and wheat spikes inoculated with wild-type and trichodiene synthase gene disrupted Fusarium graminearum. *Proceedings of the National Academy of Sciences of the United States of America* **102**, 16892-7.

Jansen M, Slusarenko AJ, Schaffrath U, 2006. Competence of roots for race-specific resistance and the induction of acquired resistance against Magnaporthe oryzae. *Molecular Plant Pathology* **7**, 191-5.

Jashni MK, Dols IH, Iida Y*, et al.*, 2015. Synergistic action of a metalloprotease and a serine protease from Fusarium oxysporum f. sp. lycopersici cleaves chitin-binding tomato chitinases, reduces their antifungal activity, and enhances fungal virulence. *Molecular Plant-Microbe Interactions* **28**, 996-1008.

Jensen MK, Hagedorn PH, De Torres-Zabala M*, et al.*, 2008. Transcriptional regulation by an NAC (NAM–ATAF1, 2–CUC2) transcription factor attenuates ABA signalling for efficient basal defence towards Blumeria graminis f. sp. hordei in Arabidopsis. *The Plant Journal* **56**, 867-80.

Jia H, Cho S, Muehlbauer GJ, 2009. Transcriptome analysis of a wheat near-isogenic line pair carrying fusarium head blight–resistant and–susceptible alleles. *Molecular Plant-Microbe Interactions* **22**, 1366-78.

Jia H, Zhou J, Xue S*, et al.*, 2018. A journey to understand wheat Fusarium head blight resistance in the Chinese wheat landrace Wangshuibai. *The Crop Journal* **6**, 48-59.

Jiang C-J, Shimono M, Sugano S, *et al.*, 2013. Cytokinins act synergistically with salicylic acid to activate defense gene expression in rice. *Molecular Plant-Microbe Interactions* **26**, 287-96.

Jin X, Jie L, Wang S, Qi HJ, Li SW, 2018. Classifying wheat hyperspectral pixels of healthy heads and Fusarium head blight disease using a deep neural network in the wild field. *Remote Sensing* **10**, 395.

Jones JDG, Dangl JL, 2006. The plant immune system. *Nature* **444**, 323-9.

Ju C, Chang C, 2015. Mechanistic Insights in Ethylene Perception and Signal Transduction. *Plant Physiology* **169**, 85-95.

Kabbage M, Yarden O, Dickman MB, 2015. Pathogenic attributes of Sclerotinia sclerotiorum: switching from a biotrophic to necrotrophic lifestyle. *Plant Science* **233**, 53-60.

Kachroo P, Liu H, Kachroo A, 2020. Salicylic acid: transport and long-distance immune signaling. *Current Opinion in Virology* **42**, 53-7.

Kakei Y, Mochida K, Sakurai T, Yoshida T, Shinozaki K, Shimada Y, 2015. Transcriptome analysis of hormone-induced gene expression in Brachypodium distachyon. *Scientific Reports* **5**, 14476.

Kauppinen S, Christgau S, Kofod LV, Halkier T, Dörreich K, Dalbøge H, 1995. Molecular cloning and characterization of a rhamnogalacturonan acetylesterase from Aspergillus aculeatus. Synergism between rhamnogalacturonan degrading enzymes. *J Biol Chem* **270**, 27172-8.

Kazan K, Gardiner DM, Manners JM, 2012. On the trail of a cereal killer: recent advances in Fusarium graminearum pathogenomics and host resistance. *Mol Plant Pathol* **13**, 399-413.

Kazan K, Lyons R, 2014. Intervention of phytohormone pathways by pathogen effectors. *The Plant Cell* **26**, 2285-309.

Kazan K, Manners JM, 2009. Linking development to defense: auxin in plant–pathogen interactions. *Trends in Plant Science* **14**, 373-82.

Keller MD, Bergstrom GC, Shields EJ, 2014. The aerobiology of Fusarium graminearum. *Aerobiologia* **30**, 123-36.

Kellogg EA, 2015. Brachypodium distachyon as a Genetic Model System. *Annu Rev Genet* **49**, 1-20.

Kerk NM, Jiang K, Feldman LJ, 2000. Auxin Metabolism in the Root Apical Meristem. *Plant Physiology* **122**, 925-32.

Khan MR, Doohan FM, 2009. Bacterium-mediated control of Fusarium head blight disease of wheat and barley and associated mycotoxin contamination of grain. *Biological Control* **48**, 42-7.

Khan N, Schisler D, Boehm M, Lipps P, Slininger P, 2004. Field testing of antagonists of Fusarium head blight incited by Gibberella zeae. *Biological Control* **29**, 245-55.

Khripach V, Zhabinskii V, De Groot A, 2000. Twenty years of brassinosteroids: steroidal plant hormones warrant better crops for the XXI century. *Annals of Botany* **86**, 441-7.

Kibbe WA, 2007. OligoCalc: an online oligonucleotide properties calculator. *Nucleic acids research* **35**, W43-W6.

Kidd BN, Kadoo NY, Dombrecht B*, et al.*, 2011. Auxin Signaling and Transport Promote Susceptibility to the Root-Infecting Fungal Pathogen Fusarium oxysporum in Arabidopsis. *Molecular Plant-Microbe Interactions* **24**, 733-48.

Kieber JJ, Schaller GE, 2018. Cytokinin signaling in plant development. *Development* **145**, dev149344.

Kikot GE, Hours RA, Alconada TM, 2009. Contribution of cell wall degrading enzymes to pathogenesis of Fusarium graminearum: a review. *Journal of basic microbiology* **49**, 231-41.

Kim E-J, Russinova E, 2020. Brassinosteroid signalling. *Current Biology* **30**, R294-R8.

Kim H-K, Yun S-H, 2011. Evaluation of Potential Reference Genes for Quantitative RT-PCR Analysis in Fusarium graminearum under Different Culture Conditions. *The Plant Pathology Journal* **27**, 301-9.

Kim J-E, Han K-H, Jin J*, et al.*, 2005. Putative Polyketide Synthase and Laccase Genes for Biosynthesis of Aurofusarin in Gibberella zeae. *Applied and Environmental Microbiology* **71**, 1701-8.

Kim J-E, Jin J, Kim H, Kim J-C, Yun S-H, Lee Y-W, 2006. GIP2, a putative transcription factor that regulates the aurofusarin biosynthetic gene cluster in Gibberella zeae. *Applied and Environmental Microbiology* **72**, 1645-52.

Kim S, Chen J, Cheng T*, et al.*, 2021. PubChem in 2021: new data content and improved web interfaces. *Nucleic acids research* **49**, D1388-D95.

Kim T-W, Wang Z-Y, 2010. Brassinosteroid Signal Transduction from Receptor Kinases to Transcription Factors. *Annual Review of Plant Biology* **61**, 681-704.

Kimura M, Tokai T, O'donnell K, *et al.*, 2003. The trichothecene biosynthesis gene cluster of Fusarium graminearum F15 contains a limited number of essential pathway genes and expressed non-essential genes. *FEBS Letters* **539**, 105-10.

Kimura M, Tokai T, Takahashi-Ando N, Ohsato S, Fujimura M, 2007. Molecular and genetic studies of Fusarium trichothecene biosynthesis: pathways, genes, and evolution. *Bioscience, biotechnology, and biochemistry* **71**, 2105-23.

King R, Urban M, Hammond-Kosack MCU, Hassani-Pak K, Hammond-Kosack KE, 2015. The completed genome sequence of the pathogenic ascomycete fungus Fusarium graminearum. *Bmc Genomics* **16**, 1-21.

Kinnersley AM, Turano FJ, 2000. Gamma Aminobutyric Acid (GABA) and Plant Responses to Stress. *Critical Reviews in Plant Sciences* **19**, 479-509.

Klessig DF, Tian M, Choi HW, 2016. Multiple targets of salicylic acid and its derivatives in plants and animals. *Frontiers in Immunology* **7**, 206.

Knoester M, Pieterse CM, Bol JF, Van Loon LC, 1999. Systemic resistance in Arabidopsis induced by rhizobacteria requires ethylene-dependent signaling at the site of application. *Molecular Plant-Microbe Interactions* **12**, 720-7.

Koen E, Trapet P, Brule D, *et al.*, 2014. beta-Aminobutyric Acid (BABA)-Induced Resistance in Arabidopsis thaliana: Link with Iron Homeostasis. *Molecular Plant-Microbe Interactions* **27**, 1226-40.

Koo YM, Heo AY, Choi HW, 2020. Salicylic Acid as a Safe Plant Protector and Growth Regulator. *The Plant Pathology Journal* **36**, 1-10.

Kõressaar T, Lepamets M, Kaplinski L, Raime K, Andreson R, Remm M, 2018. Primer3_masker: integrating masking of template sequence with primer design software. *Bioinformatics* **34**, 1937-8.

Koressaar T, Remm M, 2007. Enhancements and modifications of primer design program Primer3. *Bioinformatics* **23**, 1289-91.

Korolev N, David DR, Elad Y, 2008. The role of phytohormones in basal resistance and Trichoderma-induced systemic resistance to Botrytis cinerea in Arabidopsis thaliana. *BioControl* **53**, 667-83.

Kouzai Y, Kimura M, Yamanaka Y, *et al.*, 2016. Expression profiling of marker genes responsive to the defence-associated phytohormones salicylic acid, jasmonic acid and ethylene in Brachypodium distachyon. *BMC Plant Biol* **16**, 1-11.

Kretzler B, Rodrigues Gabriel Sales C, Karady M, Carmo-Silva E, Dodd IC, 2020. Maintenance of Photosynthesis as Leaves Age Improves Whole Plant Water Use Efficiency in an Australian Wheat Cultivar. *Agronomy* **10**, 1102.

Kriss AB, Paul PA, Xu X*, et al.*, 2012. Quantification of the relationship between the environment and Fusarium head blight, Fusarium pathogen density, and mycotoxins in winter wheat in Europe. *European Journal of Plant Pathology* **133**, 975-93.

Kulkarni RD, Kelkar HS, Dean RA, 2003. An eight-cysteine-containing CFEM domain unique to a group of fungal membrane proteins. *Trends in biochemical sciences* **28**, 118-21.

Lagudah ES, Krattinger SG, 2019. A new player contributing to durable Fusarium resistance. *Nature genetics* **51**, 1070-1.

Laluk K, Mengiste T, 2010. Necrotroph attacks on plants: wanton destruction or covert extortion? *The Arabidopsis Book/American Society of Plant Biologists* **8**, e0136.

Langevin F, Eudes F, Comeau A, 2004. Effect of Trichothecenes Produced by Fusarium graminearum during Fusarium Head Blight Development in Six Cereal Species. *European Journal of Plant Pathology* **110**, 735-46.

Laplaze L, Benkova E, Casimiro I*, et al.*, 2007. Cytokinins act directly on lateral root founder cells to inhibit root initiation. *The Plant Cell* **19**, 3889-900.

Lee T, Han Y-K, Kim K-H, Yun S-H, Lee Y-W, 2002. Tri13 and Tri7 determine deoxynivalenol-and nivalenol-producing chemotypes of Gibberella zeae. *Applied and Environmental Microbiology* **68**, 2148-54.

Lefevere H, Bauters L, Gheysen G, 2020. Salicylic Acid Biosynthesis in Plants. *Frontiers in Plant Science* **11, 338**.

Lemmens M, Haim K, Lew H, Ruckenbauer P, 2004. The effect of nitrogen fertilization on Fusarium head blight development and deoxynivalenol contamination in wheat. *Journal of Phytopathology* **152**, 1-8.

Lemmens M, Scholz U, Berthiller F*, et al.*, 2005. The Ability to Detoxify the Mycotoxin Deoxynivalenol Colocalizes With a Major Quantitative Trait Locus for Fusarium Head Blight Resistance in Wheat. *Molecular Plant-Microbe Interactions* **18**, 1318-24.

Leon-Reyes A, Du Y, Koornneef A*, et al.*, 2010a. Ethylene Signaling Renders the Jasmonate Response of Arabidopsis Insensitive to Future Suppression by Salicylic Acid. *Molecular Plant-Microbe Interactions* **23**, 187-97.

Leon-Reyes A, Van Der Does D, De Lange ES*, et al.*, 2010b. Salicylate-mediated suppression of jasmonate-responsive gene expression in Arabidopsis is targeted downstream of the jasmonate biosynthesis pathway. *Planta* **232**, 1423-32.

Leontovyčová H, Trdá L, Dobrev PI*, et al.*, 2020. Auxin biosynthesis in the phytopathogenic fungus Leptosphaeria maculans is associated with enhanced transcription of indole-3-pyruvate decarboxylase LmIPDC2 and tryptophan aminotransferase LmTAM1. *Research in Microbiology* **171**, 174-84.

Lewandowski SM, Bushnell WR, Evans CK, 2006. Distribution of Mycelial Colonies and Lesions in Field-Grown Barley Inoculated with Fusarium graminearum. *Phytopathology* **96**, 567-81.

Lewis DR, Negi S, Sukumar P, Muday GK, 2011. Ethylene inhibits lateral root development, increases IAA transport and expression of PIN3 and PIN7 auxin efflux carriers. *Development* **138**, 3485-95.

Leyser HMO, 1998. Plant hormones. *Current Biology* **8**, R5-R7.

Li G, Yen Y, 2008. Jasmonate and ethylene signaling pathway may mediate Fusarium head blight resistance in wheat. *Crop Science* **48**, 1888-96.

Li G, Zhou J, Jia H*, et al.*, 2019. Mutation of a histidine-rich calcium-binding-protein gene in wheat confers resistance to Fusarium head blight. *Nature genetics* **51**, 1106-12.

Li H, Diao Y, Wang J, Chen C, Ni J, Zhou M, 2008. JS399-19, a new fungicide against wheat scab. *Crop Protection* **27**, 90-5.

Lin F, Kong Z, Zhu H*, et al.*, 2004. Mapping QTL associated with resistance to Fusarium head blight in the Nanda2419× Wangshuibai population. I. Type II resistance. *Theoretical and Applied Genetics* **109**, 1504-11.

Lin F, Xue S, Zhang Z*, et al.*, 2006. Mapping QTL associated with resistance to Fusarium head blight in the Nanda2419× Wangshuibai population. II: Type I resistance. *Theoretical and Applied Genetics* **112**, 528-35.

Liscum E, Reed J, 2002. Genetics of Aux/IAA and ARF action in plant growth and development. *Plant Molecular Biology* **49**, 387-400.

Liu C, Ogbonnaya FC, 2015. Resistance to F usarium crown rot in wheat and barley: a review. *Plant Breeding* **134**, 365-72.

Liu P-P, Von Dahl CC, Park S-W, Klessig DF, 2011. Interconnection between Methyl Salicylate and Lipid-Based Long-Distance Signaling during the Development of Systemic Acquired Resistance in Arabidopsis and Tobacco. *Plant Physiology* **155**, 1762-8.

Liu S, Zhang X, Pumphrey MO, Stack RW, Gill BS, Anderson JA, 2006. Complex microcolinearity among wheat, rice, and barley revealed by fine mapping of the genomic region harboring a major QTL for resistance to Fusarium head blight in wheat. *Functional & Integrative Genomics* **6**, 83-9.

Liu X, Han Q, Xu J, Wang J, Shi J, 2015. Acetohydroxyacid synthase FgIlv2 and FgIlv6 are involved in BCAA biosynthesis, mycelial and conidial morphogenesis, and full virulence in Fusarium graminearum. *Sci Rep* **5**, 16315.

Llorente F, Muskett P, Sánchez-Vallet A, *et al.*, 2008. Repression of the Auxin Response Pathway Increases Arabidopsis Susceptibility to Necrotrophic Fungi. *Molecular Plant* **1**, 496-509.

Lorenzo O, Chico JM, Sánchez-Serrano JJ, Solano R, 2004. JASMONATE-INSENSITIVE1 encodes a MYC transcription factor essential to discriminate between different jasmonate-regulated defense responses in Arabidopsis. *The Plant Cell* **16**, 1938-50.

Lorenzo O, Piqueras R, Sánchez-Serrano JJ, Solano R, 2003. ETHYLENE RESPONSE FACTOR1 Integrates Signals from Ethylene and Jasmonate Pathways in Plant Defense. *The Plant Cell* **15**, 165-78.

Lorenzo O, Solano R, 2005. Molecular players regulating the jasmonate signalling network. *Current Opinion in Plant Biology* **8**, 532-40.

Lu S, Faris JD, 2019. Fusarium graminearum KP4-like proteins possess root growth-inhibiting activity against wheat and potentially contribute to fungal virulence in seedling rot. *Fungal Genetics and Biology* **123**, 1-13.

Lucyshyn D, Busch BL, Abolmaali S, *et al.*, 2007. Cloning and characterization of the ribosomal protein L3 (RPL3) gene family from Triticum aestivum. *Molecular Genetics and Genomics* **277**, 507-17.

Luna E, Van Hulten M, Zhang Y, *et al.*, 2014. Plant perception of β-aminobutyric acid is mediated by an aspartyl-tRNA synthetase. *Nature chemical biology* **10**, 450-6.

Luo K, Rocheleau H, Qi PF, Zheng YL, Zhao HY, Ouellet T, 2016. Indole-3-acetic acid in Fusarium graminearum: Identification of biosynthetic pathways and characterization of physiological effects. *Fungal Biology* **120**, 1135-45.

Lyons R, Manners JM, Kazan K, 2013. Jasmonate biosynthesis and signaling in monocots: a comparative overview. *Plant Cell Reports* **32**, 815-27.

Lyons R, Stiller J, Powell J, Rusu A, Manners JM, Kazan K, 2015. Fusarium oxysporum triggers tissue-specific transcriptional reprogramming in Arabidopsis thaliana. *Plos One* **10**, e0121902.

Lysøe E, Seong K-Y, Kistler HC, 2011. The Transcriptome of Fusarium graminearum During the Infection of Wheat. *Molecular Plant-Microbe Interactions* **24**, 995-1000.

Ma H-X, Bai G-H, Gill BS, Hart LP, 2006. Deletion of a chromosome arm altered wheat resistance to Fusarium head blight and deoxynivalenol accumulation in Chinese Spring. *Plant Disease* **90**, 1545-9.

Ma J-H, Yao J-L, Cohen D, Morris B, 1998. Ethylene inhibitors enhance in vitro root formation from apple shoot cultures. *Plant Cell Reports* **17**, 211-4.

Ma J, Li H, Zhang C, *et al.*, 2010. Identification and validation of a major QTL conferring crown rot resistance in hexaploid wheat. *Theoretical and Applied Genetics* **120**, 1119-28.

Ma L-J, Geiser DM, Proctor RH, *et al.*, 2013. Fusarium pathogenomics. *Annual review of microbiology* **67**, 399-416.

Ma Z, Michailides TJ, 2005. Advances in understanding molecular mechanisms of fungicide resistance and molecular detection of resistant genotypes in phytopathogenic fungi. *Crop Protection* **24**, 853-63.

Madgwick JW, West JS, White RP, *et al.*, 2011. Impacts of climate change on wheat anthesis and fusarium ear blight in the UK. *European Journal of Plant Pathology* **130**, 117-31.

Maier FJ, Miedaner T, Hadeler B, *et al.*, 2006. Involvement of trichothecenes in fusarioses of wheat, barley and maize evaluated by gene disruption of the trichodiene synthase (Tri5) gene in three field isolates of different chemotype and virulence. *Molecular Plant Pathology* **7**, 449-61.

Makandar R, Essig JS, Schapaugh MA, Trick HN, Shah J, 2006. Genetically Engineered Resistance to Fusarium Head Blight in Wheat by Expression of Arabidopsis NPR1. *Molecular Plant-Microbe Interactions* **19**, 123-9.

Makandar R, Nalam V, Chaturvedi R, Jeannotte R, Sparks AA, Shah J, 2010. Involvement of Salicylate and Jasmonate Signaling Pathways in Arabidopsis Interaction with Fusarium graminearum. *Molecular Plant-Microbe Interactions* **23**, 861-70.

Makandar R, Nalam VJ, Lee H, Trick HN, Dong Y, Shah J, 2011. Salicylic Acid Regulates Basal Resistance to Fusarium Head Blight in Wheat. *Molecular Plant-Microbe Interactions* **25**, 431-9.

Malonek S, Rojas MC, Hedden P, Gaskin P, Hopkins P, Tudzynski B, 2004. The NADPH-cytochrome P450 reductase gene from Gibberella fujikuroi is essential for gibberellin biosynthesis. *J Biol Chem* **279**, 25075-84.

Malz S, Grell MN, Thrane C, *et al.*, 2005. Identification of a gene cluster responsible for the biosynthesis of aurofusarin in the Fusarium graminearum species complex. *Fungal Genetics and Biology* **42**, 420-33.

Mandal S, Mallick N, Mitra A, 2009. Salicylic acid-induced resistance to Fusarium oxysporum f. sp. lycopersici in tomato. *Plant Physiology and Biochemistry* **47**, 642-9.

Mandalà G, Tundo S, Francesconi S, *et al.*, 2019. Deoxynivalenol Detoxification in Transgenic Wheat Confers Resistance to Fusarium Head Blight and Crown Rot Diseases. *Molecular Plant-Microbe Interactions* **32**, 583-92.

Maor R, Haskin S, Levi-Kedmi H, Sharon A, 2004. In Planta Production of Indole-3-Acetic Acid by Colletotrichum gloeosporioides f. sp. aeschynomene. *Applied and Environmental Microbiology* **70**, 1852-4.

Marburger DA, Venkateshwaran M, Conley SP, Esker PD, Lauer JG, Ané JM, 2015. Crop rotation and management effect on Fusarium spp. populations. *Crop Science* **55**, 365-76.

Marcel S, Sawers R, Oakeley E, Angliker H, Paszkowski U, 2010. Tissue-adapted invasion strategies of the rice blast fungus Magnaporthe oryzae. *The Plant Cell* **22**, 3177-87.

Maria Menniti A, Pancaldi D, Maccaferri M, Casalini L, 2003. Effect of Fungicides on Fusarium Head Blight and Deoxynivalenol Content in Durum Wheat Grain. *European Journal of Plant Pathology* **109**, 109-15.

Márquez-López RE, Quintana-Escobar AO, Loyola-Vargas VM, 2019. Cytokinins, the Cinderella of plant growth regulators. *Phytochemistry Reviews* **18**, 1387-408.

Martínez-Medina A, Alguacil MDM, Pascual JA, Van Wees SC, 2014. Phytohormone profiles induced by Trichoderma isolates correspond with their biocontrol and plant growth-promoting activity on melon plants. *Journal of chemical ecology* **40**, 804-15.

Mary Wanjiru W, Zhensheng K, Buchenauer H, 2002. Importance of Cell Wall Degrading Enzymes Produced by Fusarium graminearum during Infection of Wheat Heads. *European Journal of Plant Pathology* **108**, 803-10.

Marzec M, 2016. Strigolactones as part of the plant defence system. *Trends in Plant Science* **21**, 900-3.

Mashiguchi K, Tanaka K, Sakai T*, et al.*, 2011. The main auxin biosynthesis pathway in Arabidopsis. *Proceedings of the National Academy of Sciences* **108**, 18512-7.

Masuda D, Ishida M, Yamaguchi K, Yamaguchi I, Kimura M, Nishiuchi T, 2007. Phytotoxic effects of trichothecenes on the growth and morphology of Arabidopsis thaliana. *Journal of Experimental Botany* **58**, 1617-26.

Mccormick SP, Stanley AM, Stover NA, Alexander NJ, 2011. Trichothecenes: from simple to complex mycotoxins. *Toxins* **3**, 802-14.

Mcgrann GR, Stavrinides A, Russell J*, et al.*, 2014. A trade off between mlo resistance to powdery mildew and increased susceptibility of barley to a newly important disease, Ramularia leaf spot. *Journal of Experimental Botany* **65**, 1025-37.

Mcgrath KC, Dombrecht B, Manners JM*, et al.*, 2005. Repressor-and activator-type ethylene response factors functioning in jasmonate signaling and disease resistance identified via a genome-wide screen of Arabidopsis transcription factor gene expression. *Plant Physiology* **139**, 949-59.

Mcmullen M, Bergstrom G, De Wolf E, *et al.*, 2012. A Unified Effort to Fight an Enemy of Wheat and Barley: Fusarium Head Blight. *Plant Disease* **96**, 1712-28.

Mcsteen P, 2010. Auxin and monocot development. *Cold Spring Harbor perspectives in biology* **2**, a001479.

Meesters C, Mönig T, Oeljeklaus J, *et al.*, 2014. A chemical inhibitor of jasmonate signaling targets JAR1 in Arabidopsis thaliana. *Nature chemical biology* **10**, 830.

Mergoum M, Hill J, Quick J, 1998. Evaluation of resistance of winter wheat to Fusarium acuminatum by inoculation of seedling roots with single, germinated macroconidia. *Plant Disease* **82**, 300-2.

Mesterházy Á, Bartók T, Lamper C, 2003. Influence of Wheat Cultivar, Species of Fusarium, and Isolate Aggressiveness on the Efficacy of Fungicides for Control of Fusarium Head Blight. *Plant Disease* **87**, 1107-15.

Miedaner T, 1997. Breeding wheat and rye for resistance to Fusarium diseases. *Plant Breeding* **116**, 201-20.

Moore T, Martineau B, Bostock RM, Lincoln JE, Gilchrist DG, 1999. Molecular and genetic characterization of ethylene involvement in mycotoxin-induced plant cell death. *Physiological and Molecular Plant Pathology* **54**, 73-85.

Morffy N, Strader LC, 2020. Old Town Roads: routes of auxin biosynthesis across kingdoms. *Current Opinion in Plant Biology* **55**, 21-7.

Mudge AM, Dill-Macky R, Dong Y, Gardiner DM, White RG, Manners JM, 2006. A role for the mycotoxin deoxynivalenol in stem colonisation during crown rot disease of wheat caused by Fusarium graminearum and Fusarium pseudograminearum. *Physiological and Molecular Plant Pathology* **69**, 73-85.

Müllenborn C, Steiner U, Ludwig M, Oerke E-C, 2008. Effect of fungicides on the complex of Fusarium species and saprophytic fungi colonizing wheat kernels. *European Journal of Plant Pathology* **120**, 157-66.

Müller A, Hillebrand H, Weiler E, 1998. Indole-3-acetic acid is synthesized from L-tryptophan in roots of Arabidopsis thaliana. *Planta* **206**, 362-9.

Murphy AM, Pryce-Jones E, Johnstone K, Ashby AM, 1997. Comparison of cytokinin productionin vitrobyPyrenopeziza brassicaewith other plant pathogens. *Physiological and Molecular Plant Pathology* **50**, 53-65.

Müssig C, Biesgen C, Lisso J, Uwer U, Weiler EW, Altmann T, 2000. A novel stress-inducible 12-oxophytodienoate reductase from Arabidopsis thaliana provides a potential link between brassinosteroid-action and jasmonic-acid synthesis. *Journal of Plant Physiology* **157**, 143-52.

Nagahama K, Ogawa T, Fujii T, Tazaki M, Goto M, Fukuda H, 1991. L-Arginine is essential for the formation in vitro of ethylene by an extract of Pseudomonas syringae. *Microbiology* **137**, 1641-6.

Nahar K, Kyndt T, Hause B, Höfte M, Gheysen G, 2012. Brassinosteroids Suppress Rice Defense Against Root-Knot Nematodes Through Antagonism With the Jasmonate Pathway. *Molecular Plant-Microbe Interactions* **26**, 106-15.

Nakashita H, Yasuda M, Nitta T*, et al.*, 2003. Brassinosteroid functions in a broad range of disease resistance in tobacco and rice. *The Plant Journal* **33**, 887-98.

Napoleão TA, Soares G, Vital CE*, et al.*, 2017. Methyl jasmonate and salicylic acid are able to modify cell wall but only salicylic acid alters biomass digestibility in the model grass Brachypodium distachyon. *Plant Science* **263**, 46-54.

Naseem M, Dandekar T, 2012. The role of auxin-cytokinin antagonism in plant-pathogen interactions. *PLoS pathogens* **8**, e1003026.

Naseem M, Philippi N, Hussain A, Wangorsch G, Ahmed N, Dandekar T, 2012. Integrated systems view on networking by hormones in Arabidopsis immunity reveals multiple crosstalk for cytokinin. *The Plant Cell* **24**, 1793-814.

Naumann TA, Wicklow DT, Price NP, 2011. Identification of a chitinase-modifying protein from Fusarium verticillioides truncation of a host resistance protein by a fungalysin metalloprotease. *Journal of Biological Chemistry* **286**, 35358-66.

Navarro L, Bari R, Achard P*, et al.*, 2008. DELLAs Control Plant Immune Responses by Modulating the Balance of Jasmonic Acid and Salicylic Acid Signaling. *Current Biology* **18**, 650-5.

Nemhauser JL, 2018. Back to basics: what is the function of an Aux/IAA in auxin response? *New Phytologist* **218**, 1295-7.

Nganje WE, Bangsund DA, Leistritz FL, Wilson WW, Tiapo NM, 2004. Regional economic impacts of Fusarium head blight in wheat and barley. *Review of Agricultural Economics* **26**, 332-47.

Nicholson P, Chandler E, Draeger R*, et al.*, 2003. Molecular tools to study epidemiology and toxicology of Fusarium head blight of cereals. *European Journal of Plant Pathology* **109**, 691-703.

Nicholson P, Simpson D, Weston G*, et al.*, 1998. Detection and quantification ofFusarium culmorumandFusarium graminearumin cereals using PCR assays. *Physiological and Molecular Plant Pathology* **53**, 17-37.

Nishiuchi T, Masuda D, Nakashita H, *et al.*, 2006. Fusarium phytotoxin trichothecenes have an elicitor-like activity in Arabidopsis thaliana, but the activity differed significantly among their molecular species. *Molecular Plant-Microbe Interactions* **19**, 512-20.

Nongpiur R, Soni P, Karan R, Singla-Pareek SL, Pareek A, 2012. Histidine kinases in plants: Cross talk between hormone and stress responses. *Plant Signaling & Behavior* **7**, 1230-7.

Okonechnikov K, Golosova O, Fursov M, Team U, 2012. Unipro UGENE: a unified bioinformatics toolkit. *Bioinformatics* **28**, 1166-7.

Oliveira MB, Junior ML, Grossi-De-Sá MF, Petrofeza S, 2015. Exogenous application of methyl jasmonate induces a defense response and resistance against Sclerotinia sclerotiorum in dry bean plants. *Journal of Plant Physiology* **182**, 13-22.

Oliveros J, 2018. An interactive tool for comparing lists with Venn's diagrams (2007–2015)[Accessed: 2018-2021]. In. [https://bioinfogp.cnb.csic.es/tools/venny/index.html]

Olivieri FP, Lobato MC, Altamiranda E, *et al.*, 2009. BABA effects on the behaviour of potato cultivars infected by Phytophthora infestans and Fusarium solani. *European Journal of Plant Pathology* **123**, 47-56.

Opanowicz M, Hands P, Betts D, *et al.*, 2011. Endosperm development in Brachypodium distachyon. *Journal of Experimental Botany* **62**, 735-48.

Osborne LE, Stein JM, 2007. Epidemiology of Fusarium head blight on small-grain cereals. *Int J Food Microbiol* **119**, 103-8.

Overvoorde P, Fukaki H, Beeckman T, 2010. Auxin control of root development. *Cold Spring Harbor perspectives in biology* **2**, a001537.

Pal KK, Mcspadden Gardener B, 2006. Biological Control of Plant Pathogens. *The Plant Health Instructor*.

Palazzini JM, Alberione E, Torres A, Donat C, Köhl J, Chulze S, 2016. Biological control of Fusarium graminearum sensu stricto, causal agent of Fusarium head blight of wheat, using formulated antagonists under field conditions in Argentina. *Biological Control* **94**, 56-61.

Palazzini JM, Ramirez ML, Torres AM, Chulze SN, 2007. Potential biocontrol agents for Fusarium head blight and deoxynivalenol production in wheat. *Crop Protection* **26**, 1702-10.

Pan YL, Liu ZY, Rocheleau H, *et al.*, 2018. Transcriptome dynamics associated with resistance and susceptibility against fusarium head blight in four wheat genotypes. *Bmc Genomics* **19**, 1-26.

Pariyar SR, Erginbas-Orakci G, Dadshani S, *et al.*, 2020. Dissecting the Genetic complexity of fusarium crown Rot Resistance in Wheat. *Scientific Reports* **10**, 1-13.

Park S-W, Kaimoyo E, Kumar D, Mosher S, Klessig DF, 2007. Methyl Salicylate Is a Critical Mobile Signal for Plant Systemic Acquired Resistance. *Science* **318**, 113-6.

Parker JE, Warrilow AG, Cools HJ, *et al.*, 2013. Prothioconazole and prothioconazole-desthio activities against Candida albicans sterol 14-α-demethylase. *Appl. Environ. Microbiol.* **79**, 1639-45.

Parker JE, Warrilow AG, Cools HJ, *et al.*, 2011. Mechanism of binding of prothioconazole to Mycosphaerella graminicola CYP51 differs from that of other azole antifungals. *Appl. Environ. Microbiol.* **77**, 1460-5.

Parry DW, Jenkinson P, Mcleod L, 1995. Fusarium ear blight (scab) in small grain cereals—a review. *Plant Pathology* **44**, 207-38.

Pasquet JC, Changenet V, Macadre C, *et al.*, 2016. A Brachypodium UDP-Glycosyltransferase Confers Root Tolerance to Deoxynivalenol and Resistance to Fusarium Infection. *Plant Physiol* **172**, 559-74.

Pasquet JC, Chaouch S, Macadre C, *et al.*, 2014. Differential gene expression and metabolomic analyses of Brachypodium distachyon infected by deoxynivalenol producing and non-producing strains of Fusarium graminearum. *Bmc Genomics* **15**, 1-17.

Paul PA, Lipps PE, Hershman DE, Mcmullen MP, Draper MA, Madden LV, 2008. Efficacy of Triazole-Based Fungicides for Fusarium Head Blight and Deoxynivalenol Control in Wheat: A Multivariate Meta-Analysis. *Phytopathology* **98**, 999-1011.

Paul PA, Mcmullen MP, Hershman DE, Madden LV, 2010. Meta-Analysis of the Effects of Triazole-Based Fungicides on Wheat Yield and Test Weight as Influenced by Fusarium Head Blight Intensity. *Phytopathology* **100**, 160-71.

Payros D, Alassane-Kpembi I, Pierron A, Loiseau N, Pinton P, Oswald IP, 2016. Toxicology of deoxynivalenol and its acetylated and modified forms. *Archives of toxicology* **90**, 2931-57.

Pažout J, Pažoutová S, 1989. Ethylene is synthesized by vegetative mycelium in surface cultures of Penicillium cyclopium Westling. *Canadian Journal of Microbiology* **35**, 384-7.

Pearce S, Huttly AK, Prosser IM, *et al.*, 2015. Heterologous expression and transcript analysis of gibberellin biosynthetic genes of grasses reveals novel functionality in the GA3ox family. *Bmc Plant Biology* **15**, 1-18.

Peraldi A, 2012. *Brachypodium distachyon as a genetic model pathosystem to study resistance against fungal pathogens of small grain cereals.*: (PhD thesis). University of East Anglia, Norwich, PhD thesis.

Peraldi A, Beccari G, Steed A, Nicholson P, 2011. Brachypodium distachyon: a new pathosystem to study Fusarium head blight and other Fusarium diseases of wheat. *Bmc Plant Biology* **11**, 1-14.

Petti C, Reiber K, Ali SS, Berney M, Doohan FM, 2012. Auxin as a player in the biocontrol of Fusarium head blight disease of barley and its potential as a disease control agent. *Bmc Plant Biology* **12**, 1-9.

Pieterse CM, Zamioudis C, Berendsen RL, Weller DM, Van Wees SC, Bakker PA, 2014. Induced systemic resistance by beneficial microbes. *Annual Review of Phytopathology* **52**, 347-75.

Pieterse CMJ, Does DVD, Zamioudis C, Leon-Reyes A, Wees SCMV, 2012. Hormonal Modulation of Plant Immunity. *Annual Review of Cell and Developmental Biology* **28**, 489-521.

Pogány M, Koehl J, Heiser I, Elstner EF, Barna B, 2004. Juvenility of tobacco induced by cytokinin gene introduction decreases susceptibility to Tobacco necrosis virus and confers tolerance to oxidative stress. *Physiological and Molecular Plant Pathology* **65**, 39-47.

Poppenberger B, Berthiller F, Lucyshyn D*, et al.*, 2003. Detoxification of the Fusarium mycotoxin deoxynivalenol by a UDP-glucosyltransferase from Arabidopsis thaliana. *Journal of Biological Chemistry* **278**, 47905-14.

Powell JJ, Carere J, Fitzgerald TL*, et al.*, 2017a. The Fusarium crown rot pathogen Fusarium pseudograminearum triggers a suite of transcriptional and metabolic changes in bread wheat (Triticum aestivum L.). *Annals of Botany* **119**, 853-67.

Powell JJ, Carere J, Sablok G*, et al.*, 2017b. Transcriptome analysis of Brachypodium during fungal pathogen infection reveals both shared and distinct defense responses with wheat. *Scientific Reports* **7**, 17212.

Pré M, Atallah M, Champion A, De Vos M, Pieterse CM, Memelink J, 2008. The AP2/ERF domain transcription factor ORA59 integrates jasmonic acid and ethylene signals in plant defense. *Plant Physiology* **147**, 1347-57.

Pritsch C, Muehlbauer GJ, Bushnell WR, Somers DA, Vance CP, 2000. Fungal Development and Induction of Defense Response Genes During Early Infection of Wheat Spikes by Fusarium graminearum. *Molecular Plant-Microbe Interactions* **13**, 159-69.

Qadir A, Hewett EW, Long PG, 1997. Ethylene production by Botrytis cinerea. *Postharvest Biology and Technology* **11**, 85-91.

Qadir A, Hewett EW, Long PG, Dilley DR, 2011. A non-ACC pathway for ethylene biosynthesis in Botrytis cinerea. *Postharvest Biology and Technology* **62**, 314-8.

Qi L, Pumphrey M, Friebe B, Chen P, Gill B, 2008. Molecular cytogenetic characterization of alien introgressions with gene Fhb3 for resistance to Fusarium head blight disease of wheat. *Theoretical and Applied Genetics* **117**, 1155-66.

Qi P-F, Balcerzak M, Rocheleau H*, et al.*, 2016. Jasmonic acid and abscisic acid play important roles in host–pathogen interaction between Fusarium graminearum and wheat during the early stages of fusarium head blight. *Physiological and Molecular Plant Pathology* **93**, 39-48.

Qi P-F, Johnston A, Balcerzak M*, et al.*, 2012. Effect of salicylic acid on Fusarium graminearum, the major causal agent of fusarium head blight in wheat. *Fungal Biology* **116**, 413-26.

Qi P-F, Zhang Y-Z, Liu C-H*, et al.*, 2019. Functional analysis of FgNahG clarifies the contribution of salicylic acid to wheat (Triticum aestivum) resistance against Fusarium head blight. *Toxins* **11**, 59.

Ramirez ML, Chulze S, Magan N, 2004. Impact of environmental factors and fungicides on growth and deoxinivalenol production by Fusarium graminearum isolates from Argentinian wheat. *Crop Protection* **23**, 117-25.

Rawat N, Pumphrey MO, Liu S*, et al.*, 2016. Wheat Fhb1 encodes a chimeric lectin with agglutinin domains and a pore-forming toxin-like domain conferring resistance to Fusarium head blight. *Nature genetics* **48**, 1576-80.

Reineke G, Heinze B, Schirawski J, Buettner H, Kahmann R, Basse CW, 2008. Indole-3-acetic acid (IAA) biosynthesis in the smut fungus Ustilago maydis and its relevance for increased IAA levels in infected tissue and host tumour formation. *Molecular Plant Pathology* **9**, 339-55.

Ren H, Gray WM, 2015. SAUR proteins as effectors of hormonal and environmental signals in plant growth. *Molecular Plant* **8**, 1153-64.

Reusche M, Klásková J, Thole K*, et al.*, 2013. Stabilization of cytokinin levels enhances Arabidopsis resistance against Verticillium longisporum. *Molecular Plant-Microbe Interactions* **26**, 850-60.

Robert-Seilaniantz A, Navarro L, Bari R, Jones JDG, 2007. Pathological hormone imbalances. *Current Opinion in Plant Biology* **10**, 372-9.

Robert-Seilaniantz A, Maclean D, Jikumaru Y*, et al.*, 2011. The microRNA miR393 re-directs secondary metabolite biosynthesis away from camalexin and towards glucosinolates. *The Plant Journal* **67**, 218-31.

Robinson M, Riov J, Sharon A, 1998. Indole-3-Acetic Acid Biosynthesis inColletotrichum gloeosporioides f. sp. aeschynomene. *Applied and Environmental Microbiology* **64**, 5030-2.

Robison M, Griffith M, Pauls K, Glick B, 2001. Dual role for ethylene in susceptibility of tomato to Verticillium wilt. *Journal of Phytopathology* **149**, 385-8.

Rodrigues-Pousada RA, De Rycke R, Dedonder A*, et al.*, 1993. The Arabidopsis 1-aminocyclopropane-1-carboxylate synthase gene 1 is expressed during early development. *The Plant Cell* **5**, 897-911.

Routledge AP, Shelley G, Smith JV, Talbot NJ, Draper J, Mur LA, 2004. Magnaporthe grisea interactions with the model grass Brachypodium distachyon closely resemble those with rice (Oryza sativa). *Molecular Plant Pathology* **5**, 253-65.

Ruijter J, Ramakers C, Hoogaars W*, et al.*, 2009. Amplification efficiency: linking baseline and bias in the analysis of quantitative PCR data. *Nucleic acids research* **37**, e45-e.

Salameh A, Buerstmayr M, Steiner B, Neumayer A, Lemmens M, Buerstmayr H, 2011. Effects of introgression of two QTL for fusarium head blight resistance from Asian spring wheat by marker-assisted backcrossing into European winter wheat on fusarium head blight resistance, yield and quality traits. *Molecular Breeding* **28**, 485-94.

Salgado JD, Madden LV, Paul PA, 2014. Efficacy and Economics of Integrating In-Field and Harvesting Strategies to Manage Fusarium Head Blight of Wheat. *Plant Disease* **98**, 1407-21.

Saltveit ME, 2005. Aminoethoxyvinylglycine (AVG) reduces ethylene and protein biosynthesis in excised discs of mature-green tomato pericarp tissue. *Postharvest Biology and Technology* **35**, 183-90.

Sardar P, Kempken F, 2018. Characterization of indole-3-pyruvic acid pathway-mediated biosynthesis of auxin in Neurospora crassa. *Plos One* **13**, e0192293.

Sauer M, Robert S, Kleine-Vehn J, 2013. Auxin: simply complicated. *Journal of Experimental Botany* **64**, 2565-77.

Savi GD, Piacentini KC, De Souza SR, Costa ME, Santos CM, Scussel VM, 2015. Efficacy of zinc compounds in controlling Fusarium head blight and deoxynivalenol formation in wheat (Triticum aestivum L.). *International Journal of Food Microbiology* **205**, 98-104.

Saville RJ, Gosman N, Burt CJ*, et al.*, 2012. The 'Green Revolution' dwarfing genes play a role in disease resistance in Triticum aestivum and Hordeum vulgare. *Journal of Experimental Botany* **63**, 1271-83.

Sayers EW, Beck J, Brister JR*, et al.*, 2020. Database resources of the national center for biotechnology information. *Nucleic acids research* **48**, D9.

Schaller A, Stintzi A, 2009. Enzymes in jasmonate biosynthesis–structure, function, regulation. *Phytochemistry* **70**, 1532-8.

Schaller GE, Binder BM, 2017. Inhibitors of ethylene biosynthesis and signaling. In. *Ethylene Signaling.* Springer, 223-35.

Schisler D, Khan N, Boehm MJ, Slininger P, 2002. Greenhouse and field evaluation of biological control of Fusarium head blight on durum wheat. *Plant Disease* **86**, 1350-6.

Schmale Iii DG, Bergstrom GC, 2003. Fusarium head blight in wheat. In. apsnet.org: The Plant Health Instructor. (Accessed 2016.)

Scholthof K-BG, Irigoyen S, Catalan P, Mandadi KK, 2018. Brachypodium: A Monocot Grass Model Genus for Plant Biology. *The Plant Cell* **30**, 1673-94.

Schroeder H, Christensen J, 1963. Factors affecting resistance of wheat to scab caused by Gibberella zeae. *Phytopathology* **53**, 831-8.

Schuster J, Knill T, Reichelt M, Gershenzon J, Binder S, 2006. Branched-chain aminotransferase4 is part of the chain elongation pathway in the biosynthesis of methionine-derived glucosinolates in Arabidopsis. *The Plant Cell* **18**, 2664-79.

Schwarzenbacher RE, Luna E, Ton J, 2014. The discovery of the BABA receptor: scientific implications and application potential. *Frontiers in Plant Science* **5**, 304.

Schwechheimer C, 2008. Understanding gibberellic acid signaling—are we there yet? *Current Opinion in Plant Biology* **11**, 9-15.

Schweiger W, Steiner B, Ametz C*, et al.*, 2013. Transcriptomic characterization of two major Fusarium resistance quantitative trait loci (QTLs), Fhb1 and Qfhs.ifa-5A, identifies novel candidate genes. *Molecular Plant Pathology* **14**, 772-85.

Segarra G, Casanova E, Bellido D, Odena MA, Oliveira E, Trillas I, 2007. Proteome, salicylic acid, and jasmonic acid changes in cucumber plants inoculated with Trichoderma asperellum strain T34. *Proteomics* **7**, 3943-52.

Seifi HS, Curvers K, De Vleesschauwer D, Delaere I, Aziz A, Höfte M, 2013. Concurrent overactivation of the cytosolic glutamine synthetase and the GABA shunt in the ABA-deficient sitiens mutant of tomato leads to resistance against Botrytis cinerea. *New Phytologist* **199**, 490-504.

Seo HS, Song JT, Cheong J-J*, et al.*, 2001. Jasmonic acid carboxyl methyltransferase: a key enzyme for jasmonate-regulated plant responses. *Proceedings of the National Academy of Sciences* **98**, 4788-93.

Shah DA, De Wolf ED, Paul PA, Madden LV, 2014. Predicting Fusarium Head Blight Epidemics with Boosted Regression Trees. *Phytopathology* **104**, 702-14.

Shah L, Ali A, Yahya M, *et al.*, 2018. Integrated control of fusarium head blight and deoxynivalenol mycotoxin in wheat. *Plant Pathology* **67**, 532-48.

Sharaf EF, Farrag AA, 2004. Induced resistance in tomato plants by IAA against Fusarium oxysporum lycopersici. *Polish Journal of Microbiology* **53**, 111-6.

Shelp BJ, Bown AW, Faure D, 2006. Extracellular γ-Aminobutyrate Mediates Communication between Plants and Other Organisms. *Plant Physiology* **142**, 1350-2.

Shelp BJ, Bown AW, Zarei A, 2017. 4-Aminobutyrate (GABA): a metabolite and signal with practical significance. *Botany* **95**, 1015-32.

Shinshi H, 2008. Ethylene-regulated transcription and crosstalk with jasmonic acid. *Plant Science* **175**, 18-23.

Shinshi H, Usami S, Ohme-Takagi M, 1995. Identification of an ethylene-responsive region in the promoter of a tobacco class I chitinase gene. *Plant Molecular Biology* **27**, 923-32.

Shoresh M, Yedidia I, Chet I, 2005. Involvement of jasmonic acid/ethylene signaling pathway in the systemic resistance induced in cucumber by Trichoderma asperellum T203. *Phytopathology* **95**, 76-84.

Siegrist J, Orober M, Buchenauer H, 2000. β-Aminobutyric acid-mediated enhancement of resistance in tobacco to tobacco mosaic virus depends on the accumulation of salicylic acid. *Physiological and Molecular Plant Pathology* **56**, 95-106.

Siemens J, Keller I, Sarx J, *et al.*, 2006. Transcriptome Analysis of Arabidopsis Clubroots Indicate a Key Role for Cytokinins in Disease Development. *Molecular Plant-Microbe Interactions* **19**, 480-94.

Siewers V, Kokkelink L, Smedsgaard J, Tudzynski P, 2006. Identification of an abscisic acid gene cluster in the grey mold Botrytis cinerea. *Applied and Environmental Microbiology* **72**, 4619-26.

Simpson DR, Weston GE, Turner JA, Jennings P, Nicholson P, 2001. Differential control of head blight pathogens of wheat by fungicides and consequences for mycotoxin contamination of grain. *European Journal of Plant Pathology* **107**, 421-31.

Singh P, Kuo Y-C, Mishra S, *et al.*, 2012. The Lectin Receptor Kinase-VI.2 Is Required for Priming and Positively Regulates Arabidopsis Pattern-Triggered Immunity. *The Plant Cell* **24**, 1256-70.

Solomon PS, Oliver RP, 2002. Evidence that γ-aminobutyric acid is a major nitrogen source during Cladosporium fulvum infection of tomato. *Planta* **214**, 414-20.

Song C-P, Agarwal M, Ohta M, *et al.*, 2005. Role of an Arabidopsis AP2/EREBP-type transcriptional repressor in abscisic acid and drought stress responses. *The Plant Cell* **17**, 2384-96.

Song W, Ma X, Tan H, Zhou J, 2011. Abscisic acid enhances resistance to Alternaria solani in tomato seedlings. *Plant Physiology and Biochemistry* **49**, 693-700.

Soni N, Hegde N, Dhariwal A, Kushalappa AC, 2020. Role of laccase gene in wheat NILs differing at QTL-Fhb1 for resistance against Fusarium head blight. *Plant Science* **298**, 110574.

Sorahinobar M, Niknam V, Ebrahimzadeh H, Soltanloo H, Behmanesh M, Enferadi ST, 2016. Central Role of Salicylic Acid in Resistance of Wheat Against Fusarium graminearum. *Journal of Plant Growth Regulation* **35**, 477-91.

Sørensen JL, Benfield AH, Wollenberg RD, *et al.*, 2018. The cereal pathogen Fusarium pseudograminearum produces a new class of active cytokinins during infection. *Molecular Plant Pathology* **19**, 1140-54.

Spence CA, Lakshmanan V, Donofrio N, Bais HP, 2015. Crucial roles of abscisic acid biogenesis in virulence of rice blast fungus Magnaporthe oryzae. *Frontiers in Plant Science* **6**, 1082.

Spoel SH, Dong X, 2008. Making Sense of Hormone Crosstalk during Plant Immune Responses. *Cell Host & Microbe* **3**, 348-51.

Spoel SH, Koornneef A, Claessens SMC, *et al.*, 2003. NPR1 Modulates Cross-Talk between Salicylate- and Jasmonate-Dependent Defense Pathways through a Novel Function in the Cytosol. *The Plant Cell* **15**, 760-70.

Spolti P, Del Ponte EM, Dong Y, Cummings JA, Bergstrom GC, 2013. Triazole Sensitivity in a Contemporary Population of Fusarium graminearum from New York Wheat and Competitiveness of a Tebuconazole-Resistant Isolate. *Plant Disease* **98**, 607-13.

Srinivasachary, Gosman N, Steed A, *et al.*, 2009. Semi-dwarfing Rht-B1 and Rht-D1 loci of wheat differ significantly in their influence on resistance to Fusarium head blight. *Theoretical and Applied Genetics* **118**, 695-702.

Srinivasachary, Gosman N, Steed A, *et al.*, 2008. Susceptibility to Fusarium head blight is associated with the Rht-D1b semi-dwarfing allele in wheat. *Theoretical and Applied Genetics* **116**, 1145-53.

Staswick PE, 2009. The tryptophan conjugates of jasmonic and indole-3-acetic acids are endogenous auxin inhibitors. *Plant Physiology* **150**, 1310-21.

Staswick PE, Serban B, Rowe M, *et al.*, 2005. Characterization of an Arabidopsis Enzyme Family That Conjugates Amino Acids to Indole-3-Acetic Acid. *The Plant Cell* **17**, 616-27.

Staswick PE, Tiryaki I, 2004. The oxylipin signal jasmonic acid is activated by an enzyme that conjugates it to isoleucine in Arabidopsis. *The Plant Cell* **16**, 2117-27.

Stephens AE, Gardiner DM, White RG, Munn AL, Manners JM, 2008. Phases of Infection and Gene Expression of Fusarium graminearum During Crown Rot Disease of Wheat. *Molecular Plant-Microbe Interactions* **21**, 1571-81.

Su P, Guo X, Fan Y*, et al.*, 2018. Application of Brachypodium genotypes to the analysis of type II resistance to Fusarium head blight (FHB). *Plant Sci* **272**, 255-66.

Su P, Zhao L, Li W*, et al.*, 2020. Integrated metabolo-transcriptomics and functional characterization reveals that the wheat auxin receptor TIR1 negatively regulates defense against Fusarium graminearum. *Journal of Integrative Plant Biology* **63**, 340-52.

Su Z, Bernardo A, Tian B*, et al.*, 2019. A deletion mutation in TaHRC confers Fhb1 resistance to Fusarium head blight in wheat. *Nature genetics* **51**, 1099-105.

Sugano S, Sugimoto T, Takatsuji H, Jiang CJ, 2013. Induction of resistance to P hytophthora sojae in soyabean (G lycine max) by salicylic acid and ethylene. *Plant Pathology* **62**, 1048-56.

Sun Y, Xiao J, Jia X*, et al.*, 2016. The role of wheat jasmonic acid and ethylene pathways in response to Fusarium graminearum infection. *Plant Growth Regulation* **80**, 69-77.

Sutton JC, 1982. Epidemiology of wheat head blight and maize ear rot caused by Fusarium graminearum. *Canadian Journal of Plant Pathology* **4**, 195-209.

Svoboda T, Parich A, Güldener U*, et al.*, 2019. Biochemical Characterization of the Fusarium graminearum Candidate ACC-Deaminases and Virulence Testing of Knockout Mutant Strains. *Frontiers in Plant Science* **10**, 1072.

Takemoto JY, Wegulo SN, Yuen GY*, et al.*, 2018. Suppression of wheat Fusarium head blight by novel amphiphilic aminoglycoside fungicide K20. *Fungal Biology* **122**, 465-70.

Tamaoki D, Seo S, Yamada S*, et al.*, 2013. Jasmonic acid and salicylic acid activate a common defense system in rice. *Plant Signaling & Behavior* **8**, e24260.

Tanaka N, Matsuoka M, Kitano H, Asano T, Kaku H, Komatsu S, 2006. gid1, a gibberellin-insensitive dwarf mutant, shows altered regulation of probenazole-inducible protein (PBZ1) in response to cold stress and pathogen attack. *Plant, cell & environment* **29**, 619-31.

Tang Q, Zhu F, Cao X, Zheng X, Yu T, Lu L, 2019. Cryptococcus laurentii controls gray mold of cherry tomato fruit via modulation of ethylene-associated immune responses. *Food Chemistry* **278**, 240-7.

Thevenet D, Pastor V, Baccelli I, *et al.*, 2017. The priming molecule beta-aminobutyric acid is naturally present in plants and is induced by stress. *New Phytologist* **213**, 552-9.

Thole V, Peraldi A, Worland B, Nicholson P, Doonan JH, Vain P, 2012. T-DNA mutagenesis in Brachypodium distachyon. *Journal of Experimental Botany* **63**, 567-76.

Thomma BP, Eggermont K, Broekaert WF, Cammue BP, 2000. Disease development of several fungi on Arabidopsis can be reduced by treatment with methyl jasmonate. *Plant Physiology and Biochemistry* **38**, 421-7.

Tian Y, Tan Y, Yan Z, *et al.*, 2018. Antagonistic and detoxification potentials of Trichoderma isolates for control of Zearalenone (ZEN) producing Fusarium graminearum. *Frontiers in microbiology* **8**, 2710.

Tiryaki I, Staswick PE, 2002. An Arabidopsis mutant defective in jasmonate response is allelic to the auxin-signaling mutant axr1. *Plant Physiology* **130**, 887-94.

To JP, Deruère J, Maxwell BB, *et al.*, 2007. Cytokinin regulates type-A Arabidopsis response regulator activity and protein stability via two-component phosphorelay. *The Plant Cell* **19**, 3901-14.

Ton J, Flors V, Mauch-Mani B, 2009. The multifaceted role of ABA in disease resistance. *Trends in Plant Science* **14**, 310-7.

Ton J, Jakab G, Toquin V, *et al.*, 2005. Dissecting the β-Aminobutyric Acid–Induced Priming Phenomenon in Arabidopsis. *The Plant Cell* **17**, 987-99.

Ton J, Mauch-Mani B, 2004. β-amino-butyric acid-induced resistance against necrotrophic pathogens is based on ABA-dependent priming for callose. *The Plant Journal* **38**, 119-30.

Trail F, 2009. For Blighted Waves of Grain: Fusarium graminearum in the Postgenomics Era. *Plant Physiology* **149**, 103-10.

Truman W, Bennett MH, Kubigsteltig I, Turnbull C, Grant M, 2007. Arabidopsis systemic immunity uses conserved defense signaling pathways and is mediated by jasmonates. *Proceedings of the National Academy of Sciences* **104**, 1075-80.

Trusov Y, Sewelam N, Rookes JE, *et al.*, 2009. Heterotrimeric G proteins-mediated resistance to necrotrophic pathogens includes mechanisms independent of salicylic acid-, jasmonic acid/ethylene- and abscisic acid-mediated defense signaling. *The Plant Journal* **58**, 69-81.

Tsai Y-C, Weir NR, Hill K, *et al.*, 2012. Characterization of genes involved in cytokinin signaling and metabolism from rice. *Plant Physiology* **158**, 1666-84.

Tsavkelova E, Oeser B, Oren-Young L*, et al.*, 2012. Identification and functional characterization of indole-3-acetamide-mediated IAA biosynthesis in plant-associated Fusarium species. *Fungal Genetics and Biology* **49**, 48-57.

Tudzynski B, 2005. Gibberellin biosynthesis in fungi: genes, enzymes, evolution, and impact on biotechnology. *Applied Microbiology and Biotechnology* **66**, 597-611.

Tupe SG, Chaudhary PM, Deshpande SR, Deshpande MV, 2014. Development of novel molecules for the control of plant pathogenic fungi in agriculture. In. *Microbial Diversity and Biotechnology in Food Security.* Springer, 315-25.

Tzeng DD, Devay JE, 1984. Ethylene production and toxigenicity of methionine and its derivatives with riboflavin in cultures of Verticillium, Fusarium and Colletotrichum species exposed to light. *Physiologia Plantarum* **62**, 545-52.

Untergasser A, Cutcutache I, Koressaar T*, et al.*, 2012. Primer3—new capabilities and interfaces. *Nucleic acids research* **40**, e115-e.

Urban M, Daniels S, Mott E, Hammond-Kosack K, 2002. Arabidopsis is susceptible to the cereal ear blight fungal pathogens Fusarium graminearum and Fusarium culmorum. *The Plant Journal* **32**, 961-73.

Van Butselaar T, Van Den Ackerveken G, 2020. Salicylic Acid Steers the Growth–Immunity Tradeoff. *Trends in Plant Science* **25**, 566-76.

Van De Poel B, Van Der Straeten D, 2014. 1-aminocyclopropane-1-carboxylic acid (ACC) in plants: more than just the precursor of ethylene! *Frontiers in Plant Science* **5**, 640.

Van Loon LC, Geraats BPJ, Linthorst HJM, 2006a. Ethylene as a modulator of disease resistance in plants. *Trends in Plant Science* **11**, 184-91.

Van Loon LC, Rep M, Pieterse CMJ, 2006b. Significance of Inducible Defense-related Proteins in Infected Plants. *Annual Review of Phytopathology* **44**, 135-62.

Van Staden J, Nicholson RID, 1989. Cytokinins and mango flower malformation II. The cytokinin complement produced by Fusarium moniliforme and the ability of the fungus to incorporate [8-14C]adenine into cytokinins. *Physiological and Molecular Plant Pathology* **35**, 423-31.

Verbeek RE, Van Buyten E, Alam MZ*, et al.*, 2019. Jasmonate-induced defense mechanisms in the belowground antagonistic interaction between Pythium arrhenomanes and Meloidogyne graminicola in rice. *Frontiers in Plant Science* **10**, 1515.

Verhage A, Van Wees SCM, Pieterse CMJ, 2010. Plant Immunity: It's the Hormones Talking, But What Do They Say? *Plant Physiology* **154**, 536-40.

Vlot AC, Dempsey DA, Klessig DF, 2009. Salicylic Acid, a multifaceted hormone to combat disease. *Annu Rev Phytopathol* **47**, 177-206.

Vogel JP, Garvin DF, Leong OM, Hayden DM, 2006. Agrobacterium-mediated transformation and inbred line development in the model grass Brachypodium distachyon. *Plant Cell, Tissue and Organ Culture* **84**, 199-211.

Voss-Fels KP, Qian L, Gabur I*, et al.*, 2018. Genetic insights into underground responses to Fusarium graminearum infection in wheat. *Scientific Reports* **8**, 1-10.

Waldron B, Moreno-Sevilla B, Anderson J, Stack R, Frohberg R, 1999. RFLP mapping of QTL for Fusarium head blight resistance in wheat. *Crop Science* **39**, 805-11.

Walters D, Heil M, 2007. Costs and trade-offs associated with induced resistance. *Physiological and Molecular Plant Pathology* **71**, 3-17.

Walters DR, Mcroberts N, 2006. Plants and biotrophs: a pivotal role for cytokinins? *Trends in Plant Science* **11**, 581-6.

Walton JD, 1994. Deconstructing the cell wall. *Plant Physiology* **104**, 1113-8.

Wang D, Pajerowska-Mukhtar K, Culler AH, Dong X, 2007. Salicylic Acid Inhibits Pathogen Growth in Plants through Repression of the Auxin Signaling Pathway. *Current Biology* **17**, 1784-90.

Wang H, Hwang S, Eudes F, Chang K, Howard R, Turnbull G, 2006. Trichothecenes and aggressiveness of Fusarium graminearum causing seedling blight and root rot in cereals. *Plant Pathology* **55**, 224-30.

Wang KL-C, Li H, Ecker JR, 2002. Ethylene biosynthesis and signaling networks. *The Plant Cell* **14**, S131-S51.

Wang L-Y, Xie Y-S, Cui Y-Y*, et al.*, 2015a. Conjunctively screening of biocontrol agents (BCAs) against fusarium root rot and fusarium head blight caused by Fusarium graminearum. *Microbiological Research* **177**, 34-42.

Wang L, Li Q, Liu Z*, et al.*, 2018a. Integrated transcriptome and hormone profiling highlight the role of multiple phytohormone pathways in wheat resistance against fusarium head blight. *Plos One* **13**, e0207036.

Wang Q, Chen D, Wu M*, et al.*, 2018b. MFS Transporters and GABA Metabolism Are Involved in the Self-Defense Against DON in Fusarium graminearum. *Frontiers in Plant Science* **9**, 438.

Wang Q, Shao B, Shaikh FI, Friedt W, Gottwald S, 2018c. Wheat Resistances to Fusarium Root Rot and Head Blight Are Both Associated with Deoxynivalenol- and Jasmonate-Related Gene Expression. *Phytopathology* **108**, 602-16.

Wang Q, Vera Buxa S, Furch A, Friedt W, Gottwald S, 2015b. Insights Into Triticum aestivum Seedling Root Rot Caused by Fusarium graminearum. *Molecular Plant-Microbe Interactions* **28**, 1288-303.

Wang Z, Gerstein M, Snyder M, 2009. RNA-Seq: a revolutionary tool for transcriptomics. *Nat Rev Genet* **10**, 57-63.

Wasternack C, Hause B, 2013. Jasmonates: biosynthesis, perception, signal transduction and action in plant stress response, growth and development. An update to the 2007 review in Annals of Botany. *Annals of Botany* **111**, 1021-58.

Wasternack C, Strnad M, 2016. Jasmonate signaling in plant stress responses and development - active and inactive compounds. *N Biotechnol* **33**, 604-13.

Watt M, Schneebeli K, Dong P, Wilson IW, 2009. The shoot and root growth of Brachypodium and its potential as a model for wheat and other cereal crops. *Functional Plant Biology* **36**, 960-9.

Wegulo SN, Zwingman MV, Breathnach JA, Baenziger PS, 2011. Economic returns from fungicide application to control foliar fungal diseases in winter wheat. *Crop Protection* **30**, 685-92.

West JS, Canning GG, Perryman SA, King K, 2017. Novel Technologies for the detection of Fusarium head blight disease and airborne inoculum. *Tropical Plant Pathology* **42**, 203-9.

Westphal KR, Wollenberg RD, Herbst F-A, Sørensen JL, Sondergaard TE, Wimmer R, 2018. Enhancing the production of the fungal pigment aurofusarin in Fusarium graminearum. *Toxins* **10**, 485.

Wilkes J, Dale G, Old K, 1989. Production of ethylene by Endothia gyrosa and Cytospora eucalypticola and its possible relationship to kino vein formation in Eucalyptus maculata. *Physiological and Molecular Plant Pathology* **34**, 171-80.

Woodward AW, Bartel B, 2005. Auxin: regulation, action, and interaction. *Annals of Botany* **95**, 707-35.

Wu C-C, Singh P, Chen M-C, Zimmerli L, 2010. L-Glutamine inhibits beta-aminobutyric acid-induced stress resistance and priming in Arabidopsis. *Journal of Experimental Botany* **61**, 995-1002.

Wybouw B, De Rybel B, 2019. Cytokinin–a developing story. *Trends in Plant Science* **24**, 177-85.

Xu D, Zhou J, Lou X, He J, Ran T, Wang W, 2017. Myroilysin Is a New Bacterial Member of the M12A Family of Metzincin Metallopeptidases and Is Activated by a Cysteine Switch Mechanism. *The Journal of biological chemistry* **292**, 5195-206.

Xu X-M, Nicholson P, Thomsett M*, et al.*, 2008a. Relationship between the fungal complex causing Fusarium head blight of wheat and environmental conditions. *Phytopathology* **98**, 69-78.

Xu X-M, Parry D, Nicholson P*, et al.*, 2008b. Within-field variability of Fusarium head blight pathogens and their associated mycotoxins. *European Journal of Plant Pathology* **120**, 21-34.

Xu X, Nicholson P, 2009. Community ecology of fungal pathogens causing wheat head blight. *Annual Review of Phytopathology* **47**, 83-103.

Xu XM, Monger W, Ritieni A, Nicholson P, 2007. Effect of temperature and duration of wetness during initial infection periods on disease development, fungal biomass and mycotoxin concentrations on wheat inoculated with single, or combinations of, Fusarium species. *Plant Pathology* **56**, 943-56.

Xue C, Park G, Choi W, Zheng L, Dean RA, Xu J-R, 2002. Two novel fungal virulence genes specifically expressed in appressoria of the rice blast fungus. *The Plant Cell* **14**, 2107-19.

Xue S, Li G, Jia H*, et al.*, 2010. Fine mapping Fhb4, a major QTL conditioning resistance to Fusarium infection in bread wheat (Triticum aestivum L.). *Theoretical and Applied Genetics* **121**, 147-56.

Xue S, Xu F, Tang M*, et al.*, 2011. Precise mapping Fhb5, a major QTL conditioning resistance to Fusarium infection in bread wheat (Triticum aestivum L.). *Theoretical and Applied Genetics* **123**, 1055-63.

Yamaguchi S, 2008. Gibberellin metabolism and its regulation. *Annu. Rev. Plant Biol.* **59**, 225-51.

Yang C, Lu X, Ma B, Chen S-Y, Zhang J-S, 2015. Ethylene signaling in rice and Arabidopsis: conserved and diverged aspects. *Molecular Plant* **8**, 495-505.

Yang D-L, Li Q, Deng Y-W*, et al.*, 2008. Altered disease development in the eui mutants and Eui overexpressors indicates that gibberellins negatively regulate rice basal disease resistance. *Molecular Plant* **1**, 528-37.

Yang J, Duan G, Li C*, et al.*, 2019. The Crosstalks Between Jasmonic Acid and Other Plant Hormone Signaling Highlight the Involvement of Jasmonic Acid as a Core Component in Plant Response to Biotic and Abiotic Stresses. *Frontiers in Plant Science* **10**, 1349.

Yasuda M, Ishikawa A, Jikumaru Y, *et al.*, 2008. Antagonistic Interaction between Systemic Acquired Resistance and the Abscisic Acid–Mediated Abiotic Stress Response in Arabidopsis. *The Plant Cell* **20**, 1678-92.

Yazaki J, Shimatani Z, Hashimoto A, *et al.*, 2004. Transcriptional profiling of genes responsive to abscisic acid and gibberellin in rice: phenotyping and comparative analysis between rice and Arabidopsis. *Physiological Genomics* **17**, 87-100.

Yin Y, Liu X, Li B, Ma Z, 2009. Characterization of Sterol Demethylation Inhibitor-Resistant Isolates of Fusarium asiaticum and F. graminearum Collected from Wheat in China. *Phytopathology* **99**, 487-97.

Yokota T, Ohnishi T, Shibata K, *et al.*, 2017. Occurrence of brassinosteroids in non-flowering land plants, liverwort, moss, lycophyte and fern. *Phytochemistry* **136**, 46-55.

Yoshida M, Nakajima T, Arai M, Suzuki F, Tomimura K, 2008. Effect of the Timing of Fungicide Application on Fusarium Head Blight and Mycotoxin Accumulation in Closed-Flowering Barley. *Plant Disease* **92**, 1164-70.

Yoshida M, Nakajima T, Tomimura K, Suzuki F, Arai M, Miyasaka A, 2012. Effect of the Timing of Fungicide Application on Fusarium Head Blight and Mycotoxin Contamination in Wheat. *Plant Disease* **96**, 845-51.

You J, Zhang L, Song B, Qi X, Chan Z, 2015. Systematic analysis and identification of stress-responsive genes of the NAC gene family in Brachypodium distachyon. *Plos One* **10**, e0122027.

Yu B, Gruber MY, Khachatourians GG, *et al.*, 2012. Arabidopsis cpSRP54 regulates carotenoid accumulation in Arabidopsis and Brassica napus. *Journal of Experimental Botany* **63**, 5189-202.

Yu C, Zeng L, Sheng K, *et al.*, 2014. γ-Aminobutyric acid induces resistance against Penicillium expansum by priming of defence responses in pear fruit. *Food Chemistry* **159**, 29-37.

Yu M-H, Zhao Z-Z, He J-X, 2018. Brassinosteroid signaling in plant–microbe interactions. *International Journal of Molecular Sciences* **19**, 4091.

Yvon M, Chambellon E, Bolotin A, Roudot-Algaron F, 2000. Characterization and Role of the Branched-Chain Aminotransferase (BcaT) Isolated from Lactococcus lactissubsp. cremoris NCDO 763. *Applied and Environmental Microbiology* **66**, 571-7.

Zamioudis C, Pieterse CMJ, 2011. Modulation of Host Immunity by Beneficial Microbes. *Molecular Plant-Microbe Interactions* **25**, 139-50.

Zeilinger S, Gupta VK, Dahms TE, *et al.*, 2016. Friends or foes? Emerging insights from fungal interactions with plants. *FEMS microbiology reviews* **40**, 182-207.

Zhang Y, Li X, 2019. Salicylic acid: biosynthesis, perception, and contributions to plant immunity. *Current Opinion in Plant Biology* **50**, 29-36.

Zhang Z, Li Q, Li Z*, et al.*, 2007. Dual regulation role of GH3. 5 in salicylic acid and auxin signaling during Arabidopsis-Pseudomonas syringae interaction. *Plant Physiology* **145**, 450-64.

Zhao Y, 2012. Auxin biosynthesis: a simple two-step pathway converts tryptophan to indole-3-acetic acid in plants. *Molecular Plant* **5**, 334-8.

Zhao Y, 2014. Auxin biosynthesis. *The Arabidopsis Book/American Society of Plant Biologists* **12**, e0173.

Zhao Y, Selvaraj JN, Xing F*, et al.*, 2014a. Antagonistic action of Bacillus subtilis strain SG6 on Fusarium graminearum. *Plos One* **9**, e92486.

Zhao Z, Liu H, Wang C, Xu J-R, 2014b. Erratum to: comparative analysis of fungal genomes reveals different plant cell wall degrading capacity in fungi. *Bmc Genomics* **15**, 1-15.

Zhou X, Wu X, Li T*, et al.*, 2018. Identification, characterization, and expression analysis of auxin response factor (ARF) gene family in Brachypodium distachyon. *Functional & Integrative Genomics* **18**, 709-24.

Zhu J-Y, Sae-Seaw J, Wang Z-Y, 2013. Brassinosteroid signalling. *Development* **140**, 1615-20.

Zhu P, Xu L, Zhang C, Toyoda H, Gan S-S, 2012. Ethylene produced by Botrytis cinerea can affect early fungal development and can be used as a marker for infection during storage of grapes. *Postharvest Biology and Technology* **66**, 23-9.

Zhu PK, Xu Z, Cui ZJ, Zhang ZB, Xu L, 2017. Ethylene production by Alternaria alternata and its association with virulence on inoculated grape berries. *Phytoparasitica* **45**, 273-9.

Zhu Z, An F, Feng Y*, et al.*, 2011. Derepression of ethylene-stabilized transcription factors (EIN3/EIL1) mediates jasmonate and ethylene signaling synergy in Arabidopsis. *Proceedings of the National Academy of Sciences* **108**, 12539-44.

Zimmerli L, Jakab C, Metraux JP, Mauch-Mani B, 2000. Potentiation of pathogen-specific defense mechanisms in Arabidopsis by beta-aminobutyric acid. *Proceedings of the National Academy of Sciences of the United States of America* **97**, 12920-5.

Appendix

Supplementary Figures
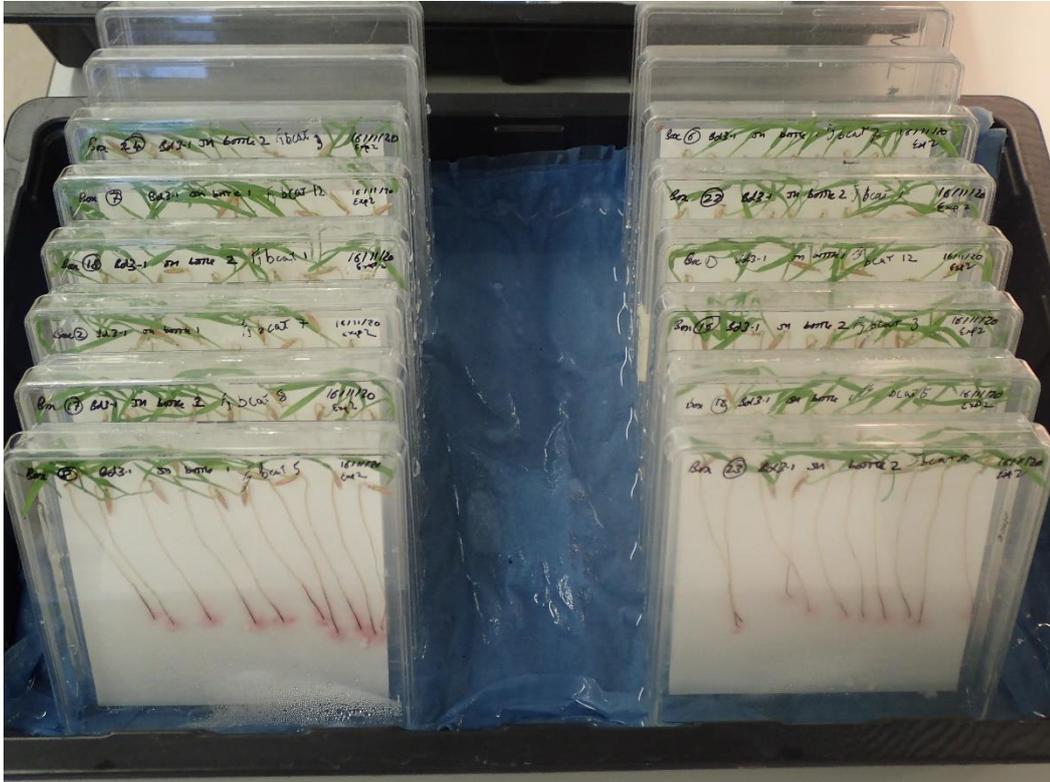
Supplementary Figure S1. Angled plates in a propagation tray for FRR assay. Note that there is usually a lid partially encasing the plates. Picture taken with an Olympus Stylus TG-4 camera.
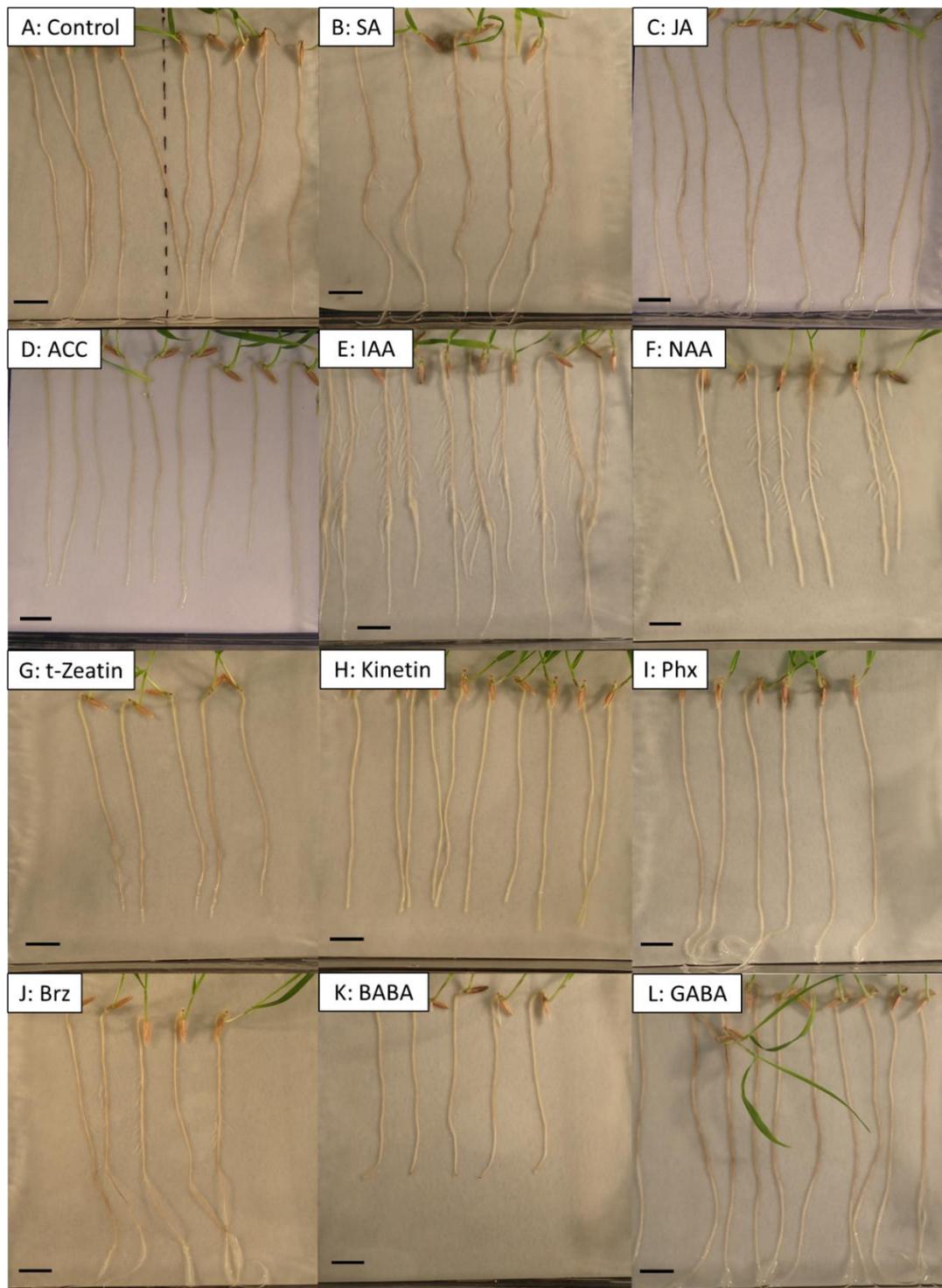
Supplementary Figure S2. The effect of phytohormones or phytohormone-associated compounds on Bd3-1 root growth at 6 dpa (or 7 dpi for SA) in the absence of *F. graminearum* inoculation (dpa denotes: since transferred to hormone amended media). Each image was obtained from different experiments. Only phytohormones shown to have a significant effect on FRR resistance (Chapter 2) are displayed. Concentrations are the same as their respective FRR trials (Table 2.1). Scale Bars = 1 cm.
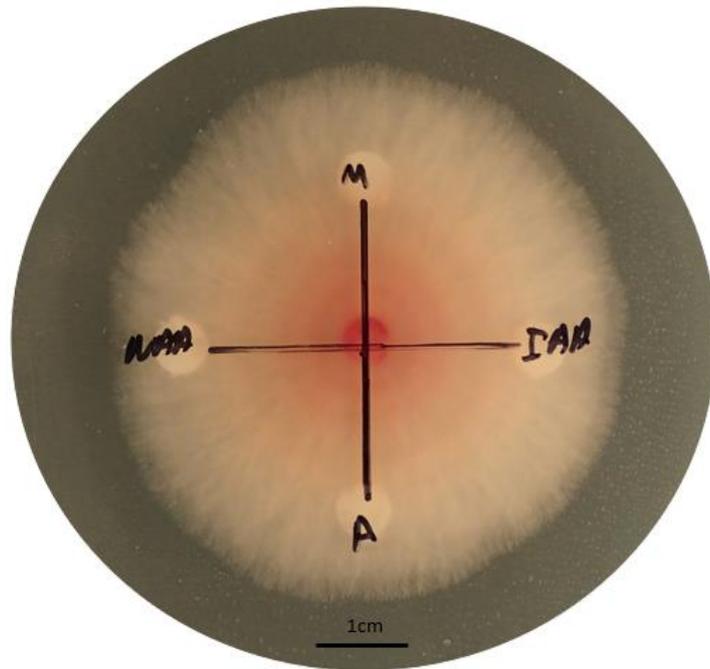
Supplementary Figure S3. *F. graminearum* PH1 mycelial growth on PDA with 8 mM Indole-3-acetic acid (IAA) and 1-Naphthaleneacetic acid (NAA) treated filter disks after 3 dpi. Image is one of three plates. The experiment was repeated twice. IAA (non-NA salt) was dissolved in Methanol (M) whereas NAA was dissolved in Acetone (A). Taken from (Haidoulis & Nicholson, 2020).
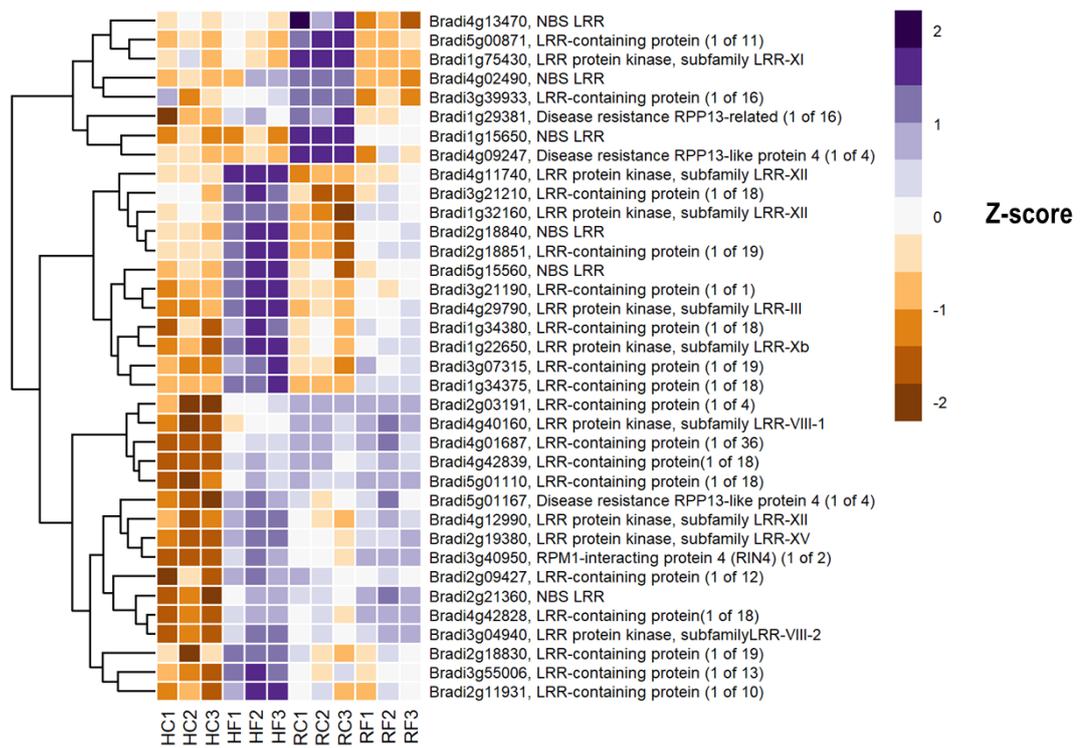
Supplementary Figure S4. The most upregulated or downregulated receptor-associated *B. distachyon* genes. These genes showed a log-fold change of -3 ≤ Log2 ≥ 3 with a p-adj < 0.05 in response to either FHB, FRR, or both. Three biological replicates for each of the four treatments are displayed as columns. Method in section 4.2. Abbreviations; HC (Head-FHB control), HF (Head-FHB fungus), RC (Root-FRR Control), RF (Root-FRR fungus).
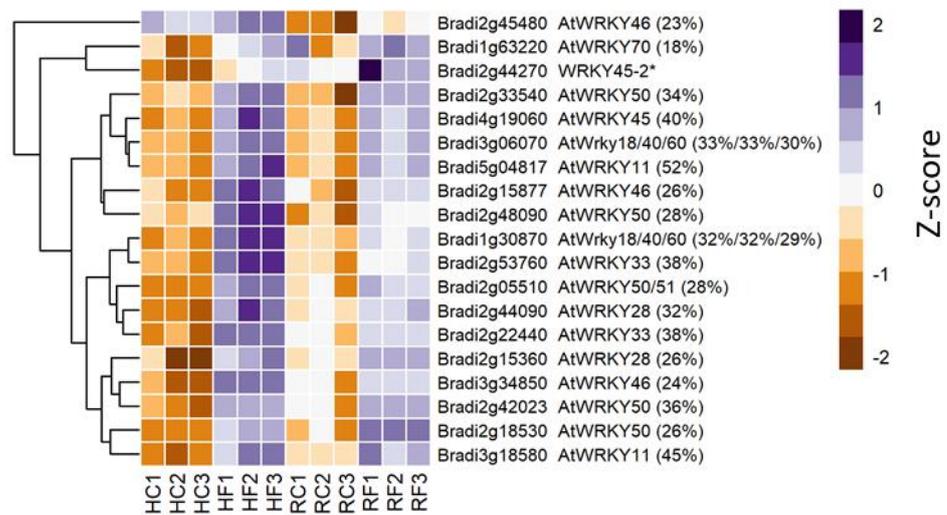
Supplementary Figure S5. The upregulated or downregulated predicted *BdWRKY* genes in response to FHB and FRR. These genes showed a log-fold change of -2 ≤ Log2 ≥ 2 with a p-adj < 0.05 in response to either FHB, FRR, or both. Three biological replicates for each of the four treatments are displayed as columns. * Derived from (Kouzai et al., 2016). All gene functions have a prefix (derived from *A. thaliana* (At)) and percentage homology (the percentage of *B. distachyon* sequence that matches the homologues sequence). Method in section 4.2. Column abbreviations; HC (Head-FHB control), HF (Head-FHB fungus), RC (Root-FRR Control), RF (Root-FRR fungus).
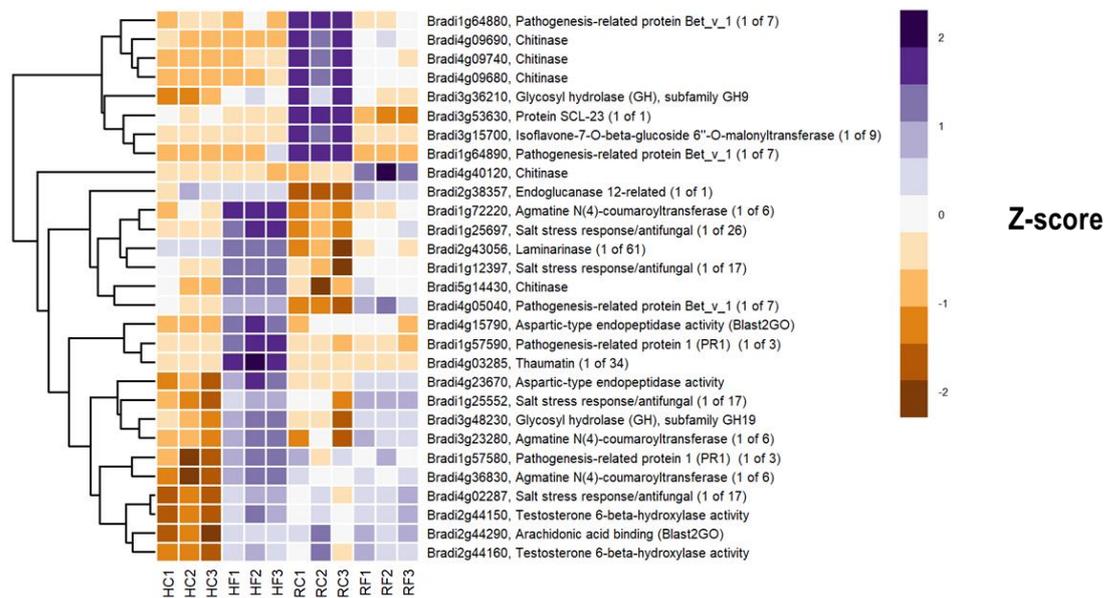
Supplementary Figure S6. The most upregulated or downregulated antimicrobial compound-related *B. distachyon* genes. These genes showed a log-fold change of -4 ≤ Log2 ≥ 4 with a p-adj < 0.05 in response to either FHB, FRR, or both. Method in section 4.2. Abbreviations; HC (Head-FHB control), HF (Head-FHB fungus), RC (Root-FRR Control), RF (Root-FRR fungus).
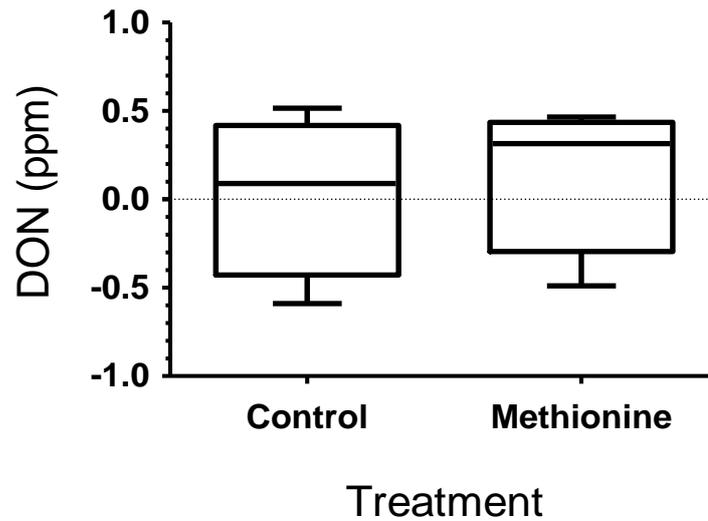
Supplementary Figure S7. No change in DON content in methionine treated CDL with *F. graminearum* after detection of ethylene presence. Undiluted CDL samples. Ridascreen Fast DON kit (R-Biopharm) used as per manufacturers guidelines. GLM ANOVA p = 0.656 between treatments with four technical replicates. This DON test was kindly performed by Dr Catherine Chinoy.

Supplementary Tables

Supplementary Table S1. Summary of other genes of interest responsive to methionine treatment from the RNA-seq analysis.

Gene ID	Predicted gene function*	Mean Control reads	Mean Methionine reads	Log-fold change	P-adj
FGRAMPH1_01G17303	ACC synthase	57.3	57	-0.02	.994
FGRAMPH1_01G25199	ACC Synthase	130.5	251.1	0.94	.782
FGRAMPH1_01G06417	ACC deaminase	130.7	202.1	0.63	.906
FGRAMPH1_01G16927	ACC deaminase	387.8	247.5	-0.65	NA
FGRAMPH1_01G13101	*FgTri8*	570.7	2088.7	1.87	.166
FGRAMPH1_01G13103	*FgTri7*	10.4	40.7	1.92	.658
FGRAMPH1_01G13105	*FgTri3**				
FGRAMPH1_01G13107	*FgTri4*	24.8	16.2	-0.63	NA
FGRAMPH1_01G13109	*FgTri6*	27.3	32.6	0.24	NA
FGRAMPH1_01G13111	*FgTri5*	7	29	2.03	.749
FGRAMPH1_01G13113	*FgTri10*	70.4	199.9	1.5	NA
FGRAMPH1_01G13115	*FgTri9*	14.8	14.7	-0.06	.988
FGRAMPH1_01G13117	*FgTri11*	3.6	17.2	2.12	.595
FGRAMPH1_01G13119	*FgTri12*	21.9	44.4	1	NA
FGRAMPH1_01G13121	*FgTri13*	30	110.5	1.88	NA
FGRAMPH1_01G13123	*FgTri14*	27.5	73.5	1.41	NA

*Gene functions for ACC were derived from (Svoboda et al., 2019), *Tri* gene function and where the function was derived from found in Table 4.4 **Gene was not listed in RNA-seq dataset.

Statistics Results

Supplementary Table S2. Accumulated analysis of variance for each plant hormone FRR experiment.

Hormone	Fig.	DPI	Transformation	N (C/I)	Factor	d.f	Mean deviance	Deviance ratio	Approx. F. Prob
SA	2.4A	3	-	61/77	Exp	1	6.52751	155.27	<.001
					Treatment	1	1.22348	29.1	<.001
					Exp.Treatment	1	0.74294	17.67	<.001
					Treatment.Rep	4	0.16581	3.94	0.005
					Exp.Treatment.Rep	4	0.26275	6.25	<.001
					Residual	126	0.04204		
	2.4A	5	-	61/77	Exp	1	2.59	9.94	.002
					Treatment	1	5.16	19.80	<.001
					Treatment.Rep	4	1.04	4.00	.004
					Residual	131	0.26		
	2.4A	7	SQRT	61/77	Exp	1	0.27	3.31	.071
					Treatment	1	1.19	14.73	<.001
					Treatment.Rep	4	0.15	1.91	.113
					Residual	131	0.08		
JA	2.4B	SD 1	-	78/73	Exp	1	20.60	31.66	<.001
					Treatment	1	11.90	18.29	<.001
					Treatment.Rep	4	0.95	1.47	.216
					Residual	144	0.65		
	2.4B	SD 2	-	78/73	Exp	1	36.22	22.62	<.001
					Treatment	1	32.38	20.22	<.001
					Treatment.Rep	4	3.29	2.05	.09
					Residual	144	1.60		

					Source	df			
	2.4B	SD 3	-	78/73	Exp	1	51.78	17.89	<.001
					Treatment	1	32.261	11.15	0.001
					Exp.Treatment	1	16.973	5.86	0.017
					Treatment.Rep	4	12.557	4.34	0.002
					Exp.Treatment.Rep	4	8.872	3.07	0.019
					Residual	139	2.894		
ACC	2.4C	SD1	SQRT	77/77	Exp	1	24.74	125.45	<.001
					Treatment	1	4.92	24.96	<.001
					Treatment.Rep	4	0.10	0.53	.713
					Residual	147	0.20		
	2.4C	SD2	-	77/77	Exp	1	153.33	76.32	<.001
					Treatment	1	20.43	10.17	.002
					Treatment.Rep	4	1.53	0.76	.551
					Residual	147	2.01		
	2.4C	SD3	-	48/47	Treatment	1	19.34	22.33	<.001
					Treatment.Rep	4	5.33	6.16	<.001
					Residual	89	0.87		
Brz	2.6B	2	SQRT	56/60	Exp	1	0.00	0.12	.735
					Treatment	1	0.02	1.11	.294
					Treatment.Rep	4	0.01	0.57	.684
					Residual	109	0.02		
	2.6B	4	-	56/60	Exp	1	0.04	0.67	.416
					Treatment	1	0.60	11.01	.001
					Treatment.Rep	4	0.08	1.51	.203
					Residual	109	0.05		
	2.6B	6	-	56/60	Exp	1	0.85	8.76	.004
					Treatment	1	2.98	30.83	<.001
					Treatment.Rep	4	0.13	1.31	.272
					Residual	109	0.10		
Phx	2.5B	2	-	59/59	Exp	1	0.39	24.86	<.001

					Source	df	MS	F	P
					Treatment	1	0.05	3.17	.078
					Treatment.Rep	4	0.01	0.73	.576
					Residual	111	0.02		
	2.5B	4	-	59/59	Exp	1	3.61	67.19	<.001
					Treatment	1	0.57	10.54	.002
					Treatment.Rep	4	0.01	0.17	.955
					Residual	111	0.05		
	2.5B	6	-	59/59	Exp	1	3.82	27.02	<.001
					Treatment	1	5.07	35.87	<.001
					Treatment.Rep	4	0.05	0.36	.833
					Residual	111	0.14		
tZ	2.9A	2	LOG10	89/88	Exp	2	0.13	2.85	.06
					Treatment	1	2.04	45.57	<.001
					Treatment.Rep	4	0.10	2.16	.076
					Residual	169	0.04		
	2.9A	4	SQRT	89/88	Exp	2	0.00	0.12	.885
					Treatment	1	2.95	126.79	<.001
					Treatment.Rep	4	0.02	0.92	.454
					Residual	169	0.02		
	2.9A	6	-	89/88	Exp	2	0.58	2.14	.12
					Treatment	1	33.06	123.03	<.001
					Treatment.Rep	4	0.11	0.41	.805
					Residual	169	0.27		
IAA	2.7A	2	SQRT	60/60	Exp	1	0.16864	12.75	<.001
					Treatment	1	1.50414	113.7	<.001
					Exp.Treatment	1	0.06101	4.61	0.034
					Treatment.Rep	4	0.01346	1.02	0.402
					Exp.Treatment.Rep	4	0.00974	0.74	0.569
					Residual	108	0.01323		
	2.7A	4	-	60/60	Exp	1	0.18096	2.1	0.15

					Treatment	1	8.26875	96.15	<.001
					Treatment.Rep	4	0.02751	0.32	0.864
					Residual	113	0.086		
	2.7A	6	SQRT	60/60	Exp	1	0.00256	0.04	0.833
					Treatment	1	3.28049	57.43	<.001
					Treatment.Rep	4	0.04124	0.72	0.579
					Residual	113	0.05712		
NAA	2.7B	2	-	59/60	Exp	1	0.15703	9.82	0.002
					Treatment	1	0.67162	42.02	<.001
					Exp.Treatment	1	0.081	5.07	0.026
					Treatment.Rep	4	0.01916	1.2	0.316
					Exp.Treatment.Rep	4	0.01454	0.91	0.461
					Residual	107	0.01598		
	2.7B	4	-	59/60	Exp	1	0.03	0.48	.491
					Treatment	1	1.84	32.53	<.001
					Treatment.Rep	4	0.08	1.41	.235
					Residual	112	0.06		
	2.7B	6	-	59/60	Exp	1	0.02	0.15	.7
					Treatment	1	3.32	21.51	<.001
					Treatment.Rep	4	0.08	0.54	.709
					Residual	112	0.15		
Kinetin	2.9B	2	SQRT	30/30	Treatment	1	0.00	0.08	.785
					Treatment.Rep	4	0.01	1.15	.342
					Residual	53	0.01		
	2.9B	4	SQRT	30/30	Treatment	1	0.28	10.38	.002
					Treatment.Rep	4	0.02	0.57	.686
					Residual	54	0.03		
	2.9B	6	-	30/30	Treatment	1	1.90	16.59	<.001
					Treatment.Rep	4	0.14	1.20	.323
					Residual	54	0.11		

GA	2.5A	3	-	28/28	Treatment	1	0.02	0.22	.641
					Treatment.Rep	4	0.14	1.33	.273
					Residual	50	0.11		
	2.5A	6	-	28/28	Treatment	1	0.22	0.26	.609
					Treatment.Rep	4	0.34	0.41	.799
					Residual	50	0.83		
	2.5A	9	-	28/28	Treatment	1	0.23	0.40	.53
					Treatment.Rep	4	0.31	0.52	.718
					Residual	50	0.58		
eBR	2.6A	3	SQRT	30/30	Treatment	1	0.01	0.31	.579
					Treatment.Rep	4	0.20	6.46	<.001
					Residual	54	0.03		
	2.6A	6	SQRT	30/30	Treatment	1	0.01	1.69	.199
					Treatment.Rep	4	0.02	3.11	.022
					Residual	54	0.01		
	2.6A	9	-	30/30	Treatment	1	0.15	0.38	.539
					Treatment.Rep	4	1.01	2.56	.048
					Residual	54	0.39		
BABA	2.11A	2	LOG10 (+0.25)	90/89	Exp	2	0.27595	4.7	0.01
					Treatment	1	0.32009	5.45	0.021
					Exp.Treatment	2	0.52218	8.89	<.001
					Treatment.Rep	4	0.13453	2.29	0.062
					Exp.Treatment.Rep	8	0.19416	3.3	0.002
					Residual	161	0.05876		
	2.11A	4	-	90/87	Exp	2	1.54	30.37	<.001
					Treatment	1	7.38	145.36	<.001
					Treatment.Rep	4	0.06	1.09	.365
					Residual	169	0.05		
	2.11A	6	-	90/87	Exp	2	4.49	26.59	<.001
					Treatment	1	21.58	127.69	<.001

					Treatment.Rep	4	0.34	2.01	.095
					Residual	169	0.17		
GABA	2.11B	2	-	60/60	Exp	1	1.35552	82.32	<.001
					Treatment	1	0.0002	0.01	0.912
					Exp.Treatment	1	0.21701	13.18	<.001
					Treatment.Rep	4	0.01043	0.63	0.64
					Exp.Treatment.Rep	2	0.01459	0.89	0.415
					Residual	110	0.01647		
	2.11B	4	-	60/60	Exp	1	5.60304	75.17	<.001
					Treatment	1	0.12352	1.66	0.201
					Exp.Treatment	1	0.50052	6.72	0.011
					Treatment.Rep	4	0.07432	1	0.412
					Exp.Treatment.Rep	4	0.03151	0.42	0.792
					Residual	108	0.07454		
	2.11B	6	-	60/60	Exp	1	6.2153	38.38	<.001
					Treatment	1	0.0745	0.46	0.499
					Exp.Treatment	1	1.0509	6.49	0.012
					Treatment.Rep	4	0.1688	1.04	0.389
					Exp.Treatment.Rep	4	0.0947	0.58	0.674
					Residual	108	0.1619		

'Treatment' is the no hormone versus hormone. 'Exp' is the experimental replicates, and 'SD' is the scoring date as opposed to the specific dpi. All ANOVA's are derived from GLM analysis with a normal identity and Link Function. Transformation denotes any what transformation was used on the Fungal length variate during GLM analysis. N (C/I) is the Number of biological replicates for control (C) and Infected (I) roots.

Supplementary Table S3. Accumulated analysis of variance results for each phytohormone tested on **FHB response in Bd3-1**.

Hormone	Fig	DPI	N (C/I)	Factor*	d.f	Mean deviance	Deviance ratio	Approx. F. Prob
SA 1**	3.4A	4	35/38	Treatment	1	2.36	2.36	0.125
				Treatment.Pot	14	1.588	1.59	0.074
				Treatment.Pot.Plant	15	2.238	2.24	0.004
				Residual	42	1.252		
	3.4A	8	35/38	Treatment	1	0.772	0.77	0.38
				Treatment.Pot	14	0.777	0.78	0.696
				Treatment.Pot.Plant	15	1.146	1.15	0.308
				Residual	41	1.667		
	3.4A	12	35/38	Treatment	1	0.623	0.62	0.43
				Treatment.Pot	14	0.833	0.83	0.633
				Treatment.Pot.Plant	15	1.557	1.56	0.077
				Residual	41	1.874		
SA 2**	3.4B	3	65/63	Treatment	1	1.228	1.23	0.268
				Treatment.Pot	13	2.564	2.56	0.002
				Treatment.Pot.Plant	11	3.183	3.18	< 0.001
				Residual	102	2.024		
	3.4B	5	65/63	Treatment	1	0.569	0.57	0.451
				Treatment.Pot	13	4.145	4.15	< 0.001
				Treatment.Pot.Plant	11	2.835	2.84	0.001
				Residual	101	2.616		
	3.4B	7	65/63	Treatment	1	1.063	1.06	0.303
				Treatment.Pot	13	4.219	4.22	< 0.001
				Treatment.Pot.Plant	11	2.723	2.72	0.002
				Residual	101	2.822		
JA	3.5A	SD 1	131/122	Exp	1	0.021	0.02	0.886
				Treatment	1	6.854	6.85	0.009

				Treatment.Pot	18	1.28	1.28	0.189
				Treatment.Pot.Plant	20	2.484	2.48	< 0.001
				Residual	212	1.28		
	3.5A	SD 2	130/122	Exp	1	4.48	4.48	0.034
				Treatment	1	15.073	15.07	< 0.001
				Treatment.Pot	18	1.188	1.19	0.261
				Treatment.Pot.Plant	20	2.327	2.33	< 0.001
				Residual	211	1.307		
	3.5A	SD 3	130/121	Exp	1	9.078	9.08	0.003
				Treatment	1	6.537	6.54	0.011
				Treatment.Pot	18	1.413	1.41	0.113
				Treatment.Pot.Plant	20	2.526	2.53	< 0.001
				Residual	210	1.426		
ACC	3.5B	3	176/184	Exp	1	15.549	15.55	< 0.001
				Treatment	1	4.887	4.89	0.027
				Treatment.Pot	18	4.324	4.32	< 0.001
				Treatment.Pot.Plant	20	2.295	2.3	< 0.001
				Residual	319	1.42		
	3.5B	7	176/184	Exp	1	17.305	17.3	< 0.001
				Treatment	1	8.781	8.78	0.003
				Treatment.Pot	18	4.401	4.4	< 0.001
				Treatment.Pot.Plant	20	1.25	1.25	0.201
				Residual	319	1.795		
	3.5B	11	176/184	Exp	1	26.116	26.12	< 0.001
				Treatment	1	2.668	2.67	0.102
				Exp.Treatment	1	7.481	7.48	0.006
				Treatment.Pot	18	4.44	4.44	< 0.001
				Exp.Treatmen.Pot	18	5.017		
				Treatment.Pot.Plant	20	2.569	5.02	< 0.001
				Exp.Treatment.Pot.Pl	14	2.341	2.57	0.003

				Residual	286	1.983	2.34	
BABA	3.6A	SD1	277/277	Exp	2	288.014	288.01	< 0.001
				Treatment	1	14.953	14.95	< 0.001
				Treatment.Pot	18	7.814	7.81	< 0.001
				Treatment.Pot.Plant	20	2.623	2.62	< 0.001
				Residual	512	1.624		
	3.6A	SD2	277/277	Exp	2	625.513	625.51	< 0.001
				Treatment	1	30.376	30.38	< 0.001
				Treatment.Pot	18	10.692	10.69	< 0.001
				Treatment.Pot.Plant	20	3.644	3.64	< 0.001
				Residual	512	2.005		
	3.6A	SD3	277/277	Exp	2	800.96	800.96	< 0.001
				Treatment	1	40.426	40.43	< 0.001
				Treatment.Pot	18	11.273	11.27	< 0.001
				Treatment.Pot.Plant	20	4.096	4.1	< 0.001
				Residual	512	2.363		
GABA	3.6B	4	103/94	Treatment	1	4.415	4.41	0.036
				Treatment.Pot	18	11.345	11.34	< 0.001
				Treatment.Pot.Plant	19	3.964	3.96	< 0.001
				Residual	158	2.189		
	3.6B	8	103/94	Treatment	1	0.342	0.34	0.558
				Treatment.Pot	18	10.097	10.1	< 0.001
				Treatment.Pot.Plant	19	3.485	3.48	< 0.001
				Residual	158	2.328		
	3.6B	12	103/94	Treatment	1	0.052	0.05	0.82
				Treatment.Pot	18	10.883	10.88	< 0.001
				Treatment.Pot.Plant	19	3.75	3.75	< 0.001
				Residual	158	2.504		
Tz	3.7	3	190/191	Exp	1	6.101	6.1	0.014
				Treatment	1	23.971	23.97	< 0.001

				Treatment.Pot	18	1.325	1.32	0.16
				Treatment.Pot.Plant	20	1.656	1.66	0.033
				Residual	340	1.459		
	3.7	7	190/191	Exp	1	27.27	27.27	< 0.001
				Treatment	1	20.274	20.27	< 0.001
				Exp.Treatment	1	6.793	6.79	0.009
				Treatment.Pot	18	1.845	1.85	0.016
				Exp.Treatmen.Pot	18	4.028	4.03	< 0.001
				Treatment.Pot.Plant	20	1.907	1.91	0.009
				Exp.Treatment.Pot.Pl	18	2.293	2.29	0.001
				Residual	303			
	3.7	11	190/191	Exp	1	20.851	20.85	< 0.001
				Treatment	1	20.328	20.33	< 0.001
				Exp.Treatment	1	9.309	9.31	0.002
				Treatment.Pot	18	1.734	1.73	0.027
				Exp.Treatmen.Pot	18	4.035	4.04	< 0.001
				Treatment.Pot.Plant	20	1.414	1.41	0.103
				Exp.Treatment.Pot.Pl	18	2.378	2.38	< 0.001
				Residual	303	1.988		
IAA 50 µm	3.8A	3	97/84	Treatment	1	0.425	0.43	0.514
				Treatment.Pot	18	4.558	4.56	< 0.001
				Treatment.Pot.Plant	17	2.352	2.35	0.001
				Residual	144	1.326		
	3.8A	7	97/84	Treatment	1	0.933	0.93	0.334
				Treatment.Pot	18	5.618	5.62	< 0.001
				Treatment.Pot.Plant	17	3.364	3.36	< 0.001
				Residual	144	1.579		
	3.8A	11	97/84	Treatment	1	0.18	0.18	0.671
				Treatment.Pot	18	5.248	5.25	< 0.001
				Treatment.Pot.Plant	17	3.981	3.98	< 0.001
				Residual	144	1.565		

NAA 5 µm	3.8B	3	55/49	Treatment	1	0.015	0.02	0.901
				Treatment.Pot	13	4.097	4.1	< 0.001
				Treatment.Pot.Plant	10	2.063	2.06	0.024
				Residual	79	1.529		
	3.8B	7	55/49	Treatment	1	1.68	1.68	0.195
				Treatment.Pot	13	3.362	3.36	< 0.001
				Treatment.Pot.Plant	10	1.914	1.91	0.038
				Residual	79	1.406		
	3.8B	11	55/49	Treatment	1	1.565	1.56	0.211
				Treatment.Pot	13	3.549	3.55	< 0.001
				Treatment.Pot.Plant	10	2.341	2.34	0.009
				Residual	79	1.789		

*'Treatment' is the no hormone versus hormone. 'Exp' is the experimental replicates, and 'SD' is the scoring date (Combined dpi). **SA 1 refers to first SA experiment with only one spray application. SA 2 refers to experiment 2 with 4 spray application of SA. All ANOVA tests are derived from GLM analysis Poisson distribution with a Log Link Function. The GLM fitted model for Bd3-1 was 'Experiment + Treatment / Pot / Plant against the response variate. N (C/I) is the Number of biological replicates for control (C) and Infected (I) florets.

Supplementary Table S4. Accumulated analysis of variance results for each phytohormone or phytohormone antagonist tested on **wheat FHB at BASF**.

Hormone	Fig**	Exp	N***	Transformation	DPI	Factor*	d.f	Mean deviance	Deviance ratio	Approx. F. Prob
SA	3.9A	1	58/59	Logit	7	Block	2	22.494	5.04	0.008
						Treatment	1	7.538	1.69	0.196
						Block.Treatment	2	4.765	1.07	0.347
						Residual	111	4.462		
	3.9A	1	58/61	Logit	15	Block	2	58.76	4.07	0.02
						Treatment	1	2.5	0.17	0.678
						Block.Treatment	2	56.37	3.91	0.023
						Residual	113	14.43		
IAA 50	3.9E	3	50/51	logit	7	Block	4	113.667	21.8	< 0.001
						Treatment	1	0.171	0.03	0.857
						Block.Treatment	4	5.644	1.08	0.37
						Residual	91	5.214		
	3.9E	3	51/51	-	10	Block	4	10793	14.57	< 0.001
						Treatment	1	72.3	0.1	0.755
						Block.Treatment	4	491.3	0.66	0.619
						Residual	92	740.8		
IAA 500	3.10A	1	58/60	SQRT	7	Block	2	70.234	12.42	< 0.001
						Treatment	1	0.842	0.15	0.7
						Block.Treatment	2	5.448	0.96	0.385
						Residual	112	5.657		
	3.10A	1	58/61	-	15	Block	2	16188	15.17	< 0.001
						Treatment	1	4	0	0.953
						Block.Treatment	2	44	0.04	0.96
						Residual	113	1067		

						Source	df			
NAA 500	3.10B	3	50/53	-	7	Block	4	16609.1	23.84	< 0.001
						Treatment	1	126.3	0.18	0.671
						Block.Treatment	4	348.9	0.5	0.735
						Residual	92	696.6		
	3.10B	3	51/50	-	10	Block	4	11944.1	18.38	< 0.001
						Treatment	1	0.7	0	0.974
						Block.Treatment	4	156.4	0.24	0.915
						Residual	91	649.9		
NAA 2	3.9F	4	50/49	SQRT	7	Block	4	19.538	9.02	< 0.001
						Treatment	1	17.142	7.92	0.006
						Block.Treatment	4	0.483	0.22	0.925
						Residual	89	2.165		
NAA 2	3.10C	5	50/46	SQRT	8	Block	4	69.454	17.5	< 0.001
						Treatment	1	0.209	0.05	0.819
						Block.Treatment	4	42.558	10.73	< 0.001
						Residual	86	3.968		
GA	3.9G	1	58/54	Logit	7	Block	2	6.082	1.62	0.202
						Treatment	1	7.736	2.07	0.154
						Block.Treatment	2	10.347	2.76	0.068
						Residual	106	3.744		
	3.9G	1	58/53	-	15	Block	2	5462	4.96	0.009
						Treatment	1	48	0.04	0.834
						Block.Treatment	2	4017	3.65	0.029
						Residual	105	1101		
BRZ	3.9H	2	54/54(20 µM)/48 (200 µM)	Logit	8	Block	4	21.568	4.59	0.002
						Treatment	2	19.152	4.08	0.019
						Block.Treatment	8	14.829	3.16	0.003
						Residual	141	4.698		
	3.9H	2	____	Logit	15	Block	4	27.553	3.46	0.01

	Fig		N	Transform	SD	Source	df			
			55/56(20 µM)/51(200 µM)			Treatment	2	24.233	3.04	0.051
						Block.Treatment	8	7.068	0.89	0.529
						Residual	147	7.97		
AVG 35 µm	3.9C	2+4	103/99	SQRT	7+8	Exp	1	49.673	10.37	0.002
						Block	4	18.772	3.92	0.004
						Treatment	1	0.883	0.18	0.668
						Block.Treatment	4	13.451	2.81	0.027
						Exp.Treatment	1	31.145	6.5	0.012
						Residual	190	4.791		
AVG 350 µm	3.9D	2	53/51	SQRT	8	Block	4	19.534	2.42	0.054
						Treatment	1	28.53	3.54	0.063
						Block.Treatment	4	10.862	1.35	0.259
						Residual	94	8.066		
	3.9D	2	52/53	Logit	15	Block	4	22.38	2.04	0.095
						Treatment	1	54.25	4.94	0.029
						Block.Treatment	4	11.56	1.05	0.385
						Residual	95	10.99		
AVG 175 µm	3.10D	4	50/51	SQRT	7	Block	4	12.675	7.22	< 0.001
						Treatment	1	64.274	36.59	< 0.001
						Block.Treatment	4	6.441	3.67	0.008
						Residual	90	1.757		
JARIN-1 300	3.9B	3+4	100/95	-	7	Exp	1	62734.8	146.32	< 0.001
						Block	4	9910.4	23.11	< 0.001
						Treatment	1	35.7	0.08	0.773
						Block.Treatment	4	919	2.14	0.077
						Exp.Treatment	1	278.8	0.65	0.421
						Residual	183	428.8		

*'Treatment' is the no hormone versus hormone, 'Exp' is the experimental replicates, and 'SD' is the scoring date (Combined dpi), 'Block' refers to the RCBD experimental design. ** 'Fig' denotes the figure the test applies to. ***N refers to the number of biological reps for control solvent/compound. Experiment

column refers to the trial the compound was tested in (some hormones were tested in the same experiment). All ANOVA tests are derived from GLM analysis normal distribution with a normal Link Function. The GLM model 'Experiment + Block * Treatment + Exp * Treatment' or 'Block * Treatment' depending on if experimental replicates were present. The symbol '-' denotes no transformation was applied to the data.

Supplementary Table S5. Accumulated analysis of variance for each phytohormone tested on **B. distachyon** FHB at BASF.

Hormone	Fig.	Experiment	DPI	Factor*	d.f	Mean deviance	Deviance ratio	Approx. F. Prob
Auxins	3.8C	8	8	Block	7	11.225	11.23	< 0.001
				Treatment	4	6.536	6.54	< 0.001
				Block.Treatment	28	7.202	7.2	< 0.001
				Residual	523	3.221		
AVG	3.5C	7	7	SprayBlock	1	37.969	37.97	< 0.001
				Block	6	17.598	17.6	< 0.001
				Treatment	1	38.042	38.04	< 0.001
				Block.Treatment	7	29.362	29.36	< 0.001
				Residual	417	4.089		
AVG	3.5D	8	8	Block	7	10.962	10.96	< 0.001
				Treatment	2	2.539	2.54	0.079
				Block.Treatment	14	6.785	6.79	< 0.001
				Residual	390	3.495		

*'Treatment' is the no hormone versus hormone. 'Exp' is the experimental replicates, and 'SD' is the scoring date (Combined dpi), 'SprayBlock' refers to the group of pots sprayed separately, 'Block' refers to the RCBD experimental design. All ANOVA tests are derived from GLM analysis Poisson distribution with a Log-Link Function. Using GLM (Poisson distribution and log-link function) for Bd21 trials, the model 'SprayBlock (separate spraying in tunnel if present) + Block * Treatment' against the response variate. Experiment column refers to the trial the compound was tested in (some hormones were tested in the same experiment). Auxins is the combination of both IAA and NAA withing the ANOVA.

Supplementary Table S6. Accumulated analysis of variance for **DON content** after plant hormone application on wheat FHB at BASF.

Hormone	Experiment	Transformation	DPI	Factor**	d.f	Mean deviance	Deviance ratio	Approx. F. Prob
SA	1	-	7	Block	2	2302	1.22	0.386
				Treatment	1	1128	0.6	0.482
				Residual	4	1885		
IAA	3	-	7	Block	3	1250	1.42	0.39
				Treatment	1	12.5	0.01	0.913
				Residual	3	879.2		
IAA*	1	-	7	Block	2	3868.8	11.9	0.021
				Treatment	1	0	0	1
				Residual	4	325		
NAA*	3	SQRT	7	Block	2	6.603	2.86	0.169
				Treatment	1	0.038	0.02	0.904
				Residual	4	2.31		
NAA	4	LOG10	7	Block	2	0.07989	1.88	0.266
				Treatment	1	0.11432	2.69	0.176
				Residual	4	0.04251		
GA	1	-	7	Block	2	309	0.21	0.817
				Treatment	1	112	0.08	0.795
				Residual	4	1455		
BRZ	2	-	8	Block	2	380	0.16	0.859
				Treatment	1	378	0.16	0.711
				Residual	4	2396		
AVG 35	4	-	7	Block	2	27.3	1.48	0.331
				Treatment	1	11.28	0.61	0.478
				Residual	4	18.46		
AVG 350	2	-	8	Block	2	439	0.22	0.812
				Treatment	1	153	0.08	0.796

333

				Residual	4	2004		
JARIN-1 300	3+4	-	7	Exp	1	34410.3	179.6	< 0.001
				Block	2	827.3	4.32	0.044
				Treatment	1	420.3	2.19	0.169
				Exp.Treatment	1	729	3.8	0.08
				Residual	10	191.6		

Data is for graphs in Fig. 3.11 or * Fig. 3.12 ** 'Treatment' is the no hormone versus hormone. 'Exp' is the experimental replicates, and 'SD' is the scoring date (Combined dpi). 'Block' refers to the trolley block where two blocks were placed. RCBD block is an artefact of the compound factor. Experiment column refers to the trial the compound was tested in (some hormones were tested in the same experiment). All ANOVA tests are derived from GLM analysis normal distribution with an identity Link Function. For DON tests, a GLM with a normal distribution and identity Link function was used with the model 'Experiment + Trolley + Treatment + Experiment * Treatment' or 'Trolley + Treatment' depending on any experimental replicates, both against the DON content response variate. The symbol '-' denotes no transformation was applied to the data.

Supplementary Table S7. Accumulated analysis of variance for FRR experiment with *bcat* strains (Fig. 6.16).

DPI	Transformation	N	Factor	d.f	Mean deviance	Deviance ratio	Approx. F. Prob
2	LOG10	40	Tray	1	0.06946	1.24	0.267
			Strain	5	0.14095	2.51	0.031
			Residual	232	0.05618		
4	-	40	Tray	1	0.0002	0	0.965
			Strain	5	0.1264	0.99	0.423
			Residual	233	0.1273		
6	SQRT	40	Tray	1	0.0943	0.61	0.435
			Strain	5	0.0878	0.57	0.723
			Residual	233	0.154		

All ANOVA's are derived from GLM analysis with a normal identity and Link Function. GLM analysis fitted model 'Tray + Strain' against the response variate 'RNL. Transformation denotes any what transformation was used on the Fungal length variate during GLM analysis. N is the Number of biological replicates (With the exception of N=39 for *bcat-L* at 2 dpi).

Supplementary Table S8. Accumulated analysis of variance for mycelial growth of *bcat* strains (Fig. 6.15).

DPA	Transformation	N	Factor	d.f	Mean deviance	Deviance ratio	Approx. F. Prob
1	SQRT	48/48/48 /48/48	Strain				
				4	0.122772	49.44	<0.001
			Strain.Rep	10	0.002216	0.89	0.541
			Residual	223	0.002483		
2	-	48/46/48 /48/46	Strain				
				4	0.61691	49.88	<0.001
			Strain.Rep	10	0.0114	0.92	0.514
			Residual	221	0.01237		
3	-	14/22/26 /22/23	Strain				
				4	0.47273	14.11	<0.001
			Strain.Rep	10	0.04267	1.27	0.257
			Residual	92	0.03351		

All ANOVA's are derived from GLM analysis with a normal identity and Link Function. GLM analysis fitted model 'strain / mycelial plug (rep)' against the response variate 'cumulative radial length'. Transformation denotes any what transformation was used on the Fungal length variate during GLM analysis. N (PH1/bcat-C/bcat-E/bcat-H/bcat-L) is the Number of biological replicates.

Supplementary Table S9. Accumulated analysis of variance for ethylene GC with different *Fusarium* isolates (Fig. 6.10).

Data	Transformation	Factor	d.f	Mean deviance	Deviance ratio	Approx. F. Prob
Area	logit	Experiment	1	0.6561	1.34	0.264
		Isolate	11	0.6178	1.26	0.324
		Residual	17	0.4907		
ET	-	Experiment	1	1.04	0.05	0.825
		Isolate	9	29.15	1.46	0.301
		Residual	8	19.91		

'All ANOVA's are derived from GLM analysis with a normal identity and Link Function. GLM distribution 'Experiment + Isolate' against the response variate. Ethylene emission experiment with FgKO. Transformation denotes any what transformation was used on the Fungal length variate during GLM analysis. The number of biological replicates for area per isolate: cc120 (3), cc52 (2), F500 (2), F710 (2), F712 (2), F713 (2), F77 (2), F86 (3), Fc2037 (2), Fc2076 (2), Fg K1/4 (3), PH1 (5). The number of biological replicates for Ethylene (ET) is the same except for F500 (1), Fc2037 (1), K1/4 (1), PH1 (2). F713 was not measured for ET.

Supplementary Table S10. Accumulated analysis of variance for ethylene GC with different bcat strains (Fig. 6.14).

Data	Transformation	N	Factor	d.f	Mean deviance	Deviance ratio	Approx. F. Prob
GC bcat area	-	5/5/4	Strain	2	267.1	4.37	0.04
			Residual	11	61.13		
GC bcat ET	-	4/5/4	Strain	2	0.4379	3.58	0.067
			Residual	10	0.1224		
All bcat area	*	**	Strain	12	11.01	0.15	0.976
			Residual	1	72.84		
All bcat ET	*	***	Strain	9	49.9707	58.06	0.102
			Residual	1	0.8607		

*Could not perform transformation checks due to low number of observations. **One biological replicate for each strain except for *bcat-J* which had two. The number of observations is the same as ** except excludes *bcat-L*, *bcat-C*, and *bcat-D*. Abbreviation: ET (Ethylene). All ANOVA's are derived from GLM analysis with a normal identity and Link Function. GLM analysis modelled the 'strain' factor treatment against the response variate. Transformation denotes any what transformation was used on the Fungal length variate during GLM analysis. N (PH1/ bcat-E/bcat-H) is the Number of biological replicates.

Primer Lists

Supplementary Table S11. PCR primers for phytohormone-associated genes and housekeeping genes in *Brachypodium distachyon*.

Hormone	Gene Abbreviation	Gene Name	GeneBank number	Primers (F/R)*
-	*ACT7*	Actin 7	DV471671	-CCTGAAGTCCTTTTCCAGCC- / -AGGGCAGTGATCTCCTTGCT-
-	*GAPDH*	GAPDH	DV482924	-TTGCTCTCCAGAGCGATGAC- / -CTCCACGACATAATCGGCAC-
SA	*PR-1*	*Pathogenesis related -1*	Bradi1g57590	- CGAGAAGAAGAACTACCACCATGAC- / - ACACCCGATGGCAGTCGA-
JA	*OPR3*	*12-Oxophytodienoate reductase 3*	Bradi3g37650	- GGGCGGCTGTTCATATCTAA- / - GGGACGGATAGTCGGTGTAA-
Ethylene	*OsETR2*	*Ethylene Receptor 2*	Bradi5g00700	- CAGTTCTGGAGGAGTCTCAGTTGA- / - CCATCATAGCTTCATGCTTTGC-
ABA	*GLTP*	*Glycolipid transfer protein*	Bradi1g11280	- AACGACTGCGTCAAGAAGCA- / - GTCGTAGCAGCATCATACAACGTA-
SA	*AtMES1*	*Methylsalicylate esterase*	Bradi2g52110	- AGCTGCCTATTTCCATGCTGTT- / - ATCGAACCCACTCGCATCA-
JA	*OsMYC2*	*Helix-loop-helix leucine zipper protein*	Bradi3g34200	- CGACGCCATCTCTTACATCA- / - CCTCAATCTGGGAATGGAGA-
Ethylene	LOC_Os01g73200	*Peroxidase*	Bradi4g27680	- ACGACCCCACCATGAACAA- / - GGTTCATCAGGTCGACGTAGTACTT-
ROS	*RbohB*	*Respiratory burst oxidase homologue protein B*	Bradi4g17020	- GATACTCAAGGTGGCCGTGT- / - ACGCTGACGTAGTCGTCCTT-

*Primer design derived from (Kakei et al., 2015) except *RbohB* was made on Primer3 (Section 4.2.5). *RbohB* was identified from orthologue comparison of *AtRbohD* on Ensembl Genomes database (Howe et al., 2020). The function of *AtRbohD* was sourced from (Dmochowska-Boguta et al., 2013). Primers and gene code of housekeeping genes obtained from (Hong et al., 2008). Hormone abbreviations: SA (Salicylic acid), JA (Jasmonic acid), ABA (Abscisic acid), ROS (Reactive oxygen species).

Supplementary Table S12. Primers used for all time-course RT-qPCR assays. Fig. 4.11.

Hormone responsive	Gene name *	Gene ID*	Gene ID in Figures	Primer Pair (F/R)	Tm (°C)	Product size (bp)
HK gene	GAPDH**	DV482924 Bradi3g14120****	GAPDH	- TTGCTCTCCAGAGCGATGAC - / - CTCCACGACATAATCGGCAC -	50-60	236
SA/JA	PR1***	Bradi1g57590	PR1	- CGAGAAGAAGAACTACCACCATGAC - / - ACACCCGATGGCAGTCGA -		
SA	NPR4	Bradi2g54340	NPR4	- ATGGAGTTGCGGTTGTTGTC - / - GCCAGTGATGTGAACAGAGC -	59.05 59.20	82
SA	AtMES1***	Bradi2g52110	MES1	- AGCTGCCTATTTCCATGCTGTT - / - ATCGAACCCACTCGCATCA -		
SA	WRKY45_1	Bradi2g30695	WRKY	- CACAAGTACGACCAGCAGTG - / - GCCGATGTATGTCACCCTGA -	58.86 59.54	96
JA	JAZ	Bradi4g31240	JAZ	- CGGCAGCTGACCATCTTTTA - / - CTCTGTGCAGGTTGGGGC -	58.26 60.67	164
JA	LOX2	Bradi3g39980	LOX2	- CCATCGATAAGAGCACACGT - / - GAGGAGGAAGCAAGGACATG -	57.79 57.96	185
Auxin	Aux/IAA	Bradi1g09090	AUXIA	- CCACCAGTCCGATCGTACC - / - TCCTTCTCGGCTTCCTCTTC -	59.56 58.81	80
Auxin	GH3-2	Bradi2g50840	GH3	- GTCCCCGTGGTCACCTAC - / - TTGGGTGGGAGGAGATGATG -	59.02 58.78	88
CK	LOG1	Bradi2g42190	LOG1	- CATCGACCTGGTCTACGGAG - / - CAATCACATGGCGTCCTCC -	59.34 58.6	98
CK	A-type RR 9	Bradi4g43090	RR9	- CAACAGCTGTAACCCCACAA - / - TGTTGTTTGCAGAGTCGGTG -	58.31 58.99	80

*All hormone genes were selected from RNA-seq results in Chapter 4 (Fig. 4.5-4.10) (RNA-seq data not shown) and made on Primer3 (Section 4.2.5) unless otherwise stated. ** From (Hong et al., 2008). *** From (Kakei et al., 2015).**** Predicted as this geneID on (Ensembl Genomes database (Howe et al., 2020)). Abbreviation: HK (Housekeeping), F (Forward primer), R (Reverse primer). Hormone abbreviations: SA (Salicylic acid), JA (Jasmonic acid), CK (Cytokinin).

Supplementary Table S13. Primers used for *F. graminearum* PH1 RT-qPCR assay.

Gene Function	Gene name	Gene ID**	Gene ID in Figures	Primer Pair (F/R)	Tm (°C)	Product size (bp)
HK gene	ubiquitin C-teminal hydrolase*	FGSG_01231.3	*gzUBH*	-GTTCTCGAGGCCAGCAAAAAGTCA - / - CGAATCGCCGTTAGGGGTGTCTG -	62.4 65.2	168
Fungal Effector	*TOX2*	FGRAMPH1_01G00199	*Tox2*	- CTACAGGCCCTTCTTGACCA - / - GTCAACTGCCCATCATCGAC -	59.02 58.99	86
Fungal Effector	Pectate Lyase	FGRAMPH1_01G16515	PecLy	-GTACCAAGACCCTCAGCACT - / - AGACTGGCCGGTACATTTCA -	59.02 59.02	101

*Gene used as reference housekeeping gene (Kim & Yun, 2011). **If gene was chosen based off a research paper, the reference was included. Abbreviation: HK (Housekeeping), F (Forward primer), R (Reverse primer).

Supplementary Table S14. PCR primers used for *Fusarium* split marker deletion experiment (Section 6.2.4.).

Primer ID	Full Primer ID	Oligo Sequence*	Properties
JH1	5'flank_ET_fwd	-ccgcgggaattcgatGAAAATACAAGATATCAGATTTATTTCAGAAAG-	3'Tm=62.8 3'Ta=62.8
JH2	5'flank_ET_rev	-gttatcgaatTCGGTGGCTGTGATCATG-	3'Tm=64.3 3'Ta=62.8
JH3	HY-seq_fwd	-gccaccgaATTCGATAACTGATATTGAAGGAGCATTTTTT-	3'Tm=67.8 3'Ta=67.8
JH4	HY-seq_rev	-gcgaattcactagtgatGGATGCCTCCGCTCGAAG-	3'Tm=68.0 3'Ta=67.8
JH5	YG_seq_fwd	-ccgcgggaattcgatCGTTGCAAGACCTGCCTG-	3'Tm=65.4 3'Ta=60.4
JH6	YG_seq_rev	-cggtctgcCTCGAGGTCGACGGTATC-	3'Tm=60.4 3'Ta=60.4
JH7	flank_ET-3'_fwd	-acctcgagGCAGACCGTGATATCCTAG-	3'Tm=56.8 3'Ta=55.8
JH8	flank_ET-3'_rev	-gcgaattcactagtgatCCTCGTCTACTTCCTCATC-	3'Tm=55.8 3'Ta=55.8
JH9	Intron3_fwd	-CAATGCTCCCACCTCGTAAG-	Tm=58.34
JH10	Intron4_rev	-CCATCTGGCATTTCAAGACCT-	Tm=58.27
JH11	Ex5'flank_fwd	-CTGCGTGGCTACAACTCATC-	Tm=59.00
JH12	IntHY_rev	-TTTGTAGAAACCATCGGCGC-	Tm=59.2
JH13	Ex3'flank_rev	-GCTTTCCAACATCGATCGCT-	Tm=58.99
JH14	IntYG_fwd	-CGTGGTTGGCTTGTATGGAG-	Tm=58.91
A2	ExtHY-flank _Rev	-GGCCGCGAATTCACTAGTG-	Tm=53.2
M13_F**	M13 (-21) Forward	-TGTAAAACGACGGCCAGT-	
M13_R**	M13 (-40)	-GTTTTCCCAGTCACGAC-	

Primers JH1-9 were made on NEBuilder, whereas JH9-JH14 and A2 were made on Primer3 (Section 4.2.5). *For JH1 to JH8, non-capitalised base pairs indicate overlapping region with adjacent sequence (Fig. 6.3) hence capitalised base pairs are gene(sequence)-specific primers. **Primer pair from Dr Marianna Pasquariello. Abbreviation: ET (Ethylene), Ex (External (Outside of coding sequence)), Fwd (Forward primer), HY (Left half of HYG gene), Int (Internal (Inside coding sequence)), Ta (annealing temp), Tm (melting temperature), Rev (Reverse primer), YG (Right half of HYG).